Variability of atmospheric aerosols at urban, regional and continental backgrounds in the Western Mediterranean Basin

Noemí Pérez Lozano

PhD Thesis
Barcelona 2010

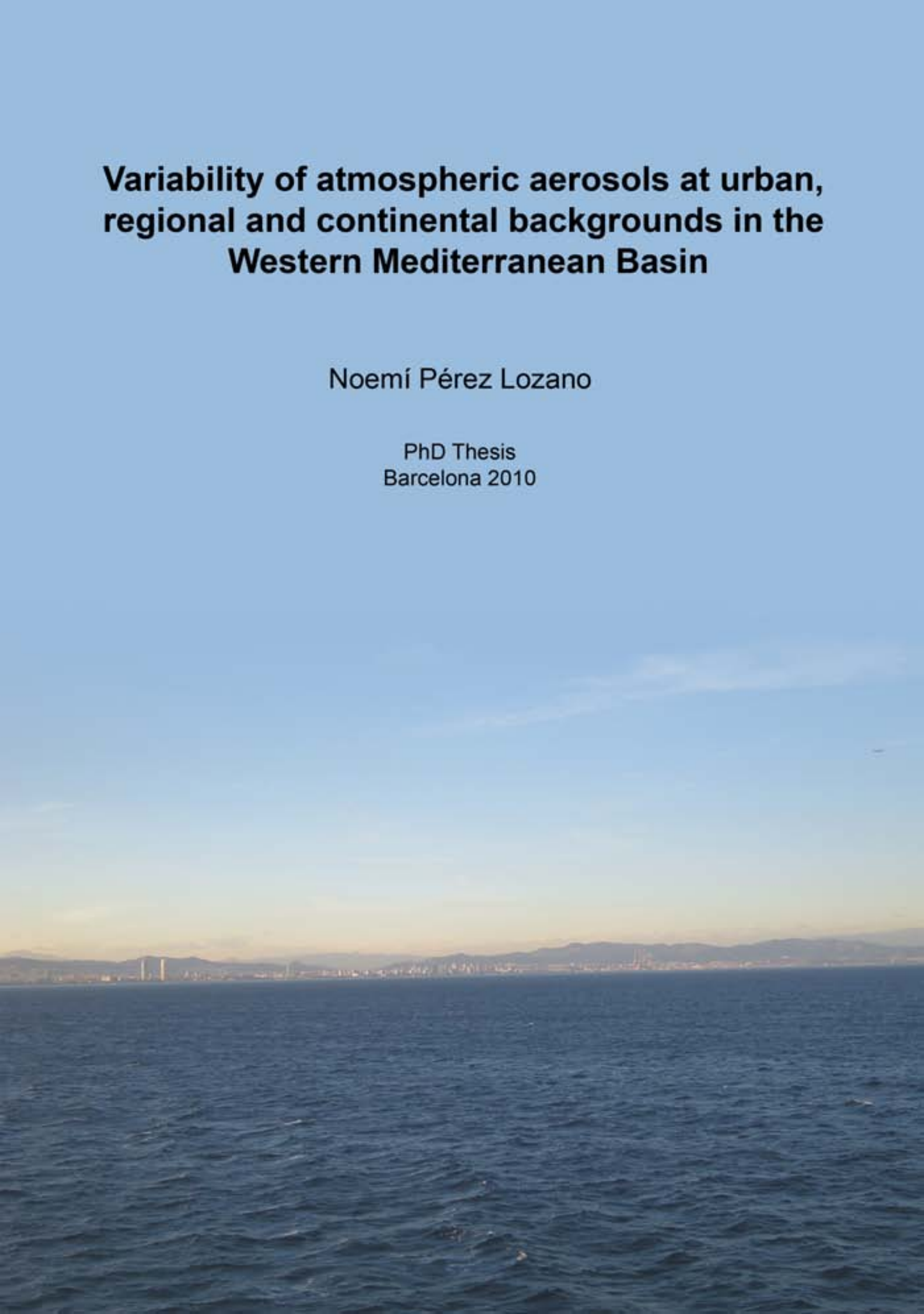

VARIABILITY OF ATMOSPHERIC AEROSOLS AT URBAN, REGIONAL AND CONTINENTAL BACKGROUNDS IN THE WESTERN MEDITERRANEAN BASIN

PhD Thesis

Noemí Pérez Lozano

Barcelona 2010

Directores de tesis:

Dr. Andrés Alastuey Urós
Instituto de Diagnóstico Ambiental y estudios del Agua (IDAEA)
Consejo Superior de Investigaciones Científicas (CSIC)

Dr. Xavier Querol Carceller
Instituto de Diagnóstico Ambiental y estudios del Agua (IDAEA)
Consejo Superior de Investigaciones Científicas (CSIC)

Tutora de tesis:

Dra. Montserrat Sarrà i Adroguer
Institut de Ciència y Tecnologia Ambientals (ICTA)
Universitat Autònoma de Barcelona (UAB)

Abstract

The Western Mediterranean basin (WMB) is characterised by an abrupt topography and complex atmospheric dynamics and meteorological processes that induce the recirculation of air masses with the consequent ageing and accumulation of pollutants at a regional scale. These recirculations, together with a low rainfall, the high solar radiation intensity, that favors atmospheric photochemical processes, and the increased convective dynamics favoring local soil resuspension, induce a PM seasonal pattern characterised by a high summer regional background. African dust outbreaks also contribute to increase summer aerosol levels. These features together with the large atmospheric anthropogenic emissions produced in the Mediterranean coast (mainly arising from densely populated areas, large industrial estates, shipping, agriculture and forest fires, among others) give rise to a scenario with a complex aerosol phenomenology, with anthropogenic and natural primary aerosol, bulky secondary aerosol formation and transformation and intensive interactions between aerosols and gaseous pollutants.

A detailed study of PM levels and composition measured simultaneously in different environments at a regional scale was performed in the WMB in order to understand the sources, behaviour, transformation and transport patterns of tropospheric aerosols in this area. In this direction, the monitoring of PM_{10}, $PM_{2.5}$ and PM_1 (particle mass concentrations finer than 10, 2.5 and 1 μm) levels and chemical characterization was carried out at three monitoring stations: Montsec (MSC, continental background, 1570 m.a.s.l.), Montseny (MSY, regional background, 720 m.a.s.l.) and Barcelona (BCN, urban background, 68 m.a.s.l.). In addition, number concentration (N) and black carbon levels (BC) were monitored at BCN, in order to assess the important influence of road traffic on the levels of ultrafine particles at the urban atmosphere. Furthermore, a detailed meteorological study was performed for each background site, with the objective to understand atmospheric processes affecting aerosols.

A few studies on PM characterisation have been previously performed in the WMB. In order to provide a new insight, this is the first time that aerosol sampling and characterisation has been conducted at a remote site in the WMB simultaneously with regional and urban environments. In addition, this is the first time that PM_1 chemical characterization and BC and N continuous and simultaneous monitoring are performed in this area.

A detailed study was performed and presented separately for the urban, regional and continental backgrounds considered. Then, an intercomparison of the simultaneous data recorded at the three sites is carried out, in order to discuss the main sources and characteristics of atmospheric aerosols in the WMB and to estimate urban, regional and external contributions to aerosols in the region.

The variability of atmospheric aerosols in the WMB is governed by diverse anthropogenic and natural emissions and the concatenation of different meteorological scenarios, affecting levels, composition and size distribution of atmospheric particulate matter. Following previous studies, different scenarios were considered: Atlantic advective conditions, African dust episodes, summer regional recirculation episodes, European and Mediterranean transport episodes, and winter anticyclonic episodes. The seasonal distribution of these episodes, together with the typical climatic patterns of the WMB gives rise to a marked seasonal pattern for PM background. In addition, local emissions are superimposed to this background pattern. Atmospheric dynamics at MSY and MSC (mainly governed by breeze circulations), regulate the daily evolution of PM levels, transporting aged air masses upwards and increasing PM levels at elevated areas. At BCN, the daily variability of atmospheric aerosols and gaseous pollutants is very influenced by road traffic emissions but also by meteorology (mainly sea-land breezes).

Mean annual levels of PM_{10}, $PM_{2.5}$ and PM_1 (for the simultaneous 2006-2007 dataset) were 40, 27 and 19 µg m^{-3}, respectively, at BCN, 15, 11 and 9 µg m^{-3} at MSY and 17, 12 and 7 µg m^{-3} at MSC. Major differences between the urban and rural sites were determined for winter, being the levels more similar during summer. Differences are due to the meteorological scenarios prevailing during each season.

During winter, the frequent anticyclonic atmospheric stability induces the stagnation of air masses that, together with road traffic emissions, produce important pollution episodes at BCN. However, atmospheric decoupling leaves MSY and, more frequently MSC, isolated from regional pollution during several days. In specific scenarios, the growth of the boundary layer and development of mountain breezes, activated by solar radiation, result in the transport of polluted air masses accumulated in the valley to the rural sites, increasing markedly PM levels at a different rate depending on the altitude and distance to the source areas. These scenarios frequently impact MSY increasing levels of PM_1 (mainly composed of carbonaceous compounds and ammonium nitrate) and reaching hourly values even higher than at BCN, due to the interaction between

pollutants during transport. Given its altitude, MSC is frequently isolated from regional pollution. However, when the high PM_1 episodes are persistent the polluted air masses may also reach distant areas such as MSC.

During summer, intense breeze circulations and atmospheric mixing favour the dispersion, transport, recirculation and ageing of pollutants at a regional scale, reducing the differences between the urban and the rural sites. Similar concentration levels of the main components (OM+EC, SIA, mineral matter) were measured in PM_{10} at MSY and MSC. During this season, levels of PM and major components are still higher in BCN with respect to the rural sites, but differences are not as marked as in winter. However, it should be noticed that mean levels of sulphate during the regional recirculation episodes are similar at the three sites proving the regional origin of this compound and the high mixing during these events. Mineral matter levels increase during the summer at the rural sites, as a consequence of a favoured regional dust resuspension (breezes and scarce precipitations) and a higher frequency of African dust episodes. This increase is more significant at MSC given the higher impact of African dust episodes at higher attitudes and the favoured local resuspension of dust by wind.

African dust outbreaks increase markedly the levels of coarse PM at all sites in the WMB, leading to exceedances of the PM_{10} daily limit values. However, at BCN, this increase in coarse PM cannot be exclusively attributed to African dust, due to the important road dust traffic emissions. At the rural sites, almost all the exceedances recorded were caused by African dust outbreaks, being the impact, as stated above, much higher at MSC. African dust contributions to mean annual PM_{10} levels during 2006-2007 were estimated as 2.1, 0.6 and 1.4 μg m^{-3} at BCN, MSY and MSC, respectively. The increase in mineral matter levels was quantified as 1.3, 0.5 and 1.1 μg m^{-3} for BCN, MSY and MSC, respectively. The difference observed between the increase in PM_{10} levels and the increase in mineral matter levels attributed to African dust outbreaks may be due to the formation of secondary aerosols favoured by the presence of high concentrations of mineral dust.

Source apportionment studies (Principal Component Analysis (PCA) and Positive Matrix Factorization (PMF)) were carried out with all available data, individually for the different sites, but also for simultaneous PM_{10} data measured at BCN, MSY and MSC during the period 2006-2007. The results obtained in the simultaneous study showed five common aerosol sources at a regional scale, representative of the region of study:

Mineral matter, ammonium sulphate + fuel oil combustion, ammonium nitrate, aged aerosols (sea spray + secondary aerosols) and a primary road traffic + industrial tracers source showing its main contribution at the urban site. The major contribution to PM_{10} in BCN is mainly related to road traffic (50% of total PM_{10}), resulting from primary traffic emissions (29%), secondary nitrate (9%) and also aged secondary aerosols (13%), although the latter may be partially attributed to other sources. Other urban source identified is the anthropogenic dust (13%), which may be also emitted by traffic in an important extent (road dust resuspension by vehicles) but also by wind resuspension and construction/demolition works. Ammonium sulphate has also a significant urban contribution (6%). The regional contribution to PM_{10} at the urban site (25%) is mainly composed of mineral dust, ammonium sulphate and nitrate species. Finally, African dust (1%) and sea spray (5%) had low contributions at the urban site. At MSY and MSC, the major sources are mineral matter and secondary sulphate. Secondary nitrate is a very important source in MSY but has a lower relevance in MSC. The African dust source is slightly higher at MSC.

The variability of different aerosol measurement parameters (N, BC, PM_{10}, $PM_{2.5}$ and PM_1) and gaseous pollutants was studied at BCN urban background. The hourly variability of all aerosol metrics and gaseous pollutants recorded is very influenced by road traffic emissions and meteorology (especially by the evolution of breezes). PM_x, N, BC, CO and NO_x levels increase markedly during traffic rush hours, reflecting direct exhaust emissions. Then, levels of most parameters decrease at midday due to the reduction of traffic emissions and the changes in wind direction and speed, due to dilution processes. However, some parameters are not only governed by traffic direct exhaust emissions. Thus, $PM_{2.5-10}$ remains high during all the day due to road dust resuspension processes, but also has contributions from other sources (dust resuspension by wind). $PM_{1-2.5}$ and PM_1 levels increase during traffic rush hours but also at night, when the decrease of the boundary layer depth favours condensation and coagulation processes, and consequently N levels decrease and levels of the fine PM fractions increase. In addition to the traffic peak, N levels show a second but very important peak at noon, reflecting the variation of the solar radiation intensity, which may be attributed to ultrafine particle formation by the photochemical nucleation of precursor gases. This peak appears when the levels of BC (primary emissions) are very low. Thus, N is influenced by direct ultrafine particle emissions but also in a very important fraction by the formation of secondary particles by photochemical processes.

The time series obtained in this study were completed with available data from previous studies in order to study temporal trends. The influence of road traffic emissions on the levels of fine particulate matter at the urban background is reflected in PM_1 mean annual levels, which show a significant increasing inter-annual trend from 2003 to 2007, and a good correlation with the progressive rise in road traffic flow and the growth of the diesel fleet in Barcelona. However the coarser fractions showed a decreasing trend at BCN and MSY than may be attributed to meteorology and the frequency and intensity of African dust outbreaks, but could also be related to temporal changes in anthropogenic emissions, such as road traffic or industrial emissions. Accordingly, a decreasing trend was observed in the levels of some industrial and road traffic tracers at BCN and MSY. In order to identify trends in aerosol sources, source apportionment studies (PCA and PMF) were applied to the complete time series obtained. As a result, the industrial source identified in BCN presented a decreasing trend from 2003 to 2007.

The variety of sources and factors affecting the variability of atmospheric pollutants in the WMB make the simultaneous monitoring of different parameters necessary, in order to better understand emission sources, transformation or transport processes, and to be able to establish effective emission abatement techniques. The results also show that the monitoring of PM_1 (nucleation and accumulation modes) or BC, providing information about contributions from combustion processes, and PM_{10}, providing information on combustion and also mechanically-generated aerosols may be a better strategy than the combination of $PM_{2.5}$ and PM_{10} measurements as air quality standards.

The parallel monitoring of aerosols at an urban, regional and continental background was a useful strategy in order to understand the phenomenology of aerosols at the WMB. Given the meteorological characteristics of the WMB, the urban and industrial emissions, concentrated in the coastal areas have a considerable impact in PM levels and composition in rural and remote areas located at different altitudes, both in summer, with important atmospheric recirculation and mixing of air masses at a regional scale, and during winter, with breeze-activated transport of stagnated urban pollutants. The high contribution of urban emissions and the transport of air masses at a regional scale demonstrate the importance of devising and applying emission abatement strategies for urban road traffic, in order to improve efficiently air quality in the study area, not only at a local, but also at a regional scale.

Resumen

La cuenca del Mediterráneo Occidental se caracteriza por una topografía abrupta y una compleja dinámica atmosférica y procesos meteorológicos que inducen a la recirculación de masas de aire con el consiguiente envejecimiento y acumulación de contaminantes a escala regional. Estas recirculaciones, junto con una baja precipitación, una alta intensidad de radiación solar que favorece procesos fotoquímicos atmosféricos, y una dinámica convectiva que favorece la resuspensión del suelo, inducen un patrón estacional del material particulado atmosférico (PM) que se caracteriza por un alto fondo regional en verano. Las intrusiones de polvo desde el norte de África contribuyen también a aumentar los niveles de aerosoles en verano. Estas características, junto con las importantes emisiones antropogénicas de la costa mediterránea (originadas principalmente en zonas densamente pobladas, grandes polígonos industriales, transporte, agricultura e incendios forestales, entre otros) dan lugar a un escenario con una fenomenología compleja del aerosol atmosférico, con emisiones primarias naturales y antropogénicas, formación y transformación de aerosoles secundarios y una importante interacción entre aerosoles y gases contaminantes.

Se ha realizado un estudio detallado de los niveles y composición de PM medidos simultáneamente en diferentes ambientes a escala regional en la cuenca del Mediterráneo Occidental, con el fin de entender las fuentes, propiedades, y patrones de transformación y transporte de aerosoles troposféricos en este ámbito. En esta dirección, la medida de los niveles y caracterización química de PM_{10}, $PM_{2.5}$ y PM_1 (concentración en masa de partículas más finas de 10, 2,5 y 1 micra) se ha llevado a cabo en tres estaciones de monitoreo: Montsec (MSC, fondo continental a 1570 m.s.n.m.), Montseny (MSY, fondo regional, 720 m.s.n.m.) y Barcelona (BCN, fondo urbano, 68 m.s.n.m.). Además, los niveles de concentración en número de partículas (N) y el coeficiente de absorción o carbono negro (*black carbon*, BC) fueron monitoreados en BCN, con el fin de evaluar la influencia del tráfico rodado en los niveles de partículas ultrafinas de la atmósfera urbana. Por otra parte, se realizó un estudio meteorológico detallado para cada sitio, con el objetivo de comprender los procesos atmosféricos que afectan a los aerosoles.

Algunos estudios sobre la caracterización de PM han sido realizados anteriormente en la cuenca del Mediterráneo Occidental. A fin de proporcionar una nueva visión, esta es la primera vez que el muestreo y caracterización de aerosoles se ha realizado en un

sitio remoto en esta zona simultáneamente con ambientes regional y urbano. Además, esta es la primera vez que la caracterización química de PM_1 y la monitorización continua y simultánea de N y BC se llevan a cabo en esta zona.

Se han realizado estudios detallados para la zona urbana, el fondo regional y el continental y se han presentado por separado. A continuación, se ha llevado a cabo una intercomparación de los datos simultáneos registrados en los tres sitios, a fin de discutir las principales fuentes y características de los aerosoles atmosféricos en la cuenca del Mediterráneo Occidental y estimar, en la zona urbana, las contribuciones regionales y externas a los aerosoles en la región.

La variabilidad de los aerosoles atmosféricos en la cuenca del Mediterráneo Occidental se rige por diversas emisiones antropogénicas y naturales y la concatenación de diferentes escenarios meteorológicos, que afectan a los niveles, la composición y la distribución de tamaños del material particulado atmosférico. A partir de estudios anteriores, se han considerado los siguientes escenarios: condiciones de advección Atlántica, episodios de intrusión de polvo de África, episodios de recirculación regional de verano, episodios de transporte de masas de aire de Europa y el Mediterráneo, y episodios anticiclónicos de invierno. La distribución estacional de estos episodios, junto con los patrones típicos del clima de la cuenca del Mediterráneo Occidental da lugar a un marcado patrón estacional para el fondo de PM. Además, las emisiones locales se superponen a este patrón de fondo. La dinámica atmosférica en MSY y MSC (regida principalmente por las circulaciones de brisas) regula la evolución diaria de los niveles de PM, transportando las masas de aire y aumentando los niveles de PM en zonas elevadas. En BCN, la variabilidad diaria de los aerosoles atmosféricos y gases contaminantes está muy influenciada por las emisiones del tráfico y también por la meteorología (principalmente brisas mar-tierra).

Los niveles medios anuales de PM_{10}, $PM_{2.5}$ y PM_1 (para el conjunto de datos simultáneos medidos en 2006-2007) fueron 40, 27 y 19 µg m^{-3}, respectivamente, en BCN, 15, 11 y 9 µg m^{-3} en MSY y 17, 12 y 7 µg m^{-3} en MSC. Las mayores diferencias entre el fondo urbano y las zonas rurales se observaron durante el invierno, siendo los niveles más similares durante el verano. Las diferencias se deben a los escenarios meteorológicos que prevalecen durante cada temporada.

Durante el invierno, la frecuente estabilidad atmosférica anticiclónica induce el estancamiento de las masas de aire que, junto con las emisiones del tráfico, producen

importantes episodios de contaminación en BCN. Sin embargo, esta estabilidad atmosférica deja MSY y, más frecuentemente MSC, aislados de la contaminación regional durante varios días. En determinados escenarios, el crecimiento de la capa límite y el desarrollo de brisas de la montaña, activados por la radiación solar, resulta en el transporte de las masas de aire contaminado acumuladas en el valle a las estaciones rurales, aumentando notablemente los niveles de PM, a ritmos diferentes en función de la altitud y la distancia a las zonas de origen. Estos escenarios impactan con frecuencia en MSY, incrementando marcadamente los valores horarios de PM_1 (compuesto principalmente de compuestos de carbono y nitrato amónico), incluso más que en BCN debido a la interacción entre los contaminantes durante el transporte. Dada su altitud, MSC se encuentra frecuentemente aislada de la contaminación regional. Sin embargo, cuando los episodios de PM_1 son persistentes las masas de aire contaminado también pueden llegar a zonas distantes como MSC.

Durante el verano, la circulación de las brisas favorece la dispersión atmosférica, el transporte, la recirculación y el envejecimiento de contaminantes a escala regional, reduciendo las diferencias entre el fondo urbano y las zonas rurales. Se midieron concentraciones similares de los componentes principales (compuestos carbonosos, aerosoles inorgánicos secundarios, materia mineral) de PM_{10} en MSY y MSC. Durante esta estación, los niveles de PM y sus componentes principales son más altos en BCN con respecto a las estaciones rurales, pero las diferencias no son tan marcadas como en invierno. Sin embargo, cabe señalar que los niveles medios de sulfato durante los episodios de recirculación regional son similares en los tres sitios, demostrando el origen regional de este compuesto y la importante mezcla atmosférica durante estos eventos. El aumento de los niveles de materia mineral durante el verano en las zonas rurales es debido a una favorecida resuspensión del polvo por el efecto de brisas y escasas precipitaciones, y a una mayor frecuencia de episodios de intrusión de masas de polvo africano. Este aumento es más significativo en el MSC dado el mayor impacto de los episodios de polvo africano a mayores altitudes y la resuspensión de polvo local favorecida por el viento.

Las intrusiones de masas de aire desde el Norte de África incrementan notablemente los niveles de las fracciones gruesas de PM en la cuenca del Mediterráneo Occidental, dando lugar a la superación de los valores límite diarios establecidos para PM_{10}. Sin embargo, en BCN, este aumento no puede atribuirse exclusivamente al polvo africano, debido a las importantes emisiones de polvo de carretera por el tráfico. En las estaciones rurales, casi todos los casos de superación registrados fueron causados

por las intrusiones africanas, siendo el impacto mucho más alto en el MSC. Las contribuciones africanas a los niveles medios anuales de PM_{10} durante el bienio 2006-2007 se han estimado como 2.1, 0.6 y 1.4 μg m^{-3} en BCN, MSY y MSC, respectivamente. El aumento en los niveles de materia mineral se ha cuantificado en 1.3, 0.5 y 1.1 μg m^{-3} para BCN, MSY y MSC, respectivamente. La diferencia observada entre el aumento en los niveles de PM_{10} y el aumento en los niveles de materia mineral atribuido a las intrusiones africanas puede deberse a la formación de aerosoles secundarios favorecida por la presencia de altas concentraciones de polvo mineral.

Se han llevado a cabo estudios de contribución de fuentes (Análisis de Componentes Principales (PCA) y Factorización de Matriz Positiva (PMF)) con todos los datos disponibles, de forma individual para todas las estaciones, y también para los datos medidos simultáneamente en BCN, MSY y MSC durante el período 2006-2007. Los resultados obtenidos en el estudio simultáneo mostraron cinco fuentes de aerosoles comunes a escala regional, representantes de la región de estudio: materia mineral, sulfato amónico + combustión de fuel oil, nitrato amónico, aerosoles envejecidos (aerosol marino + aerosoles secundarios) y una fuente de tráfico + marcadores industriales, que tienen su principal contribución en el fondo urbano. La mayor contribución al PM_{10} en BCN está relacionada con el tráfico (50% del total de PM_{10}), resultante de las emisiones de tráfico primario (29%), nitrato secundario (9%) y también otros aerosoles secundarios (13%), aunque este último puede atribuirse en parte a otras fuentes. Otra fuente urbana identificada es el polvo antropogénico (13%), que puede ser emitido por el tráfico en una parte importante (resuspensión de polvo de carretera por vehículos), pero también por la resuspensión del viento o emisiones de obras (construcción y demolición). El sulfato amónico tiene también una importante contribución urbana (6%). La contribución regional al PM_{10} en la zona urbana (25%) está compuesta principalmente de polvo mineral, sulfato y nitrato amónico. Por último, el polvo africano (1%) y el aerosol marino (5%) presentan proporciones bajas en el fondo urbano. En MSY y MSC, las principales fuentes son la materia mineral y el sulfato secundario. El nitrato secundario es una fuente muy importante en MSY, pero tiene una relevancia menor en MSC. La contribución del polvo africano es ligeramente superior en el MSC.

La variabilidad de los diferentes parámetros de medición de aerosoles (N, BC, PM_{10}, $PM_{2.5}$ y PM_1) y gases contaminantes se ha estudiado en el fondo urbano de BCN. La variabilidad horaria de todas las métricas de aerosoles y gases contaminantes

registrados está muy influenciada por las emisiones de tráfico y la meteorología (especialmente por la evolución de las brisas). Los niveles de PM_x, N, BC, CO y NO_x se incrementan notablemente durante las horas punta de tráfico, reflejando las emisiones directas. A mediodía, los niveles de la mayoría de los parámetros disminuyen debido a la reducción de las emisiones del tráfico y al proceso de dilución debido a los cambios de dirección y velocidad del viento y el crecimiento de la capa de mezcla. Sin embargo, algunos parámetros no se rigen solamente por las emisiones del tubo de escape del tráfico. Por ejemplo, $PM_{2.5-10}$ sigue siendo elevado durante todo el día debido a los procesos de resuspensión del polvo de carretera, pero también tiene aportes de otras fuentes (resuspensión de polvo por el viento). Los niveles de $PM_{1-2.5}$ y PM_1 aumentan durante las horas punta de tráfico, pero también por la noche, cuando la disminución de la capa de mezcla favorece los procesos de condensación y coagulación, y por consiguiente los niveles de N disminuyen, y los niveles de las fracciones finas de PM aumentan. Además de los picos de tráfico, los niveles de N muestran un segundo pico, pero muy importante al mediodía, reflejando la variación de la intensidad de la radiación solar, que puede ser atribuido a la formación de partículas ultrafinas por procesos de nucleación fotoquímica de gases precursores. Este pico aparece cuando los niveles de BC (emisiones primarias) son muy bajos. Por lo tanto, N está influenciado por emisiones directas de partículas ultrafinas, y también en una fracción muy importante por la formación de partículas secundarias mediante procesos fotoquímicos.

Las series temporales obtenidas en este estudio se completaron con datos procedentes de estudios anteriores con el fin de estudiar tendencias temporales. La influencia de las emisiones del tráfico por carretera en los niveles de partículas finas en el fondo urbano se refleja en los niveles medios anuales de PM_1, que muestran una tendencia creciente interanual significativa de 2003 a 2007, y una buena correlación con el aumento progresivo en el parque de vehículos y el crecimiento de la flota diesel en Barcelona. Sin embargo, las fracciones más gruesas mostraron una tendencia decreciente en BCN y MSY, que puede atribuirse a causas meteorológicas y a la frecuencia e intensidad de las intrusiones africanas, pero que también podría estar relacionada con cambios temporales en las emisiones antropogénicas, como el tráfico rodado o emisiones industriales. Así, se observó una tendencia decreciente en los niveles de algunos marcadores industriales y de tráfico en BCN y MSY. Con el fin de identificar tendencias en las fuentes de aerosoles, se aplicaron estudios de contribución de fuentes (PCA y PMF) a la serie temporal completa obtenida. Como

resultado, la fuente industrial obtenida en BCN presenta una tendencia decreciente desde 2003 hasta 2007.

La variedad de fuentes y factores que afectan la variabilidad de los contaminantes atmosféricos en la cuenca del Mediterráneo Occidental hace que el monitoreo simultáneo de diversos parámetros sea necesario para comprender mejor las fuentes de emisión, transformación o procesos de transporte a fin de poder establecer técnicas eficaces de reducción de emisiones. Los resultados también muestran que el control de PM_1 (modos de nucleación y acumulación) o BC, que proporcionan información sobre las contribuciones de procesos de combustión, y el PM_{10} que aporta información sobre la combustión y además sobre aerosoles generados mecánicamente, puede ser una estrategia mejor que la combinación de las medidas de $PM_{2.5}$ y PM_{10}, como estándares de calidad del aire.

El monitoreo paralelo de aerosoles en los fondos urbano, regional y continental ha sido una estrategia útil para entender la fenomenología de los aerosoles en la cuenca del Mediterráneo Occidental. Dadas las características meteorológicas de esta zona, las emisiones urbanas e industriales, concentradas en las zonas costeras, tienen un impacto considerable en los niveles y composición de PM en las zonas rurales y remotas situadas a diferentes alturas, tanto en verano, con una importante recirculación atmosférica y mezcla de masas de aire a escala regional, y durante el invierno, con el transporte de contaminantes antropogénicos activado por las brisas. La gran contribución de las emisiones urbanas y el transporte de masas de aire a escala regional demuestran la importancia de elaborar y aplicar estrategias de reducción de emisiones para el tráfico, a fin de mejorar la calidad del aire de manera eficiente en la zona de estudio, no sólo a nivel local, sino también a escala regional.

INDEX

1. INTRODUCTION

1. INTRODUCTION

Atmospheric particulate matter (PM) is defined as solid and/or liquid particles suspended in the atmosphere (Mészáros, 1999). Atmospheric aerosols are emitted by a wide variety of anthropogenic and natural sources directly as particles (primary) or are formed in the atmosphere by transformations of gaseous pollutants (secondary). The nature of the source influences both the physical properties (size, mass, density or specific surface) and the chemical composition of the particles. Atmospheric aerosols are widely studied owing to their adverse effects on human health, the environment and climate.

1.1. Origin of aerosols

The global planetary emissions of particulate matter to the atmosphere have been summarized by IPCC (2001) as shown in Table 1.1. In a planetary scale natural primary emissions prevail. Conversely, anthropogenic emissions are a low proportion of the total, being mainly secondary. However, these proportions are very different considering PM origin at urban or industrial areas, where traffic and industrial emissions are the main sources of particulate matter.

Table 1.1. PM emission on a global scale (IPCC, 2001).

GLOBAL PARTICULATE MATTER EMISSIONS (Tg per year)			
Primary particles	Mineral (soil) dust		1000 - 3000
	Sea spray		1000 - 6000
	Organic matter (OM) 0-2µm	Biomass burning Fossil fuel Biogenic (>1um)	45 – 80 10 - 30 0 - 90
	Black carbon (BC) 0-2µm	Biomass burning Fossil Fuel Aircraft	5 - 9 6 - 8 0.006
	Anthropogenic mineral dust (>1µm)		40 -130
Secondary particles	SO_4^{2-}	Anthropogenic Biogenic Volcanic	69 - 214 28 - 118 9 - 48
	NO_3^-	Anthropogenic Natural	10 - 19 2 - 8
	Organic compounds (VOC)	Anthropogenic Biogenic	0.3 - 2 8 - 40

A good quantification of aerosol emissions is very important to estimate the aerosol impacts on air quality and climate, and to develop coherent pollution abatement strategies. The identification of the proportion between anthropogenic and natural emissions is crucial, as only anthropogenic emissions can be influenced, for example being reduced by abatement techniques (de Meij et al., 2006). Besides global, regional or local emission inventories, such as the Intergovernmental Panel on Climate Change, (IPCC, 2001), the European Pollutant Emission Register (EPER, http://www.eper-es.es/), the European Monitoring and Evaluation Programme (EMEP, http://www.emep-emissions.at/emission-data-webdab/, Figure 1.1), the Co-ordinated European Programme on Particulate Matter Emission Inventories, Projections and Guidance (CEPMEIP, http://www.air.sk/tno/cepmeip/) or the Aerosol Comparisons between Observations and Models (AEROCOM, http://nansen.ipsl.jussieu.fr/AEROCOM), and emission models like TM5 (Krol et al., 2005), EMITEMA-EIM (Costa and Baldasano, 1996) or EMICAT2000 (Parra et al., 2006), aerosol emission sources have been estimated by source contribution studies (Henry, 1984; Thurston and Spengler, 1987; Harrison et al., 1997; Querol et al., 2001b; Rodriguez et al., 2004; Viana et al., 2007 and 2008a; Bi et al., 2007; Raman and Hopke, 2007; Srivastava and Jain, 2007; Kim and Hopke, 2008; Lee et al., 2008; Yatkin and Bayram, 2008). The methodologies applied for the identification and quantification of emission sources based in receptor modelling are diverse (Principal Component Analysis, Positive Matrix Factorization, Chemical Mass Balance, Cluster Analysis, etc.). Source contribution studies allow the identification and quantitative estimation of source contribution to exposure levels to PM at local and regional scales.

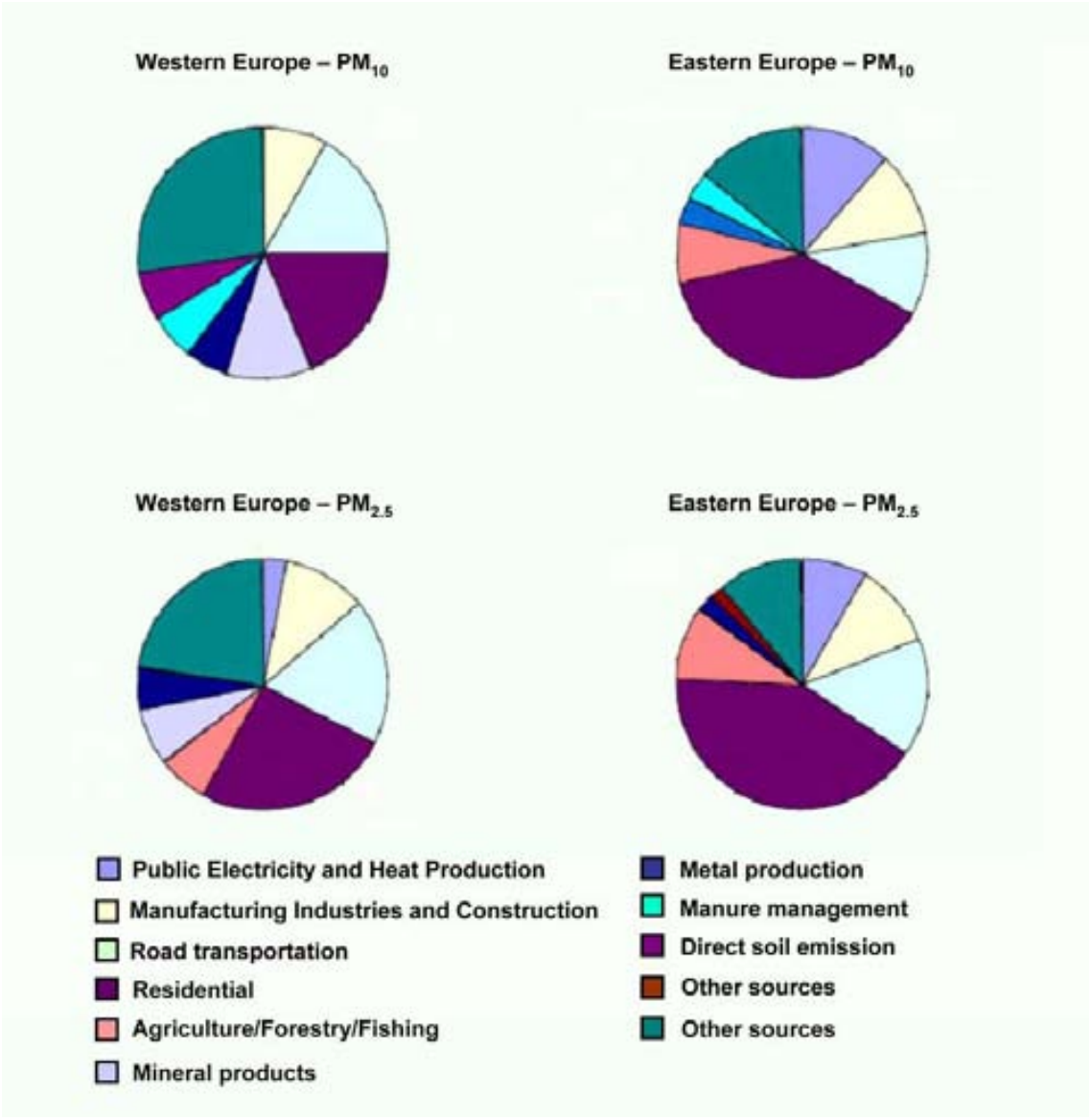

Figure 1.1. Key category analysis of 2006 CLRTAP (Convention of Long-Range Transboundary Air Pollution) inventories for Western Europe and Eastern Europe for PM_{10} and $PM_{2.5}$ (EMEP, Technical Report, CEIP 1/2008). WEST = Austria, Belgium, Switzerland, Germany, Denmark, Spain, Finland, France, United Kingdom, Greece, Ireland, Iceland, Italy, Liechtenstein, Malta, Netherlands, Norway, Portugal, Sweden. EAST = Bulgaria, Belarus, Cyprus, Czech Republic, Estonia, Croatia, Hungary, Lithuania, Latvia, Macedonia, Poland, Romania, Slovenia, Slovakia, Turkey, Ukraine.

An important difference on estimating the source contributions from inventory emissions and by source apportionment using receptor modelling is that in the first case estimations are obtained on bulk local or regional emissions, whereas in the second case estimations refer to contributions to ambient air levels. In many cases it has been demonstrated that these two types of estimations do not coincide.

1.1.1. Natural emissions

On a global scale natural origin aerosols, such as windborne naturally emitted crustal material, sea spray, volcanic emissions, wild biomass burning, biogenic emissions, secondary aerosols generated from gaseous natural precursors (SO_2, NO_X, VOCs emitted by volcanoes, storms, soils and plants), spores or pollens, are important sources of particulate matter to the troposphere.

Mineral particles enter into the atmosphere by the action of winds on the surface of the Earth (Prospero et al., 1981) and by crustal volcanic emissions. The major emission area is in the Northern Hemisphere, mainly the 'dust belt', an area with arid soils between latitudes 10 and 35ºN from western African coast to Middle East and Central and Southern Asia, where the mineral matter is injected into the atmosphere when high temperatures and certain conditions of air mass circulation are presented (Prospero, 1999; Prospero et al., 2002). Mineral matter can be transported long distances by air masses. Other source of mineral PM is the resuspension of semi-arid soils. In Southern Europe, some areas with low precipitation rates and low vegetal cover may act also as important dust resuspension sources with local or regional impact on ambient PM levels.

1.1.2. Anthropogenic emissions

At a global scale, the most important anthropogenic sources of aerosols are industrial emissions, road, maritime and air traffic derived emissions, domestic emissions and the emissions derived from construction and demolition or agriculture and farming in a minor scale (IPCC, 2001).

At local or regional scales fossil fuel combustion, energy plants, metallurgy and other industrial activities (mainly cement, ceramic and brick production), agricultural activities, waste treatment plants and fertilizer production plants are important aerosol sources. Industrial activities, construction/demolition, mining activities, cement and ceramic production and smelters are typical anthropogenic mineral PM emission sources (a significant proportion of these emissions are fugitive emissions produced by handling and transport of material).

An important proportion of the anthropogenic aerosol is made up of secondary particles formed from anthropogenic gaseous pollutants. The biomass burning oriented to obtain new land for agriculture purposes represents an important anthropogenic source.

In urban backgrounds source contribution studies designate road traffic, as the principal emission source to urban atmosphere as exhaust (precursor gaseous species and particles) and non-exhaust emissions. *Vehicle exhaust emissions* are considered the main source of ultrafine particles in urban backgrounds, even when improvements in emission control technology have decreased the particle emission rates significantly (EURO-5 and EURO-6 standards for vehicle emissions; EC, 2007). The main vehicle exhaust source to ambient particles is diesel motors (Mariq et al., 2007). Nanoparticles (<30nm) emitted in diesel exhausts are generally semivolatile, containing primarily unburned fuel, unburned lubricating oil and sulphate, and form during dilution and cooling of exhaust gases (Mariq et al., 2007; Rodriguez et al., 2007; Olivares et al., 2007; Casati et al., 2007). Diesel vehicles also emit primary carbonaceous particles (soot) in the size ranges 30 nm-0.1 μm diameter, which consist primarily of aggregates of graphite with mean diameters of 25-35 nm that form during combustion (Fraser et al., 2003; Brandenbergera et al., 2005). The heavy duty vehicles can also emit soot in the *accumulation mode* (0.1-1 μm) and even in the ranges >1 μm (Morawska et al., 1998). However, Robinson et al. (2007) showed that photo-oxidation of diesel emissions rapidly generates large volumes of organic aerosol because of the photo-oxidation of gaseous compounds volatilized from the emitted particles. Particle emissions (25–400 nm) from gasoline cars are up to two orders of magnitude lower than those from diesel cars (Wehner et al., 2009) with mean diameters in the nucleation mode.

Several studies indicate that a large part of the total road traffic emissions originates from *non-exhaust emissions* involving mechanical abrasion and corrosion processes (Wåhlin et al., 2006; Schauer et al., 2006; Kupiainen, 2007; Amato et al., 2009). Direct emissions from brake and tyre wear and road pavement abrasion are found partly in the fine fraction and mostly in the coarse fraction. Other emissions originate from clutch wear and the corrosion of vehicle components. The road dust (material collected on the road surface) is resuspended to the atmosphere by traffic (Schauer et al., 2006; Thorpe and Harrison, 2008). Road dust can contain particles emitted by vehicles but also mineral dust (natural or anthropogenic), biogenic compounds or products derived from road sanding during the winter.

1.2. Aerosol composition

The major components of atmospheric particulate matter are mineral dust, carbonaceous matter (organic and elemental carbon), sea spray, sulphate, nitrate, ammonium and water. The predominance of these chemical components in the

different size fractions of PM is linked to the prevailing emission sources and the formation mechanisms of the particles.

1.2.1. Mineral dust

Mineral matter is the major component of the total PM mass present in the atmosphere (44% of global planetary emissions, Duce, 1995; IPCC, 2001; Prospero et al., 2002). However, at local or regional scales this proportion can be lower.

Natural mineral PM composition depends on the geology of the emission area. The major components are Al, Ca, Si, Fe, Ti, K and Mg. Other important trace elements are Co, Rb, Ba, Sr, Li, Sc, Cs, and rare earth elements (REEs, Chester et al., 1996; Bonelli et al., 1996). The main mineral composition of PM is quartz (SiO_2), calcite ($CaCO_3$), dolomite ($CaMg(CO_3)_2$), clay minerals, mainly kaolinite ($Al_2Si_2O_5(OH)_4$), illite ($K(Al,Mg)_3SiAl_{10}(OH)$), smectite ($(Na,Ca)Al_4(Si,Al)_8O_{20}(OH)_4 \cdot 2H_2O$ and palygorskite $(Mg,Al)_5(OH)_2[(Si,Al)_4O_{10}]_2 \cdot 8H_2O$, and feldspars like the microcline/orthoclase ($KAlSi_3O_8$) or the albite/anorthite $(Na,Ca)(AlSi)_4O_8$). In minor quantities calcium sulphate ($CaSO_4 \cdot 2H_2O$) and iron oxides (Fe_2O_3) can be found (Glaccum y Prospero, 1980; Ávila et al., 1997; Querol et al., 2002).

Mineral dust plays an important role in climate forcing (IPCC, 2007). Mineral dust is one of the major natural ice nucleating aerosols (Levin et al., 1996; Hoose et al., 2008) and consequently may influence climate by both direct and indirect effects on the radiative balance (Prospero and Lamb, 2003).

In urban areas, one of the principal sources of mineral matter (with construction and demolition) is the road pavement abrasion, brake and tyre wear by traffic. This mineral dust linked to traffic consists mainly of a mixture of mineral particles (pavement and dust deposited in the pavement) mixed with carbonaceous particles (from tyres and traffic emissions deposited on the road) and metals (Fe, Cu, Sb, Ba from brakes, Ti, Rb, Sr from pavement, and Zn from tyres, Wåhlin et al., 2006; Schauer et al., 2006; Thorpe and Harrison, 2008; Amato et al., 2009).

Primary mineral particles associated to steel work and ceramic production sources can also influence levels in the $PM_{2.5}$ size fraction. However, the majority of the sources of mineral matter emit coarse particles.

1.2.2. Marine aerosol

Marine aerosol (or sea spray) is the second more abundant component of PM emissions (38% of terrestrial global emissions, IPCC, 2001). However on a local/regional scale sea spray rarely exceeds 5% of the PM_{10} ambient air concentration. Sea spray aerosols are mainly primary, generated by bubble bursting processes at the ocean surface or by the waves in coastal areas (Mészaros, 1999).

Sea spray concentrations at a given region depend on the geographic area, proximity to the coast and meteorology. Sea spray particles are mainly in the coarse fraction (the main part of the mass is present in the fraction bigger than 2.5 μm) and are constituted mainly by Cl^-, Na^+, SO_4^{2-}, Br^-, CO_3^{2-}, Mg^{2+}, Ca^{2+}, and K^+ (Mészáros, 1999). The major component is NaCl (Warneck, 1988) followed by $MgCl_2$, Mg_2SO_4, or Na_2SO_4. In addition, there are secondary PM contributions constituted by sulphate and monosulphonate produced by oxidation of the biogenic dimethyl sulphide (DMS). There are also trace elements like Al, Co, Cu, Fe, Mn, Pb, V and Zn (Seinfeld and Pandis, 1998; Mészáros, 1999). Some studies show that oceans are important sources of elements as Cu, V and Zn (Nriagu, 1989).

1.2.3. Carbonaceous aerosols

Carbonaceous compounds represent around 2 to 5% of the global planetary emissions (IPCC, 2001). However, on a local/regional scale carbonaceous aerosols may account up to 20-40% of the ambient PM mass concentration (Putaud et al., 2004; Querol et al., 2004a and b). In urban areas it is one of the most abundant fractions of PM. An 80% of the carbonaceous species in urban and industrial areas is present in the finer fractions (Harrison and Yin, 2008), usually in the size range <0.1μm (*nucleation and Aitken modes*). The carbonaceous fraction of the particulate matter (excluding mineral carbon from carbonates) consists of both elemental and organic carbon.

Elemental carbon (EC) is primary and it is emitted directly at the source from incomplete combustion processes such as fossil fuel and biomass burning. The main emission sources of EC are road traffic, (mainly diesel engines), power generation, specific industrial processes, biomass combustion and residential and domestic emissions. The investigation on this component of the aerosol is very important due to its impact on radiative forcing and global climate change (Jacobson, 2001; IPCC, 2001 and 2007).

Particulate organic carbon (OC) can be emitted directly as primary aerosol particles or formed as secondary aerosol particles from condensation of low-volatility organic gases (VOCs). The main emission sources of OC are similar to those of EC, like fossil fuel and biomass burning and in a minor proportion agricultural emission sources and natural biogenic forest emissions. In urban areas, the volatile hydrocarbons and other non-methane organic compounds are mostly of an anthropic origin. They are mainly emitted by fuel vaporization (fugitive emissions) and combustion processes (fossil fuel and biomass) and they are important precursors of secondary organic aerosols (SOA). Moreover, bio-aerosols (pollen, spores, microorganisms and vegetal or insect debris, among others) or biogenic emissions of volatile precursors of SOA can contribute to increase the levels of organic carbonaceous aerosols, especially in rural areas. However, in urban and industrial areas anthropogenic sources of OC prevail (Rodríguez et al., 2002b; Lonati et al., 2005; Viana et al., 2006).

1.2.4. Secondary inorganic aerosols (SIA)

Sulphate (SO_4^{2-}), nitrate (NO_3^-) and ammonium (NH_4^+) are usually the major secondary inorganic compounds in PM. They are formed in the atmosphere from their precursor gaseous species (SO_2, NO_X and NH_3) through a gas-to-particle conversion. The secondary inorganic aerosols represent around 5% of the global planetary emissions (IPCC, 2001). However on a local/regional scale they might account up to 30-40% of the PM_{10} mass concentration (Putaud et al., 2004; Querol et al., 2004a and b).

Once the sulphur dioxide (SO_2) is emitted to the atmosphere (by industrial processes, energy generation, domestic and residential emissions and/or road traffic) its oxidation in the atmosphere gives rise to the formation of sulphuric acid aerosol, that will react later in the atmosphere with ammonia to form particulate ammonium sulphate and in a minor proportion calcium or sodium sulphate by interaction with calcium carbonate and sodium chloride respectively. Both the sulphuric acid and the ammonium sulphate present a fine grain size (<1µm), whether the calcium and sodium sulphates present a coarse grain size (>1µm, Mildford and Davidson, 1987).

Nitrogen oxides (NO_X) are emitted mainly by traffic in urban areas and by electricity generation, industrial processes and domestic and residential emissions. These oxides are precursors of the atmospheric nitrate, originated from nitric acid (HNO_3), a product of NO_2 oxidation, once the nitric acid is formed, neutralized and transformed in ammonium, sodium or calcium nitrate (Meszarós, 1999). The size distribution of

particulate nitrate depends on the neutralizing agent of the nitric acid. Thus, ammonium nitrate presents mainly a fine grain size (<1µm), while sodium or calcium nitrate species are mainly in the coarse range (>1 µm). In cold and humid regions of Europe, nitrate aerosols are mainly NH_4NO_3 and fine in size, while in warmer and dryer regions, about 50% of the nitrate present in the PM_{10} fraction is in the coarse mode (Querol et al., 2004a and b; Putaud et al. 2004). This is a consequence of the instability of ammonium nitrate under warm and dry ambient conditions. In this situation gaseous HNO_3 may react with components as sea spray (NaCl) or mineral matter ($CaCO_3$) and the result of this reaction is the formation of secondary inorganic aerosols with a coarse grain size, as mineral matter or sea spray are mainly in the coarse size range (Harrison and Pio, 1983; Mamane and Mehler, 1987; Wall et al., 1988, Querol et al., 1998a). Thus, in warm regions of Europe nitrate presents a marked seasonal pattern (Querol et al., 2004a and b) with higher NO_3^- levels during the winter and a summer decrease as a consequence of the instability of ammonium nitrate under warm and dry ambient conditions. Gaseous nitric acid predominates over particulate nitrate during this period of the year (Song et al., 2001; Wittig et al., 2004) and $Ca(NO_3)_2$ or $NaNO_3$ formation is observed.

1.3. Aerosols and environment, climate and health

Aerosol particles have always been part of the atmosphere. Without particles in the atmosphere, there would be no rain, and the climate would be different (Mészarós, 1999; IPCC, 2007). However, atmospheric composition has changed since human beings live on Earth. Nowadays, the largest fraction of directly emitted anthropogenic aerosol particles derive from combustion sources such as power plants, vehicles, or domestic stoves (Brimblecombe, 2001). The atmospheric concentration of condensable gaseous species has also changed due to the anthropogenic emission of sulphur dioxide, nitrogen oxides and volatile organic compounds. Due to the world-wide industrialization in the last two centuries, the particulate air pollution in urban areas has drastically increased. Furthermore, due to long range transport, aerosol particles spread over thousands of kilometres, influence the Earth radiative balance and regulate the global climate. Thus, aerosols have a large impact on local pollution problems, but also contribute to regional environmental issues (e.g., acidification), long range transport and global environmental issues (e.g., the destruction of Antarctic ozone and climatic change).

In addition to their influence on climate, atmospheric aerosols are associated with a range of adverse effects on human health and the environment. Aerosol mass and

some of its components are known to have links to toxicity, chronic respiratory and acute cardio-vascular problems. Aerosols are also closely linked to problems of visibility reduction, acid rain, and urban smog in many locations of the world.

1.3.1. Health effects

The increases in mortality and morbidity during several mid twentieth-century air pollution episodes demonstrated to both scientists and governments that air pollution from heavy industry and residential coal combustion were hazards to public health (Brimblecombe, 2001). Atmospheric particulate matter effects on health have been evaluated by means of epidemiological studies carried out since the 1980s proving that elevated aerosol mass concentrations are associated with an increase in mortality and other serious health effects (Donaldson et al. 1998; Pope and Dockery 1999 and 2006; Wichmann et al., 2000; Küntzli et al., 2000 and 2006; Pope et al. 2002 and 2004; WHO, 2003 and 2006). Associations are reported between recent exposure to atmospheric particulate matter and short term increases in mortality and morbidity from cardiovascular, cerebrovascular or respiratory diseases (Schwartz, 1996; Katsouyanni et al., 1997; Künzli, 2000; Peters et al., 2004; Pope and Dockery, 2006; Dockery and Stone, 2007; Lee et al., 2009). The health effects of aerosol particles depend strongly on their size, surface area and composition. Many epidemiological studies report that some of these adverse health effects are associated to ultrafine aerosol particles (<100 nm) derived from combustion of fossil fuels (Seaton et al. 1995; Schwartz et al., 2000; Dockery, 2001; Hoek et al. 2002; Pope and Dockery, 2006; Miller et al., 2007; Dockery and Stone, 2007). These particles can reach the alveolar region of the lungs, enter the blood circulatory system and distribute throughout the whole human body, being this distribution higher for insoluble material. Specific components such as soot, certain organics, or metals are believed to increase the risk of diseases (Ovrevik and Schwarze, 2006; Kampa and Castanas, 2008; Ostro et al., 2007). Moreover, fresh soot particles are particularly surface-reactive and may carry carcinogenic compounds (such as PAHs; Highwood and Kinnersley, 2006). The literature suggests that a range of health effects occur at PM levels below US and European regulatory standards. However, several studies have found that high coarse PM levels also produce adverse health effects, showing the inflammatory potential of coarse particles (Schins et al., 2004; Schwarze et al., 2007). Jalava et al. (2007) found a much higher inflammatory potential for the coarse fraction than for the finer fractions. Some studies show that coarse PM derived from non-combustion traffic-related sources, such as the re-suspension of road dust originating from the mechanical wear and degradation of tyres,

brakes and pavement abrasion, has a much higher inflammatory effect than other size fractions, possibly owing to metal toxicity, and associate it to cardiovascular and cerebrovascular mortality (Gustafsson et al., 2008; Pérez L. et al., 2009). Pérez L. et al. (2008) observed a daily increase on mortality during Saharan dust outbreaks and Middleton et al. (2008) also found an increase on hospital admissions for cardiovascular causes during these episodes.

1.3.2. Effects on radiative balance

Atmospheric aerosols play an important role in global and regional climate changes as they influence the atmospheric radiative balance by directly scattering or absorbing the incoming solar radiation or the outcoming terrestrial radiation (Charlson et al., 1992; Levin et al., 1996; Horvath, 1998; Arimoto, 2001; IPCC, 2001 and 2007), or acting as a cloud condensation nuclei (CCN) or ice nuclei (IN) and thereby indirectly modifying the amount and lifetime of clouds (Charlson et al., 1992; Levin et al., 1996; Ramanathan et al., 2001; Sekiguchi et al., 2003; Satheesh and Moorthy, 2005; IPCC, 2001 and 2007; Hoose et al., 2008)

Aerosols may scatter or absorb solar radiation depending on their chemical composition and refractive index. A fraction of the incoming solar radiation is scattered back to space leading to a cooling effect. Another fraction of the solar radiation is absorbed by the particles leading to warming effect. These effects are called direct aerosol forcing of climate. The direct effect depends strongly on the size distribution and the chemical composition of the aerosol (Adams et al. 2001). Carbonaceous particles (mainly BC) contribute decisively to atmospheric warming (Rose et al., 2006). Diesel vehicles contribute in a much more important way than gasoline vehicles to ultrafine particles emissions and therefore to global warming, emitting soot particles in the ultrafine range, between 30-130 nm (Morawska et al., 1998; Zhu et al., 2002).

As already mentioned aerosols may act as CCN or IN. Cloud droplets scatter and absorb solar radiation depending on their size and the amount and type of incorporated absorbing material. Aerosols may induce modifications in the cloud albedo, the number of CCN and IN, the lifetime of clouds and the frequency of the precipitation. These effects are called indirect aerosol forcing of climate (IPCC, 2001). The size distribution (number and size) of cloud droplets depends strongly on the number size distribution of the aerosol. An increase in hygroscopic aerosol number concentration tends to increase the CCN, which in turn leads to increased cloud albedo and to changes in the

Earth's radiation budget (Levin et al. 1996; IPCC, 2001).There is also a semi-direct effect caused by the absorption of radiation by soot, lowering the cloud cover locally (Ackerman et al, 2000). Thus, cloud lifetimes and precipitation frequencies are affected by CCN properties, altering the hydrological cycle and water supply (Levin et al. 1996; Ramanathan et al., 2001; Teller and Levin, 2005; Rosenfeld et al., 2008).

Mineral dust is the main natural IN, and consequently in addition to the direct radiative effect, dust may have also a cooling indirect effect (Levin et al., 1996; IPCC, 2007). However, several studies (Hoose et al., 2008; Möhler et al., 2008) show that coating of dust particles with soluble secondary organic or inorganic species reduce clearly the IN potential of dust.

Radiative forcing (RF, W m^{-2}) is a measure of the change in the balance of incoming and outgoing energy in the Earth-atmosphere system due to a certain agent, quantifying the importance of this agent as a potential climate change mechanism. Positive forcings tend to warm the surface while negative forcings tend to cool it. IPCC (2007) estimates the global mean direct radiative forcing from the different components of RF (scattering or absorption of incoming radiation for all gases, aerosols and precursors, the indirect forcing through cloud albedo effects or changes in land use or solar irradiance, Figure 1.2). The combined aerosol direct and cloud albedo effect exert a RF that is negative, with a median RF of -1.3 W m^{-2}. The mean anthropogenic RF would be of +2.6 W m^{-2} without the aerosol effect, which reduces it to +1.6 W m^{-2} (IPCC, 2007).

The quantification of aerosol radiative forcing is more complex than the quantification of radiative forcing by greenhouse gases because aerosol mass and particle number concentrations are highly variable in space and time (IPCC, 2007). Spatially and temporally resolved information on the atmospheric burden and radiative properties of aerosols is needed to estimate radiative forcings. Important parameters are particle number size distributions, particle shape, changes in size with relative humidity, complex refractive index, state of mixture and solubility of aerosol particles. Estimating radiative forcing also requires an ability to distinguish natural and anthropogenic aerosols (IPCC, 2007).

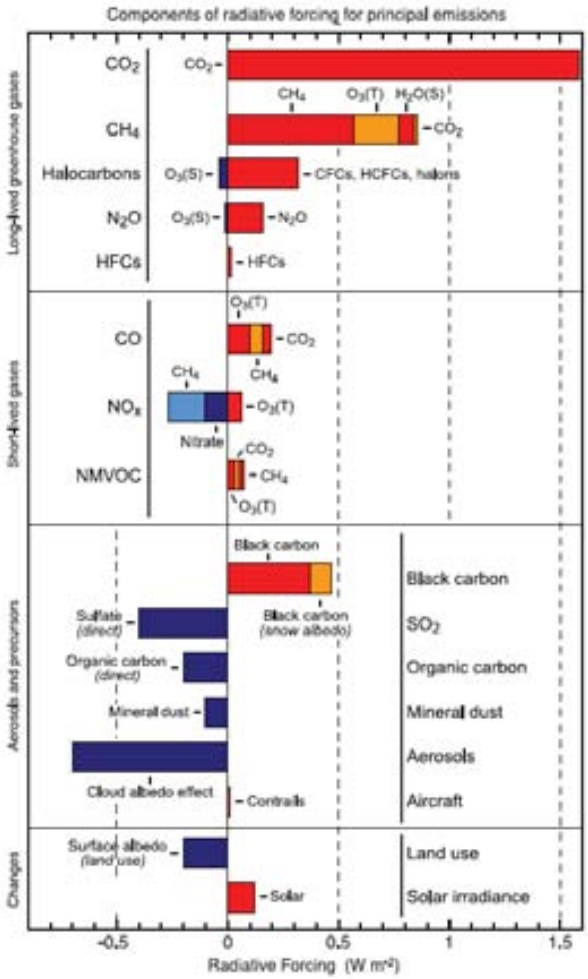

Figure 1.2. Summary of the principal components of radiative forcing for emissions of principal gases, aerosols and aerosol precursors and other changes. Values represent radiative forcing for 2005 due to emissions and changes since 1750 (start of industrial era). (S) and (T) next to gas species represent stratospheric and tropospheric changes, respectively. Human activities cause significant changes in long-lived gases, ozone, water vapor, surface albedo, aerosols and contrails. The only increase in natural forcing of any significance between 1750 and 2005 occurred in solar irradiance. Positive forcings lead to warming of climate and negative forcings lead to a cooling (IPCC, 2007).

1.3.3. Effects on ecosystems

Atmospheric particles can directly interact with ecosystems. Well known interactions are aerosol deposition on plant leaves and soils and the change of acidity of soils and rain. The incorporation of acid species to rain drops (wet deposition of atmospheric particles) is called acid rain. Aerosols and gaseous pollutants that produce acid rain can be natural (such as SO_2 derived from volcanic eruptions or CO_2 emitted in forest fires) or anthropogenic (caused by the emission of pollutants derived from the use of fossil fuels). Acid rain has been studied from the 1970s (Likens, 1974; Butler and Likens, 1991; Avila et al., 1996), showing that the acidification of ecosystems disturbs

their operation. In lakes and oceans, this acidification of the environment can produce a modification of the life conditions of the species and even their death. Moreover, the deposition of nitrate and ammonia can contribute to the eutrofization of lands, lakes and surface waters. The atmospheric particle deposition on the Earth surface and surface waters can also alter the composition of underground waters (Wright, 1995). In the land, acid rain may react with soil nutrients preventing their absorption by plants and may dissolve potentially toxic metals (such as Al^{3+}) facilitating their absorption and producing damages even perceptible on the surface. Atmospheric particulate matter produces also damages on plants because of the deposition of particles on the leaves, affecting their capability to perform the photosynthesis (Emberson et al., 2003). This effect gives rise to important economical losses because of crop ruin. Atmospheric mineral dust transported from arid areas over long distances has also important effects on biogeochemical cycles, as it represents and important source of primary nutrients like calcium, iron, nitrogen, potassium and phosphorus (Ávila et al., 1998; Prospero, 1999; Jickells, 2005) to both continental and marine ecosystems.

1.3.4. Visibility reduction

Atmospheric aerosols affect visibility interfering with light transmission in the atmosphere (scattering and absorption of radiation). The air pollution impact on visibility is usually characterized by the light extinction of the particles (Johnson, 1981; Horvath, 1992; IMPROVE reports). Visibility usually ranges from 10 to 100 km (WHO, 2002) but at urban polluted backgrounds the high concentration of anthropogenic particles can reduce the visibility to a few meters (Husar et al., 1981; Wu et al., 2005; Deng et al., 2008). Sulphate and ammonium nitrate aerosols are important contributors to visibility reduction because their high hygroscopicity results in the production of high number of CCN (IMPROVE reports).

1.3.5. Degradation of building materials

In urban areas, atmospheric particulate matter deposition produces the degradation of construction materials exposed to the atmosphere, like cement and metallic structures of buildings and monuments, because of their interaction with the surface. This material degradation may be produced by acidic or soluble aerosols, deposition of particles or interaction of aerosol derived gaseous species (HNO_3 and HCl among others; Alastuey, 1994; Brimblecombe and Camuffo, 2003).

1.4. Current Air Quality Standards and Regulations

Atmospheric particulate matter is continuously monitored in air quality networks due to its adverse effects. In order to protect human health and the environment, and to establish emission reduction strategies, the emissions and ambient levels of atmospheric pollutants are currently regulated. In June 2008 the European air quality directive 2008/50/EC was officially published by the EC (2008) with the aim of taking into account the most recent scientific research and experience of the Member States. It unifies criteria from the old directives 96/62/EC (for evaluation and management of air quality), 1999/30/EC (limit values for SO_2, NO_x, PM and Pb), 2000/69/EC (benzene and CO), 2002/3/EC (O_3) and 2002/3/0EC (information and data sharing between Member States) and it will incorporate in the future the directive 2004/107/EC (relative to As, Cd, Hg, Ni and PAHs) when sufficient experience in its application will be acquired.

The previous European Directive 1999/30/EC established air quality standards for PM_{10} with an annual mean limit value of 40 μg m^{-3} and a daily limit value 50 μg m^{-3} not to be exceeded more than 35 times a year (Table 1.2). The new air quality Directive 2008/50/EC sets the same limit values for PM_{10} than the previous one and establishes also limit and target values for $PM_{2.5}$, together with exposure reduction targets and exposure concentration obligations for urban backgrounds (Table 1.2). It defines the Average Exposure Indicator (AEI), expressed in μg m^{-3} and based in measurements performed at urban backgrounds and agglomerations, as a three-calendar year running annual mean concentration averaged over all sampling points established. The AEI will be used to know if the exposure concentration obligation and the national exposure reduction target established by the Directive are met. The exposure concentration obligation establishes 20 μg m^{-3} as the obligation value for the AEI to be met in 2015. The national exposure reduction target, to be met in 2020, depends on the initial ambient concentration, being between 0% when initial AEI are lower than 8.5 μg m^{-3} and 20% for initial AEI between 18 and 22 μg m^{-3}. When levels are higher, additional measures should be taken until the levels reach 18 μg m^{-3}. The Directive 2008/50/EC also establishes limit and target values for $PM_{2.5}$ to be met at all sites (including background and hotspot sites). In a first stage an annual target value of 25 μg$PM_{2.5}$ m^{-3} will come into force in 2010, and will become an annual limit value in 2015. Then, in a second stage it establishes an annual limit value of 20 μg $PM_{2.5}$ m^{-3} that will be effective in 2020. The second stage will be revised by the Commission in the year 2013

with actualized information on PM effects on health and the environment, technical viability and the experience obtained with the target values in the Member States.

Table 1.2. PM_{10} and $PM_{2.5}$ limit and target values. $PM_{2.5}$ exposure reduction targets and exposure concentration obligations for the AEI (average exposure indicator) in urban backgrounds, as established by the European Directive 2008/50/EC.

	Directive 1999/30/EC	Directive 2008/50/EC		
	PM_{10}	PM_{10}	$PM_{2.5}$ Stage I	$PM_{2.5}$ Stage II*
Annual target value (μg m^{-3})			25 (2010)	
Annual limit value (μg/m^3)	40	40	25 (2015)	20 (2020)
Daily limit value (DLV) (μg/m^3)	50	50		
DLV permitted exceedances	35	35		
Exposure concentration obligation for AEI			20 (2015)	
Exposure reduction target for AEI				18 (2020)**

*Stage II will be revised by the Commission in 2013 with actualized information on PM effects on health and the environment, technical viability and the experience obtained with the target values in the Member States. **The reduction objective for AEI depends on the initial concentration and is for example of 20% for the levels between 18 and 22 μg $PM_{2.5}$ m^{-3}. When the levels are higher than 22 μg m^{-3} additional measures should be taken until reaching 18 μg m^{-3}.

The establishment of a monitoring network with equilibrated number of hotspots, urban and rural monitoring sites is important to appropriately monitor atmospheric aerosols. The 2008/50/CE Directive establishes criteria about the sitting of monitoring networks, the type and the number of sampling points and the measurement reference methods. Industrial sites are located inside industrial areas to measure the local impact of an industrial area. Urban traffic sites must be located near roads with high traffic inside the cities to measure direct pollution of both the city and road traffic. Urban sites are located inside urban areas but in background areas that represent exposure level of citizens. The directive also requires measurements at background rural/regional sites that are located in areas far from any direct anthropogenic pollution source to provide information on background levels of pollutants at a regional scale. This information is essential to evaluate the increments in the levels of urban, industrial or traffic hotspots and to evaluate the contribution of long range transport of atmospheric pollutants. The monitoring of atmospheric pollution at regional backgrounds is very important in Europe, with regions with very diverse climatic/meteorological characteristics as the background pollution of an urban or hotspot site will depend on the regional background of the surrounding area. Furthermore, chemical composition monitoring in rural areas for $PM_{2.5}$ has now become mandatory for NO_3^-, SO_4^{2-}, Cl^-, NH_4^+, Na^+, K^+, Mg^+, Ca^{2+}, OC and EC (Annex IV of the 2008/50/CE Directive).

The directive 2008/50/CE recognises that exceedances of the PM_{10} daily limit levels can be caused by natural events. Natural events are *volcanic eruptions, seismic activities, geothermal activities, wild-land fires, high wind events or the atmospheric resuspension or transport of natural particles from dry regions*. These exceedances can be discounted by the State Members after scientific validation together with the exceedances caused by winter road sanding or salting. In Southern Europe, the natural episodes with the greatest impact on PM levels are the intrusions of African air masses, frequently with high dust loads (Querol et al., 1998b; Rodriguez et al., 2001; Escudero et al., 2005; Gerasopoulos et al., 2006; Gobbi et al., 2007). The most common approach to quantify dust contributions is the study of PM chemical speciation (Rodriguez, 2002; Viana, 2003; Castillo, 2006) but it is costly and time consuming. Escudero et al. (2007b) proposed a methodology for estimating the net dust load in PM_{10} during African dust outbreaks based on the analysis of time series of PM_{10} levels from regional background sites in the Iberian Peninsula and quantifying the impact of African dust outbreaks on the levels of PM_{10} in air quality monitoring networks.

Ultrafine particle emissions are a cause of concern, owing to the impact they have on human health (Wichmann et al., 2000), to the extent that the World Health Organization has recognised that more research is needed to establish the possible links between ultrafine particle sources, exposure and health (WHO, 2003). Particles below 0.1 μm arise mainly from anthropogenic sources and in urban backgrounds road traffic is the main emission source of ultrafine particles. EURO-5 and EURO-6 (EC, 2007) are European regulation processes that fix important reduction values in the emission of particles and nitrogen oxides in diesel vehicles. Many studies (Ruuskanen et al., 2001, as an example) recommend the establishment of limit values for particle number concentration in ambient air to be considered in addition to particle mass concentration standards. The PM working group from CAFE programme (Clean Air for Europe; CAFE, 2004) has already drawn attention to PM_1 as a possible metric for air quality standards.

1.5. Aerosol formation and transformation processes

Atmospheric aerosols range in size from a few angstroms (Å) to some tens of micrometers. They can be classified by a series of size ranges, generally related to their formation mechanisms (Figure 1.3). *Primary particles* are emitted directly from the source to the atmosphere in aerosol phase. *Secondary particles* are formed in the atmosphere from precursor gases, such as sulphur dioxide, nitrogen oxides, ammonia

or VOCs. The reactions to form secondary particles may undergo gas to particle conversions (homogeneous nucleation) or reactions between gases and atmospheric particles (heterogeneous) to form new particles, by coagulation or condensation processes (Warneck, 1988).

Particles are removed from the atmosphere by different mechanisms as the deposition on the Earth's surface by gravimetry (dry deposition) or the incorporation into cloud droplets during the formation and occurrence of precipitation (wet deposition or scavenging) Therefore, particle sizes and concentrations change due to nucleation, coagulation, condensation, evaporation, deposition of transport processes.

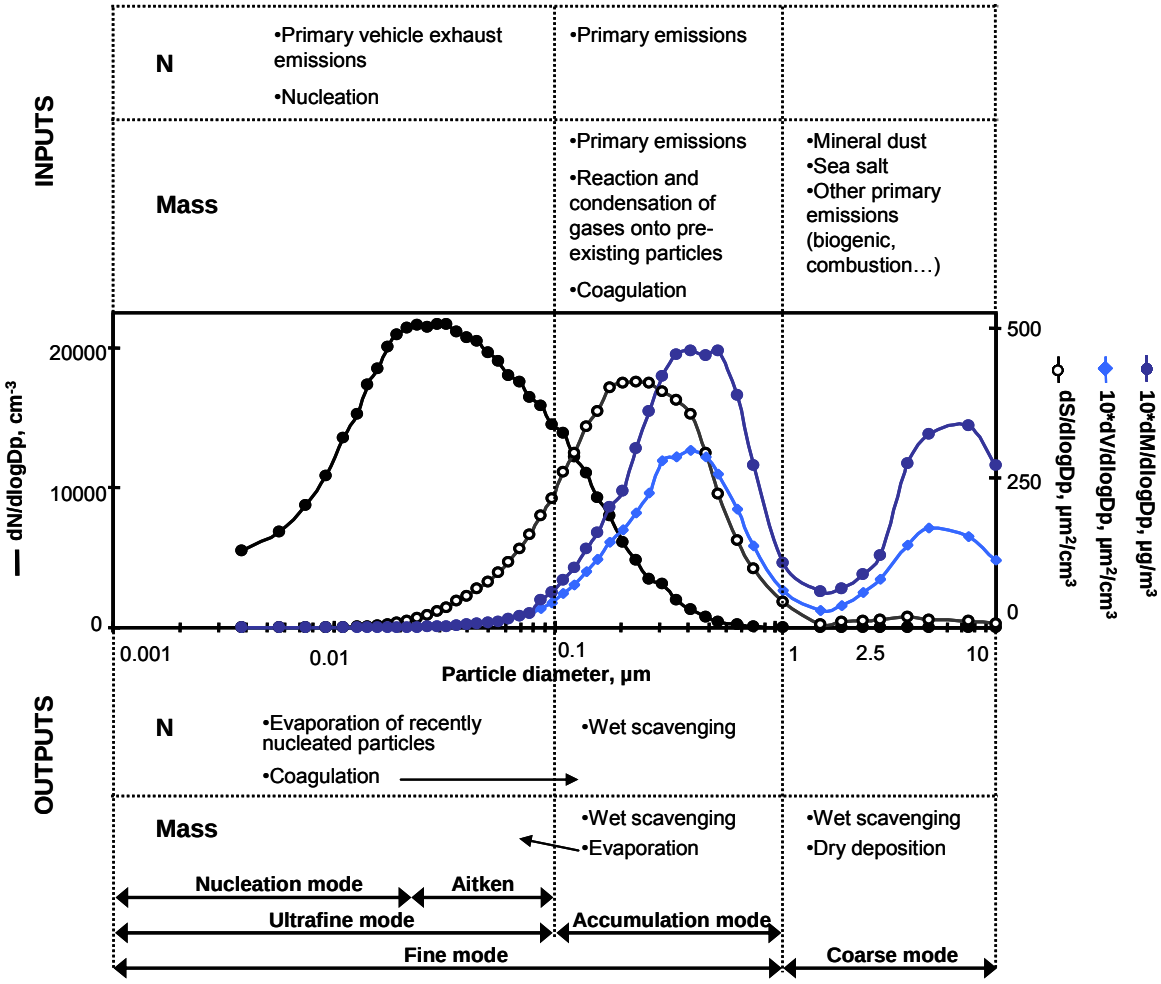

Figure 1.3. Illustration of the main processes affecting number and mass concentrations of atmospheric particles. "Idealized" number (N), surface (S), volume (V) and mass (M) size distribution of aerosols based on urban background measurements. Input and output mechanisms affecting the number, mass concentrations and size distributions. The size distribution of aerosols is based in studies performed by Raes et al. (2000); Harrison et al. (2000); Wehner and Wiedensohler (2003); Cabada et al. (2004); Hussein et al. (2005); Stanier et al. (2004); Van Dingenen et al. (2004); Salma et al. (2005) and Rodríguez et al. (2007). Adapted from a figure by Sergio Rodríguez.

1.5.1. Primary particles

Primary particles occur in the ultrafine, fine and coarse modes.

Ultrafine primary particle emissions are especially important in urban areas, where road traffic is the most important emission source. They may be emitted directly in the aerosol phase by vehicle exhausts or formed during the emission of the vehicle exhaust. The latter are considered primary because they are typically present in the particle phase in normal ambient air temperature conditions (Rodriguez and Cuevas, 2007).

The size distribution of ultrafine primary particles in urban areas shows two modes (Kittelson, 1998; Harris and Maricq, 2001; Burtscher, 2005; Rose et al. 2006; Casati et al., 2007; Rodriguez and Cuevas, 2007):

a) A *nucleation mode* in the size range <30nm. Nucleation particles are formed immediately during emission, dilution, cooling and mixing of exhaust gases with ambient air and depend on the technology of the vehicle and the fuel but also on the ambient air conditions (ambient temperature, relative humidity or dilution conditions, Jamriska et al., 2008; Rodriguez et al., 2007; Olivares et al., 2007; Casati et al., 2007). These semi-volatile particles are mainly attributed to binary H_2O-H_2SO_4 nucleation, nucleation of some semi-volatile organic compounds and subsequent particle growth during the dilution and cooling of the vehicle exhaust up to 30 nm (Mathis et al., 2005; Rönkkö et al, 2006). The fresh nucleation particles in the vehicle exhaust are thus constituted mainly by sulphuric acid and organic compounds and are responsible for the high ultrafine particle number concentration typically observed in urban air (Aalto et al., 2005; Harrison and Jones, 2005; Puustinen et al., 2007; Cyrys et al., 2008; Wu et al., 2008).

b) A *soot* (black carbon) *mode* in the size range from 30 to 100 nm (*Aitken mode*). Soot particles consist mainly of carbonaceous aggregates made up of elemental carbon, absorbed organic material and some trace elements (e.g. V, Zn, Ca or phosphate) formed during fuel combustion in the engine and emitted directly in the aerosol phase (Fraser et al., 2003; Brandenbergera et al., 2005). These components are associated with incomplete fuel combustion or contained in oil lubricant (core of particles) and the subsequent condensation of semi-volatile phases on the surface of the unburned carbon particles. Diesel vehicles represent the main source to ambient soot particles (Maricq, 2007). The heavy duty vehicles can also emit primary carbonaceous particles (soot) in the *accumulation mode* (0.1-1 μm) and even in the ranges >1 μm (Morawska et al., 1998). However, Robinson et al. (2007) showed that photo-oxidation of diesel

emissions rapidly generates large volumes of secondary organic aerosol, probably owing to the oxidation of low volatility gas-phase species volatilized from primary particles when diluted in ambient air.

Both types of particles fall mostly in the size range <100 nm and are found in high concentrations near emission sources (Morawska et al., 1998). Nanoparticle size distributions change rapidly with the distance to the emission sources as nucleation mode particles grow fast by coagulation and condensation processes (Zhu et al., 2002; Charron and Harrison ,2003; Zhang and Wexler, 2004; Zhang et al., 2004). In contrast, accumulation particles (0.1-1μm) present a long residence time in the atmosphere (days to a few weeks, Mészáros, 1999).

Coarse particles are mainly primary and generated by mechanical processes from a variety of sources. Natural origin particles are mineral dust resuspended and transported from arid areas, sea spray at coastal sites and biogenic compounds. In urban areas road traffic produces the resuspension of mineral dust and abrasion products from tyre and brake wear deposited on roads (Kupiainen, 2007). Construction and demolition activities are also important sources of anthropogenic mineral dust (Amato et al., 2009). Organic matter and elemental carbon linked to combustion emissions are other natural or anthropogenic primary particles. Coarse particles are relatively rapidly removed of the atmosphere through sedimentation. Residence lifetime of coarse particles decreases when the diameter increases (hours for particles >20μm to 2-4 days for particles of 2-3μm diameter, Mészáros, 1999).

According to the size distribution of these compounds and considering number concentration measurements, primary particles are expected to occur both in the ultrafine (<0.1μm) and accumulation modes (0.1-1μm), owing to the fact that the coarse mode (>1μm) particles contribute mainly to mass and not to number concentrations (Figure 1.3).

1.5.2. Secondary particles

1.5.2.1 Nucleation

New particle formation occurs in the atmosphere by nucleation from precursor gases. Several nucleation mechanisms have been proposed: homogeneous binary water-sulphuric acid nucleation, homogeneous ternary water-sulphuric acid-ammonia

nucleation, ion-induced nucleation of inorganic or organic vapours, or kinetically controlled homogeneous nucleation (Kulmala and Kerminen 2008, and references therein). Their occurrence depends on atmospheric conditions and concentrations of precursor gases. Photochemistry plays a key role in nucleation because it generates radicals that react with gaseous precursors to produce the vapours responsible for the nucleation of particles. Nucleation processes are generally highly influenced by the concentration of atmospheric precursor gases, the ambient air conditions (temperature, humidity, solar radiation) and the availability of pre-existing particle surfaces that favour condensation rather than nucleation processes, among other factors (Rodriguez et al., 2007; Casati et al., 2007; Olivares et al., 2007; Jamriska et al., 2008; Kulmala and Kerminen, 2008). *Nucleation mode* particles are in the size range <30nm and present the maximum number concentration usually around 5-15 nm particle diameter (Raes et al., 2000; Harrison et al., 2000; Wehner and Wiedensohler, 2003; Cabada et al., 2004; Hussein et al., 2005; Stanier et al., 2004; Van Dingenen et al., 2004; Salma et al., 2005 and Rodríguez et al., 2007; Figure 1.3).

In urban background environments, a large proportion of secondary nucleation particles are formed in ambient air from traffic gaseous exhaust emissions once these are diluted in ambient air, photo-oxidized by reactive species under solar radiation and the supersaturation conditions are reached (this usually takes place a few hours after the emission, Boy and Kulmala, 2002; Rodriguez et al., 2005). Thus, nucleation particles in urban areas originate from sulphuric acid, ammonia ions and products of volatile organic compounds oxidation as precursor gases (Kittelson, 1998; Kulmala et al., 1998 and 2004; Zhang et al., 2004). Their residence time in the atmosphere is very short (a few hours) because of their rapid growth by coagulation and condensation processes (Zhu et al., 2002; Charron and Harrison, 2003; Zhang and Wexler, 2004; Zhang et al., 2004).

Nucleation episodes are favoured under clean air conditions (Birmili et al., 2001; Stanier et al., 2004; Rodriguez et al., 2005). Nucleation and condensation of gas-phase components onto pre-existing particles are competing processes. In polluted air conditions, when the availability of aerosol surface area concentrations is high enough, condensation of gases onto particles is favoured rather than the formation of new particles by nucleation. Nucleation episodes reported (Birmili et al. 2001; Stanier et al., 2004; Rodriguez et al., 2005) are associated with cold front passages with abrupt drops in relative humidity, high wind speeds, raise in the total solar radiation intensity and abrupt increases in ozone levels.

In rural areas, under specific temperature, insolation and relative humidity conditions, important nucleation episodes have also been reported (Birmili and Wiedensohler, 2000; Ketzel et al., 2004; Mäkelä et al., 2000; Boy and Kulmala, 2002; Kulmala et al., 2004; Rodríguez et al., 2005).

1.5.2.2 Condensation

Measurements have indicated that emitted nanoparticle (<50 nm diameter) size distributions evolve significantly with time and distance from emission sources (Morawska et al., 2008b). The variation in particle size depends on the balance between particle size growth by coagulation and condensation processes and shrinkage by evaporation (Minoura and Takekawa, 2005). This balance is affected by the concentration of gases or particles in the atmosphere between other factors like ambient relative humidity or temperature (Jamriska et al., 2008).

Particles may act as condensation nuclei where gaseous species like sulphuric acid, water, ammonia, nitric acid or organic compounds with low vapour pressures condense (Rose et al., 2006). The condensation or adsorption of gas-phase components onto pre-existing particles results in particle growth by heterogeneous nucleation or reaction of gases with the particle surface (Warneck, 1988; Cabada et al., 2004). As a result, particle size and mass increase and particle number decreases.

As above mentioned, condensation is in competition with the nucleation of new particles (Rodriguez et al., 2005; Minoura and Takekawa, 2005; Jamriska et al., 2008). The condensation of semi-volatile species onto particle surfaces is favoured under high concentrations of pollutants, when the aerosol surface concentration available is high enough to favour condensation instead of nucleation of new particles. Thus, condensation processes are favoured at night, when the decrease in the boundary layer depth increases the concentration of aerosols and gaseous precursors and the temperature decreases lowering the equilibrium vapour pressure that favours condensation.

In rural sites, the aerosols exhibits usually lower number concentrations and higher mean particle size than those recorded at urban sites. This is due to coagulation and condensation processes during the transport from urban/road traffic to rural sites (Birmili et al., 2001; Rodriguez et al., 2005), although nucleation episodes are also occurring, for example when temperature drops markedly and rapidly.

Atmospheric aerosol formation and growth may also increase CCN and lead to enhancements in cloud droplet concentrations (Laaksonen et al., 2005; Tunved et al., 2006).

1.5.2.3 Agglomeration/coagulation

During their residence time in the atmosphere and as the distance to the emission sources increases the particles interact and coagulation between particles occurs. The coagulation of ultrafine particles results in particle growth to *Aitken* (30-100nm) and then to *accumulation modes* (0.1-1μm, Figure 1.3). Coagulation is produced by Brownian motion and diffusion, and the probability of coagulation is higher for the smaller particles (Mészáros, 1999). Higher concentrations of particles lead to faster coagulation, owing to the higher collision probability. Therefore, the agglomeration of particles is favoured under high concentration of pollutants or at night, when the decrease of the boundary layer depth increases the concentration of particles in ambient air. Coagulation is one of the main mechanisms reducing the number concentration (together with condensation and volatilization).

Several studies report urban pollution events (Ruuskanen et al., 2001; Vecchi et al., 2004; Rodriguez et al., 2007) characterized by high PM mass concentrations. In most of these episodes condensation processes take place and particles grow enough to produce significant concentrations of particles higher than 100 nm that account for the high PM mass concentrations observed.

1.5.2.4 Volatilization

Re-evaporation of recently nucleated particles is an important mechanism that contributes to reduce number concentration. Dilution of volatile gases when increasing the distance from the emission source (e.g. vehicle exhaust) may cause the smaller particles in the ultrafine size range to evaporate when the ambient concentration of volatile components is low enough (Zhang et al., 2004; Minoura and Takekawa, 2005; Robinson et al., 2007). Similarly, semivolatile organic compounds volatilize from small liquid nanoparticles (<15nm) almost immediately after the emission and the shrinking of these nanoparticles enhances their rates of coagulation by over an order of magnitude (Jacobson et al., 2005) resulting in particle growth and a decrease in the number concentration.

Volatilization depends on atmospheric conditions. Evaporation is favoured during daylight due to the increase in temperature and the decrease of the gas-phase precursor concentrations owing to the dilution induced by the higher boundary layer depth (Rodríguez et al., 2007). Likewise, wind changes or an increase in wind speed helps to diffuse pollutants and favours the vaporization of volatile components of particles (Minoura and Takekawa 2005).

Solid/gas phase distribution of several chemical species depends also on atmospheric conditions (e.g. ambient temperature or relative humidity). This fact is especially important for ammonium nitrate and semi-volatile organic compounds (Adams et al., 1999). Ammonium nitrate (NH_4NO_3) is not stable in particulate phase at a temperature higher than 20-25ºC and low relative humidity (Stelson et al., 1979; Mészáros and Horváth, 1984; Willison et al., 1985; Seidl et al., 1996; Querol et al., 1998a; Song et al., 2001; Wittig et al., 2004) and depending on the climatic region considered it may present a seasonal evolution in particulate phase with winter maximums and summer minimums. A number of semivolatile organic compounds may also experience the same processes (Viana et al., 2006; Harrison and Yin, 2008).

1.6. Monitoring parameters

The complexity of the mixture of gaseous, solid and liquid substances (some of them semi-volatile) yielding a large range of particle size and number concentrations, both changing with atmospheric conditions, makes characterization of aerosols and aerosol processes interesting science issues. Aerosol monitoring parameters may be chosen according to the aim of the study to be carried out.

1.6.1. Particle number concentration (N, cm^{-3})

Studies on ultrafine particles are typically based on aerosol number concentration and size distribution measurements (Harrison et al., 2000; Van Dingenen et al., 2004 ; Minoura and Takekawa, 2005; Mejia et al., 2007; Wu et al., 2008; Morawska et al., 2008; Kulmala and Kerminen, 2008). N is frequently expressed as $N_{>X}$ (particles with diameters larger than x nm) or as grain size segregated measurements ($N_{XX\text{-}YY}$, particles with diameters between xx and yy nm). Researchers have shown how in urban environments, aerosols typically exhibit a number size distribution with an absolute mode within the size range 20-40 nm. Moreover, the ultrafine fraction (N<100 nm) usually accounts for 80-90% of the total number concentration (Wichmann et al.,

2000; Wehner and Wiedensohler, 2003; Kulmala et al., 2004 Rodríguez et al., 2007; Figure 1.3). The monitoring of number concentrations (N) or number size distributions is not required in air quality networks. However, it is indispensable to account for the ultrafine fraction, especially in urban areas, where road traffic emissions are important.

1.6.2. Black carbon concentration (BC, µg m^{-3} or ng m^{-3})

Black carbon (BC) is the main component of soot responsible for light absorption (IPCC, 2007) and consequently it has an important effect on climate. It is formed by incomplete combustion processes and it is attributed to road traffic exhaust emissions and other combustion sources (industrial, residential, domestic, shipping, biomass, among others). Continuous measurements of BC are very important in urban areas, where traffic is the most important emission source of carbonaceous particles, but also in rural areas were biomass (or less frequently coal) combustion is usual. BC monitoring is a very useful tool to study direct traffic emissions not accounting for processes that occur after the dilution of the exhaust gases in the urban atmosphere, for example photochemical nucleation. BC monitoring is not required by current EC standards on air quality, although it has been largely monitored in the past (Directive 80/779/EEC, EC 1980) and used in many epidemiological studies.

1.6.3. PM_{10}, $PM_{2.5}$ and PM_1 (aerosol mass concentration, µg m^{-3})

In air quality studies PM_{10}, $PM_{2.5}$ and PM_1 are defined as the mass fractions of particulate matter that pass through a selective inlet for an aerodynamic diameter of 10, 2.5 or 1 µm respectively, with 50% efficiency. PM_{10} and $PM_{2.5}$ are actually selected as the monitoring parameters in worldwide environmental standards (e.g. 2008/50/CE in Europe) where the coarse fraction is considered the one between 2.5 and 10 µm ($PM_{2.5-10}$), whereas $PM_{2.5}$ is considered the fine fraction. This particular size discrimination is the product of recognition that fine and coarse particles generally have distinct properties, sources and formation mechanisms. However, in atmospheric sciences, the fine mode includes particles <1µm (PM_1, Whitby, 1978; Wilson and Suh, 1997). This is due to the fact that fine (<1 µm) and ultrafine (<0.1 µm) particles have a large proportion of secondary species and are dominated by emissions from combustion processes (carbonaceous material, trace metals, and sulphate, nitrate and ammonium ions). However, coarse particles (>1 µm) are mostly primary and generated by mechanical processes from a variety of sources (such as mineral dust, abrasion products from tyre and brake wear, sea spray at coastal sites or biogenic aerosols),

although secondary particles formed by chemical interaction of gases with primary particles of crustal or marine origin may also be found (Wakamatsu et al., 1996; Querol et al., 1998a). In conclusion, PM_{10} levels are highly influenced by particles generated by mechanical processes and belonging to the coarse mode. In urban environments PM_{10} is affected by particles resuspended by road traffic, but in a lesser extent by vehicle direct exhaust emissions. $PM_{2.5}$ measurements provide information also on particles generated by mechanical processes, but the contribution from particles derived from combustion sources becomes more significant. PM_1 measurements (nucleation and accumulation modes, Figure 1.3) provide more information about contributions from combustion processes.

1.6.4. Size distribution, N and PM_x

PM mass concentrations are currently monitored in air quality networks because the current air quality legislations have established PM mass concentration standards (µg or ng m^{-3}). The current European Air Quality Directive 2008/50/EC establish limit values for PM_{10} and $PM_{2.5}$. However, atmospheric aerosol concentration can also be expressed as particle number (cm^{-3}), surface (cm^2 cm^{-3}) or volume (cm^3 cm^{-3}) concentration. The particle size distribution is very different depending on the parameter represented (Figure 1.4).

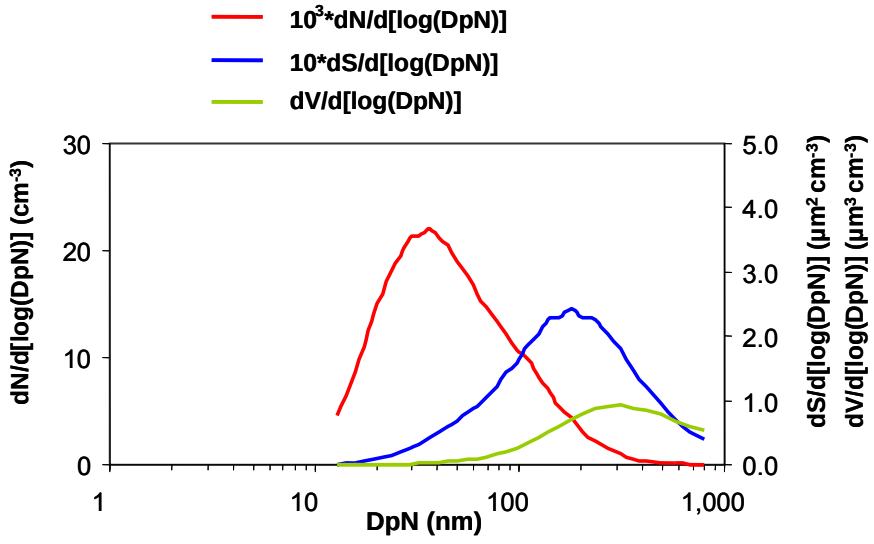

Figure 1.4. Experimental measures of number (N), surface (S) and volume (V) size distributions carried out by J. Pey (2007) in Barcelona

Several studies (Whitby, 1978; Wilson and Suh, 1997; Morawska et al., 2008) have designed PM_1 as the fine fraction (and not $PM_{2.5}$ that would be a mixture of fine and coarse particles). Consequently, in order to distinguish the contribution from different

types of sources (combustion and mechanically generated aerosols) an appropriate monitoring strategy may be the combination of PM_1 together with PM_{10} as particle mass standards instead of the current $PM_{2.5}$ and PM_{10} (Morawska et al., 2008). In addition, fine particles are a cause of concern due to the higher impact on human health, the environment and climate, and the monitoring of PM_1 becomes important to study and control emission sources to fine particles.

The variability of particle number concentrations and PM levels are not always proportional (Figure 1.4). Ultrafine particles are abundant in the air in terms of particle number concentration (80-90% of the total number concentration, Wichmann et al., 2000; Wehner & Wiedensohler, 2003; Kulmala et al., 2004; Rodríguez et al., 2007) but their contribution to the aerosol mass concentration is low. Moreover, PM mass measurements do not allow the study of aerosol processes taking place in the ultrafine particle range. In urban areas, particle number measurements are more directly influenced by vehicle exhaust traffic emissions, being this parameter more adequate than mass concentration measurements to illustrate the impact of this emission source on air quality. In addition, in urban background environments there is also a large contribution of coarse particles to the bulk aerosol mass levels, originating mainly from road dust resuspension or demolition and construction activities. However, coarse particles have a higher impact on PM mass concentration and not very significant effects on number concentration levels. Therefore, it becomes evident that the monitoring of coarse, fine and ultrafine particles, as well as BC, may yield very complementary information for a detailed study of the different pollution sources and atmospheric processes. The simultaneous monitoring of PM_{10} and PM_1 mass concentrations, BC and number concentration levels may be an appropriate approach to the monitoring of air quality in urban areas.

1.7. Atmospheric Aerosols in Europe and the Mediterranean

As described in the previous sections, atmospheric particles are emitted by a wide variety of natural and anthropogenic sources, and the nature of the source influences both the physical and the chemical composition of the particles. In addition to the local and regional anthropogenic PM sources, both the levels and composition of atmospheric PM depend on the meteorology (mainly temperature, humidity, photochemistry, re-suspension of soil particles, rain scavenging potential, re-circulation of air masses, dispersive atmospheric conditions) and on the geography (mainly

proximity to the coast, topography, soil cover and proximity to arid zones) of a given region. Several studies have been carried out to synthesize and compare the characteristics and variability of the composition and physical properties of PM in different regions of Europe (Ruuskanen et al., 2001; Querol et al., 2004b; Van Dinengen et al. 2004; Putaud et al., 2004; Götschi et al., 2005; Sillanpää et al., 2006; Puustinen et al., 2007; Rodriguez et al., 2005 and 2007; Jalava et al., 2007 and 2008). Wide variations in PM levels and characteristics are observed when considering different European regions such as Southern Mediterranean, Eastern European or Scandinavian countries with very different environmental and geographical patterns and PM source characteristics.

The predominant conditions at the North of the Alps and the Pyrenees (relatively flat terrain, westerly winds and frequent passages of cold fronts and depressions resulting in rain) favour the renovation of air masses. In contrast, the areas surrounding the Western Mediterranean basin (WMB) are characterised by an abrupt topography and complex atmospheric dynamics and meteorological processes that are described in several studies (Millán et al.,1997 and 2000; Mantilla et al., 1998; Salvador, 1999; Toll and Baldasano, 2000; Soriano et al., 2001; Gangoiti et al., 2001; Rodríguez et al., 2002a and 2003; Palau, 2003; Jorba et al., 2004; Pérez et al., 2004; Jiménez et al., 2005, 2006 and 2007; Sicard et al., 2006). Atmospheric circulation over the WMB is highly influenced by the Azores high pressure system and balanced between two synoptic systems (Millan et al., 1997; Pérez et al., 2004; Sicard et al., 2006). In winter the Azores high is situated at lower latitudes on the Atlantic Ocean and allows lows and cold fronts to reach the WMB, favouring air mass renovation. In summer, it is placed to the East and North Atlantic with the highest intensity, whereas thermal lows are developed over the Iberian Peninsula (IP) and the Sahara. This scenario favours a very weak pressure gradient in the WMB and consequently local and regional circulations dominate the atmospheric dynamics (Millán et al., 1997). The interaction of the sea and mountain breezes, the abrupt topography, the dominant north-western flows at high atmospheric levels, the uplift of air masses in the central IP and the compensatory subsidence over the sea induce recirculation of air masses around the WMB and the consequent ageing and accumulation of pollutants at a regional scale. These recirculations, together with the low rainfall registered, the high solar radiation intensity that induces atmospheric photochemical processes and the increased convective dynamics favoring local soil resuspension, induce a PM seasonal pattern, characterised by a high summer regional background across the WMB areas (Bergametti et al., 1989; Querol et al., 1998a and b; Rodríguez et al., 2001 and 2002a;

Viana et al., 2005). These high summer aerosol levels are enhanced by the frequent African dust outbreaks (Rodríguez et al., 2001; Viana et al., 2002; Escudero et al., 2005). Mediterranean Countries have a higher impact of African dust outbreaks than Northern European countries because of the proximity to the African continent. Transport scenarios of mineral dust from North Africa and impact on PM levels have been widely documented over the WMB (Loÿe-Pilot et al., 1986; Bergametti et al., 1989; Dayan et al., 1991, Guerzoni et al., 1997; Rodriguez et al., 2001 and 2002a; Escudero et al. 2005). During these episodes important increases of the mineral dust load in the atmosphere are recorded, frequently contributing to the exceedances of the daily limit value established (Escudero et al., 2007a). The occurrence of high levels of mineral matter aerosols in rural areas of dry and arid regions of Southern Europe is common as a consequence of local dust resuspension (Querol et al., 2004b). In addition, the low precipitation rates also enhance the mineral dust resuspension processes by road traffic in urban areas due to the scarce road washout (Amato et al., 2009). The occurrence of a high load of mineral matter in the atmospheric aerosol may favour the interaction with gaseous pollutants and give rise to a high proportion of coarse secondary PM (Harrison and Pio, 1983; Mamane and Mehler, 1987; Wall et al., 1988, Querol et al., 1998a). Warm conditions may favour the partitioning of atmospheric pollutants towards the gaseous phases, which in turn may interact also with the coarse components and increase the secondary coarse PM load (Harrison and Kito, 1990; Wakamatsu et al., 1996). This scenario together with the large atmospheric anthropogenic emissions produced in the Mediterranean coast (mainly arising from densely populated areas, large industrial estates, shipping, agriculture and forest fires, among others) give rise to a scenario with a complex aerosol phenomenology, with large anthropogenic and natural emissions, bulky secondary aerosol formation and transformation and intensive interaction of aerosols and gaseous pollutants.

The dispersion of traffic emissions in urban areas is very influenced by the wind interaction with buildings and streets. In many Southern EU countries the urban population usually lives closer to traffic emissions than in the North of Europe, due to the occurrence of narrower streets (street canyons) and reduced green areas making dispersion of pollutants difficult. However, in cold regions as Northern European countries the levels of mineral dust registered in urban areas may also be high, especially during the spring months. This is a consequence of the use of traction control methods in the winter (road sanding, brine solutions to melt ice or the use of studded winter tyres, snow chains or friction tyres). These methods enhance the formation of mineral particles from pavement wear or from traction sand that

accumulates on the road during winter (Kupiainen, 2007; Ketzel et al., 2007; Hussein et al., 2008).

1.8. Previous studies and gaps of knowledge

Owing to the effects that aerosols have on human health, the environment and the climate, intense and widespread aerosol research is developed. Air quality networks worldwide monitor PM levels, and a large amount of research has been carried out on the variability of levels of ambient aerosol, and their physical and chemical properties as well as on aerosol effects.

1.8.1. Studies on the interpretation of the variability of PM levels

As previously stated, PM_{10} levels are measured continuously in air quality networks by standardized methods. The new European Air quality directive (2008/50/EC) indicates that $PM_{2.5}$ and PM_{10} measurements for air quality monitoring have to be performed according to EN14907 and EN12341 standards respectively or with methods for which equivalence is demonstrated. Currently, monitoring of PM_{10} and $PM_{2.5}$ is being already carried out in Europe. Conversely, PM_1 measures are very scarce. Available data on PM_1 are usually measured with techniques that are not validated by normalized methods (e.g. optical particle counters). PM_1 measurements taken using these techniques should be corrected and validated with a normalized method. There are already gravimetric measurement technologies available to undertake PM_1 measurements accurately (very similar to those used for $PM_{2.5}$ or PM_{10} monitoring). However, long data series of PM_1 levels are currently extremely scarce (Spindler et al., 2004; Vecchi et al., 2004 and 2008; Morawska et al., 2008a; Yin and Harrison, 2008). PM_1 is considered as the fine PM fraction by atmospheric scientists. Most of its components are associated to combustion sources and may have important health effects. Consequently, long data series from monitoring of PM_1 are of great interest in order to assess the concentration levels and the properties and variability of this fine aerosol size fraction.

1.8.2. PM composition (or speciation)

Many studies have been carried out on PM_{10} or $PM_{2.5}$ levels and composition (Putaud et al., 2004; Puxbaum et al., 2004; Querol et al., 2004a and b; Hueglin et al. 2005; Sillanpää et al., 2006). In contrast there are only a few studies on PM_1 composition

across the world (Morawska et al., 2008a; Vecchi et al., 2004; Spindler et al., 2004; Ariola et al., 2006; Yin and Harrison, 2008). In this research area the terms PM speciation and composition are equivalent. Although chemically this is not completely right, we use indistinctively both of these terms with and equivalent meaning. A continuous and detailed study on PM_1 levels and speciation is necessary to obtain significant data to understand the composition, main properties and major sources of this fraction as well as the possible health impact of PM_1 compared with $PM_{2.5}$ and PM_{10}. There are a large number of studies showing that the health impact of finer PM ($PM_{2.5}$) is more relevant than that of PM_{10} (Dockery and Stone, 2007; Miller et al., 2007), but scarce data is available for the actually fine fraction (PM_1). Moreover, a quantitative intercomparison of simultaneous PM_{10}, $PM_{2.5}$ and PM_1 speciation measured at the same location could be useful to assess sources and processes that influence each PM fraction.

1.8.3. Particle number concentration

Ultrafine particles (<0.1 μm) have been related to more important health effects than coarser particles (Wichmann et al., 2000) and consequently particle number concentration monitoring and size distribution studies have gained broad attention. Many studies have been carried out on aerosol number concentrations and size distributions in rural and urban backgrounds associating road traffic as the main source to ultrafine particles (Harrison et al., 2000 and 2005; Wichmann et al., 2000; Koponen et al., 2001; Boy and Kulmala, 2002; Molnár et al., 2002; Tuch et al., 2003; Hauck et al., 2004; Ketzel et al., 2004; Zhou et al., 2004; Minoura and Takekawa, 2005; Rodríguez et al., 2005, 2007 and 2008). WHO (2006) recommends the measurement of particle number concentrations as a possible air quality parameter in epidemiological studies. However, neither total number concentration nor ultrafine particle monitoring is required by the current Air quality Directives (in Europe 2008/50/EC). In addition to mass concentration standards, the monitoring of the ultrafine number concentration may be important in air quality networks, especially in urban areas where road traffic is the main ultrafine and sub-micron PM source. The development in monitoring technologies available makes nowadays possible the continuous measurement of ultrafine or sub-micron particle number concentration. However, more research and continuous monitoring are needed in order to obtain statistically significant data to fully understand the major properties and sources of ultrafine particles, the variability of number concentration measurements and the relationship between the number and mass concentrations, and to draw attention to the importance of particle monitoring. In

the Mediterranean Basin long term studies of number concentration of sub-micron or ultrafine particles are absent.

1.8.4. Urban, regional and continental background sites

Aerosol measurements at traffic, industrial, urban, regional, rural, remote or natural background sites are useful tools to understand emission sources, transport and transformation of aerosols in the troposphere. Monitoring sites are classified using different criteria (Larssen et al., 1999; Van Dinengen et al. 2004; Putaud et al. 2004; European Air Quality Directive 2008/50/EC), such as the distance of the station to large pollution sources (cities, power plants and major motorways) or the road traffic volume.

Urban background sites are located in urban areas but isolated from the direct influence of traffic or industrial emissions (~2500 vehicles/day within a radius of 50m and far from industrial sources, Larssen et al., 1999), in order to represent the average exposure levels of the urban population. Many studies on PM levels and speciation focused on urban monitoring sites (Vecchi et al., 2004 and 2008; Ariola et al., 2006; Sillanpää et al., 2006; Vardoulakis and Kassomenos, 2008; Favez et al., 2008). The PM exposure representativeness is currently a hot issue in air quality research because not only the difficulty of measuring the exposure at an urban scale, but also for the relevance of indoor/outdoor contribution to human exposure.

Regional or rural background sites are isolated from the direct influence of local anthropogenic sources, but they should represent the regional background of the areas where they are located (distance from large pollution sources 10–50km, Larssen et al., 1999). They are usually located in the country side and as far as possible from roads, populated or industrial areas but they are affected by regional sources, long-range transport and urban plumes. Measurements performed only at a local scale at industrial, traffic or urban backgrounds may not always allow the interpretation of the origin of pollution episodes. On the contrary, aerosol measurements performed simultaneously at regional background sites at a sufficient distance from large sources of pollutants, are the best way to accurately document both aerosol long-term trends and the influence of synoptic meteorological features in air quality. Many studies have already been carried out in regional backgrounds sites around Europe (Bergametti et al., 1989; Querol et al., 2004a and 2008; Rodríguez et al., 2002b, 2003 and 2004; Rodríguez and Cuevas, 2007; Spindler et al., 2004; Salvador et al., 2006; Gerasopoulos et al.;2006; Raman et al., 2008; Dongarra et al., 2007; Kocak et al.,

2007; Glavas et al., 2008; Perrino et al., 2008; Türküm et al., 2008), but there is lack of long time PM data for Southern Europe, with differentiated meteorological characteristics, including the relevant impact of African dust outbreaks.

Continental or remote background sites are located in isolated areas, at a distance from large pollution sources (>50km, Larssen et al., 1999). Studies at remote sites, with very little influence of nearby industrial emissions or significant population, are important to characterize the continental background aerosol. The natural background aerosol is defined as the aerosol that should occur under natural circumstances without anthropogenic pollution (Hoornaert et al., 2004). However, there is always and input from anthropogenic long range transported PM. Due to the global climate effects, more attention is being paid to remote background atmospheric aerosols, and aerosol research in remote sites are being carried out in order to investigate the contribution of the natural and anthropogenic emissions to the global aerosol and to understand the mechanisms of long-range transport of anthropogenic pollutants (Cunningham et al., 1981; Putaud et al., 2003; Hoornaert et al., 2004; Alastuey et al., 2005; Marenco et al., 2006; Nyanganyura et al., 2007; Cong et al., 2007). Understanding the chemical and physical properties of background aerosols from remote areas can be a valuable reference for the study and evaluation of the evolution of the atmosphere with respect of the development of industry, populations and energy uses.

Finally, the study and intercomparison of simultaneous PM data on levels and composition at urban, regional and remote backgrounds within the same geographic area can be very useful to identify and quantify local and external sources of pollutants, especially if several PM sizes are evaluated simultaneously. A few studies following this strategy have already been performed (Pakkanen et al., 2001; Röösli et al., 2001; Lenschow et al., 2001; Querol et al., 2004a and b and 2008; Hueglin et al. 2005; Gerasopoulos et al., 2006; Ledoux et al., 2006; Lall et al., 2006; Charron et al., 2007; Yin and Harrison, 2008; Perrino et al., 2008). The Western Mediterranean regions have special meteorological and geographic characteristics (Millán et al., 1997), and a consequently detailed study of PM levels and composition measured simultaneously at urban, regional and natural backgrounds within the same geographic area could be useful to understand the behaviour and transport patterns or atmospheric PM in the Western Mediterranean.

1.8.5. Atmospheric aerosol research in the study area

The present study is continuation of previous studies focused on the characterization of atmospheric aerosols in the Iberian Peninsula carried out by the Environmental Inorganic Geochemistry research group at IDAEA-CSIC.

- TSP and PM_{10} levels and speciation started to be measured in 1995 at the Teruel coal-fired power station (Querol et al., 1996, 1998a and b) and the relevance of the African dust contribution to the PM levels measured in Spain was highlighted.
- Between 1999 and 2000, PM_{10}, $PM_{2.5}$ and PM_1 levels and PM_{10} and $PM_{2.5}$ speciation were measured at L'Hospitalet-Gornal urban (Barcelona) and Monagrega rural (Teruel) monitoring sites (Rodríguez, 2002).
- In 2001, PM_{10}, $PM_{2.5}$ and PM_1 levels and PM_{10} and $PM_{2.5}$ speciation were measured at the Sagrera urban monitoring site in Barcelona (Viana, 2003).
- In 2002 a regional background monitoring site was established in the Montseny Natural Park. PM_{10} $PM_{2.5}$ and PM_1 levels and TSP and $PM_{2.5}$ speciation started to be monitored (Castillo, 2006). TSP speciation was measured instead of PM_{10} because of the simultaneous studies of dry and wet deposition carried out at the same place (Castillo, 2006).
- In 2003 an urban background site was established at BCN-CSIC in Barcelona. From March 2003 to June 2005 PM_{10}, $PM_{2.5}$ and PM_1 levels, PM_{10} and $PM_{2.5}$ speciation and particle number concentration and size distributions were monitored (Pey, 2007). During the same period PM_{10}, $PM_{2.5}$ and PM_1 levels and PM_{10} and $PM_{2.5}$ speciation were monitored at the Montseny regional background site (Pey, 2007).
- From July 2005 (this work) the monitoring of PM_{10}, $PM_{2.5}$ and PM_1 levels, PM_{10} and $PM_{2.5}$ speciation and particle number concentration continued at BCN-CSIC in Barcelona. Moreover, in September 2005, PM_1 speciation started to be measured at the same site and from July 2007 BC levels were also monitored. At Montseny, the PM_{10}, $PM_{2.5}$ and PM_1 levels and the PM_{10} and $PM_{2.5}$ speciation measurements also continued.
- In November 2005 a remote/continental background monitoring site was established in Montsec (Catalan pre-Pyrenees). PM_{10}, $PM_{2.5}$ and PM_1 levels and PM_{10} speciation have been monitored since then (this work).

To continue and increase the understanding on the characterization of PM at Barcelona, Montseny and Montsec it is necessary to complete the studies already carried out by:

- The study of PM_1 speciation. There are no PM_1 speciation studies in this area and, in addition, they are very scarce in Southern Europe.
- The particle number concentration monitoring at the urban site. N measurements are very scarce in Southern Europe and it is important to obtain a long temporal series of particle number measurements in order to better interpret the temporal and seasonal variability and sources of ultrafine particles.
- The BC levels monitoring at the urban site. BC is an indicator of direct road traffic emissions and the study of this parameter will be useful to assess the impact of road traffic on ambient urban levels.
- The integration of all the years of PM monitoring to study temporal tendencies in PM levels, speciation, particle number and African dust outbreaks. The large number of data and the extension of the temporal series obtained until now will allow a representative study on the variability of PM levels and composition in the NE Iberian Peninsula.
- The parallel study on the three background sites will allow to better understand the different pollution scenarios occurring in this area and to interpret PM emission sources to urban, regional and continental backgrounds.

2. OBJECTIVES AND STRUCTURE OF THE STUDY

2. OBJECTIVES AND STRUCTURE OF THE STUDY

Based on the description of the research needs presented in the previous chapter, the following objectives are selected for the present study:

The main objective of this study is the interpretation of the variability of the concentration levels of PM_{10}, $PM_{2.5}$ and PM_1 and their chemical composition at urban, regional and continental backgrounds in North-Eastern Iberian Peninsula, studying the different scenarios that affect atmospheric aerosols at the three types of background. At the urban site, a study of the variability of particle number concentration and black carbon levels will also be carried out.

The specific objectives of this work are:

- The study of PM levels and composition simultaneously monitored at an urban (Barcelona), a regional (Montseny) and a continental background site (Montsec) in the same area to clarify the origin of PM pollution at the three types of background and understand the impact on air quality of the different meteorological scenarios that give rise to different air mass episodes.
- The study of PM levels and composition time series to identify the causes that difficult the compliance with the limit levels established by the Air Quality European Union Directive 2008/50/EC.
- The study of the partitioning of the different components of particulate matter between $PM_{2.5\text{-}10}$ (2.5 to 10µm), $PM_{1\text{-}2.5}$ (1 to 2.5 µm) and PM_1 (<1µm) fractions at an urban site (Barcelona), between $PM_{2.5\text{-}10}$ and $PM_{2.5}$ at a regional site (Montseny) to study the size distribution of the different PM components and to investigate their possible origin. The study of the PM_{10} speciation at a continental background site (Montsec).
- The study of the PM_1 levels and chemical composition at an urban background site (Barcelona) to evaluate the main sources to fine particles. The evaluation of the possibility of using PM_1 as an air quality monitoring parameter is also key point of this study.
- The study of the variability of particle number concentration levels in Barcelona urban site. The simultaneous study of BC levels monitored at the same site to evaluate their relationship and try to assess sources to ultrafine particles. The

possibility of employing particle number concentration as an air quality monitoring parameter together with PM is also an important topic of this study.

- The study of the mineral dust load simultaneously monitored at an urban, a regional and a continental background site in the same area can help to quantify the anthropogenic and the natural contribution to the mineral dust load and to assess the contribution of African dust, regional soil resuspension and anthropogenic mineral dust.
- The integration of all the data previously obtained at Barcelona, Montseny and Montsec by the Environmental Inorganic Geochemistry research group at IDAEA-CSIC to study temporal tendencies on PM levels, speciation and particle number concentrations.
- The study of simultaneous measurements performed at Barcelona, Montseny and Montsec, in order to investigate the main sources, transport and transformation patterns of atmospheric aerosols at a regional scale. The comparison of data obtained simultaneously at all three sites may also help to quantify urban, regional and external contributions to aerosols in this region and to estimate the impact of urban emissions in the rural areas.

To reach the objectives proposed in this project the following tasks that will be detailed in the Methodology chapter, were carried out:

- The continuous monitoring and interpretation of PM_{10}, $PM_{2.5}$ and PM_1 levels at Barcelona, Montseny and Montsec.
- The continuous characterization of the local atmospheric dynamics and the daily interpretation of air mass origins, with the objective of detection of the different episodes influencing atmospheric aerosol variability at the three backgrounds.
- The study of the chemical composition of PM_{10}, $PM_{2.5}$ and PM_1 at Barcelona, PM_{10} and $PM_{2.5}$ at Montseny and PM_{10} at Montsec. Regular sampling and analysis of major and trace components.
- The continuous monitoring and interpretation of particle number concentrations at the urban background site in Barcelona.
- The continuous monitoring of BC levels (from July 2007) at the Barcelona site.
- The identification and quantification of aerosol sources in the three backgrounds by source apportionment techniques.
- The integration of all the data previously obtained at Barcelona, Montseny and Montsec in time series.

The results presented in this work are organized as follows. After a methodology chapter, a detailed study was performed and presented separately for the urban, regional and continental backgrounds considered in three individual chapters that resume the results obtained for each site, with a summary and conclusions section at the end of each chapter. Then, in a discussion chapter, an intercomparison of the simultaneous data recorded at the three sites is carried out, in order to discuss the main sources and characteristics of atmospheric aerosols in the WMB and to estimate urban, regional and external contributions to aerosols in the region. Finally, there is a conclusion chapter resuming the main conclusions extracted from the study. In this section, the most relevant conclusions for each site and on the comparative study of atmospheric aerosols at the urban, regional and continental backgrounds are presented.

3. METHODOLOGY

3. METHODOLOGY

3.1. Monitoring sites

The characterization of atmospheric particulate matter in the Western Mediterranean Basin (WMB) according to the objectives proposed was carried out simultaneously at urban, regional and continental backgrounds at a regional scale. Three monitoring sites were selected in North-Eastern Iberian Peninsula (Figure 3.1):

- Barcelona (BCN-CSIC): An urban background site with road traffic influence
- Montseny (MSY): A regional background site
- Montsec (MSC): A continental background site

The **BCN-CSIC** monitoring site is located in Barcelona, on the North-Eastern Mediterranean coast of the Iberian Peninsula, at 68 m.a.s.l. (Figure 3.1). The mountain ranges surrounding the area act as a climatic barrier, protecting the area from the continental climatic conditions and influencing the winds arriving in the area. The Pyrenees Range, the Catalan Coastal Ranges and the valleys crossing the coastal ranges (the Ebro, Llobregat and Besòs Valleys) are the main geographical systems (Figure 3.2). The typical winds in the region are the Tramontana (northern winds affecting the north-eastern peninsula) and the Cierzo (north-western winds canalized by the Ebro valley).

The **Montseny** monitoring site is situated on the pre-Coastal Catalan Range at 720 m.a.s.l. (Figure 3.1 and Figure 3.2). These mountain ranges have an orientation northeast-southwest. In this region of Iberia daily atmospheric dynamics are characterized by the sea-land breezes activated by the heating of the slopes orientated to the east and southeast by the sun during the morning hours (Baldasano et al., 1994; Millan et al., 1997; Jorba et al., 2004). Air masses are injected to different heights depending on the breeze intensity. At a certain altitude the atmospheric circulation transports these air masses back to the Mediterranean, where there is a subsidence area. The predominating air mass transport is from the sea to the land (valley and mountain breezes) during the day and the opposite (through the valleys) during the night.

The **Montsec** monitoring site is situated at 1570 m.a.s.l. on the Montsec range, a Pre-Pyrenean mountain range of 40 km long between Aragon and Lleida that is oriented East-West (Figure 3.1 and Figure 3.2). Atmospheric dynamics are characterized by

predominant North-Atlantic advections during the winter months and daily cycles during the warm months produced by the mountain breezes activated by the heating of the slopes orientated to the South and South-west.

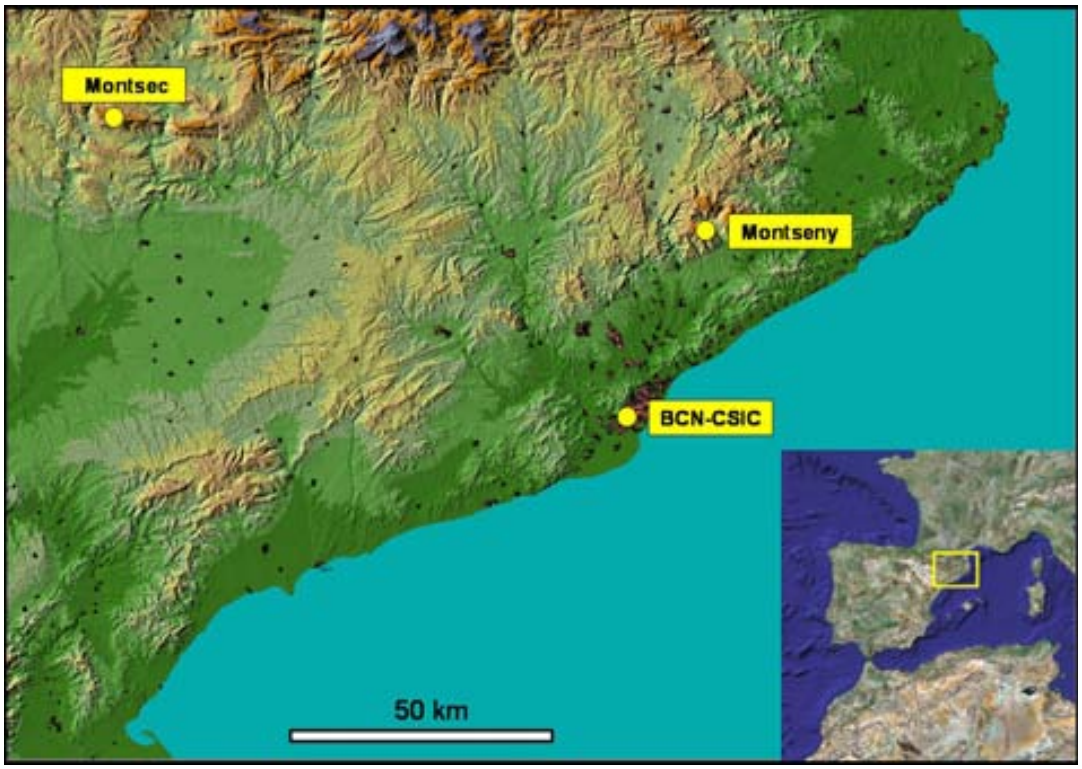

Figure 3.1. Location of the three monitoring sites.

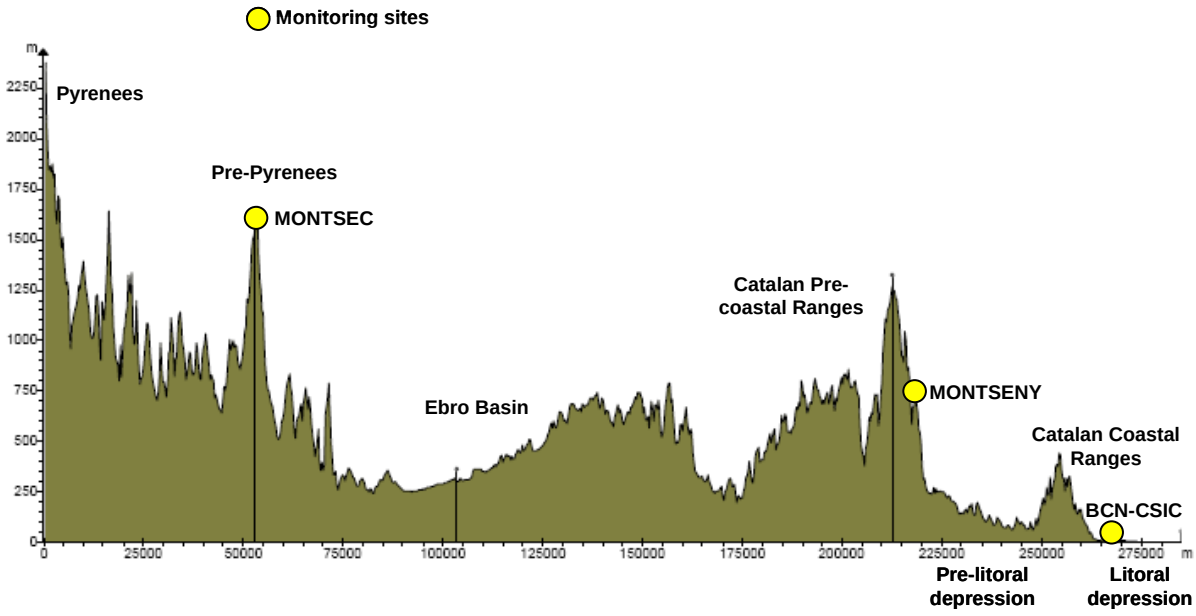

Figure 3.2. Topography of the study area and location of the three monitoring sites.

From the cluster analysis of atmospheric retro-trajectories, Jorba et al. (2004) described the synoptic transport patterns in the Barcelona area (Figure 3.3). The results show three groups of westerly flows (fast, moderate and slow) being 48% of the analyzed situations at 5500 m, 38% at 3000 m and 23% at 1500 m.

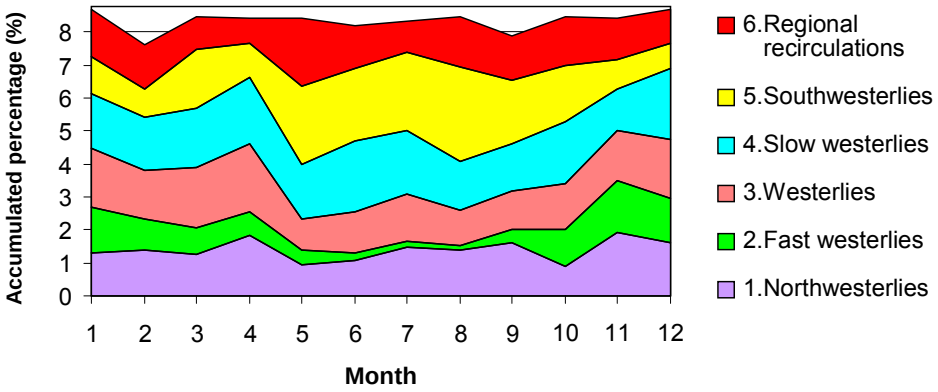

Figure 3.3. Cluster analysis of retro-trajectories ending in Barcelona (Jorba et al., 2004).

In winter, the worst situation for air quality is the high pressure system induced by the presence of the continental anticyclone (lower dispersion scenario). In this situation, the precipitations are absent, the daily thermal amplitude is high and the wind speed is lower than the average. A thermal inversion of a few hundred metres is formed over the ground and it prevents air mass ascending movements, with a significant increase of pollutants at surface levels, especially primary gaseous pollutants and particulate matter. These situations are characterized by their temporal persistency, sometimes longer than one week.

In summer, there is a high occurrence of regional air mass regional recirculation situations, being the 45% of the total situations (Figure 3.3). They are characterized by the stagnation of air masses during periods of several days, with the formation of diurnal sea-earth and nocturnal earth-sea breezes and mountain winds (Figure 3.4). As a typical characteristic of the region when compared with more septentrional regions there is an important decoupling between the low and middle troposphere, especially in summer, with zonal fluxes in middle and high layers of the troposphere and stagnation in the lower levels.

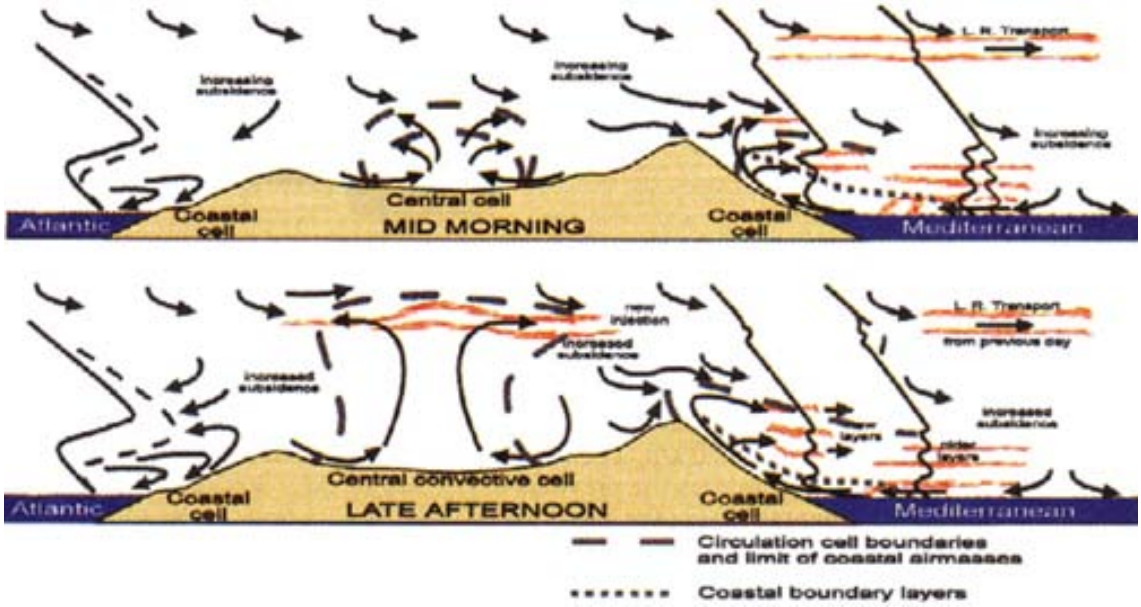

Figure 3.4. Typical summer atmospheric circulation at mid morning and late afternoon over the Iberian Peninsula (Millán et al., 1997).

PM levels and composition in this area are conditioned by the influence of anthropogenic emissions, the local, regional and synoptic meteorological conditions and the dispersion of pollutants into the boundary layer. Winter pollution episodes are mainly dominated by stable anticyclonic conditions, which favour air mass stagnation and result in high levels of PM. The summer months are characterized by the absence of large-scale forcing and the predominance of mesoscale circulations (Figure 3.4), the formation of a thermal low at a peninsular level forcing the convergence of surface winds from the coastal areas towards the central plateau with strong levels of subsidence over the Western Mediterranean Basin and sea-land breeze dynamics which result in the recirculation and accumulation of pollutants over the eastern Iberian coast. Breeze circulations and transitions (diurnal sea breeze and weak nocturnal earth breeze) are reflected in PM concentrations.

3.1.1. Barcelona monitoring site (BCN-CSIC)

The PM monitoring site in Barcelona is an urban background station under the influence of road traffic emissions from one of the largest avenues at the western edge of the city (traffic density 120000 vehicles per day, Figure 3.5). The monitoring station is located on the roof of the Institute of Earth Sciences *Jaume Almera* (41º23'N and 2º7'E at 68 m.a.s.l.). The building has two storeys and is found within the University campus at approximately 150 m distance from the Diagonal Avenue. The mean annual

temperature is 17.4ºC, the mean relative humidity 70% and the annual precipitation 450 mm (*Servei Meteorològic de Catalunya*). The main local source of atmospheric particulate matter in Barcelona is road traffic, with a high impact on the levels of carbonaceous compounds, nitrate and mineral matter (Pey, 2007). Other disperse sources (small industries, house heatings, etc.) contribute to the increase the levels of sulphate, nitrate and carbonaceous compounds. Construction activities have also an important impact on the levels of coarse mineral compounds.

Figure 3.5. BCN-CSIC PM monitoring site at Barcelona.

The BCN-CSIC site is operating continuously since March 2003. It is equipped with real time optical particle counters for the continuous measurement of PM_{10}, $PM_{2.5}$ and PM_1 levels (hourly basis). Twenty four hour samples of PM_{10}, $PM_{2.5}$ and PM_1 were simultaneously collected by means of high-volume samplers equipped with PM_{10}, $PM_{2.5}$ and PM_1 (the latter since October 2005) inlets. Sampling was carried out at a rate of two 24h samples of each PM fraction per week. Before October 2005, only PM_{10} and $PM_{2.5}$ gravimetric samples were available (Pey, 2007). Aerosol number concentration (5 min basis) was monitored from 2003 to 2005 with a butanol-based condensation particle counter (Pey, 2007) and from July 2005 with a water-based condensation particle counter. Real time black carbon concentrations (BC) were sporadically monitored from July 2007 with a BC MAAP monitor (5 min basis).

Data relative to PM levels, chemical characterization and particle number concentration levels at other monitoring sites in Barcelona from 1999 to 2002 and at BCN-CSIC site from 2003 to June 2005 were compiled and used to help the interpretation of results (Table 3.1 and Figure 3.6). L'Hospitalet-Gornal and Sagrera sites are equivalent to BCN-CSIC site regarding the type of aerosols and levels measured, and it is possible

to build a unique series for the urban background from Barcelona. Zona Universitaria sampler is located on the ground and surrounded by tall buildings. PM levels measured at this site are lower owing to the buildings that stop direct impact of emissions from near roads.

Table 3.1. Data from Barcelona urban monitoring sites from 1999 to 2007.

Period	Site	Parameters	References
1999-2000	L'Hospitalet-Gornal	PM_{10}, $PM_{2.5}$, PM_1 levels PM_{10}, $PM_{2.5}$ speciation	Rodríguez, 2002
2001	La Sagrera	PM_{10}, $PM_{2.5}$, PM_1 levels PM_{10}, $PM_{2.5}$ speciation	Viana, 2003
2002	Zona Universitaria	PM_{10} levels	Barcelona *Air quality Monitoring Network*
March2003-June 2005	BCN-CSIC	PM_{10}, $PM_{2.5}$, PM_1 levels PM_{10}, $PM_{2.5}$ speciation Particle number concentration levels	Pey, 2007
July 2005-December 2007	BCN-CSIC	PM_{10}, $PM_{2.5}$, PM_1 levels PM_{10}, $PM_{2.5}$ speciation PM_1 speciation (from October 2005) Particle number concentration levels BC levels (from July 2007)	This work

Figure 3.6. Localization of the four Barcelona monitoring sites.

Data on levels of gaseous pollutants at some sites in the Barcelona metropolitan area were supplied by the Department of Environment of the Government of Catalonia. Data from L'Hospitalet-Gornal site were used considering that it is near to BCN-CSIC site.

Meteorological variables (atmospheric pressure, wind components, solar radiation, temperature and relative humidity) from a close meteorological station were provided by the Department of Astronomy and Meteorology from The Physics Faculty at the *Barcelona University* and precipitation data from the Fabra meteorological station (*Servei Meteorologic de Catalunya)*. Data on traffic intensity was provided by the *Ajuntament de Barcelona (Serveis de Mobilitat)* and *Dirección General de Tráfico (DGT).*

3.1.2. Montseny monitoring site (MSY)

The Montseny monitoring site is a regional background site for the measurement of atmospheric aerosols (Figure 3.7). It is located in *La Castanya* an experimental ground owned by the *Generalitat de Catalunya* in the Montseny Natural Park (40 km to the North-East of Barcelona, 25 km from the Mediterranean coast, 41º46'N and 2º21'E, 720 m.a.s.l.).The Montseny is part of the pre-coastal Catalan range. This area is characterized by a mean annual temperature of 11.5ºC, a mean relative humidity of 76% and an annual precipitation of 690 mm. It has been operating from February 2002 (Castillo, 2006; Pey, 2007) and the results obtained provide important information about tropospheric aerosols in the Mediterranean area. This site is integrated in the Network of Control and Surveillance of Air Quality of the *Direcció General de Qualitat Ambiental* of *the Conselleria de Medi Ambient* of the *Generalitat de Catalunya* and in EUSAAR (EUSAAR, *European Super-sites for Atmospheric Aerosol Research*) which integrates a European network of monitoring sites located in regional background areas distant from direct local emissions.

The Montseny site has been equipped with optical particle counters for real time measurements of the levels of PM_{10}, $PM_{2.5}$ and PM_1 continuously since March 2002. From 2002 to the end of 2003, TSP and $PM_{2.5}$ were sampled periodically with high volume samplers and from January 2004 PM_{10} and $PM_{2.5}$ were sampled at a rate of 2 PM_{10} and 1 $PM_{2.5}$ samples per week.

Data available from previous studies (Castillo, 2006; Pey, 2007) relative to levels and composition of Montseny from 2002 to July 2005 were compiled and used to support interpretations (Table 3.2).

Table 3.2. Data obtained at Montseny regional background monitoring site from 2002 to 2007.

Period	Parameters	References
March 2002- January 2004	PM_{10}, $PM_{2.5}$ and PM_1 levels TSP and $PM_{2.5}$ speciation	Castillo, 2006
January 2004-June 2005	PM_{10}, $PM_{2.5}$ and PM_1 levels PM_{10} and $PM_{2.5}$ speciation	Pey, 2007
July 2005-December 2007	PM_{10}, $PM_{2.5}$ and PM_1 levels PM_{10} and $PM_{2.5}$ speciation	This work

Data on meteorology (atmospheric pressure, wind components, solar radiation, precipitation, temperature and relative humidity) from two meteorological stations next to Montseny, PN-Tagamanent and Santa Maria de Palautordera, was provided by the *Servei Meteorològic de Catalunya.*

Atmospheric particulate matter at Montseny is mainly fine (Castillo, 2006). In addition to the natural origin PM, the main sources are urban, industrial, and agricultural and farming emissions at a regional scale and it is mainly composed of ammonia sulphates and nitrates and carbonaceous compounds that can be associated to anthropogenic or biogenic emissions. The main source to the mineral dust is the regional and local soil resuspension and in a minor extent the African dust outbreak contribution (Pey, 2007).

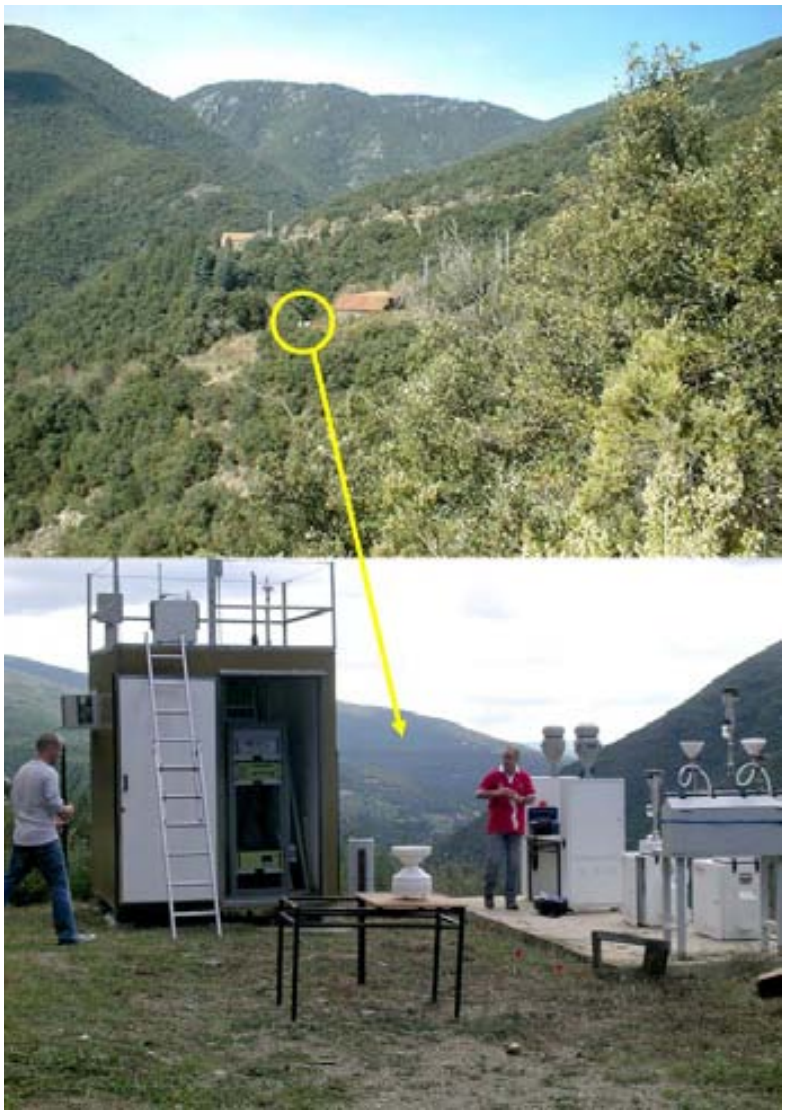

Figure 3.7. Montseny monitoring site (MSY).

3.1.3. Montsec monitoring site (MSC)

The Montsec monitoring site is a continental/remote background site for the measurement of atmospheric aerosols (Figure 3.8). It is located at the Montsec Astronomic Observatory of the *Generalitat de Catalunya* (42º3'N and 0º44'E, 1540 m.a.s.l.) in the Montsec mountain range, a calcareous range with an orientation from west to east that belongs to the Pre-Pyrenean range. This area is characterized by a mean annual temperature of 8.8ºC, a mean relative humidity of 64% and an annual precipitation of 380 mm (data from 2006 and 2007).

From November 2005 to March 2007 a mobile laboratory equipped with aerosol monitoring equipment was installed at the Montsec site. Real-time levels of PM_{10}, $PM_{2.5}$ and PM_1 were monitored with an optical counter (1 hour basis) and PM_{10} samples were

periodically collected (1-3 samples per week) for chemical characterization with an automatic sequential high volume sampler. From 15th March 2007 the mobile unit was removed and the equipment was installed in open air. Data on meteorology (atmospheric pressure, wind components, solar radiation, precipitation, temperature and relative humidity) measured at the Montsec meteorological station was provided by the *Servei Meteorològic de Catalunya.*

The main PM sources in Montsec are natural sources (biogenic), the recirculation of pollutants at a regional scale and also long-range transport of pollutants at high altitudes (African dust outbreaks, biomass burning and anthropogenic plumes among others).

Figure 3.8. Montsec monitoring site (MSC).

3.2. PM monitoring: instruments and methods

3.2.1. Instruments

3.2.1.1. Real time monitoring of PM concentration levels

The levels of PM_{10}, $PM_{2.5}$ and PM_1 were measured continuously on an hourly basis at all sites by means of optical particle counters (Grimm Technologies, Inc. 1107 and 1108 models, Figure 3.9). GRIMM dust monitors measure concentration levels of particles between 0.3 and 15 μm diameters. The operation principle is based in the measurement of particle number. The air flow passes through a laser beam and the scattered signal of particles are collected at 90º by a mirror and transferred to a recipient diode. Then, a 15-channel pulse height analyzer for size classification detects scattered signals and the number of single particle counts registered in each channel is converted to mass using an algorithm and expressed in μg m^{-3}. The data obtained in this study was corrected using the gravimetric PM_{10}, $PM_{2.5}$ or PM_1 data obtained simultaneously with high volume samplers.

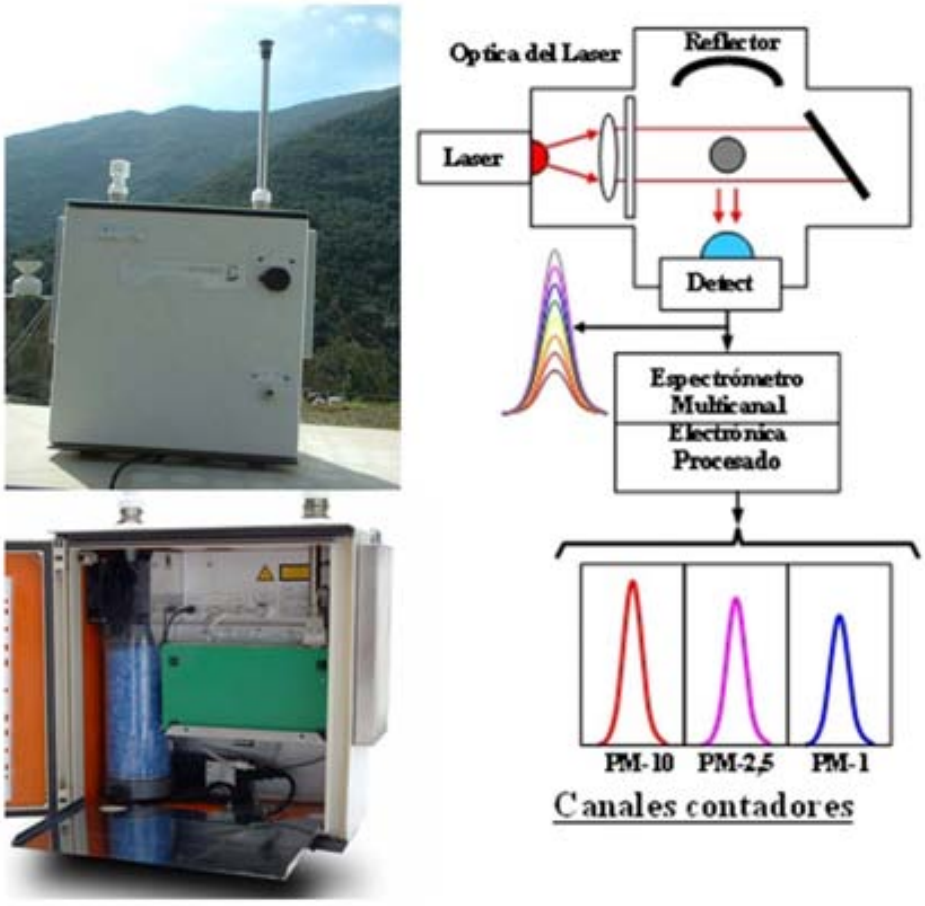

Figure 3.9. GRIMM 1107 dust monitor and flow diagram (SIR S.A.).

3.2.1.2. Sampling for gravimetric determination of PM levels and speciation

Twenty four hour samples of PM_{10}, $PM_{2.5}$ and PM_1 were collected in BCN-CSIC by means of high-volume samplers (MCV CAV-A, Figure 3.10) working at 30 $m^3 h^{-1}$ and equipped with PM_{10}, $PM_{2.5}$ or PM_1 inlets (DIGITEL DPM10/30/00, DPM2.5/30/00 and DPM01/30/00 for PM_{10}, $PM_{2.5}$ and PM_1 or MCV PM1025-CAV for PM_{10} or $PM_{2.5}$, Figure 3.11). An automatic sequential high volume sampler (DIGITEL DH-80, Figure 3.10), working at 30 $m^3 h^{-1}$, was used in Montseny for the sampling of PM_{10} fractions while $PM_{2.5}$ was sampled by means of a MCV-CAV high-volume sampler (Figure 3.10). In Montsec, PM_{10} was sampled using automatic sequential high volume samplers (DIGITEL DH-80 from November 2005 and MCV CAV-A/M-S from March 2007), all working at 30 $m^3 h^{-1}$.

In these instruments the air sample enters through the inlet (Figure 3.11), vacuumed by the high-volume sampler pump and goes through the nozzles of diameters depending on the fraction to sample (PM_{10}, $PM_{2.5}$ or PM_1), where the speed increases. Then, the particles bigger than the designed cut size impact on a plate impregnated with vaseline (baffle pot) and the smaller ones pass and are collected on the filter (Figure 3.11). The PM_1 DIGITEL inlet (DPM01/30/00) is a 2-stage impactor inlet and the air sampled passes through two impaction stages (first a $PM_{2.5}$ stage at 30 $m^3 h^{-1}$ and then a PM_1 stage at 30 $m^3 h^{-1}$, Figure 3.11).

Figure 3.10. MCV-CAV high volume sampler (left), DIGITEL DH-80 sequential high volume sampler (center) and MCV CAV-A/M-S sequential high volume sampler (right).

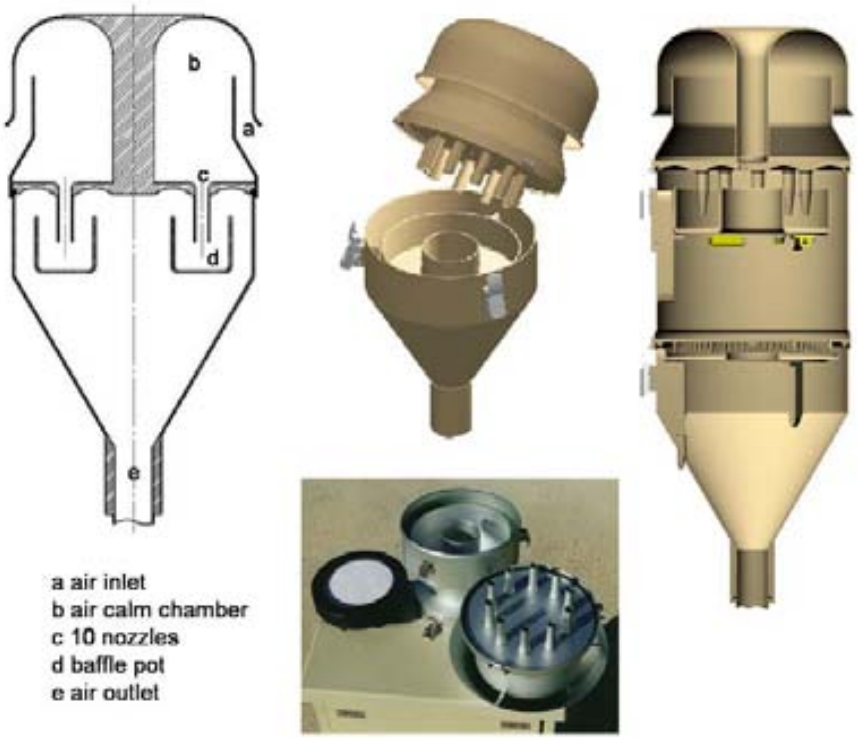

Figure 3.11. Inlet scheme (left), PM_{10} DIGITEL inlet (center top) and MCV inlet (center bottom), PM_1 DIGITEL 2-stage impactor inlet (right).

In all cases samples with high volume samplers were collected using 15 cm diameter quartz micro-fibre filters (QF20 Schleicher and Schuell) previously conditioned following the procedure described later.

3.2.1.3. Real time monitoring of levels of particle number concentration (N)

The levels of sub-micron particle number concentration in the range 3nm-3μm were monitored from June 2005 from June 2007 at the BCN-CSIC urban background site by means of a water-based condensation particle counter (TSI WCPC 3785, Figure 3.12). Before this study, particle concentration in the range 13-800 nm was monitored at the same site from November 2003 to December 2004 by means of a butanol-based condensation particle counter (TSI CPC 3022A) connected to a Differential Mobility Analyzer (DMA TSI 3071 system, Pey, 2007) in order to monitor number size distributions. Since 2005, a water-based CPC was used at BCN-CSIC, instead of a butanol-based CPC, because flooding of the butanol was a problem owing to the high relative humidity at the monitoring site. Several studies have compared the performance of butanol and water-based CPCs for different types of aerosol (Morawska et al., 2009) obtaining comparable results, with observed differences due to

the chemical composition of the aerosols, size detection limits of the instruments and response under different particle concentrations due to calibration differences between instruments. Regarding measurements of total particle number concentration by means of a DMA-CPC system or only a CPC, the main differences are due to the size detection limits of the system (Morawska et al., 2008b and 2009). The CPC may extend to lower sizes than the window set by the DMA. Thus, differences may be larger for environments where particle number concentration in the nucleation mode is important.

The WCPC is designed to measure the concentration of airborne ultrafine particles and counts the number of particles to provide a value displayed as particle number by cubic centimetre of sampled air (expressed as cm^{-3}). The principle of operation is the enlargement of small particles using a condensation technique to a size that is large enough to be detected optically. The WCPC uses a laser and an optical detector to detect particles and ultrafine particles are not easily detected because their diameters are equal or smaller than light wavelength. For this reason, a saturation system is used. The aerosol enters the sample inlet and immediately reaches a region supersaturated with water vapour. The aerosol flow is saturated with water vapour and temperature equilibrated in a cooled saturator. Then the flow passes through the growth section: a condenser with heated walls which contain water to produce elevated vapour pressure. The particles act as condensation nuclei where water condenses. The enlarged particles can be then detected by the optical detector. Each particle droplet produces a light pulse and these are counted. The particle number concentration is calculated by knowing the aerosol flow rate (1 litre per minute). For the instrument TSI WCPC 3785, the minimum detectable particle diameter is 3 nm (for wettable aerosols) and the maximum particle diameter that is detected is 3 microns, though a cyclone was used to cut particle size at 1 micron. Continuous live-time corrected single particle counting is possible up to $2 \cdot 10^4$ cm^{-3}. A photometric mode extends the concentration range to 10^7 particles cm^{-3} although this is considered as a limitation as this concentration is calculated and it is not equivalent to the single particle counting. Figure 3.12 shows the scheme of operation of a WCPC.

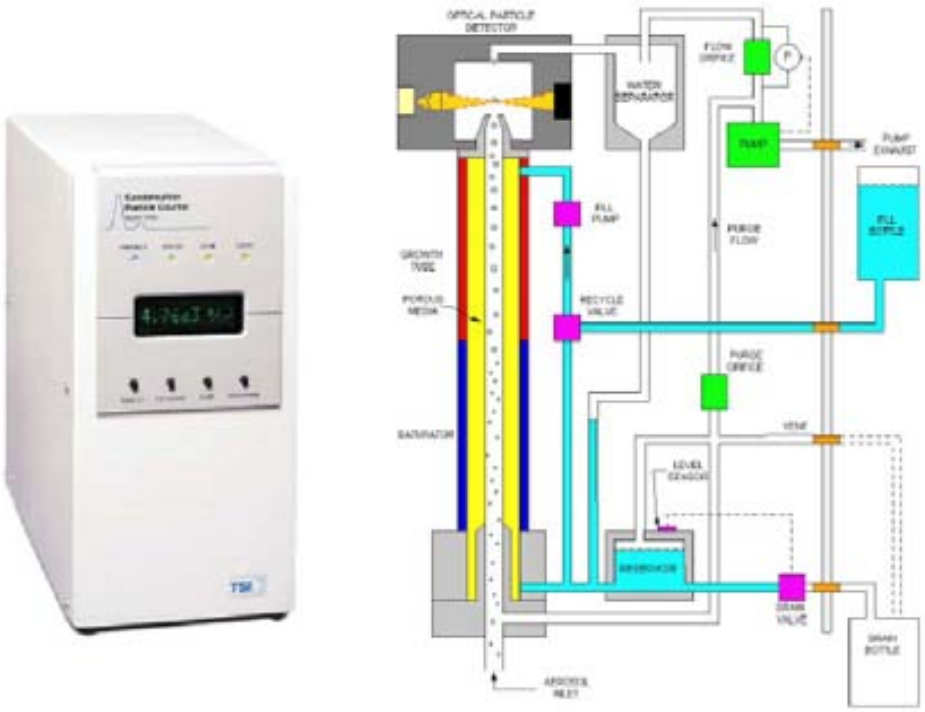

Figure 3.12. Water-based condensation particle counter and flow diagram (TSI WCPC 3785 operation and service manual).

3.2.1.4. Real time monitoring of levels of black carbon (BC)

Levels of black carbon (BC) were continuously monitored (as aerosol absorption coefficient) on a 5-min basis from July 2007 at the BCN-CSIC urban site by means of a Multi-Angle Absorption Photometer (MAAP). The BC MAAP monitor used (CARUSSO, Thermo ESM Andersen Instruments, Figure 3.13) monitors the absorption coefficient expressed as mass concentration of elemental carbon (EC, μg or ng m^{-3}) in ambient air.

The Multi-Angle Absorption Photometer (MAAP) was developed at the Institute of Atmospheric Physics of the German Aerospace Centre (DLR). The method is based, on the collection of airborne particles on a filter and the optical analysis of the particles deposited. Contrary to the previous methods for measuring aerosol absorption coefficients (by means of transmission analysis of the filter loaded with particles), the MAAP uses a complex inversion algorithm that is based on a radiation transport analysis of the aerosol layer and filter matrix system and thus incorporates the scattering effect of the aerosol into the analysis. Thus, the MAAP measures the aerosol absorption coefficients directly, while considerable corrections are necessary with transmission measurements. The principle of determination is based on a combination

of the reflectometer method at certain defined scattering angles and the transmission. With this method, also multiple scattering is taken into consideration.

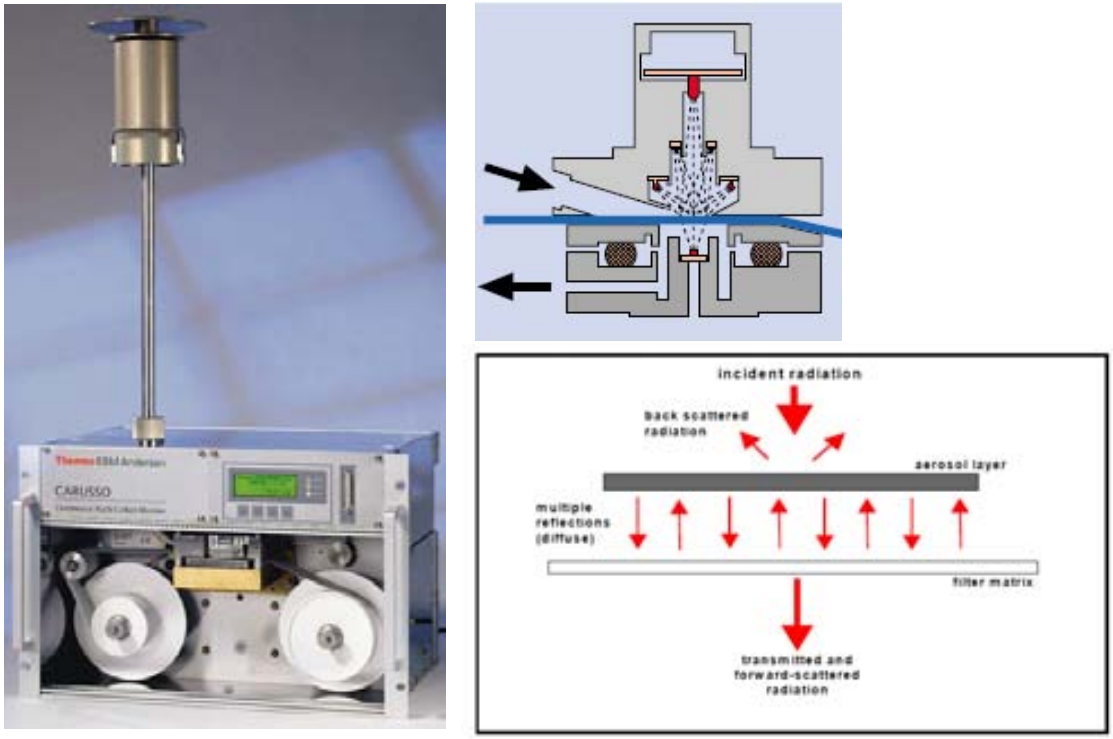

Figure 3.13. MAAP BC monitor and operation scheme (Thermo ESM Andersen Instruments).

3.2.2. Chemical analysis and speciation

3.2.2.1. Filter preparation

As already mentioned, filter sampling was carried out by means of high volume samplers using 150 mm diameter Quartz micro fibre filters (Schleicher and Schuell, QF20) at all monitoring sites. The filters were pre-heated at 200ºC during four hours to eliminate the volatile compounds. Then, the filters were conditioned under controlled temperature (20º) and humidity (25%) during 24 hours. After that, the blank filters were weighted during three consecutive days. Then, they were preserved individually in aluminium foil until they were used for sampling. From every set of fifteen filters, three of them were retained to be used as blanks for the subsequent chemical analysis.

After sampling, the filters were conditioned at the above controlled temperature and humidity again and stabilized during 24 hours. These were weighted during at least two consecutive days to get a definitive weight. From the differential mass and the volume

of air sampled it was possible to determine the mean concentration during the sampling period.

3.2.2.2. Filter treatment

Once the gravimetric determination is performed, filters can be treated for analysis. ½ of each filter was acid digested (2.5 ml HNO_3 and 5 ml HF) into a PFA bomb at 90ºC during at least 8 hours. After cooling, the PFA bombs were opened and 2.5 ml $HClO_4$ were added. Subsequently, acids were completely evaporated by drying the open PFA bomb on a heating plate at 230ºC. The dry residue was dissolved with 2.5 ml HNO_3, adding bi-distilled water (MilliQ) to make a volume of 50 ml in a graduated flask, obtaining a solution of 5% HNO_3. This solution was analyzed for the determination of major and trace elements by ICP-AES and ICP-MS.

In every acid digestion batch, blank filters were treated by the same procedure. The blank filter analysis is useful to control the levels of the elements in the blank filters and to subtract the concentrations from those obtained for the filters sampled. In addition, detection limits are calculated from the standard deviations from blank filter analyses together with the analytical uncertainties.

10 mg of a certified reference material (NBS1633b, fly ash) was also digested in each set prior loading of this material on ½ blank filters. The reference material analysis assures the quality of the results permitting the identification of possible analytical or calibration errors.

Another ¼ of each filter was water leached for the determination of levels of soluble ions by ion chromatography (sulphate, nitrate and chloride) and FIA colorimetry (ammonium). The filter portion is cut in pieces and introduced into a PVC flask with 30 ml of bi-distilled water. After closing, the PVC flask it was placed in an ultrasound bath during ten minutes and then heated at 60ºC during 6 hours. After this, the resulting solution is filtrated and then it is ready to be analyzed.

The remaining ¼ of each filter was used for the determination of levels of total carbon and/or organic and elemental carbon (OC and EC).

3.2.2.3. Analytical techniques

Inductively Coupled Plasma Atomic Emission Spectrometry (ICP-AES) was used for the determination of major elements (Al, Fe, K, Ca, Na, Mg, S, P, Ba, Cr, Cu, Mn, Ni, Sr, Pb, Ti, V, Zn) in the acidic digestions of filter samples. These analyses were carried out with IRIS Advantage TJA Solutions THERMO equipment at the Laboratory of ICP MS/AES in the Institute of Environmental Assessment and Water Studies (IDAEA-CSIC).

Inductively Coupled Plasma Mass Spectrometry (ICP-MS) was used for the determination of trace elements (Li, Be, B, Sc, Ti, V, Cr, Mn, Co, Ni, Cu, Zn, Ga, Ge, As, Se, Rb, Sr, Y, Zr, Nb, Mo, Cd, Sn, Sb, Cs, Ba, La, Ce, Pr, Nd, Sm, Eu, Gd, Tb, Dy, Ho, Er, Tm, Yb, Lu, Hf, Ta, W, Tl, Pb, Bi, Th and U) in the acidic digestions of filter samples. These analyses were carried out with X Series II THERMO equipment at the Laboratory of ICP MS/AES in the Institute of Environmental Assessment and Water Studies (IDAEA-CSIC).

Ion Chromatography (IC) was used for the determination of levels of water soluble ions (Cl^-, NO_3^- and SO_4^{2-}) in the leachates of the filter samples. These analyses were performed partly at the Institute of Environmental Assessment and Water Studies (IDAEA-CSIC) and partly at the University of Granada by means of Ionic Chromatography HPLC (High Pressure Liquid Chromatography) using a WATERS IC-pakTM anion column and WATERS 432 conductivity detector.

Ammonia Selective Electrode (SE) was used for the determination of levels of NH_4^+ in the leachates of the filter samples. These analyses were carried out at the Institute of Environmental Assessment and Water Studies (IDAEA-CSIC) by using a selective Electrode MODEL 710 A+, THERMO Orion.

Carbon Elemental Analyzer was used for the determination of levels of total carbon directly on sections of filter samples. These analyses were carried out at the *Centro de Investigaciones Energéticas, Medioambientales y Tecnológicas* (CIEMAT) by means of a LECO carbon analyzer.

Organic Carbon and Elemental Carbon Analyzer was used for the analysis of levels of OC and EC directly on sections of the filter samples by the TOT technique (Birch and Cary, 1996) using a Sunset Laboratory OCEC Analyzer at the Institute of Environmental Assessment and Water Studies (IDAEA-CSIC). This instrument is based in the NIOSH 5040 method (Birch and Cary, 1996) for the measurement of organic and elemental carbon on quartz filters. The OCEC Analyzer analyzes aerosol particles collected on quartz-fibre filters for both organic carbon and elemental carbon (OC and EC). This instrument employs a flame ionization detector (FID) with high sensitivity. Samples are heated over four temperature ramps to remove all organic

carbon and convert it to carbon dioxide. This carbon dioxide is then reduced to methane which is detected using the FID. Known volumes of methane are then used to calibrate to a known quantity of carbon. From the response from the FID detector and the laser transmission data, the quantity of organic and elemental carbon in a sample can be determined. Detection limits are of the order of 0.2 µg per cm^2 of filter (0.04 µg m^{-3}) for OC and 0.1 µg per cm^2 (0.02 µg m^{-3}) for EC.

3.2.2.4. Indirect determinations

With the analytical techniques described above it was possible to determine directly up to 63 components of PM in each sample. Furthermore, the levels of 4 additional components were indirectly determined using empirically obtained factors such as: $SiO_2=3*Al_2O_3$ and $CO_3^{2-}=1.5*Ca$ (Dulac et al., 1992; Molinaroni et al., 1993; Querol et al., 2001b). The non-mineral carbonaceous compounds were expressed as the sum of organic matter and elemental carbon (OM+EC). The concentration of OM+EC was calculated from the levels of OC and EC or from the total carbon content when OC and EC levels were not available. To calculate the organic matter component (OM), OC is multiplied by a factor with the intention of adding the heteroatoms of the organic matter (H, N, O) not analyzed with this method. This factor was estimated by various authors to be between 1.2 and 2.1, being higher for remote sites and lower for urban sites (Putaud et al., 2000; Turpin et al. 2001; Russell, 2003). We applied here a factor of 1.6 for Barcelona (urban background) and of 2.1 for Montseny and Montsec (regional and continental backgrounds). To calculate OM+EC from the total carbon content, first the mineral carbon from carbonates is subtracted from the total carbon ($OC+EC=Ctotal-0.2*CO_3^{2-}$). The ratio between EC and the total carbon (TC) was estimated from the OCEC analysis performed to be 0.1 for Montseny and Montsec and 0.3 for Barcelona. With these ratios and factors the next calculations were made:

Barcelona: $OM+EC=EC+OC*1.6$

$OM+EC= 0.3*TC+0.7*TC*1.6$

Montseny and Montsec: $OM+EC=EC+OC*2.1$

$OM+EC= 0.1*TC+0.9*TC*2.1$

From 75 to 85% of the PM_{10}, $PM_{2.5}$ and PM_1 mass was accounted from the addition of the above direct and indirect determinations. The remaining undetermined mass is

attributed to formation, crystallization and moisture water that was not removed during the sample conditioning.

After the above analysis the chemical components of PM were grouped as:
(a) crustal or mineral matter (sum of elements typically found in rock-forming minerals, including Al_2O_3, SiO_2, CO_3^{2-}, Ca, Fe, K, Mg, Mn, Ti and P)
(b) Sea spray component (sum of Cl^- and Na^+)
(c) Carbonaceous compounds (organic matter and elemental carbon, OM+EC)
(d) Secondary inorganic aerosols, SIA (sum of SO_4^{2-}, NO_3^- and NH_4^+ concentrations).

In addition, the contribution of primary (POA) and secondary (SOA) organic aerosols to the total OM concentration in Barcelona were estimated by the EC trace method (Salma et al., 2004), modified according to criteria applied by Docherty et al. (2008). This method is based in the evaluation of primary organic carbon (POC) using EC as a tracer. The ratios OC/EC observed vary usually from lower values, attributed to POC and EC emissions recorded near emission sources, to higher values, attributed to secondary organic carbon (SOC) formed in the atmosphere by photochemical oxidation reactions. This POC/EC ratio is generally calculated from the minimum ratio obtained on the OC vs. EC plot. From this primary ratio (POC/EC)p, primary and secondary organic carbon fractions were calculated using the following equations:

Primary organic carbon: POC= (POC/EC)p*EC
Secondary organic carbon: SOC=OC-POC

In addition, experimental results (Mohr et al., 2009) indicate that in order to account for the presence of oxygen, nitrogen or hydrogen in the organic compounds the carbonaceous fractions calculated may be multiplied by the following factors:
Primary organic aerosols: POA =POC*1.2
Secondary organic aerosols: SOA=SOC*1.9

3.2.2.5. Calculation of uncertainties

Calculation of uncertainties associated to experimental results was performed for each species or compound analyzed in each sample. In the present study individual uncertainties are calculated from detection limits following the method described by Polissar et al. (1998) according to the equations as follows.

$$\sigma(x_{ij} < DL_j) = X_{ij} + \frac{1}{3}DL_j$$

$$\sigma(DL < x_{ij} < 3DL_j) = 0.2X_{ij} + \frac{1}{3}DL_j$$

$$\sigma(x_{ij} > 3DL_j) = 0.1X_{ij} + \frac{1}{3}DL_j$$

where the X_{ij} are concentration values of a species or compound for each sample and DL_j are detection limits associated to the measurement.

There are several sources of error contributing to the overall uncertainty of the ambient measurements but the one associated with the analytical procedure is likely to be the most important source of uncertainty. As explained above, diverse analytical and instrumental techniques have been used for the determination of all species concentrations (ICP-AES, ICP-MS, IC, ammonium selective electrode, carbon elemental and thermo-optical analyzers). Moreover, the subtraction of blank filters also causes an additional source of uncertainty.

To account for these sources of uncertainty, detection limits were calculated from the analytical error (α_j) and the standard deviation of the blank filters that were analyzed together with the samples ($\alpha_{BLK,j}$) from the following equation obtained from propagation laws (Currie et al., 1995):

$$DL_j = \sqrt{\alpha_j^2 + \alpha_{BLK,j}^2}$$

Mean values and uncertainties for major and trace elements measured at Barcelona, Montseny and Montsec are presented in the results section for each monitoring site, in the source apportionment chapter, when the PMF method is applied.

3.3. Source apportionment techniques

Receptor modelling techniques are used to identify and quantify the contributions from emission sources to the levels of major and trace components of ambient particulate matter. In receptor models PM data is described as a function of source profiles and source contributions as in the equation $X=GF+E$, where X is the concentration matrix (measured ambient concentrations), G is the source contribution matrix, F is the source profile matrix (elemental abundances in source emissions) and E the portion of the

measured elemental concentration that cannot be fit by the model (Hopke et al., 2003 and 2006). Many receptor models are available; the main differences being the knowledge about pollution sources required (input requirements: speciation data, uncertainty data and/or emission profiles, Figure 3.14), the model computation requirements and the results obtained (Bruinen de Bruin et al., 2006; Schauer et al., 2006). Three of the most widespread receptor models are principal component analysis (PCA, Thurston and Spengler, 1985), positive matrix factorization (PMF, Paatero and Tapper, 1994) or chemical mass balance (CMB, US-EPA, 1987). The main differences are that CMB requires detailed quantitative knowledge of the emission source profiles, whereas for PCA and PMF qualitative knowledge of the sources is sufficient. PCA requires only speciation data while PMF requires in addition uncertainty data. Other models include UNMIX, multi-linear engine (ME, Paatero, 1999), Lenschow approach (Lenschow et al., 2001) back-trajectory analysis, constrained physical receptor model (COPREM, Wåhlin, 2003) and isotopic mass balance using C-14 (Szidat et al., 2004).

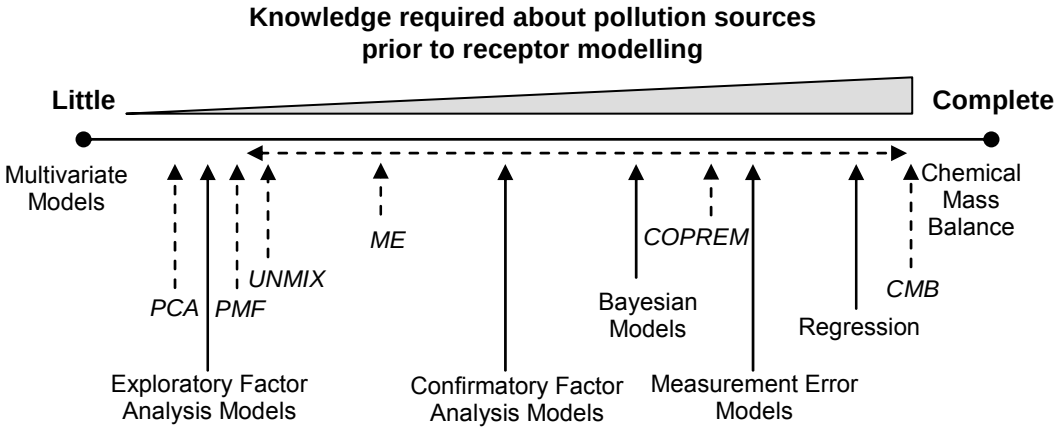

Figure 3.14. Knowledge required about pollution sources prior to receptor modelling. Modified from Schauer et al. (2006).

3.3.1. Identification of source emission profiles

To perform a source contribution study when the emission source profiles are unknown, the different compounds and elements analyzed are grouped in categories, and different combinations of them are used as tracers or markers to identify aerosol sources:

-Mineral matter: characterized by elements and compounds associated to the Earth's crust as CO_3^{2-}, SiO_2, Al_2O_3, Ca, K, Mg, Fe, Ti, P, Ba and Sr as main tracers (Querol et al., 2004a and b) and usually identified as local dust resuspension by wind or road

traffic, industrial, demolition and construction anthropogenic emissions or African dust outbreaks.

-Sea spray: characterized by high levels of Cl^-, Na and SO_4^{2-} (Querol et al., 2004a and b).

-Non-mineral carbonaceous compounds: EC and OC (or OM), usually identified as road traffic emissions and other combustion sources (Schauer et al., 2006).

-Secondary inorganic aerosols (SIA): high levels of NO_3^-, NH_4^+ or SO_4^{2-}, usually identified as regional background or local anthropogenic pollution episodes but also as road traffic and other combustion or industrial emissions.

-Trace elements (Pb, Fe, Zn, Cu, Cr, Ni, V, Mn, Sb, Ba, etc.): different combinations of trace elements with other compounds can be tracers of different source profiles as road traffic (exhaust or non-exhaust emissions), combustion sources, industrial emissions, etc.

3.3.2. Principal component analysis and multilinear regression analysis (PCA-MLRA)

In this technique correlations among the measured elemental concentrations at the receptor are studied by factor analysis (FA, Pio et al., 1989; Paatero and Tapper, 1993) and the principal components explaining the variance of the data are interpreted as possible sources. From an array with major and trace element concentrations (gaseous pollutants, meteorological data or particle number levels may also be included) a number of principal factors are obtained. These factors are the result of linear combinations of all the parameters considered. Initially every factor corresponds to a particulate matter source, presenting the components that characterize a source with coefficients (factor loadings) higher than the others (next to 1). The concentrations of the different components introduced in the analysis must be then normalized.

The maximum number of factors will be the same than the number of components but not all the factors must have a physical meaning. The number of factors is determined by the variance of the original components (being normalized they will all have variance 1). Then, the first criteria established to determine the number of factors is that they have variance (eigenvalue) higher than 1. Once this restriction made it is necessary to study the physical significance of each one from the chemical profile. For this purpose it is necessary to know the possible emission profiles that determine the existence of these factors. The accumulated variance of the factors obtained must be higher than 75% to consider the analysis representative. In this way, we obtain each one of the

factors, the components that characterize them, the variance value and the mean concentration that explains each factor.

From these factors/sources it is possible to estimate quantitatively the daily contribution of each factor to the total daily mass. The methodology used was described by Thurston and Spengler (1985). The daily values of the scores obtained from the daily concentrations of the elements are used. These factors are proportional to the daily mass contribution of each source. Then, since the concentration values are normalized, the scores are normalized too and they refer to mean mass values. This means that the score for a zero mass must be calculated. The score of this sample will be subtracted from the daily scores, obtaining the absolute scores.

With the absolute scores and the concentration of PM corresponding to each one it is possible to do a multilinear regression. We obtain the coefficients that allow transforming the absolute daily scores in mass contribution for each one of the factors. In the same way that daily contributions of the sources to the PM levels are estimated it is possible to establish the contribution of each source to each element by a multilinear regression, taking in this case the daily concentration of the element as the dependent variable and the daily mass contribution of each source as the independent variable.

3.3.3. Positive matrix factorization (PMF)

As showed by Paatero and Tapper (1993), the main limit of PCA technique, which provides the simplest approach to Factor Analysis (FA), is that it can not provide a unique solution (problem usually referred as rotational ambiguity in FA). Moreover, negative source contributions and negative specie abundances in the retrieved factors are allowed in PCA this leading to sources which are not always physically explainable. In order to minimize the rotational ambiguity in FA analysis and to solve the problem of negative loadings, the advanced PMF algorithm was developed as a new approach to FA (Paatero and Tapper, 1994; Paatero and Hopke, 2003). PMF provides estimates of the chemical composition of the sources contributing to the ambient PM and the PM mass concentration attributed to each factor and it was successfully used since its development for a number of source apportionment analyses (Lee et al., 1999; Xie et al., 1999; Zhao and Hopke, 2004; Kim and Hopke, 2008; Hopke et al., 2003; Paatero et al., 2003 among others). Even if the chemical profile of the contributing sources is not required as input, the receptor models based on FA require a priori knowledge of the main tracer elements of the possible emission sources. This information is used to attribute the retrieved factors to specific emission sources.

This model requires two types of data matrix, one with the concentrations of the different variables (major and trace elements, gaseous pollutants, meteorological variables, particle number concentrations, etc.) and another one with the errors associated to each of the variables.

In this study, the model PMF2 (Bilinear Positive Matrix Factorization, Paatero, 1999) was applied. It is based in the PMF model, and the equation applied was:

$$x_{ij} = \sum_{k=1}^{p} g_{ik} f_{kj} + e_{ij} \quad (1)$$

x_{ij}: mean concentration of j species on sample i

f_{kj}: mass fraction of j species on k source (source profile)

g_{ik}: contribution of k source to sample i

e_{ij}: residual, fraction that cannot be explained by model

In order to reduce the degree of rotational freedom, PMF constraints both g_{ih} and f_{hj} in equation (1) to be positive, as negative source contributions and compositions have no physical meaning. Moreover, the PMF model estimates g_{ih} and f_{hj} in order to minimize a loss function Q, defined as:

$$Q = \sum_{i} \sum_{j} \left[\frac{e_{ij}}{h_{ij} u_{ij}} \right]^2 \quad (2)$$

where u_{ij} are the uncertainties estimated for x_{ij} and the residual matrix e_{ij} is defined as:

$$e_{ij} = x_{ij} - \sum_{h=1}^{p} g_{ih} f_{hj} \quad (3)$$

The multiplicative function h_{ij} in equation (2) is added in order to account for the outliers, i.e. positive extreme values leading to frequency distribution of the data with a long right tile which can strongly influence the solution and it is defined as $h_{ij}^2 = 1$ if $\left| e_{ij} / u_{ij} \right| \leq \alpha$. and $h_{ij}^2 = \left| e_{ij} / u_{ij} \right| / \alpha$, otherwise, where α is the outlier distance (in this study α was set equal to 4).

According to Viana et al. (2008a) the number of elements to use within the model and their uncertainties were determined based on the method detection limit (MDL) by looking at their signal-to-noise (S/N) ratio as well as at the number of times these were found below the detection limit.

The S/N ratios for each j_{th} species were calculated as follows:

$$\left(\frac{S}{N}\right)_j = \frac{\sum_i x_{ij(x_{ij}>DL_j)}}{DL_j N_{DL_j}} \quad (4)$$

where the X_{ij} concentration values are those higher than the corresponding detection limit (DL_j) and N_{DLj} is the number of concentration values higher than the DL_j for each j_{th} specie. Species for the PMF analysis were selected in function of the S/N ratio (defined as *strong* when higher than 2, following the US EPA procedure, Eberly, 2005), N_{DLj}, and percentage of data below detection limit (BDL). Data BDL were replaced with the DL/2 value (Kim et al., 2004).

The number of factors providing the best solution can be determined by looking at the values of the observed Q when the number of factors is changed (for example from 3 to 10) and by evaluating the physical meaningful of the retrieved factors. This procedure is applied considering that the observed Q value can not be less than the theoretical one which should be approximately equal to the dimension (i × j) of the input data matrix.

The model PMF2 includes rotational ambiguity (Paatero et al., 2002) controlled by means of the FPEAK parameter for which the optimal value is generally within the range in which the Q values are relatively constant around their minimum value (Hopke, 2000). Moreover, the frequency distribution of the residuals (Hopke, 2000) and the G-space plotting (Paatero et al., 2005) were also used to identify the optimal solution.

3.4. Trend analysis: Mann-Kendall test

Analysis of temporal trends for PM and its chemical components are performed by means of the MAKESENS template application (Mann-Kendall test for trend and Sen's slope estimates, Salmi et al., 2002), consisting in the nonparametric Mann-Kendall test for the calculation of the trend and the nonparametric Sen's method for the magnitude of the trend. This method was originally developed for the detection and estimation of trends in the time series of annual values of parameters such as atmospheric concentrations and precipitation.

MAKESENS performs two types of statistical analysis. First the presence of a monotonic increasing or decreasing trend is tested with the nonparametric Mann-Kendall test and secondly the slope of a linear trend is estimated with the nonparametric Sen's method (Gilbert, 1987). In the Mann-Kendall test missing values are allowed and the data need not conform to any particular distribution. The Sen's method is not greatly affected by gross data errors or outliers, and also it can be computed when data are missing. However, examination of the time series is very important before performing the calculations. The Mann-Kendall test is only applicable to the detection of a monotonic trend of a time series with no seasonal or other cycle, and therefore the method is usually applied to mean annual concentrations. However, it can be applied on data with marked seasonal cycles by comparing the same month throughout the different years of analysis. In the Sen's method it is assumed that the trend is linear and the residuals are from the same distribution with zero mean. The time series should fulfil these presumptions in order to produce correct statistical results with MAKESENS.

3.5. Interpretation of the origin of air masses: meteorological maps, aerosol models and satellite images

Additional tools were used for the interpretation of PM levels and for the subsequent analysis of the results from chemical characterization, such as meteorological maps, aerosol models and satellite images. All these tools are all freely available on the Internet.

3.5.1. Back-trajectory analysis: Hysplit model, interpretation of the origin of air masses

Air mass back-trajectory analysis was performed at 750, 1500 and 2500 m.a.s.l. using the Hysplit model (Hybrid Single Particle Lagrangian Integrated Trajectory Model; Draxler and Rolph, 2003; http://www.arl.noaa.gov/HYSPLIT.php). From the back-trajectories (calculated for 120 hours) it is possible to establish approximately the origin of air masses that reach a determined area when these are transported from a long distance. For the study area considered, the next origins are distinguished (Figure 3.15): Northern Atlantic (NA), North-western Atlantic (NWA), Western Atlantic (WA), South-Western Atlantic (SWA), North African (NAF), Mediterranean (MED), Centre Europe (EU) and Regional (REG) or Winter Anticyclonic episodes (WAE).

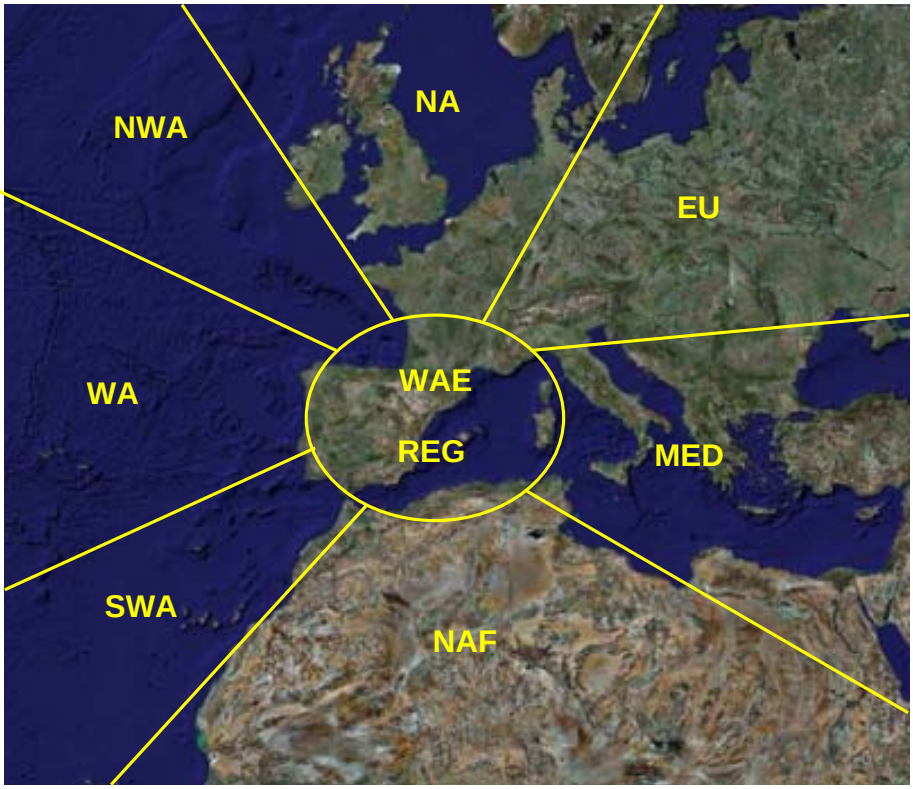

Figure 3.15. Map of air mass origin for the area of the study.

3.5.2. Boundary layer depth

Boundary layer depths were calculated for the different areas using the meteorological model of NOAA Air Resources Laboratory (ARL, www.arl.noaa.gov/readyamet.html) by introducing the geographical coordinates of the site. In the menu Stability time series, a meteorological data file (GDAS or FNL) must be selected. Then, the starting date and time must be introduced and the duration of the stability plot chosen. Data can be downloaded as a text file.

3.5.3. Aerosol concentration maps

The **NAAPS** model produces aerosol maps from the Marine Meteorology Division of the Naval Research Laboratory (NRL, http://www.nrlmry.navy.mil/aerosol). These provide information on the aerosol optical depth and the surface concentration of mineral dust from desert areas, sulphate particles and carbonaceous aerosols derived from biomass burning (Figure 3.16). There are four daily maps (0, 6, 12 and 18h) with predictions up to 96 hours.

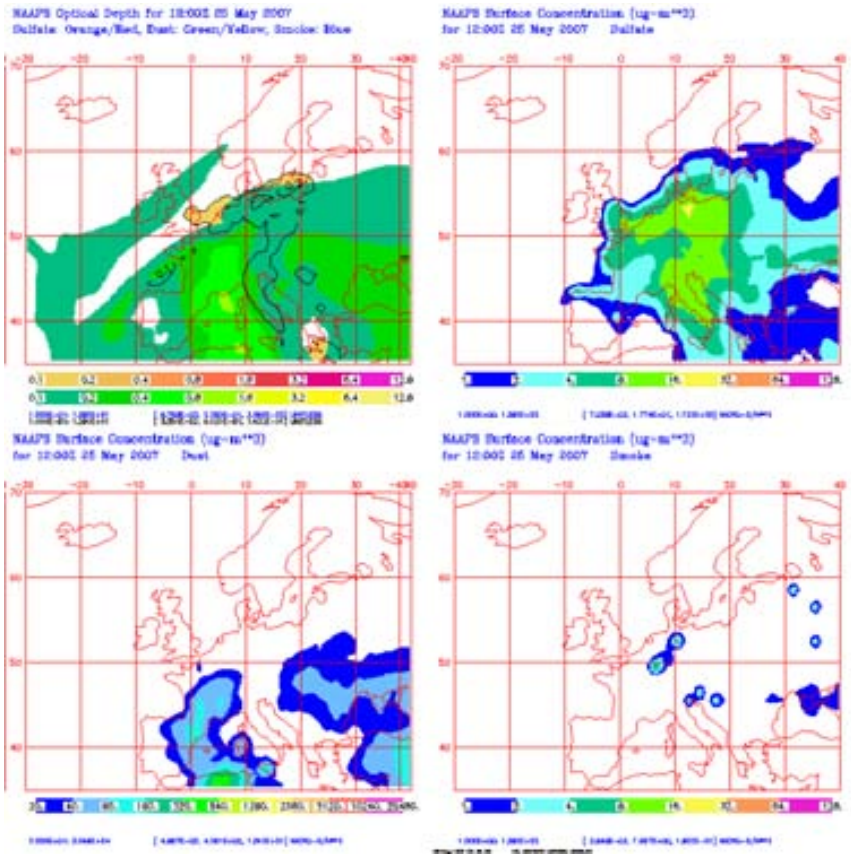

Figure 3.16. NAAPS aerosol maps for the day 26/05/2007.

SKIRON simulations produce also aerosol surface concentration maps (http://forecast.uoa.gr/dustindx.php, Kallos et al., 1997). These simulations provide information on total column loads and surface level dust (Figure 3.17) and in addition dry and wet dust deposition fluxes at a surface level. With these maps it is possible to identify emission source areas of mineral dust.

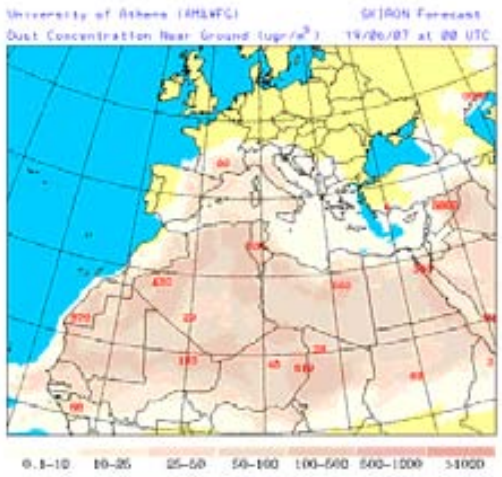

Figure 3.17. SKIRON surface dust concentration map for the day 19/06/2007.

BSC-DREAM model (http://www.bsc.es/projects/earthscience/DREAM/, Nickovic et al., 2001) produce also surface and column dust concentration maps, as well as dry and wet deposition fluxes. The forecasting maps are made of a meteorological map with surface pressure and the rainfall and an aerosol map showing areas affected by dust and expected concentrations at a surface level (Figure 3.18). With these maps it is also possible to identify emission source areas of mineral dust.

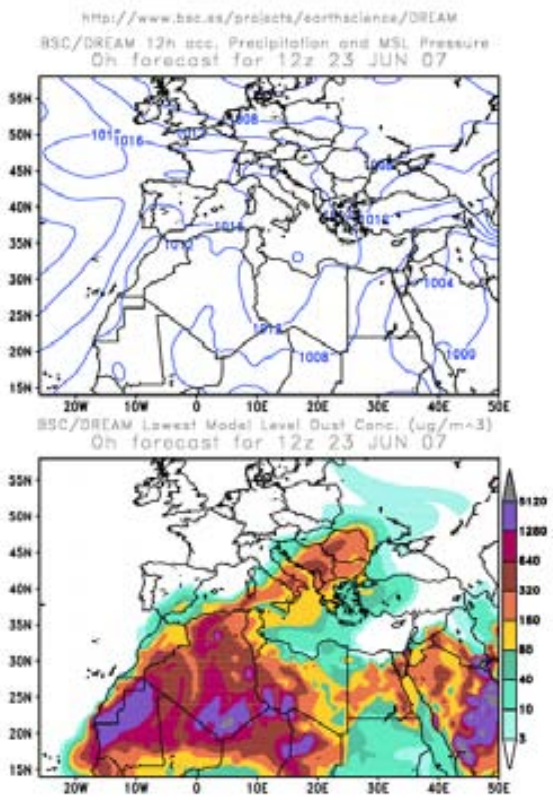

Figure 3.18. BSC-DREAM surface dust concentration maps for the day 23/06/07.

3.5.4. Satellite imagery

NASA SeaWIFS project offers free satellite images (SeaWIFS Project Image Archive, http://seawifs.gsfc.nasa.gov/SEA-WIFS.html, McClain et al., 1998) that may be used for the identification of dust episodes. These images (Figure 3.19) are very useful to visualize the dust transport over the sea but they have a few limitations. The transport height of dust and the possible impact on surface are unknown, it is difficult to visualize the dust plume over the land and it can be superposed with clouds. Besides these limitations, this tool was very useful for the present study, allowing the validation of the models concerning the areas covered by dust plumes and the detection of forest fires.

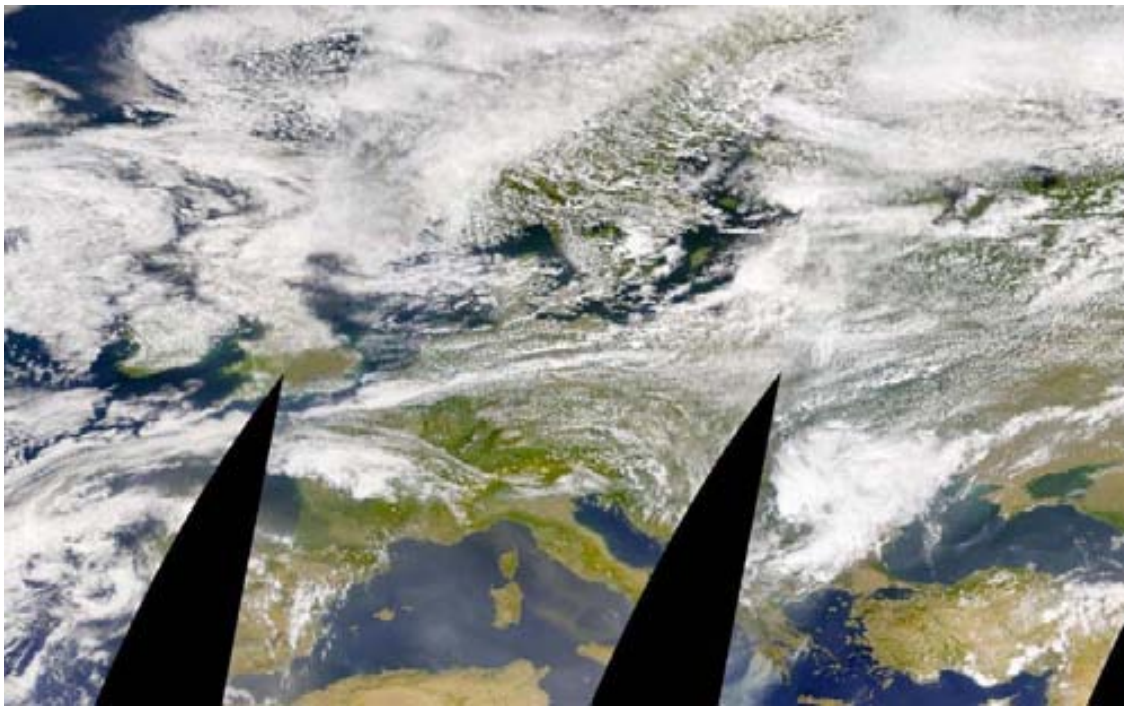

Figure 3.19. SeaWIFS Satellite image for Europe for the day 26/08/2007. A dust mass can be observed over the Mediterranean Sea and smoke from fires in Greece.

MODIS Rapide Response System satellite images

MODIS Rapid Response System satellite images (Earth and Aqua satellites, http://rapidfire.sdci.gsfc.nasa.gov.html) are used in a similar way that SEAWIFS maps to detect the transport of mineral dust from desert areas. They are also very useful to localize fires because they appear marked in red and the smoke plume is often noticeable (Figure 3.20). The same limitations commented for SEAWIFS apply to MODIS.

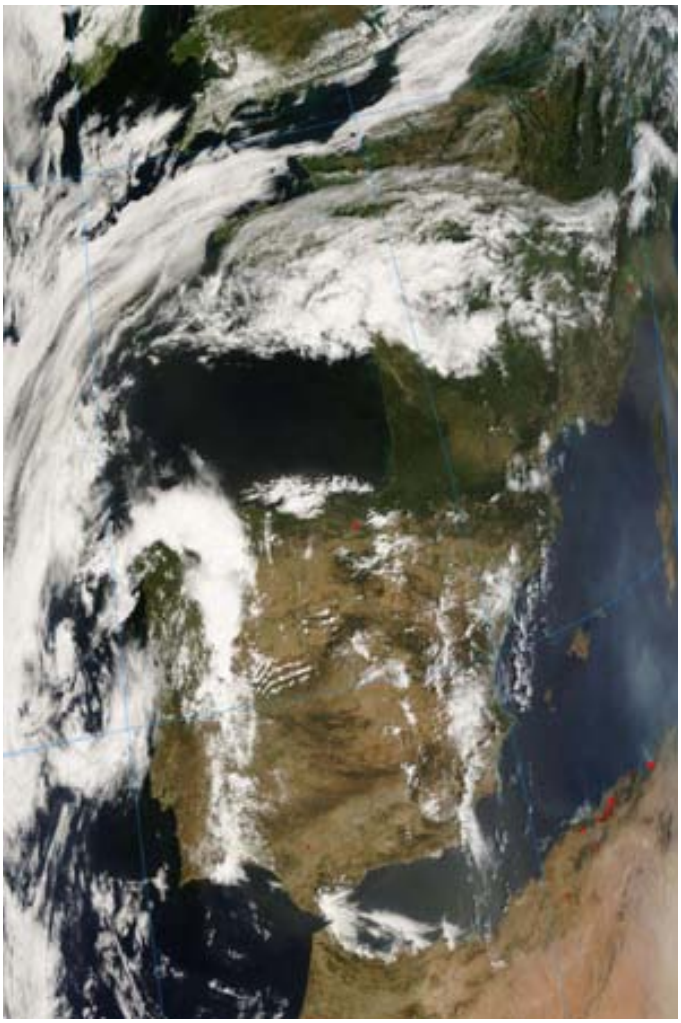

Figure 3.20. MODIS Earth satellite image over the Iberian Peninsula and North Africa for the day 26/08/2007. Dust over the Mediterranean Sea and smoke from fires on the African coast can be observed.

4. RESULTS

4.1. URBAN BACKGROUND

4. RESULTS

4.1. Barcelona urban background site

Urban background sites are located in urban areas, avoiding direct emission sources, where they reflect a general exposure of the population to atmospheric pollutants. BCN-CSIC urban background site is situated in the Barcelona university campus and reflects the Barcelona urban background and the traffic influence from the city.

In this chapter, PM_{10}, $PM_{2.5}$ and PM_1 levels and speciation, particle number and black carbon levels recorded at Barcelona are presented and discussed. Special attention is paid on the speciation and grain size partitioning of PM components between the different PM fractions. PM levels, PM speciation and particle number concentration time series will be discussed to see if seasonal or inter-annual trends are present. Daily evolution of all parameters will be studied together with levels of atmospheric gaseous pollutants and road traffic cycles. Finally, source apportionment techniques will be applied to the results to try to identify sources for the different PM components. The objective of all these analysis is the interpretation of the variability of levels, composition and source contribution to urban aerosols in Barcelona.

4.1.1. Meteorology, atmospheric dynamics and transport of pollutants

4.1.1.1. Meteorology and atmospheric dynamics in Barcelona

Barcelona is located on the North-Eastern coast of the Iberian Peninsula and the wind fields of this region are very influenced by the position of the Azores high and the main geographical setting (mountain ranges and valleys) surrounding the area. The analysis of air mass circulation at a local scale was performed by analyzing wind speed and direction data from meteorological stations near the monitoring sites. In BCN-CSIC the main wind directions are South-East and North-West (Data from the Department of Meteorology and Climatology, Facultat de Física, Universitat de Barcelona, Figure 4.1.1). North-western wind direction corresponds to Atlantic advections that are the most frequent situations in the Iberian Peninsula. Daily evolution of wind speed and direction (Figure 4.1.2) shows that during the winter months the main wind direction in North-West and during the warmer months coastal breezes develop and are characterized by a change of wind direction from South-East during the day (sea-land

breeze) to North-West during the night (drainage flows). The wind speed increases with the development of the sea-land breeze to reach maximum values at noon and decreases gradually until reaching the minimum values in the evening.

Maximum temperatures are registered during July-August and minimum temperatures during December-February with marked daily temperature cycles increasing during the day to decrease at night (Figure 4.1.2). Relative humidity shows the inverse cycle decreasing during the central hours of the day and increasing during the night. The maximum relative humidity values are registered during February-March and September-October, when the precipitation rates are usually higher. Solar radiation increases from winter to summer months and shows its maximum value at noon (Figure 4.1.2). The boundary layer depth increases during the central hours of the day as a result of a higher insolation, higher temperatures and the maximum wind speed, allowing the dispersion of pollutants. The seasonal evolution shows a lower development of the boundary layer during the summer months (Figure 4.1.2). This is an effect of sea-land breezes in coastal areas and it has already been described in Millán et al., 1997 and 2000; Pérez et al., 2004 and Sicard et al., 2006.

Figure 4.1.1. Relative frequencies of main wind directions at BCN-CSIC (Departament de Meteorología i Climatología, Facultat de Física, Universitat de Barcelona).

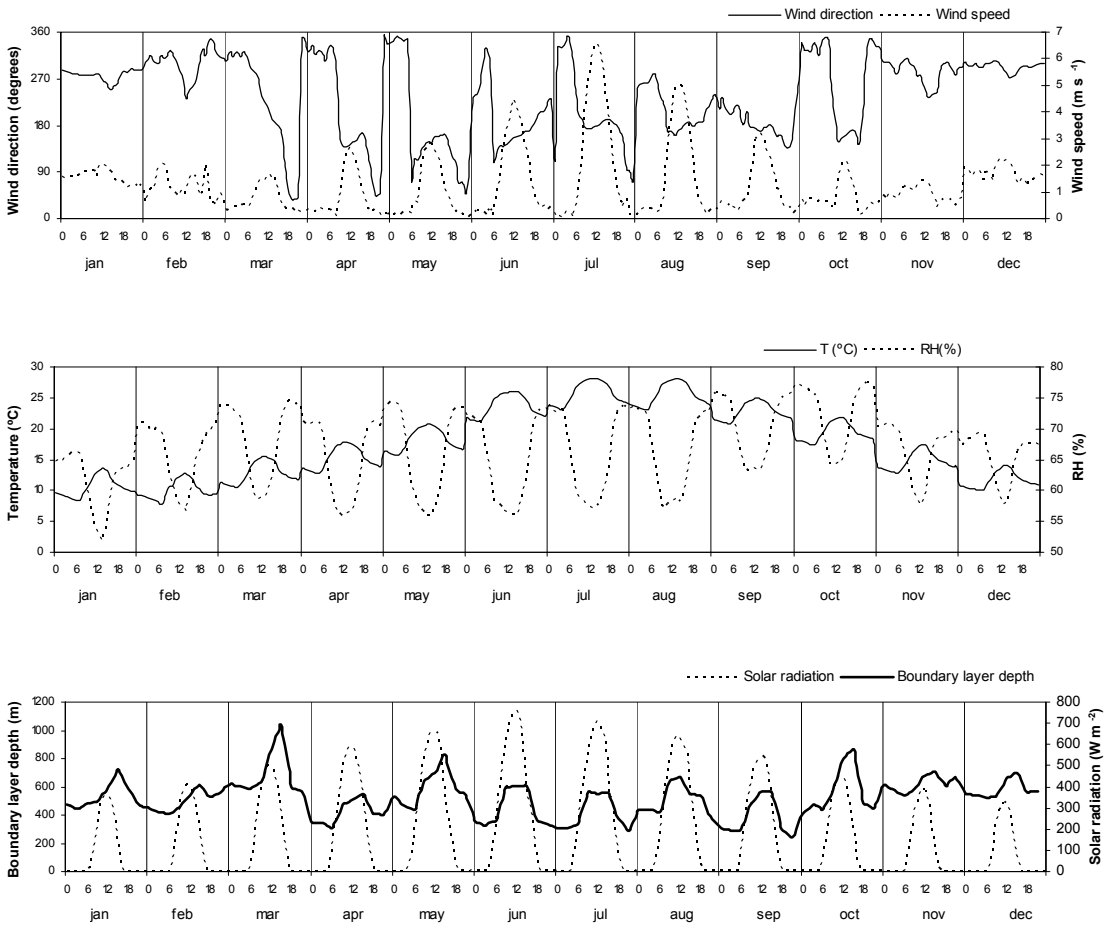

Figure 4.1.2. Daily evolution of wind speed and directions, temperatures and relative humidity recorded close to BCN-CSIC (Departament de Meteorología i Climatología, Facultat de Física, Universitat de Barcelona) and solar radiation recorded at Fabra observatory (Meteocat) for the years 2003-2007. Boundary layer depth calculated using the meteorological model of NOAA Air Resources Laboratory (ARL, www.arl.noaa.gov/readyamet.html) for BCN-CSIC coordinates.

4.1.1.2. Origin of air masses and atmospheric transport scenarios

Air mass origin is estimated by calculating mass back-trajectories, together with the study of satellite images and aerosol maps. Annual relative frequencies of the main origins of air masses arriving to the region of this study from 1999 to 2007 are shown in Figure 4.1.3. The predominant situation is the Atlantic Advection (ATL), especially from Western (WA) and North-western Atlantic (NWA), with annual frequencies between 30 and 55%. It is the result of the Azores anticyclone influence that favours Western and North-western winds over the Iberian Peninsula, lasting between 2 to 10 consecutive days. These observations are in accordance with the study carried out by Jorba et al. (2004) describing the synoptic transport patterns in Barcelona by cluster analysis of back-trajectories and describing almost a 50% of the analyzed situations to be Atlantic flows. North-African air mass transport (NAF) is also very frequent but it depends on

the year considered, being more important in 2001 (22%), 2003 (28%) and 2007 (18%), with a mean duration of 2-5 days. Air mass recirculations at a regional scale (REG) are also frequent, especially during the warmer months, being characterized by the recirculation an ageing of air masses over the WMB (Rodriguez et al., 2002a). These episodes account for annual frequencies from 3% (2000) to 18% (2005), lasting between 2-3 days to more than a week. During winter anticyclonic episodes (WAE), occurring mainly from November to March, atmospheric stability produces intense pollution episodes. These episodes were recurrent over the WMB with a frequency from 2% (2003) to 16% (2006) and a mean duration of 4-8 days. The frequency of episodes of air mass transport from Europe ranged between 3 % (2000) and 13% (2001), with a mean duration of 2-4 days. The transport of Mediterranean air masses was the least frequent scenario (2% in 2002, 2006 and 2007 to 5% in 2005) with a mean duration of 2-3 days, and it was usually associated to strong winds and rainfall.

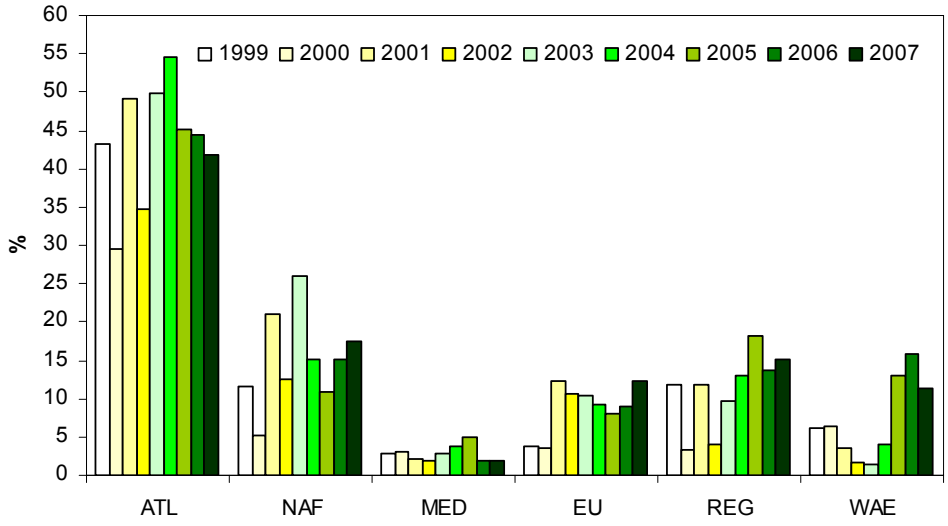

Figure 4.1.3. Annual relative frequencies for Atlantic advections (ATL), African dust outbreaks (NAF), Mediterranean (MED) and European (EU) air mass origins, regional recirculations (REG) and winter anticyclonic episodes (WAE) in the study region during the period 1999-2007.

4.1.2. PM levels at the urban background

PM levels have been continuously registered at Barcelona from 1999 (at four different urban sites) by means of optical particle counters, with levels being corrected with the factors obtained by comparison with the simultaneous gravimetric monitoring using high volume samplers. Daily PM levels recorded at this site are shown in Figure 4.1.4. Days with African dust influence are marked.

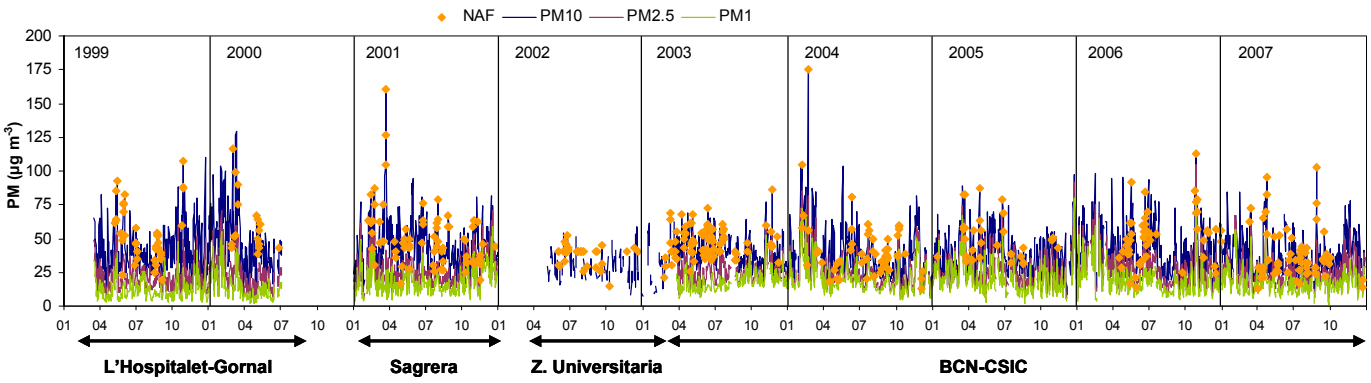

Figure 4.1.4. PM levels time series recorded at L'Hospitalet-Gornal, Sagrera, Zona Universitaria and BCN-CSIC in Barcelona from 1999 to 2007. Days with African dust outbreak influence are marked with yellow diamonds.

Mean annual PM_{10}, $PM_{2.5}$ and PM_1 levels registered at Barcelona from 1999 with optical particle counters and gravimetric methods are shown on Table 4.1. The levels measured by the gravimetric methods are slightly higher for PM_{10} and $PM_{2.5}$. The differences observed are due to the fact that high volume sampling was done only on weekdays, when traffic density and other anthropogenic emissions are higher, whereas the real time measurements also covered weekends.

Table 4.1. PM mean annual levels registered at Barcelona from 1999 to 2007 by means of optical particle counters (corrected) and gravimetric methods. Data were obtained at four different sites: [a]L'Hospitalet-Gornal (Rodriguez, 2002); [b]Sagrera (Viana, 2003); [c]Zona Universitaria (Ajuntament de Barcelona Air Quality Monitoring Network); [d]BCN-CSIC (Pey, 2007 and this work).

PM levels	Optical particle counter			Gravimetry		
µg m^{-3}	PM_{10}	$PM_{2.5}$	PM_1*	PM_{10}	$PM_{2.5}$	PM_1
1999 [a]	42	21	11	50	34	
2000 [a]	48	23	13			
2001 [b]	44	26	17	46	28	
2002 [c]	29**					
2003 [d]	40	25	17	46	28	
2004 [d]	39	25	19	49	35	
2005 [d]	39	27	19	45	31	
2006 [d]	42	29	19	45	29	18
2007 [d]	38	25	17	43	28	17
Mean	42	25	17	46	30	17

*PM_1 measurements are corrected with gravimetric PM_1 data from October 2005 in Barcelona. A factor obtained between levels corrected with gravimetric PM_1 and $PM_{2.5}$ in 2006-2007 is applied to correct data from 1999-2007 (previously corrected with $PM_{2.5}$). **PM_{10} measured at Zona Universitaria site in Barcelona is anomalously low. It is not considered for the mean annual PM levels calculation.

The high PM levels recorded at Barcelona have an anthropic origin. The main sources contributing to PM in this urban area are road traffic, some industrial activities,

demolition and construction activities, power generation, waste treatment plants and port activity. PM_{10} and $PM_{2.5}$ levels measured at Barcelona can be considered as relatively high when compared with the average ranges observed at Spanish and central and northern European urban background sites (Querol et al., 2004, 2004b and 2006; Götschi et al., 2005, Figure 4.1.5), but similar to the levels recorded in southern European countries (Vardoulakis et al., 2008; Götschi et al., 2005). PM_1 levels measured at Barcelona are comparable to the levels measured at some Italian cities (Florence, Genoa or Milan during the summer, Vecchi et al., 2008), higher than levels measured at Northern European cities as Helsinki (Pakkanen et al., 2003) and Birmingham (Yin and Harrison, 2008), and lower than PM_1 levels measured at Milan in winter (Vecchi et al., 2008, Figure 4.1.5). Differences are observed when comparing Northern and Southern Europe. Northern European cities show in general lower PM_{10}, $PM_{2.5}$ and PM_1 levels than Southern European cities. PM levels are relatively high in urban agglomerations in Southern Europe. Higher PM anthropogenic emissions in narrow streets, a warm and dry climate, low dispersive conditions, soil resuspension and a sporadic contribution from Northern African dust could account for the high PM levels. However, these factors affect mainly the coarse fraction. In urban backgrounds the lack of rain minimizes particle washout from roads and streets making resuspension by vehicles or winds an important source to coarser atmospheric aerosols. In addition the proximity to Northern Africa makes dust outbreaks frequent. There might also be differences in the proportion of diesel vehicles in the fleets or the quality of fuel used in different countries.

$PM_{2.5}/PM_{10}$ and PM_1/PM_{10} ratios were lower at Barcelona (0.6 and 0.4 respectively), when comparing with Central and Northern Europe, with $PM_{2.5}/PM_{10}$ between 0.7-0.8 and PM_1/PM_{10} around 0.5. This is probably the consequence, as explained above, of the lower frequency of precipitations registered in Southern Europe, increasing ambient coarse PM levels by resuspension processes.

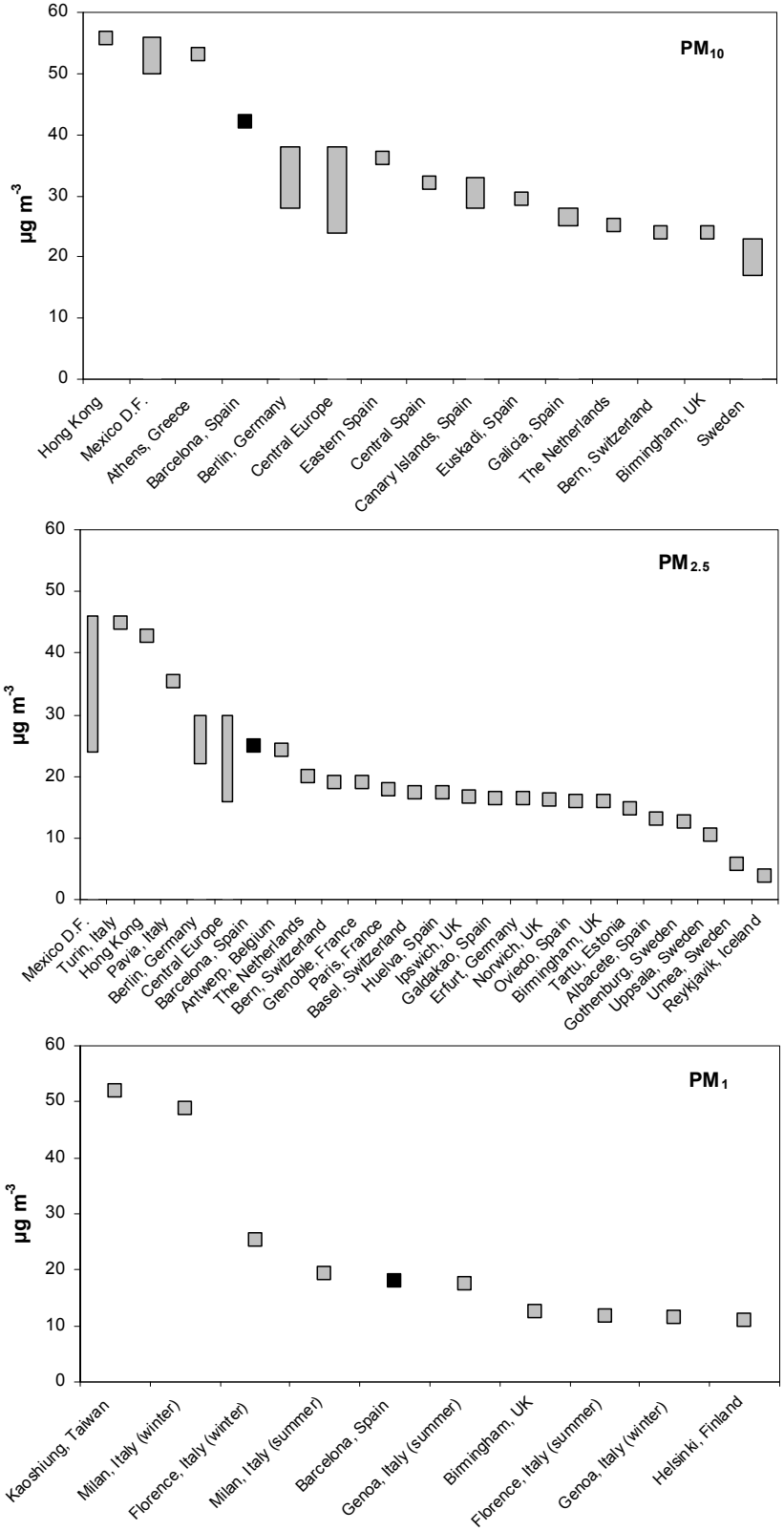

Figure 4.1.5. PM_{10}, $PM_{2.5}$ and PM_1 levels recorded at different urban sites compared to PM levels recorded at Barcelona in this study (Pakkanen et al., 2003; Lin and Lee, 2004; Götschi et al., 2005; Querol et al., 2004a, 2004b, 2008a and 2008b; Vardoulakis et al., 2008; Vecchi et al., 2008 and Yin and Harrison, 2008).

$PM_{2.5}/PM_{10}$ and PM_1/PM_{10} ratios depend on the study site and the sources affecting PM levels. During the period 1999-2001, measured at L'Hospitalet-Gornal and Sagrera sites, $PM_{2.5}/PM_{10}$ (between 0.5-0.6) and PM_1/PM_{10} (between 0.3-0.4) were lower than the ratios measured at BCN-CSIC during the period 2003-2007 (0.6-0.7 and 0.5 for $PM_{2.5}/PM_{10}$ and PM_1/PM_{10} respectively, Table 4.2). The higher difference between sites is observed for the $PM_1/PM_{2.5-10}$ ratio, from 0.6 in L'Hospitalet to 1 in Sagrera and 1.2-1.8 in BCN-CSIC. This is probably due to the proximity of L´Hospitalet and Sagrera sites to road traffic and the presence of a park near L'Hospitalet-Gornal, involving higher coarse emissions from resuspension processes. Measurements at BCN-CSIC site present higher ratios in general, reflecting the urban background environment.

Table 4.2. Mean annual $PM_{2.5}/PM_{10}$, PM_1/PM_{10} and $PM_1/PM_{2.5-10}$ ratios registered at Barcelona from 1999 to 2007 at four different sites: [a]L'Hospitalet-Gornal (Rodriguez, 2002); [b]Sagrera (Viana, 2003); [c]Zona Universitaria (Ajuntament de Barcelona Air Quality Monitoring Network); [d]BCN-CSIC (Pey, 2007 and this work).

	$PM_{2.5}/PM_{10}$	PM_1/PM_{10}	$PM_1/PM_{2.5-10}$
1999 [a]	0.5	0.3	0.6
2000 [a]	0.5	0.3	0.6
2001 [b]	0.6	0.4	1.0
2002 [c]			
2003 [d]	0.6	0.5	1.2
2004 [d]	0.6	0.5	1.5
2005 [d]	0.7	0.5	1.8
2006 [d]	0.7	0.5	1.4
2007 [d]	0.7	0.5	1.3
Mean	0.6	0.4	1.2

4.1.2.1. Inter-annual variability

PM levels at urban sites are very influenced by road traffic emissions but also by meteorology. The inter-annual variability of PM levels depends strongly on the meteorology and the frequency of African dust episodes in a year. Temporal changes in anthropogenic emissions as road traffic or industrial emissions also influence PM variability. Figure 4.1.6 shows the evolution of mean $PM_{2.5-10}$, $PM_{1-2.5}$ and PM_1 annual levels from 1999 to 2007 in Barcelona for all days (total), days with African dust influence (NAF) and days without African dust influence (without NAF). With the objective of being able to study trends in PM_1 levels, in 2006 and 2007 PM_1 levels are corrected with PM_1 gravimetric data and for the rest of the years a ratio obtained between levels corrected with gravimetric PM_1 and $PM_{2.5}$ in 2006-2007 is applied to correct data. Vehicle fleet evolution in Barcelona city and % Diesel in Barcelona

province is also shown from 1999 to 2007 (Dirección General de Tráfico). In Barcelona, $PM_{2.5-10}$ and $PM_{1-2.5}$ levels recorded are lower at the BCN-CSIC site (2003-2007) than at the other sites (1999-2001). This decrease in the levels of the coarser fractions may be related to the effect of a change in resuspension processes at the different sites, as L'Hospitalet-Gornal was located near a park and closer to road traffic. However, mean $PM_{2.5-10}$ or $PM_{1-2.5}$ annual levels recorded from 2003 to 2007 at BCN-CSIC site do not seem to follow a definite trend, probably because the annual variation of coarser PM is more influenced by meteorology and the frequency and intensity of African dust outbreaks. Conversely, PM_1 levels are higher at BCN-CSIC site (2003-2007) than at the other sites in Barcelona (1999-2001) and PM_1 levels follow a clear increasing trend from 1999 to 2006. It is not easy to attribute this upward trend exclusively to an increase in PM anthropogenic emissions given that data were obtained at different sites in Barcelona. Nevertheless, it should be noted that this trend is also observed for the 2003-2006 period when the measurements were carried out at the BCN-CSIC site. In addition, the fact that the increasing trend is observed for the fine fractions but not for the coarser ones suggests an anthropogenic origin. Moreover, this increase could be related to the progressive rise in road traffic flow during the last decade and to the marked growth of the diesel fleet (from around 26% in 1999 to around 43% in 2007). However, 2007 data show a slight decrease compared to 2006, indicating that this 1999-2006 increasing trend may be due in part to meteorological causes, owing to the fact that during the year 2007 higher precipitation rates were registered (520 mm in 2007, from 240 to 510 in the rest of the years). The application of the Mann-Kendall test for the detection of temporal trends (Salmi et al., 2002) to mean annual PM levels measured at BCN results in a significant PM_1 increasing trend of 49% from 1999 to 2007 (at α=0.01 significant level) that is equivalent to 5 μg m^{-3} from 1999 to 2007. Conversely, $PM_{2.5-10}$ presented a decrease of 45% at α=0.01 significance level from 1999 to 2007 (9 μg $PM_{2.5-10}$ m^{-3}), probably more related to meteorological factors. In addition, mean annual PM_1 levels showed significant correlations and positive slopes with the year of measurement (r^2=0.71), vehicle fleet (r^2=0.82) and the % of diesel (r^2=0.74, Figure 4.1.7) indicating the existence of this trend and its relationship with the increase in vehicle fleet and the proportion of diesel vehicles.

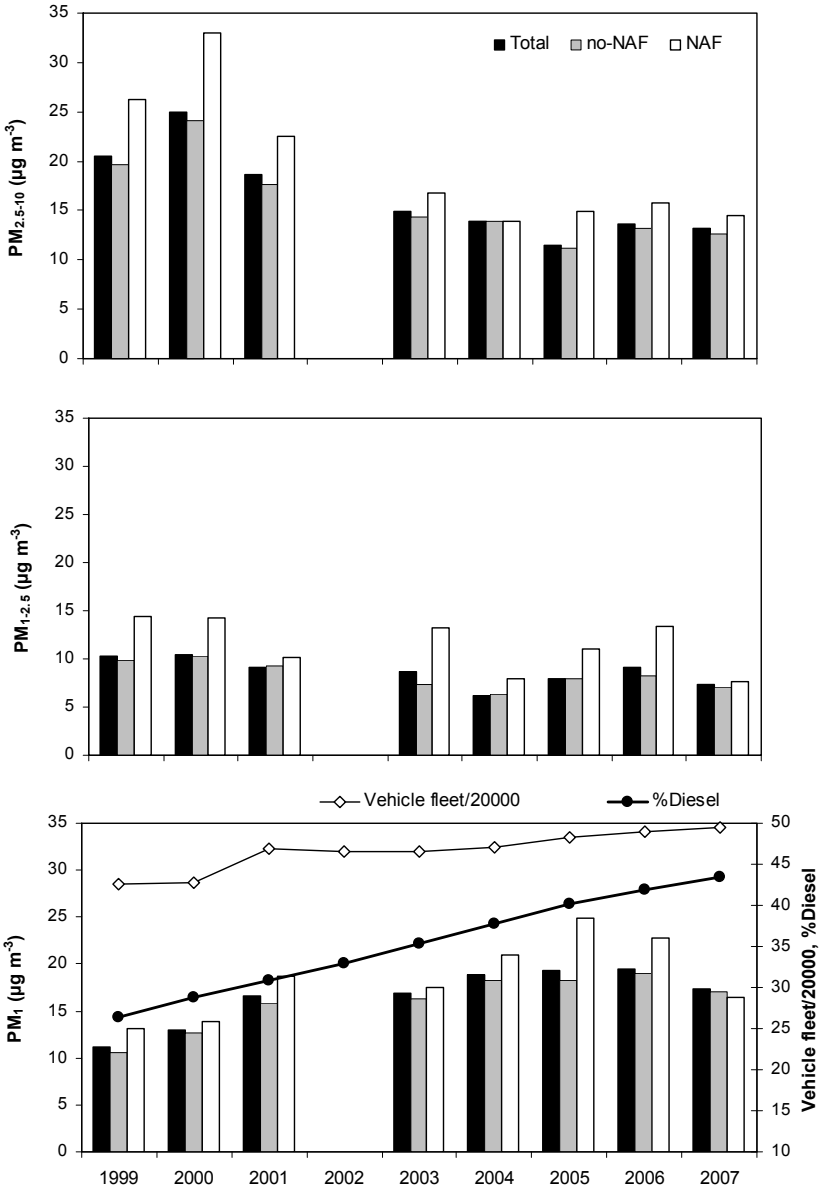

Figure 4.1.6. Evolution of mean annual $PM_{2.5-10}$, $PM_{1-2.5}$ and PM_1 levels from 1999 to 2007 for the total of days (total), days with African dust influence (NAF) and days without African dust influence (no-NAF) recorded at Barcelona urban sites. Vehicle fleet in Barcelona city and % diesel evolution in the Barcelona province.

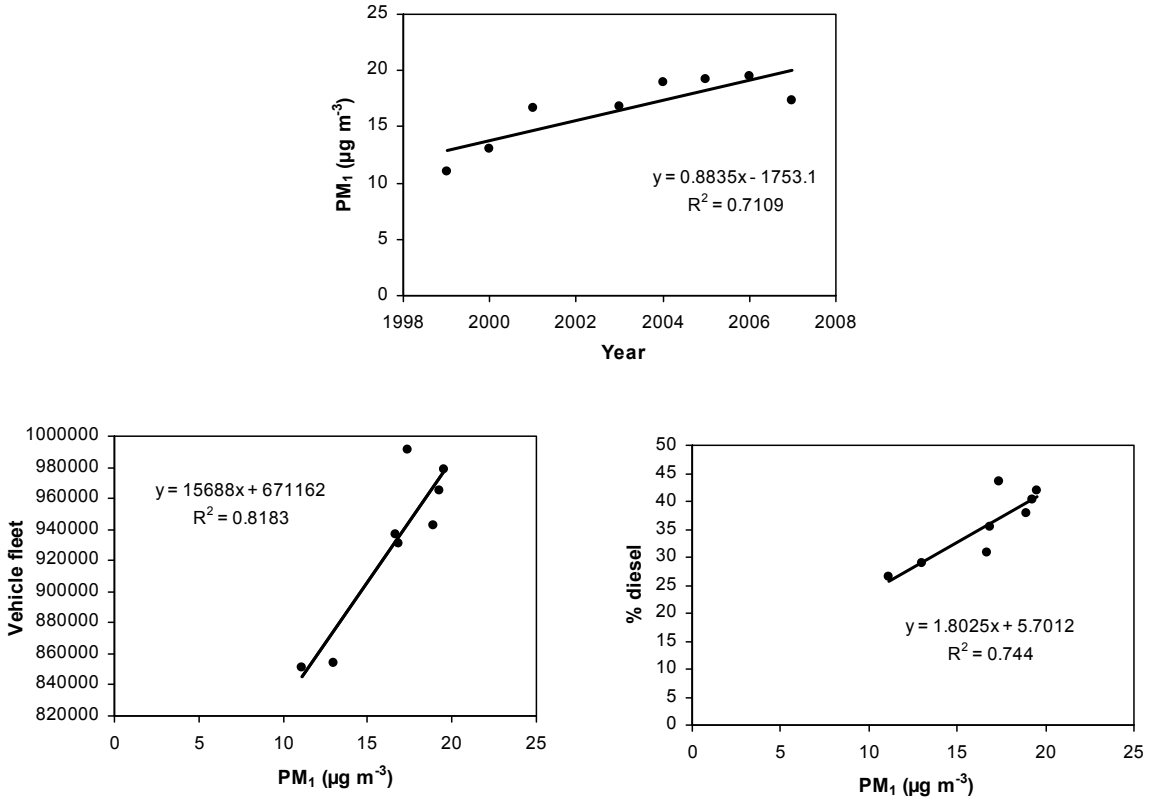

Figure 4.1.7. Correlation between mean annual PM1 levels and year of measurement, mean annual vehicle fleet and % diesel in the fleet in Barcelona from 1999 to 2007.

4.1.2.2. Seasonal variability

The mean monthly evolution of PM_{10}, $PM_{2.5}$ and PM_1 levels and $PM_{2.5-10}$ and $PM_{1-2.5}$ fractions levels recorded at Barcelona from 1999 to 2007 are shown on Table 4.3 and Figure 4.1.8.

Table 4.3. Monthly mean PM_{10}, $PM_{2.5}$, PM_1, $PM_{1-2.5}$ and $PM_{2.5-10}$ levels registered at Barcelona from 1999 to 2007.

µg m^{-3}	PM_{10}	$PM_{2.5}$	PM_1	$PM_{1-2.5}$	$PM_{2.5-10}$
January	39	26	22	4	15
February	48	35	27	8	16
March	48	29	20	9	18
April	41	23	16	7	18
May	42	24	16	8	19
June	44	25	16	9	19
July	39	25	17	8	16
August	33	20	13	7	14
September	34	22	16	6	13
October	38	25	17	7	14
November	42	28	20	7	16
December	35	27	21	6	10

High PM_1 levels are usually registered during the winter months (especially February-March and November). These elevated PM_1 levels are related to the frequent anticyclonic situations occurring in the area during this period of the year, favouring the stagnation of pollutants near the emission sources and producing episodes of intense local pollution, especially increasing the secondary PM. In addition, the occurrence of African dust episodes increases coarse PM levels. High $PM_{2.5-10}$ levels are usually observed during the warmer months (from May to July) and they can be associated to a high frequency of African dust outbreaks occurring during this period of the year, the regional recirculation of air masses in the Mediterranean that prevent air mass renovation, the low precipitations registered, a higher soil resuspension due to the aridity of soils, resuspension of road and anthropogenic dust by road traffic, and the formation of secondary aerosols from gaseous precursors caused by enhanced photochemistry (Querol et al., 2001a; Viana et. al., 2002; Escudero et al., 2005). The decrease of PM levels usually observed in April, August and September are related to the higher frequency of precipitations and the Atlantic air mass advections registered during this months that produce air mass renovation and wash out the dust from roads diminishing resuspension. Moreover, August is the usual month of holidays in Spain and traffic activity in Barcelona is reduced. The summer in 2003 was characterized by a heat wave and lower precipitation rates, consequently higher summer coarse PM increase was registered. From 2004 to 2006 strong pollution episodes associated to winter anticyclonic scenarios were recorded, increasing PM_1 levels markedly. Conversely to $PM_{2.5-10}$ and PM_1, the fraction $PM_{1-2.5}$ does not present a clear seasonal trend. This is probably the result of its composition by a mixture of sources.

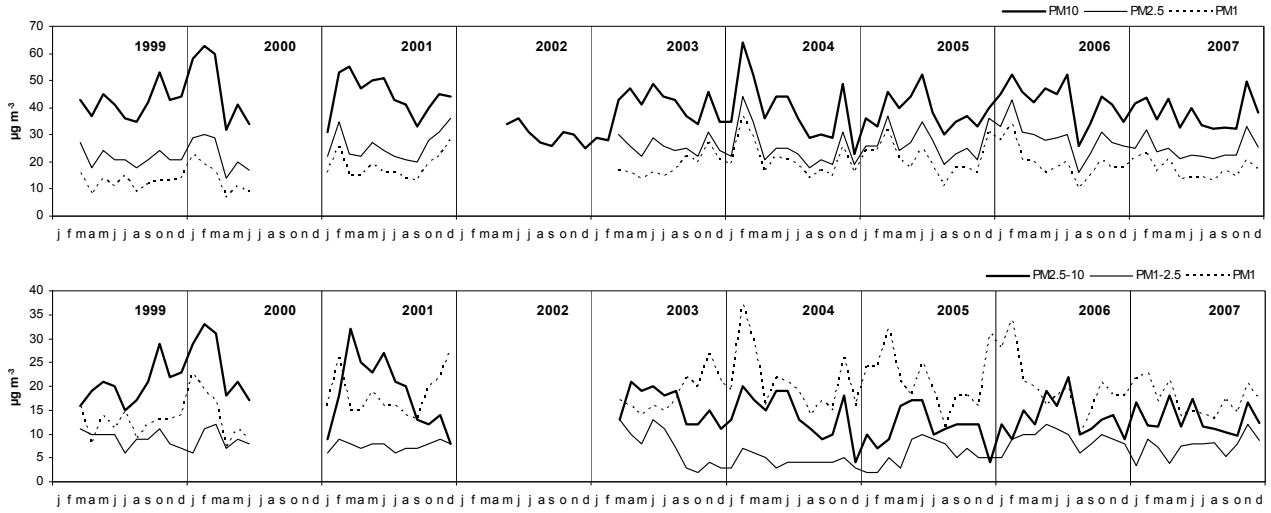

Figure 4.1.8. Monthly mean PM_{10}, $PM_{2.5}$ and PM_1 levels (top) and $PM_{2.5-10}$, $PM_{1-2.5}$ and PM_1 levels (bottom) registered at Barcelona from March 1999 to December 2007.

Mean daily $PM_{2.5}/PM_{10}$, PM_1/PM_{10} and $PM_1/PM_{2.5-10}$ ratios obtained at Barcelona from 1999 to 2007 (Figure 4.1.9) show a clear seasonal trend, decreasing during the summer, when the mineral dust influence is higher because of a higher resuspension and frequency of African dust episodes, and increasing during winter, with a finer PM distribution in general owing to anthropogenic emission sources. The decrease of the ratios during the summer is more marked for the PM_1/PM_{10} than for the $PM_{2.5}/PM_{10}$ ratio, probably because PM_1 is less affected by the mineral dust contributions from African dust or soil resuspension and presents a lower seasonal variation. The influence of African dust episodes on the ratios is evident during 2003, with a very warm and dry summer and a higher frequency of African dust outbreaks than the rest of the years. The ratios decrease more markedly for the 2003 summer than for the rest of the summers due to the higher input of coarse particles by the mineral dust. The high winter pollution episodes recorded from 2004 to 2006 influence the $PM_1/PM_{2.5-10}$ ratios with markedly higher values than in 1999-2001 and 2003 and 2007.

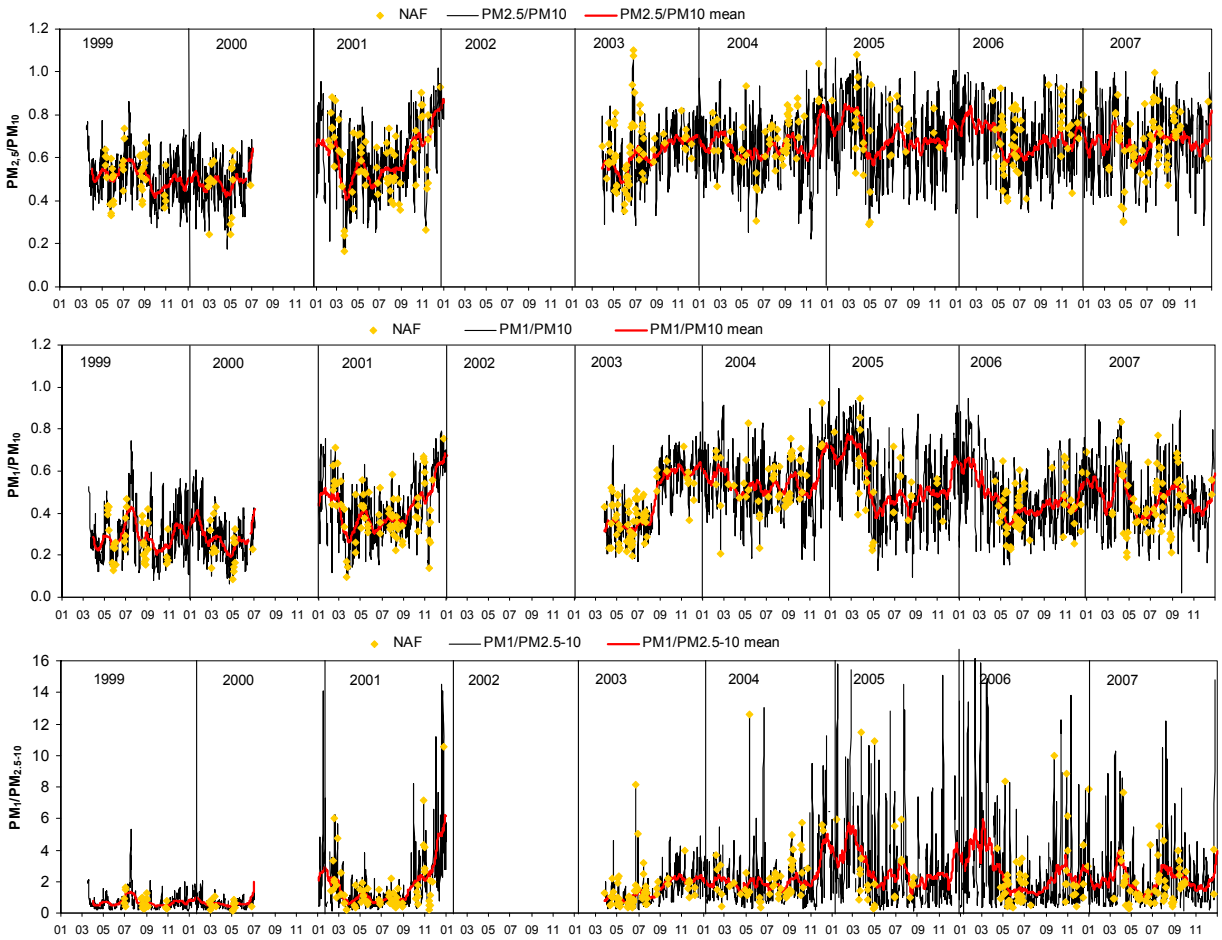

Figure 4.1.9. Ratios $PM_{2.5}/PM_{10}$, PM_1/PM_{10} and $PM_1/PM_{2.5-10}$ in Barcelona from 1999 to 2007. The days with African outbreaks (NAF) and the sliding average for 30 days were marked.

4.1.2.3. Daily cycles

Daily cycles of PM levels at BCN-CSIC urban background site are very influenced by traffic and meteorology (especially breeze circulations). PM_{10}, $PM_{2.5}$ and PM_1 levels start to increase during morning traffic peak hours (around 6h UTC, Figure 4.1.10 and Figure 4.1.11) and reach the maximum at around 7-8h UTC. This increase in PM levels is attributed to road dust resuspension by road traffic and direct vehicle exhaust emissions into a relatively thin mixing layer. Breeze circulation in Barcelona plays a very important role on the daily cycles of PM levels. Before traffic peak hours, wind speed is lower and coming from the NW, thus carrying the direct emissions from the Diagonal Avenue (120000 vehicles day^{-1}) and other important traffic arteries of Barcelona. As previously explained, sea-land breeze starts to blow at around 8h UTC from the SE increasing its speed during the daylight hours. The sea breeze, together with the development of the boundary layer during the day and a slight decrease of the traffic flow, make PM_{10}, $PM_{2.5}$ and PM_1 levels decrease as a consequence of

atmospheric dilution processes (Figure 4.1.10, Figure 4.1.1 and Figure 4.1.2). However, this behaviour is not observed for the coarse fraction ($PM_{2.5-10}$) remaining high until the evening. This is probably due to the direct resuspension of dust (coarse particles) proceeding from traffic and demolition/construction activities by wind and by the continuous road traffic flow during all day, and thus coarse particle levels remain high until the traffic intensity and wind speed decrease in the evening. This can be clearly seen in the $PM_{2.5-10}$ cycle ($PM_{2.5-10}$ morning increase and evening decrease are much sharper than the variation for the other fractions, Figure 4.1.10 and Figure 4.1.11). At night, when traffic activity is lower, exhaust and non-exhaust emissions decrease together with wind speed and this is reflected on a sharp decrease of PM_{10} or $PM_{2.5-10}$ levels. However, $PM_{2.5}$ and PM_1 do not follow the same pattern than PM_{10}. These particle size ranges have a longer residence lifetime in the atmosphere and their levels are also affected by secondary particles formation after traffic peak hours from precursor gaseous pollutants previously emitted by vehicles. As a result, $PM_{2.5}$ and PM_1 levels do not decrease at night. This is also a consequence of the lower temperatures, higher relative humidity and thinning of the boundary layer during the night, favouring secondary formation of particles together with the lower dilution processes that make concentration of pollutants increase (Viana et al., 2005).

$PM_{2.5-10}$ and PM_1 have a more marked daily cycle than $PM_{1-2.5.}$ The daily evolution of $PM_{1-2.5}$ levels is very smooth and only a small peak is observed at 7-8h UTC. This may be a consequence of the diverse sources that affect the different size fractions. $PM_{2.5-10}$ and PM_1 may be more affected by traffic emissions and breeze evolution than $PM_{1-2.5.}$

The important influence of traffic emissions on PM levels can be clearly observed by the study of the weekly evolution of the daily cycles (Figure 4.1.10). Similar cycles following the traffic emissions pattern (Figure 4.1.12) are observed from Monday to Friday. However, on Saturdays and Sundays the traffic pattern is different, the traffic density is lower and PM cycles change, being especially clear for $PM_{2.5-10}$ levels, with a much smoother and lower increase during the day and also for PM_1 where the morning peak cannot even be observed but the decrease on PM_1 levels by atmospheric dilution in the middle is clear.

The inter-annual evolution of daily cycles is shown in Figure 4.1.11. The same daily patterns of $PM_{2.5-10}$, $PM_{1-2.5}$ and PM_1 levels are observed for every year, driven by breezes and road traffic emissions. However, higher $PM_{2.5-10}$ levels are observed during the year 2006. Specific meteorological conditions during this year make PM levels

recorded in most monitoring sites in Spain and Europe higher than the rest of the years considered (Airbase databases, http://air-climate.eionet.europa.eu/databases/airbase/). PM_1 levels are also higher in 2006 due to the intense winter PM episodes recorded.

As a conclusion, it is clear the influence of traffic on $PM_{2.5-10}$ levels (Figure 4.1.12) as a consequence of road dust resuspension, whether PM_1 is marked by the traffic peak hours in the morning but follow the ratio traffic intensity/wind speed during the day, being influenced by direct traffic emissions but also by atmospheric dilution processes produced by breezes.

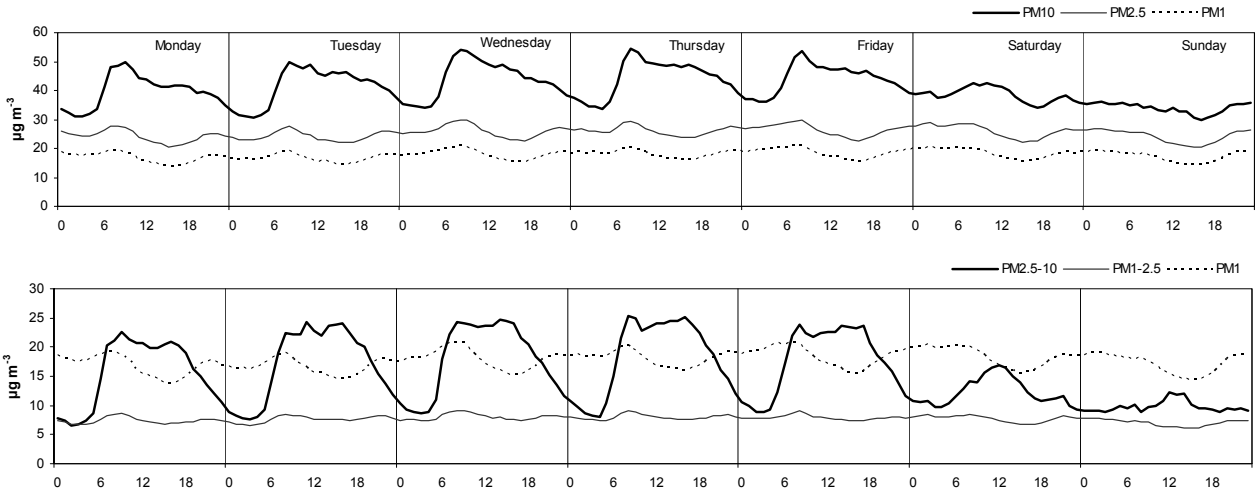

Figure 4.1.10. Mean PM_{10}, $PM_{2.5}$ and PM_1 (top) and $PM_{2.5-10}$, $PM_{1-2.5}$ and PM_1 (bottom) daily cycles and weekly evolution recorded at BCN-CSIC during 2003-2007.

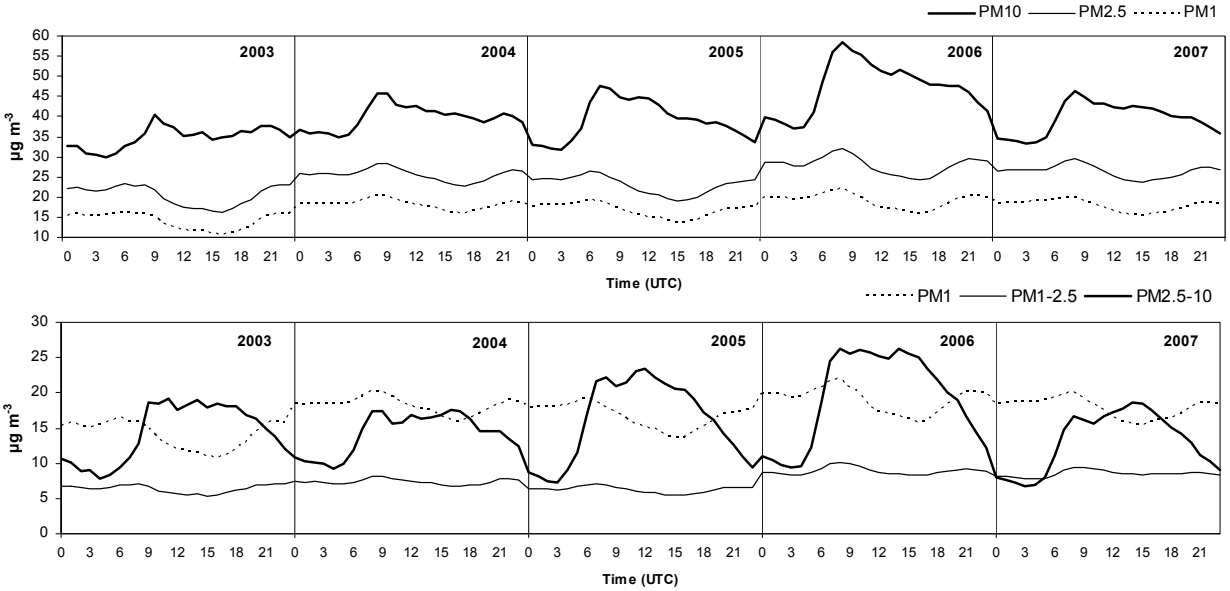

Figure 4.1.11. Mean PM_{10}, $PM_{2.5}$ and PM_1 (top) and $PM_{2.5-10}$, $PM_{1-2.5}$ and PM_1 (bottom) daily cycles and annual evolution recorded at BCN-CSIC during 2003-2007.

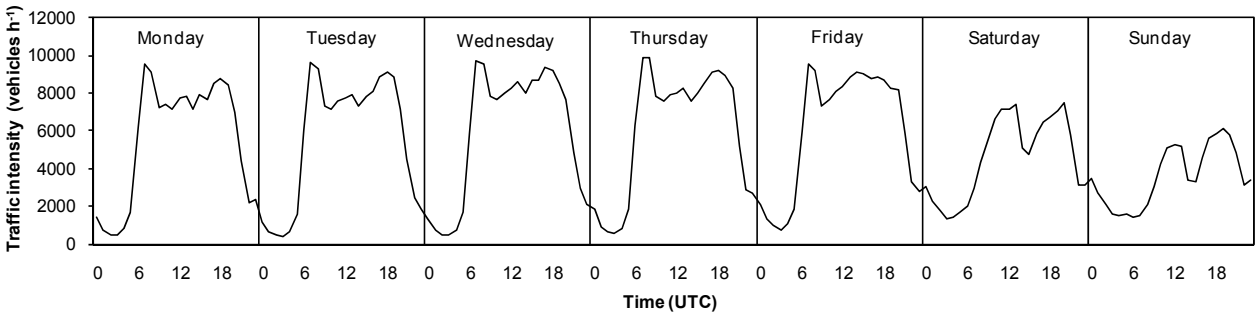

Figure 4.1.12. Road traffic intensity measured at the Diagonal Avenue from July to December 2007 (Ajuntament de Barcelona, Serveis de Mobilitat).

4.1.2.4. Influence of different air mass transport episodes on PM levels

Air mass origin and transport together with meteorological conditions influence noticeably the variability of PM levels, increasing the levels when the air transports particles from distant areas or decreasing them by the renovation of the air masses. Mean PM levels associated to each of the air mass episodes and fractions considered are shown in Table 4.4 and Figure 4.1.13.

Table 4.4. Mean daily levels for each air mass episode registered in Barcelona (1999 to 2007). North Atlantic (NA), North-Western Atlantic (NWA), Western Atlantic (WA), South-Western Atlantic (SWA), African dust outbreaks (NAF), Mediterranean (MED), European (EU) and Winter anticyclonic episodes (WAE).

μg m^{-3}	NA	NWA	WA	SWA	NAF	MED	EU	REG	WAE
PM_{10}	34	37	38	41	**48**	36	41	40	47
$PM_{2.5}$	21	22	23	24	30	25	27	25	**34**
PM_{1}	16	15	16	16	20	19	21	18	**26**
$PM_{1-2.5}$	5	7	7	8	**10**	6	6	7	8
$PM_{2.5-10}$	13	15	15	17	**18**	16	14	15	13

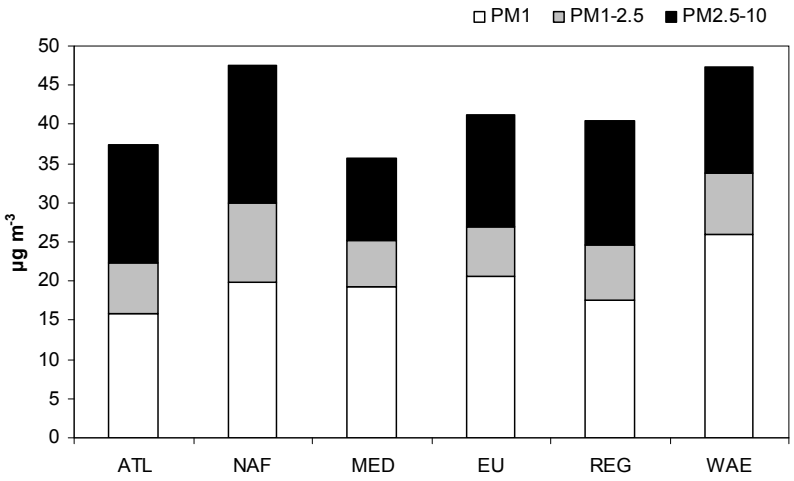

Figure 4.1.13. Mean PM levels by air mass origin registered at Barcelona (1999-2007). Atlantic advections (ATL), African dust outbreaks (NAF), Mediterranean (MED), European (EU) and winter anticyclonic episodes (WAE).

The highest PM_{10} $PM_{2.5-10}$ and $PM_{1-2.5}$ levels registered at Barcelona were observed during North African dust outbreaks. North African air masses loaded with mineral dust increase PM levels, especially in the coarser fractions. PM_1 levels do not have an important variation with NAF, EU, MED or REG episodes, but they are markedly higher during winter pollution episodes. In contrast, $PM_{2.5-10}$ and PM_{10} levels are clearly higher for NAF episodes. This is a consequence of the coarser size contribution of North African dust to PM levels.

Regional recirculation episodes (REG) present also high PM levels associated to the accumulation and recirculation of pollutants over the region. Sometimes these episodes last a few days producing the aging of air masses. Aged air masses carry secondary aerosols (mainly ammonium sulphate) with a fine grain size.

The lowest PM levels are observed for Atlantic advections and Mediterranean episodes. These air mass advections renovate the air masses cleaning the atmosphere from pollutants and generally reducing PM levels. Atlantic advections are sometimes associated to precipitations that contribute to wash out the suspended particles and to minimize the dust resuspension. Mediterranean episodes are also frequently associated to intense precipitations.

European episodes are associated to winds that allow the renovation of air masses but sometimes the transport of pollutants from Central and Eastern Europe contributes to

increment PM levels, especially the finer fractions because the air masses transported are charged with anthropogenic pollutants.

Winter anticyclonic episodes are registered in this area during the winter months (especially November and February-March). They are associated to high pressures and atmospheric stability, producing the stagnation of air masses during several days and the accumulation of pollutants. In these circumstances, intense pollution episodes are recorded due to the lack of dispersion that induces the accumulation of urban emissions during several days. Under these episodes the highest daily levels of PM_1 are registered (26 μg m^{-3}).

4.1.2.5. Influence of African dust outbreaks on PM levels: exceedances of the PM_{10} daily limit level and annual PM_{10} contributions

The contribution of North-African mineral dust to the annual PM levels depends on the frequency and intensity of African outbreak episodes in a year. The annual number of days with clear African dust contribution varies widely. In the region studied, for the period 1999-2007 the number of African days varied from 32 (2005) to 85 (2003), with a mean annual frequency of 52 days (Table 4.5).

The influence of African dust outbreaks is more relevant if the daily increase of PM levels is concerned. The evaluation of the measured data shows that daily African dust contributions to PM_{10} higher than 25 μg m^{-3} (and up to 60 μg m^{-3}) are usually reached a few days every year. Dust outbreaks may contribute to exceed the 50 μg m^{-3} PM_{10} daily limit level. For the period 1999-2007 in Barcelona, the annual daily exceedances of the 50 μg m^{-3} PM_{10} daily value were between 63-104, always over the 35 annual permitted exceedances. Between 10 and 30 (16-45%) of the daily exceedances of the PM_{10} limit were recorded during days with African dust influence and 36-77 (55-84%) of the daily exceedances were exclusively attributed to anthropogenic activity. Most of the exceedances recorded during days with African dust influence in Barcelona are not attributed exclusively to natural causes, being the anthropogenic mineral load dominant at this urban background.

Table 4.5. Number of days with African dust influence in the study region. Number of exceedances of the PM_{10} 50 μg m^{-3} daily limit value and the % of the exceedances recorded during African dust outbreaks.

	Annual days with NAF influence	Number of Exceedances PM_{10}> 50 μg m^{-3}	% D.L.V. exceedances recorded during NAF
1999	48	72	29
2000	33	63	16
2001	71	102	27
2002	40		
2003	85	66	45
2004	56	74	18
2005	32	72	18
2006	53	104	26
2007	62	66	23

The difference between the mean PM annual levels and the mean levels obtained for days without African dust influence may be considered as the African dust contribution to PM_{10}, $PM_{2.5}$ and PM_1 (Table 4.6). At Barcelona, the annual increase of PM levels due to the African dust influence is around 0.6-2.4, 0.5-1.8 and 0.2-0.9 μg m^{-3} (1.5, 0.9 and 0.6 mean values respectively) for PM_{10}, $PM_{2.5}$ and PM_1 measured in the period 1999-2007. PM_{10}, $PM_{2.5}$ and PM_1 levels are not affected by African dust outbreaks in the same extent. Mineral dust is mainly coarse in grain size and the increase in annual PM levels is less marked in PM_1 than in PM_{10} or $PM_{2.5}$. The highest African dust contributions to PM levels (2.4 and 1.8 and μg m^{-3} for PM_{10} and $PM_{2.5}$ respectively) were recorded during the year 2003, owing to the higher frequency and intensity of dust outbreaks and the lower precipitations registered during this year.

Table 4.6. Mean PM annual levels range at Barcelona (data from 1999 to 2007). Mean annual levels range for days without African dust influence (no NAF). Increase in the annual PM levels attributed to African dust outbreaks.

μg m^{-3}	PM mean annual levels	PM levels (without NAF)	Annual increase of PM related to NAF episodes
PM_{10}	38-48	37-47	0.6-2.4
$PM_{2.5}$	21-29	20-27	0.5-1.8
PM_1	11-19	11-19	0.2-0.9

4.1.2.6. Size fraction correlation studies: discrimination of sources

The study of correlations between PM fractions revealed some relationships that are due to the contribution of common sources to the different PM fractions (Table 4.7 and Figure 4.1.14). Thus, fractions with the contribution of common sources showed good

correlation coefficients (r^2>0.5) and fractions that had no common sources did not show a significant correlation, as PM_1 with $PM_{2.5-10}$ or with PM_{1-10} (r^2< 0.15 in both cases).

PM_{10} showed significant correlation coefficients with $PM_{2.5}$ (r^2=0.71) and PM_1 (r^2=0.51), as a result of the contribution of combustion sources to all three fractions, and with the fractions $PM_{2.5-10}$ (r^2=0.65) and PM_{1-10} (r^2=0.85), indicating a high contribution of other non-combustion sources (mainly dust resuspension). $PM_{2.5}$ showed a good correlation with PM_1 (r^2=0.69) and $PM_{1-2.5}$ (r^2=0.59) as they are all affected by combustion sources. However, PM_1 only showed significant correlations with $PM_{2.5}$ and PM_{10}, because it is included in these fractions and did not show correlation with any other fraction (r^2<0.15). This is probably a consequence of the different sources contributing to PM_1 (affected mainly by combustion emissions) and the coarser fractions (affected by other sources not related to combustion).

Table 4.7. Correlation coefficients (r^2) between simultaneous levels of different PM fractions.

r^2	PM_{10}	$PM_{2.5}$	PM_1	$PM_{2.5-10}$	PM_{1-10}	$PM_{1-2.5}$
PM_{10}	X	0.71	0.51	0.65	0.85	0.41
$PM_{2.5}$	0.71	X	0.69	0.14	0.42	0.59
PM_1	0.51	0.69	X	0.10	0.14	0.08
$PM_{2.5-10}$	0.65	0.14	0.10	X	0.78	0.07
PM_{1-10}	0.85	0.42	0.14	0.78	X	0.47
$PM_{1-2.5}$	0.41	0.59	0.08	0.07	0.47	X

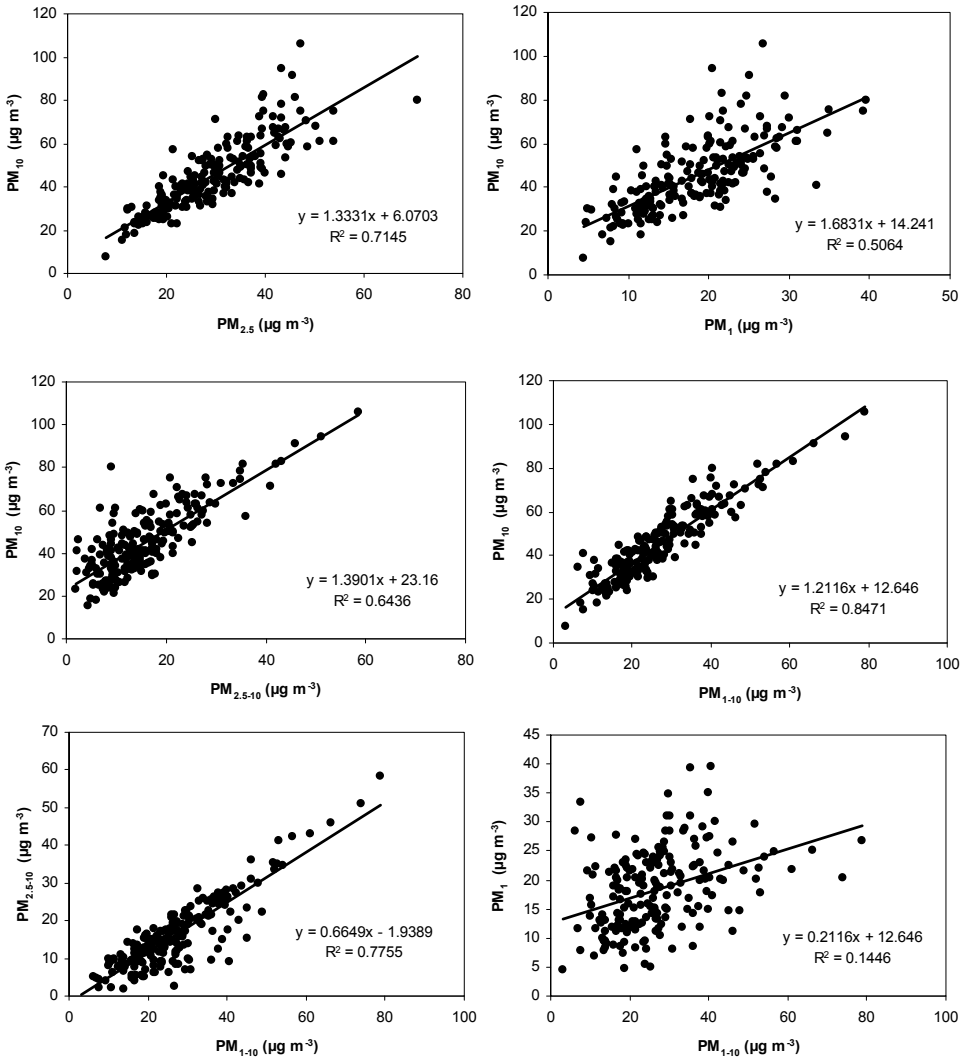

Figure 4.1.14. Correlation graphs between different PM mass fractions.

Therefore, from the correlations between the different PM size fractions it is possible to deduce the main sources contributing to each fraction and consequently their major chemical components. From the results obtained, the fine fraction (PM_1), with a main combustion source would be mainly composed of carbonaceous compounds (OM+EC) and secondary inorganic compounds (SIA). Exposure to fine PM is related to important health effects as cardiovascular diseases and its effects are related to the size distribution of the particles but also to the composition. Then, the coarser particles (PM_{1-10}) that are related to non-combustion sources as the resuspension of road dust would be mainly composed of mineral matter and also trace elements related to traffic abrasion products (from tyres and brakes wear). Exposure to this fraction is more related to respiratory diseases but also to inflammatory and toxic effects of the trace elements (oxidative stress).

In conclusion, PM_1 is mainly affected by combustion sources (road traffic and other anthropogenic emissions at the urban site) and PM_{1-10} is mainly related to other sources not related with combustion (mainly road dust resuspension by traffic and construction and demolition activities), representing other sources non-related with combustion. PM_{10} and $PM_{2.5}$ are the parameters that are currently monitored in air quality networks. However, correlation studies show that $PM_{2.5}$ is a mixture of sources (combustion and non-combustion), while the monitoring of PM_1 and PM_{10} may make possible a better discrimination of combustion and non-combustion sources, with different health effects. Therefore, a good sampling strategy for air quality monitoring may include PM_1 and PM_{10} (thus PM_1 and PM_{1-10}) parameters as they vary in relation with different emission sources and processes that could then be monitored separately.

4.1.3. PM speciation at the urban background

The results of the PM_{10}, $PM_{2.5}$ and PM_1 chemical speciation analysis performed at three different monitoring sites in Barcelona (L'Hospitalet-Gornal, Sagrera and BCN-CSIC) from 1999 to 2007 are shown on Table 4.8. The results obtained for the different components analyzed in the fractions PM_{10} and $PM_{2.5}$ at the three Barcelona sites are comparable. However the levels of carbonaceous compounds and SIA were slightly higher at L'Hospitalet site, probably because of a higher road traffic influence.

Table 4.8. Mean annual levels of PM_{10}, $PM_{2.5}$ and PM_1 and their major components registered at different sites of Barcelona between 1999 and 2007.

	PM_{10}			$PM_{2.5}$			PM_1
	BCN-CSIC [a]	Sagrera [b]	L'Hospitalet[c]	BCN-CSIC [a]	Sagrera [b]	L'Hospitalet[c]	BCN-CSIC [d]
	2003-2007	2001	1999-2000	2003-2007	2001	1999-2000	2005-2007
$\mu g\ m^{-3}$	45.3	46.2	49.5	30.3	27.6	33.9	18.0
OC	5.1			5.0			4.2
EC	2.9			2.7			2.1
OM+EC	11.1	13.7	15.9	10.9	12.2	13.2	8.8
SO_4^{2-}	5.1	5.2	6.9	4.4	4.2	5.6	2.9
NO_3^-	4.8	3.9	5.8	3.0	2.2	4.0	1.6
NH_4^+	1.4	2.0	2.7	1.7	2.0	3.2	1.2
SIA	11.6	11.1	15.4	9.0	8.4	12.8	5.7
Mineral dust	13.8	15.2	12.9	5.1	4.2	3.8	0.7
Sea spray	1.8	2.4	2.3	0.6	0.7	0.8	0.1
Unaccounted	6.6	3.8	3.0	5.0	2.1	4.2	2.6

[a]Pey (2007) and this study. [b]Querol (2004a). [c]Querol et al. (2001) and Rodríguez et al. (2003). [d]This study.

When compared to other urban sites in Spain and Central and Northern Europe, levels of mineral matter in PM_{10} and $PM_{2.5}$ are comparable to other sites in Spain and Northern Europe, but higher than the levels measured in Central Europe (Figure 4.1.15). Scandinavian countries present a high mineral load in PM_{10} or $PM_{2.5}$ as a consequence of road sanding and the use of studded tires in winter. The higher mineral load in urban areas of Southern Europe compared to central Europe is attributed to the lower precipitation. Rainfall favours not only the atmospheric scavenging of atmospheric pollutants but also the washout of road dust and the prevention of resuspension. In PM_1 the mineral matter is much reduced with respect to $PM_{2.5}$ and PM_{10} and the geographical differences diminish in terms of absolute concentration levels.

Levels of OM+EC measured at Barcelona were higher than levels recorded in most urban background areas in Europe with a fine grain size distribution (>80% in $PM_{2.5}$). At urban sites, major sources of these compounds are traffic and coal and fuel oil combustion. Levels of these compounds will depend mainly on the proximity and emission rate of these sources in the area. OC/EC ratios measured in Barcelona (2.1, 2.4 and 2.5 in PM_{10}, $PM_{2.5}$ and PM_1 respectively) show that 70% of the non mineral carbon is attributable to OC. These ratios are comparable to the values measured at other urban background sites in Europe (2.2, 1.7 and 1.7 for PM_{10}, $PM_{2.5}$ and PM_1 in Birmingham, or 2.0 for PM_1 in Milano, Harrison and Yin, 2008; Vecchi et al., 2004). However, measurements carried out in Milano for $PM_{2.5}$ showed ratios of 4.5-6.5 (Vecchi et al., 2004; Lonati et al., 2007).

At most urban background sites in Europe, levels of SIA in PM_{10} and $PM_{2.5}$ extend from 4 to 13 μg m^{-3}, Barcelona being in the upper range of these values. The lowest values are registered in Scandinavian cities (3-4 μg m^{-3}).

Sea spray contribution to PM_{10} is fairly homogeneous in Europe, with annual mean concentrations in PM_{10} between 1 and 4 μg m^{-3}. Sea spray concentrations measured in Barcelona, on the Mediterranean coast (1-2 μg m^{-3}) are clearly lower than those reported at Atlantic coastal sites in Spain or Northern Europe (up to 4 μg m^{-3}). In $PM_{2.5}$ sea spray contribution is markedly reduced and the levels are <1-2 μg m^{-3} at most sites, except for Northern European coastal sites, where higher levels are registered.

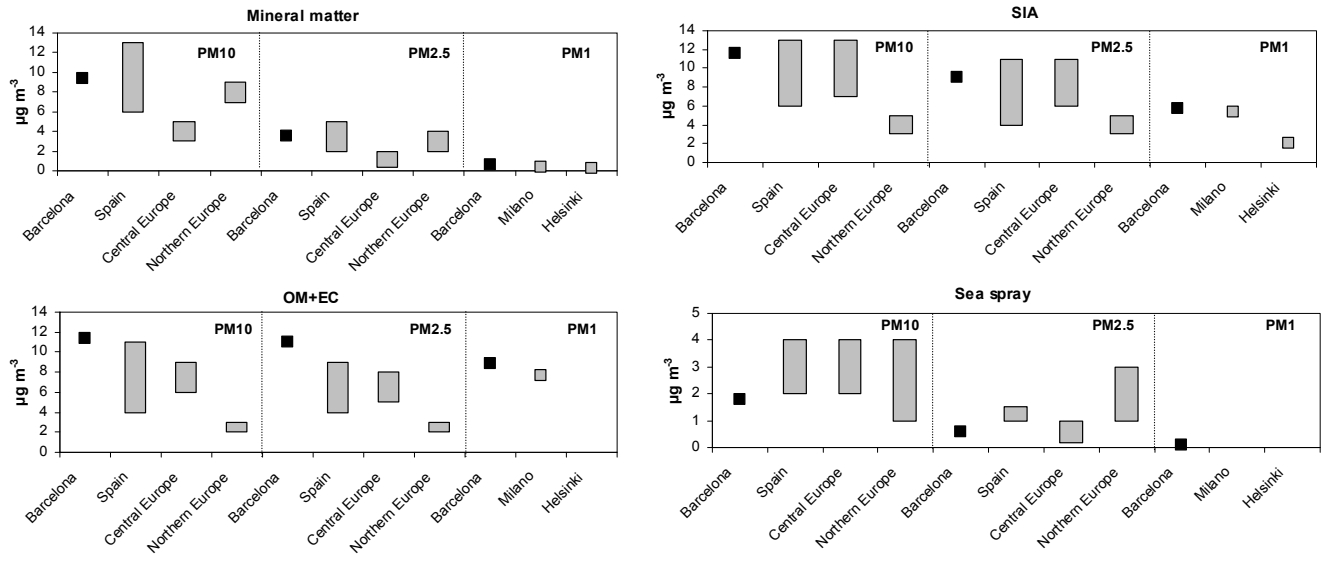

Figure 4.1.15. PM_{10}, $PM_{2.5}$ and PM_1 levels of the main PM components in BCN-CSIC compared to other urban background sites in Europe (Pakkanen et al., 2003; Vecchi et al., 2007; Querol et al., 2004 and 2008).

4.1.3.1. Speciation of PM_x and partitioning of major components in $PM_{2.5-10}$, $PM_{1-2.5}$ and PM_1

The speciation analysis of PM_1 started to be carried out at BCN-CSIC in October 2005. Studies on the comparative speciation of $PM_{2.5-10}$, $PM_{1-2.5}$ and PM_1 and the partitioning of major and trace PM components between the $PM_{2.5-10}$ $PM_{1-2.5}$ and PM_1 fractions are described using the speciation analysis from simultaneous PM_{10}, $PM_{2.5}$ and PM_1 sampling carried out from October 2005 to December 2007. Speciation data from simultaneous PM_{10}, $PM_{2.5}$ and PM_1 samples is presented in Table 4.9 and Figure 4.1.16. The partitioning of PM components into the $PM_{2.5-10}$, $PM_{1-2.5}$ and PM_1 fractions is presented in Figure 4.1.18.

Table 4.9. Mean levels of PM_{10}, $PM_{2.5}$, PM_1, $PM_{1-2.5}$ and $PM_{2.5-10}$ and their major components registered at BCN-CSIC from October 2005 to December 2007.

	PM_{10}	$PM_{2.5}$	PM_1	$PM_{1-2.5}$	$PM_{2.5-10}$
µg m^{-3}	43.8	28.8	18.0	10.8	15.0
OC	5.2	5.2	4.2	1.0	<0.1
EC	2.9	2.8	2.1	0.7	0.1
OM+EC	11.1	11.0	8.8	2.2	0.1
SO_4^{2-}	4.6	4.1	2.9	1.2	0.5
NO_3^-	5.2	3.0	1.6	1.4	2.2
NH_4^+	1.1	1.5	1.2	0.3	<0.1
SIA	11.0	8.6	5.7	2.9	2.4
Mineral matter	14.1	4.7	0.7	4.1	9.3
Sea spray	1.8	0.5	0.1	0.4	1.3
Unaccounted	5.4	3.8	2.6	1.2	1.6

The coarse fraction ($PM_{2.5-10}$, Figure 4.1.16) was mainly made up of mineral dust (61%), sea spray (9%) and coarse SIA (Na, Ca, K, Mg sulphates and nitrates, 17%). The carbonaceous material (only EC) was found at very low levels in this fraction (1%).

The proportion of sea spray and mineral dust were reduced in the $PM_{2.5}$ (2 and 16% respectively) with respect to the PM_{10} (4 and 32% respectively). Most of the carbonaceous components present in PM_{10} also fall within the $PM_{2.5}$ range (almost no OM+EC is present in the $PM_{2.5-10}$ fraction) but, as stated above a fraction of the SIA, particularly nitrate, was coarse, and consequently not present in $PM_{2.5}$. Thus $PM_{2.5}$ was still a mixture of SIA (29%), carbonaceous material (39%) and still a large proportion of mineral dust (16%). The mineral load in $PM_{2.5}$ continues to be high given the influence of primary PM emissions at urban sites.

The mineral matter load in PM_1 (4%) was much more reduced than in $PM_{2.5}$ (16%). Around 80% of the carbonaceous material present in $PM_{2.5}$ continued to be found in PM_1. However, concentrations of SIA (especially nitrate levels) were reduced by 30% in PM_1 with respect to $PM_{2.5}$. Thus, the $PM_{1-2.5}$ fraction was made up of mineral dust (37%) and SIA (38%), with a fraction of carbonaceous matter (21%). The PM_1 fraction was predominantly made up of OM+EC (48%), SIA (32%) and minor proportions of mineral dust and sea spray.

It is important to highlight that the composition of the PM_{10} and $PM_{1-2.5}$ fractions is very similar (Figure 4.1.16) suggesting that $PM_{2.5}$ still contains a high proportion of what is generally considered as the coarse fraction. Moreover, the composition of $PM_{2.5-10}$ and PM_{1-10} are also similar. These results indicate that the simultaneous measurement of PM_{10} and PM_1 is probably a more interesting strategy for the study of air quality than the measurement of PM_{10} and $PM_{2.5}$. Accordingly, the fraction PM_1 is more influenced by combustion sources and the fraction PM_{1-10} by other non-combustion sources.

The unaccounted fraction was a 12, 13 and 14% of the PM_{10}, $PM_{2.5}$ and PM_1 mass respectively. Unaccounted material is attributed to adsorbed and composition water and is usually correlated with a higher content in hygroscopic compounds. The proportion of unaccounted mass increased from coarser to finer fractions (Figure 4.1.17), as the proportion of hygroscopic compounds in the fraction (ammonium sulphate and organic matter) increased.

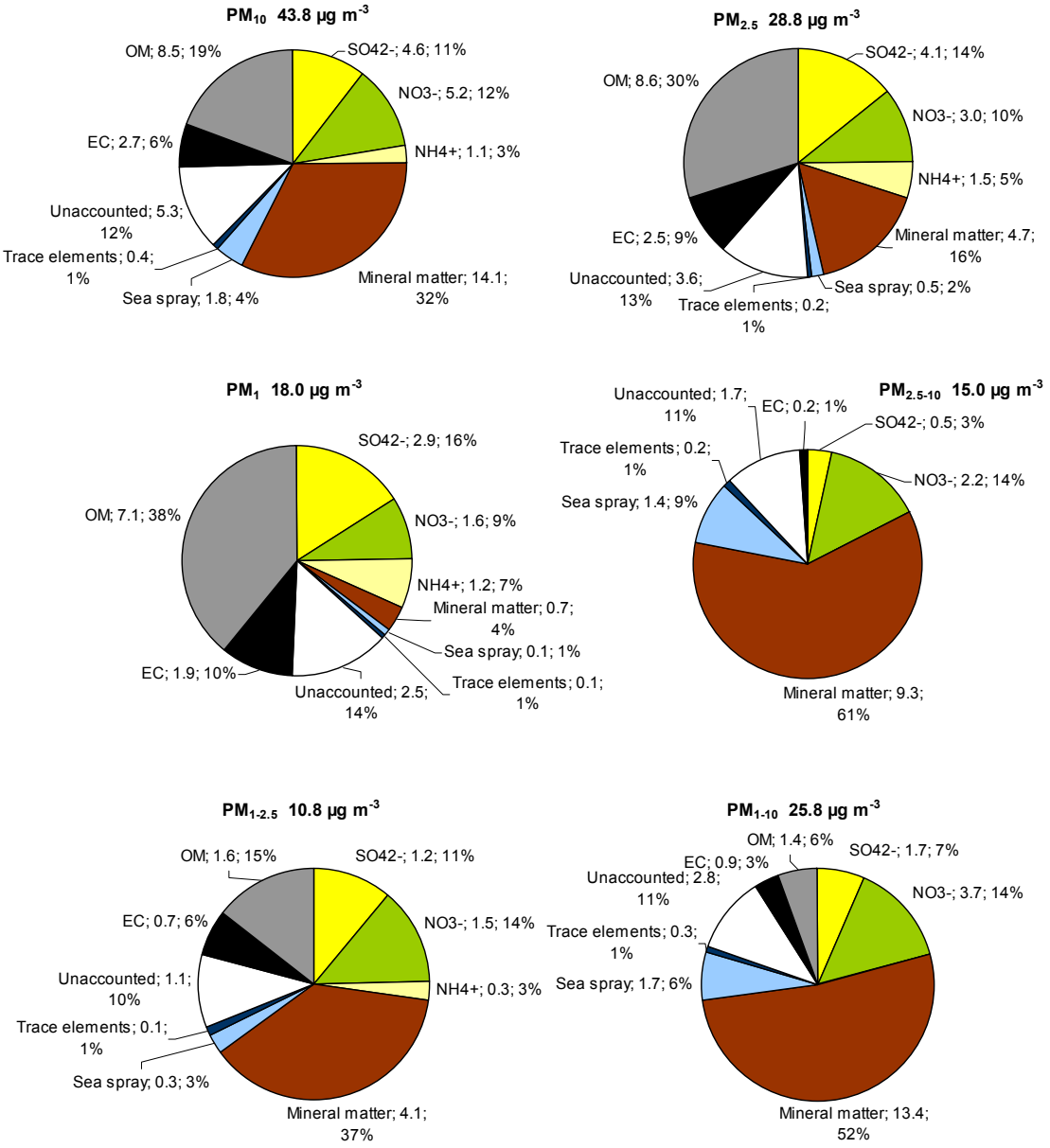

Figure 4.1.16. Mean composition of PM_{10}, $PM_{2.5}$, PM_1, $PM_{2.5-10}$, $PM_{1-2.5}$ and PM_{1-10} measured at the BCN-CSIC site, from October 2005 to December 2007.

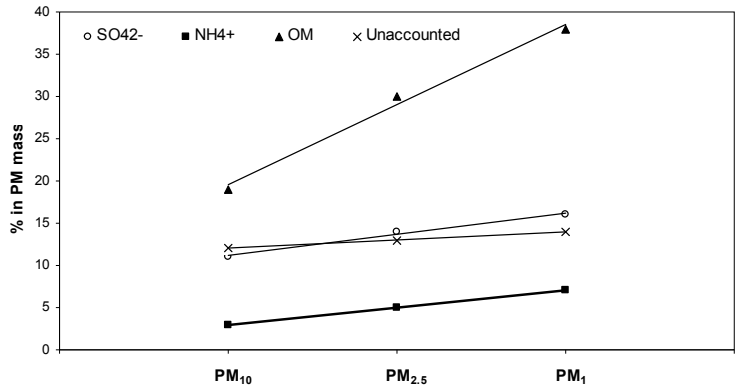

Figure 4.1.17. Variation of the % of SO_4^{2-}, NH_4^+ and OM and the unaccounted fraction in PM_{10}, $PM_{2.5}$ and PM_1.

In conclusion, PM_1 is mainly composed of carbonaceous compounds (OM+EC) and secondary inorganic aerosols (SIA), representing combustion sources and PM_{1-10} is mainly composed of mineral matter, sea spray, with some contribution of coarse SIA and OM+EC, representing other sources non-related with combustion. PM_{10} and $PM_{2.5}$ are the parameters that are currently monitored in air quality networks. However correlations and speciation studies show that $PM_{2.5}$ is a mixture of sources (combustion and non-combustion) while when monitoring PM_1 and PM_{10} these sources might be separated. Therefore, a good sampling strategy for air quality monitoring may include PM_1 and PM_{10} (thus PM_1 and PM_{1-10}) parameters as they vary in relation with different emission sources and processes that could then be monitored separately.

Mineral matter is mainly coarse, although it is still present in $PM_{2.5}$ in significant amounts. The partitioning of mineral matter (Figure 4.1.18) was 5/29/66% for $PM_1/PM_{1-2.5}/PM_{2.5-10}$, respectively. As stated above, the high mineral dust load in Barcelona arises mainly from anthropogenic emissions, such as road dust resuspension, demolition and construction. Dust accumulation on roads is favoured by the relatively long periods without rain in this region. A lower contribution is attributed to African dust events and natural resuspension from arid soils, but as previously stated the contribution may be very high during these episodes.

S*ea spray* is mainly coarse. The partitioning was 8/17/75% for $PM_1/PM_{1-2.5}/PM_{2.5-10}$, respectively. A significant fraction is still present in $PM_{2.5,}$ but markedly diminished in PM_1.

Carbonaceous material (OM+EC) was mainly present in the fine fraction (80/20/0% in the $PM_1/PM_{1-2.5}/PM_{2.5-10}$ fractions respectively). In this urban environment, the carbonaceous material is mainly anthropogenic, emitted by road traffic and in a minor proportion by power stations, specific industrial processes, biomass combustion and biogenic emissions. Regarding OC and EC partitioning, the percentages obtained were 82/18/0% for OC and 69/25/6% for EC in the $PM_1/PM_{1-2.5}/PM_{2.5-10}$ fractions respectively.

Sulphate was distributed among the fractions with a fine grain size (63/26/11% in the $PM_1/PM_{1-2.5}/PM_{2.5-10}$ fractions, respectively) as a consequence of the prevalence of ammonium sulphate (fine aerosols) versus the coarser Ca, Na or Mg sulphate species.

Nitrate was distributed among the three PM fractions with a shift towards the coarse fraction (30/28/42% in $PM_1/PM_{1-2.5}/PM_{2.5-10}$, respectively). The fine size fraction is due to the presence of fine ammonium nitrate, but coarser Na and Ca nitrates also occur in appreciable levels.

Ammonium showed a fine size distribution (81/18/1% in the $PM_1/PM_{1-2.5}/PM_{2.5-10}$ fractions respectively) as a consequence of the fine grain size of ammonium sulphate and nitrate. Most of the ammonium present in PM_{10} also falls in the $PM_{2.5}$ range. On occasions lower concentrations are observed in PM_{10} than in $PM_{2.5}$. This behaviour was observed in urban areas and has been attributed to a negative sampling artefact due to the volatilization of NH_4Cl by the reaction of NH_4NO_3 with NaCl on the PM_{10} filter (Querol et al, 2001).

The *unaccounted mass* followed a size distribution similar to that reported for nitrate (48/21/31% in $PM_1/PM_{1-2.5}/PM_{2.5-10}$, respectively). These species are hydrophilic and tend to accumulate water (the main cause of the unaccounted mass).

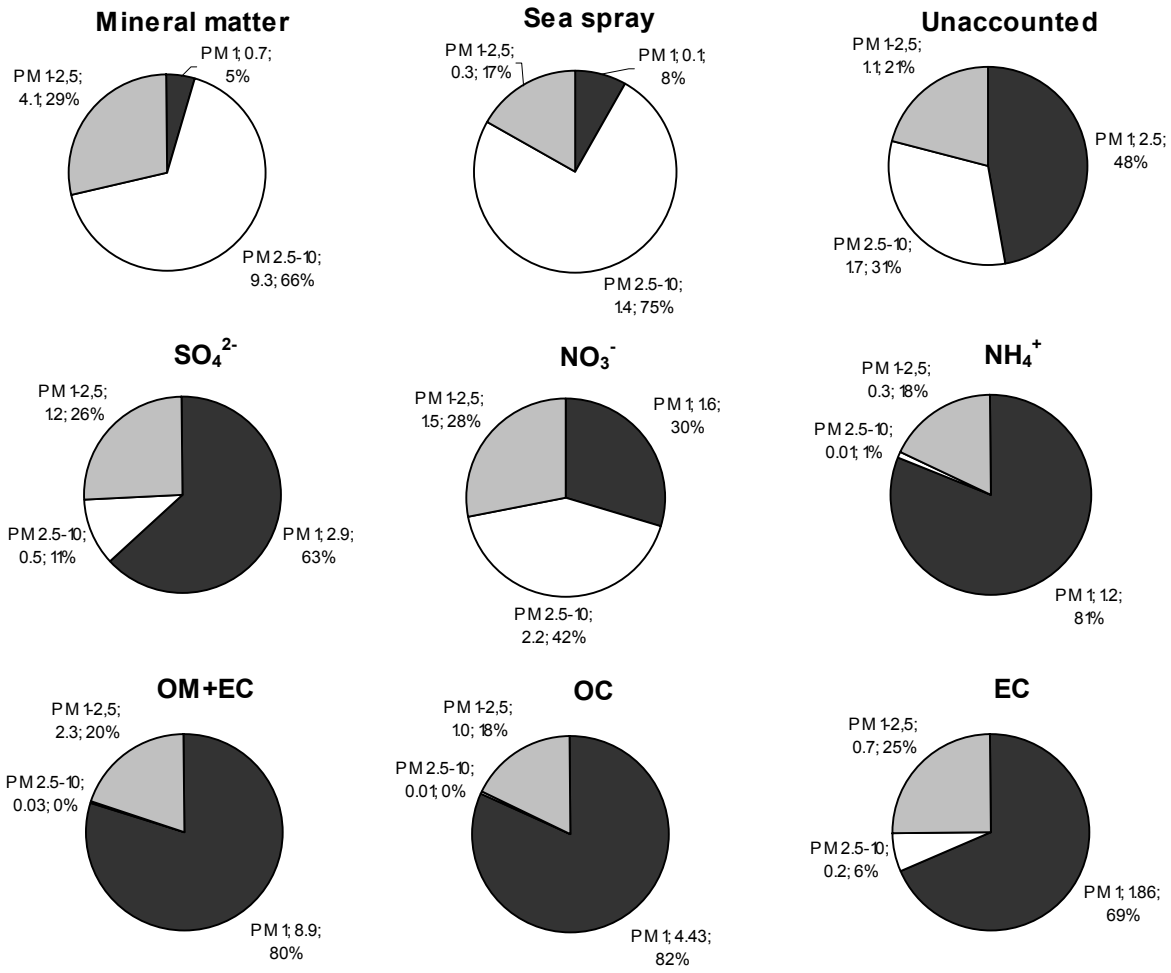

Figure 4.1.18. Partitioning of major PM components between the fractions $PM_{2.5-10}$, $PM_{1-2.5}$ and PM_1 at the BCN-CSIC site, from October 2005 to December 2007.

4.1.3.2. Carbonaceous compounds: estimation of primary and secondary organic aerosols

The contribution of primary (POA) and secondary (SOA) organic aerosols to the total OM concentration were estimated by the EC trace method (Salma et al., 2004), modified according to criteria applied by Docherty et al. (2008). This method is based in the evaluation of primary organic carbon (POC) using EC as a tracer. The ratios OC/EC observed vary usually from lower values, attributed to POC and EC emissions recorded near emission sources, to higher values, attributed to secondary organic carbon (SOC) when secondary organic aerosols are formed in the atmosphere by photochemical oxidation reactions.

This POC/EC ratio is generally calculated from the minimum ratio obtained on the OC/EC plot (Figure 4.1.19). However, calculations for ½*(POC/EC) ratios will also be presented, as some experimental results (de Gouw and Jiménez, 2009) indicate that this ratio could be lower at urban backgrounds because of the difficulty to account for the rapid formation of SOA or small amounts of background SOA.

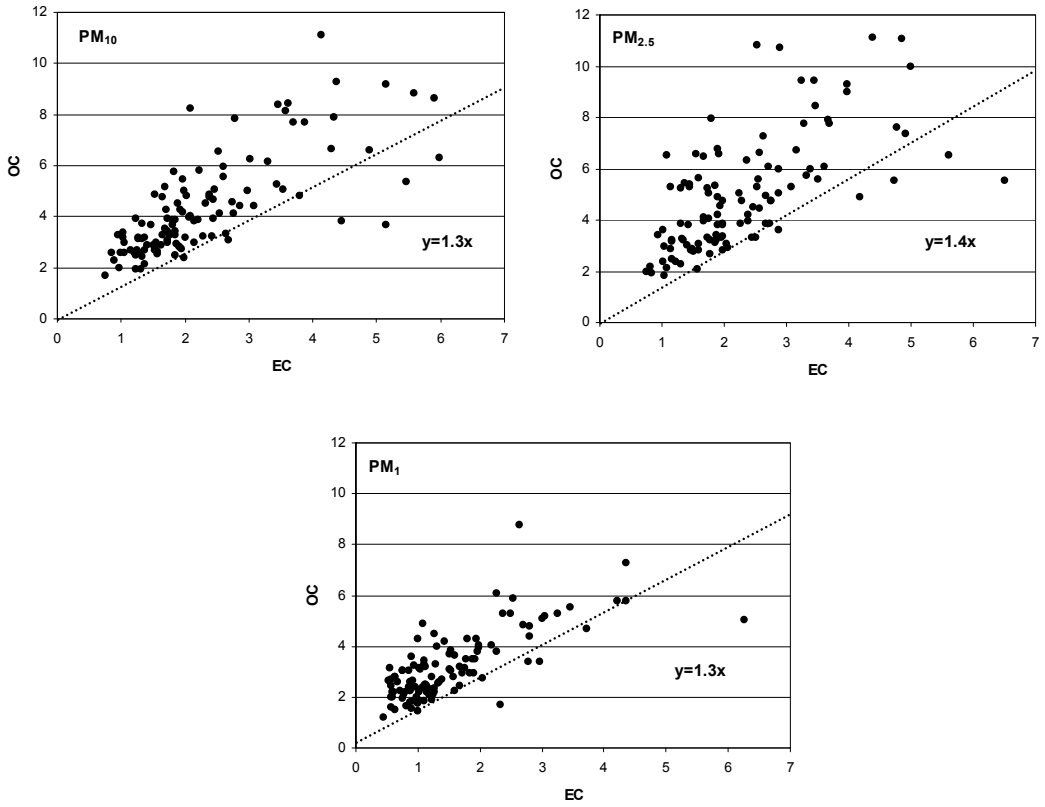

Figure 4.1.19. OC/EC primary ratios in PM_{10}, $PM_{2.5}$ and PM_1 in BCN-CSIC.

From this primary ratio $(POC/EC)_p$, primary and secondary organic carbon fractions were calculated using the following equations:

Primary organic carbon: $POC = (POC/EC)_p * EC$

Secondary organic carbon: $SOC = OC - POC$

In addition, experimental results (Mohr et al., 2009) indicate that in order to account for the presence of oxygen, nitrogen or hydrogen in the organic compounds the carbonaceous fractions calculated may be multiplied by the following factors:

Primary organic aerosols: POA =POC*1.2

Secondary organic aerosols: SOA=SOC*1.9

The results obtained from these calculations using the $(POC/EC)_p$ ratio and ½*$(POC/EC)_p$ are shown in Table 4.10, indicating that approximately between 40-80% of the OM registered at BCN-CSIC urban background is made of SOA (secondary organic compounds) formed in the atmosphere from volatile organic compounds (VOCs), depending on the criteria selected for the calculation of the POC/EC ratio.

Therefore, the carbonaceous fraction (OM+EC) is composed by 22-25% EC, 27-32% SOA and 38-40% POA, as measured and calculated for PM_{10}, $PM_{2.5}$ and PM_1 fractions (Table 4.10 and Figure 4.1.20), obtaining very similar proportions in all fractions, as OM+EC is mainly fine in size (80% of the OM+EC mass is in PM_1). Conversely, when considering the $PM_{2.5-10}$ and $PM_{1-2.5}$ fractions the proportions differ. In the $PM_{2.5-10}$ fraction 50% of the OM+EC is due to SOA and 44% to EC, with only 3% POA, however, the mass contribution of this fraction is very low (0.3 μg m^{-3}). To conclude, the fine fraction (PM_1), which contain 80% of the OM+EC is composed by 22, 38 and 32% EC, POA, and SOA, respectively, and the coarse fraction (PM_{1-10}) 34, 41 and 14% EC, POA and SOA, respectively. Thus, primary organic aerosols were emitted in both coarse and fine fractions in similar proportions but the proportion of secondary organic aerosols decreases in the coarse fraction, increasing the proportion of EC.

Table 4.10. Total carbon (TC=OC+EC), EC, OC and OM mean levels measured in PM_{10}, $PM_{2.5}$ and PM_1 and the fractions $PM_{1-2.5}$, $PM_{2.5-10}$ and PM_{1-10} from 2003 to 2007. Levels of the POA and SOA fractions calculated for the minimum $(POC/EC)_p$ and ½*$(POC/EC)_p$.

					$(POC/EC)_p$		½*$(POC/EC)_p$	
μg m^{-3}	TC	EC	OC	OM	POA	SOA	POA	SOA
PM_{10}	8.0	2.8	5.2	8.4	4.3	3.2	2.1	6.6
$PM_{2.5}$	7.7	2.6	5.2	8.3	4.3	3.0	2.2	6.4
PM_1	6.3	2.0	4.3	6.9	3.4	2.8	1.7	5.5
$PM_{1-2.5}$	1.4	0.6	0.9	1.4	0.9	0.2	0.5	0.9
$PM_{2.5-10}$	0.3	0.2	<0.1	0.1	<0.1	0.2	<0.1	0.2
PM_{1-10}	1.7	0.8	0.9	1.5	0.9	0.4	0.5	1.1

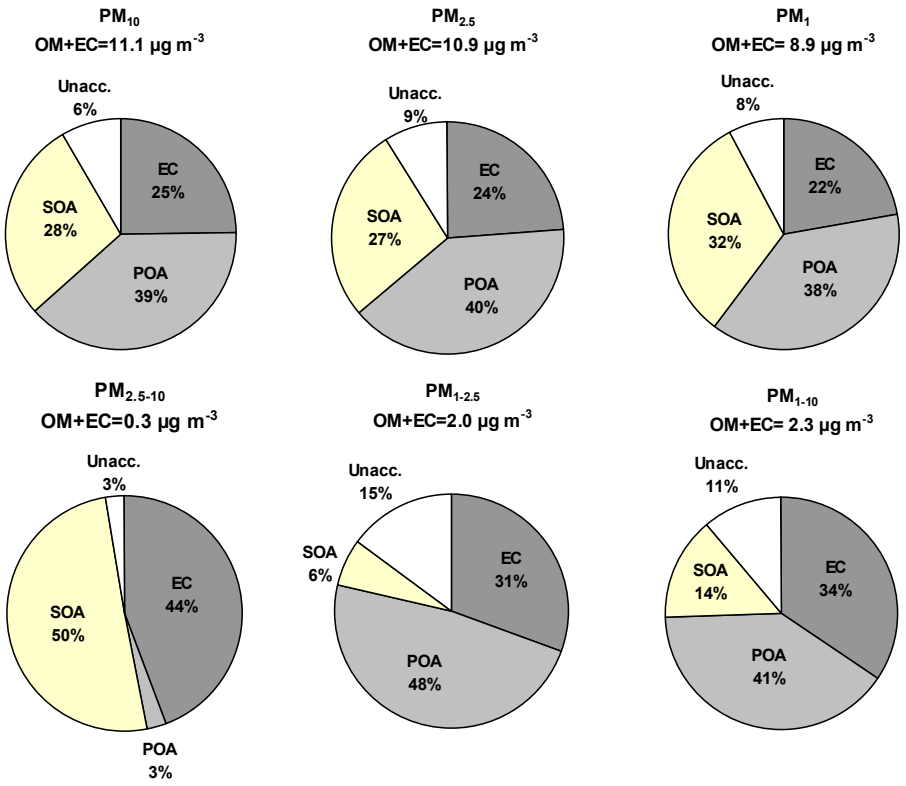

Figure 4.1.20. OM+EC composition in PM_{10}, $PM_{2.5}$ and PM_1 and the fractions $PM_{2.5-10}$, $PM_{1-2.5}$ and PM_{1-10}, using the $(POC/EC)_p$ ratio for calculations.

The partitioning of POA, SOA and EC between the fractions $PM_{2.5-10}$, $PM_{1-2.5}$ and PM_1 (Figure 4.1.21) shows that all carbonaceous compounds are mainly present in the fine fraction. The contributions of POA were 0/22/78% in $PM_{2.5-10,}$ $PM_{1-2.5}$ and PM_1 respectively, SOA present a partitioning of 6/4/90% in $PM_{2.5-10,}$ $PM_{1-2.5}$ and PM_1, and EC presents a slightly coarser grain size than the organic compounds, with a higher proportion in the coarser size ranges (6/22/72% in $PM_{2.5-10,}$ $PM_{1-2.5}$ and PM_1) when compared with POA and SOA.

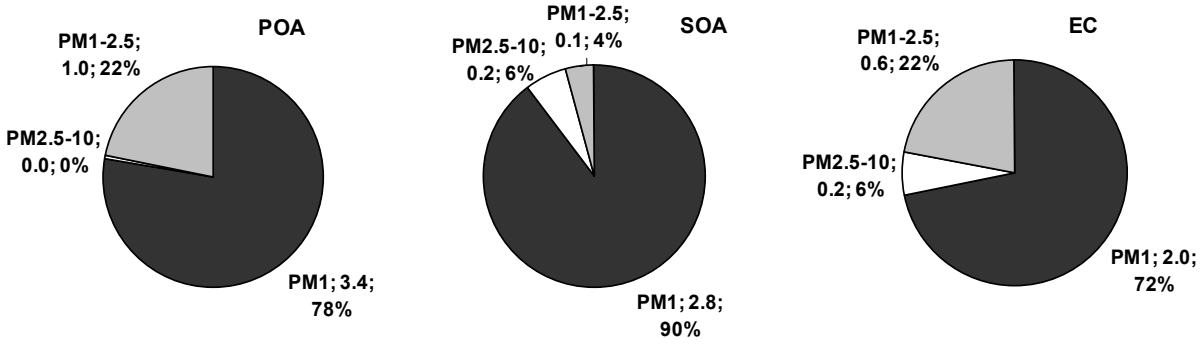

Figure 4.1.21. Partitioning of POA, SOA and EC between the fractions $PM_{2.5-10}$, $PM_{1-2.5}$ and PM_1.

When comparing the results obtained at BCN-CSIC to results obtained at other European urban backgrounds using the EC tracer method the SOA contribution to OM varies widely (Table 4.11). The highest %SOA (72-77%) were calculated at Barcelona (calculation using minimum $(POC/EC)_p$ ratios) and Milano (summer data), and the lowest in Santiago de Chile (6-20%). The rest of the data reported were between 35-55%. Variation of % SOA between studies was high owing to the differences on the application of the method (e.g. selection of $(POC/EC)_p$ ratio), characteristics of the monitoring site and meteorological factors.

Table 4.11. Summary of results obtained by the EC tracer method at Barcelona and other urban sites in Europe. Ratio $(POC/EC)_p$, %POA and %SOA fractions in the total OM in $PM_{2.5}$.

$(POC/EC)_p$	POA (%)	SOA (%)	Urban sites	Reference
0.7-1.4	26-52	36-77	Barcelona	This work
1.56-1.6	80-94	6-20	Santiago de Chile	Seguel et al., 2009
0.84		35	Madrid (summer)	Plaza et al., 2006
1.02		55	Madrid (winter)	Plaza et al., 2006
1.1-2.9		37-46	Budapest	Salma et al., 2004
0.67	14	72	Milano (summer)	Lonati et al., 2007

The levels of carbonaceous compounds calculated at BCN present a marked seasonal trend (Figure 4.1.22). OM and EC present higher levels during winter months, as a result of the intense winter local and regional pollution events favoured by atmospheric anticyclonic conditions, and lower levels during the summer owing to the favoured dilution processes driven by sea-land breezes and the regional recirculation of air masses. Regarding the calculated primary and secondary organic aerosols, during the winter the levels of POA exceed SOA during some periods but the opposite occurred during other periods. The fact that POA>SOA may be attributed to Atlantic advective conditions, when strong winds allow the renovation of air masses and thus primary organic aerosols are measured at the source but secondary organic compounds are not formed near the VOCs source area. Conversely, during some winter episodes SOA> POA, probably due to the atmospheric stagnation of air masses that avoid the dispersion of pollutants, and consequently secondary organic aerosols are formed near the VOCs source areas and the levels measured increase. During the summer months levels of POA and SOA are generally lower, because of the dispersion of pollutants by breezes, as explained above. However, the formation of SOA is favoured by the higher insolation and O_3 concentration levels during the summer.

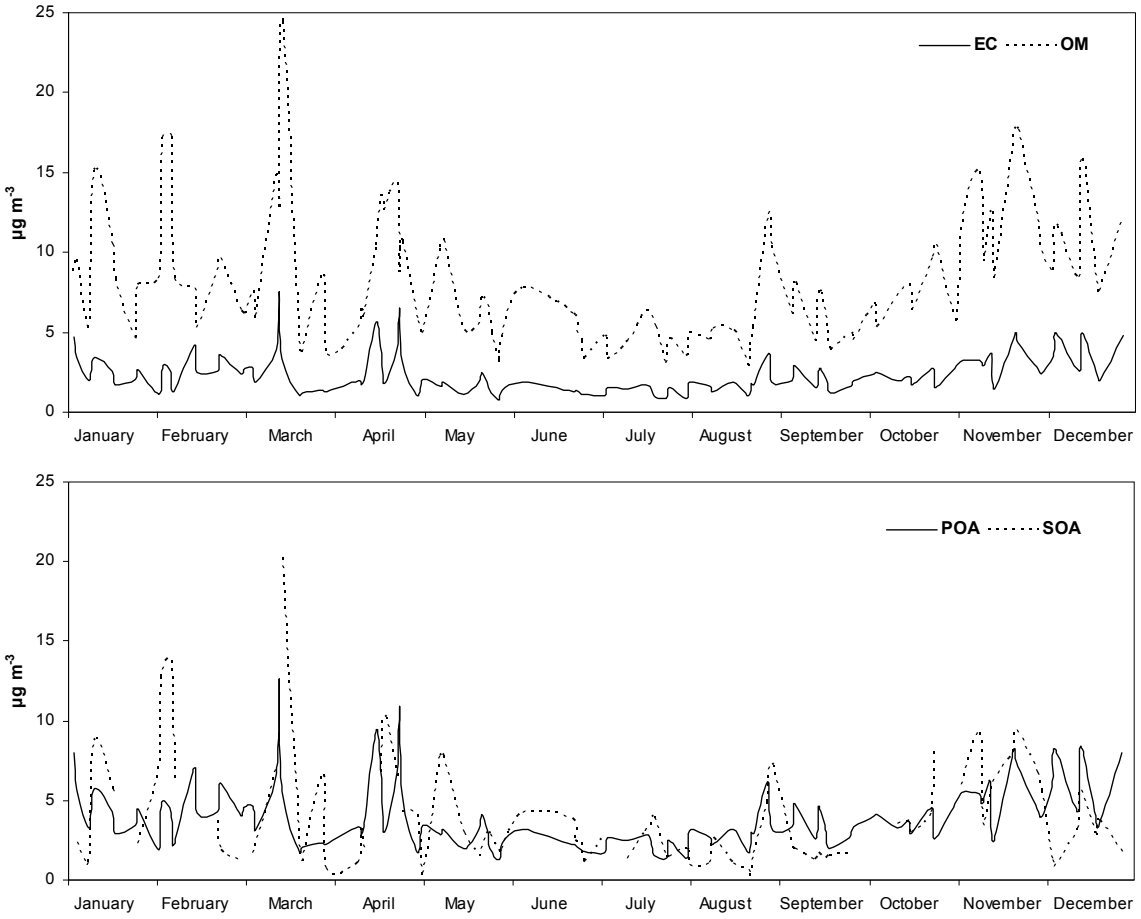

Figure 4.1.22. Seasonal variability of OM and EC measured in $PM_{2.5}$ and the calculated POA and SOA during 2007.

4.1.3.3. Trace elements

The mean levels of trace elements (including metals) measured at Barcelona-CSIC in 2003-2007, at Sagrera in 2001 and at L'Hospitalet in 1999-2000 are shown in Table 4.12. The elements studied do not present a large time and spatial variation in the Barcelona metropolitan area, with a few exceptions such as Zn (higher contents in L'Hospitalet) and Pb (higher contents before 2001 when unleaded petrol became obligatory).

Table 4.12. Mean levels of trace elements in PM_{10}, $PM_{2.5}$ and PM_1 registered at Barcelona urban sites between 1999 and 2007.

	PM_{10}			$PM_{2.5}$			PM_1
ng m^{-3}	CSIC [a] 2003-2007	Sagrera [b] 2001	L'Hospitalet [c] 1999-2000	CSIC [a] 2003-2007	Sagrera [b] 2001	L'Hospitalet [c] 1999-2000	CSIC [d] 2005-2007
Li	0.7	0.7		0.3	0.2		0.1
P	29	32	44	14	19	30	7
Ti	46	84	54	17	26	16	2
V	12	15	13	9	10	9	7
Cr	6	8	6	3	3	6	1.4
Mn	20	23	24	10	10	14	4
Co	0.4	0.4		0.2	0.3		0.1
Ni	5	7	7	4	5	6	3
Cu	71	49	74	36	31	52	11
Zn	97	98	263	68	55	191	36
As	1.0	1.5		0.7	1.0		0.5
Se	0.8	1.1		0.5	0.8		0.3
Rb	1.3	1.8		0.6	0.7		0.2
Sr	6	6	7	2	2	4	0.8
Cd	0.4	0.7		0.4	0.6		0.2
Sn	7	4		4	4		2
Sb	6	10		3	4		0.8
Ba	30	41	38	13	9	23	11
La	0.4	0.6		0.2	0.2		0.1
Ce	1.0	1.3		0.4	0.5		0.2
Tl	0.3	0.3		0.2	0.3		0.1
Pb	23	58	149	18	40	130	11
Bi	0.6	0.4		0.4	0.2		0.2
Th	0.1	0.3		0.1	0.2		0.1
U	0.1	0.2		0.1	0.3		0.1

[a]Annual means, Querol et al. (2004 and 2007), Pey (2007) and this work. [b]Annual means, Viana (2003) and Querol (2004 and 2007). [c]Annual means, Querol et al. (2001a), Rodríguez (2002) and Rodríguez et al. (2003). [d]Annual means, this work.

The levels of trace elements did not exceed the limit and target values of the CE standards (2008/50/EC and 2004/107/EC). However, as shown in Figure 4.1.23, the levels of V and Ni (mainly due to fuel oil combustion) and Mn, Cu, Zn, Sb and Li (mainly attributed to road dust) recorded in Barcelona are in the upper range of the concentrations registered at urban background sites with low industrial influence in Spain (Querol et al., 2007).

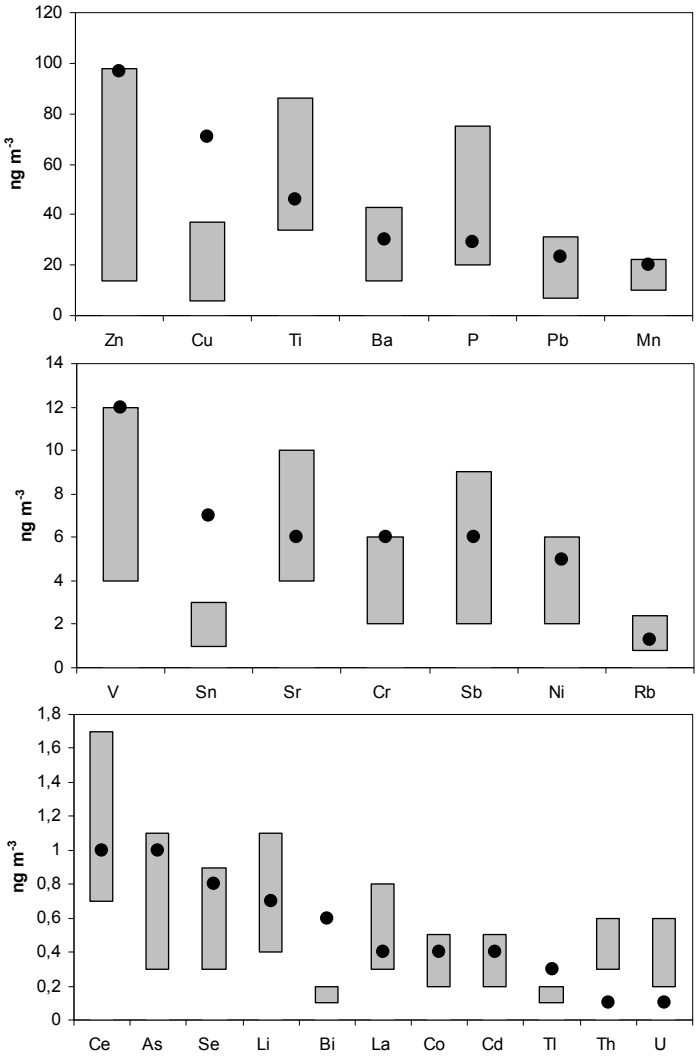

Figure 4.1.23. Mean levels of trace elements in PM_{10} at the BCN-CSIC site for 2003-2007 compared with the concentration ranges registered at other urban background sites in Spain (Querol et al., 2007).

The trace elements showed a clear partitioning between the PM_{1-10} and the PM_1 fraction, probably reflecting the origin of some of these elements. Figure 4.1.24 shows the ratios PM_1/PM_{10} and $PM_{2.5}/PM_{10}$ for the elements analysed. Elements associated with fossil fuel combustion (V, Ni) or other high temperature industrial processes (As, Cd, Pb and U) occur in very fine particles (50 to 70% in the PM_1 fraction). Other elements usually associated with mineral matter emitted by road dust, construction and/or demolition, such as Ti, Li, Rb, Sr, La, Ce, P, and Th, or with road traffic abrasion products (mainly from tires and brakes) such as Sb, Cu, Mn, Cr, Co, Sn, Tl, Ba, Bi, Se, and Zn, (Wahlin et al., 2006, Schauer et al., 2006) tend to accumulate in the coarse mode (60 to 95% in the fraction PM_{1-10}).

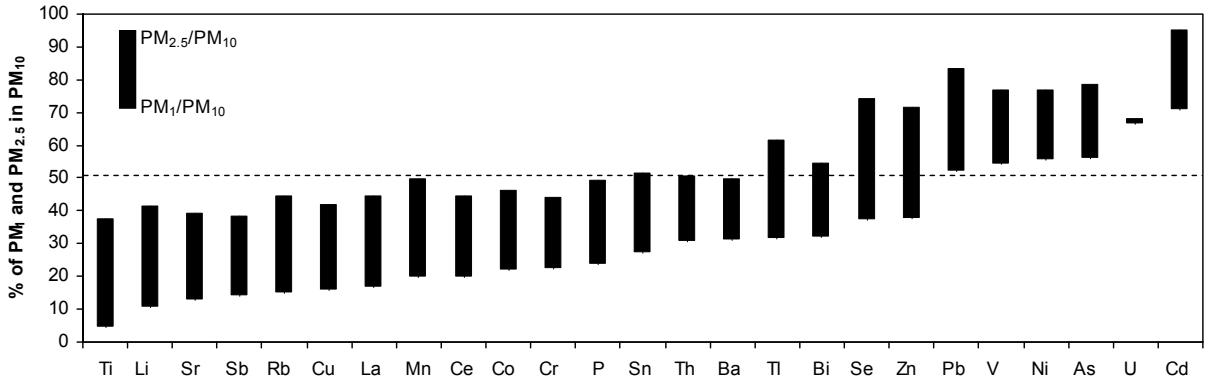

Figure 4.1.24. Mean $PM_{2.5}/PM_{10}$ and PM_1/PM_{10} ratios for levels of trace elements at the BCN-CSIC site, from October 2005 to December 2007.

4.1.3.4. Seasonal evolution of PM components

PM components measured at Barcelona show a clear seasonal trend. Annual cycles of the major PM_{10} and $PM_{2.5}$ components measured from April 2003 to December 2007 and PM_1 components measured from October 2005 to December 2007 at BCN-CSIC are shown in Figure 4.1.25. Mann-Kendall test applied to annual means did not show any significant trend for any of the main components.

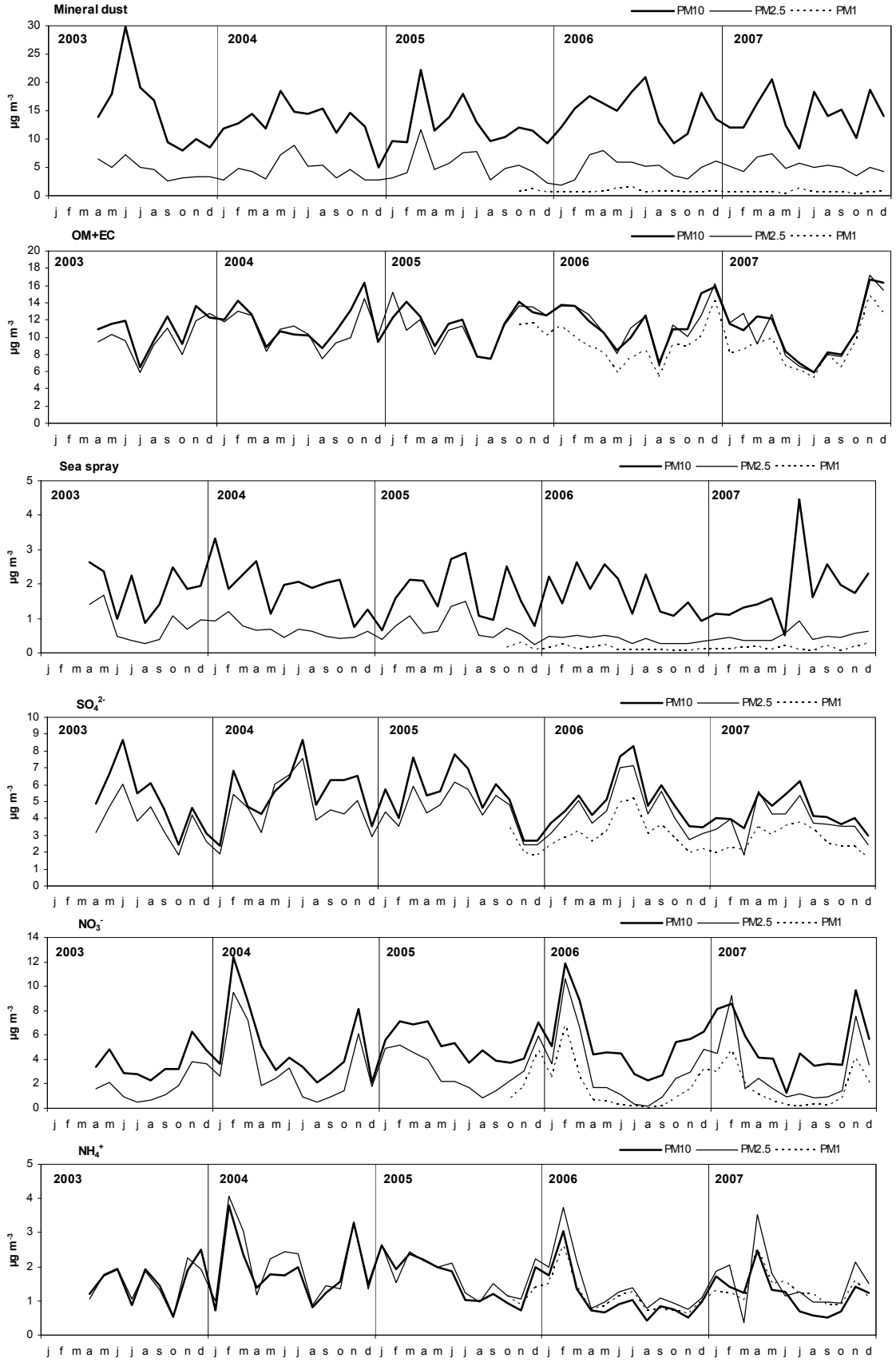

Figure 4.1.25. Annual cycles of the major PM_{10}, $PM_{2.5}$ and PM_1 components measured at BCN-CSIC from 2003 to 2007.

The mineral matter presents a clear seasonal trend and is usually associated to the frequency and intensity of African dust outbreaks and also to meteorology (mainly lack of precipitation). During the winter the levels of crustal material are usually lower because of the lower wind speed, higher humidity and precipitations that prevent dust resuspension. High levels are also registered in March during some years and are related to the frequent occurrence of African dust outbreaks during this month. In April mineral matter levels decrease again due to the high frequency of precipitations during this month. The levels of crustal material are high during all the summer (May, June and July) associated to a higher resuspension of road dust because of a lower precipitation rate and also to the high frequency of African dust outbreaks during this period of the year. In August and September the levels decrease because of the lower road traffic intensity (August holidays) and the occurrence of precipitations (September).

The carbonaceous compounds (OM+EC) present the maximum levels during the winter months, associated to the strong pollution episodes recorded in this period of the year due to the atmospheric stability. The minimum levels are presented in April, related to the higher precipitation rates, and August, because of the lower traffic intensity during this month.

The seasonal evolution of sea spray levels shows a different pattern depending on the year considered. Its variability may be associated to enhanced sea-land breezes during the summer and intense Atlantic advections transporting sea spray during the winter, and depend on the main atmospheric scenarios occurring during the year. However, the ratio Cl/Na presented higher levels during the winter than during the summer. This may be attributed to the thermal instability of ammonium nitrate. During the summer the nitric acid/ammonium nitrate is high and nitric acid may interact with the abundant sodium chloride and cause the loss of volatile HCl (Harrison and Pio, 1983; Mamane and Mehler, 1987).

Sulphate presents maximum levels during the summer months. It is related to the higher oxidation rate of the SO_2 due to a stronger insolation and thus a higher photochemical activity during summer months (Hidy, 1994).

Nitrate levels show a seasonal evolution opposite to sulphate. The levels are maximum in winter and minimum in summer. This behaviour is due to the thermal instability of ammonium nitrate that gives rise to gaseous nitric acid and ammonia (Warneck, 1988).

HNO_3 may then react with coarse fraction particles forming coarse calcium, sodium or magnesium nitrate compounds (Harrison and Pio, 1983; Zhuang et al., 1999). As a result, a different grain size distribution can be distinguished with finer nitrate during the winter months and coarser during the summer months. This is a consequence of the prevalence of ammonium nitrate in the winter, with a fine size distribution, and the formation of coarser nitrate compounds during the warmer months.

Ammonium levels present a seasonal evolution parallel to nitrate. High levels during the winter months are observed associated to the stability of ammonium nitrate. During the warmer months ammonium nitrate is not stable and the formation of gaseous ammonia and nitric acid prevails over ammonium nitrate (Warneck, 1988; Mészáros, 1999).

4.1.3.5. Day to day variability: PM episodes

Air mass origin and atmospheric conditions influence decisively the composition of atmospheric aerosols (Table 4.13 and Figure 4.1.26). African dust outbreaks and European air mass transport supply new particles to the atmosphere. Other episodes may clean the atmosphere, as Atlantic advections and other episodes associated to precipitations and winds, which renovate air masses. $PM_{2.5-10}$, $PM_{1-2.5}$ and PM_1 fractions mean levels classified by air mass episodes show that episodes registering higher PM levels account for the highest concentrations of most elements (Table 4.13 and Figure 4.1.26). North African dust outbreaks register the highest $PM_{2.5-10}$ levels, the highest mineral dust and sulphate levels for all the fractions and the highest nitrate levels in the coarse fraction ($PM_{2.5-10}$). Relatively high PM_1 levels are also recorded under African episodes. European episodes register also high PM_1 levels, the highest NH_4^+ levels in PM_1 and the highest OM+EC levels in $PM_{2.5-10}$ and PM_1. Winter anticyclonic episodes register the highest $PM_{1-2.5}$ levels, ammonium levels and OM+EC in $PM_{1-2.5}$ and also the highest nitrate levels in $PM_{1-2.5}$ and PM_1. Regional recirculations register the highest levels of sea spray, although the difference among African episodes and Atlantic advections are not very significant. Atlantic and Mediterranean advections register lower PM levels and the levels of all components are lower.

Table 4.13. Mean components measured in PM_{10}, $PM_{2.5}$ and PM_1 during Atlantic advections (ATL), African dust outbreaks (NAF), Mediterranean (MED) and European (EU) air mass origins, regional recirculations (REG) and winter anticyclonic episodes (WAE).

	ATL	NAF	MED	EU	REG	WAE
Annual frequency (%days/year)	49	17	3	10	13	8
$PM_{2.5-10}$						
µg m^{-3}	12	**22**	11	13	15	15
SO_4^{2-}	0.5	**0.8**	0.5	0.4	0.5	0.3
NO_3^-	1.8	**3.3**	2.1	1.9	2.5	2.2
NH_4^+	<0.01	<0.01	<0.01	<0.01	<0.01	<0.01
Mineral dust (%)	8	**16**	5	8	11	8
Sea spray (%)	1.3	1.6	1.1	1.0	**1.8**	1.1
OM+EC (%)	<0.01	<0.01	<0.01	**0.5**	<0.01	0.3
Trace elements (%)	0.1	0.2	0.1	0.2	0.1	0.2
Unaccounted (%)	0.5	1.3	1.4	1.4	<0.01	2.4
$PM_{1-2.5}$						
µg m^{-3}	9	13	8	10	10	**15**
SO_4^{2-} (%)	0.8	**1.8**	1.7	1.3	1.4	1.5
NO_3^- (%)	1.1	1.3	1.0	1.6	0.6	**3.2**
NH_4^+ (%)	0.2	0.2	0.5	0.5	0.1	**0.7**
Mineral dust	4	**6**	2	3	4	5
Sea spray	0.3	0.4	0.3	0.3	0.3	0.4
OM+EC	1.9	2.6	2.2	2.2	2.1	**3.6**
Trace elements	0.1	0.1	0.1	0.1	0.1	0.1
Unaccounted	1.4	0.7	<0.01	0.5	1.1	0.6
PM_1						
µg m^{-3}	15	**21**	12	**21**	17	**20**
SO_4^{2-}	2.0	**4.1**	2.4	3.0	3.9	2.8
NO_3^-	1.4	0.7	0.5	2.6	0.3	**2.9**
NH_4^+	0.9	1.5	0.7	**1.8**	1.0	1.3
Mineral dust	0.7	**0.9**	0.5	0.6	0.8	0.6
Sea spray	0.1	0.1	0.1	0.1	0.1	0.1
OM+EC	8	10	8	**11**	7	10
Trace elements	0.1	0.1	0.1	0.1	0.1	0.1
Unaccounted	1.4	3.9	<0.01	1.8	3.8	2.8

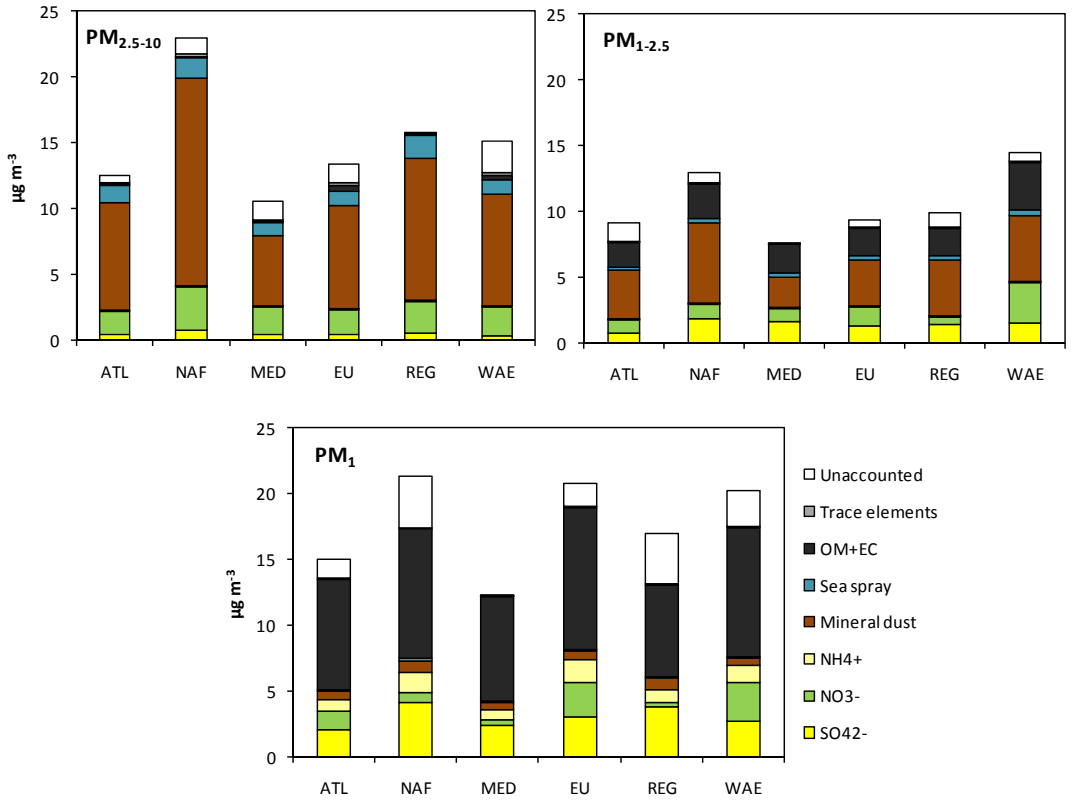

Figure 4.1.26. Mean components measured in $PM_{2.5-10}$, $PM_{1-2.5}$ and PM_1 during Atlantic advections (ATL), African dust outbreaks (NAF), Mediterranean (MED) and European (EU) air mass origins, regional recirculations (REG) and winter anticyclonic episodes (WAE).

The concentration of the main components analyzed for the different episodes was normalized by the respective PM mass fraction concentration for the different episodes in order to be able to identify the main tracers of each episode (Figure 4.1.27 and Table 4.14. PM during Atlantic advections (ATL) showed high concentrations of sea spray (Na and Cl^-) but also high concentrations of some trace elements as Cr, Mn, Cu, Zn, As, Se, Sn, Sb, Pb, Cd and other anthropogenic tracers that may be the consequence of air mass transport through industrial and urban areas. Tracers for African dust outbreaks (NAF) are mineral origin components as Al_2O_3, SiO_2, Ca, Fe, K, Mg, Li, P, Ti, Rb, Sr, Cs, Ba, La or Ce. Mediterranean advections (MED) showed high levels of OM+EC, sulphate, ammonium and sea spray (Na and Cl^-). European episodes (EU) present high levels of anthropogenic components as OM+EC, ammonium and some trace elements as Cu, Sn, Sb or Ba. Regional recirculation (REG) episodes increase the levels of mineral matter (Al_2O_3, SiO_2, Ca, Mg, Li, P, Ti, etc.) but also anthropogenic components as sulphate, V and Ni (tracers of fuel oil combustion). The main components associated to winter anticyclonic episodes (WAE) are nitrate and

ammonium and also some anthropogenic trace elements as Cd and Pb, associated to industrial emissions or Sn and Sb, associated to traffic emissions.

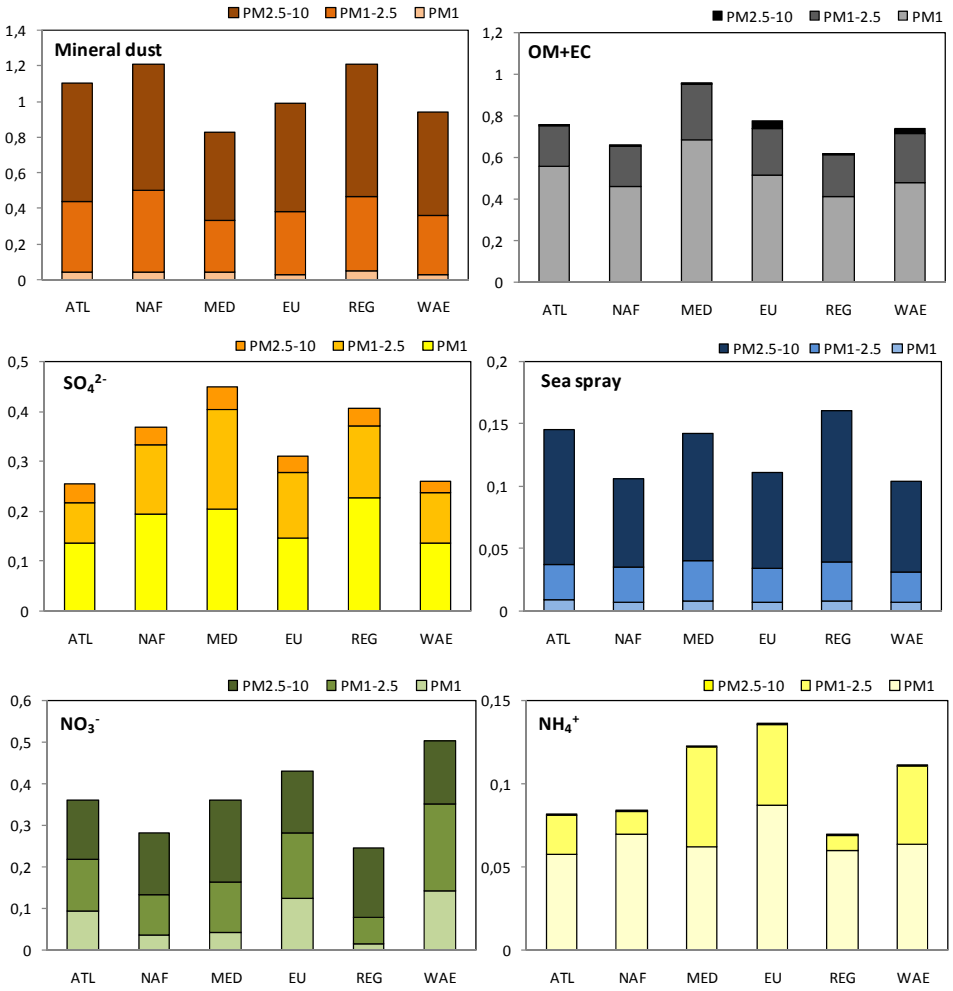

Figure 4.1.27. Mean levels of the main PM components for the different episodes normalized by the respective PM concentration.

Table 4.14. Mean tracers identified in PM_{10} for the main air mass episodes (Atlantic Advections, African dust outbreaks, air mass transport from the Mediterranean and Europe, regional recirculations and winter anticyclonic episodes).

ATL	NAF	MED	EU	REG	WAE
Na, Cl^-, Cr, Mn, P, Cu, Zn, As	Al_2O_3, SiO_2, Ca, Fe, K, Mg, Li, P, Ti, Rb, Sr, Cs, Ba, La, Ce	OM+EC, SO_4^{2-}, NH_4^+, Cl^-, Na, Cd, Co	OM+EC, NH_4^+, NO_3^-, Cu, Sn, Sb, Ba	Al_2O_3, SiO_2, Ca, Mg, Li, Ti, Y, V, Ni, SO_4^{2-}, Na	NO_3^-, NH_4^+, Cd, Pb, Sn, Sb

4.1.4. N and BC: Influence of road traffic emissions on urban atmospheric pollutants

4.1.4.1. N: levels

The levels of sub-micron particle number concentration in the range 13-800 nm were monitored during November 2003 to December 2004 at the BCN-CSIC urban background site by means of a butanol-based condensation particle counter (TSI CPC 3022A; Pey, 2007). After that, particle number concentration in the range 3 nm-1 μm was monitored from June 2005 to June 2007 by means of a water-based condensation particle counter (TSI WCPC 3785). Daily N levels measured from March to November 2003 with a TSI CPC 3022 butanol particle counter in the range >7nm at another urban site on the coast of Barcelona (CREAL, von Klot et al., 2005) were added to the BCN-CSIC dataset to complete the time series. The daily time series plots of the simultaneous N, $PM_{2.5-10}$, $PM_{1-2.5}$ and PM_1 daily levels monitored in Barcelona from 2003 to 2007 and BC levels monitored from July 2007at BCN-CSIC are represented in Figure 4.1.28. The daily time series plots of ambient levels of NO, NO_2, CO, O_3 and SO_2 monitored simultaneously at L'Hospitalet-Gornal are shown in Figure 4.1.29.

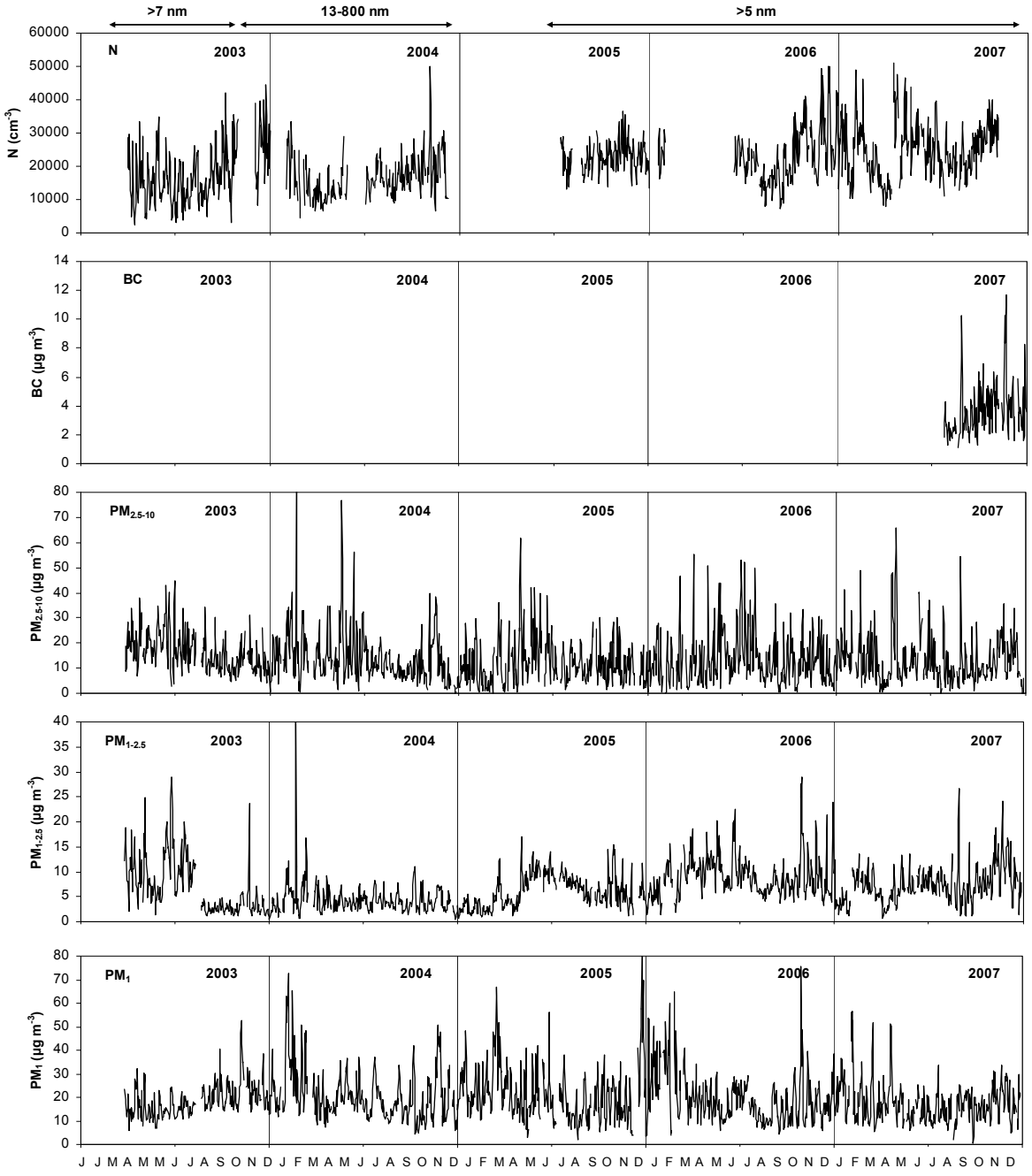

Figure 4.1.28.Mean daily levels of N, BC, $PM_{2.5-10}$, $PM_{1-2.5}$ and PM_1 measured in Barcelona from 2003 to 2007.

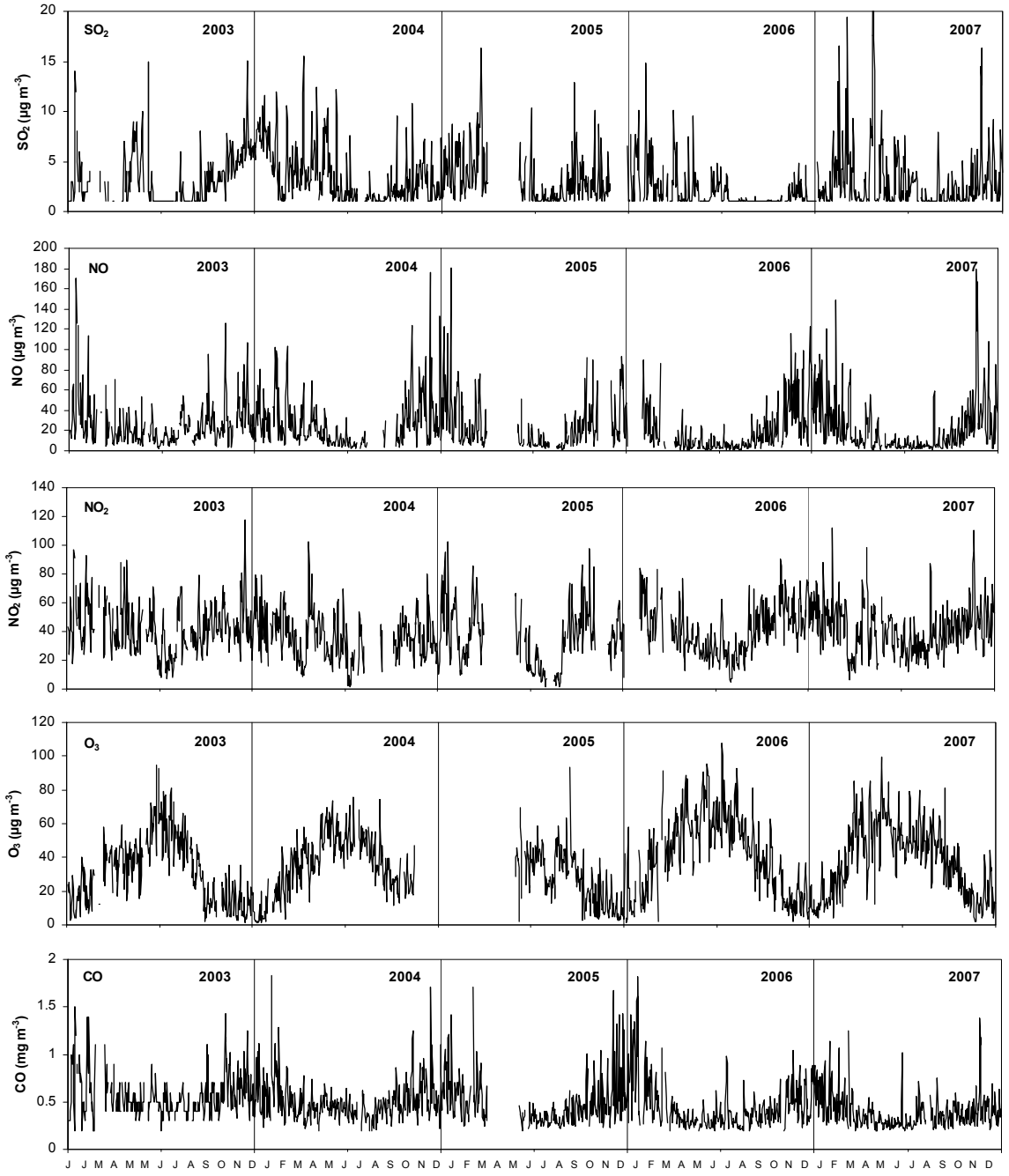

Figure 4.1.29. Mean ambient levels of SO_2, NO_2, NO, O_3 and CO measured at L'Hospitalet-Gornal from 2003 to 2007.

Mean monthly N levels and mean annual N levels (calculated from available daily means) recorded at Barcelona from 2003 to 2007 are presented in Table 4.15. The mean levels registered in Barcelona from 2003 to 2007 were 21000 cm^{-3}. When considering measurements taken only with the butanol-based CPCs (N>7 and 13-800 nm) the annual means for 2003 and 2004 were 16388 and 17800 cm^{-3}, respectively

(Pey, 2007) and when considering only the water-based WCPC (N>5nm) measurements, the annual means from 2005 to 2007 ranged between 22800 and 24800 cm^{-3}. However it must be considered that during 2003, 2005 and 2007 data was not available during 4 to 6 months. The levels obtained using the WCPC are usually higher than the levels obtained with the butanol-based CPC, mainly due to the different size detection limits of each instrument. In addition, N levels measured during 2003 at the CREAL site may be lower because this site is situated on the coast of Barcelona and consequently not exposed to direct road traffic emissions during the day, when the sea-land breeze brings air masses directly from the sea. Nevertheless, N levels measured at Barcelona fall in the mid-high range of those registered at other urban background sites (Figure 4.1.30).

Table 4.15. Mean monthly levels and annual means of particle number concentration recorded at CREAL (April to October 2003) and BCN-CSIC (December 2003 to December 2007).

cm^{-3}	$N_{>7}$	$N_{13\text{-}800}$	$N_{>5}$			Mean monthly levels
	2003	2004	2005	2006	2007	
Data availability (%)	65	64	41	56	79	
January				24315	23797	23958
February		19722			28822	24636
March		13475			17361	15642
April	16630	11232			23258	16873
May	16233	14936			28850	20309
June	14259			23754	26216	20842
July	12060	16383	21862	21064	23879	18762
August	14921	14729	19609	14960	21510	16823
September	17934	17562	22814	17067	23034	19610
October	22877	19538	22792	28695	30268	25025
November		22399	25758	26306	30121	25111
December	26465	15628	22074	30086		25348
Annual means	16388	17782	22825	23309	24790	21000

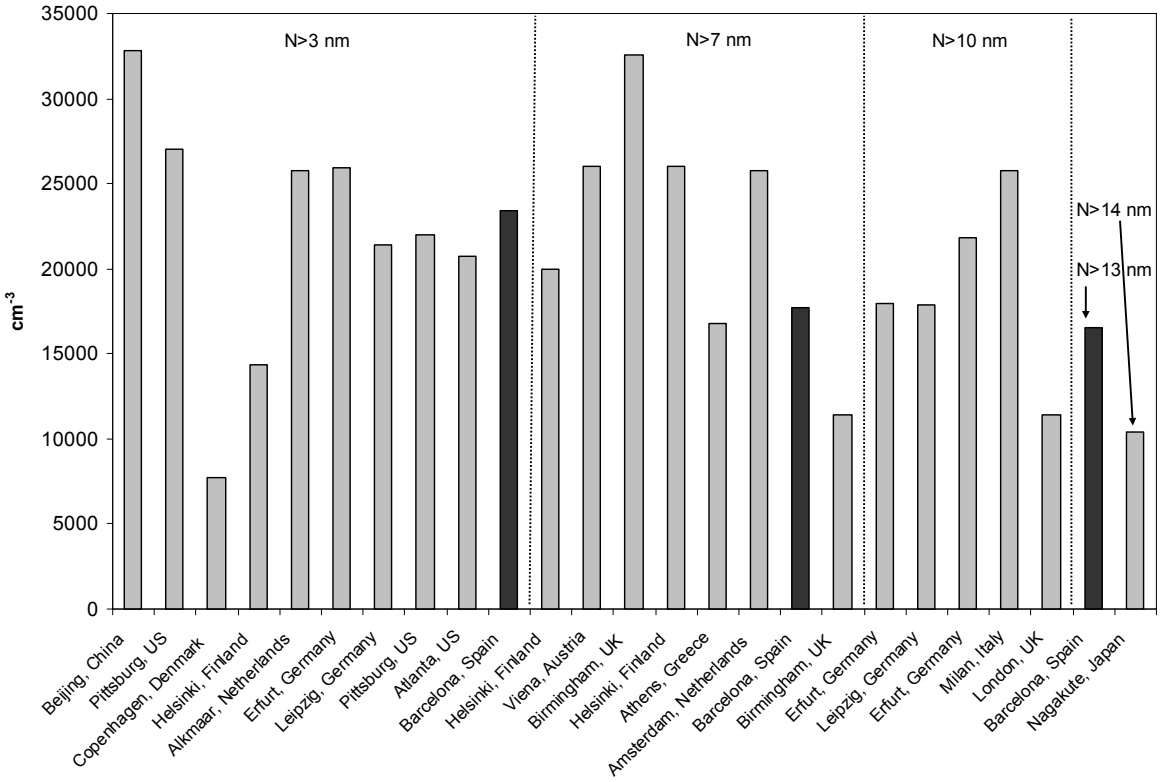

Figure 4.1.30. Comparison of mean N mean levels measured at Barcelona (black bars) with other studies (Harrison et al., 1999; Wichmann et al., 2000; Koponen et al., 2001; Ruuskanen et al., 2001; Woo et al., 2001; Tuch et al., 2003; Wehner and Wiedensohler, 2003; Hauck et al., 2004; Hussein et al., 2004; Ketzel et al., 2004; Stanier et al., 2004; Zhou et al., 2004; Minoura and Takekawa, 2005; Laakso et al., 2006; Pey , 2007; Puustinen et al., 2007; Rodriguez et al., 2007; von Klot et al., 2005; Wu et al., 2008).

4.1.4.2. N: seasonal evolution

The seasonal evolution of N daily means measured in Barcelona in 2003 (N>7nm in CREAL coastal urban site), 2004 (N=13-800 nm in BCN-CSIC) and from 2005 to 2007 (N>5 nm in BCN-CSIC) are shown in Figure 4.1.31. Although monthly levels for a given month may vary widely from year to year (>100%) depending on the meteorology and also on the characteristics of the instrument used (mainly size detection limits), the higher particle number concentrations are observed in general during two periods of the year: The colder months (October to February) and the spring months (May and June). The high N levels recorded during the winter months are probably a consequence of the important pollution episodes identified during this period of the year (WAE). These situations are characterized by atmospheric stability, mild winds and a minimum thickness of the boundary layer (Pey et al., 2008), avoiding the dispersion of polluted air masses. The high anthropogenic emissions (mainly fresh road traffic emissions) and the low temperatures registered, favouring the nucleation of new particles, account for the high number concentration of ultrafine particles registered.

During the spring N levels rise attributed to the stronger solar radiation that generates photochemical nucleation of new particles, increasing particle number concentrations during the day (Hämeri et al., 1996; Pey et al., 2008). The periods of the year registering the minimum levels of particle number concentration were characterized by higher rates of precipitations with the consequent cleaning of air masses (March-April and August) and by the reduction of road traffic emissions (July and August as typical holiday months). In addition, the higher temperatures registered during the summer are also probably contributing to the reduction the particle number registered by volatilization of the new particles formed.

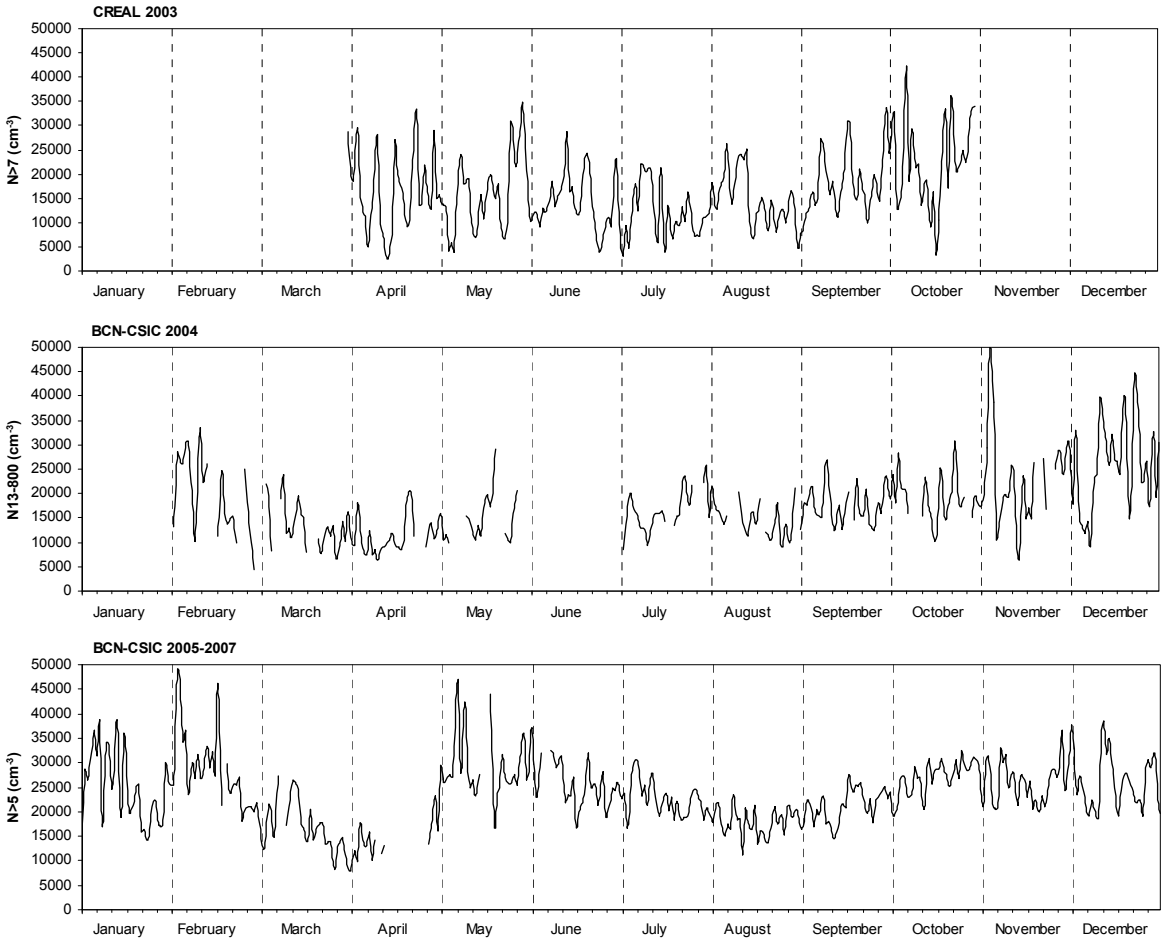

Figure 4.1.31. Seasonal evolution of mean daily particle number concentration levels recorded at Barcelona from 2003 (N>7nm in CREAL coastal urban site), 2004 (N=13-800 nm in BCN-CSIC) and from 2005 to 2007 (N>5 nm in BCN-CSIC).

4.1.4.3. N: daily cycles

The study of daily cycles shows that road traffic is the major emission source contributing to increase the levels of particle number concentration (Figure 4.1.32). Maximum N levels are usually recorded during traffic peak hours both in the morning

(around 7 to 9, local time) and the evening (around 19 to 23, local time). This increase is related to the high number of ultrafine primary particles emitted directly or formed by nucleation processes during the dilution and cooling of the vehicle exhaust (Mariq et al., 2007) and favoured by the lower wind speeds and temperatures registered in the morning and evening (Casati et al, 2007). After the peak hours, when traffic emissions are slightly reduced and temperature rises, number concentration decreases due to condensation, coagulation and volatilization processes (Minoura and Takekawa, 2005), but probably also to the development of sea breezes favouring dispersion of pollutants. However, from 11 to 13 hours (UTC), when the solar radiation intensity is highest, there is an increase of N levels produced by the formation of new ultrafine particles by photochemical nucleation processes (Rodríguez et al., 2007, Figure 4.1.33), together with the emission of new particles due to a slight increase in traffic intensity (Figure 4.1.34). This increase is better observed during the warmer months, when solar radiation is stronger, increasing N levels even more than peak hour road traffic emissions (Figure 4.1.33). However, it is better detected for data from 2005 to 2007, when the instrument size detection limit was 5 nm, as the new particles formed by photochemical nucleation processes are smaller than the 13 nm size limit of the instrument used during 2003-2004.

The influence of road traffic emissions on number concentration levels is clearly seen in the weekly evolution of N daily cycles (Figure 4.1.34). N daily cycles on Sunday and Saturdays change because of the different traffic pattern and lower traffic intensity during the weekends. The morning road traffic is much less intense and this is reflected in N levels. The evening traffic peak is also reduced but in a lower extent, due to road traffic emissions produced by night-life activities in the area on Saturday nights and the return of the weekend holidays on Sundays. The peak at noon is still observed, being higher than the morning peak, coinciding with the increase in traffic intensity at this time of the day during the weekends and probably also to the highest insolation.

From the measurements presented in this study, particle size range is an essential characteristic to take in account in the design of number concentration measurement methods. Size ranges basically depend on size detection limits of the particle counter and the levels of particle number measured depend drastically on this characteristic. Nevertheless, this information is not always reported in publications. However, despite accounting for a very important fraction of number concentration, the particles in the smallest size range detected (5 to 13 nm), are probably not so harmful for health, as they are mainly composed of soluble compounds that may be easily eliminated from

the body. Size ranges, however, should be taken in account in the design of particle number concentration standards, in order to be able to compare measurements and be sure of the accuracy of data reported.

The relationship of N levels with BC, PM_x and gaseous pollutants measured at Barcelona will be discussed in detail in the next section, where the influence of road traffic intensity in all measurement parameters will be investigated.

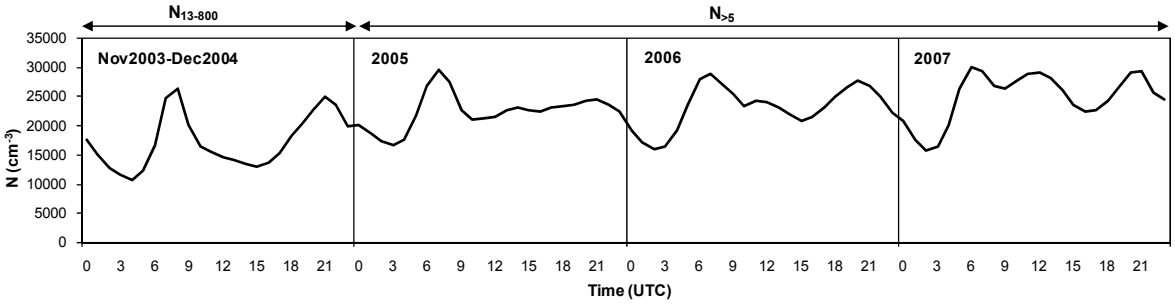

Figure 4.1.32. Inter-annual evolution of the mean daily cycles of particle number concentration levels recorded at Barcelona from November 2003 to December 2007.

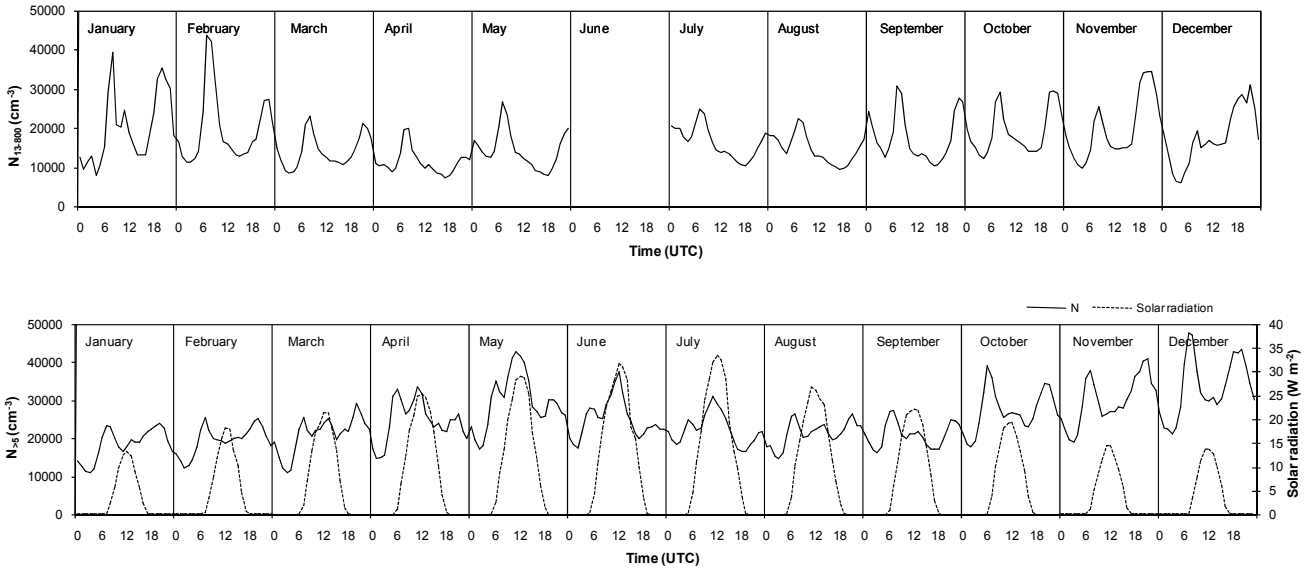

Figure 4.1.33. Seasonal evolution of the mean daily cycles of particle number concentration levels recorded at BCN-CSIC from November 2003 to December 2004 ($N_{13\text{-}800}$, top) and from July 2005 to December 2007 ($N_{>5}$, bottom) and simultaneous solar radiation intensity recorded at Fabra (Meteocat).

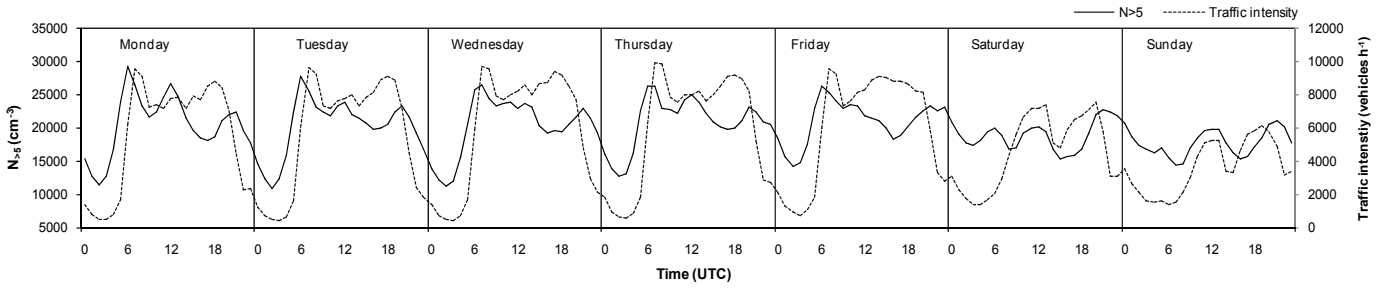

Figure 4.1.34. Weekly evolution of the mean number concentration daily cycles recorded at BCN-CSIC during 2005-2007 and road traffic intensity measured at the Diagonal Avenue.

4.1.4.4. Influence of road traffic emissions on aerosol parameters at Barcelona

Continuous measurements of black carbon levels were carried out at BCN-CSIC monitoring site only from July to December 2007. BC is a tracer of combustion emissions (mostly direct traffic emissions in urban areas). Besides, as already observed, the variability of all the other aerosol parameters measured at BCN-CSIC (N and PM levels and chemical speciation) is clearly influenced by road traffic emissions and meteorology (mainly breeze circulations, anticyclonic stagnant scenarios and intense advective conditions). BC data will be presented together with simultaneous N, and PM_x data registered at BCN-CSIC during the period July-December 2007 and the evolution of all parameters the will be studied in parallel in order to analyze the influence of road traffic emissions on the variability of all monitoring parameters. In addition, levels of atmospheric gaseous pollutants measured at a nearby site (L'Hospitalet-Gornal), meteorological data and traffic intensity data will be used to interpret the results.

BC, N, $PM_{2.5-10}$ and PM_1 daily evolution during July-December 2007 are shown in Figure 4.1.35. The mean daily evolution of some parameters is comparable when concerning the main peaks registered. However, depending on the processes that rise/decrease the levels of each parameter measured, the evolution may be different. The monthly mean levels of BC, N and PM_{10}, $PM_{2.5}$ and PM_1 are shown in Table 4.16.

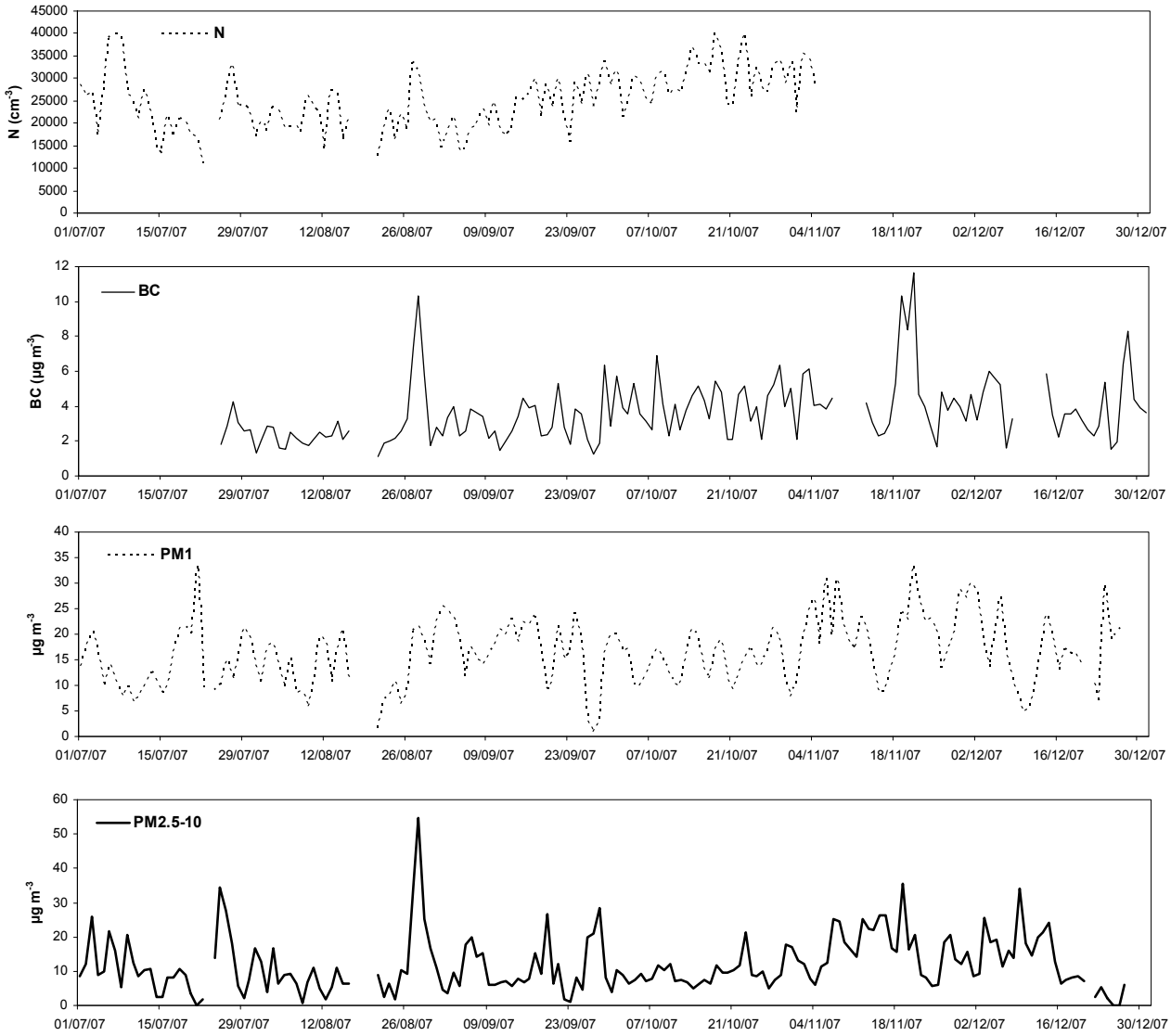

Figure 4.1.35. N, BC, PM_1 and $PM_{2.5-10}$ daily mean levels measured at BCN-CSIC from July to November 2007.

Table 4.16. Mean monthly levels of BC, N, PM_{10}, $PM_{2.5}$ and PM_1 measured at BCN-CSIC from July to December 2007.

	BC ($\mu g\ m^{-3}$)	N (cm^{-3})	PM_{10} ($\mu g\ m^{-3}$)	$PM_{2.5}$ ($\mu g\ m^{-3}$)	PM_1 ($\mu g\ m^{-3}$)
July	2,6	23879	34	22	14
August	2,8	21510	32	21	13
September	3,0	23034	33	22	17
October	4,1	30268	32	23	15
November	4,6	30121	49	33	21
December	4,0		38	26	17
Mean	3,6	24065	36	24	16

The study of correlations between daily levels of the parameters measured simultaneously during July-December 2007 revealed some relationships that are due to the contribution of common sources and processes (Table 4.17). N and BC showed a correlation coefficient (r^2) of 0.47 due to their dependence on road traffic direct emissions. However, this parameter is not very high due to the additional particles formed by photochemical nucleation processes, which increase N levels but do not affect BC levels. N and BC also showed good correlation with nitrogen oxides with r^2=0.37-0.38 and 0.66-0.79 respectively, due to their common traffic exhaust source. However the correlation of r^2=0.36 and 0.32 with O_3 and BC was inverse, due to the increase in O_3 levels in the afternoon when N levels start to decrease. N did not show a relationship with any PM fraction. However, BC presented r^2=0.23 with PM_1 and 0.4 with $PM_{1\text{-}2.5}$ and higher than r^2=0.3 with all atmospheric gaseous pollutants.

Table 4.17. Correlation coefficients (r^2) obtained in the correlation between the daily mean levels of the parameters measured simultaneously during July-December 2007.

r^2	N	BC	PM_1	$PM_{1\text{-}2.5}$	$PM_{2.5\text{-}10}$	SO_2	NO	NO_2	O_3	CO
N										
BC	**0.47**									
PM_1	<0.01	0.23								
$PM_{1\text{-}2.5}$	0.09	**0.40**	0.28							
$PM_{2.5\text{-}10}$	0.09	0.17	<0.01	0.24						
SO_2	0.13	**0.56**	0.12	0.29	0.15					
NO	**0.37**	**0.66**	0.18	**0.32**	0.15	**0.80**				
NO_2	**0.38**	**0.79**	0.23	**0.32**	0.15	**0.56**	**0.69**			
O_3	**0.36**	**0.32**	0.14	0.29	0.08	0.25	**0.47**	**0.51**		
CO	0.04	**0.52**	0.16	0.25	0.07	**0.48**	**0.58**	**0.44**	0.17	

4.1.4.4.1. Daily cycles related to road traffic emissions

As previously mentioned, the evolution of breezes in Barcelona is characterized by a change in direction from North-western to South at around 8h UTC and an increase in wind speed starting around the same time to reach its maximum value at 13h UTC and then decreasing gradually until reaching its minimum in the evening (Figure 4.1.37). Wind direction and speed affect markedly the levels of aerosols measured at BCN-CSIC. The highest direct road traffic emissions to the monitoring site arrive from the Diagonal Avenue, located to the North of the site but also from other important traffic arteries of Barcelona (Figure 4.1.37). Direct emissions arrive to the site in the morning, when wind direction is mainly NW and mild wind speeds are recorded. Then, at around 8h UTC, the breeze changes and starts to blow from the SE increasing its speed until

noon and bringing marine air masses to the site mixed with urban and traffic pollution from the city centre. Thus, the effect of the increase of wind speed, together with the entrance of marine air masses and the increase of the mixing layer height may produce the dilution of traffic pollutants measured at the BCN-CSIC site during the central hours of the day.

The evolution of the aerosol parameters measured at BCN-CSIC will be studied in relation to the ratio traffic intensity/wind speed, as both variables together affect significantly the variability of atmospheric pollutants because of the atmospheric dilution of traffic emissions by wind circulation (Rodriguez et al., 2008). The daily cycles of traffic intensity and traffic intensity/wind speed ratios measured at the Diagonal Avenue during weekdays and weekends are shown in Figure 4.1.38. Daily evolution of road traffic intensity presents a sharp increase during the morning rush hour, a slight reduction after this and then the traffic intensity remains high during the rest of the day, increasing slowly until the evening when road traffic starts to decrease to reach minimum levels during the night. The daily pattern and evolution of road traffic intensity changes markedly during the weekends (Figure 4.1.36 and Figure 4.1.38), with much lower intensity than during weekdays, peaking in the morning between 9-10h UTC and later between 16-20h UTC.

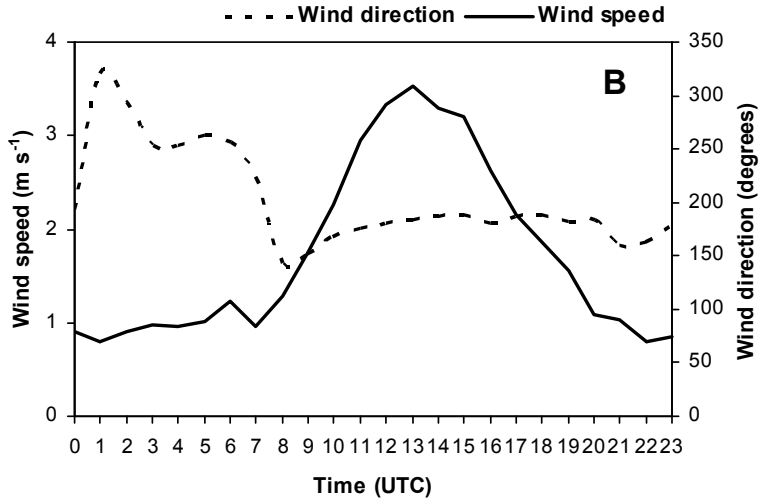

Figure 4.1.36. Daily variation of wind speed and wind direction at The Faculty of Physics (UB) during the sampling period.

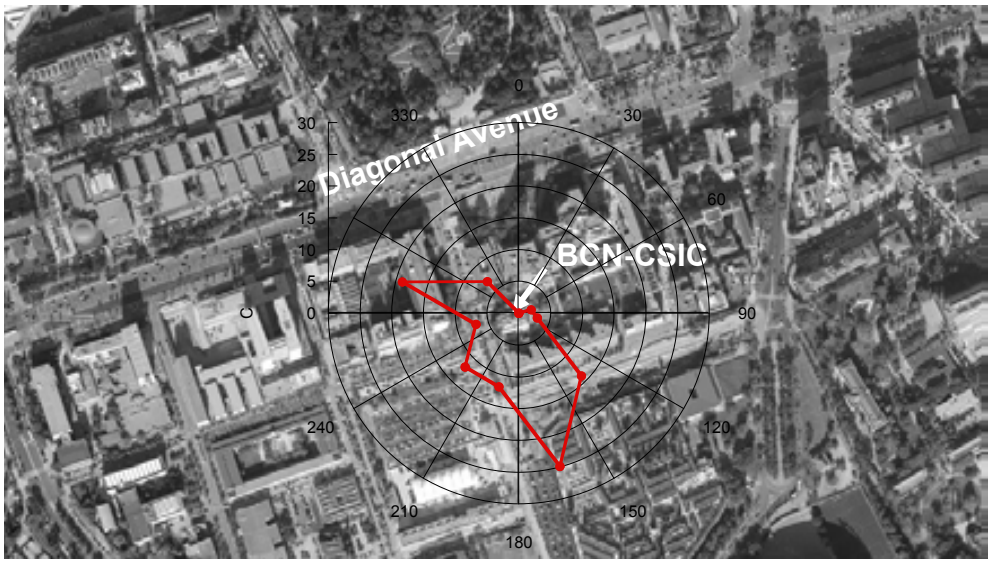

Figure 4.1.37. BCN-CSIC and Diagonal Avenue location and main wind frequencies.

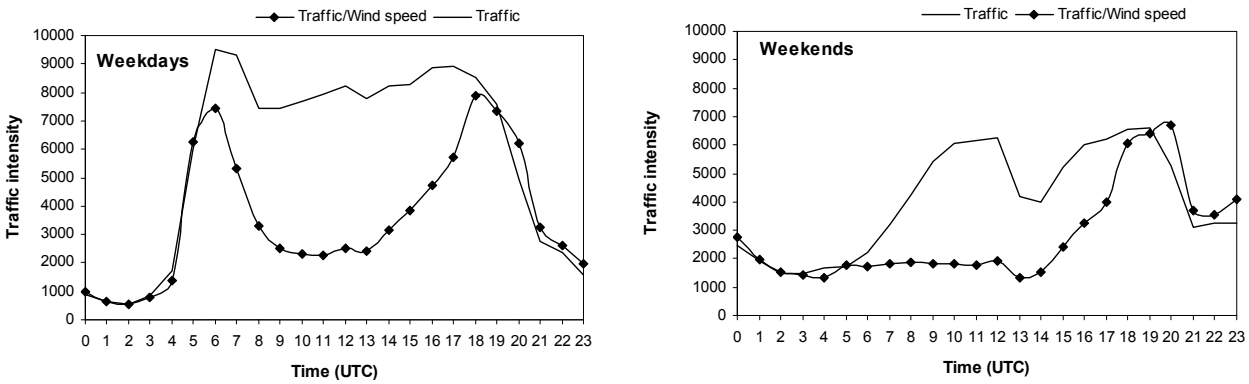

Figure 4.1.38. Daily cycles of traffic intensity and traffic intensity/wind speed ratio measured at Diagonal Avenue during weekdays and weekends from July to December 2007.

The increase in aerosol levels during the morning rush hours as a result of direct road traffic emissions is observed for all the metrics and monitoring parameters measured at BCN-CSIC (Figure 4.1.39), but this increase is more marked in the cases of N and BC (reflecting direct exhaust emissions). In the case of $PM_{2.5-10}$ the maximum levels are observed during the central hours of the day, coinciding with the maximum wind speed, solar radiation intensity and temperatures. Conversely, PM_1 levels are higher during the morning and evening, as a consequence of secondary aerosol formation, and decrease during the central hours of the day, due to wind dilution effects. The evolution of the fraction $PM_{1-2.5}$ is less significant. Thus, daily cycles reflect the sources affecting each parameter. $PM_{2.5-10}$ starts to increase in the morning due to the resuspension on road traffic by vehicles but shows the maximum levels in the central hours of the day as a

result of resuspension processes by wind (road dust and dust from construction/demolition processes. The N levels noon peak coincident with the maximum solar radiation reflects the photochemical processes inducing nucleation of new particles. The origin of the peaks of these two parameters is not the same but the processes behind their variation (resuspension and photochemistry) are activated by the diurnal cycles of solar radiation and temperature.

Daily cycles of some atmospheric gaseous pollutants emitted mostly by traffic exhausts (NO, NO_2 and CO) are also marked by road traffic evolution (Figure 4.1.40). Nitrogen oxides and CO levels peak with traffic rush hours and SO_2 levels start to increase with breeze transport, probably due to emissions from the port. O_3 levels increase in the afternoon due to photochemical processes, being markedly reduced during the winter months.

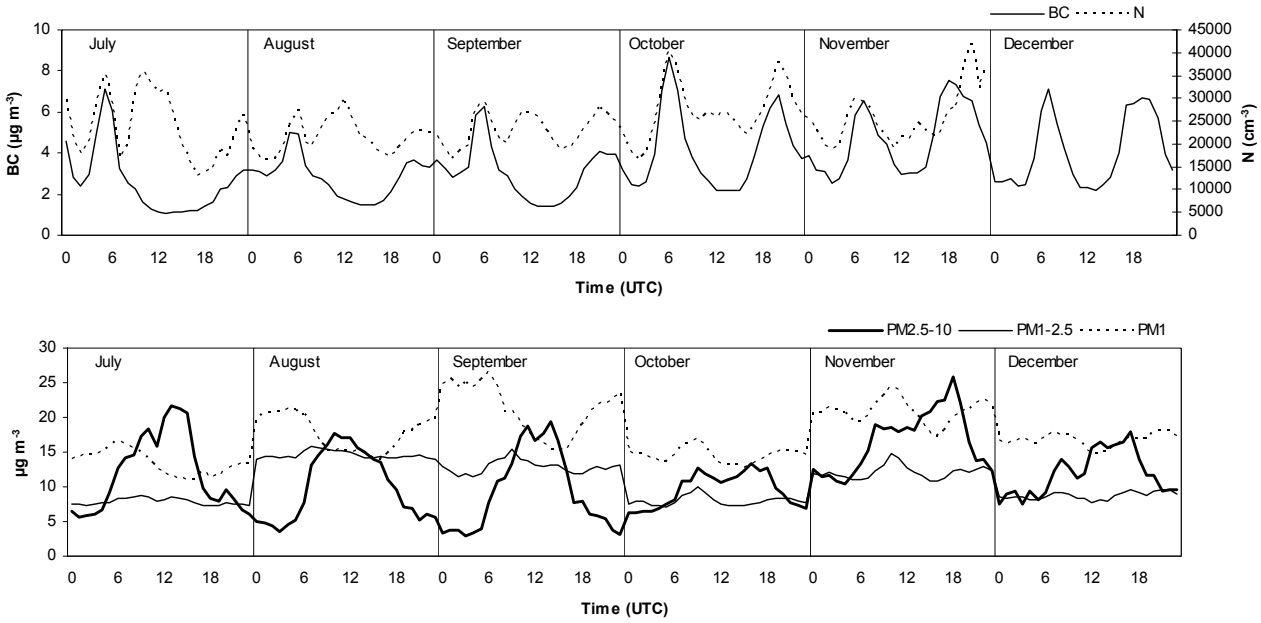

Figure 4.1.39. Seasonal evolution of N and BC daily cycles (top) and $PM_{2.5-10}$, $PM_{1-2.5}$ and PM_1 cycles (bottom) simultaneously monitored at BCN-CSIC during July-December 2007.

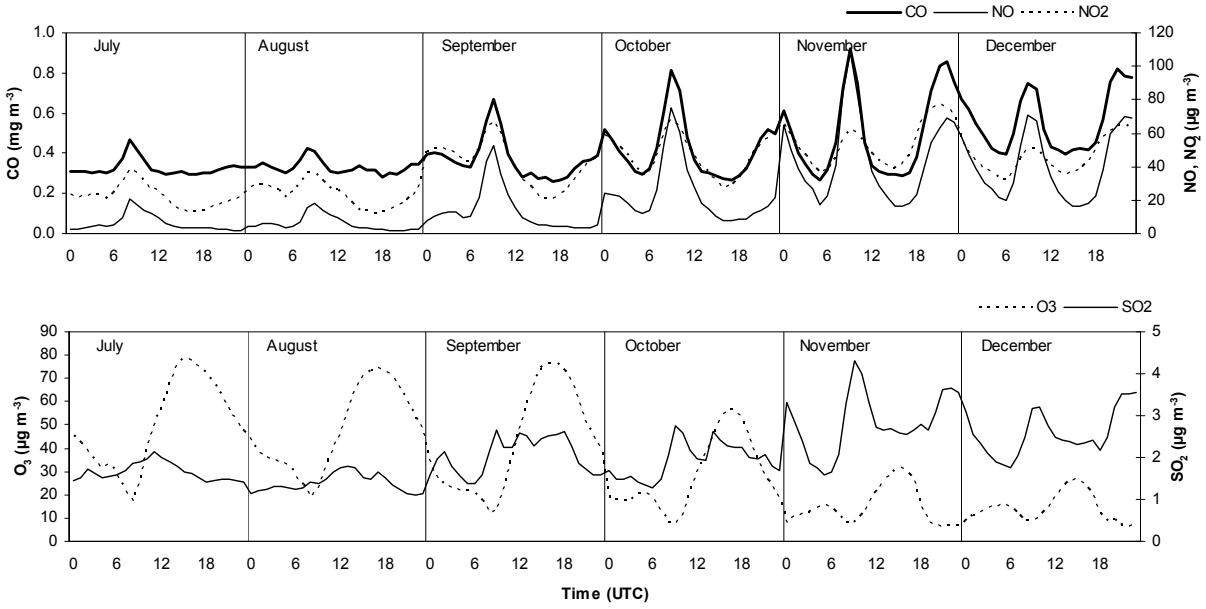

Figure 4.1.40. Seasonal evolution of CO, NO and NO_2 (top) and O_3 and SO_2 daily cycles (bottom) simultaneously monitored at L'Hospitalet site during July-December 2007.

Daily cycles will be studied in detail in the next paragraphs, together with the daily evolution of road traffic intensity. As previously mentioned number concentration (N) increases with road traffic intensity in the morning owing to ultrafine particle vehicle emissions and formation of new particles during dilution and cooling of the vehicle exhaust (Mariq et al., 2007, Figure 4.1.41). This peak is favoured by the increase in traffic emissions and the lower wind speed registered in the morning (Casati et al, 2007), decreasing as the traffic/wind speed ratio decreases (reduction of emissions and increase in wind speed). N shows a second peak at noon-afternoon that may be attributed to new particle formation by photochemically-induced nucleation (Rodríguez et al., 2007) and by dilution of aerosols due to the growth of the mixing layer, but also to maximal transport of pollutants from the central urban area. The evening N peak due to the increase of traffic intensity is also observed. During the night N decreases owing to the reduction of the road traffic flow and probably also to the thinning of the boundary layer depth that favours condensation and coagulation processes reducing ultrafine particle number (Minoura and Takekawa, 2005). N morning peaks were lower during weekends. However the afternoon and evening increases were more enhanced (Figure 4.1.41). In the case of the afternoon peak this could be a consequence of the lower concentrations of atmospheric pollutants registered during weekends, that favour nucleation processes instead of condensation on the surface of particles (Hämeri et al., 1996; Pey et al., 2008). In the case of the evening peak it may be related to road traffic

due to night life activities in the area and the return from the weekend holidays on Sunday evenings.

The levels of BC follow the same evolution as N levels in the morning (Figure 4.1.41), but conversely to N levels, BC levels decrease sharply during the central hours of the day owing to dilution processes and following the traffic intensity/wind speed ratio. This behaviour may be attributed to: a) the increase in wind speed and the change of wind direction during the day (at around 8h) from North-West to South, b) the growth of the mixing layer and c) in a lower extent the decrease of the traffic flow. In the evening rush hour, BC levels start to increase again showing a second maximum at 20h. This is due to the increase in traffic intensity and the reduction of dilution processes in the evening. BC levels decrease during the night, owing to the reduction of vehicle emissions. Reduced traffic emissions on weekends result in a lower BC morning peak. Conversely, a higher evening peak is recorded as a consequence, like occurred with N levels, of night life activities around the monitoring site and traffic from the return from the weekend holidays on Sunday evenings.

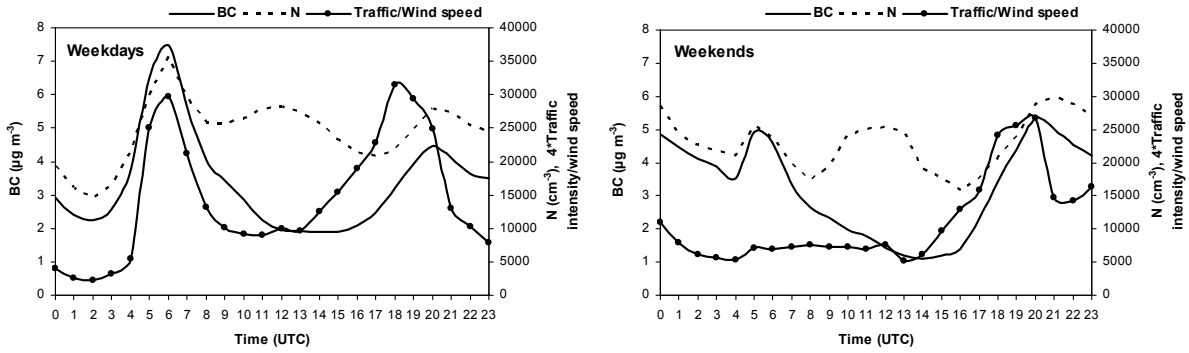

Figure 4.1.41. Mean daily evolution of black carbon concentration (BC) and particle number concentration (N) at BCN-CSIC site and road traffic intensity/wind speed ratio evolution at Barcelona Diagonal Avenue on weekdays and weekends.

The daily evolution of PM levels is not as clear as observed for N or BC levels (especially the finer fractions). During the week $PM_{2.5-10}$ starts to increase in the morning when traffic flow starts (Figure 4.1.42) owing to the direct dust resuspension by road traffic. Conversely to BC evolution, $PM_{2.5-10}$ levels do not decrease during the day with the ratio traffic/wind speed and remain high until the evening, probably because $PM_{2.5-10}$ levels daily cycle (coinciding with the temperature and wind speed evolution and inverse to the humidity) is also very affected by wind resuspension that arises not only from road traffic but from construction/demolition activities occurring

frequently in this area during the sampling period. Coarse particle emissions decrease visibly at night as a consequence of the reduction in the traffic flow and wind speed. $PM_{1-2.5}$ and PM_1 levels increase slightly in the morning after the traffic rush hour (the finer fractions mass is mainly due to secondary particle formation, Zhang et al., 2004) and then decrease gradually during the day probably due to the increase in the boundary layer height and the increase of wind speed that produces the dispersion and dilution of fine atmospheric pollutants (Figure 4.1.42). Conversely to the other parameters, $PM_{1-2.5}$ and PM_1 levels do not decrease at night. This may be a result of the decrease of the boundary layer height and the lower temperatures and higher relative humidity, which favour condensation and coagulation processes between particles and precursor gases and contribute to the formation of particles in the accumulation mode (Jamriska et al., 2008). PM weekend levels were reduced as a consequence of the lower traffic intensity, especially the coarse fraction.

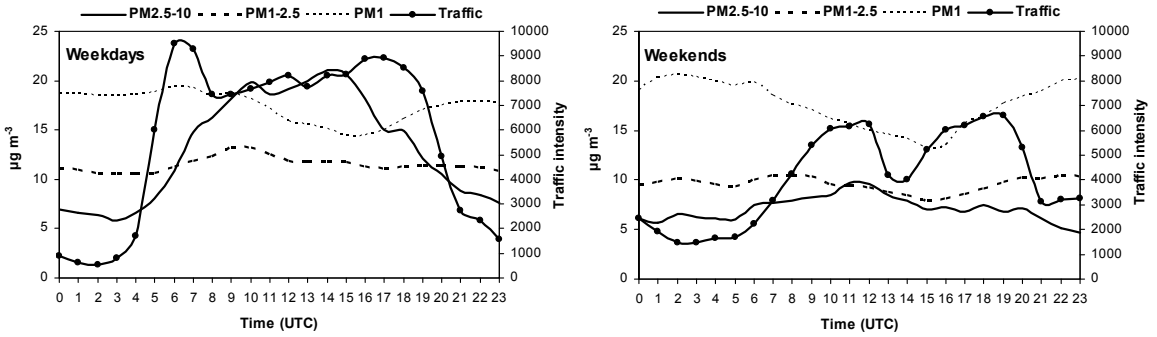

Figure 4.1.42. Mean daily evolution of PM_{10}, $PM_{2.5}$ and PM_1 levels at BCN-CSIC site and road traffic intensity at Barcelona Diagonal Avenue on weekdays and weekends.

During the week, the levels of atmospheric gaseous pollutants related to vehicle exhaust emissions (CO, NO, NO_2) also follow the traffic intensity/wind speed ratio evolution, with maxima during the morning rush hour, decreasing during the day because of dilution processes, and increasing in the evening again (Figure 4.1.43). Levels remain high during the night as a consequence of the reduction of the boundary layer height and lower wind speeds that prevent the dispersion of pollutants. The reduction of road traffic flow intensity during the weekends, results in lower morning and evening peaks and a different evolution of CO, NO and NO_2 levels. During the week, SO_2 levels increase in the morning together with CO, NO and NO_2, revealing that traffic is partially a source to this pollutant, although its decrease is slower than for the rest of the gases. Conversely, SO_2 maximum peak during the weekends is observed at noon, coinciding with the maximum wind speed and southern wind

direction. As a result, SO_2 evolution may be related to shipping emissions from the port (to the south of the BCN-CSIC site) and thus the daily cycle of this pollutant may be driven by its transport by the wind. O_3 levels increase in the afternoon both during weekdays and weekends, following the N noon peak and the solar radiation intensity, as its formation depends on photochemistry. However, during the weekends, the peak is higher. This observation may be related to the effect of the lower general pollution levels observed during the weekends reducing the interaction of O_3 with other species as NO_X or carbonaceous compounds.

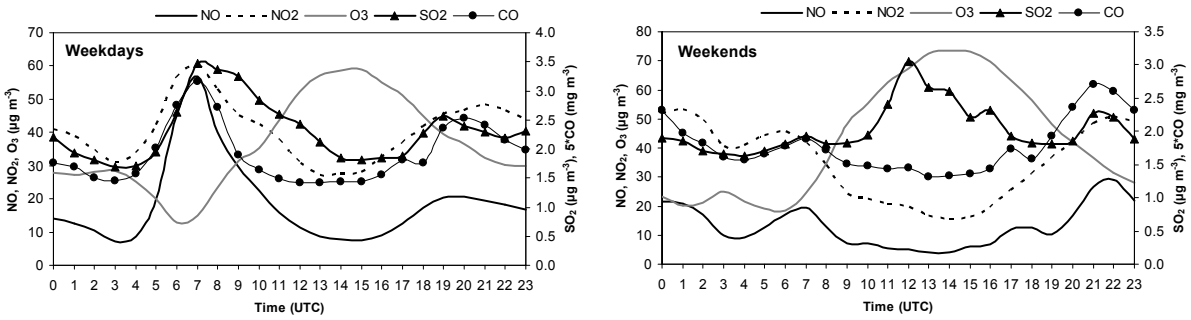

Figure 4.1.43. Mean daily evolution of levels of atmospheric gaseous pollutants (NO, NO_2, SO_2, CO and O_3) in weekdays and weekends at L'Hospitalet-Gornal site during the sampling period.

The relationship between N and BC levels was also studied by representing the daily evolution of the N/BC ratio (Figure 4.1.44). A clear increase in N/BC ratio is observed during the central hours of the day, coincident with the maximum radiation intensity. This peak in N levels is probably caused by photochemical nucleation processes that increase the N levels while the BC levels are reduced by wind speed and direction changes. During the night there is no significant variation of the N/BC ratio. The weekend N/BC peak was higher, explaining the favoured photochemical nucleation processes that are observed when atmospheric pollutant levels are lower (Hämeri et al., 1996; Pey et al., 2008).

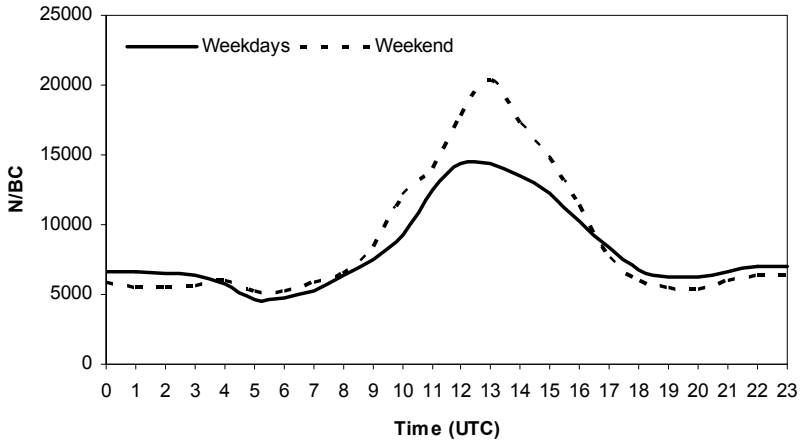

Figure 4.1.44. Mean daily evolution of N/BC ratio.

The correlation between N and BC hourly mean levels showed two slopes (Figure 4.1.45). When representing only data recorded during the night, only one slope was obtained. The nocturnal data show the relationship between N and BC when photochemical processes are not present, the mixing layer is reduced and nucleation is reduced compared to condensation processes. The higher slope present when representing all data may correspond to the higher N measured owing to photochemical nucleation during daytime.

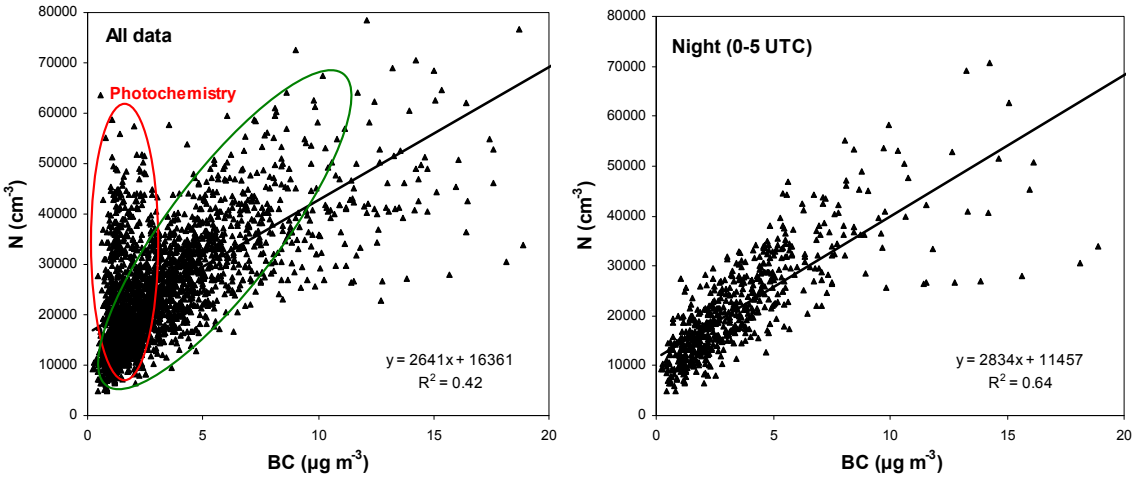

Figure 4.1.45. Correlation graphs between BC and N hourly means measured at BCN-CSIC during all the period (left) and only during the night (right).

The photochemical nucleation processes affecting the N noon peak are confirmed by studying the influence of the solar radiation intensity on the seasonal variation of the N

peak. The difference between N levels and BC levels in the afternoon is reduced as the solar radiation intensity decreases from July to November (Figure 4.1.46). However the difference between N and BC peaks at traffic rush hours do not show a significant variation.

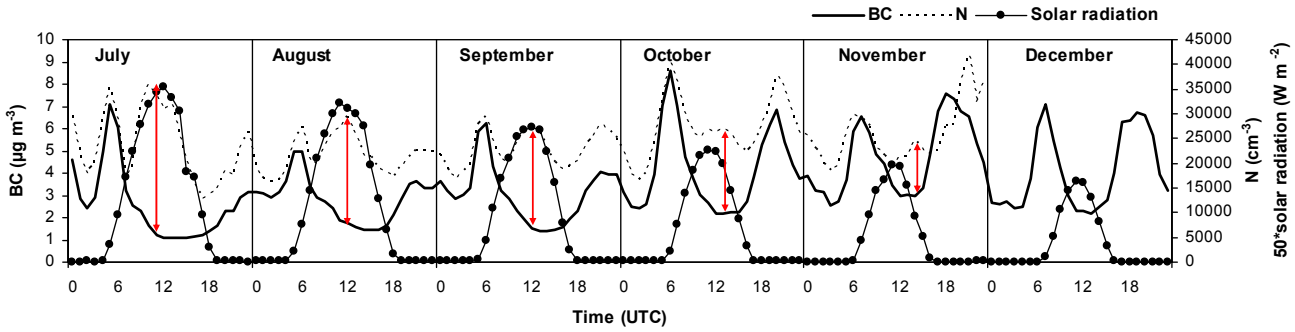

Figure 4.1.46. Seasonal evolution of the daily cycles of N and BC levels recorded at BCN-CSIC site and the solar radiation measured at Fabra from July to December 2007. Red arrows show the difference between BC and N levels at noon.

The contribution of road traffic to the levels of all parameters was estimated for rush hours during weekdays as the increment from mean hourly background levels when traffic intensity was minimum (from 0-4h UTC) and mean hourly levels during the rush hours, when direct emissions can be measured (from 5-10h and 18-21h UTC). Thus, N hourly mean levels increased from 17600 cm^{-3} during the background hours to 27500 cm^{-3} during rush hours and consequently 36% of the particles measured during rush hours may be attributed to direct traffic emissions. Similarly, BC mean hourly levels increased from 2.8 to 4.2 µg m^{-3}, with 33% being attributed to recent traffic emissions. The mean hourly increment of the $PM_{2.5-10}$ fraction when considering traffic rush hours was of 52%. However, the contributions of traffic emissions to PM_1 or $PM_{1-2.5}$ have not been estimated, as finer particles are formed by condensation and coagulation processes and direct emissions affect the variability of these fractions to a lower extent. Although this is just a simplified estimation, as background levels are also affected by traffic emissions and these increments may be only attributed to rush hour direct emissions, these estimations show the important impact that traffic emissions have on urban air quality.

4.1.4.4.2. Variability of aerosol parameters related to wind direction and speed

The important influence of road traffic emissions and sea-land breezes on the variability of the levels of atmospheric aerosols and gaseous pollutants was also

observed when rose wind plots were studied, indicating the main source direction for each of the different parameters considered. Hourly means for BC, N, $PM_{2.5-10}$, $PM_{1-2.5}$ and PM_1 for each month during July to November 2007 were considered for the rose winds plots (Figure 4.1.47). Rose wind plots are also presented for gaseous pollutants measured at L'Hospitalet-Gornal in the same period (Figure 4.1.48). For all components it may be distinguished an urban background, with similar levels measured in all wind directions (marked with a green circle in the graphs) and then higher peaks indicating the direct contributions from the main emission sources of each parameter (marked with a red line). The highest levels of BC were obtained when the wind direction ranged from SW to NE, reaching hourly levels of 9 μg m^{-3}. This may indicate a main BC emission source related to direct road traffic emissions (from the Diagonal Avenue and other important roads) occurring mainly during the morning traffic rush hours. N did not present such a clear source direction, reaching the highest levels with NE, SW and S wind directions (up to 45000 cm^{-3}). This may indicate the main direct sources of ultrafine particles being road traffic (NE and SW as for BC) but also another source that may be related to the photochemical nucleation of new particles when sea breezes predominated at noon, coinciding with the highest insolation and the entry of cleaner air masses, favouring nucleation of new particles instead of condensation-agglomeration processes. PM_1 levels also presented the highest hourly levels (up to 28 μg m^{-3}) corresponding to wind directions ranging from SW to NW, showing the influence of direct road traffic emissions to this parameter. In the cases of BC and PM_1 the fact that levels were lower when wind direction ranged from SW to SE may reflect the influence of the entry of cleaner sea breezes with a Southern wind direction and a higher wind speed, favouring the dilution of pollutants. In contrast, the highest levels of $PM_{2.5-10}$ and $PM_{1-2.5}$ (up to 25 and 16 μg m^{-3}) were recorded when the main wind directions ranged from NW to SE, corresponding to the directions of the main direct traffic emissions but also probably related to the effect of Southern sea breezes, coinciding with the highest wind speeds that may favour dust resuspension processes.

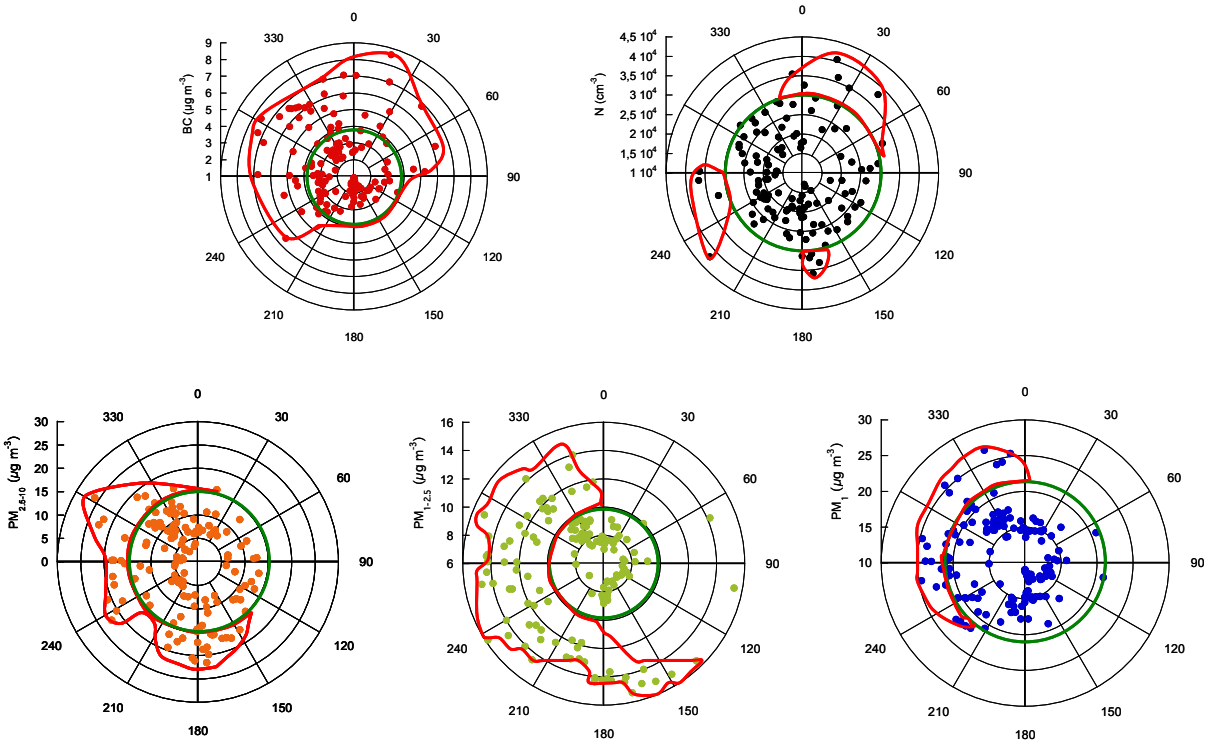

Figure 4.1.47. Rose winds for BC, N, $PM_{2.5-10}$, $PM_{1-2.5}$ and PM_1 hourly mean levels measured from July to December 2007 at BCN-CSIC.

Regarding the mean hourly levels of gaseous pollutants measured at L'Hospitalet-Gornal (Figure 4.1.48), the highest levels of CO, NO, NO_2 and SO_2 were recorded when the main wind directions ranged from SW to NW due to direct traffic emissions from nearby important traffic arteries. However, the SW direction may also be associated to emissions from industries, the port and the airport. In addition, like BC and N, CO, NO and NO_2 present high levels in some cases that the main wind direction was NE, also being related to direct traffic emissions, The highest levels of O_3 were observed for wind directions ranging from SW to E. This may be due to the favoured formation of O_3 in the afternoon, coinciding with the higher insolation, when sea breezes are dominant.

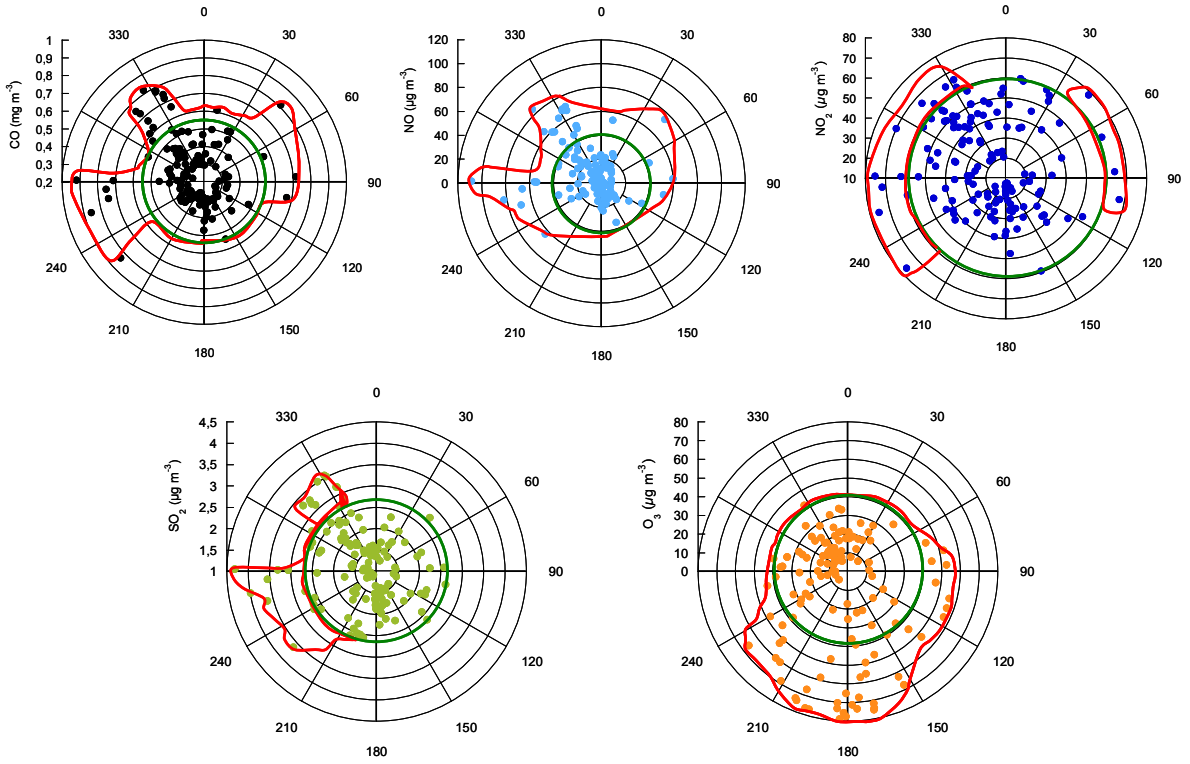

Figure 4.1.48. Rose winds for CO, NO, NO_2, SO_2 and O_3 hourly mean levels measured from July to December 2007 at L'Hospitalet-Gornal.

The study of the influence of wind speed on the levels of some aerosol parameters shows that BC, N, $PM_{2.5-10}$ and PM_1 levels have a tendency to reduce when the wind speed increases (Figure 4.1.49). This effect is the consequence of atmospheric dilution processes, due to the entry of cleaner marine air masses together with the maximum wind speeds. However, this reduction is less pronounced for the fraction $PM_{2.5-10}$ and N levels. As it was observed above when studying rose wind plots (Figure 4.1.47), high levels of $PM_{2.5-10}$ were recorded for the NW direction, registered during the night and early morning, when wind speed is minimum and therefore this high levels may be attributed to road dust resuspension processes by vehicles during the morning traffic rush hours. In addition, peak levels were also observed for the Southern wind direction. In this case, these high $PM_{2.5-10}$ levels may be attributed to dust resuspension by vehicles but probably also by wind during the central hours of the day, when the highest wind speeds are recorded, coincident with the development of sea-land breezes. Thus, three main factors are leading the evolution of coarse PM: the direct emission of particles by road dust resuspension by vehicles, dust resuspension by wind and cleaning of air masses by dispersion. Regarding N levels, higher number concentration levels are recorded for the NW, NE and S direction. Thus, high N levels are recorded during lower wind speeds due to direct exhaust emissions (probably

attributed to important winter pollution episodes) but also in some cases during higher wind speeds, due to the favoured nucleation processes when dispersion of pollutants occurs (Rodriguez et al., 2007) depending on the process behind the formation of ultrafine particles.

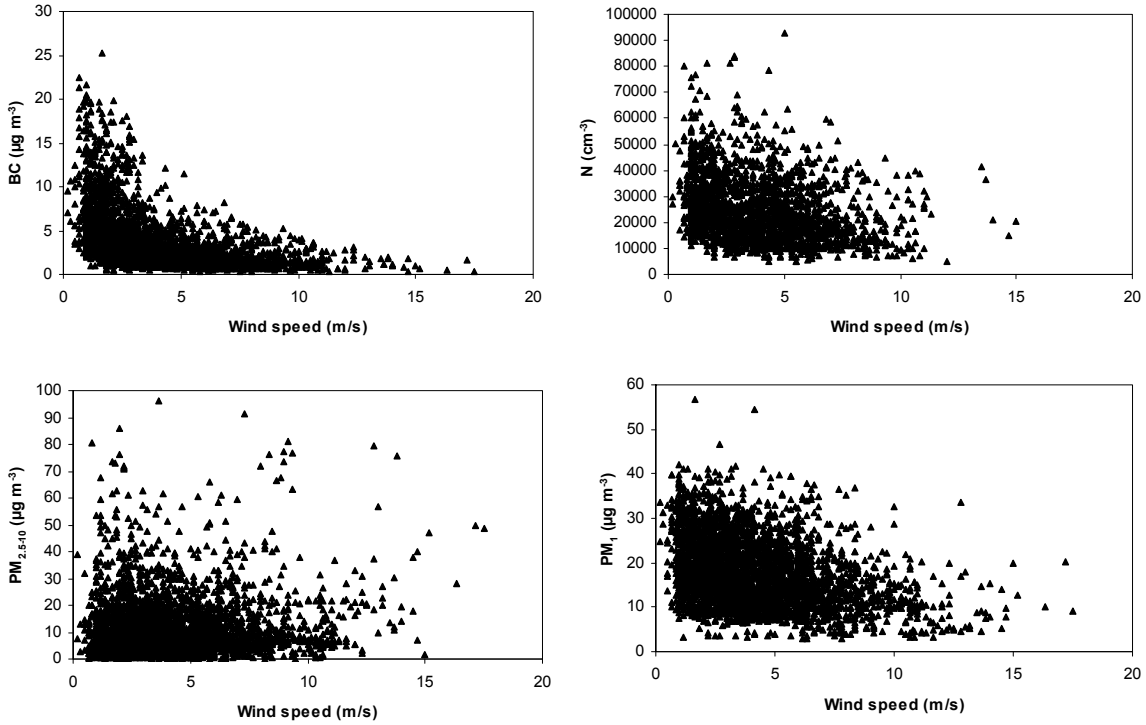

Figure 4.1.49. Wind speed influence on N and BC, $PM_{2.5-10}$ and PM_1 hourly mean levels measured in BCN-CSIC from July to December 2007.

4.1.4.4.3. PM speciation: road traffic tracers

The influence of road traffic emissions on aerosol composition is clearly noticed in the results from PM speciation. When studying the seasonal evolution of some PM_{10}, $PM_{2.5}$ and PM_1 components compared to parameters directly related to traffic emissions, it becomes evident that the carbonaceous compounds (OM+EC) follow a similar pattern than N levels (Figure 4.1.50). This is a consequence of the important influence that road traffic emissions (both primary and secondary) have on both parameters. OM+EC and particle number concentration present their maximum levels during the winter months, associated to the strong pollution episodes recorded in this period of the year. The levels decrease in April, related to the higher precipitation rates, and also in August, because of the lower traffic intensity during this month. However, in the summer 2007 N and OM+EC levels did not follow the same trend. The summer increase of N levels is attributed to the stronger photochemical activity during summer months that generates nucleation episodes during the day. This is not observed in

OM+EC levels but it is observed in sulphate levels, that is a main component of the ultrafine particles together with carbonaceous components (Figure 4.1.50). The peak in particle number concentrations observed during the cold months (February-March and November) is also observed in nitrate and ammonium levels (Figure 4.1.50). This is as a result of the strong pollution episodes related to anticyclonic conditions occurring during these months in Barcelona.

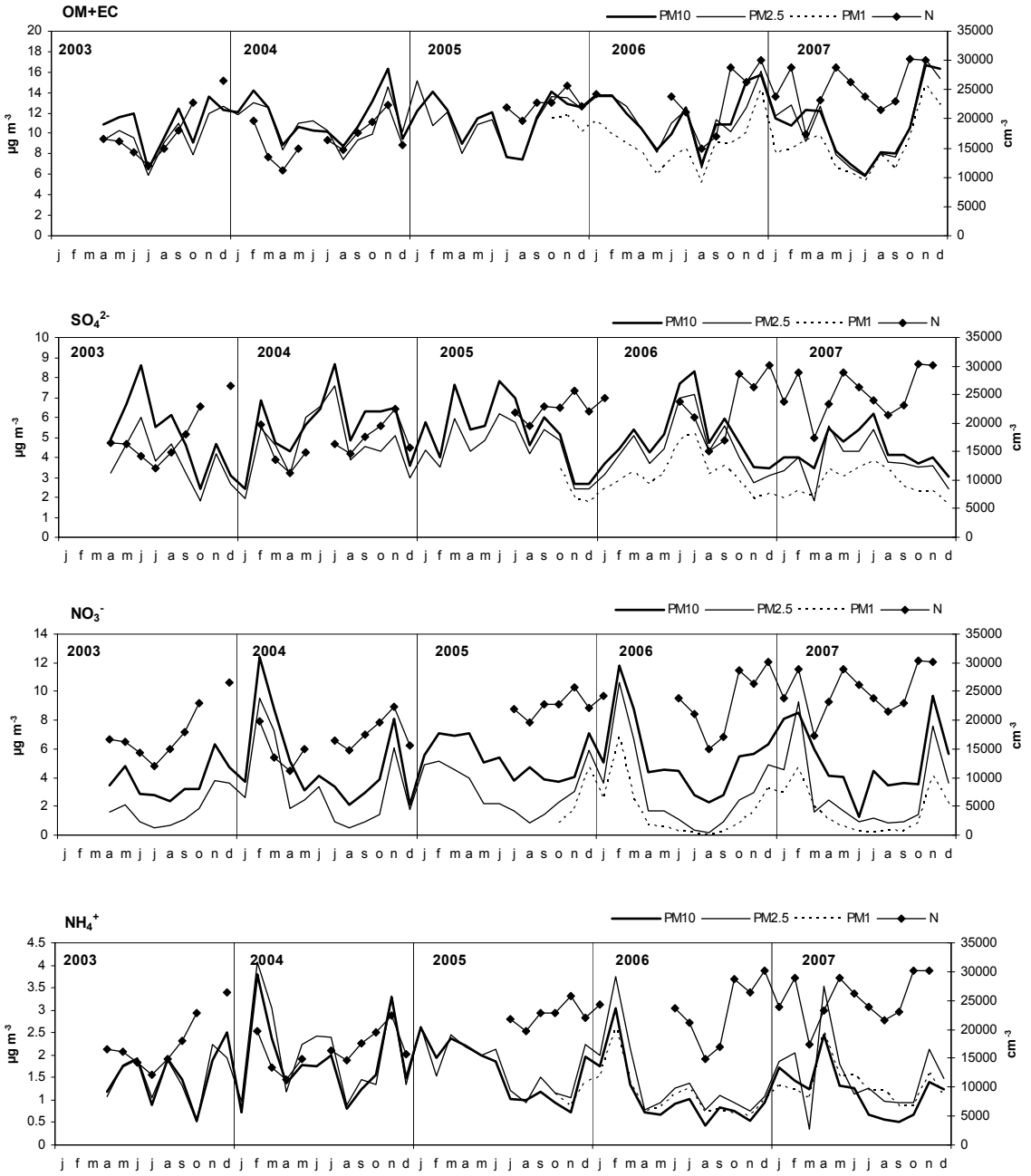

Figure 4.1.50. Mean annual cycles of particle number concentration and OM+EC, SO_4^{2-} and NO_3^- and NH_4^+ levels in PM_{10}, $PM_{2.5}$ and PM_1 recorded in BCN-CSIC from 2003 to 2007.

Black carbon levels also showed a parallel evolution to the simultaneous OM+EC levels measured in PM_{10}, $PM_{2.5}$ and PM_1 (Figure 4.1.51) indicating the same traffic direct emission source. Moreover, the correlation of BC mean daily levels monitored with the simultaneously measured OC and EC mean daily levels was good (Figure 4.1.52).

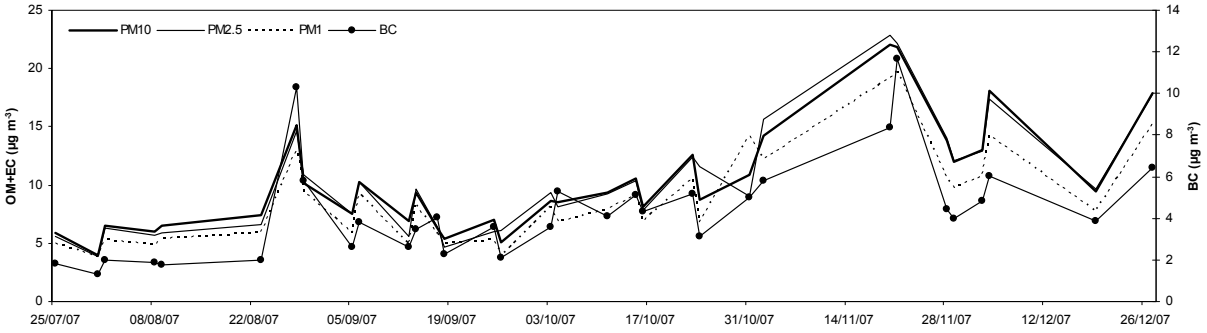

Figure 4.1.51. Daily evolution of BC levels and OM+EC levels in PM_{10}, $PM_{2.5}$ and PM_1 recorded at BCN-CSIC from July to December 2007.

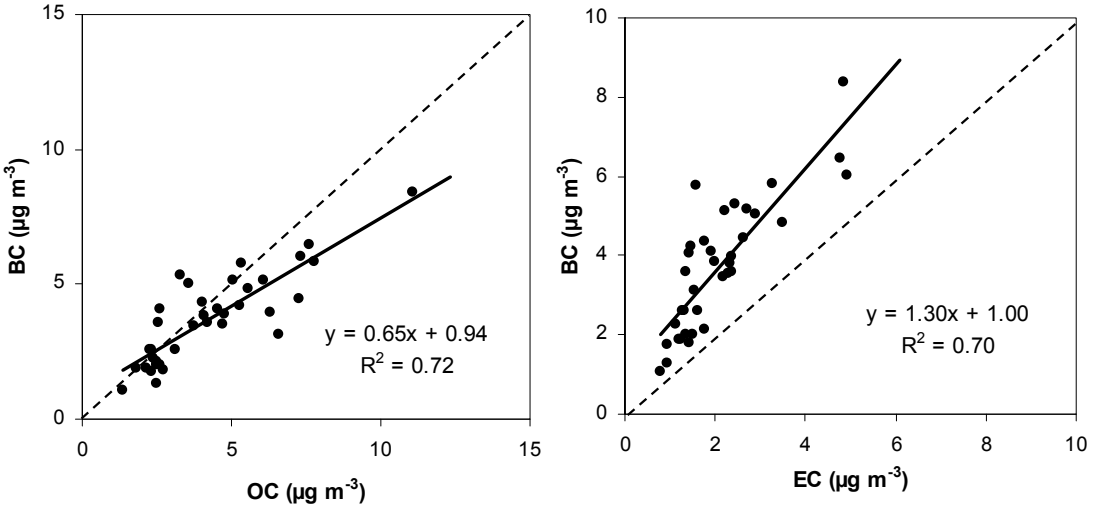

Figure 4.1.52. Correlation between BC and OC and EC measured in $PM_{2.5}$ at BCN-CSIC in the period July-December 2007.

Some tracers associated to road traffic emissions analyzed in PM_{10}, such as total carbon, Fe, Sb, Ni, Sn and Cu, showed a very good correlation with BC daily levels (Figure 4.1.53), indicating traffic related sources. Fe is usually associated to dust resuspension, Fe, Sb, Cu, Ni and and Sn are attributed to vehicle wear (brakes, tyres

and other components) and carbonaceous compounds (total carbon) are generally associated to direct vehicle exhaust emissions.

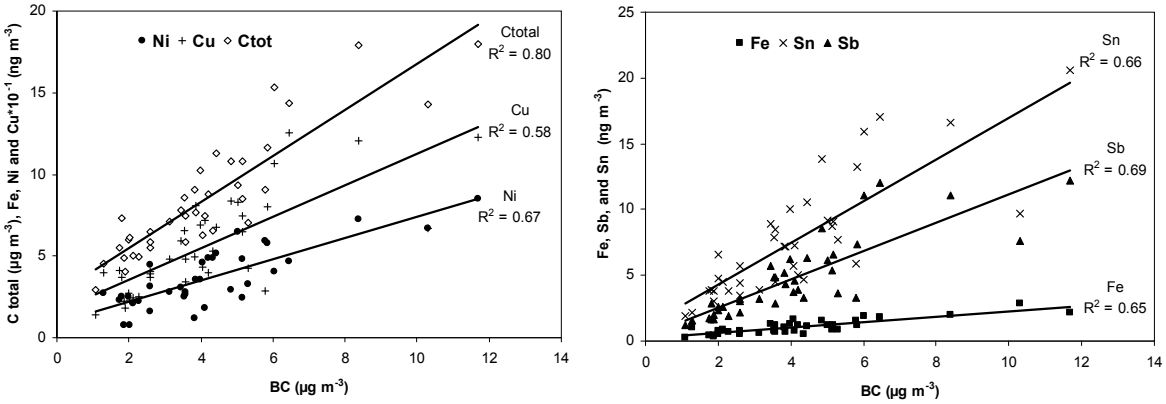

Figure 4.1.53. Correlation of mean BC daily levels with the simultaneous Ctotal, Ni, and Cu and Fe, Sn and Sb mean daily levels measured in PM_{10} at BCN-CSIC during the period July-November 2007.

4.1.5. Source contribution to ambient PM levels

The identification of emission sources contributing to increase PM_{10}, $PM_{2.5}$ and PM_1 levels by using receptor modelling tools is one of the main objectives of the study of PM chemical composition. In this case, two techniques based on receptor modelling were applied, principal component analysis (PCA) and positive matrix factorization (PMF), obtaining comparable results. First, PCA results will be presented briefly and then PMF results will be presented and discussed and the main differences with the PCA analysis commented.

4.1.5.1. PCA

4.1.5.1.1. Elements and data for analysis

Some of the elements measured are not used for the PCA analysis because the mean concentrations obtained were similar in all the samples analyzed, the levels were very high in the blanks, or levels were under the detection limit. The number of components considered for the principal component analysis in PM_{10}, $PM_{2.5}$ and PM_1 were 32, 30 and 27, respectively and are shown in Table 4.18.

Table 4.18. Components analyzed and selected for the PCA analysis (X). Exclusion causes: very low levels, in most cases <DL (●) or very high blank levels (○).

	PM_{10}	$PM_{2.5}$	PM_1		PM_{10}	$PM_{2.5}$	PM_1		PM_{10}	$PM_{2.5}$	PM_1
OM+EC	X	X	X	Ni	X	X	X	Pr	●	●	●
Al_2O_3	X	X	X	Cu	X	○	○	Nd	●	●	●
Ca	X	X	X	Zn	X	X	X	Sm	●	●	●
K	X	X	X	Ga	X	X	X	Eu	●	●	●
Na	X	X	X	Ge	●	●	●	Gd	●	●	●
Mg	X	X	X	As	X	X	X	Tb	●	●	●
Fe	X	X	X	Se	○	○	○	Dy	●	●	●
SO_4^{2-}	X	X	X	Rb	X	X	X	Ho	●	●	●
NO_3^-	X	X	X	Sr	X	X	X	Er	●	●	●
Cl^-	X	X	X	Y	●	●	●	Tm	●	●	●
NH_4^+	X	X	X	Zr	○	○	○	Yb	●	●	●
Li	X	X	X	Nb	●	●	●	Lu	●	●	●
Be	●	●	●	Mo	○	○	○	Hf	●	●	●
P	X	X	○	Cd	X	X	X	Ta	●	●	●
Sc	●	●	●	Sn	X	X	X	W	●	●	●
V	X	X	X	Sb	X	X	X	Tl	●	●	●
Ti	X	X	X	Cs	●	●	●	Pb	X	X	X
Cr	X	X	X	Ba	X	○	○	Bi	●	●	●
Mn	X	X	X	La	X	X	●	Th	●	●	●
Co	X	X	X	Ce	X	X	●	U	●	●	●

4.1.5.1.2. Identification of emission sources

Factors identified by PCA analysis in PM_{10}, $PM_{2.5}$ and PM_1 are shown in Table 4.19, Table 4.20 and Table 4.21 respectively. Factor loadings associated to each of the compounds are indicated and main tracers are highlighted.

Table 4.19. Factors identified in PM_{10} by PCA, associated factor loadings and % variance (% Var) of the samples explained by each of the factors obtained. Main tracers where highlighted.

Mineral matter		**Road traffic**		**Secondary**		**Industrial**		**Marine aerosol**		**Fuel oil**	
Al_2O_3	**1.0**	**OM+EC**	**0.8**	**NH_4^+**	**0.9**	**Pb**	**0.9**	**Na**	**0.9**	**Ni**	**0.8**
Ti	**0.9**	**Sn**	**0.8**	**NO_3^-**	**0.8**	**Zn**	**0.9**	**Cl^-**	**0.9**	**V**	**0.7**
Rb	**0.9**	**Sb**	**0.8**	**SO_4^{2-}**	**0.7**	**Cd**	**0.7**	*Mg*	*0.5*	*Co*	*0.4*
Sr	**0.9**	**Cr**	**0.7**	V	0.3	**As**	**0.6**	Ba	0.1	SO_4^{2-}	0.3
Li	**0.9**	**Fe**	**0.7**	OM+EC	0.3	Mn	0.3	Sr	0.1	Cr	0.3
K	**0.9**	**Cu**	**0.6**	Cd	0.2	Sb	0.2	SO_4^{2-}	0.1	As	0.3
La	**0.9**	*Mn*	*0.4*	K	0.2	Cr	0.2	NO_3^-	0.1	Cd	0.2
Ce	**0.9**	*Ba*	*0.4*	As	0.2	Ca	0.2	K	0.1	La	0.2
Mg	**0.8**	NO_3^-	0.3	Ni	0.2	NH_4^+	0.1	Al_2O_3	0.0	Ce	0.2
Ca	**0.8**	Ca	0.2	Sb	0.2	Co	0.1	V	0.0	Ti	0.1
P	**0.7**	Co	0.2	Mn	0.1	OM+EC	0.1	Cu	0.0	Al_2O_3	0.1
Fe	**0.7**	As	0.2	P	0.1	Rb	0.1	Ti	0.0	Sr	0.1
Mn	**0.7**	Ce	0.2	Fe	0.1	K	0.1	As	0.0	OM+EC	0.1
Ba	*0.4*	P	0.2	Ti	0.1	Fe	0.1	Cd	0.0	Mg	0.1
Cr	*0.4*	Ni	0.2	Rb	0.1	Li	0.1	Pb	0.0	K	0.1
Co	*0.4*	Cd	0.2	La	0.1	Sn	0.1	Rb	0.0	Sb	0.1
SO_4^{2-}	*0.4*	V	0.2	Al_2O_3	0.1	NO_3^-	0.1	Li	0.0	Fe	0.1
As	0.3	Sr	0.2	Pb	0.1	Cu	0.1	La	0.0	NO_3^-	0.1
V	0.3	La	0.2	Cu	0.0	Ni	0.1	Ce	0.0	Rb	0.1
Sn	0.3	K	0.2	Ca	0.0	SO_4^{2-}	0.1	Zn	-0.1	NH_4^+	0.1
OM+EC	0.2	Rb	0.2	Sn	0.0	P	0.1	Co	-0.1	P	0.1
Ni	0.2	Zn	0.1	Mg	0.0	La	0.1	Fe	-0.1	Sn	0.1
Sb	0.2	Pb	0.1	Li	0.0	V	0.1	Sn	-0.1	Li	0.1
Zn	0.2	NH_4^+	0.1	Ce	0.0	Sr	0.1	Ni	-0.1	Ca	0.1
Na	0.1	Ti	0.1	Sr	0.0	Ti	0.0	Ca	-0.1	Cu	0.1
Pb	0.1	Li	0.1	Co	0.0	Cl^-	0.0	P	-0.1	Ba	0.0
Cu	0.0	Al_2O_3	0.1	Zn	0.0	Ce	0.0	Sb	-0.1	Mn	0.0
NO_3^-	0.0	Cl^-	0.0	Cl^-	0.0	Al_2O_3	0.0	Cr	-0.1	Na	0.0
Cd	0.0	Mg	0.0	Cr	0.0	Mg	0.0	OM+EC	-0.1	Pb	0.0
NH_4^+	0.0	SO_4^{2-}	-0.2	Na	0.0	Ba	0.0	NH_4^+	-0.1	Zn	0.0
Cl^-	-0.1	Na	-0.2	Ba	-0.1	Na	-0.1	Mn	-0.2	Cl^-	-0.1
% Var	44	% Var	13	% Var	7	% Var	6	% Var	5	% Var	3

Table 4.20. Factors identified in $PM_{2.5}$ by PCA, associated factor loadings and % variance (% Var) of the samples explained by each of the factors obtained. Main tracers where highlighted.

Mineral matter		Industrial		Fuel oil		Road traffic		Secondary		Marine aerosol	
Ti	**0,9**	**Zn**	**1,0**	**V**	**0,8**	**OM+EC**	**0,8**	**NH_4^+**	**0,9**	**Cl^-**	**0,9**
Al_2O_3	**0,9**	**Pb**	**0,9**	**Ni**	**0,8**	**Sb**	**0,7**	**NO_3^-**	**0,8**	**Na**	**0,6**
Rb	**0,9**	*Cd*	*0,5*	**SO_4^{2-}**	**0,6**	**Sn**	**0,6**	**SO_4^{2-}**	**0,6**	*Mg*	*0,5*
Sr	**0,9**	*As*	*0,4*	*Cr*	*0,4*	*Cr*	*0,5*	*OM+EC*	*0,4*	*Co*	*0,4*
Ca	**0,9**	Mn	0,3	Co	0,3	*Mn*	*0,5*	K	0,3	As	0,3
Ce	**0,9**	Ga	0,2	NH_4^+	0,3	*As*	*0,4*	Mn	0,3	Cd	0,3
La	**0,8**	Sb	0,2	Sn	0,2	*Fe*	*0,4*	V	0,2	Sb	0,1
Fe	**0,8**	Sn	0,2	La	0,2	NO_3^-	*0,4*	Sb	0,2	Al_2O_3	0,1
Ga	**0,8**	K	0,1	Na	0,2	Ni	0,3	As	0,2	Ti	0,1
Li	**0,8**	Rb	0,1	Ga	0,2	Cd	0,3	Cl^-	0,2	SO_4^{2-}	0,1
Mg	**0,8**	Cl^-	0,1	As	0,2	Co	0,3	Cd	0,1	Ga	0,1
K	**0,8**	OM+EC	0,1	Ce	0,2	Ce	0,2	Rb	0,1	Fe	0,1
P	**0,7**	NH_4^+	0,1	Al_2O_3	0,1	K	0,2	Ni	0,1	Sr	0,1
Mn	**0,6**	SO_4^{2-}	0,1	Ti	0,1	P	0,2	P	0,1	Ca	0,1
Sb	0,3	NO_3^-	0,1	Mg	0,1	Ca	0,2	Zn	0,1	P	0,1
Na	0,3	Li	0,1	Cd	0,1	Ga	0,2	Pb	0,1	NO_3^-	0,0
Co	0,3	Ni	0,0	Sr	0,1	La	0,2	Ga	0,1	Ni	0,0
SO_4^{2-}	0,3	Fe	0,0	OM+EC	0,1	Rb	0,2	Fe	0,0	Rb	0,0
Sn	0,3	Cr	0,0	Sb	0,1	V	0,1	Sn	0,0	NH_4^+	0,0
Cr	0,2	Na	0,0	Li	0,1	Zn	0,1	Li	0,0	K	0,0
V	0,2	La	0,0	Rb	0,1	NH_4^+	0,1	Co	0,0	Pb	0,0
OM+EC	0,2	V	0,0	Fe	0,1	Pb	0,1	Ti	0,0	V	0,0
As	0,2	Ce	0,0	P	0,0	Sr	0,1	Ce	0,0	Zn	0,0
Ni	0,1	Ca	0,0	Pb	0,0	Cl^-	0,1	Al_2O_3	0,0	La	0,0
Zn	0,1	Sr	0,0	Zn	0,0	Li	0,0	La	-0,1	Mn	0,0
Pb	0,1	Mg	0,0	K	0,0	Ti	0,0	Sr	-0,1	Ce	0,0
Cl	0,0	Ti	0,0	NO_3^-	0,0	Al_2O_3	0,0	Ca	-0,1	Cr	-0,1
NH4+	-0,1	Co	0,0	Ca	0,0	Mg	-0,1	Na	-0,1	Li	-0,1
Cd	-0,1	Al_2O_3	0,0	Mn	-0,1	SO_4^{2-}	-0,2	Mg	-0,2	OM+EC	-0,1
NO_3^-	-0,1	P	0,0	Cl^-	-0,1	Na	-0,3	Cr	-0,2	Sn	-0,1
% Var	40	% Var	14	% Var	7	% Var	6	% Var	5	% Var	4

Table 4.21. Factors identified in PM_1 by PCA, associated factor loadings and % variance (% Var) of the samples explained by each of the factors obtained. Main tracers where highlighted.

Road traffic (primary)		Mineral matter		Secondary aerosols + Fuel oil combustion		Industrial emissions	
OM+EC	**0,8**	**Ca**	**0,9**	**Ni**	**0,9**	**Pb**	**0,9**
Mn	**0,8**	**Mg**	**0,8**	**V**	**0,8**	**Zn**	**0,9**
K	**0,7**	**Al_2O_3**	**0,8**	**SO_4^{2-}**	**0,8**	**Cd**	**0,6**
Fe	**0,7**	**Ti**	**0,6**	**Co**	**0,7**	*Cl^-*	*0,5*
Rb	**0,7**	**Na**	**0,6**	**NH_4^+**	**0,6**	*Sb*	*0,4*
NO_3^-	**0,6**	**Sr**	**0,6**	*Cr*	*0,4*	Na	0,3
As	**0,6**	*Fe*	*0,5*	As	0,3	Rb	0,3
Sb	**0,6**	*Li*	*0,5*	Sr	0,3	Sn	0,2
Sn	*0,5*	Sb	0,2	Cd	0,3	As	0,2
Li	*0,5*	V	0,2	Ti	0,2	Li	0,2
NH_4^+	*0,4*	Sn	0,2	Sb	0,2	OM+EC	0,1
Co	0,3	Ni	0,2	OM+EC	0,2	K	0,1
Cd	0,3	Rb	0,2	Sn	0,2	Mn	0,1
Ti	0,2	Cr	0,1	Na	0,1	Fe	0,1
Cl^-	0,2	SO_4^{2-}	0,1	Rb	0,1	Co	0,1
Ni	0,2	K	0,1	Al_2O_3	0,1	Ni	0,0
Pb	0,1	Zn	0,1	Li	0,1	V	0,0
Zn	0,1	Co	0,1	NO_3^-	0,1	Al_2O_3	0,0
Ca	0,1	As	0,0	Mg	0,1	Cr	0,0
V	0,1	Mn	0,0	Fe	0,0	NO_3^-	0,0
Cr	0,1	Pb	0,0	K	0,0	Sr	0,0
Na	0,0	Cl^-	-0,1	Mn	0,0	SO_4^{2-}	0,0
Mg	0,0	Cd	-0,1	Pb	0,0	NH_4^+	-0,1
SO_4^{2-}	0,0	OM+EC	-0,1	Zn	-0,1	Mg	-0,1
Al_2O_3	-0,1	NH_4^+	-0,2	Cl^-	-0,1	Ca	-0,1
Sr	-0,1	NO_3^-	-0,3	Ca	-0,1	Ti	-0,1
% Var	27	% Var	15	% Var	10	% Var	7

The main factors identified in PM_{10}, $PM_{2.5}$ and PM_1 and the characteristic chemical species of each factor (factor loadings>0.4) are summarized in Table 4.22. In PM_{10} and $PM_{2.5}$ the same six factors were identified: mineral matter, primary road traffic, secondary aerosols, industrial emissions, marine aerosols and fuel oil combustion, accounting or 78% and 76% of the total variance respectively. Mineral matter, road traffic and industrial emissions account mainly for primary emissions in PM_{10} and $PM_{2.5}$. However, in $PM_{2.5}$ nitrate also appears associated to this factor. In PM_1 only 4 factors were identified: mineral matter, road traffic, industrial emissions and fuel oil combustion, accounting for only 59% of the total variance. This is probably due to the fact that in PM_1 many of the elements analysed were discarded for the PCA analysis due to the low levels measured, sometimes under detection limits. Marine aerosols are mainly coarse in size and don't appear as a factor in this size fraction. Secondary aerosols appear divided between two factors in PM_1: ammonium nitrate is associated to the road traffic factor and ammonium sulphate to the fuel oil combustion factor, accounting for local and regional secondary emissions.

Table 4.22. Main factors identified in PM_{10}, $PM_{2.5}$ and PM_1. Components with factors higher or equal to 0.6 are highlighted in block letters and components with factors between 0.4 and 0.6 are written in italic.

	PM_{10}	**$PM_{2.5}$**	**PM_1**
Mineral matter	**Al_2O_3, Ti, Rb, Sr, Li, K, La, Ce, Mg, Ca, P, Fe, Mn,** *Ba, Cr, Co, SO_4^{2-}*	**Ti, Al_2O_3, Rb, Sr, Ca, Ce, La , Fe, Ga, Li, Mg, K, P, Mn**	**Ca, Mg, Al_2O_3, Ti, Na, Sr,** *Fe, Li*
Road traffic	**OM+EC, Sn, Sb, Cr, Fe, Cu,** *Mn, Ba*	**OM+EC, Sb, Sn,** *Cr, As, Mn, Fe, NO_3^-*	**OM+EC, Mn, K, Fe, Rb, NO_3^-, As, Sb,** *Sn, Li, NH_4^+*
Secondary aerosols	**NH_4^+, NO_3^-, SO_4^{2-}**	**NH_4^+, NO_3^-, SO_4^{2-},** *OM+EC*	
Industrial emissions	**Pb, Zn, Cd, As**	**Zn, Pb,** *Cd, As*	**Zn, Pb, Cd,** *Cl^-, Sb*
Marine aerosols	**Na, Cl^-,** *Mg*	**Cl^-, Na,** *Mg, Co*	
Fuel oil combustion	**Ni, V,** *Co*	**V, Ni, SO_4^{2-},** *Cr*	**Ni, V, SO_4^{2-}, Co, NH_4^+,** *Cr*

4.1.5.2. PMF

4.1.5.2.1. Elements and data for analysis

In PMF, elements were selected for the analysis according to their signal to noise ratio (S/N), the % of values above the detection limit (%>DL) and the errors associated to each of the measurements (Viana et al. 2008a), as previously explained in the methodology chapter (Table 4.23). In PMF, 29 elements were chosen for PM_{10} and $PM_{2.5}$ and 23 for PM_1. The differences in the elements selected for the PCA and PMF analysis are due to the application of different criteria used to obtain the better solutions with each method.

Table 4.23. Mean concentration for values over the detection limit (Mean>DL), proportion of values over the detection limit (%DL), error percentage (% error), signal to noise ratio (S/N) and for the main elements used in the PMF analysis measured in PM_{10}, $PM_{2.5}$ and PM_1. Components selected for the analysis. Exclusion causes: low levels, often under DL (●).

	Mean>DL (μg m^{-3})			S/N			% >DL			% error			Selections		
	PM_{10}	$PM_{2.5}$	PM_1	PM_{10}	$PM_{2.5}$	PM_1	PM_{10}	$PM_{2.5}$	PM_1	PM_{10}	$PM_{2.5}$	PM_1	PM_{10}	$PM_{2.5}$	PM_1
Ctot	8.7727	7.9462	6.3183	7.7	7.0	5.6	100	100	100	30	32	36	X	X	X
Al	0.7624	0.2868	0.1122	15.1	5.7	2.2	100	96	17	20	50	271	X	X	●
Ca	2.5412	0.7766	0.0911	55.6	17.0	2.0	100	100	62	13	20	123	X	X	X
K	0.3885	0.2042	0.0972	16.4	8.6	4.1	100	100	98	18	25	46	X	X	X
Na	1.0410	0.3085	0.1624	10.1	3.0	1.6	100	90	15	27	71	223	X	X	●
Mg	0.3011	0.0975	0.0215	22.5	7.3	1.6	100	100	15	16	31	167	X	X	●
Fe	1.0252	0.3498	0.0587	159	54.3	9.1	100	100	100	11	12	24	X	X	X
SO_4^{2-}	5.1080	4.3887	2.8813	220	189	124	100	100	100	16	17	17	X	X	X
NO_3^-	5.0874	2.9796	1.6652	239	140	78.2	100	99	94	18	22	70	X	X	X
Cl^-	0.8317	0.3657	0.1196	22.1	9.7	3.2	98	83	51	78	363	869	X	X	X
NH_4^+	1.4132	1.7140	1.2332	169	205	148	100	100	100	21	21	21	X	X	X
Li	0.0006	0.0002	0.0001	11.8	4.9	1.6	97	97	62	31	49	139	X	X	X
Ti	0.0459	0.0172	0.0021	56.1	21.1	2.6	100	99	90	13	42	234	X	X	X
V	0.0121	0.0089	0.0065	34.7	25.7	18.7	100	100	100	14	16	20	X	X	X
Cr	0.0058	0.0026	0.0018	7.8	3.5	2.5	99	94	66	47	168	520	X	X	X
Mn	0.0200	0.0100	0.0039	93.5	47.1	18.5	100	100	99	11	13	29	X	X	X
Co	0.0003	0.0002	0.0002	3.2	2.0	1.4	97	67	16	57	116	264	X	X	●
Ni	0.0055	0.0040	0.0029	7.5	5.5	4.0	98	96	95	111	136	90	X	X	X
Cu	0.0703	0.0354	0.0106	39.4	19.9	6.0	100	100	96	14	18	67	X	X	X
Zn	0.1139	0.0909	0.0631	2.5	2.0	1.4	76	58	21	94	139	232	X	X	●
As	0.0009	0.0007	0.0005	14.6	10.9	7.5	100	99	100	19	25	26	X	X	X
Rb	0.0013	0.0005	0.0002	46.8	20.6	6.9	100	100	100	13	17	28	X	X	X
Sr	0.0058	0.0020	0.0012	9.1	3.3	2.0	99	91	17	42	115	732	X	X	●
Cd	0.0003	0.0003	0.0002	4.6	4.3	3.0	96	95	90	65	64	63	X	X	X
Sn	0.0071	0.0036	0.0026	7.0	3.6	2.6	98	96	72	36	104	291	X	X	X
Sb	0.0064	0.0024	0.0010	11.1	4.3	1.7	100	99	57	24	43	123	X	X	X
La	0.0004	0.0001	0.0001	9.7	4.3	2.1	97	91	67	36	106	136	X	X	X
Ce	0.0009	0.0004	0.0002	9.2	4.1	2.4	97	93	71	50	100	148	X	X	X
Pb	0.0213	0.0163	0.0086	118	90.3	47.5	100	100	100	12	12	14	X	X	X

4.1.5.2.2. Identification of emission sources

The source identification and quantification was carried out with the Positive Matrix Factorization (PMF) model, obtaining similar results to the PCA analysis, especially for the fractions PM_{10} and $PM_{2.5}$, but differing more in the fraction PM_1. Source profiles for PMF solutions obtained for PM_{10}, $PM_{2.5}$ and PM_1 are shown in Figure 4.1.54, Figure

4.1.55 and Figure 4.1.56. A summary of the factors identified in PM_{10}, $PM_{2.5}$ and PM_1 is shown in Table 4.24.

Six factors were identified in PM_{10} and they were very similar to the factors obtained by means of the PCA analysis. These source factors were aged sea spray, fuel oil combustion, secondary ammonium nitrate, mineral matter, road traffic primary emissions and industrial emissions. The difference with the PCA analysis was found for secondary aerosols, which in the PCA results appear grouped in the same factor (ammonium nitrate and sulphate), while in the PMF results sulphate aerosols are divided between the aged marine aerosols factor and the fuel oil combustion factor.

Six factors were also identified in $PM_{2.5}$. These factors were fuel oil combustion, secondary ammonium nitrate, industrial emissions, road traffic primary emissions, mineral matter and secondary ammonium sulphate. The difference with PM_{10} was that in the $PM_{2.5}$ fraction the factor accounting for aged sea spray does not appear, and secondary aerosols are divided in two factors: ammonium nitrate and ammonium sulphate. However, there were some differences with the PCA analysis, as the marine factor of the PCA analysis does not appear in the PMF analysis for this fraction. In addition, the regional-secondary factor is now divided in two factors: ammonium sulphate and ammonium nitrate.

In PM_1, four factors were identified: secondary ammonium nitrate, secondary ammonium sulphate, a mixed factor accounting for road traffic primary emissions, mineral matter and industrial emissions and another factor accounting for fuel oil combustion together with some industrial tracers. However, the results were quite different than those obtained with PCA. In the PMF analysis the primary traffic factor appears mixed with mineral matter and industrial tracers and, as in $PM_{2.5}$, two secondary aerosol factors were identified instead of one: ammonium sulphate and ammonium nitrate. The fuel oil combustion factor appears also mixed with industrial tracers and it is not mixed with the secondary ammonium sulphate as it was in the PCA analysis.

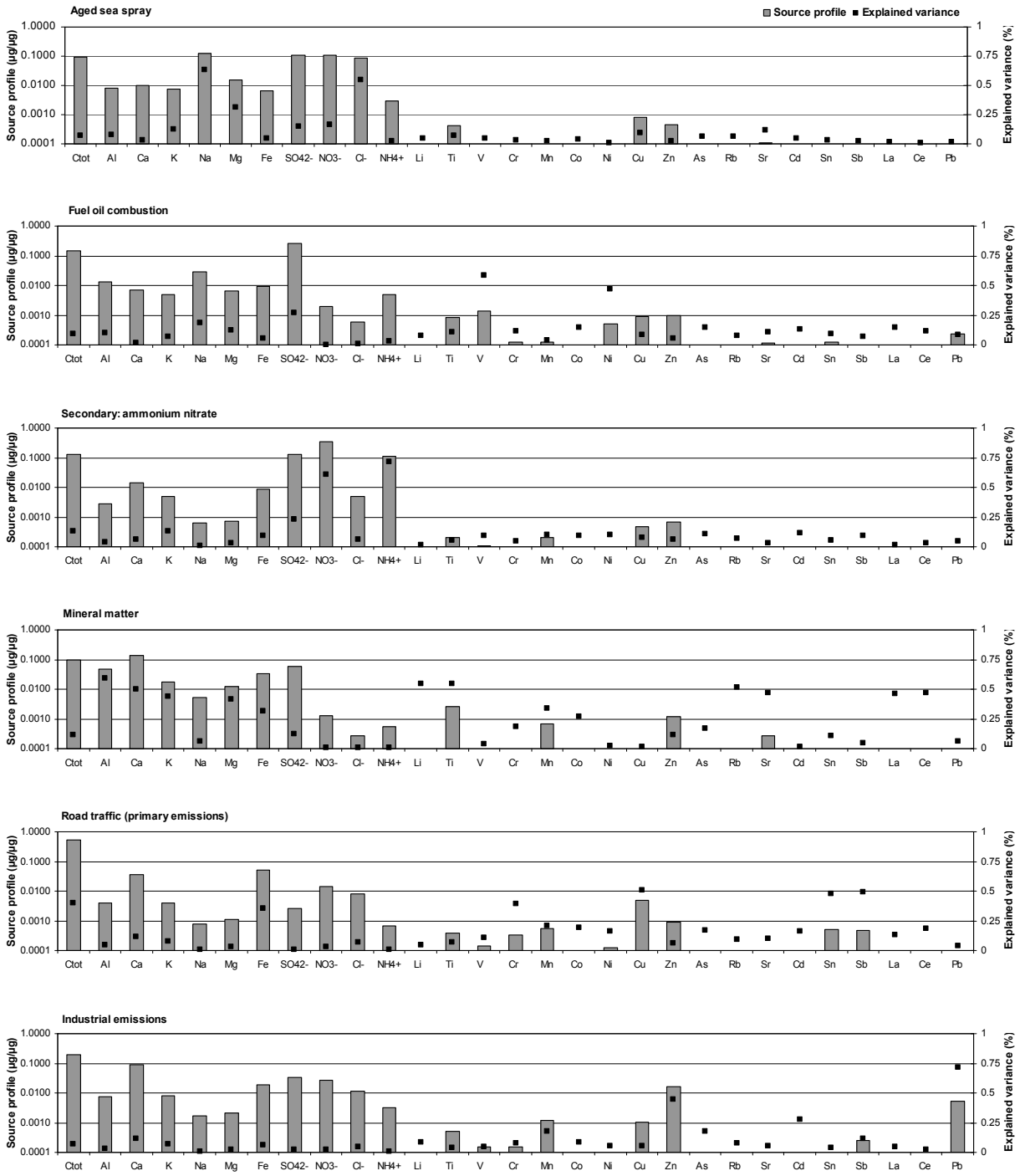

Figure 4.1.54. Source profiles for PMF solutions in PM_{10}.

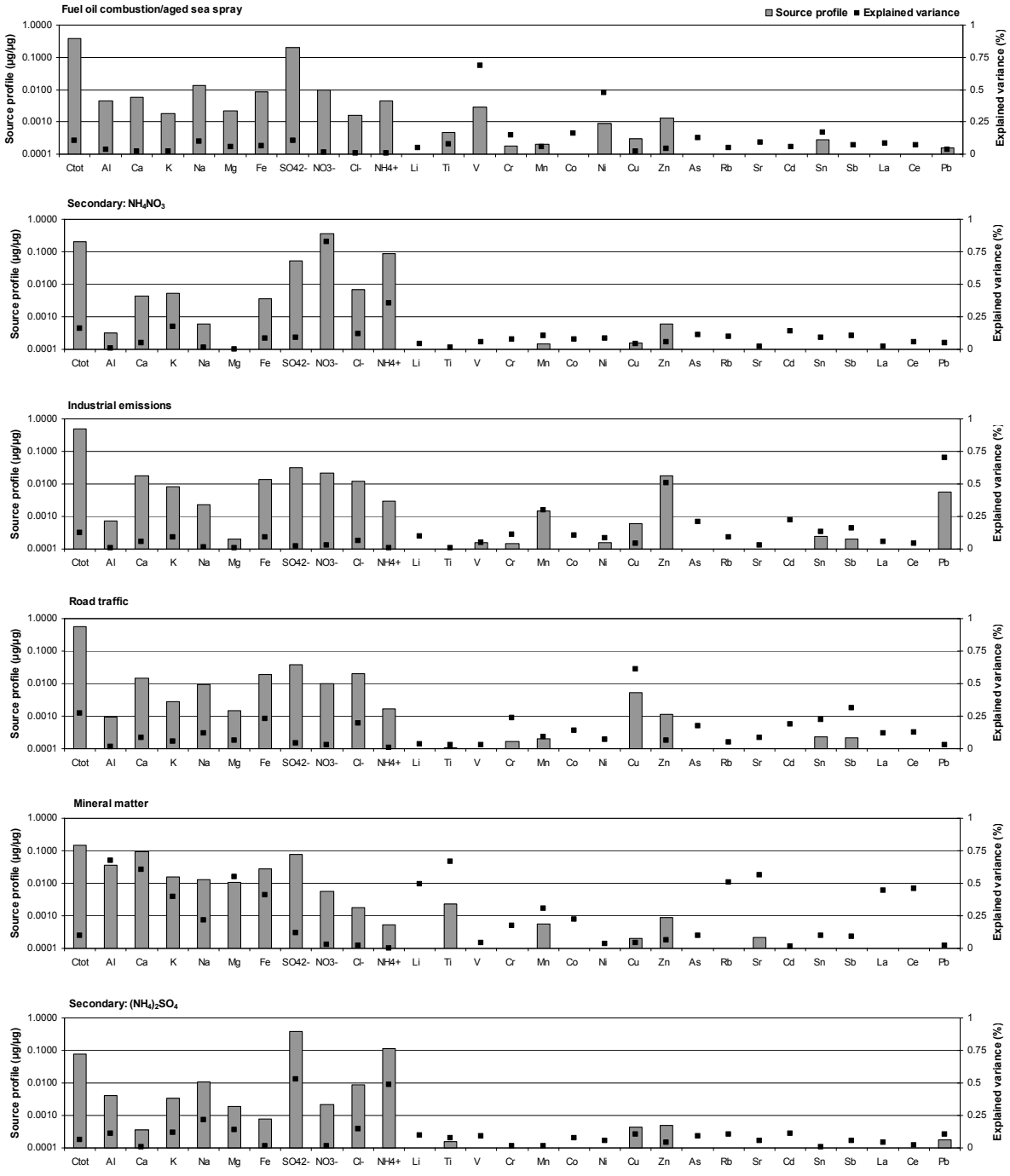

Figure 4.1.55. Source profiles for PMF solutions in $PM_{2.5}$.

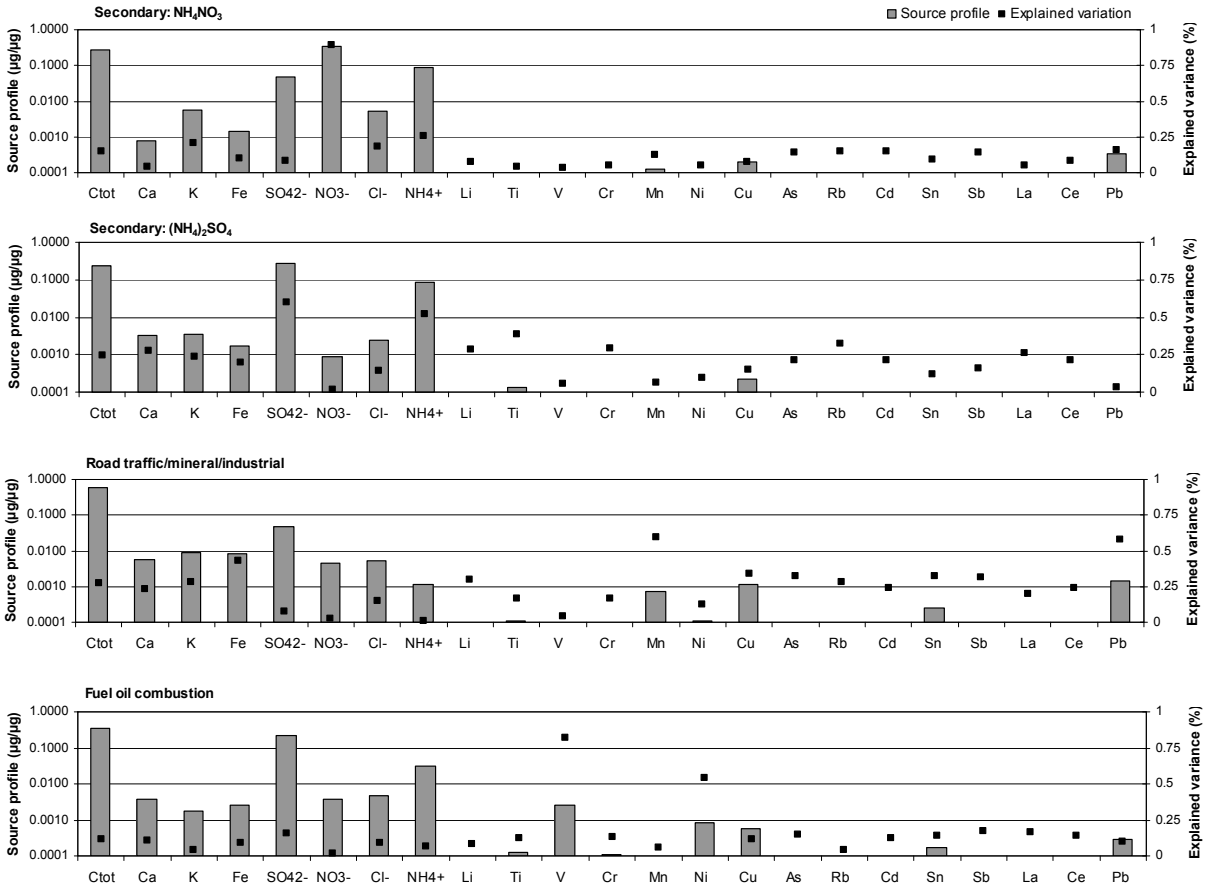

Figure 4.1.56. Source profiles for PMF solutions in PM_1.

Table 4.24. Factors identified using the PMF model.

	PM_{10}	$PM_{2.5}$	PM_1
Mineral matter	**Al, Ca, K, Li, Ti, Rb, Sr, La, Ce,** *Mg*	**Al, Ca, K, Mg, Fe, Li, Ti, Rb, Sr, La, Ce,** *Na*	**Ctot, Ca, K, Fe, Li, Ti, Mn, Cu, Rb,** *As, Cd, Sn, Sb, Pb*
Road traffic (mostly primary)	**Ctot, Fe, Cr, Cu, Sn, Sb**	**Ctot, Cl^-, Cu, Sb, Sn,** *Fe, Cr*	
Industrial emissions	**Pb, Zn, Cd, As, Mn**	**Mn, Zn, As, Cd, Pb,** *Co, Sb, Sn, Ctot,*	
Secondary-regional: Ammonium sulphate		**NH_4^+, SO_4^{2-},** *Na*	**NH_4^+, SO_4^{2-}**
Secondary: Ammonium nitrate (mostly from road traffic)	**NH_4^+, NO_3^-,** *SO_4^{2-}*	**NH_4^+, NO_3^-**	**NH_4^+, NO_3^-**
Aged marine aerosols	**Na, Cl^-, Mg,** *SO_4^{2-}*	**V, Ni, Na,** *SO_4^{2-}, Cr, Co, Sn, Ctot*	
Fuel oil combustion (primary + secondary)	**SO_4^{2-}, Ni, V**		**Ni, V, Cr, La, Ce,** *Ctot, As, Cd, Sn, Sb*

The ***mineral factor*** is identified in PM_{10} and $PM_{2.5}$ fractions by the presence of Al, Ca, K, Li, Ti, Rb, Sr, La and Ce, and in $PM_{2.5}$ also by Mg and Fe. It represents several sources of mineral matter (mainly alumino-silicates with some proportion of Ca and Mg carbonates) including anthropic (road dust resuspension by vehicles, mineral matter from construction-demolition works) and natural (African dust outbreaks, soil resuspension by wind) origins. In PM_1 this factor is not identified separately by the PMF analysis, as mineral matter is generally coarse. In this case it appears mixed with traffic tracers in PM_1 due to its relationship with road dust resuspension by vehicles.

In the PCA analysis the mineral factor was identified in all fractions by the presence of alumino-silicates (Al_2O_3, Ti, Li, Rb, K) with some amount of Ca-Mg-Sr carbonates in PM_{10} and $PM_{2.5}$ and explains the highest % variance of the samples in PM_{10} and $PM_{2.5}$ (44 and 40% respectively). In PM_1 this factor is dominated by the presence of Ca-Mg-Sr carbonates and in minor proportion alumino-silicates and it explains a 15% of the total variance.

The ***road traffic factor*** is identified in all fractions by the presence of Ctotal (from vehicle exhaust emissions) and trace elements as Fe, Cu, Sn and Sb (from the mechanical abrasion of road pavement and vehicle components). Cr appears also related to this factor in PM_{10} and $PM_{2.5}$ and Cl^- only in $PM_{2.5}$. In PM_1 the traffic tracers appear associated to mineral matter tracers as Ca, K, Li, Ti and Rb, probably because of road dust resuspension by vehicles and also to industrial emission tracers, as Pb, Cd, As and Mn. The road traffic factor obtained in PMF explains mostly primary road traffic emissions.

In the PCA analysis the road traffic factor is identified in PM_{10} (mostly as primary emissions), and $PM_{2.5}$ and PM_1 (primary with a proportion of secondary components) by OM+EC, Sb, Sn, Fe and Mn in all fractions, Cr in both PM_{10} and $PM_{2.5}$ and As and NO_3^- in both $PM_{2.5}$ and PM_1. Ba and Cu also have a contribution in PM_{10} (these elements were not considered for the $PM_{2.5}$ or PM_1 analysis). In PM_1 the main traffic tracers appear mixed with secondary components (NO_3^- and NH_4^+) explaining this factor the highest % of variance. This factor could also be related to the winter anticyclonic episodes (WAE) that produce intense pollution events and very high PM_1 levels. The % variance of the traffic factor is high in PM_{10} (13%) and explains the highest variance in PM_1 (27%). In $PM_{2.5}$ it only represents a 6%.

The ***secondary aerosol factor*** is identified in PM_{10} by NH_4^+, NO_3^- and SO_4^{2-} from the formation of secondary aerosols from gaseous precursors (NH_3, NO_X and SO_2) in the atmosphere. In $PM_{2.5}$ and PM_1, secondary aerosols are separated in two factors: ammonium sulphate and ammonium nitrate. Ammonium sulphate is the result of the formation of secondary sulphate in the atmosphere by the photochemical oxidation of sulphur oxides emitted by combustion sources as power plants and shipping, and also from long-range transport and vehicle exhaust in a low proportion. Ammonium nitrate is also formed in the atmosphere from gaseous nitrogen oxides emitted in >80% by road traffic and in a minor proportion from other combustion sources. NH_4^+ is derived from NH_3 arising in >95% from farming and agricultural emissions.

In the PCA analysis the regional factor is identified by NH_4^+, NO_3^- and SO_4^{2-} both in PM_{10} and $PM_{2.5}$. In $PM_{2.5}$ OM+EC is also present, because of the important formation of secondary carbonaceous compounds at urban backgrounds. In PM_1, secondary compounds appear in two different factors: ammonium sulphate is associated to fuel oil combustion tracers and ammonium nitrate is associated to the road traffic factor. This factor explains a 7% of the variance in PM_{10} and a 5% in $PM_{2.5}$.

The ***industrial emissions factor*** is identified in PM_{10} and $PM_{2.5}$ by Pb, Zn, Cd, As and Mn. These elements are tracers of metallurgic processes according to other studies (Pacyna, 1986). In $PM_{2.5}$ Sb and Sn, which are related to traffic emissions, also appear associated with the industrial tracers. In Barcelona there are a number of metallurgical sources that may account for the industrial tracer contribution, mainly ferrous and non ferrous smelters.

In the PCA analysis this factor is identified in all fractions by Pb, Zn and Cd and also by As in PM_{10} and $PM_{2.5}$. In PM_1 Cl^- and Sb also appear together with the industrial tracers. This factor explains a 6% of the variance in PM_{10}, 14% in $PM_{2.5}$ and 7 % in PM_1.

The ***marine factor*** is only identified as a single factor in PM_{10} by PMF, with Na, Cl^-, Mg and SO_4^2 as main tracers. It accounts for aged sea spray, as secondary sulphate is also associated to this factor. In $PM_{2.5}$ sea spray aerosols are not detected as a single factor in PMF, being mixed with the fuel oil combustion factor (associated to sea breezes carrying shipping emissions). In PM_1 this source is not detected, as it is mainly coarse in size.

In the PCA analysis this factor is identified in PM_{10} and $PM_{2.5}$ and explains a 5 and 4% of the variance respectively. It accounts for sea spray primary emissions and the main tracers are Na, Cl^- and Mg.

The ***fuel oil combustion factor*** is identified in all fractions by V and Ni. Secondary SO_4^{2-} also appears associated to the main tracers in PM_{10} and $PM_{2.5}$, and Cr and Sn in $PM_{2.5}$ and PM_1. In $PM_{2.5}$ Co and Na also appear in this factor and in PM_1, Ctot, La, Ce, As, Cd and Sb. V and Ni are typical tracers of fuel oil combustion (Pacyna, 1986) and its presence in Barcelona may be derived of electricity generation processes and emissions from shipping traffic.

In the PCA analysis this factor was identified also in all fractions by the tracers V and Ni. Co appears also in PM_{10} and $PM_{2.5}$ and SO_4^{2-} and Cr in $PM_{2.5}$ and PM_1. NH_4^+ appears also in PM_1 and this factor is also associated to the secondary ammonium sulphate. This factor explains a 3% of the variance in PM_{10}, a 7% in $PM_{2.5}$ and a 10% in PM_1.

When considering road traffic and fuel oil contributions it seems that the coarser sizes include mostly primary PM, whereas the proportion of secondary aerosols derived from gaseous precursors increases towards the finer PM sizes.

4.1.5.2.3. Quantification of source contributions to PM_{10}, $PM_{2.5}$ and PM_1

The correlation between gravimetric and simulated PM_{10}, $PM_{2.5}$ and PM_1 was good, with r^2=0.84, 0.83 and 0.74 respectively and an underestimation lower than 3% by the PMF (Figure 4.1.57).

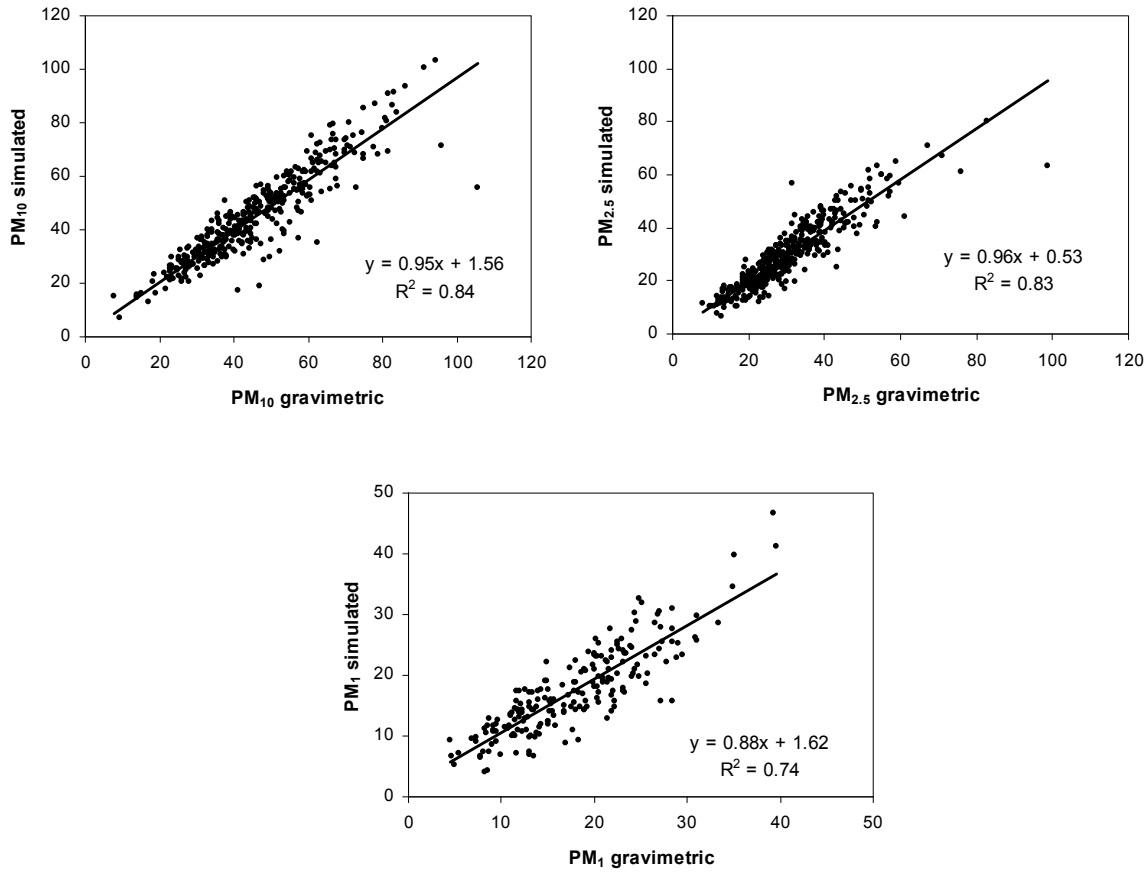

Figure 4.1.57. Correlations between simulated and gravimetric PM_{10}, $PM_{2.5}$ and $PM_{1.}$

The mean contributions for each factor obtained by the PMF analysis are shown in Table 4.25 and Figure 4.1.58. Mineral origin aerosols accounted for 11.3 and 5.9 μg m^{-3} (25 and 20%) of the PM_{10} and $PM_{2.5}$ mass respectively. The contribution of road traffic primary emissions to the PM_{10}, $PM_{2.5}$ and PM_1 mass was 7.7, 4.2 and 3.6 μg m^{-3} (17, 14 and 20%) respectively, being this factor mixed with mineral matter and industrial tracers in the PM_1 fraction. Secondary ammonium nitrate accounted for 10.1, 7.4 and 4.4 μg m^{-3} (22, 24 and 25%) of the $PM_{10,}$ $PM_{2.5}$ and PM_1 mass respectively. In $PM_{2.5}$ and PM_1, secondary ammonium sulphate accounted for 7.2 and 7.1 μg m^{-3} (24 and 39%) respectively. Secondary sulphate aerosols in the PM_{10} fraction were detected both in the secondary nitrate and the fuel oil combustion factor. The contribution of industrial origin aerosols to the PM_{10} and $PM_{2.5}$ mass was of 3.3 and 2.3 μg m^{-3} (7 and 8%) respectively, being industrial tracers mixed with the road traffic factor in the PM_1 fraction. Aged marine aerosols were 6.4 μg m^{-3} (14%) of the PM_{10} fraction, accounting for a mixture of sea spray and secondary aerosols, mainly sulphate. In the $PM_{2.5}$ fraction sea spray appears in the fuel oil combustion factor, due to the important

contribution of shipping emissions to this factor. Aerosols associated to fuel-oil combustion emissions accounted for 5.8, 2.5 and 2.3 (13, 8 and 13%) of the PM_{10}, $PM_{2.5}$ and PM_1 mass respectively.

Table 4.25. Mean contributions (µg m^{-3} and %) of the factors obtained by PMF in PM_{10}, $PM_{2.5}$ and PM_1.

	µg m^{-3}			%		
	PM_{10}	**$PM_{2.5}$**	**PM_1**	**PM_{10}**	**$PM_{2.5}$**	**PM_1**
Mineral matter	11.3	5.9	3.6	25	20	20
Primary road traffic	7.7	4.2		17	14	
Industrial emissions	3.3	2.3		7	8	
Secondary ammonium sulphate		7.2	7.1		24	39
Secondary ammonium nitrate	10.1	7.4	4.4	22	24	25
Aged sea spray	6.4	2.5		14	8	
Fuel-oil combustion	5.8		2.3	13		13
Unaccounted	0.7	0.7	0.5	2	2	3

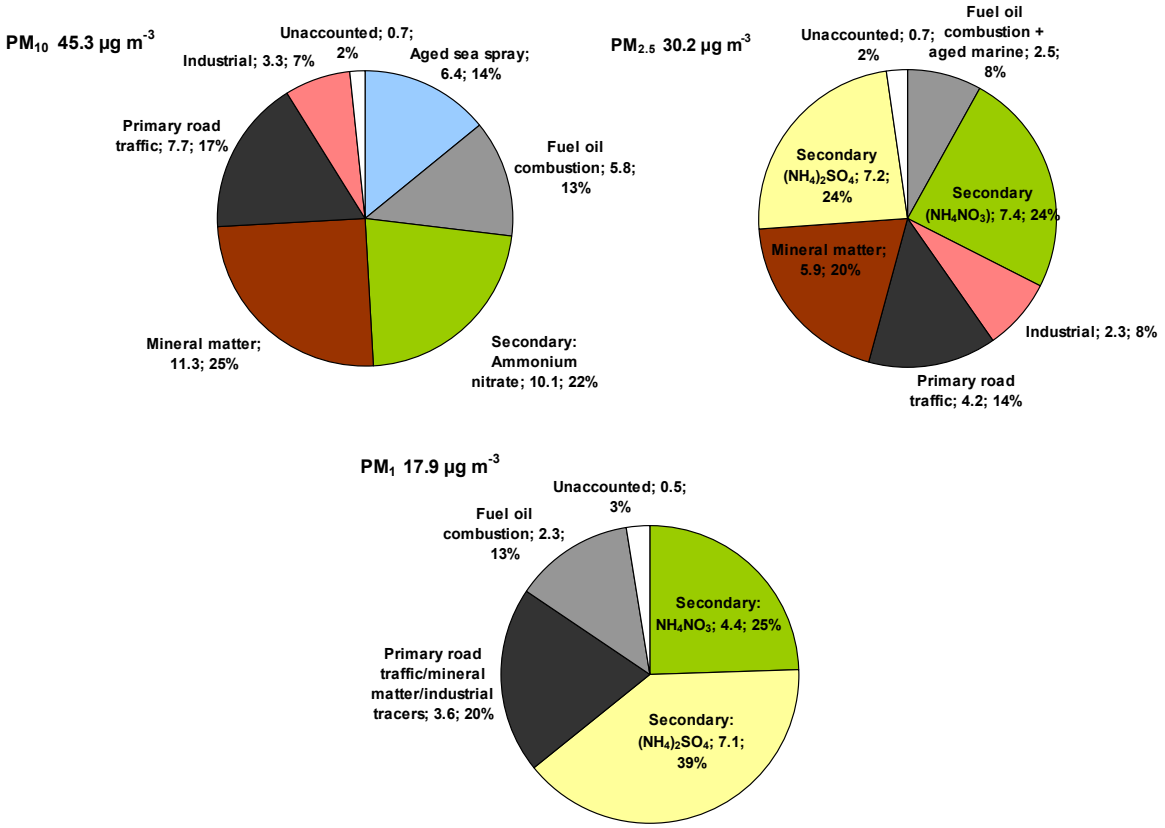

Figure 4.1.58. Average contribution of sources obtained by PMF to PM_{10}, $PM_{2.5}$ and $PM_{1.}$

The road traffic factor is mainly primary, accounting from exhaust (carbonaceous compounds) and non-exhaust (road dust resuspension) primary emissions. However, a high proportion of the secondary ammonium nitrate factor may be also attributed to road traffic emissions. Moreover, an important part of the mineral matter factor may also be attributed to dust resuspension processes by vehicles. At BCN the mean annual African contribution to PM levels was calculated previously as 1.5, 0.9 and 0.6 μg m^{-3} for PM_{10}, $PM_{2.5}$ and PM_1, as mean values for the period 1999-2007. Thus, excluding some transport of dust from resuspension processes in the region, mineral matter may be attributed to anthropogenic emissions, mainly road traffic and fugitive emissions from construction and demolition activities.

The relative contribution of the species analyzed to each of the factors identified in PM_{10}, $PM_{2.5}$ and PM_1 is presented in Figure 4.1.59, indicating the main sources contributing to the levels of each component.

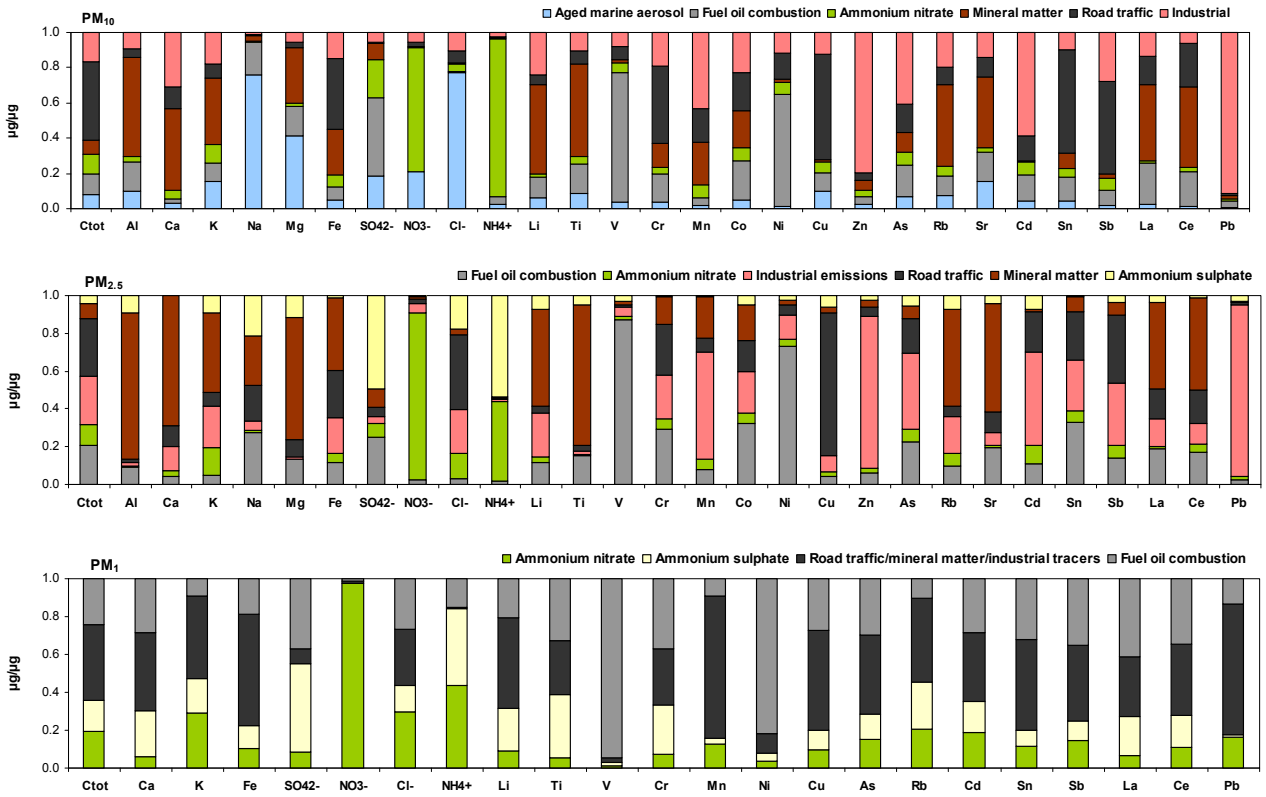

Figure 4.1.59. Relative contribution of each species to the factors identified by PMF in PM_{10}, $PM_{2.5}$ and PM_1.

4.1.5.2.4. Seasonal and inter-annual evolution of PM sources

Seasonal and inter-annual evolutions for the main daily contributions for each source identified in PM_{10}, $PM_{2.5}$ and PM_1 are shown in Figure 4.1.60, Figure 4.1.61 and Figure 4.1.62.

The aged marine source in PM_{10} usually presents higher levels during the summer. This is produced by the development of summer sea breezes with direct transport of sea spray from the Mediterranean. In winter Atlantic advections may account for the sea spray recorded in Barcelona, as air mass transport from the Atlantic sea is common during this period of the year.

The mineral source presents a clear seasonal trend in PM_{10} and $PM_{2.5}$ with higher levels during summer and lower in winter. This behaviour is mainly due to lower precipitations that favour road dust resuspension by traffic and wind, a higher frequency of African dust outbreaks during summer months and summer atmospheric conditions (breezes) that favour resuspension and recirculation processes.

The ammonium nitrate source identified in PM_{10}, $PM_{2.5}$ and PM_1 shows a clear seasonality with higher levels during the winter months (especially from November to March) owing to the stagnant conditions that produce the winter anticyclonic episodes previously described, together with the effect of the thermal instability of particulate ammonium nitrate at high temperatures. In $PM_{2.5}$ and PM_1, the secondary ammonium sulphate presents a seasonal pattern with higher levels during the summer as a result of the favoured photochemical processes and ageing of air masses at a regional scale.

The primary traffic source shows higher levels during winter months. This behaviour is also the result of the anticyclonic atmospheric conditions during this period of the year, producing the stagnation of atmospheric pollutants at a local scale in Barcelona.

The fuel oil combustion source shows an annual cycle with higher levels during the summer, associated to the favoured sea-land breezes that carry pollutants from the port.

The industrial source does not show a clear seasonal trend. However, the levels of industrial contribution seem to decrease from 2003 to 2007, indicating a possible reduction of industrial emissions, probably due to the application of some emission abatement plans.

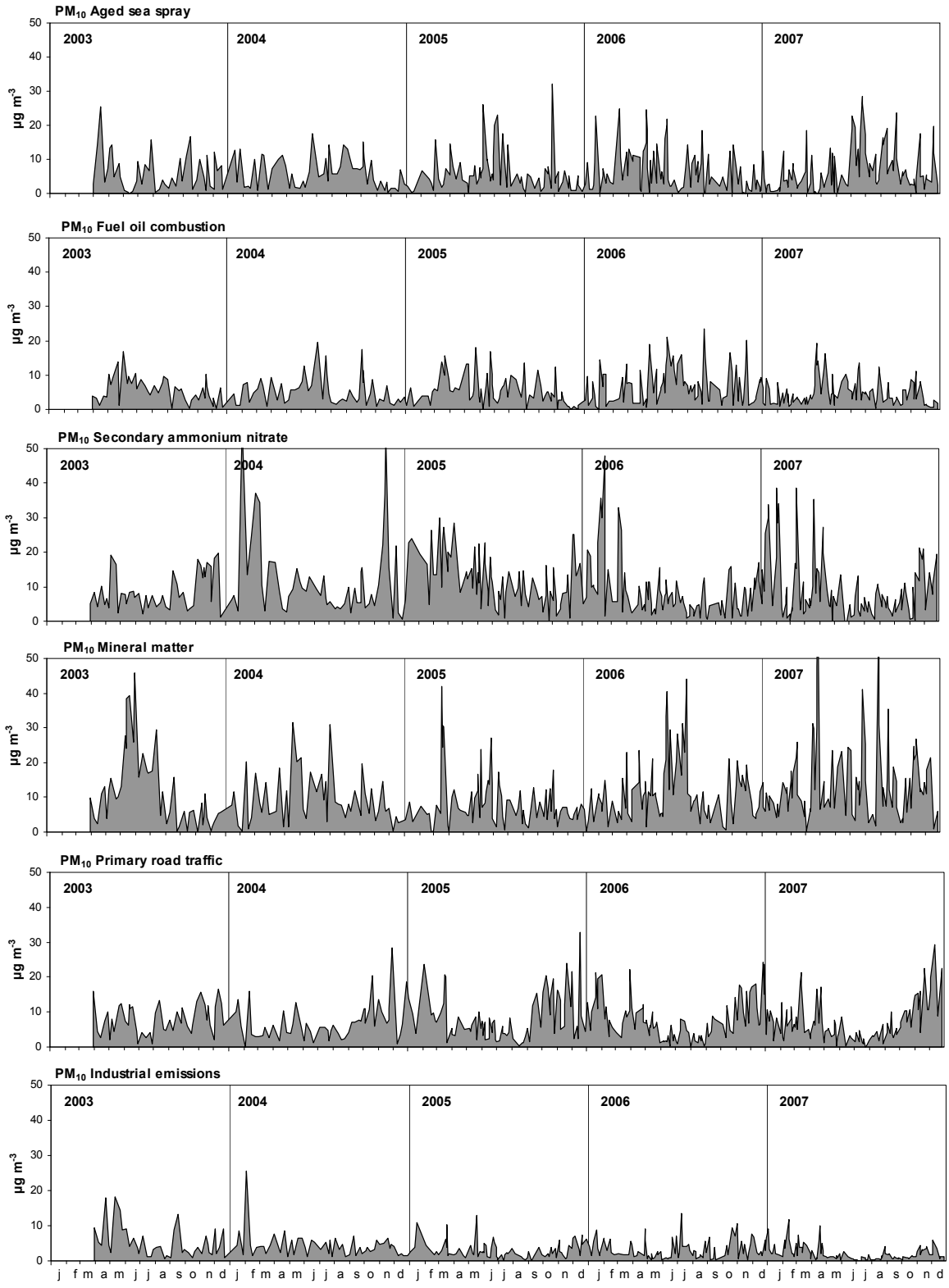

Figure 4.1.60. Seasonal and inter-annual evolution of the main daily contributions for each source identified in PM_{10}.

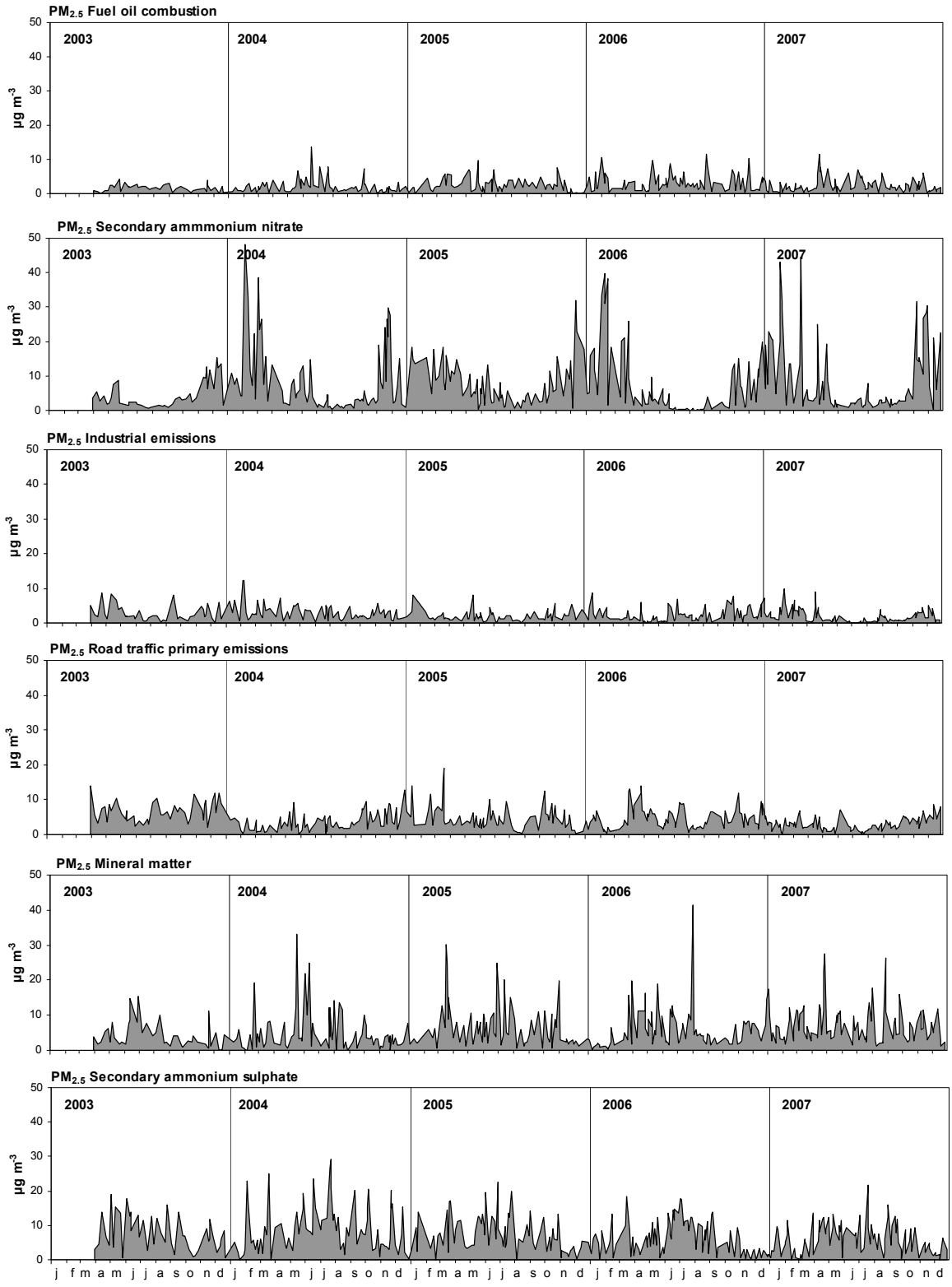

Figure 4.1.61. Seasonal and inter-annual evolution of the main daily contributions for each source identified in $PM_{2.5}$.

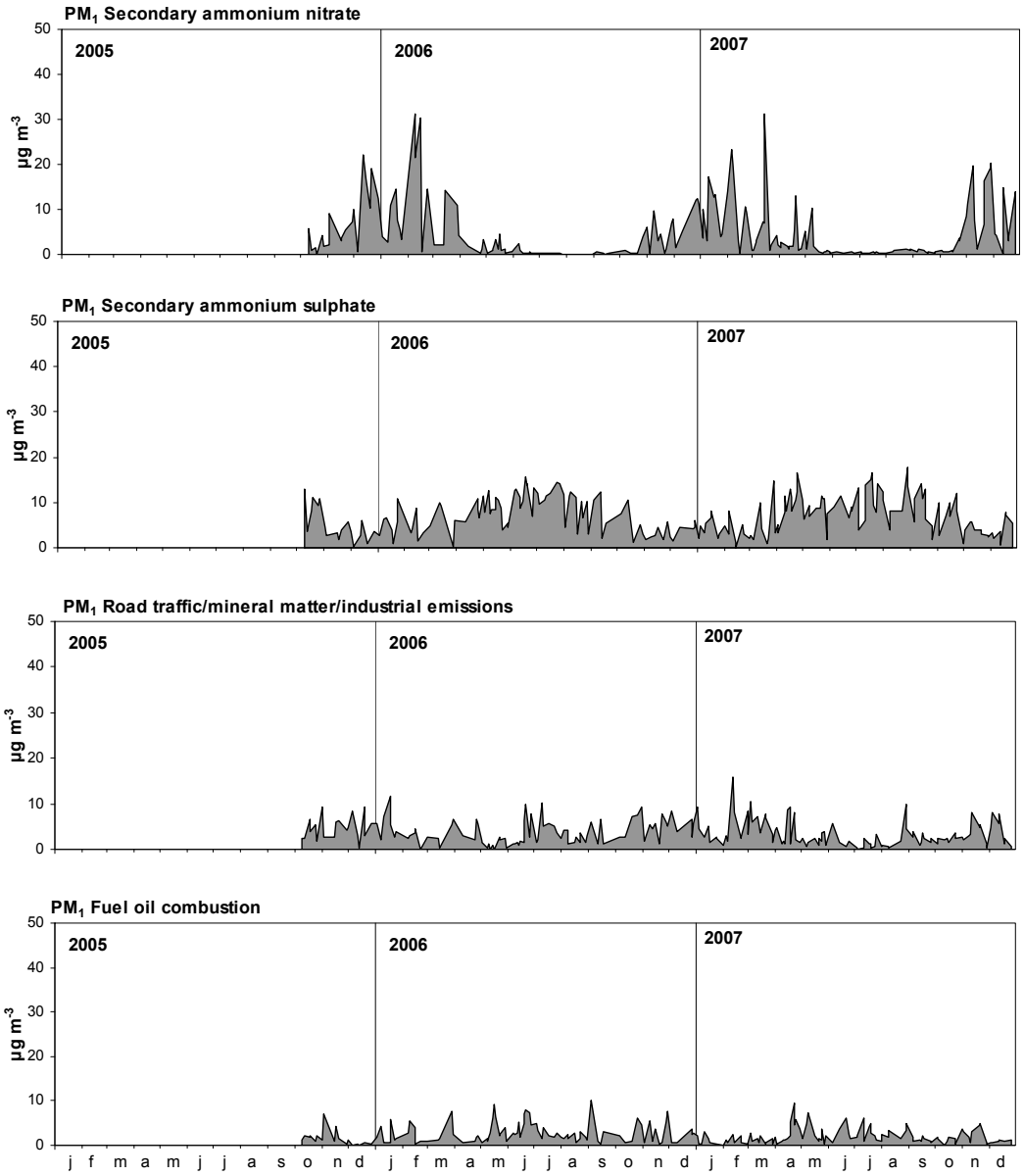

Figure 4.1.62. Seasonal and inter-annual evolution of the main daily contributions for each source identified in PM_1.

4.1.6. Summary and conclusions

The BCN-CSIC monitoring site is an urban background site that reflects the general exposure of the urban population of Barcelona to atmospheric pollutants and allows understanding the influence of road traffic emissions in the urban atmosphere.

In this chapter, PM_{10}, $PM_{2.5}$ and PM_1 levels and speciation, particle number concentration (N) and black carbon levels (BC) recorded at BCN-CSIC urban background site were measured, presented and interpreted. Special attention was paid on the speciation and grain size partitioning of PM components between the different PM fractions. Seasonal and inter-annual trends in the time series of PM levels and speciation and particle number concentration were investigated. The daily evolution of all parameters was studied together with levels of atmospheric gaseous pollutants and road traffic cycles. Finally, source apportionment techniques were applied to the results in order to identify the main sources of PM. The main objective of all these analyses is the interpretation of the variability of levels, composition and source contribution to urban aerosols in Barcelona.

Comparing PM levels recorded in this study (42, 25 and 17 μg m^{-3} mean annual PM_{10}, $PM_{2.5}$ and PM_1 levels, respectively fro 1999-2007) with other European regions with different meteorological and geographical patterns, it may be concluded that PM levels are relatively high at Barcelona. High PM anthropogenic emissions (mainly due to intense road traffic), narrow streets, together with a dry and warm Mediterranean climate, low dispersive conditions, soil re-suspension and sporadic contribution from North African dust could account for the high PM levels registered. The important influence of road traffic emissions on the levels of fine particulate matter is reflected in PM_1 mean annual levels, which show a significant increasing trend, and a probable correlation with the progressive rise in road traffic flow and the growth of the diesel fleet in Barcelona. However, the coarse fraction ($PM_{2.5-10}$) showed a decreasing trend probably attributed to meteorology and the frequency and intensity of African dust outbreaks.

The contribution of African dust to PM levels depends on the frequency and intensity of African dust episodes. In Barcelona, for the period 1999-2007, between 16 and 45% of the annual exceedances of the 50 μg m^{-3} daily limit for PM_{10} were recorded during African dust outbreaks episodes, but not in all cases were exclusively caused by this natural contribution. The annual mean African contribution to PM_{10} levels is estimated

to range from 0.6 to 2.4 μg m^{-3}, depending on the year considered. Thus, the African dust contribution to PM_{10} is important both at the annual and daily bases, and important interannual variations were observed.

Results on PM speciation and size partitioning illustrate that the coarse fraction ($PM_{2.5-10}$) is mainly composed of mineral dust (61%), sea spray (9%), and secondary inorganic aerosols (mostly Na, Ca, K, Mg sulphate and nitrate, 17%), evidencing the importance of dust resuspension from road traffic and wind, as well as other sources. The $PM_{1-2.5}$ fraction is made up of mineral dust (37%) and secondary inorganic aerosols (28%), with a fraction of carbonaceous matter (21%). The PM_1 fraction is mainly composed of OM+EC (48%) and secondary inorganic aerosols (mostly ammonium nitrate and sulphate, 32%) and very minor proportions of mineral dust and sea spray, evidencing the high influence of combustion sources (mainly exhaust emissions). Relatively high levels of mineral dust and a high proportion of coarse nitrate are PM patterns peculiar of Barcelona when compared with central and western European urban sites. However, the levels of mineral dust in PM_1 are comparable to those recorded in other climatic regions of Europe.

Day to day variation of PM levels and speciation in the WMB is governed by the concatenation of different meteorological scenarios, affecting PM concentrations and size distribution of atmospheric particulate matter at the Barcelona urban area. The seasonal distribution of these episodes together with the climatic patterns of the WMB gives rise to a marked seasonal pattern for PM background. Maximum PM levels with a finer grain size, are recorded in winter, associated with the important local pollution episodes registered as a consequence of atmospheric stability (WAE), avoiding dispersion of the important urban emissions (especially road traffic) and increasing the levels of secondary aerosols (especially ammonium nitrate). During summer atmospheric dispersion conditions are favoured, due to regional recirculation episodes (REG) and the levels of fine PM are reduced. However, coarse PM levels increase associated to the regional recirculation of air masses, the low precipitations registered favouring soil resuspension, the formation of secondary aerosols caused by enhanced photochemistry (especially ammonium sulphate) and a higher frequency of African dust outbreaks. The lower levels recorded during April, August and September are related to a higher frequency of precipitations and Atlantic air mass advections, producing the renovation of air masses and the washout of road dust, together with a lower frequency of road traffic in August attributed to summer holidays.

Levels of ultrafine particles in urban atmospheres are highly influenced by vehicle exhaust emissions. These may have serious impacts on human health and the environment. Particle number concentration (N) was monitored in real time at BCN-CSIC from 2003. Moreover, real-time monitoring of the levels of black carbon (BC) started in July 2007. The mean levels of N registered at BCN-CSIC were around 21000 cm^{-3} and are in the mid-high range of those registered at other urban background sites around Europe. N levels were higher during the winter months, when important pollution episodes were registered due to atmospheric stability, together with the low temperatures that favoured the formation of ultrafine particles. During spring and summer higher insolation favoured the formation of particles by photochemical processes. However, the high temperatures registered may favour the volatilization of new formed nanoparticles decreasing the levels measured. In addition, the higher precipitation and lower emissions during April and August-September reduce markedly the levels of all pollutants.

The simultaneous monitoring of N, BC, PM_{10}, $PM_{2.5}$ and PM_1 levels together with the levels of SO_2, NO, NO_2, O_3 and CO showed that the variability of all aerosol metrics and gaseous pollutants recorded at the Barcelona urban background is highly influenced by road traffic emissions and meteorology (especially the evolution of breezes). N, BC, PM_x, CO and NO_x levels increase markedly during traffic rush hours, reflecting direct exhaust emissions. The N traffic peak is related to particles emitted directly or formed by nucleation processes from precursors, and the BC peak to direct soot emissions. Near all parameters decrease with the slight reduction in traffic emissions after rush hours and the changes in wind direction and speed, due to dilution processes, with the exception of $PM_{2.5-10}$ and N. $PM_{2.5-10}$ remains high during all the day due to the road dust resuspension processes but also dust resuspension by wind. At noon, with the maximum solar radiation intensity, there is also an increase of N levels produced by new ultrafine particles formed by photochemical nucleation processes from precursor gases. Then, O_3 increases in the afternoon, also associated to photochemical processes. The evening traffic peak, together with the decrease of wind speed increases again the levels of all particulate and most gaseous pollutants. Finally, nocturnal conditions (decrease of the traffic flow, lower temperatures, low wind speed and minimum boundary layer height) decrease markedly the levels of $PM_{2.5-10}$, gaseous pollutants, N and BC. In these conditions coagulation-condensation processes are favoured, increasing mass concentration in the accumulation mode (reflected in $PM_{1-2.5}$ and PM_1 increases). The different traffic pattern with a lower intensity during the

weekend results in a different evolution for all parameters, with lower levels registered in general in weekends.

Source apportionment analysis was carried out by means of two methodologies (PCA and PMF), obtaining similar results. The main factors identified in PM_{10} and $PM_{2.5}$ were mineral matter, primary road traffic and secondary aerosols (ammonium sulphate and nitrate). Other factors as fuel oil combustion, aged sea spray and industrial emissions were also identified. However, in PM_1 the contributions of mineral matter or sea spray were very low. Although road traffic emissions clearly control the variability of atmospheric pollutants in the urban area of Barcelona, the influence of other sources is also evident. That is the case of some metallurgical processes on the concentration of some trace elements, fuel oil combustion on the levels of V and Ni, and sporadically the influence of natural episodes such as African dust episodes on mineral matter. Some source contributions presented marked seasonal evolution, such as mineral dust, ammonium sulphate and fuel oil combustion, which presented higher levels during summer, and ammonium nitrate and road traffic during the winter. In addition, a decreasing trend in the industrial source factor was detected from 2003 to 2007, probably due to the application of emission abatement plans.

A number of different sources and factors affecting the variability of atmospheric pollutants make the simultaneous measurement of several parameters very interesting, concerning the complementary information supplied for the interpretation of the variability of levels of pollutants.

- Ultrafine particle measurements (N) are an adequate indicator to monitor the variability of primary traffic emissions and other atmospheric processes such as photochemical nucleation.
- BC measurements detect the direct exhaust emissions of road traffic (soot) and other combustion processes.
- The monitoring of PM levels is necessary to study other important PM sources in the area, such as dust resuspension or African dust outbreaks.
- Speciation measurements of fine and coarse PM fractions provide very important information on PM composition, allowing the identification and quantification of PM sources and processes in the area, such as the enrichment of PM in secondary components as a consequence of aging of aerosols due to anticyclonic atmospheric stagnation or recirculation processes in the region.

Thus, the combination of the above measurements provides complete information, in order to better understand atmospheric particulate matter emission sources and transformation or transport processes, and consequently to identify effective emission abatement strategies for air quality improvement.

From the measurements presented in this study, particle size range is a critical characteristic to take into account in the design of number concentration measurement methods. The lower size ranges basically depend on size detection limits of the particle counter and, consequently the levels of particle number measured depend drastically on this characteristic. Nevertheless, this information is not always reported in publications. However, it may happen that despite accounting for a very important fraction of number concentration, the particles in the smallest size range detected (5 to 13 nm), may probably not be so toxic as other coarser (30-100 nm) particles, as the nucleation particles are mainly composed of soluble compounds that may be easily eliminated from the body. Size ranges, however, should be taken in account in the design of particle number concentration standards, in order to be able to compare measurements and to be sure of the accuracy of data reported.

The results obtained also indicate that the strategy of combining PM_{10} and PM_1 monitoring may be a better tool for urban air quality monitoring across Europe, instead of PM_{10} and $PM_{2.5}$. In PM_1 (nucleation and accumulation modes) the dust load is considerably reduced when compared with PM_{10} and $PM_{2.5}$. PM_1 measurements provide information about contributions from combustion processes and allow a better distinction between combustion and mechanically-generated aerosols than $PM_{2.5}$. Moreover, the measurement of PM_1 allows us to monitor levels of the same components (mostly carbonaceous and secondary inorganic components) in different scenarios. Simultaneously measured PM_{10} could also add information on the levels of specific coarse components for a given site, such as mineral dust and sea salt. $PM_{2.5}$ measurements represent an intermediate stage, providing information on particles generated by mechanical processes but also being the contribution of combustion generated aerosols very significant. In addition, the fraction $PM_{1\text{-}2.5}$ presents a lower variability and provides less information than PM_1 and $PM_{1\text{-}10}$.

4.2. REGIONAL BACKGROUND

4.2. Montseny regional background site

Atmospheric aerosol monitoring networks in Europe are generally based in urban sites and designed to determine PM levels with the end of evaluating the compliance with the existent directives and providing data for epidemiologic studies. Nevertheless, recent works (Querol et al., 2008c) draw attention to the need for regional background sites, monitoring networks located in background areas without the direct impact of local emissions, for air quality measurements. This strategy allows the estimation of the increment in pollution attributed to urban emissions and helps to understand the transport processes of aerosols at a regional and intercontinental scale and to design appropriate strategies to reduce pollution levels.

The interpretation of PM levels and composition resulting from a complex atmospheric scenario, such as the one from the Mediterranean area, can only be accomplished by focusing on regional background sites, comprising ideal locations to fulfil the growing demand for an integrated atmospheric monitoring network for air quality and climate studies. The importance of this type of environments for the study of long-term aerosol trends from a climate perspective was highlighted by the recent creation of the EUSAAR network (European Supersites for Atmospheric Aerosol Research, http://www.eusaar.net/), which seeks to integrate the measurements of atmospheric aerosol properties at 20 high quality European ground-based stations. One of these is the Montseny site (MSY), which was selected to be part of the network owing to its unique setting representing South-Western European environments (data available since March 2002). In addition, the EMEP programme (European Monitoring and Evaluation Programme, http://www.emep.int/) under the convention on Long-range Transboundary Air Pollution focuses in the evaluation of the long-range transport of atmospheric pollutants in Europe by means of a network of regional background monitoring sites, with the aim to solve transboundary air pollution problems.

In this chapter, PM levels and speciation recorded at the Montseny regional background site from 2002 to 2007 are presented and discussed. Special attention is given to the study of inter-annual trends, the identification and interpretation of seasonal patterns, the influence of atmospheric transport scenarios on the PM levels and speciation and the detailed characterization of specific PM episodes, such as African dust outbreaks, regional pollution episodes and winter anticyclonic scenarios. Finally, source apportionment techniques will be applied for the identification of aerosol main sources.

4.2.1. Meteorology, atmospheric dynamics and transport of pollutants

4.2.1.1. Meteorology and atmospheric dynamics in Montseny

The MSY area presents a typical Mediterranean climate with warm summers, temperate winters and irregular precipitation rates (Figure 4.2.1). The average monthly temperatures registered during the study period (2002-2007) ranged from 1-7 ºC in winter (December, January and February) and 17-23 ºC in summer (June, July and August). Annual mean precipitations varied from 676 mm in 2004 to 882 mm in 2002, and also mean monthly precipitation levels varied from 0 mm in January 2005 to 210 mm in October 2005. The highest mean temperatures and lowest precipitation rates were recorded in summer 2003, drier and warmer than usual (1, 43 and 60 mm of rainfall and 21, 21 and 23ºC were registered in June, July and August, respectively). Conversely, 2002 summer was characterized by the opposite conditions (56, 49 and 123 mm of rainfall and 18, 18 and 17ºC were recorded in June, July and August, respectively).

During the colder months, the MSY station (720 m a.s.l.) is generally located outside of the mixing layer and is therefore affected by the regional anthropogenic pollution with a low frequency. Nevertheless, during several anticyclonic scenarios, highly polluted air masses from the coast and valleys are transported towards MSY by the mountain/sea breeze. During the warmer months, owing to the maximum height of the mixing layer (Figure 4.2.2) the MSY is frequently located into the mixing layer being affected by the regional pollution that reaches the station very often. In any case, the highest development of the mixing layer occurs during the central hours of the day.

Two main wind directions were recorded at Tagamanent (Figure 4.2.3 and Figure 4.2.4); south-south west and north-north west. Both are conditioned by the topography of the valley where the monitoring site is located. The southerly direction is registered when the mountain and sea breezes are developed, entering the valley from the South. The northern direction corresponds to the advections from the North and North-West, channelled into the valley. Figure 4.2.3 shows the typical daily cycles of wind direction and speed for each month. During the winter months the main wind components are north and north-west, with relatively low wind speeds. However, breezes from the south-west are recorded during the central hours of the day. From April to October the main wind direction is south, especially during the central hours of the day and coincident with the highest wind speeds associated to maximum breeze development. During the night, south and south-eastern wind directions are recorded.

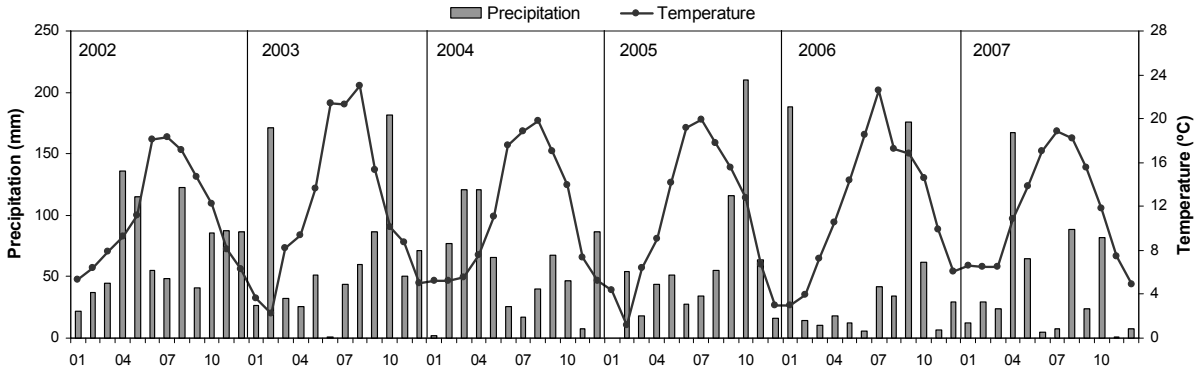

Figure 4.2.1. Mean monthly temperature (ºC) and precipitation (mm) registered at Tagamanent-Montseny Natural Park (Servei Meteorològic de Catalunya) from 2002 to 2007.

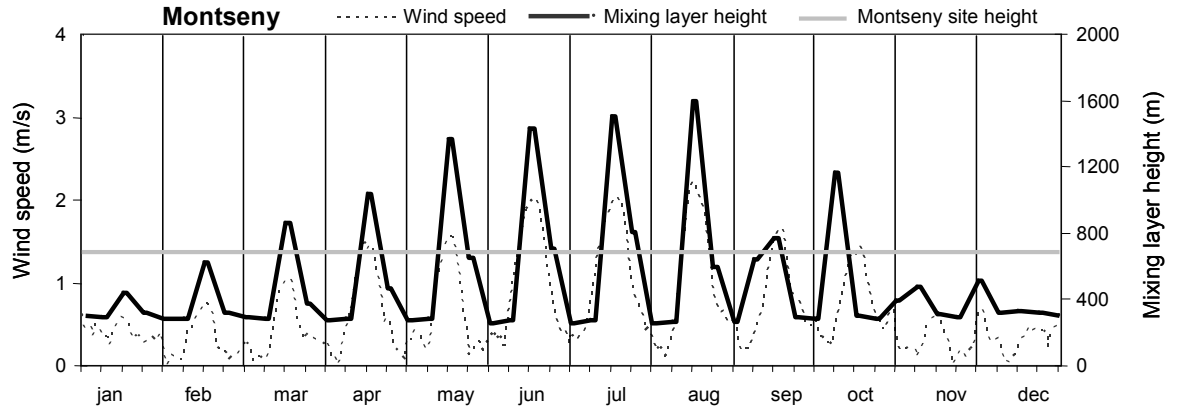

Figure 4.2.2. Mean daily evolution of the mixing layer height (modelled with Hysplit4) at Montseny and wind speed at ground level measured at Tagamanent (Servei Meteorològic de Catalunya).

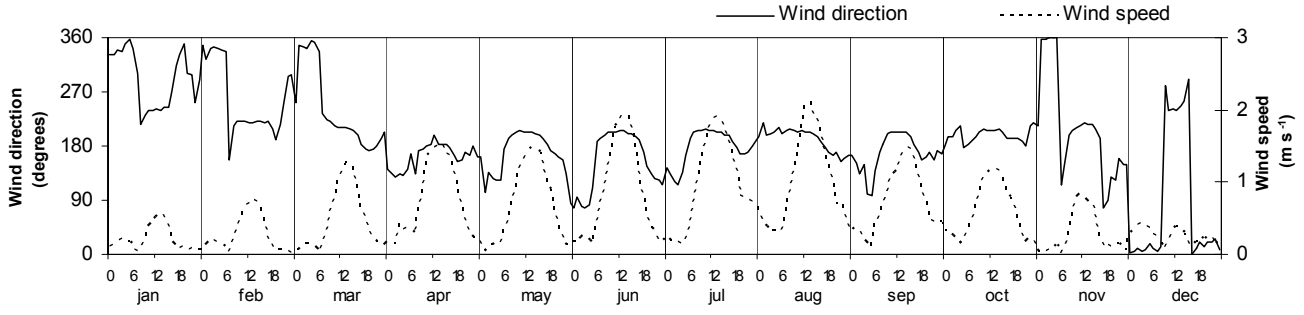

Figure 4.2.3. Annual evolution of hourly mean wind direction and wind speeds measured at Tagamanent for the period 2002-2007.

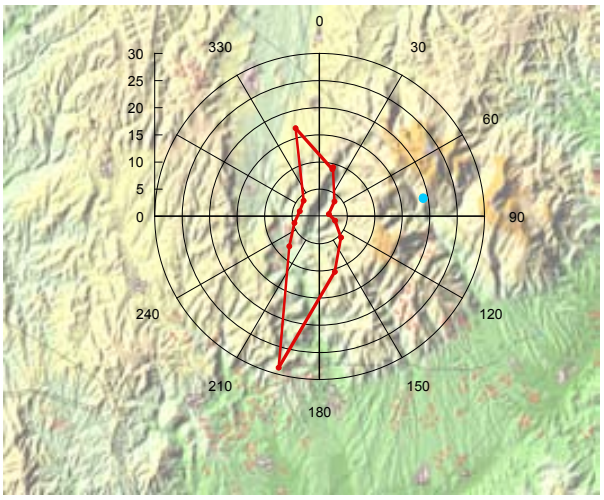

Figure 4.2.4. Relative frequencies of main wind directions measured at Tagamanent (Servei Meteorològic de Catalunya) during the year 2004.

4.2.1.2. Origin of air masses and atmospheric transport scenarios

Day to day variation of PM levels at MSY is driven by the concatenation of different meteorological scenarios that may increase or reduce the levels and size of atmospheric particulate matter in north-eastern Iberia. In line with prior studies these scenarios are as follows: Atlantic advective conditions, African dust episodes, regional recirculation episodes, European and Mediterranean transport episodes, and local pollution episodes (Millán et al., 1997; Rodríguez et al., 2002a and 2003, Escudero et al., 2005 and 2007a). Escudero et al. (2007a) defined the summer anticyclonic episodes, equivalent to the regional recirculation episodes defined by Rodriguez et al., (2003), with impact on the PM_{10} levels at RB sites, and the winter anticyclonic episodes, equivalent to the local pollution episodes. The latter have a major influence in urban and industrial areas but a reduced influence at rural sites owing to the high stability of these scenarios, giving rise to the frequent formation of near ground inversion layers (Rodríguez et al., 2003, Escudero et al., 2007a). Nevertheless, given the difference between them and the relative proximity of large urban and industrial agglomerations, in this study we are considering the summer recirculation episodes (REG) and the winter anticyclonic episodes (WAE). Frequencies of the episodes that affect the study area were calculated for the 2002-2007 period (Figure 4.2.5).

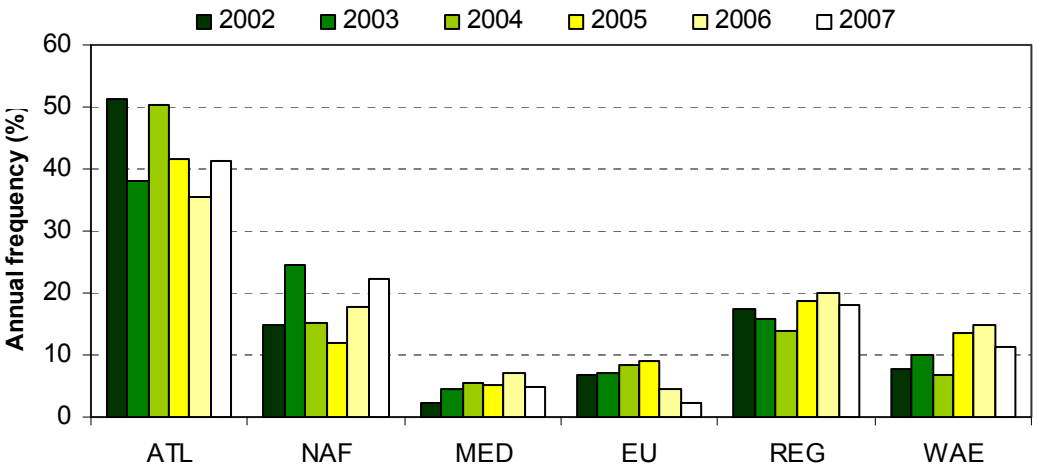

Figure 4.2.5. Annual relative frequencies of each air mass origin selected for the study region for the period 2002-2007. Air mass origin considered: Atlantic advection (ATL); African dust outbreaks (NAF); Mediterranean (MED); European (EU); regional recirculation (REG); and winter anticyclonic episodes (WAE).

The Atlantic advection prevailed along the year at MSY, with a range of frequency between 36% (2006) to 53% (2002) days/year (mainly from NW Atlantic regions, 17%), with episodes lasting from 2 to 10 consecutive days. The transport of Mediterranean air masses towards MSY was the least frequent scenario with a frequency of 2% (2002) to 7% (2006) of the days/year and a mean duration of 2-3 days/episode. African dust air masses may transport mineral dust from arid areas located over North Africa to the Iberian Peninsula (Querol, et al., 1998a, b). Dust outbreaks affecting the Western Mediterranean occur with a higher frequency in February-March and June-October (Rodríguez et al., 2001; Escudero et al., 2005), although sporadic episodes were detected along the entire year. The inter-annual frequency of this kind of episode varied considerably at MSY, ranging from 12% (2005) to 24% (2003) days/year (Figure 4.2.5), with a mean duration from 2 to 5 days/episode. The regional re-circulation episodes are developed from May to October, with the highest frequency in mid summer (Millán et al., 1997; Rodríguez et al., 2002a). These episodes occur over the Western Mediterranean basin during low pressure gradient situations and are characterised by the recirculation and ageing of the air masses over the Western Mediterranean basin (Rodríguez et al., 2002a). These episodes account for between 14% (2004 and 2007) and 20% (2006) days/year, lasting from 2-3 days to more than a week. European air masses may occasionally transport pollutants from Central Europe. The frequency of these episodes ranged between 5% (2006) and 9% (2005) days/year and the mean duration was of 2-4 days. Weak gradient anticyclonic conditions in wintertime were recurrent over the WMB with a frequency from 7% (2004) to 16%

(2007) days/year, and a mean duration of 4-8 days. The absence of intense advections favours the stagnation of pollutants around populated and industrialized areas (mostly concentrated in the coastal and pre-coastal depressions in the study area) inducing important pollution episodes in these areas. Owing to the thermal inversions associated with these anticyclonic scenarios higher temperatures are more frequent in the mountain areas (i.e at MSY) than in the depressions. After some days under an anticyclonic situation local slope breezes can be activated by solar radiation pushing polluted air masses from the valley (Vallès industrial area and Barcelona metropolitan area) towards rural areas.

4.2.2. PM levels at the regional background

4.2.2.1. Mean PM levels at MSY and other RB sites

PM levels have been continuously registered at Montseny from 2002 by means of optical particle counters, with levels being corrected with the factors obtained by comparison with the simultaneous gravimetric monitoring using high volume samplers. Daily PM levels recorded at this site are shown in Figure 4.2.6. Days with African dust influence are marked.

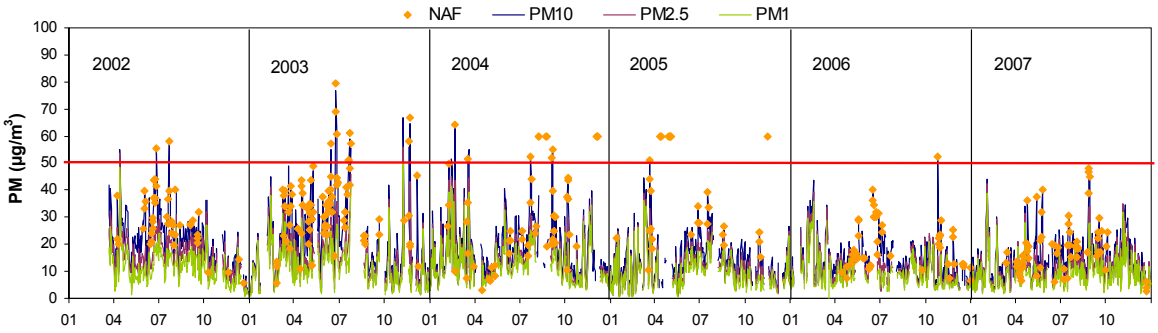

Figure 4.2.6. Daily PM levels time series recorded at Montseny from March 2002 to December 2007. Days with African dust outbreak influence are marked with yellow diamonds.

The mean annual PM_{10}, $PM_{2.5}$ and PM_1 levels registered at Montseny from 2002 to 2007 are shown in Table 4.2.1 together with the gravimetric annual levels recorded. TSP and $PM_{2.5}$ were measured during the period 2002-2003 and PM_{10} and $PM_{2.5}$ from 2004 to 2007. The levels measured by the gravimetry method using high volume samplers were higher (Table 4.2.1). These differences with the levels measured in continuous may be due to the fact that high volume sampling (especially $PM_{2.5}$ because of the use of a manual instrument) was performed mostly on weekdays, when

anthropogenic emissions in the region are higher, whereas the real time measurements also covered weekends, with lower emissions (at a regional scale).

Table 4.2.1. PM mean annual levels registered at Montseny from March 2002 to December 2007 by means of optical particle counters (after correction) and gravimetric methods.

PM levels	Optical particle counter			Gravimetry		
μg m^{-3}	PM_{10}	$PM_{2.5}$	PM_1	TSP	PM_{10}	$PM_{2.5}$
2002 [a]	20	16	12	29		15
2003 [a,b]	20	15	12	26		16
2004 [b]	19	15	13		19	19
2005 [b,c]	14	11	10		16	13
2006 [c]	14	11	9		15	14
2007 [c]	14	11	9		15	12
Mean	17	13	11	28	16	15

[a]Castillo (2006), [b]Pey (2007) and [c]This work.

The mean PM levels recorded at Montseny during the period 2002-2007 fell in the usual ranges of mean levels registered at other regional background sites in the Iberian Peninsula (IP, Table 4.2.2). Mean annual PM_{10} RB levels on the Mediterranean side of the IP between 2002 and 2007 reached 15, 16, 17 and 21 μg m^{-3} at Zarra, Monagrega, MSY and Cabo de Creus, respectively. The levels recorded at Cabo de Creus were relatively higher due to regional contribution of pollutants from the urban and industrial hotspots surrounding Barcelona, Girona and towns in south-eastern France. The other three sites showed very similar PM_{10} levels (15-17 μg m^{-3}); however inter-annual variations, probably caused by inter-annual meteorological differences, are very important (14-17, 13-19, 14-20 μg m^{-3} at Zarra, Monagrega and MSY, respectively (Table 4.2.2), although this variability is not parallel at all the sites.

When comparing the Mediterranean background (excluding Cabo de Creus) with PM_{10} levels measured at other Spanish EMEP stations (Table 4.2.2 and Figure 4.2.7), the above PM_{10} levels may be considered as intermediate. Thus, the stations located in the Atlantic and Central regions of Spain presented relatively low PM_{10} levels (12-14 μg m^{-3} as mean levels for O Saviñao, Riscollano, Campisábalos and Peñausende stations), whereas those measured in the southern regions were higher (18 and 22 μg m^{-3} for Barcarrota and Viznar). This distribution is possibly caused by the increasingly higher frequency and intensity of African dust outbreaks and the decreasing rainfall from the Atlantic regions to the eastern and to southern regions of Iberia.

PM_{10} levels in the study area may also be regarded as intermediate when compared with those in other rural areas in Europe (according data available from AirBase,

http://air-climate.eionet.europa.eu/databases/airbase/). Thus, taking the data from Airbase, PM_{10} levels range from 25 to 35 μg m^{-3} in most rural areas in The Netherlands, whereas they range from 7 to 16 μg m^{-3} at rural sites in Scandinavian countries (Figure 4.2.7). The data from the study area are also intermediate when compared with those from rural sites in the central (Italy and Cyprus) and eastern (Macedonia) Mediterranean countries, with PM_{10} ranging from 30 (Cyprus) to 15 μg m^{-3} (Macedonia, Figure 4.2.7).

As regards $PM_{2.5}$ (Table 4.2.2), the mean annual levels ranged from 8 to 10 μg m^{-3} in the Atlantic and central Spain, from 10 to 11 μg m^{-3} in southern Spain, and from 8 to 13 μg m^{-3} in eastern Spain. It is clear that PM_{10} and $PM_{2.5}$ do not show the same spatial variations over the IP. Thus, the highest $PM_{2.5}$ levels are recorded at MSY, Cabo Creus and Els Torms (eastern IP), where the highest regional anthropogenic emissions are present, followed by Viznar and Barcarrota (southern IP), where probably African dust has a higher incidence in $PM_{2.5}$ levels. Most of the remaining monitoring sites recorded levels close to 8 μg m^{-3}.

The ratio $PM_{2.5}/PM_{10}$ reached the lowest values in the southern IP, with values of 0.5-0.6. In most of the other areas of the IP, the $PM_{2.5}/PM_{10}$ ratio ranged from 0.6 to 0.7, with the exception of industrialized regions (such the Barcelona region), where the RB ratio reached 0.8 (MSY). The coarser grain size distribution for the southern sites is probably the result of the higher mineral load in PM_{10} owing to the drier climate (especially in summer) and the proximity to the African desert regions.

PM_1 levels have been continuously measured at MSY since 2002. Mean annual levels were 11 μg m^{-3}, ranging between 9 and 13 μg m^{-3}. The $PM_1/PM_{2.5}$ ratio reached 0.8 constantly as an annual mean value the 6 years of measurement. Similar $PM_{2.5}$ and PM_1 levels and $PM_{1/2.5}$ ratios were reported for the rural site of Bemantes in northwest Spain for the year 2001 by Salvador et al. (2007). PM_1 levels measured at Monte Cimone in Italy were 7 μg m^{-3}, which were 30% lower than those recorded at MSY (Marenco et al., 2006). This is probably because Monte Cimone can be considered as a remote site (2165 m.a.s.l.), but MSY represents the RB.

Table 4.2.2. PM_{10} and $PM_{2.5}$ mean annual levels (μg m^{-3}) at Iberian Peninsula EMEP stations for 2002-2007. ATL: Atlantic, MED: Mediterranean, C: central, S: South.

		PM_{10}							$PM_{2.5}$							Ratio
Region	Station	2002	2003	2004	2005	2006	2007	Mean	2002	2003	2004	2005	2006	2007	Mean	$PM_{2.5}/PM_{10}$
ATL	O Saviñao	14	15	14	14	13	12	14	9	9	9	10	9	8	9	0.7
ATL	Niembro	19	20	16	17	18	20	18	10	11	10	9	9	12	10	0.6
MED	Cabo de Creus	19	25	21	21	19	19	21	13	17	13	12	10	10	13	0.6
MED	Zarra	15	16	17	15	14	14	15	8	8	8	8	8	9	8	0.5
MED	Els Torms	15	20	22	17	17	17	18	10	13	13	10	10	12	11	0.6
MED	Monagrega	13	16	15	19	19	16	16								
MED	Montseny	20	20	19	14	14	14	17	16	15	15	11	11	11	13	0.8
C	Peñausende	12	13	13	13	11	11	12	8	8	8	8	7	6	8	0.6
C	Campisábalos	11	12	13	12	12		12	7	7	8	8	8		8	0.6
C	Riscollano	12	14	16	15	13		14	7	7	8	8	9		8	0.6
S	Viznar	21	21	24	22	20	21	22	10	9	11	11	10	11	10	0.5
S	Barcarrota	16	17	19	19	16	18	18	12	8	11	10	9	8	10	0.6

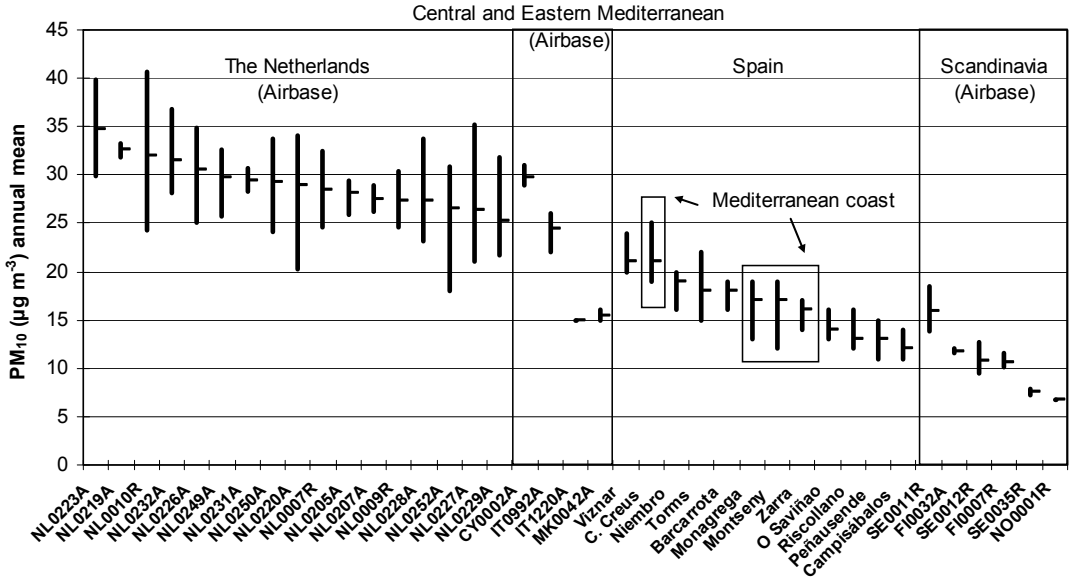

Figure 4.2.7. Annual PM_{10} ranges and mean values measured at the study sites compared with data from Airbase (http://air-climate.eionet.europa.eu/databases/airbase/airview/index_html) for rural sites of The Netherlands (as an example of central Europe), the Scandinavian countries, and the Central and Eastern Mediterranean.

4.2.2.2. Inter-annual variability

Annual variation of PM levels may depend on the meteorology, the volume of anthropogenic emissions and the frequency of African dust episodes in a year. Figure 4.2.8 shows the mean annual $PM_{2.5-10}$, $PM_{1-2.5}$ and PM_1 levels measured at Montseny from 2002 to 2007 for all days (total), days with African dust outbreak influence (NAF) and days without African dust influence. PM levels seem to follow a decreasing trend

from 2002 to 2007, which may be attributed to meteorology; however this trend could also be caused by a variation of the anthropogenic regional PM load because of the abatement of industrial atmospheric emissions.

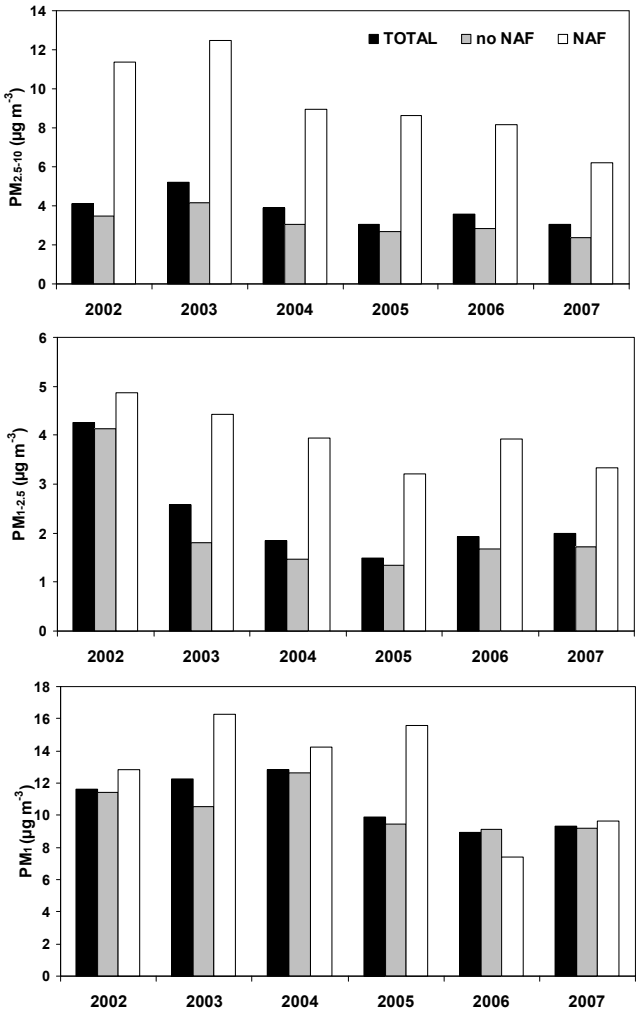

Figure 4.2.8. Mean annual $PM_{2.5-10}$, $PM_{1-2.5}$ and PM_1 levels measured at Montseny from 2002 to 2007 for all days (total), days with African dust influence (NAF) and days without African dust influence.

Temporal trend analyses were applied to the annual and monthly datasets available between 2002 and 2007. The Mann-Kendall test showed significant and robust results for PM_{10} and $PM_{2.5}$ at the MSY site, despite the relatively short dataset. Both mean annual PM_{10} and $PM_{2.5}$ concentrations showed an average decrease of 34%, for the entire monitoring period (at α=0.05 significance level). In absolute terms this decrease is equivalent to 6 µg m^{-3} PM_{10} and 5 µg m^{-3} $PM_{2.5}$ between 2002 and 2007, and these trends may be considered as significant (Figure 4.2.9). In the fine fraction (PM_1) a somewhat smaller decrease was detected (28%) even though it was not significant (α

>0.1). The $PM_{1-2.5}$ and $PM_{2.5-10}$ fractions presented important decreases from 2002 to 2007 (57% and 32% respectively), but they were not significant. The different trends observed in this study of the coarser (PM_{10}, $PM_{2.5}$) and fine (PM_1) fractions suggest a variety of causes for the decreasing trend, related to large-scale meteorological processes or cycles, to local or meso-scale processes, and to the possible decrease of the nearby anthropogenic emission sources.

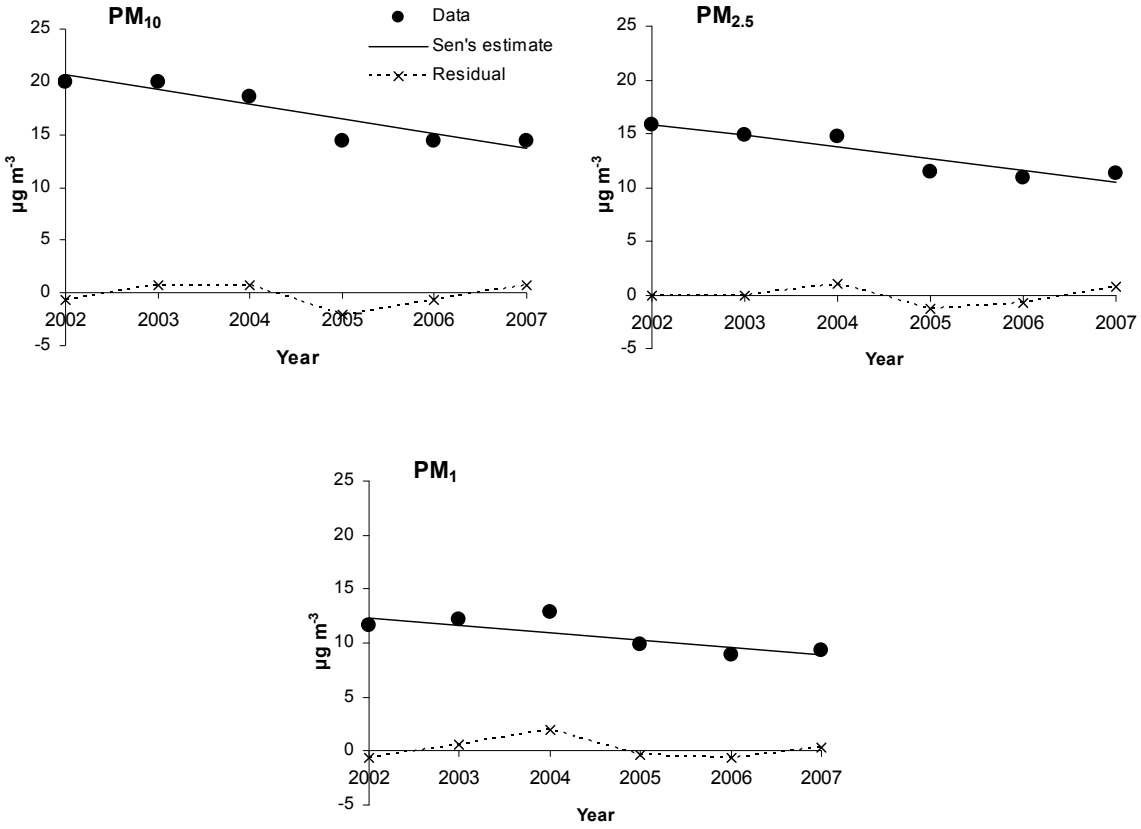

Figure 4.2.9. Temporal trends for PM_{10}, $PM_{2.5}$ and PM_1 detected at Montseny by means of the Mann-Kendall test and Sen's method using MAKESENS (Salmi et al., 2002).

The analysis of the monthly datasets provided evidence of decreasing temporal trends for specific months of the year. PM levels of all grain size fractions at MSY showed the strongest and most consistent decrease during March for the entire study period, with a reduction of 66% in PM_{10}, 65% in $PM_{2.5}$ and 60% in PM_1 (α=0.05). June and July also showed similar trends in PM_{10} and $PM_{2.5}$ although not in PM_1 (an average decrease of 48-51%, α=0.05). During the winter months (November to January) the levels decreased in a minor proportion than during the warmer months of the year for all the size fractions and these trends were not significant, except for PM_{10} during December,

with a decrease of 15% (α=0.05). The fact that almost no significant tendencies were detected during the winter months and that the decrease was lower indicates that anthropogenic emissions may not be the only cause of the decrease in PM levels. Moreover, the higher decrease in the levels observed during the warmer months and the significant trends observed during March, June and July, point to natural causes as African dust episodes, the influence of sea-breeze circulations (typical of summer) or meteorology as a possible reason for this decreasing trends.

It is worthy to note that the interpreted inter-annual trends cannot be considered as a general time trend (only 6 years are considered) but probably these are reflecting meteorological cycles with a 6-10 year scale.

4.2.2.3. Seasonal variability

Monthly means for PM_{10}, $PM_{2.5}$ and PM_1 levels and the fractions $PM_{2.5-10}$ and $PM_{1-2.5}$ registered at Montseny from 2002 to 2007 are shown on Table 4.2.3.

Table 4.2.3. Monthly mean PM_{10}, $PM_{2.5}$, PM_1, $PM_{1-2.5}$ and $PM_{2.5-10}$ levels registered at Montseny from March 2002 to December 2007.

µg m^{-3}	PM_{10}	$PM_{2.5}$	PM_1	$PM_{1-2.5}$	$PM_{2.5-10}$
January	11	9	8	1	1
February	19	16	15	2	2
March	20	16	14	3	4
April	17	13	11	2	4
May	17	12	9	3	5
June	24	15	12	3	9
July	24	16	13	3	8
August	17	13	10	3	4
September	18	14	11	3	4
October	15	11	9	3	3
November	16	12	10	2	3
December	10	8	7	1	2

PM levels at MSY follow a clear seasonal trend. The highest levels were registered during the summer months (especially June and July, Table 4.2.3 and Figure 4.2.10). This summer increase is associated with the highest frequency of African dust outbreaks, the recirculation of air masses that prevent air renovation, the low precipitations registered, the highest resuspension owing to the dryness of soils during this period and the increased formation of secondary aerosols from gaseous precursors caused by the maximum solar

radiation (Querol et al., 1998b, 1999 and 2001a; Escudero et al., 2005; Viana et. al., 2005). The summer increase was more pronounced in the coarse fraction ($PM_{2.5-10}$) than in the finer fractions ($PM_{1-2.5}$ and PM_1), probably because of the coarser size of the mineral dust and summer-nitrate particles (Figure 4.2.10). In the remaining months of the year the levels were relatively low owing to the higher frequency of Atlantic advection and precipitation. However, pronounced peaks were usually recorded during the winter months (especially in November and February-March) when PM levels (especially the finest fraction) rise episodically because of intense pollution episodes of anthropogenic (winter anticyclonic scenarios) or natural (African dust) origin. The seasonal variation of PM levels at MSY is also influenced by the evolution of the thickness of the boundary layer. Thus, when the monitoring site is decoupled from the boundary layer (especially in winter) it is less affected by regional anthropogenic emissions. In contrast, the high vertical development of the boundary layer in summer allows PM pollutants to reach the monitoring site.

The occurrence of the above seasonal trend (characterized by summer, November and February-March higher PM levels) may vary from one year to another (Figure 4.2.10), depending on the intensity of the pollution and the African dust episodes in winter, and on the dryness and frequency of dust episodes in summer. Thus, the high PM levels recorded in the summer 2003 were caused by very frequent and intense African dust episodes, increasing aerosol levels, especially in the coarser fraction. The relatively lower PM levels recorded in the summers of 2005 and 2007 were related to meteorology and to the lower frequency and intensity of dust outbreaks (2005). However, from 2002 to 2006 intense February-March winter anticyclonic episodes were recorded, considerably raising PM levels in winter, especially in the finer fractions (Figure 4.2.10).

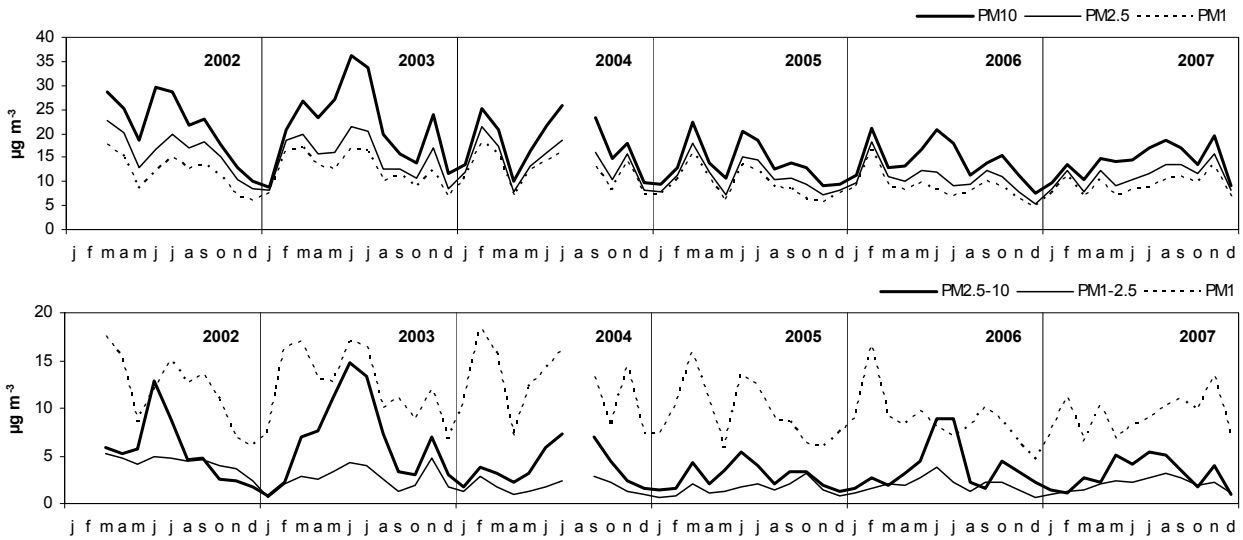

Figure 4.2.10. Monthly mean PM_{10}, $PM_{2.5}$ and PM_1 levels (top) and $PM_{2.5-10}$, $PM_{1-2.5}$ and PM_1 levels (bottom) registered at MSY from March 2002 to December 2007.

The seasonal evolution of atmospheric scenarios also played a major role in the $PM_{2.5}/PM_{10}$ and $PM_1/PM_{2.5}$ ratios. Thus, the typical winter $PM_{2.5}/PM_{10}$ ratio reached values of 0.8-0.9 (Figure 4.2.11) owing to the fine PM size of the low PM episodes under Atlantic advection scenarios and to the high (and fine) PM pollution episodes in winter. Sporadically, these ratios decreased to 0.3 in accordance with the occurrence of intense winter dust outbreaks (Figure 4.2.11). In summer, $PM_{2.5}/PM_{10}$ fell to mean values of 0.7 (due to higher levels of background dust and coarse nitrate), with values reaching 0.3 during intense summer dust outbreaks. Summer $PM_{2.5}/PM_{10}$ decreased to mean values of 0.5 for specific years such as the 2003, with a higher frequency of African dust outbreaks and very dry conditions or reached 0.7 in years with very light summer conditions (2005). $PM_1/PM_{2.5-10}$ ratio also showed a seasonal trend with very high levels during winter as a result of fine pollution episodes and lower levels during the summer with a PM size distribution versus the coarser grain size.

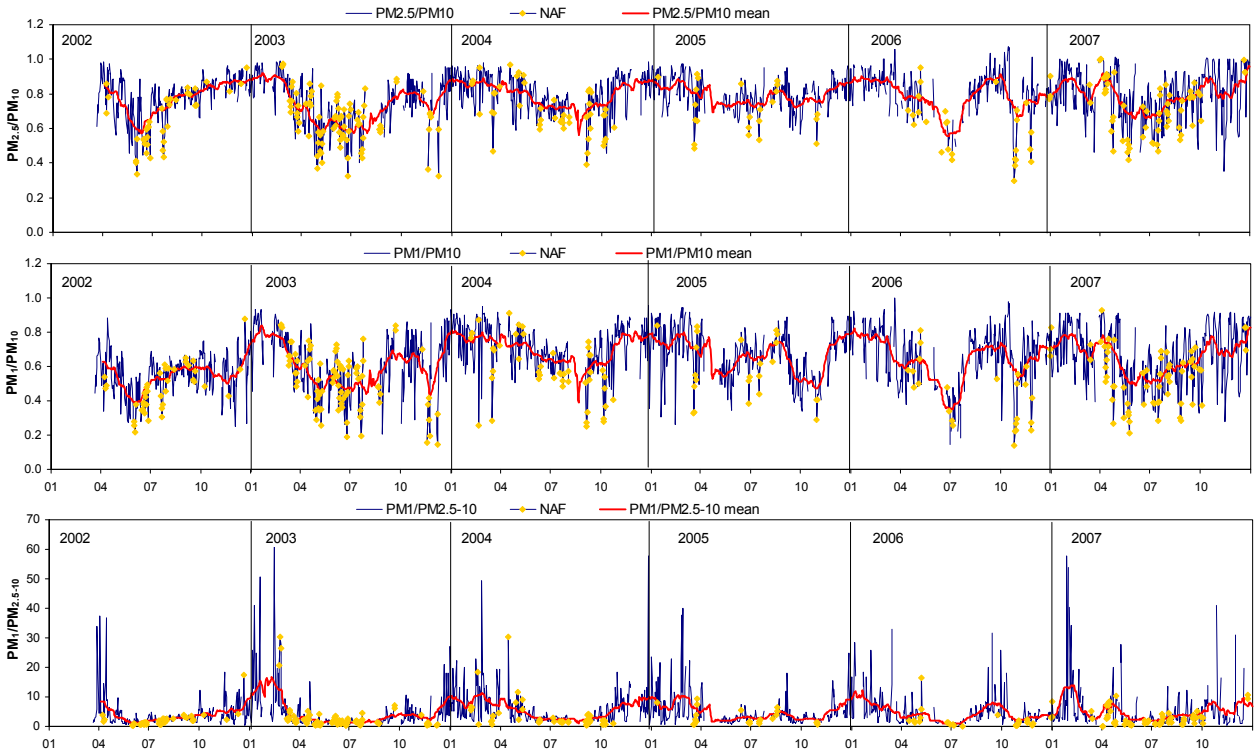

Figure 4.2.11. Mean annual evolution for the ratios $PM_{2.5}/PM_{10}$ PM_1/PM_{10} and $PM_1/PM_{2.5-10}$ in Montseny from 2002 to 2007. The days with African outbreaks (NAF) and the sliding average for 30 days were marked.

4.2.2.4. Daily cycles

The daily evolution of PM levels at MSY is markedly driven by the breeze circulation (mountain and sea breezes) that dominates the atmospheric dynamics at this site (Figure 4.2.12). During the night (0-7 h UTC), relatively low PM levels were recorded, with mean levels of 12, 9 and 6 μg m^{-3} for PM_{10}, $PM_{2.5}$ and PM_1, in winter and 15, 12 and 9 μg m^{-3} in summer for the period 2002-2007. From early morning (7-8 h UTC in summer, 9-10 h UTC in winter) to afternoon, PM levels increased progressively, coinciding with the mountain breeze flow and the increase in wind speed, reaching the highest values at around 13-14 h UTC in summer and 15-16 h UTC in winter (Figure 4.2.13). Mean maximum hourly levels of 25, 18 and 17 μg m^{-3} in winter and of 30, 18 and 15 μg m^{-3} in summer were registered for PM_{10}, $PM_{2.5}$ and PM_1, respectively.

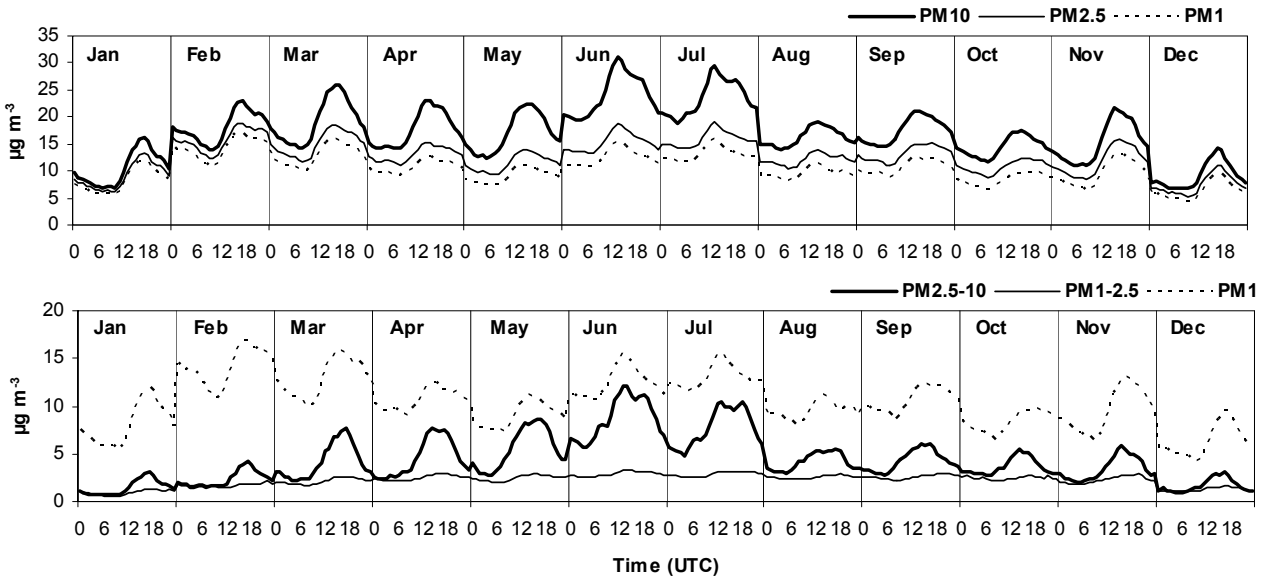

Figure 4.2.12. Mean monthly daily cycles of PM_{10}, $PM_{2.5}$ and PM_1 levels (up) and $PM_{2.5\text{-}10}$, $PM_{1\text{-}2.5}$ and PM_1 levels (down) recorded at Montseny from 2002 to 2007.

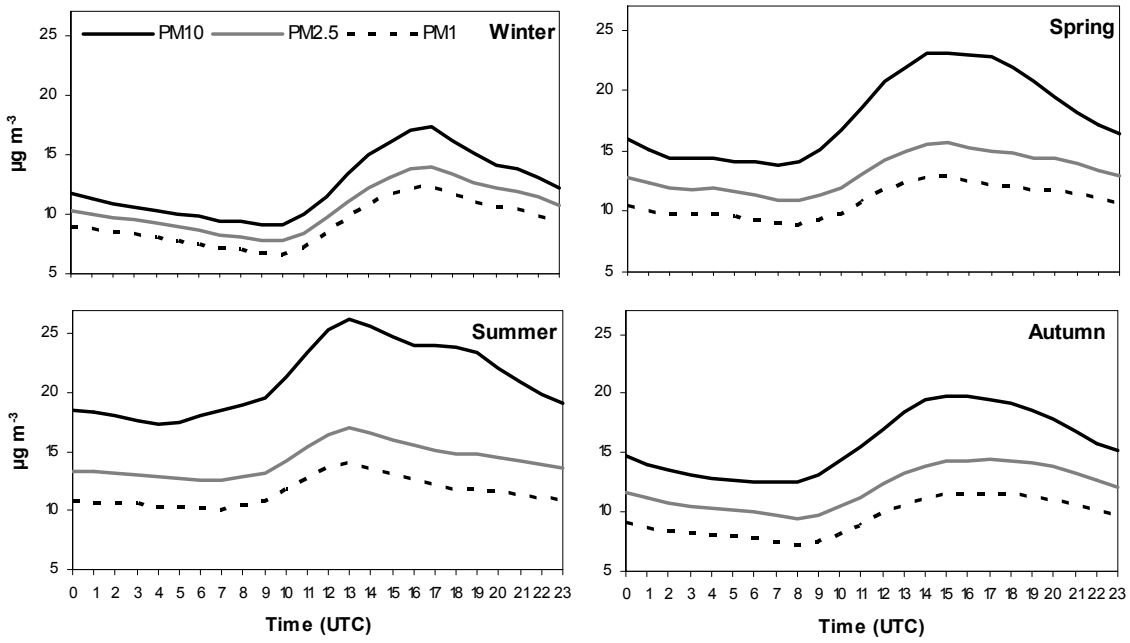

Figure 4.2.13. Mean PM daily cycles recorded at Montseny site during winter, spring, summer and autumn from 2002 to 2007.

The above described daily trend may be attributed to the following processes: early in the day atmospheric pollutants are accumulated in the pre-coastal depression (highly populated and industrialized, crossed by important main roads); subsequently the diurnal breeze development (activated by insolation) increases the PM levels at MSY by transporting the aged air masses upwards from the valley. The influence of cleaner nocturnal drainage flows and the decrease of the mixing layer height result in the lower nocturnal PM levels. These lower levels are measured during the nocturnal to early

morning period due to the combination of the 720 m a.s.l. of the MSY station and the decrease of the boundary layer, causing the decoupling of MSY site from the mixing boundary layer. Consequently, the low levels measured during the night may be representative of the continental background. In this study, the continental background may be considered as the mean background levels of aerosols of a region with a diameter of around 250 to 500 km, whereas the regional scale would have a 50 km size.

In many aerosol studies performed in mountainous areas, PM levels are measured only during the nocturnal period to diminish the regional/local influence from mountain breezes and by the growth of the mixing boundary layer (Prospero et al., 1995). These levels, without local/regional influence may be considered as continental background levels. For most days of the year this situation is prevailing, however, for a number of days strata with aged pollution aerosols or African dust outbreaks may increase also the nocturnal aerosol levels, but these are also influencing the continental background of the area.

Thus, the above continental background is characterized by levels of PM_{10}, $PM_{2.5}$ and PM_1 reaching annual mean values of 13, 10 and 8 μg m^{-3} (with slightly higher summer levels and lower winter levels). The results are comparable to the measurements performed at remote sites in central and northern Spain (EMEP stations), with mean levels of 12-13 and 8-10 μg m^{-3} for PM_{10} and $PM_{2.5}$. If these values are subtracted from the annual mean levels, the annual mean regional contributions may be quantified in around 4, 3 and 2 μg m^{-3} for PM_{10}, $PM_{2.5}$ and PM_1. For the fine fractions these contributions in winter are twice as large as those in summer probably because of the occurrence of the anticyclonic pollution episodes.

The inter-annual evolution of the continental background levels showed a clear decrease from 18, 13 and 9 μg m^{-3} (2002) to 12, 9 and 7 μg m^{-3} (2007) for PM_{10}, $PM_{2.5}$ and PM_1, respectively, whereas the regional contributions did not show a significant trend (Figure 4.2.14). The Mann-Kendall test was applied to the continental background mean levels calculated for MSY, showing important results at a significance level of 0.05 for the PM_{10} fraction (average decrease of 36% for the entire monitoring period). In absolute terms this decrease is equivalent to 6 μg PM_{10} m^{-3} between 2002 and 2007. $PM_{2.5}$ and PM_1 also showed decreasing, but not significant, trends of 51 and 28%, respectively (equivalent to 4 μg $PM_{2.5}$ m^{-3} and 2 μg PM_1 m^{-3}). If only the summer months are considered, this trend was significant for PM_{10} (60%) and

$PM_{2.5}$ (38%). In the fine fraction (PM_1) a similar decrease was detected (38%) even though it was not significant (α>0.1).

The detection of a decreasing trend for the continental background and not for the regional contribution is probably pointing to a main meteorological cause for the detected PM_{10} decreasing trend during the 6 year study period.

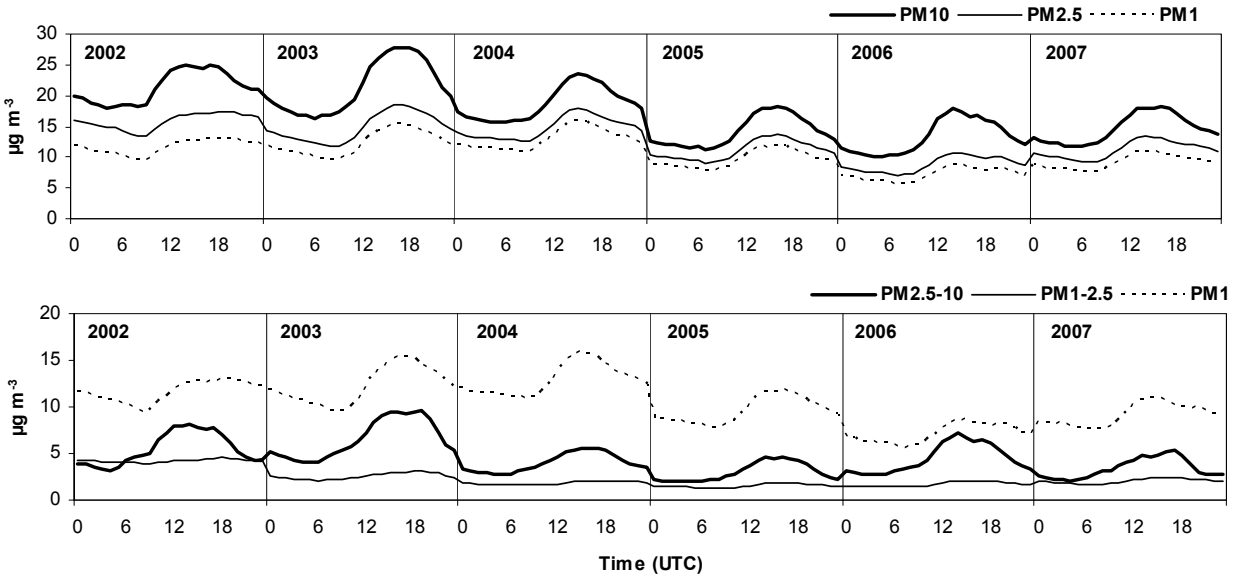

Figure 4.2.14. Mean annual daily cycles of PM_{10}, $PM_{2.5}$ and PM_1 levels (up) and $PM_{2.5-10}$, $PM_{1-2.5}$ and PM_1 levels (down) recorded at Montseny from 2002 to 2007.

4.2.2.5. Influence of air mass origin on PM levels

In order to evaluate the influence of the different meteorological scenarios influencing PM RB levels in the WMB, PM_{10}, $PM_{2.5}$ and PM_1 daily means were classified in the previously described atmospheric scenarios according to the origin of the air masses. Mean PM levels obtained for each episode considered are reported in Table 4.2.4 and Figure 4.2.15. Atlantic and Mediterranean episodes are related to low PM levels because of the renovation of air masses and the occurrence of precipitations. In contrast, African dust outbreaks, European episodes and summer regional recirculations may increase PM concentrations at RB sites. In addition, as will be shown below, the winter anticyclonic episodes may markedly increase the PM levels (mainly PM_1) even in regional areas.

Table 4.2.4. Mean levels of PM fractions at MSY (2002 to 2007) for each air mass origin considered: Atlantic advection (NA, north; NWA, northwest; WA, west; SWA, southwest); African dust outbreaks (NAF); Mediterranean (MED); European (EU); Regional recirculation (REG); and winter anticyclonic episodes (WAE).

µg m^{-3}	NA	NWA	WA	SWA	NAF	MED	EU	REG	WAE
PM_{10}	14	15	12	11	**24**	13	16	20	19
$PM_{2.5}$	12	12	9	9	16	11	13	15	16
PM_1	10	10	8	7	12	9	11	12	**14**
$PM_{1\text{-}2.5}$	2	2	1	2	**4**	2	2	3	2
$PM_{2.5\text{-}10}$	2	3	3	2	**8**	2	3	5	3

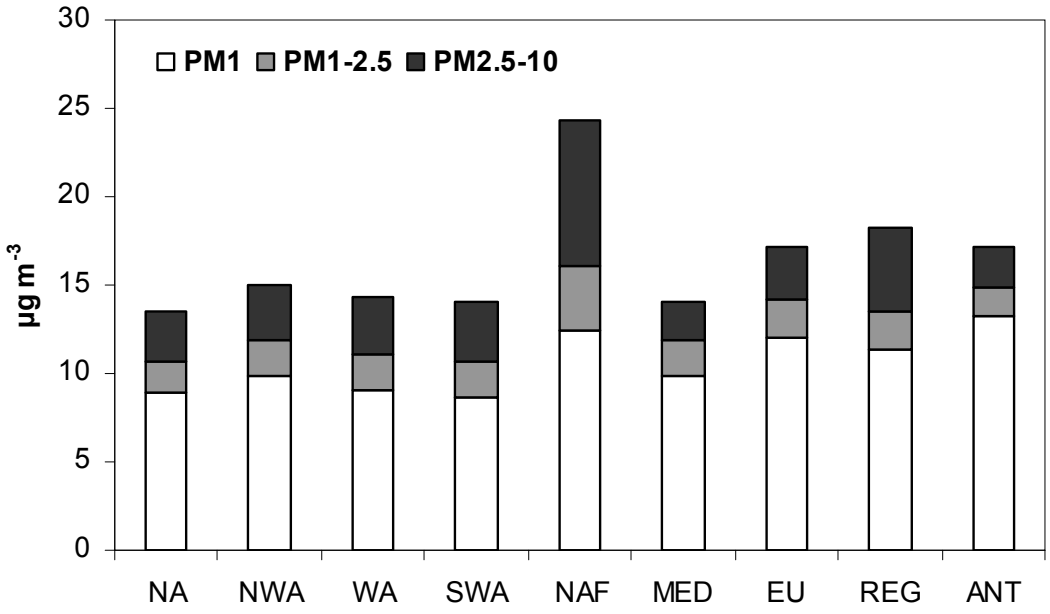

Figure 4.2.15. Mean $PM_{2.5\text{-}10}$, $PM_{1\text{-}2.5}$ and PM_1 levels registered in MSY for each air mass origin considered (2002 to 2007).

Annual mean levels (2002-2007) registered under Atlantic advections at MSY reached 14, 11 and 9 µg m^{-3} of PM_{10}, $PM_{2.5}$ and PM_1, respectively. PM under this scenario has a typical fine grain size (with both $PM_{2.5}/PM_{10}$ and PM_1/PM_{10} ratios reaching values between to 0.7 and 0.9).

The Mediterranean air mass transport scenario is normally associated with strong winds and rainfalls, causing the decrease in PM levels. Consequently, annual mean levels were 14, 12 and 10 µg m^{-3} of PM_{10}, $PM_{2.5}$ and PM_1, respectively, with prevalent fine grain size particles ($PM_{2.5}/PM_{10}$ and PM_1/PM_{10} ratios between 0.7 and 0.9).

Annual mean levels registered under African dust outbreaks were 24, 16 and 12 μg m^{-3} of PM_{10}, $PM_{2.5}$ and PM_1, respectively. Owing to the typical coarse size of the mineral dust particles, a coarse grain size distribution was obtained ($PM_{2.5}/PM_{10}$ and PM_1/PM_{10} ratios of 0.7 and 0.5, respectively). The highest levels of PM_{10}, $PM_{2.5\text{-}10}$ and $PM_{1\text{-}2.5}$ were registered under this scenario (Table 4.2.4 and Figure 4.2.15), and relatively high $PM_{2.5}$ and PM_1 levels were also recorded.

Annual mean levels registered under regional recirculation episodes were relatively high, with mean values of 20, 15 and 12 μg m^{-3} of PM_{10}, $PM_{2.5}$ and PM_1, respectively (Table 4.2.4 and Figure 4.2.15). Fine particles were predominant with $PM_{2.5}/PM_{10}$ and PM_1/PM_{10} mean ratios of 0.8 and 0.6, respectively, given that the formation of secondary aerosols is enhanced under this meteorological scenario, increasing markedly the levels of PM_1.

Mean PM levels registered during European air mass transport were very close to the annual mean levels with mean values of 16, 13 and 11 μg m^{-3} of PM_{10}, $PM_{2.5}$ and PM_1, respectively (Table 4.2.4 and Figure 4.2.15). The fine grain size distribution ($PM_{2.5}/PM_{10}$ ratio 0.8 and PM_1/PM_{10} 0.7) is a consequence of the relatively high proportion of secondary inorganic aerosol content in these air masses.

At MSY, mean PM_{10}, $PM_{2.5}$ and PM_1 levels under winter anticyclonic scenarios reached 19, 16 and 14 μg m^{-3}, respectively (Table 4.2.4 and Figure 4.2.15). These anticyclonic episodes are characterized by a fine PM grain size ($PM_{2.5}/PM_{10}$ ratio 0.8 and PM_1/PM_{10} 0.7) because of the predominance of secondary inorganic compounds and anthropogenic carbonaceous species. These episodes account for the highest PM_1 concentrations recorded at MSY, both in hourly and daily basis, and consequently have a great impact on PM levels in the elevated rural areas of the WMB.

4.2.2.6. Influence of African dust outbreaks on PM levels

African dust episodes increase the PM levels importantly in a daily basis and can contribute to exceed the daily limit values established. At MSY, the 50 μg PM_{10} m^{-3} daily limit value was exceeded between zero (2007) and 9 (2003) times in a year, considering the period of sampling from March 2002 to December 2007. The exceedances of the PM_{10} daily limit value recorded at MSY occur almost in all cases during NAF episodes and can be attributed to the African dust contribution.

Table 4.2.5. Number of days with African dust influence in the study region. Number of exceedances of the 50 μgPM_{10}/m^3 daily limit value and % of the exceedances recorded during NAF episodes at Montseny.

	Number of days with NAF influence	Number of exceedances PM_{10}>50μg/m^3	% D. L. V exceedances recorded during NAF
2002	43	3	67
2003	85	9	89
2004	55	7	71
2005	31	1	100
2006	53	1	100
2007	63	0	

The difference between the PM mean annual levels and the mean levels obtained for days without African dust in the same year period may be considered as the annual African dust contribution to PM levels (Table 4.2.6 and Figure 4.2.16). At MSY the annual increase of PM levels owing to the African dust influence was around 0.8-3.5, 0.1-2.4 and <0.1-1.7 μg m^{-3} (1.5, 0.7 and 0.4 mean values respectively) for PM_{10}, $PM_{2.5}$ and PM_1 during the period 2002-2007. Concerning the fractions $PM_{1-2.5}$ and $PM_{2.5-10}$ the mean increase due to African dust was of 0.3 and 0.7 μg m^{-3}, respectively. The mean contribution of African dust depends on the year considered, as the frequency and intensity of African dust outbreaks differ. The highest contribution is observed for the year 2003 (3.5, 2.4 and 1.7 μg m^{-3} for PM_{10}, $PM_{2.5}$ and PM_1 respectively). These results are in accordance with previous studies carried out by Castillo (2006), where the mean annual contribution of North-African dust to PM_{10} was estimated to be between 1-2 μg PM_{10} m^{-3} and 0.2-1 μg $PM_{2.5}$ m^{-3}. $PM_{2.5-10}$, $PM_{1-2.5}$ and PM_1 levels are not affected by African dust outbreaks in the same extent (Figure 4.2.16). Mineral dust is mainly coarse in grain size and the increase in annual PM levels is more marked in PM_{10} than in the finer fractions.

Table 4.2.6. Mean PM annual levels recorded at MSY (2002 to 2007). Mean annual levels for days without African dust influence (no NAF). Increase in the annual PM levels attributed to African dust outbreaks.

	PM mean annual levels (μg m^{-3})	no NAF PM levels (μg m^{-3})	Annual increase of PM related to NAF (μg m^{-3})
PM_{10}	14-20	13-19	0.8-3.5
$PM_{2.5}$	11-16	11-16	0.1-2.4
PM_1	9-13	9-13	<0.1-1.7
$PM_{1-2.5}$	1-4	1-4	<0.1-0.8
$PM_{2.5-10}$	3-5	3-6	0.4-1.1

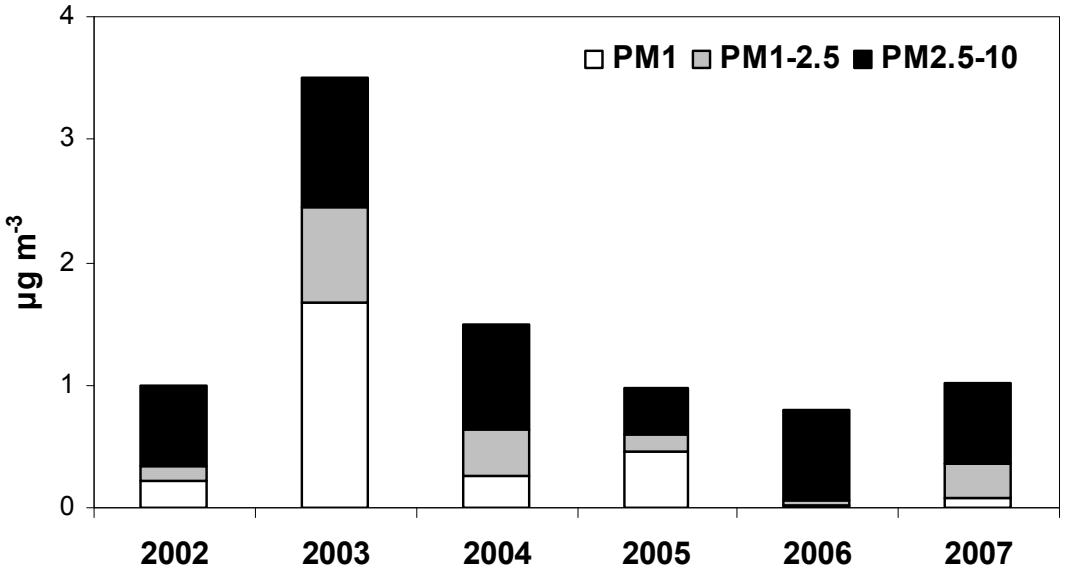

Figure 4.2.16. Annual increment of PM_{10}, $PM_{2.5}$ and PM_1 levels attributed to African dust outbreaks at MSY.

The African dust contribution to the annual mean PM levels was also quantified by applying the method proposed by Escudero et al. (2007b). To this end, the daily PM_{10} RB levels were obtained by applying a monthly moving 30^{th} percentile to the PM_{10} time series at MSY for days without African dust transport. Thereafter, the daily PM RB levels obtained were subtracted from the daily PM levels recorded at MSY only on days when African dust outbreaks occurred, the difference being the daily net African dust load. The results are very similar to the obtained with the method applied above. Thus, the annual mean contributions of the African dust outbreaks calculated for 2002-2007 in PM_{10}, $PM_{2.5}$ and PM_1 were 1.5, 0.7 and 0.4 µg m^{-3}, respectively. The highest contributions were determined in 2003, with 3.5, 2.4 and 1.7 µg m^{-3} and the lowest from 2005 to 2007, with 0.9, 0.3 and 0.2 µg m^{-3} in PM_{10}, $PM_{2.5}$ and PM_1, respectively. These results reflect the variability of the frequency and intensity of African dust episodes. Thus the highest frequency was obtained in 2003 (24% of the days) and the lowest in 2005 (12% of the days). The mean dust contribution per day/African episode was calculated for each year, with a maximum contribution of 15 µg PM_{10} m^{-3} for 2003 and 2004, and a minimum of 10 µg PM_{10} m^{-3} for 2006 and 2007.

4.2.3. PM speciation at the regional background

4.2.3.1. PM speciation at MSY and other RB sites

The speciation of PM_{10} and $PM_{2.5}$ at MSY was performed simultaneously from October 2003 to December 2007. Until this date, instead of PM_{10}, TSP was sampled from March 2002 to October 2003. Major TSP, PM_{10} and $PM_{2.5}$ components measured from 2002 to 2007 are shown in Table 4.2.7 and Figure 4.2.17.

Table 4.2.7. TSP (2003-2003), PM_{10} (2004-2007) and $PM_{2.5}$ (2002-2007) major components measured at MSY. OC: organic carbon, EC: elemental carbon, OM+EC: organic matter + elemental carbon, SIA: secondary inorganic aerosols (SO_4^{2-}+ NO_3^-+ NH_4^+). Mineral matter= sum of Al_2O_3, SiO_2, CO_3^{2-}, Ca, Fe, K, Mg, Mn, Ti and P, sea spray=Na^+ + Cl^-.

	TSP		**PM_{10}**				**$PM_{2.5}$**					
	2002	**2003**	**2004**	**2005**	**2006**	**2007**	**2002**	**2003**	**2004**	**2005**	**2006**	**2007**
N	66	91	83	83	100	102	41	36	37	45	46	50
µg m^{-3}	26.3	25.3	19.7	15.5	14.6	15.4	14.0	14.4	16.2	12.4	13.4	11.9
OC	3.8	3.3	2.8	2.2	2.0	2.1	2.6	2.4	2.8	2.2	2.2	2.4
EC	0.3	0.3	0.3	0.2	0.2	0.2	0.2	0.2	0.2	0.2	0.1	0.2
OM+EC	8.4	7.1	6.3	4.9	4.5	4.7	5.8	5.3	6.2	4.9	4.9	5.2
SO_4^{2-}	3.1	2.8	3.0	2.7	2.3	2.4	3.0	2.6	3.0	2.7	2.8	2.6
NO_3^-	1.3	2.0	1.8	1.9	1.5	1.6	0.4	1.2	1.7	1.3	1.2	1.1
NH_4^+	0.6	0.9	1.2	1.4	0.6	0.7	1.1	1.1	1.4	1.5	0.9	1.0
SIA	5.0	5.8	6.0	5.9	4.3	4.7	4.5	5.0	6.0	5.5	4.9	4.7
Mineral matter	7.6	6.8	4.7	3.1	3.9	4.2	1.4	0.9	1.8	0.8	1.4	1.2
Sea spray	0.6	0.7	0.5	0.5	0.4	0.5	0.2	0.2	0.2	0.3	0.2	0.2
Unaccounted	4.5	4.8	2.1	1.0	1.5	1.2	2.2	3.1	1.9	0.5	2.2	0.7

As shown in Figure 4.2.17, mean TSP and PM_{10} compositions are very similar in relative terms. Thus, the main constituents in both fractions are the crustal component (28-24%) and the organic matter (OM, 28-29%), followed by sulphate (12-16%), nitrate (7-11%), ammonium (3-6%), sea spray (3%) and EC (1-2%). The unaccounted mass was 18 and 9% of the total TSP and PM_{10} respectively. In $PM_{2.5}$ the crustal component is highly reduced (down to 9%), the dominant components being OM (37%) and sulphate (20%), followed by nitrate (8%), ammonium (8%), sea spray (2%) and EC (2%). The unaccounted mass was 13% of the $PM_{2.5}$ fraction. Due to the high proportion of hygroscopic components (at least sulphate, nitrate, ammonium and sea spray) the proportion of the unaccounted mass is relatively high in all fractions. The fact that some components, such as NH_4^+, NO_3^- and OM+EC, in many cases present lower levels in the fraction PM_{10} than in the fraction $PM_{2.5}$ is probably the result of the partitioning of

these compounds, occuring mostly in particles smaller than 2.5 μm. Thus, the differences observed may be probably due to the fact that some PM_{10} and $PM_{2.5}$ samples are not simultaneous and common experimental uncertainties. In addition, the interaction of ammonium nitrate with coarse sodium chloride particles in the PM_{10} filter may lead to volatilization of ammonium chloride reducing the measured levels of these compounds (Harrison and Pio, 1983; Warneck, 1988; Harrison and Kito, 1990; Wakamatsu et al., 1996).

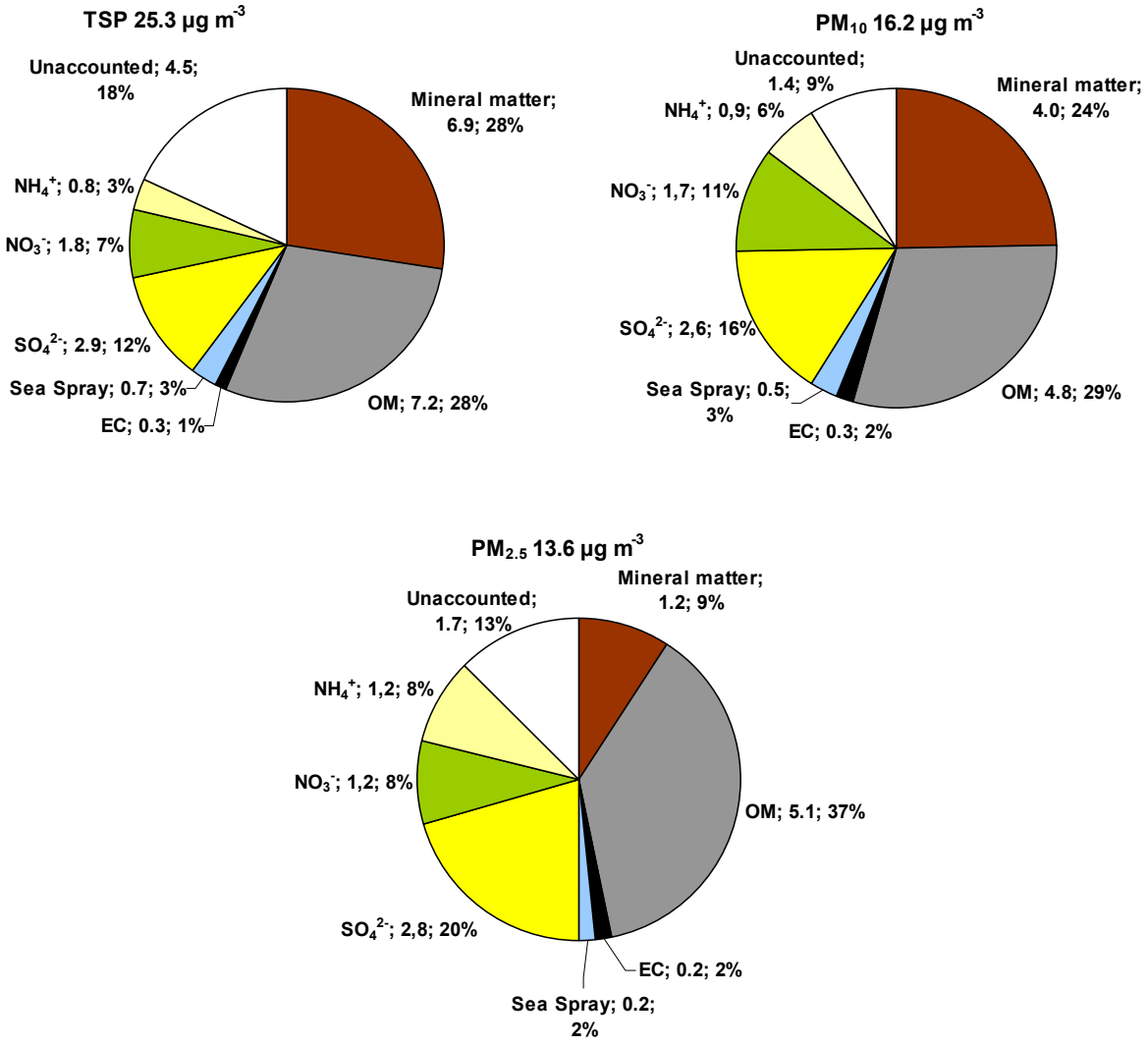

Figure 4.2.17. Mean composition of TSP (2002-2003), PM_{10} (2004-2007) and $PM_{2.5}$ (2002-2007) measured in MSY.

Table 4.2.8 shows the mean levels of PM_{10} and $PM_{2.5}$ components at MSY and at some other RB sites. The most distinctive feature of PM at MSY is the relatively high levels of the crustal component (4 and 1 μg m^{-3} for PM_{10} and $PM_{2.5}$, respectively) when

compared with central and northern European sites (2 and <0.5 μg m^{-3} for PM_{10} and $PM_{2.5}$ in most cases). This enrichment is also evident at Southern European sites as Monte Cimone (3.5 μg m^{-3} in PM_{10}).

Sulphate levels measured at MSY (3 μg m^{-3}) fall within the usual range reported for RB sites in central, and southern Europe and UK (2-4 μg m^{-3}), and are slightly lower than those in Eastern USA (4.5 μg m^{-3}) and higher than those registered at RB sites in Switzerland and Scandinavia (1-2 μg m^{-3}).

Nitrate levels (1-2 μg m^{-3}) are relatively low when compared with those in central Europe and the UK (2-4 μg m^{-3}), and slightly higher than those measured at RB sites in the central Mediterranean, Switzerland and Scandinavia (0.5-1 μg m^{-3}), but similar to the levels recorded in Italy. Ammonium follows a very similar spatial distribution pattern.

EC and OC levels at MSY (0.2 and 2 μg m^{-3}) are lower than those at RB sites in central Europe (0.5 to 2 and 2 to 4 μg m^{-3} in most cases), slightly higher than those in Scandinavia (0.1 and 0.9 μg m^{-3}), but akin to those reported for Italy and Eastern USA.

Levels of sea spray (0.5 and 0.2 μg m^{-3} in PM_{10} and $PM_{2.5}$, respectively) are lower in the mountainous areas surrounding the Mediterranean, such as MSY than those at the Atlantic sites in Europe (4 to 12 μg m^{-3} as reported by Visser et al., 2001 and Querol et al., 2008a).

Accordingly, it may be concluded that PM at MSY (and other RB Mediterranean sites) is characterized by relatively high levels of crustal material and lower levels of OM+EC and ammonium nitrate when compared with similar RB sites in central Europe (Table 4.2.8).

As expected from the location, the carbonaceous fraction in $PM_{2.5}$ at MSY is mainly composed of organic carbon (1.7 μg m^{-3} in winter and 2.8 μg m^{-3} in summer). EC levels present slight variations from winter to summer (0.16 and 0.21 μg m^{-3}, respectively). These levels are within the range of those at other RB sites in Europe, such as Puy du Dôme (France) and Schauinsland (Germany), (Pio et al., 2007), and Moitinhos (Portugal, Duarte et al., 2008) (Table 4.2.9). The mean OC+EC levels recorded at MSY exceed those registered at remote sites in Europe such as Sonnblick (Austria) and the Azores (Portugal) (Pío et al. 2007). Nevertheless, these levels are very low when

compared with other RB sites in Europe, and much lower when contrasted with those at regional sites in Asia (Table 4.2.9). The OC/EC ratio reaches mean values close to 11 at MSY, which is similar to that at Monagrega, a RB site 350 km to the SW of MSY (Rodriguez et al. 2003). This ratio is much higher than those at most RB sites in Europe (OC/EC values generally >4), including Southern Europe (OC/EC values from 4 to 9 in most cases) and Asia (from 3 to 7) (Table 4.2.9). The OC/EC ratio found at most of these sites reaches higher values in summer than in winter, which is also the case at MSY (with summer and winter ratios of 14 and 11, respectively). The higher OC/EC ratio at MSY and Monagrega, especially in summer, could be due to high summer biogenic emissions of SOA precursors (Peñuelas et al., 1999), elevated ozone levels, intense insolation and frequent recirculation of aged air masses.

Regarding SIA, nitrate/sulphate ratios for most years lie in the range 0.5-0.7. This resembles those reported at RB sites in Switzerland, Italy and Spain, and some sites in Austria. By contrast, the nitrate/sulphate ratio is twice as high as that obtained at remote sites in Scandinavia (Birkenes), Crete and Italy (Mt. Cimone), and half that recorded at rural sites in Germany and the UK (Table 4.2.8). Thus, the nitrate/sulphate ratio is higher than at remote sites but lower than at the RB sites of central Europe and the UK. This may reflect a moderate regional influence from urban and industrial nitrate contributions.

Table 4.2.8. Mean levels of PM_{10} and $PM_{2.5}$ components measured at Montseny (MSY) and some other regional background (RB) sites.

	Germany			Austria			Switzerland		
	Melpitz[1]			Illmitz[2]	Streithofen[3]		Payerne[4]	Chaumont[4]	
	annual	annual	annual	annual	annual		annual	annual	annual
	2004-2006	2004-2006	2004-2006	99-2000	99-2000		1998-99		
N	153	153	153				17	104	78
µg m^{-3}	PM_{10}	$PM_{2.5}$	PM_1	PM_{10}	PM_{10}	$PM_{2.5}$	PM_{10}	PM_{10}	$PM_{2.5}$
PM	20.5	16.1	12.2	24.2	23.7	18.1	13.7	10.8	7.7
SO_4^{2-}	3.1	2.8	2.3	4.4	3.9	3.3	2.2	2.0	2.3
NO_3^-	3.4	2.8	2.0	2.7	4.1	2.9	1.1	0.8	0.6
NH_4^+	2.0	1.8	1.4	1.9	2.6	2.1	1.0	0.8	0.8
OC				5.6*	4.3	3.0	2.4	1.2*	1.1*
EC				1.9	2.0**	1.8	1.3	0.6	0.4
OM+EC[#]	6.4	4.5	3.6	13.7	11.0	8.1	6.4	3.2	2.8
Mineral	1.1	0.7	0.5				1.6	1.6	0.7
Sea spray	0.5	0.2	0.1		0.3	0.2	0.2	0.2	0.1
SIA	8.6	7.4	5.7	9.0	10.6	8.3	4.3	3.6	3.7
Unacc.	3.9	3.2	2.3	1.5	1.8	1.5	2.9	2.2	0.4

	Norway	UK	USA	Italy				Greece
	Birkenes[5]	Churchill-P.S. Birmingham[6]	Sterling Forest, NYC[7]	Mt Cimone[8]		Montelibretti[9]		Patras[10]
	annual	annual	annual	summer	summer	annual	annual	annual
	2004	2005-2006	2001	2004	2004	2006	2005	2004-2005
N			88	47	47			105
µg m^{-3}	PM_{10}	PM_{10}	$PM_{2.5}$	PM_{10}	PM_1	PM_{10}	PM_{10}	$PM_{2.5}$
PM	5.4	19.0	11.4	16.0	7.1	29.0	29.9	13.9
SO_4^{2-}	1.1	2.8	4.5	3.5	2.4	3.5	3.4	3.2
NO_3^-	0.4	3.2		0.8	0.3	1.8	1.7	0.4
NH_4^+	0.8	1.3		1.4	1.0	1.0	1.1	1.6
OC	1.6	3.6	1.7	1.5*	1.5	5.8	8.2	
EC	0.2	1.0	0.2	0.2*	0.2	1.0	1.4	
OM+EC[#]	3.5	8.6	3.8	3.4	3.4	13.2	18.6	
Mineral	0.1	1.0	0.3	3.5	0.1	9.4	8.8	
Sea spray	0.8	2.0	0.1	0.3	<0.1	1.0	1.0	
SIA	2.2	7.3		5.7	3.7	6.3	6.2	
Unacc.	-1.2	0.1	2.7	3.1	-0.1	-0.9	-4.7	

	Spain						
	Bemantes[11]		Villar Arzobispo[12]		Monagrega[13]	Montseny	
	annual	annual	annual	annual	annual	Annual	annual
	2001	2001	2004-2005	2004-2005	1999-2000	2004-2007	2002-2007
N	87	45	72	72	112	442	255
µg m^{-3}	PM_{10}	$PM_{2.5}$	PM_{10}	$PM_{2.5}$	PM_{10}	PM_{10}	$PM_{2.5}$
PM	18.9	13.5	21.0	18.0	22.0	16.2	13.6
SO_4^{2-}	3.0	2.9	2.3	2.5	3.8	2.6	2.8
NO_3^-	0.9	0.4	1.4	1.3	2.2	1.7	1.2
NH_4^+	1.3	1.2	1.1	1.2	1.3	0.9	1.1
OC					1.7	2.3	2.4
EC					0.6	0.3	0.2
OM+EC[#]	4.5	4.0	2.4	2.8	4.2	5.0	5.3
Mineral	2.5	1.5	7.3	5.2	5.8	4.0	1.2
Sea spray	2.4	0.9	0.6	0.4	0.6	0.5	0.2
SIA	5.2	4.5	4.8	5.0	7.3	5.2	5.1
Unacc.	4.3	2.6	5.9	4.6	4.1	1.5	1.8

[1] Spindler et al. (2007); [2] EMEP (2007); [3] Puxbaum et al. (2004); [4]. Hueglin et al. (2005); [5]Yttri et al. (2007); [6] Yin and Harrison (2008); [7] Lall and Thrurston (2006); [8] Marenco et al., (2006); [9] C. Perrino (Pers Com); [10] Glavas et al. (2008); [11] Salvador et al. (2007); [12] Viana et al. (2008b); [13] Rodriguez et al. (2004)

[#] OM=OC*2.1; *OC and EC levels measured in PM_1

Table 4.2.9. EC and TC levels (μg m^{-3}), as well as OC/EC and OC/TC ratios, in $PM_{2.5}$ or PM_{10} in regional background (RB, or RBH if these are mountain >1000 m.a.s.l. RB sites), rural (R, or near city R, RNC) sites, obtained from different studies performed with a methodology similar to the one used in this study compared with the mean data obtained at MSY. Grey shadowed numbers show OC/EC ratios from 8 to 14 in a range similar to those measured at MSY (11 mean annual).

	City	Site	Period	OC	EC	TC	OC/EC	Reference
$PM_{2.5}$	Shanghai	R	11/2002, 7 days	16.5	3.6	20.1	4.6	Feng et al., 2006
$PM_{2.5}$	Shanghai	R	08/2003, 7 days	4.9	2.0	6.9	2.5	Feng et al., 2006
$PM_{2.5}$	Hok Tsui, Hong Kong	RB	02-03/2005	5.6	1.4	7.0	4.0	Duan et al., 2007
$PM_{2.5}$	Hok Tsui, Hong Kong	RB	11/2000-02/2001	5.5	1.4	6.9	4.0	Ho et al., 2006
$PM_{2.5}$	Hok Tsui, Hong Kong	RB	01-02/2005	6.3	1.9	8.2	3.3	Cao et al., 2003
PM_{10}	Hok Tsui, Hong Kong	RB	11/2000-02/2001	5.6	1.5	7.1	3.8	Ho et al., 2006
PM_{10}	Hok Tsui, Hong Kong	RB	01-02/2001	9.1	3.0	12.1	3.0	Cao et al., 2003
$PM_{2.5}$	Hok Tsui, Hong Kong	RB	08-09/2004	5.9	0.8	6.7	7.4	Duan et al., 2007
$PM_{2.5}$	Hok Tsui, Hong Kong	RB	06-08/2001	1.5	0.4	1.9	3.5	Ho et al., 2006
PM_{10}	Hok Tsui, Hong Kong	RB	06-08/2001	1.7	0.4	2.1	4.0	Ho et al., 2006
$PM_{2.5}$	Hok Tsui, Hong Kong	RB	Summer 2002	3.4	0.7	4.1	4.9	Cao et al., 2004
PM_{10}	Hok Tsui, Hong Kong	RB	Summer 2002	4.1	1.1	5.2	3.7	Cao et al., 2004
TSP	Daihai, Inner Mongolia	RBH	2005-2007	19.9	3.1	23.0	6.4	Han et al., 2008
$PM_{2.5}$	Daihai, Inner Mongolia	RBH	2005-2007	11.8	1.9	13.7	6.4	Han et al., 2008
$PM_{2.5}$	Meru, Kenya	R	05-06/1999	6.0	1.4	7.4	4.3	Gatari & Bomana, 2003
$PM_{2.5}$	San Joaquin Valley, CA	R	01/2000-05/2001	5.0	1.2	6.2	4.2	Chow et al., 2006
$PM_{2.5}$	Sterling Forest, NYC	R	2001, 1 year	1.7	0.2	1.9	8.5	Lall & Thrurston, 2006
PM_{10}	Birkenes, Norway	R		0.9	0.1	1.0	9.6	Yttri, 2007
PM_{10}	Birmingham, UK	R	11/2005-05/2006	3.6	1.0	4.6	3.6	Harrison and Yin, 2008
$PM_{2.5}$	Birmingham, UK	R	11/2005-05/2006	3.2	0.9	4.1	3.6	Harrison and Yin, 2008
PM_{1}	Birmingham, UK	R	11/2005-05/2006	2.7	0.8	3.5	3.4	Harrison and Yin, 2008
PM_{10}	Chaumon, Switzerland	RBH	1 year	1.2	0.6	1.8	2.0	Hueglin et al., 2005
$PM_{2.5}$	Chaumon, Switzerland	RBH	1 year	1.1	0.4	1.5	2.8	Hueglin et al., 2005
PM_{10}	Streithofen, Austria	R	06/1999-05/2000	4.3	2.0	6.3	2.2	Puxbaum et al., 2004
$PM_{2.5}$	Streithofen, Austria	R	06/1999-05/2000	3.0	1.8	4.8	1.7	Puxbaum et al., 2004
PM_{10}	Illmitz, Austria	R		3.9	2.0	5.9	1.9	Putaud et al., 2003
$PM_{2.5}$	Bologna, Italy	R	Winter 1998-1999	7.2	0.9	8.1	8.0	Decesari et al., 2001
$PM_{2.5}$	Bologna, Italy	R	Summer 1998-1999	2.9	0.3	3.2	9.7	Decesari et al., 2001
PM_{10}	Montelibretti, Rome	RNC	2006, 1 year	5.8	1.0	6.8	5.8	C. Perrino (Pers com)
PM_{10}	Montelibretti, Rome	RNC	2005, 1 year	8.2	1.4	9.6	5.9	C. Perrino (Pers com)
$PM_{2.5}$	Monagrega, Spain	RB	1999-2000, 1 year	2.2	0.2	2.4	11.0	Rodríguez et al. 2002a
PM_{1}	Monte Cimone, Italy	RBH	Summer 2004	1.5	0.2	1.7	7.5	Marenco et al., 2006
PM_{10}	Moitinhos, Portugal	R	07-08/2004	3.0	0.4	3.4	8.6	Duarte et al., 2008
PM_{3}	Moitinhos, Portugal	R	07-08/2004	2.5	0.3	2.8	8.3	Duarte et al., 2008
$PM_{2.5}$	Azores, Portugal	R	Summer, 2003-2005	0.4	0.06	0.4	6.7	Pio et al., 2007
$PM_{2.5}$	Azores, Portugal	R	Winter, 2003-2005	0.3	0.04	0.3	6.9	Pio et al., 2007
$PM_{2.5}$	Aveiro, Portugal	R	Summer, 2003-2005	3.1	0.6	3.8	4.8	Pio et al., 2007
$PM_{2.5}$	Aveiro, Portugal	R	Winter, 2003-2005	7.5	1.3	8.8	5.6	Pio et al., 2007
PM_{10}	Puy du Dôme, France	RBH	Summer, 2003-2005	2.4	0.3	2.7	9.2	Pio et al., 2007
PM_{10}	Puy du Dôme, France	RBH	Winter, 2003-2005	0.8	0.2	1.0	4.3	Pio et al., 2007
PM_{10}	Schauinsland, Germany	RBH	Summer, 2003-2005	3.4	0.4	3.8	9.7	Pio et al., 2007
PM_{10}	Schauinsland, Germany	RBH	Winter, 2003-2005	1.4	0.2	1.6	6.2	Pio et al., 2007
$PM_{2.5}$	Sonnblick, Austria	RBH	Summer, 2003-2005	1.4	0.2	1.6	6.0	Pio et al., 2007
$PM_{2.5}$	Sonnblick, Austria	RBH	Winter, 2003-2005	0.5	0.06	0.5	7.3	Pio et al., 2007
$PM_{2.5}$	K-Puszta, Hungary	R	Summer, 2003-2005	4.9	0.7	5.6	7.1	Pio et al., 2007
$PM_{2.5}$	K-Puszta, Hungary	R	Winter, 2003-2005	7.4	1.6	9.0	4.7	Pio et al., 2007
$PM_{2.0}$	Budapest, Hungary	RNC	04-05/2002	4.1	0.3	4.4	12.4	Salma et al., 2004
$PM_{2.5}$	Montseny, Spain	RB	Winter, 2002-2007	1.7	0.2	1.8	10.6	This work
$PM_{2.5}$	Montseny, Spain	RB	Summer, 2002-2007	2.8	0.2	3.0	13.6	This work

4.2.3.2. Partitioning of major components in $PM_{2.5}$ and $PM_{2.5-10}$

In this section, PM_{10} and $PM_{2.5}$ simultaneous data measured from 2004 to 2007 in Montseny will be presented and discussed (Table 4.2.10). The composition of $PM_{2.5-10}$, PM_{10} and $PM_{2.5}$ and partitioning of PM components between the $PM_{2.5-10}$ and $PM_{2.5}$ fractions will be described below using the PM_{10} and $PM_{2.5}$ chemical speciation measured simultaneously from 2004 to 2007 (Figure 4.2.18 and Figure 4.2.19).

Table 4.2.10. Mean levels of PM_{10}, $PM_{2.5}$ and $PM_{2.5-10}$ and their major components measured simultaneously at Montseny from 2004 to 2007.

	PM_{10}	**$PM_{2.5}$**	**$PM_{2.5-10}$**
N	160	160	160
µg m^{-3}	17.0	13.6	3.4
OC	2.4	2.4	<0.1
EC	0.3	0.2	0.1
OM+EC	5.4	5.3	<0.1
SO_4^{2-}	2.8	2.8	<0.1
NO_3^-	1.9	1.3	0.4
NH_4^+	1.2	1.2	<0.1
SIA	5.9	5.3	0.6
Mineral matter	4.3	1.3	2.7
Sea spray	0.5	0.2	0.3
Unaccounted	1.6	1.6	<0.1

In Montseny only 30, 40 and 70% of the crustal mineral, sea spray, and nitrate levels measured in PM_{10} are still present in $PM_{2.5}$. The other major PM_{10} components are in the fine fraction in a proportion >80%.

PM_{10} was mainly composed by SIA (34%), carbonaceous compounds (30%), mineral matter (25%) and sea spray (3%).

$PM_{2.5}$ was made of a mixture of SIA (39%), carbonaceous material (38%) and mineral matter (9%). The mass of mineral dust was reduced in the $PM_{2.5}$ with respect to the PM_{10} (4.3 and 1.3 µg m^{-3} in PM_{10} and $PM_{2.5}$ respectively). Most of the carbonaceous components present in PM_{10} also fall within the $PM_{2.5}$ range (almost no OM+EC is present in the $PM_{2.5-10}$ fraction). Most sulphate was also present in this fine fraction.

The coarse fraction ($PM_{2.5-10}$) was mainly made up of mineral dust (78%), sea spray (6%) and nitrate (14%). The carbonaceous material (2%), ammonia and sulphate were found at very low levels in this coarse fraction.

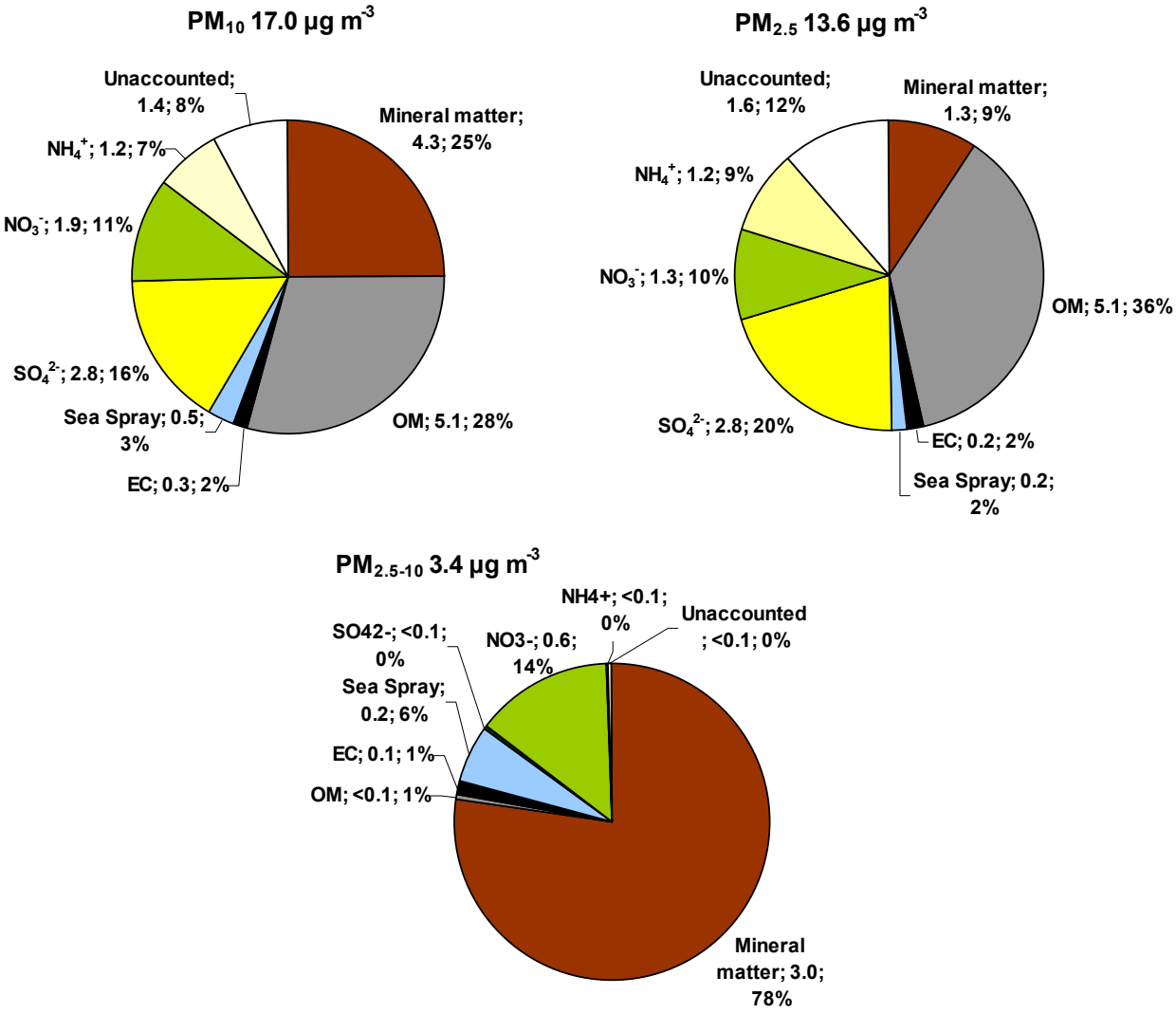

Figure 4.2.18. Mean composition of PM_{10}, $PM_{2.5}$ and $PM_{2.5-10}$ measured at MSY simultaneously from 2004 to 2007.

The partitioning of the mineral matter was 30/70% for $PM_{2.5}/PM_{2.5-10}$ respectively. Mineral dust load in this regional site has a prevailing natural origin and it is attributed to natural resuspension from regional soils and in a minor proportion to African dust events. Soil dust resuspension is favoured by the relatively long periods without rain in this region. African dust contribution to crustal levels can be very high during the occurrence of long-range transport events.

Sea spray was distributed among the two fractions. The partitioning was 51/49% for $PM_{2.5}/PM_{2.5-10}$, respectively.

The carbonaceous material (OM+EC) was mainly present in the fine fraction (99% in the $PM_{2.5}$ fraction). The carbonaceous material measured at a regional background site may be biogenic (secondary organic compounds, pollens and other biological debris) or anthropogenic (regional fossil fuel and biomass combustion), with a finer grain size.

Sulphate was mainly present in the $PM_{2.5}$ fraction as a consequence of the prevalence of ammonium sulphate (fine aerosols) versus the coarser Ca, Na or Mg sulphate species.

Nitrate was distributed between the fine a coarse fractions but also shifted towards the $PM_{2.5}$ fraction. The partitioning was 30/70% for $PM_{2.5}/PM_{2.5\text{-}10}$, respectively. The finer size distribution is due to the prevalence of fine ammonium nitrate, but coarser Na and Ca nitrate also occur in appreciable levels.

Ammonium showed a fine size distribution. Almost all was present in the $PM_{2.5}$ fraction as a consequence of the fine grain size of ammonium sulphate and nitrate.

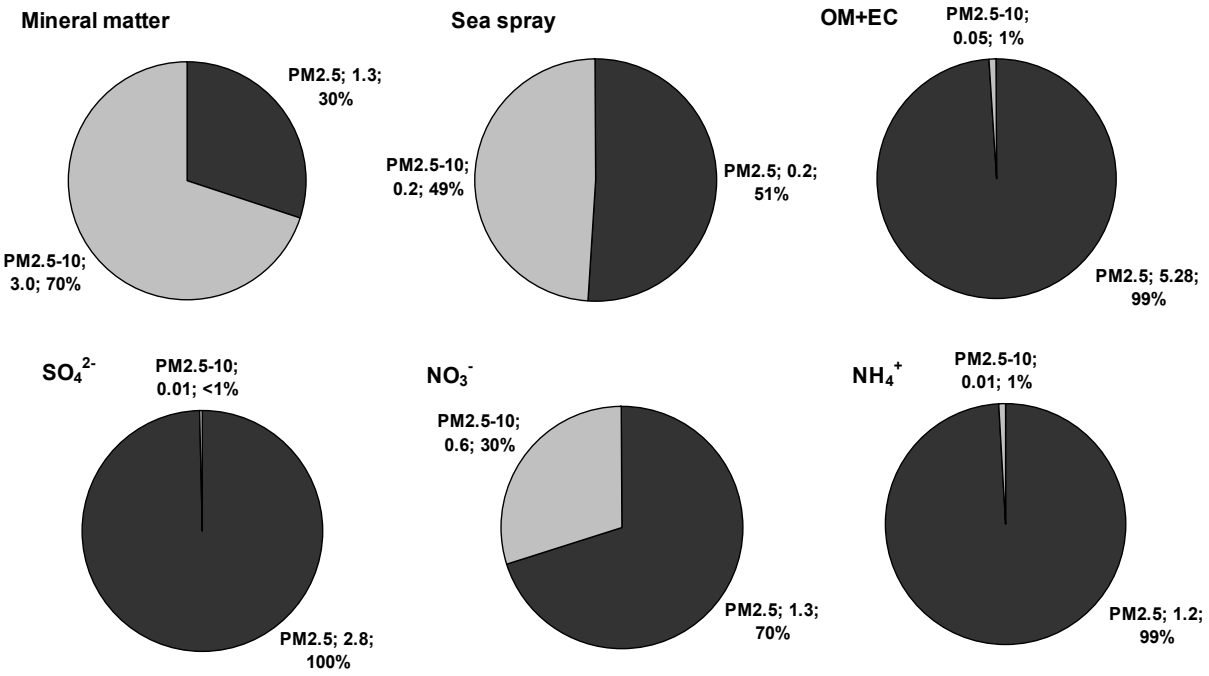

Figure 4.2.19. Partitioning of mean PM components between $PM_{2.5\text{-}10}$ and $PM_{2.5}$ fractions at MSY from 2004 to 2007.

4.2.3.3. Carbonaceous aerosols

There are several indirect methods for the calculation of the contribution of primary and secondary organic aerosols (POA and SOA) to the total organic aerosol (OA) or organic matter (OM) concentration. In Barcelona urban background, the EC tracer method (Salma et al., 2004), based in the use of EC as a tracer of primary OC emissions, was applied, supposing a common origin for OC and EC (in this case, road traffic emissions) and a negligible SOA contribution for the minimum OC/EC ratio obtained. However, the OC/EC ratio increases with the distance to the direct anthropogenic emission sources and in the case of the regional background at MSY, this method is not valid. Primary carbonaceous emissions in Montseny arise from natural (biogenic) or anthropogenic sources (fossil fuel and biomass combustion) emitted in the area or transported from regional or distant areas. However, POC cannot be determined from the OC/EC ratio as the same source cannot be supposed for OC and EC, and SOA cannot be neglected for the minimum OC/EC ratio. Consequently, this estimation would have a very large uncertainty. For POA and SOA determinations other methods may be applied, as the ^{14}C method to discriminate the origin of the carbon content in atmospheric aerosols (Hallquist et al., 2009). However, these measurements were not available at MSY. Analyses of ^{14}C are currently under development for samples collected during the DAURE campaign in 2009.

4.2.3.4. Trace elements

The mean annual levels of trace elements measured at MSY in PM_{10} and $PM_{2.5}$ from 2004 to 2007 are shown on Table 4.2.11. The elements studied do not present a large temporal variation in the area. As occurred with major elements, for some years certain elements present higher levels in $PM_{2.5}$ than PM_{10}, such as Ni, Zn, As, Sn and Pb. This may be due, as above, to the presence of anthropogenic elements mainly in particles of a diameter <2.5 μm, and to differences in sampling frequency between $PM_{2.5}$ and PM_{10} and common experimental uncertainties.

Table 4.2.11. Mean annual levels of trace elements (ng m^{-3}) measured at MSY in PM_{10} and $PM_{2.5}$ between 2004 and 2007.

ng m^{-3}	PM_{10}				$PM_{2.5}$			
	2004	2005	2006	2007	2004	2005	2006	2007
N	83	83	100	102	37	45	46	50
P	14.4	12.2	11.9	12.6	7.7	5.5	5.8	6.0
Li	0.3	0.2	0.2	0.3	0.1	0.1	0.2	0.1
Ti	22.6	14.4	18.1	18.0	8.9	4.1	6.8	4.7
V	3.4	3.9	3.2	3.3	2.7	2.5	3.5	2.7
Cr	1.1	1.0	0.8	1.2	0.8	0.8	1.0	1.1
Mn	5.4	4.3	4.5	5.0	3.2	2.0	2.7	2.2
Co	0.1	0.1	0.1	0.1	0.1	0.1	0.1	0.1
Ni	1.7	1.8	1.5	1.2	1.9	1.5	1.8	1.2
Cu	4.9	3.5	3.4	3.2	3.5	3.3	3.3	2.8
Zn	15.0	13.7	9.1	13.8	26.5	15.0	13.2	13.2
As	0.3	0.3	0.2	0.2	0.3	0.2	0.3	0.2
Se	0.4	0.2	0.2	0.2	0.3	0.2	0.2	0.2
Rb	0.6	0.3	0.4	0.5	0.3	0.1	0.2	0.2
Sr	2.0	1.3	1.6	1.9	0.8	0.4	0.8	0.7
Cd	0.2	0.1	0.1	0.1	0.2	0.1	0.1	0.1
Sn	1.3	0.9	0.6	0.8	1.6	0.8	0.7	0.8
Sb	0.6	0.6	0.4	0.4	0.5	0.5	0.4	0.3
Ba	5.0	4.7	5.4	8.2	3.2	3.4	3.1	4.9
La	0.2	0.1	0.2	0.2	0.1	0.1	0.1	0.1
Ce	0.4	0.3	0.3	0.4	0.2	0.1	0.2	0.2
Tl	0.07	0.15	0.03	0.04	0.10	0.11	0.03	0.03
Pb	5.1	4.8	3.8	4.3	6.4	4.6	4.6	4.2
Bi	0.1	0.2	0.1	0.1	0.1	0.2	0.1	0.1
Th	0.06	0.08	0.08	0.08	0.04	0.06	0.05	0.04
U	0.07	0.09	0.05	0.07	0.04	0.12	0.05	0.06

Table 4.2.12 shows the mean levels of trace elements analyzed in PM_{10} and $PM_{2.5}$ at MSY and selected RB sites. Levels of V measured at MSY (3.5 ng m^{-3} in PM_{10}) are relatively higher than those at most sites in central Europe (0.7-1.2 ng m^{-3}) and similar to those measured at Monte Cimone and in Eastern USA (3 ng m^{-3}). The other elements analyzed fall within similar concentration ranges. The higher V measured in Southern Europe when compared with Central Erurope may be due to the relatively high emissions from fuel-oil combustion in the Mediterranean basin (power generation, industrial and shipping emissions, Querol et al., 2009). Regarding the ratio V/SO_4^{2-}, it was generally higher in Southern Europe compared with Northern Europe, probably due to the influence of shipping emissions from the Mediterranean.

Table 4.2.12. Mean levels of PM_{10} and $PM_{2.5}$ trace elements (ng m^{-3}) measured at MSY and at some other RB sites.

ng m^{-3}	Austria		Switzerland			Italy		USA
	Streithofen[1]		Payerne[2]	Chaumont[2]		Mt Cimone[3]		S. Forest[4]
	PM_{10}	$PM_{2.5}$	PM_{10}	PM_{10}	$PM_{2.5}$	PM_{10}	PM_1	$PM_{2.5}$
Li								
V	1.2	0.7	0.7	0.8	0.8	3.1		3
Cr	0.5	0.3						
Mn	4.0	2.0	2.8	2.4	0.8	6.2		1
Co	<0.1	<0.1						
Ni	0.7	0.4	1.2	1.3	1.3	1.4		4
Cu	4	2	6	7	6	3		1
As	0.7	0.5	0.5	0.2	0.2			
Zn	27	17				10	6	9
Se			0.2	0.2	0.2			1
Sr						3		1
Ba								<0.1
Pb	17	12	10	5	5	4	2	2
Rb			0.3	0.3	0.2			
Cd	0.3	0.2	0.3	0.1	0.1			
Sb			0.3	0.2	0.2			
La			0.1	0.1	0.2			
Ce								
Tl			<0.1	<0.1	<0.1			
Sn								
Th								
U								

	Spain						
	Bemantes[5]		Villar Arzobispo[6]		Monagrega[7]	Montseny	
	PM_{10}	$PM_{2.5}$	PM_{10}	$PM_{2.5}$	PM_{10}	PM_{10}	$PM_{2.5}$
Li	0.1	0.1	0.3	0.2		0.2	0.1
V	5.0	4.0	2.6	2.8	2.0	3.5	3.0
Cr	1.0	1.0	2.1	2.0	1.0	1.0	0.9
Mn	5.0	3.0	3.8	3.2	5.0	4.8	2.6
Co	0.1	0.2	0.1	0.1		0.1	0.1
Ni	3	4	3	4		1.5	1.6
Cu	8	9	2	1	3	3.6	3.2
As	0.4	0.3	0.2	0.3		0.3	0.3
Zn	16	17	11	12	30	12	
Se	0.5	0.4	0.3	0.4		0.3	0.2
Sr	1	1	1	1	5	1.7	0.7
Ba	6	5	4	5		6	4
Pb	8	7	5	6	10	4	5
Rb	1.0	0.5	0.5	0.5		0.5	0.2
Cd	0.2	0.2	0.1	0.1		0.1	0.1
Sb	0.6	0.4	0.4	0.3		0.5	0.4
La	0.1	0.1	0.1	0.1		0.2	0.1
Ce	0.2	0.2	0.2	0.2		0.4	0.2
Tl	0.1	0.1	0.1	0.2		0.1	0.1
Sn	0.5	0.4	0.4	0.7		0.9	1.0
Th	0.2	0.2	0.1	0.1		0.1	<0.1
U	0.2	0.2	0.1	0.1		0.1	0.1

[1] Puxbaum et al. (2004); [2] Hueglin et al. (2005); [3] Marenco et al., (2006); [4] Lall and Thrurston (2006); [5] Salvador et al. (2007); [6] Viana et al. (2008b); [7] Rodríguez et al. (2004)

The trace elements showed a clear partitioning trend between the $PM_{10-2.5}$ and the $PM_{2.5}$ fraction, reflecting the origin of some of the elements. Figure 4.2.20 shows the ratios $PM_{2.5}/PM_{10}$ for the elements analysed. There is a clear differentiation between the typical crustal elements (Li, Sc, Mn, Ga, Sr, Ba, Rb, Y, La, Ce, Cs, Th), with a coarser particle size (<50% of the levels measured in PM_{10} are present in $PM_{2.5}$), and the dominantly anthropogenic elements (V, Cr, Co, As, Pb, Mo, Cd, Sb, Tl, Sn), which show a preference for the finer particle size (>80%; Allen et al., 2001; Moreno et al., 2006). The crustal material in MSY comes from arid soil resuspension and African dust outbreaks. Thus, typically crustal trace elements, such as Rb, Sr, Cs, Nb, La and Ce, are enriched mainly in the coarse fraction during African dusts events. The samples registering the lowest crustal tracers were those collected during winter anticyclonic episodes, when crustal material is normally at a relative minimum. Conversely, typical anthropogenic trace elements (Ni, As, Pb, Sn, and Sb) show their highest levels under these pollution episodes.

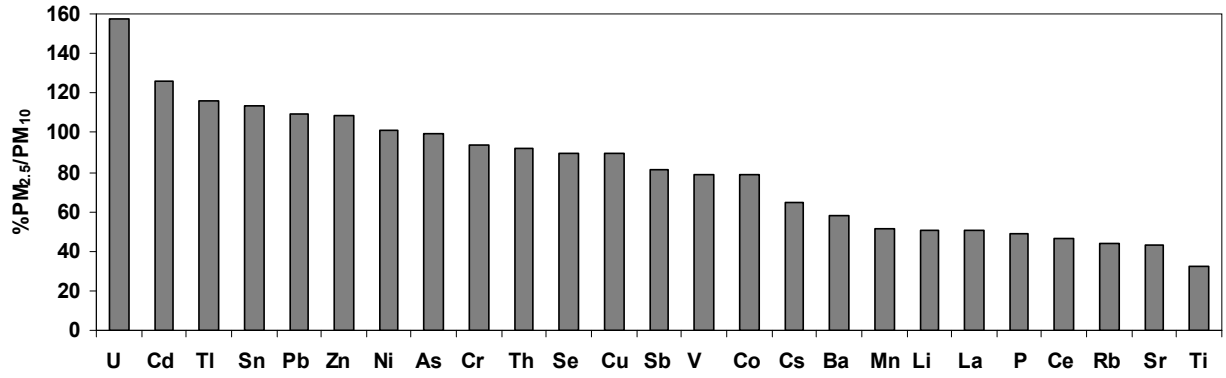

Figure 4.2.20. $PM_{2.5}/PM_{10}$ % ratios for mean levels of trace elements measured at MSY from 2004 to 2007.

4.2.3.5. Inter-annual trends

The analysis of inter-annual variations in $PM_{2.5}$ speciation data from 2002 to 2007 revealed decreasing trends for some of the variables, at 0.05 or 0.1 significance levels (α). According to Salmi et al. (2002), lower significance levels may be exclusively acquired with datasets containing >9 data points (6 in the present study). When annual means were analyzed, significant temporal trends were obtained for the carbonaceous aerosols (EC, OC, TC), which showed a clear decrease of 36-39% of the mass between 2002 and 2007 (α=0.05, Figure 4.2.21). Similar results were obtained for Cd (48% decrease, α=0.05). Given that carbonaceous aerosols and Cd are known tracers

of traffic emissions (Sternbeck et al., 2002), these trends could suggest a reduction in traffic emissions in the study area. However, this trend was not observed in the case of other tracers of traffic emissions (e.g., Sb and Sn).

On a seasonal basis, the natural components in $PM_{2.5}$ (sea-spray and crustal material) did not present any significant trends at MSY, whereas carbonaceous aerosols showed every year decreasing values during April (α=0.05), and less significantly in March, June and September (α=0.1). Longer time-series would be necessary to obtain a more detailed and statistically relevant picture of the temporal trends of aerosols at MSY. In any case the trends observed could probably be linked to meteorological cycles coupled with emission-abatement strategies, although this is a wider matter that needs a more detailed study.

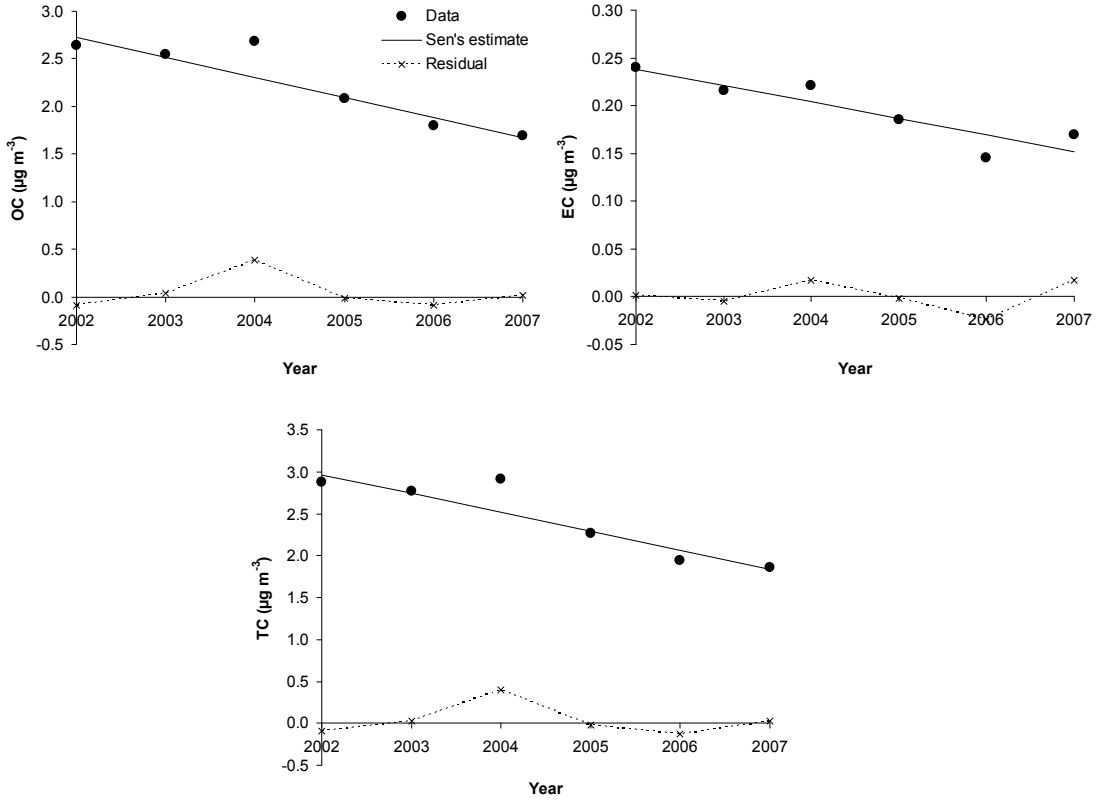

Figure 4.2.21. Temporal trends of annual levels of organic, elemental and total carbon (OC, EC and TC) in $PM_{2.5}$ detected at MSY by means of Mann-Kendall's test and Sen's method using MAKESENS (Salmi et al., 2002).

4.2.3.6. Seasonal evolution of PM components

Major PM components showed marked seasonal variations at MSY. The concentration of mineral matter was highest in summer (up to 25 and 12 μg m^{-3} in PM_{10} and $PM_{2.5}$, as daily values, respectively) (Figure 4.2.22). This can be attributed both to elevated dust re-suspension (both of local and regional origin due to high convective dynamics and low rainfall), and to the higher frequency of African dust episodes (N. Pérez et al., 2008b). In particular, high levels of mineral matter were registered sporadically in February-March (up to 55 μg m^{-3} in PM_{10}, as a daily value) and September-October, being attributed mainly to the contribution of intense African dust outbreaks.

Nitrate levels at MSY were highest during the colder months and considerably reduced in the summer (Figure 4.2.22). This trend is related to the thermal instability of the ammonium nitrate (Harrison and Pio, 1983; Querol et al., 1998b, 2004a). Ammonium nitrate may be volatilised in the atmosphere in the summer given the relatively high temperatures reached in summer in this Mediterranean region. The low values in summer could also be related to a negative artefact due to the volatilization of the ammonium nitrate once collected in the filter, but current sampling strategies with the filter under controlled temperature show also this summer low for NO_3^-. Moreover, the occurrence of a relatively high proportion of coarse nitrate species (Ca and Na nitrate compounds) could be deduced from these data, with $PM_{2.5}/PM_{10}$ ratios for nitrate being very close to 1 during the colder months and around 0.2 in summer. Extremely intense nitrate episodes were recorded every year from November to March under winter anthropogenic episodes (up to 15 μg m^{-3} of daily mean nitrate levels, Figure 4.2.22) and are associated with the transport (by mountain breezes) of aged air masses from the surrounding industrial/urban areas during anticyclonic scenarios. In addition, there may also be a contribution related to the formation of NH_4NO_3 from the input of NH_3 from agriculture and farming.

Sulphate levels presented the opposite seasonal trend to nitrate, increasing progressively from April-May to reach a broad maximum in mid summer (Figure 4.2.22). This seasonal pattern could be related to enhanced photochemistry, low regional air mass renovation (Millán et al, 1997; Querol et al., 1998a and 1999; Rodríguez et al., 2003) and to the expansion of the mixing layer depth, which results in the Montseny being within the boundary layer during the daytime. Second order and much shorter peaks of sulphate concentration were commonly recorded from November to March, coinciding with the aforementioned winter anticyclonic episodes.

Generally, sulphate species presented a predominantly fine particle size, with $PM_{2.5}/PM_{10}$ close to 1 and varying little over the year.

Ammonium concentration showed only a slight annual variation, being higher in the colder months related to the presence of ammonium nitrate (and to a lesser extent ammonium sulphate), and in the summer, associated with the highest concentration of ammonium sulphate. In April-May and September-October minimum levels were generally recorded. Owing to the artefact reaction between ammonium nitrate and sodium chloride on PM_{10} filters and the subsequent loss of gaseous ammonium chloride (Querol et al., 2001a), higher levels of ammonium were on average recorded in $PM_{2.5}$ than those obtained in PM_{10}. This artefact is less significant in $PM_{2.5}$ due to the considerably lower presence of sodium chloride in the $PM_{2.5}$ fraction.

Sea spray showed highest concentrations in the summer months due to increasing sea breeze circulation over the coast (located 30 km from MSY) (Figure 4.2.22). Chlorine/sodium ratios showed a seasonal trend, with higher winter values (close to the typical marine ratio in winter) and very low summer ratios. These may be attributed to the thermal instability of ammonium nitrate, yielding relatively high nitric acid/ammonium nitrate ratios (Harrison and Pio, 1983). In summer, nitric acid may interact with relatively abundant sodium chloride and cause loss of volatile hydrochloric acid. As expected, sea spray had a prevalent coarse particle size, with constant $PM_{2.5}/PM_{10}$ ratios varying between 0.4-0.6.

Carbonaceous aerosols were most abundant in summer (Figure 4.2.22), coinciding with the lower renovation of the atmosphere on a regional scale and probably with high biogenic emissions of gaseous organic precursors. Secondary peaks of concentration were usually observed from November to March (Figure 4.2.22), associated with winter anticyclonic pollution episodes. Carbonaceous compounds were mostly fine, with $PM_{2.5}/PM_{10}$ ratios very close to 1. As stated above, the mean OC/EC ratio was close to 11, although in most years it dropped to 7-8 in November-December and increased to 14-20 in June-September (with some exceptions, e.g., January 2005 (ratio of 22), or November-December 2004 (ratio of 15-17). The highest ratios recorded in the spring-summer period were due to an increase in the OC levels, probably attributable to secondary biogenic OC contributions.

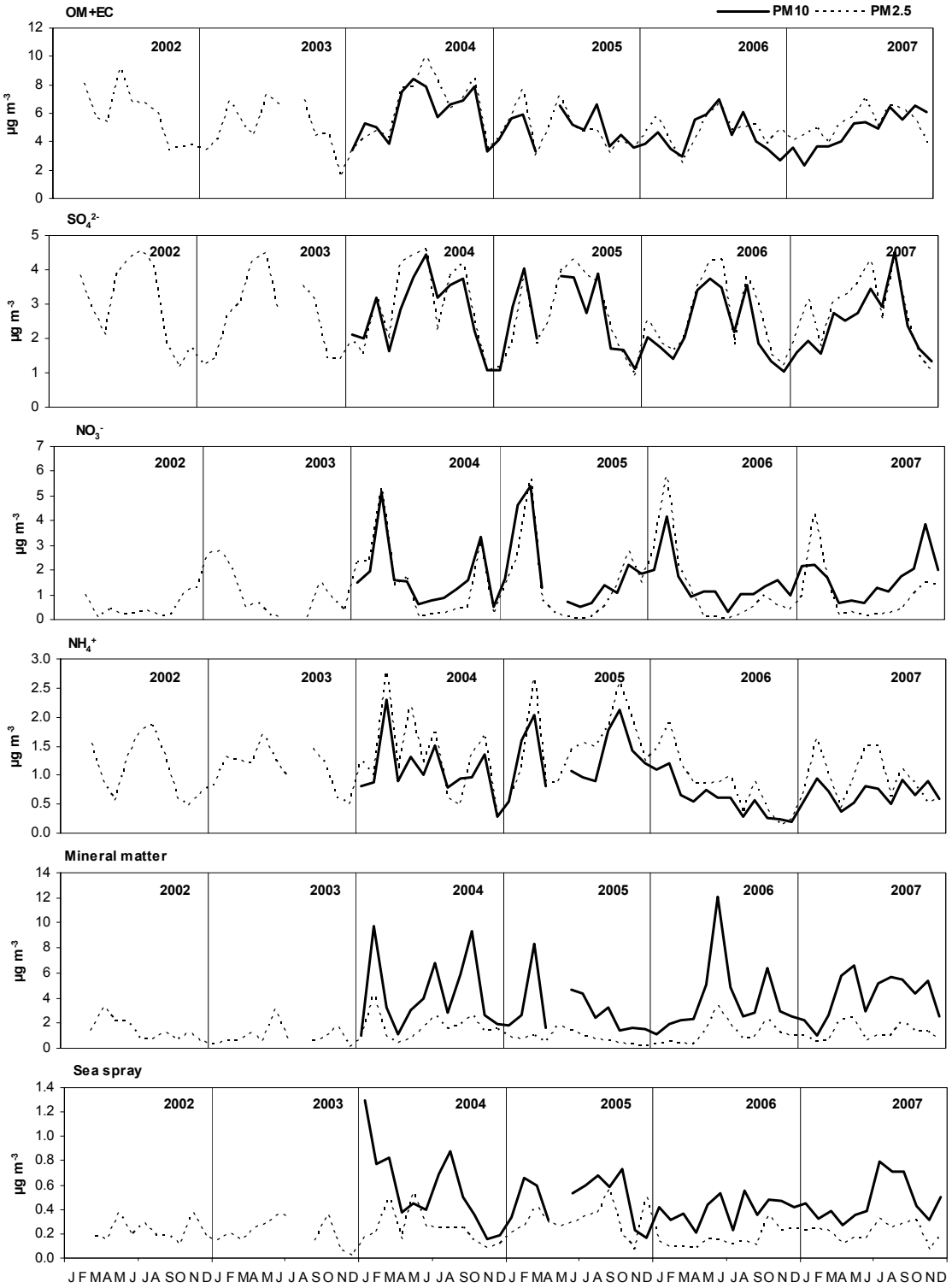

Figure 4.2.22.Time evolution of the levels of OM+EC, SO_4^{2-}, NO_3^-, NH_4^+, mineral matter and sea spray measured in PM_{10} and $PM_{2.5}$ at MSY during 2002-2007.

4.2.3.7. Day to day variability: PM episodes

Day to day variation of PM levels and speciation at MSY is mainly due to the occurrence of Atlantic advection episodes, African dust outbreaks, regional recirculations, European and Mediterranean transport events, and to local pollution or anticyclonic episodes (Rodríguez et al., 2003; Escudero et al., 2007a). As previously shown, the frequencies of these varying meteorological conditions affecting the study area were calculated for the 2002-2007 period, and mean PM levels and levels of the major components analyzed in PM_{10} and $PM_{2.5}$ obtained for each episode considered are given in Table 4.2.13 and Figure 4.2.23.

NAF episodes registered the highest mean levels of PM_{10} and $PM_{2.5}$ (26 and 17 μg m^{-3} respectively, with only 12 μgPM_1 m^{-3}). During these episodes the mineral fraction dominated the PM_{10} mass (40% as compared to only 17% of $PM_{2.5}$), SIA constituted 24% of PM_{10} and 32% of $PM_{2.5}$ (with sulphate being dominant in both), and OM was the other major component (16% and 25% of PM_{10} and $PM_{2.5}$).

WAE occurred from October to March and favour the accumulation of pollutants in the pre-coastal depression below MSY, towards which they are moved by mountain breezes. Enhancement of PM levels during these episodes (up to means of 20 μg m^{-3} PM_{10} and 16 μg m^{-3} $PM_{2.5}$) was especially remarkable in the finest aerosols, with PM_1 reaching 14 μg m^{-3}. Ambient PM composition under these conditions is rich in SIA (44% in PM_{10} and $PM_{2.5}$ especially NH_4NO_3 (30-32%)) and carbonaceous aerosols (OM+EC: 25 and 24% in PM_{10} and $PM_{2.5}$), whereas mineral matter is markedly reduced (16 and 5%, respectively).

Summer regional episodes were due to the recirculation of air masses over the WMB, resulting in mean levels of 18, 15, 12 μg m^{-3} for PM_{10}, $PM_{2.5}$, PM_1. PM composition was characterized by a high sulphate concentration (20 and 27% in PM_{10} and $PM_{2.5}$) that is mainly due to intense photochemical activity and the low renovation of air masses on a regional scale. Carbonaceous aerosol levels were also high (OM reaches 22 and 26 % in PM_{10} and $PM_{2.5}$), probably because of high biogenic emissions. Mineral matter was also high in the coarser fraction (22 and 8% in PM_{10} and $PM_{2.5}$) owing to local soil resuspension and to the frequent simultaneous occurrence of African dust outbreaks.

European and Mediterranean episodes were less frequent and registered relatively low mean PM levels (13, 12, 11 μg m^{-3} and 13, 10, 9 μg m^{-3} for PM_{10}, $PM_{2.5}$ and PM_1, respectively). PM composition was characterized by relatively high proportions of SIA

(European 30 and 41%, Mediterranean 31 and 33% in PM_{10} and $PM_{2.5}$) and carbonaceous aerosols (European 22 and 31%, Mediterranean 25 and 30% in PM_{10} and $PM_{2.5}$). The main difference between the two types of transport scenarios was the mineral matter content, which was much higher during Mediterranean episodes (European 14 and 5%, Mediterranean 23 and 15% in PM_{10} and $PM_{2.5}$) and was probably due to the presence of African dust during Mediterranean episodes.

Atlantic air mass advection events were the most frequent meteorological scenarios at MSY, giving rise to the renovation of air masses, with the subsequent lowering of PM levels to 13, 11 and 9 μg m^{-3} PM_{10}, $PM_{2.5}$ and PM_1. SIA accounted for 34 and 37% in PM_{10} and $PM_{2.5}$, while carbonaceous species constituted 26 and 31% of the PM_{10} and $PM_{2.5}$. Mineral matter represented 22 and 9% of the PM_{10} and $PM_{2.5}$, and sea spray reached its highest levels (although still just 4 and 2% in PM_{10} and $PM_{2.5}$). Finally, the proportion of unaccounted mass, mainly comprising water and unanalysed components can be regarded as relatively high (around 20% in most scenarios, but ranging from 14 to 31%).

Table 4.2.13. Annual frequency, PM_{10}, $PM_{2.5}$ and PM_1 levels and PM_{10} and $PM_{2.5}$ composition (in %) for the main scenarios occurring at MSY. NAF African dust outbreaks; WAE, winter anticyclonic episodes; REG, regional re-circulations, EU, European air mass transport; MED, Mediterranean air mass transport; ATL, Atlantic advective conditions.

	NAF	WAE	REG	EU	MED	ATL
Annual frequency (%days/year)	12-24	7-15	14-20	8-17	2-7	39-53
μg PM_{10} m^{-3}	26	20	18	13	13	13
OM (%)	16	23	22	22	23	24
EC (%)	1	2	1	0	2	2
SO_4^{2-} (%)	14	14	20	14	17	15
NO_3^- (%)	6	22	5	10	9	12
NH_4^+ (%)	4	8	6	6	5	6
Unaccounted (%)	17	14	21	31	18	17
Mineral (%)	40	16	22	14	23	22
Sea S. (%)	2	2	3	3	3	4
SIC (%)	24	44	30	30	31	34
μg $PM_{2.5}$ m^{-3}	17	16	15	12	10	11
OM (%)	25	23	26	29	29	29
EC (%)	1	1	1	2	1	2
SO_4^{2-} (%)	21	18	27	19	21	20
NO_3^- (%)	4	21	2	12	6	9
NH_4^+ (%)	7	11	9	10	6	8
Unaccounted (%)	24	20	25	22	19	22
Mineral (%)	17	5	8	5	15	9
Sea S. (%)	1	2	2	2	2	2
SIC (%)	32	44	37	41	33	37
μg PM_1 m^{-3}	12	14	12	11	9	9

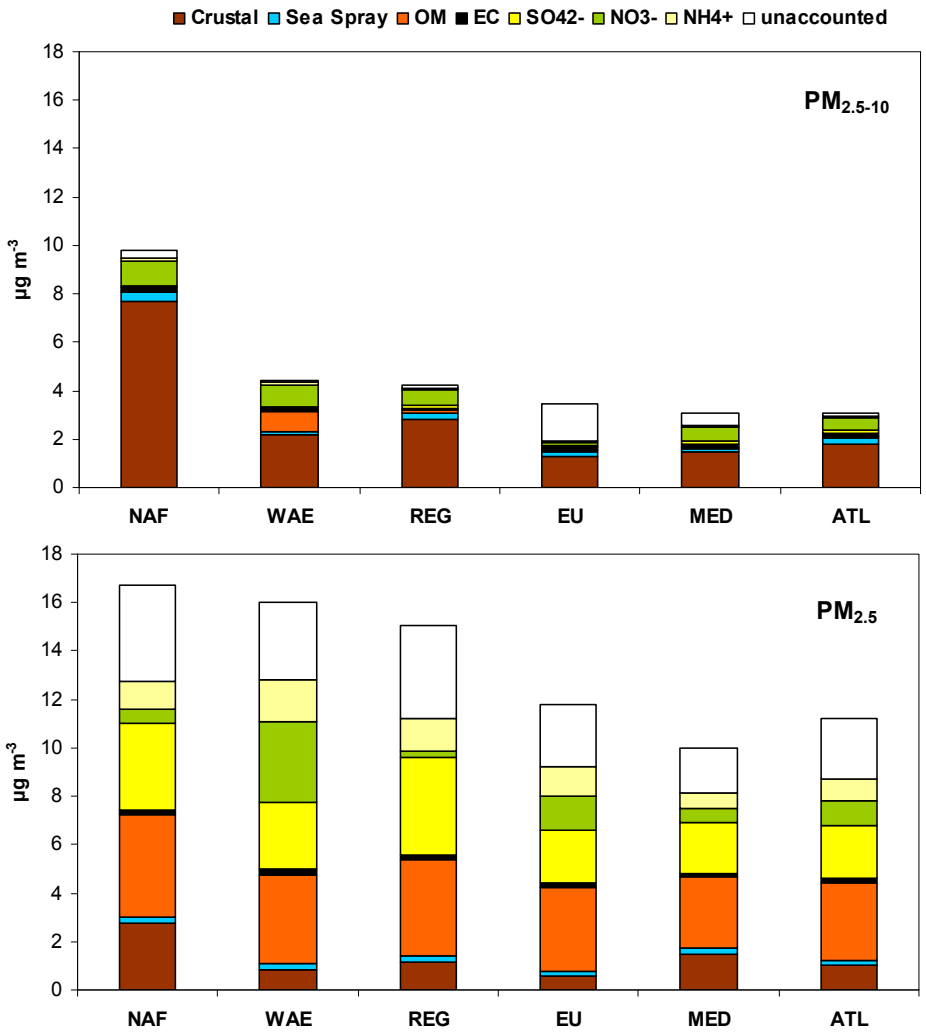

Figure 4.2.23. Mean components measured in $PM_{2.5-10}$ and $PM_{2.5}$ at MSY during African dust outbreaks (NAF), winter anticyclonic episodes (WAE), regional recirculation episodes (REG), European (EU) and Mediterranean (MED) air mass transport and Atlantic advections (ATL).

4.2.4. Source contribution to ambient PM levels

The identification of emission sources was carried out in Montseny by applying two different receptor modelling tools, principal component analysis (PCA) and positive matrix factorization (PMF), obtaining similar results. PCA results will be briefly discussed and subsequently PMF results will be presented and discussed, and the main differences with the PCA analysis commented.

4.2.4.1. PCA

4.2.4.1.1 PM components and data for analysis

The PM components used in the PCA analysis are presented in Table 4.2.14. Some of the components measured were not considered for the analysis because their daily levels registered were frequently under or very close to the detection limits or their levels were very high in the blanks. A total of 26 PM_{10} and 20 $PM_{2.5}$ components were finally selected for the PCA analysis.

Table 4.2.14. Components analyzed and selected for the PCA analysis. Exclusion causes: very low levels in most cases <DL (●), very high blank levels (○).

	PM_{10}	$PM_{2.5}$		PM_{10}	$PM_{2.5}$		PM_{10}	$PM_{2.5}$
Ctotal	X	X	Ni	X	X	Pr	●	●
Al_2O_3	X	●	Cu	X	●	Nd	●	●
Ca	X	X	Zn	●	●	Sm	●	●
K	X	X	Ga	●	●	Eu	●	●
Na	X	X	Ge	●	●	Gd	●	●
Mg	X	X	As	X	X	Tb	●	●
Fe	X	X	Se	○	○	Dy	●	●
SO_4^{2-}	X	X	Rb	X	X	Ho	●	●
NO_3^-	X	X	Sr	X	●	Er	●	●
Cl^-	X	●	Y	●	●	Tm	●	●
NH_4^+	X	X	Zr	○	○	Yb	●	●
Li	X	X	Nb	●	●	Lu	●	●
Be	●	●	Mo	○	○	Hf	●	●
P	●	●	Cd	X	X	Ta	●	●
Sc	●	●	Sn	X	●	W	●	●
V	X	X	Sb	X	●	Tl	●	●
Ti	X	X	Cs	●	●	Pb	X	X
Cr	○	○	Ba	○	○	Bi	●	●
Mn	X	X	La	X	X	Th	●	●
Co	●	●	Ce	X	X	U	●	●

4.2.4.1.2 Identification of emission sources

Factors identified by the PCA analysis in PM_{10} and $PM_{2.5}$ are shown in Table 4.2.15 and Table 4.2.16 respectively. Factor loadings associated to each compound are indicated and main tracers highlighted.

Table 4.2.15. Factors identified in PM_{10} by PCA, associated factor loadings and % variance of the samples explained by each of the factors obtained for MSY. Main tracers were highlighted.

Mineral matter		**Industrial/road traffic**		**Marine/regional**		**Secondary nitrate/WAE**	
Al_2O_3	**1.0**	**Sb**	**0.9**	**Na**	**0.8**	**Cl^-**	**0.8**
Ti	**1.0**	**Pb**	**0.8**	**SO_4^{2-}**	**0.6**	**NO_3^-**	**0.6**
Fe	**1.0**	**Cu**	**0.8**	V	*0.4*	*NH_4^+*	*0.5*
La	**1.0**	**Sn**	**0.8**	Ni	*0.4*	Pb	0.2
Rb	**1.0**	**Ctotal**	**0.8**	Mg	0.3	Ni	0.2
Sr	**0.9**	**Cd**	**0.7**	NH_4^+	0.3	As	0.1
Ce	**0.9**	**V**	**0.7**	As	0.1	Cd	0.1
Mg	**0.9**	**As**	**0.6**	Sr	0.1	Mn	0.1
K	**0.9**	**Ni**	**0.6**	Rb	0.1	Na	0.1
Mn	**0.9**	**NO_3^-**	**0.6**	Ca	0.1	K	0.1
Li	**0.9**	**NH_4^+**	**0.6**	La	0.1	Sb	0.1
Ca	**0.9**	**SO_4^{2-}**	**0.6**	K	0.1	Mg	0.1
As	*0.4*	Mn	0.3	Ctotal	0.1	Sr	0.1
V	0.3	K	0.3	Fe	0.1	Al_2O_3	0.1
Na	0.3	Ca	0.2	Ti	0.1	Fe	0.1
Cl^-	0.3	Fe	0.2	Sb	0.1	Ca	0.0
Ni	0.2	Rb	0.2	Li	0.1	Ti	0.0
Ctotal	0.2	Li	0.2	Ce	0.1	Ce	0.0
SO_4^{2-}	0.2	Ti	0.1	Al_2O_3	0.1	Sn	0.0
Pb	0.1	Al_2O_3	0.1	Cl^-	0.1	SO_4^{2-}	0.0
Sn	0.1	Sr	0.1	Cu	0.0	V	0.0
Sb	0.1	Mg	0.1	Mn	0.0	Li	0.0
Cu	0.1	La	0.1	Sn	0.0	Rb	0.0
Cd	0.1	Ce	0.1	NO_3^-	0.0	La	0.0
NO_3^-	-0.1	Cl^-	0.0	Pb	-0.1	Cu	-0.1
NH_4^+	-0.1	Na	0.0	Cd	-0.3	Ctotal	-0.1
%Var	51	**%Var**	20	**%Var**	5	**%Var**	5

Table 4.2.16. Factors identified in $PM_{2.5}$ by PCA, associated factor loadings and % variance of the samples explained by each of the factors obtained for MSY. Main tracers were highlighted.

Mineral matter		**Secondary sulphate/industrial**		**Secondary nitrate/WAE**		**Marine**	
Ti	**0.9**	**SO_4^{2-}**	**0.9**	**NO_3^-**	**0.8**	**Na**	**0.9**
Fe	**0.9**	**V**	**0.8**	*K*	*0.4*	*Mg*	*0.4*
Rb	**0.9**	**Ni**	**0.8**	*Cd*	*0.4*	K	0.3
Ca	**0.9**	**Pb**	**0.7**	*NH_4^+*	*0.4*	SO_4^{2-}	0.3
La	**0.9**	**As**	**0.7**	*Pb*	*0.4*	Ca	0.2
Mg	**0.9**	**Ctot**	**0.7**	Mn	0.3	V	0.2
Ce	**0.8**	**NH_4^+**	**0.6**	Ctot	0.3	Mn	0.1
Mn	**0.8**	*Cd*	*0.4*	As	0.2	NH_4^+	0.1
K	**0.7**	Rb	0.3	Ca	0.1	Ni	0.1
Li	*0.5*	Mn	0.3	Rb	0.0	Ti	0.0
V	0.2	Li	0.3	Mg	0.0	Rb	0.0
Ctot	0.2	K	0.2	Ni	0.0	Fe	0.0
Ni	0.2	Fe	0.2	Fe	0.0	Ctot	0.0
Pb	0.2	Na	0.2	Ti	0.0	NO_3^-	0.0
Na	0.2	La	0.1	Na	-0.1	Ce	-0.1
As	0.1	Ti	0.1	SO_4^{2-}	-0.1	La	-0.1
SO_4^{2-}	0.1	NO_3^-	0.1	Ce	-0.2	Pb	-0.1
Cd	0.1	Ce	0.1	La	-0.2	Cd	-0.1
NO_3^-	-0.1	Mg	0.0	V	-0.2	Li	-0.1
NH_4^+	-0.2	Ca	-0.1	Li	-0.2	As	-0.2
%Var	42	**%Var**	19	**%Var**	7	**%Var**	6

The main factors identified in PM_{10} and $PM_{2.5}$ and the characteristic chemical species of each factor (factor loadings>0.4) are summarized in Table 4.2.17. Very similar four factors were identified in both fractions, accounting for 81 and 74% of the explained variance in PM_{10} and $PM_{2.5}$ respectively. Mineral matter explains 51 and 42% of the variance in PM_{10} and $PM_{2.5}$ respectively and it is identified by crustal origin elements (Ti, Fe, Rb, Ca, La, Mg, K, Li, etc.). Industrial and road traffic emissions together with secondary ammonium sulphate appear as a mixed source and explain 20 and 19% of the variance in PM_{10} and $PM_{2.5}$, respectively. This factor is identified by anthropogenic elements derived from industrial activities (Pb, Cd, As, carbonaceous compounds, Querol et al., 2007), fuel oil combustion (SO_4^{2-}, V and Ni, Pacyna, 1986) and road traffic (Sn, Sb, Cu, carbonaceous compounds, Pacyna, 1986; Schauer et al., 2006) and also by secondary inorganic compounds associated to anthropogenic emissions (ammonium sulphate, Alastuey et al., 2004). The marine factor explains 5 and 7% of the variance in PM_{10} and $PM_{2.5}$ respectively and it is identified by the presence of Na in both fractions, sulphate aerosols in PM_{10} and Mg in $PM_{2.5}$. In PM_{10} it is associated to fuel oil emissions tracers (SO_4^{2-}, V and Ni, Pacyna, 1986), probably derived of shipping

emissions. Chlorine does not appear in this factor as the formation of $NaNO_3$ at high temperatures prevails during the warmer months producing the volatilization of chlorine (Viana et al., 2005). The secondary nitrate factor accounts for 5 and 6% of the PM_{10} and $PM_{2.5}$ variance respectively. It is identified by the presence of ammonium nitrate in both fractions, anthropogenic chlorine in PM_{10} and some other anthropogenic elements in $PM_{2.5}$, as Cd or Pb, related to industrial emissions (Querol et al., 2007) and K indicating biomass combustion (Saarikoski et al., 2008) and it may be associated to winter anthropogenic episodes (WAE).

Table 4.2.17. Main factors identified by PCA in PM_{10} and $PM_{2.5}$. Components with factor loadings higher or equal to 0.6 are highlighted in block letters and components with factor loadings between 0.4 and 0.6 are written in italics.

	PM_{10}	**$PM_{2.5}$**
Mineral matter	**Al_2O_3, Ti, Fe, La, Rb, Sr, Ce, Mg, K, Mn, Li, Ca,** *As*	**Ti, Fe, Rb, Ca, La, Mg, Ce, Mn, K,** *Li*
Industrial/road traffic/SIA	**Sb, Pb, Cu, Sn, Ctot, Cd, V, As, Ni, NO_3^-, NH_4^+, SO_4^{2-}**	**SO_4^{2-}, V, Ni, Pb, As, Ctot, NH_4^+,** *Cd*
Marine/fuel-oil combustion	**Na, SO_4^{2-},** *V, Ni*	**Na,** *Mg*
Secondary nitrate/WAE	**Cl^-, NO_3^-,** *NH_4^+*	**NO_3^-,** *K, Cd, NH_4^+, Pb*

4.2.4.2. PMF

4.2.4.2.1 PM components and data for analysis

IN PMF, 25 PM_{10} and 20 $PM_{2.5}$ chemical species were selected for the study according to their signal to noise ratio, the % of values over the detection limit and the errors associated to the measurement (Table 4.2.18). A total of 442 and 255 valid cases were used for the PM_{10} and $PM_{2.5}$ analysis, respectively.

Table 4.2.18. Mean concentration for values over the detection limit (Mean>DL), error percentage (% error), signal to noise ratio (S/N) and percentage of values over the detection limit (%DL) for the main elements used in the PMF analysis measured in PM_{10} and $PM_{2.5}$ at MSY. Components selected for the PMF analysis. Exclusion causes: very low levels in most cases <DL (●), very high blank levels (○).

	Mean>DL (μg m^{-3})		% error		S/N		%>DL		Selected	
	PM_{10}	$PM_{2.5}$	PM_{10}	$PM_{2.5}$	PM_{10}	$PM_{2.5}$	PM_{10}	$PM_{2.5}$	PM_{10}	$PM_{2.5}$
Ctot	2.8019	2.8697	68	70	2.5	2.5	95	91	X	X
Al	0.2096	0.1372	87	310	4.1	2.7	77	26	X	●
Ca	0.4195	0.1329	36	141	9.2	2.9	97	63	X	X
K	0.1632	0.0909	34	49	6.9	3.8	99	97	X	X
Na	0.3739	0.1993	97	173	3.6	1.9	81	43	X	X
Mg	0.1094	0.0413	35	90	8.2	3.1	98	71	X	X
Fe	0.2030	0.0715	17	27	31.5	11.1	100	100	X	X
SO_4^{2-}	2.5779	2.7749	19	18	111	119	100	100	X	X
NO_3^-	1.7788	1.4682	28	64	83.5	69.0	98	96	X	X
Cl^-	0.2379	0.2300	692	736	6.2	6.1	60	59	○	○
NH_4^+	0.9243	1.1457	23	22	110	137	100	100	X	X
Li	0.0002	0.0002	105	181	5.0	3.2	85	60	X	X
Ti	0.0191	0.0063	39	329	23.4	7.7	99	94	X	X
V	0.0035	0.0029	63	165	10.1	8.4	97	93	X	X
Cr	0.0015	0.0015	958	922	1.9	1.9	52	54	○	○
Mn	0.0049	0.0025	18	24	22.9	11.7	100	98	X	X
Co	0.0002	0.0002	344	400	1.8	1.6	29	20	●	●
Ni	0.0019	0.0019	381	373	2.5	2.6	74	75	X	X
Cu	0.0042	0.0052	521	379	2.4	2.9	74	71	X	○
Zn	0.0546	0.0569	15930	18617	1.2	1.3	0.2	2.4	●	●
As	0.0003	0.0003	64	80	4.1	4.3	85	91	X	X
Rb	0.0005	0.0002	29	48	17.7	7.8	97	93	X	X
Sr	0.0021	0.0016	133	363	3.2	2.5	81	34	X	●
Cd	0.0002	0.0002	157	142	2.0	2.4	61	69	X	X
Sn	0.0017	0.0018	355	625	1.6	1.8	34	40	X	●
Sb	0.0009	0.0009	293	331	1.5	1.5	36	16	X	●
La	0.0002	0.0001	85	143	4.6	2.7	88	67	X	X
Ce	0.0004	0.0003	109	226	4.1	2.4	84	56	X	X
Pb	0.0045	0.0049	25	21	24.8	27.0	99	100	X	X

4.2.4.2.2 Identification of emission sources

The source identification and quantification was carried out with the Positive Matrix Factorization (PMF) model, obtaining similar results to the PCA analysis.

After a series of runs varying the number of factors, the most robust solutions resulted in 4 sources for both PM_{10} and $PM_{2.5}$ fractions. The main sources identified in PM_{10} and $PM_{2.5}$ were representative of a RB environment: mineral matter, anthropogenic industrial/road traffic, secondary sulphate and secondary nitrate. Source profiles for PMF solutions obtained for PM_{10} and $PM_{2.5}$ are shown in Figure 4.2.24 and Figure 4.2.25, and a summary of the factors identified in PM_{10} and $PM_{2.5}$ is shown in Table 4.2.19.

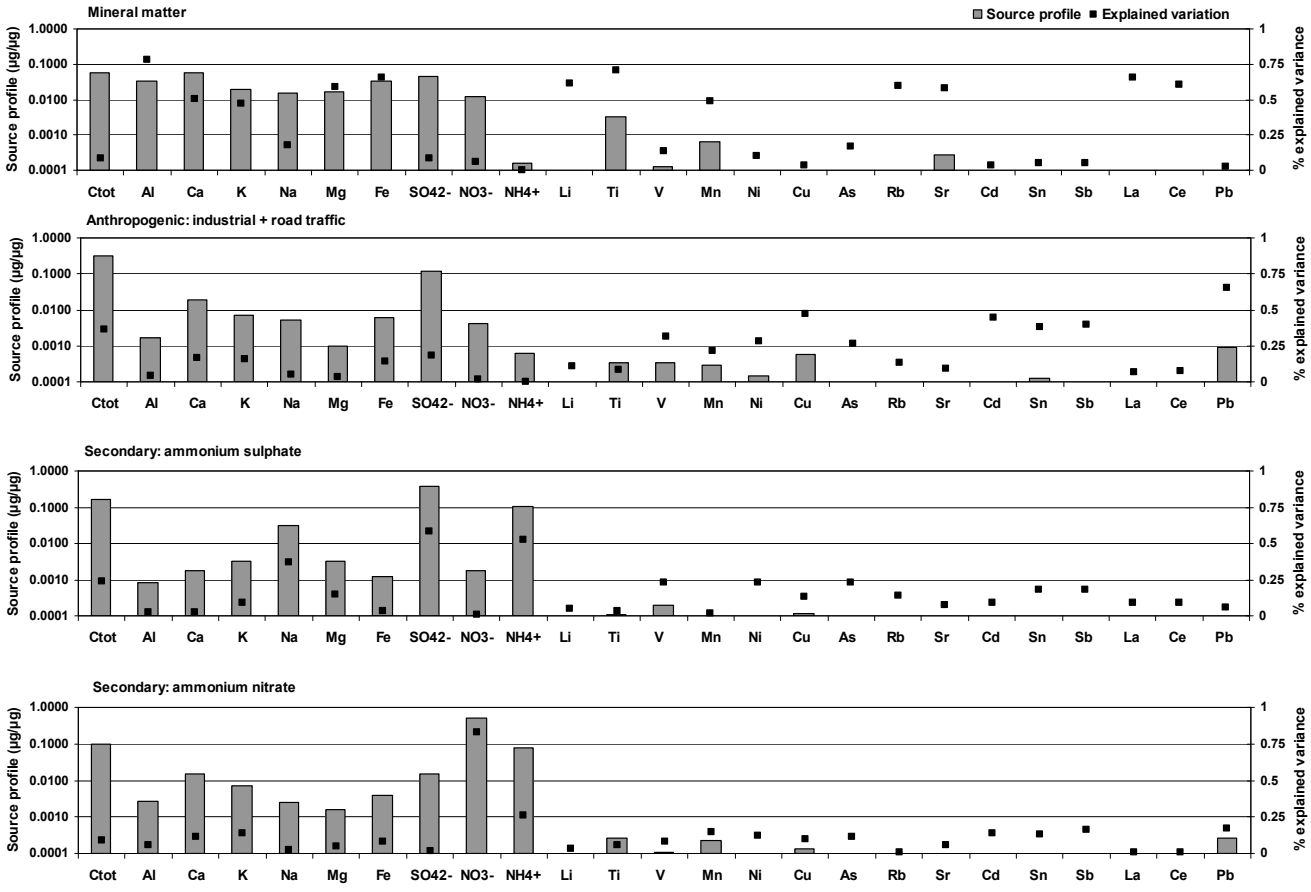

Figure 4.2.24. Source profiles for PMF solutions in PM_{10} for MSY.

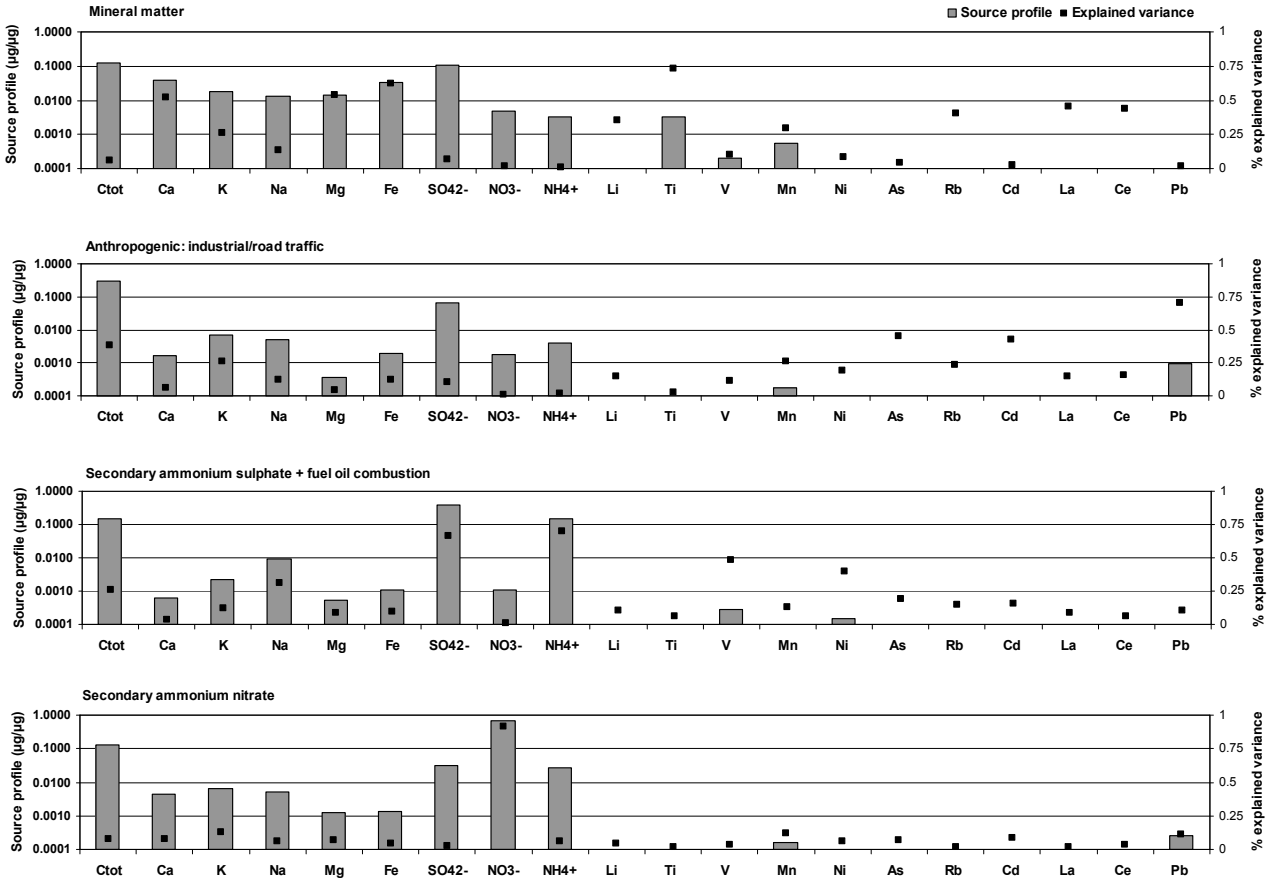

Figure 4.2.25. Source profiles for PMF solutions in $PM_{2.5}$ for MSY.

Table 4.2.19. Factors identified by the PMF model in PM_{10} and $PM_{2.5}$.

	PM_{10}	$PM_{2.5}$
Mineral matter	**Al, Ca, K, Mg, Fe, Li, Ti, Mn, Rb, Sr, La, Ce**	**Ca, K, Mg, Fe, Li, Ti, Mn, Rb, Sr, La, Ce**
Anthropogenic Industrial/road traffic	**Ctot, V, Ni, Cu, As, Cd, Sn, Sb, Pb**	**Ctot, As, Cd, Pb**
Secondary ammonium sulphate	**SO_4^{2-}, NH_4^+, Na,** Ctot	**SO_4^{2-}, NH_4^+, V, Ni,** Ctot
Secondary ammonium nitrate	**NO_3^-, NH_4^+,** SO_4^{2-}, Ctot	**NO_3^-,** NH_4^+, SO_4^{2-}, Ctot

Mineral matter: The main tracers of this source were Al, Ca, K, Mg, Fe, Li, Ti, Mn, Rb, Sr, La and Ce in PM_{10} and $PM_{2.5}$. This factor accounts for crustal material originating from local and regional resuspension processes and also from long-range transport of dust from Northern Africa.

***Mixed anthropogenic industrial/road traffic source*:** one mixed anthropogenic source was identified in both PM_{10} and $PM_{2.5.}$ The tracers of this source indicate a mixture of industrial (total carbon, Zn, Cu, V, Ni, Pb, Querol et al., 2007) and road traffic emissions (total carbon, Cu, Sn, Sb, Pacyna, 1986; Schauer et al., 2006).

***Secondary sulphate*:** this factor had SO_4^{2-} and NH_4^+ as main tracers in both PM_{10} and $PM_{2.5}$ fractions, followed by V and Ni in the fraction $PM_{2.5}$. In the coarse fraction, sulphate levels were also correlated with Na, which was interpreted as the result of the more intense sea breeze in summer transporting sea spray, Viana et al., 2005), coupled with the higher summer sulphate levels (Figure 4.2.29 and Figure 4.2.30).

***Secondary nitrate*:** The main tracers of this source were NO_3^- and NH_4^+. Contribution of the secondary nitrate source reaches a maximum in winter with raised peaks coinciding with the aforementioned winter anticyclonic episodes (Figure 4.2.29 and Figure 4.2.30). In PMF K does not appear in the $PM_{2.5}$ fraction as in happened in the PCA analysis.

4.2.4.2.3 Quantification of source contributions to PM_{10} and $PM_{2.5}$

Daily contributions of each factor to the PM_{10} and $PM_{2.5}$ levels were calculated by a multilineal regression analysis. The correlation coefficients (r^2) between the measured and modelled concentrations were 0.90 and 0.73 for PM_{10} and $PM_{2.5}$, respectively, and 96% of the mass of each PM fraction was simulated in the analysis (Figure 4.2.26).

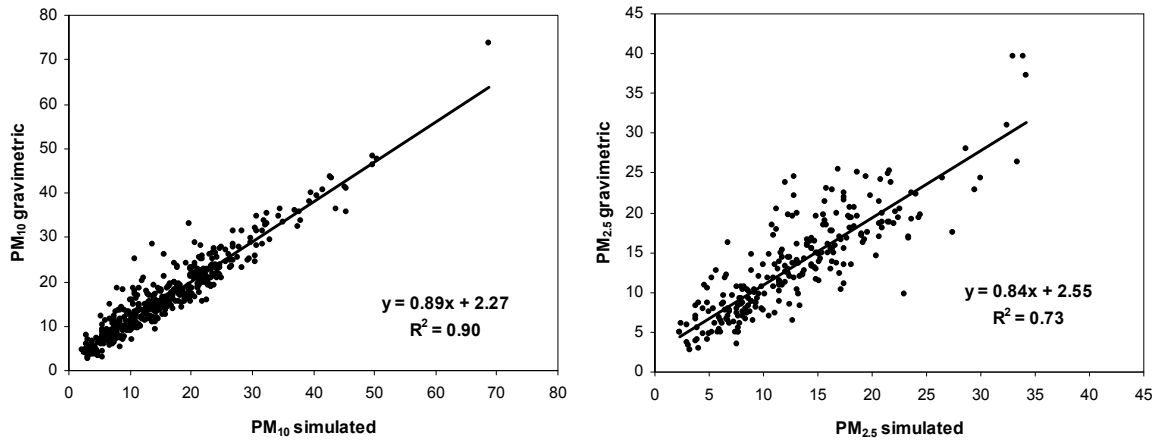

Figure 4.2.26. Correlation between simulated and gravimetric PM_{10} and $PM_{2.5}$.

The mean contributions for each factor obtained by the PMF analysis are shown in Table 4.2.20 and Figure 4.2.27. Ammonium sulphate aerosols were the major contributors to PM_{10} and $PM_{2.5}$ (28% and 40% of the PM mass). Mineral matter was identified as a major contributing source to PM_{10} (28% of the mass), and its contribution was also significant in $PM_{2.5}$ (12%). The ammonium nitrate source accounted for 18% of PM_{10} and 14% of $PM_{2.5}$. The mixed anthropogenic source contributed 22% and 30% to the PM_{10} and $PM_{2.5}$ mass respectively. The unaccounted mass was low (4% in both fractions).

Table 4.2.20. Mean contributions (µg m^{-3} and %) of the factors obtained by PMF in PM_{10} and $PM_{2.5}$ for MSY.

	µg m^{-3}		%	
	PM_{10}	$PM_{2.5}$	PM_{10}	$PM_{2.5}$
Mineral matter	4.6	1.6	28	12
Anthropogenic: industrial/road traffic	3.6	4.0	22	30
Secondary sulphate	4.6	5.5	28	40
Secondary nitrate	3.0	1.9	18	14
Unaccounted	0.6	0.5	4	4

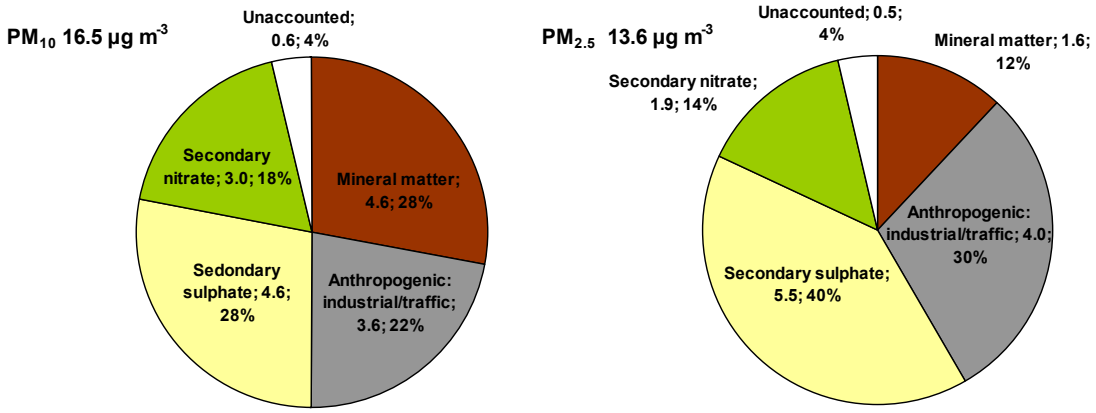

Figure 4.2.27. Average contribution of sources obtained by PMF to PM_{10} and $PM_{2.5}$ for MSY.

The relative contributions of the different species analyzed to each of the factors identified in PM_{10} and $PM_{2.5}$ are shown in Figure 4.2.28, indicating the main sources contributing to each component.

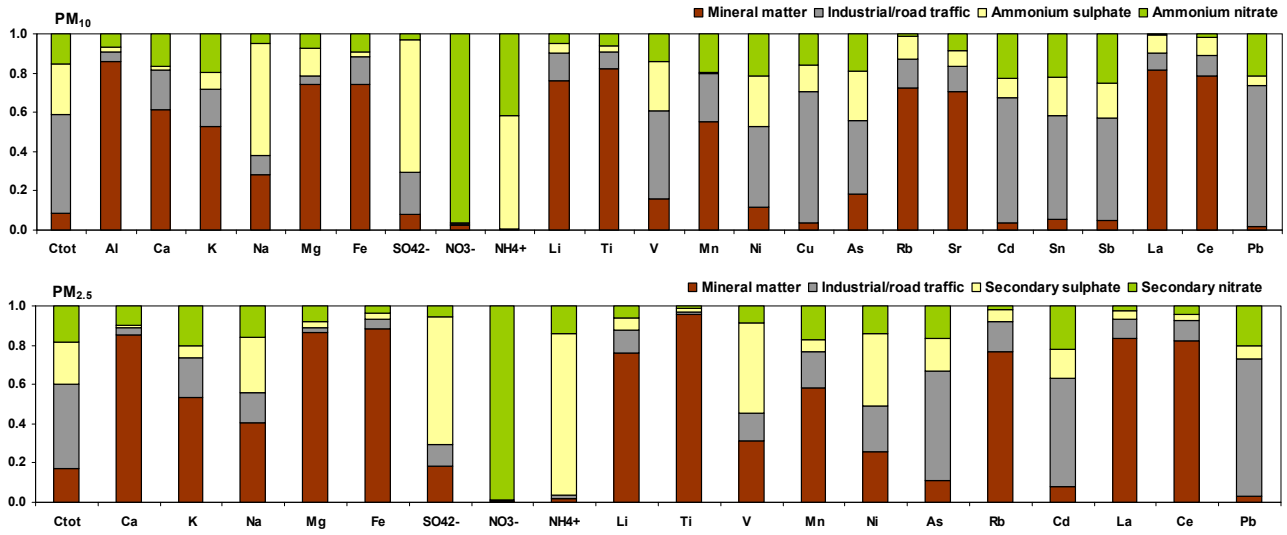

Figure 4.2.28. Relative contribution of each species to the factors identified by PMF in PM_{10} and $PM_{2.5}$.

4.2.4.2.4 Seasonal and inter-annual evolution of PM sources

Seasonal and inter-annual evolution for the main daily contributions for each source identified in $PM_{2.5}$ and PM_{10} are shown in Figure 4.2.29 and Figure 4.2.30.

Owing to their nature, the anthropogenic PM_{10} and $PM_{2.5}$ sources (road traffic and industrial emissions) do not present defined seasonal trends (Figure 4.2.29 and Figure 4.2.30). However, the seasonal character of the retrieved sources should be highlighted given that separate summer (sulphate) and winter (nitrate) sources were obtained. Thus, sulphate is more associated with regional pollution on a larger scale than nitrate (Putaud et al., 2004), which is more related to episodes reaching the monitoring site in winter. However, the ambient conditions could also have exerted considerable influence on the production of both secondary nitrate and sulphate; given that ammonium nitrate is not stable in particulate phase at relatively high temperatures (25ºC) and sulphate formation is favoured by photochemical processes during the summer months. Using source apportionment analysis, it has not been possible to ascertain whether there are two different sources of precursors of anthropogenic emissions (one more regional and the other more local) or a single regional-scale mixture of gaseous precursors. There is also an obviously mixture of oil combustion sources (secondary sulphate and industrial/road traffic) as V and Ni, the typical tracers, appear in both of them. The time series of the mineral matter source shows higher levels during the warmer months and also registers the impact of African dust

outbreaks, identified as single peak episodes with significantly higher concentrations both in PM_{10} and $PM_{2.5}$ (Figure 4.2.29 and Figure 4.2.30).

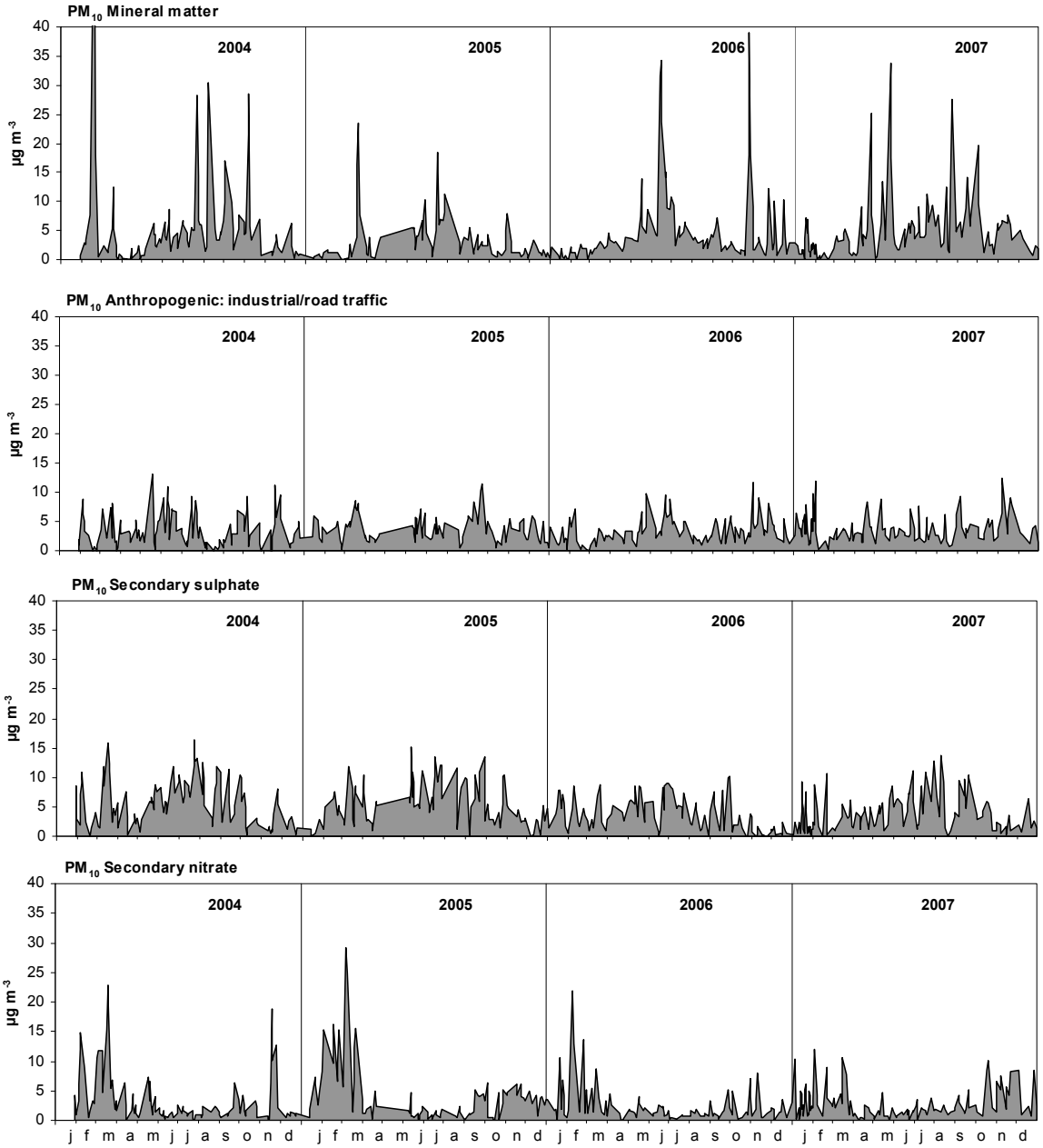

Figure 4.2.29. Seasonal and inter-annual evolution of the main daily contributions for each source identified in PM_{10} at MSY.

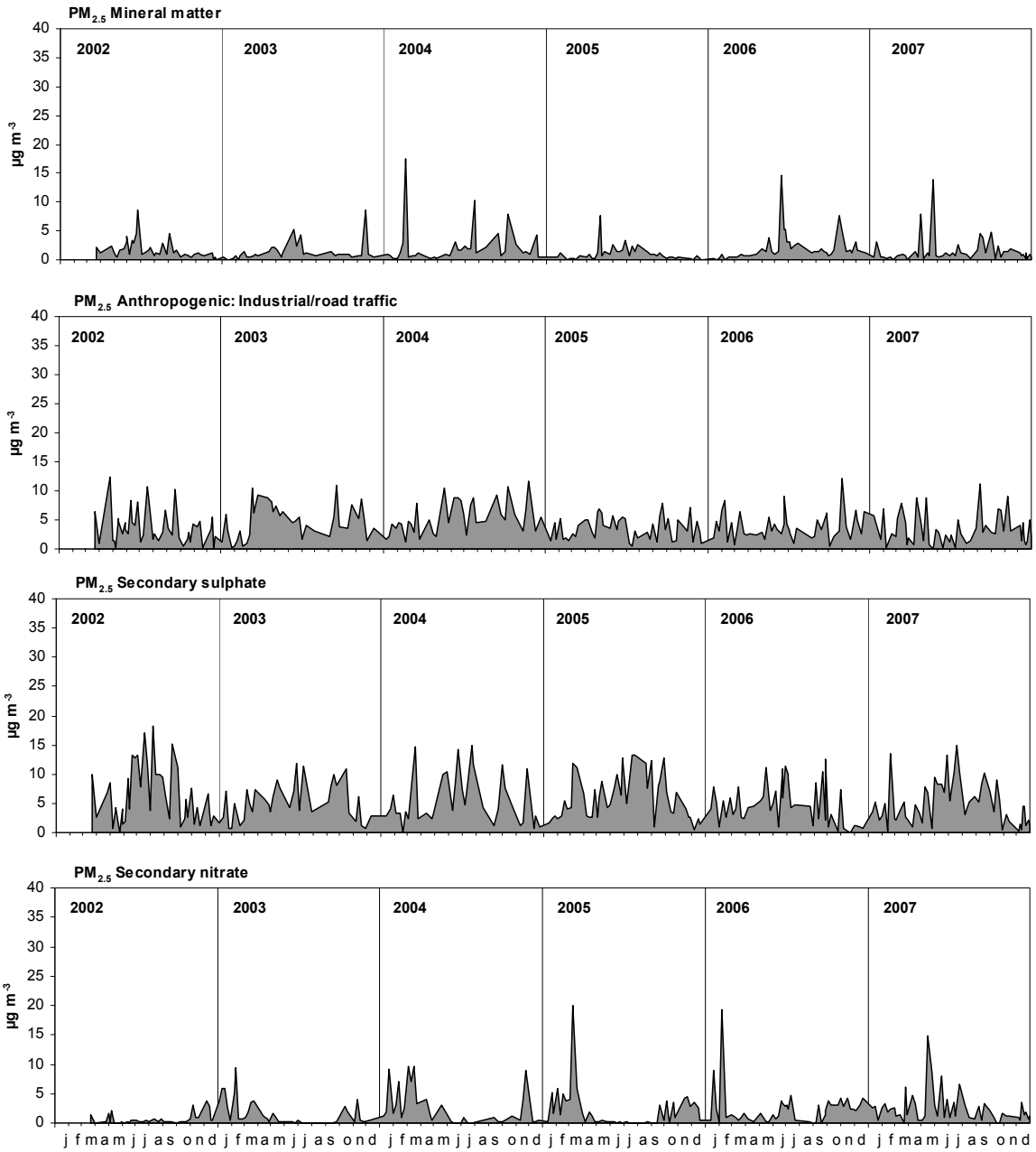

Figure 4.2.30. Seasonal and inter-annual evolution of the main daily contributions for each source identified in $PM_{2.5}$ at MSY.

4.2.5. Summary and conclusions

PM_{10} regional background (RB) levels along the Spanish Mediterranean coast may be regarded as intermediate when compared with those obtained at other RB areas in the Iberian Peninsula. However, $PM_{2.5}$ levels are higher at the Mediterranean sites, reflecting a greater influence of anthropogenic emissions. PM levels along the Western Mediterranean coast are also intermediate when compared with those recorded at background sites in Northern, Central and Eastern Europe and in the Eastern Mediterranean basin. Regarding the mean PM levels registered in the 2002-2007 period (17, 13 and 11 μg m^{-3} of PM_{10}, $PM_{2.5}$ and PM_1, respectively), the MSY site could be considered as representative of the RB PM pollution in the WMB.

Atmospheric dynamics at MSY (elevated rural area in the WMB) are highly influenced by the breeze circulation (mountain and sea breezes) which regulates the daily evolution of PM levels. Early in the day atmospheric pollutants accumulate in the pre-coastal depression. Subsequently, the diurnal breeze (activated by insolation) transports aged air masses upwards from the valley, increasing the PM levels in elevated RB areas. During the night the nocturnal drainage flows and the decrease in the mixing layer height result in lower PM levels at the RB sites. PM levels measured during the night allowed to estimate the continental background levels in 12-13, 8-10 and 6-8 μg m^{-3} of PM_{10}, $PM_{2.5}$ and PM_1, respectively.

Day to day variation of PM levels in the WMB is governed by the concatenation of different meteorological scenarios, affecting the PM concentrations and size distribution of atmospheric particulate matter in North-eastern Iberia. The seasonal distribution of these episodes together with the climatic patterns of the WMB gives rise to a marked seasonal pattern for background PM. Maximum PM_{10} background levels are recorded in summer, associated with the elevated frequency of African dust outbreaks, the recirculation of air masses over the WMB, the lowest precipitation, the intense resuspension due to the dryness of soils, the enhanced formation of secondary aerosols and the highest development of the boundary layer in (that allows PM regional anthropogenic pollution to reach elevated rural areas). Secondary maximums are observed in February-March and November attributed to Saharan dust episodes (low PM_1/PM_{10}) and winter anticyclonic scenarios (high PM_1/PM_{10} ratios). Minimum values are recorded during the rest of the year owing to the higher frequency of Atlantic advection and precipitation rates. This background trend is overlapped by PM peak episodes, mainly attributed to Saharan dust outbreaks and anticyclonic episodes.

This study shows that the winter anticyclonic scenarios, with a known impact on PM levels at urban and industrial areas, could have a notable influence also on PM levels recorded at elevated RB areas in the WMB. These pollution episodes occur mainly from November to March when low temperatures are registered at night and relatively high temperatures are reached at noon, favouring the activation of mountain winds that transport polluted air masses accumulated in nearby areas. Under these scenarios, the hourly levels of PM_1 at MSY may reach 75 μg m^{-3} and exceed the levels of PM_1 measured simultaneously at the city centre of BCN. This is one of the most impacting features of these WAE and it may be attributed to the enhanced formation of secondary pollutants under these atmospheric conditions.

A significant inter-annual 6 year decreasing trend was detected in PM_{10} and $PM_{2.5}$ with the Mann-Kendall test, but in PM_1 the decrease observed was not significant. Significant decreasing temporal trends were registered for March (PM_{10}, $PM_{2.5}$ and PM_1), June and July (PM_{10} and $PM_{2.5}$), and December (PM_{10}). However, during the winter period the decrease observed was less pronounced. Mean annual PM_{10} and $PM_{2.5}$ concentrations showed an average decrease of 34% for the entire monitoring period. In absolute terms this decrease is equivalent to 6 μg PM_{10} m^{-3} and 5 μg $PM_{2.5}$ m^{-3} between 2002 and 2007, being regarded as significant. Similar decreasing trends were detected by Papadimas et al. (2008) for the North-West of the Iberian Peninsula based on MODIS data. The different trends observed in our study for the coarsest (PM_{10}, $PM_{2.5}$) and fine (PM_1) fractions suggest a variety of causes related to large-scale meteorological processes or cycles, or to local or meso-scale processes.

The inter-annual evolution of the continental background levels (night levels at MSY) showed a clear decrease from 18, 13 and 9 μg m^{-3} (2002) to 12, 9 and 7 μg m^{-3} (2007) for PM_{10}, $PM_{2.5}$ and PM_1, respectively, whereas the regional contributions did not show this decreasing trend. As deduced from these results, this trend could be partially attributed to the variability of the frequency and intensity of the Saharan dust episodes during this relatively short period (2002-2007). Thus, the highest mean annual African dust contribution was registered in 2003, with 3.5, 2.4 and 1.7 μg m^{-3}, in PM_{10}, $PM_{2.5}$ and PM_1, respectively, and the lowest from 2005 to 2007, with 0.9, 0.3 and 0.2 μg m^{-3} in PM_{10}, $PM_{2.5}$ and PM_1, respectively. Nevertheless, this trend to lower contributions of Saharan dust does not wholly account for the decreasing trend observed for PM_{10} and $PM_{2.5}$. Thus, when the Mann-Kendall test was applied to the chemical components of $PM_{2.5}$ at the MSY site (data available since 2002), some components tracers of

anthropogenic emissions showed also a significant decreasing trend from 2002 to 2007. These PM components were carbonaceous compounds (OC, EC and TC), with a decrease between 36-37%, and Cd (decrease of 48%).

However, the relatively short period considered (6 years) imply that the interpreted inter-annual trends may not be considered as general temporal trends, but, as stated above, probably these are reflecting meteorological cycles with a 6-10 year scale. This relatively short tendency may be attributed to more dispersive atmospheric conditions occurring during the summer months in the last years considered in this study.

In accordance with other RB monitoring stations in the WMB, MSY shows high levels of crustal material. Lower levels of OM+EC and ammonium nitrate are recorded at MSY when compared with equivalent sites from central Europe. Despite the large amount of crustal dust (mostly regional and African-derived), overall concentrations of PM_{10} remain relatively low, with an annual average of 17 ± 3 μg m^{-3} recorded. However, in the case of finer particles measured at MSY the levels are quite high (annual $PM_{2.5}$ averages of 13 ± 2 μg m^{-3}) and a very high proportion has an anthropic origin (biomass burning, traffic and industry). These are transported over regional distances from the surrounding coastal valleys and from Barcelona Metropolitan Area and much of the pollution is concentrated during relatively transient events such as WAE and daily peaks around midday in summer.

All major PM components showed marked seasonal variations. Average concentrations of mineral matter, sulphate, sea spray and carbonaceous aerosols are all higher in summer, whereas nitrate levels and the ratio Cl/Na are higher in winter. The anomalously high OC/EC ratio (14 in summer, 11 in winter) at MSY, also recorded elsewhere in Spain (Monagrega), is attributed to a combination of raised biogenic emissions of SOA precursors, high ozone levels, intense insolation and frequent recirculation of aged air masses. Superimposed onto this seasonal background is the annual pattern of African dust intrusions, which are especially prominent in spring and summer. Thus, the final chemical composition of atmospheric PM at MSY is conditioned by complex local and regional topographic and meteorological variations, by the arrival of anthropogenic emissions from the Mediterranean coast and in addition to the occurrence of African dust outbreaks.

Trace elements analyzed at MSY did not show a large temporal variation in MSY during the period considered and fell within similar concentration ranges than elements

measured at other RB sites in Europe. However, levels of V measured at MSY were relatively higher than those at most sites in central Europe, probably due to the relatively high emissions from fuel-oil combustion in the region (power generation, industrial, but mostly shipping emissions).

Source apportionment analysis was carried out for PM_{10} and $PM_{2.5}$ identifying 4 main sources. Sulphate aerosols were found to be the major contributors to both size fractions, followed by nitrate aerosols and crustal material. One mixed traffic-industrial source was detected in both PM_{10} and $PM_{2.5}$ fractions.

Two different sources of precursors of anthropogenic emissions, one more regional for sulphate and the other more local for nitrate, are represented by the two secondary inorganic aerosol (SIA) sources identified. However, it is also possible that these are the product of a single regional-scale mixture of gaseous precursors resulting in different types of aerosols as a function of ambient conditions and seasonality.

4.3. CONTINENTAL BACKGROUND

4.3. Montsec continental background site

Remote background sites are located far away from urban or industrial areas to avoid the direct influence of emissions of anthropogenic pollutants. These sites are important to study the transport processes of aerosols at regional and continental scales and the distribution of aerosols at different heights. The difference between regional (RB) and continental backgrounds (CB) is that the CB sites are usually situated over the boundary layer height in order to be isolated from the regional background pollution. However, a certain regional contribution to aerosol composition is usually present (Cunningham and Zoller, 1981), and the contribution of sources such as local wind-blown dust, particles from vegetation, sea spray in coastal areas or transported desert dust are frequent (Prospero, 1968).

The Montsec monitoring site (MSC) is a continental (or remote) background site for the measurement of atmospheric aerosols. It is located in the Montsec mountain range, which is part of the pre-Pyrenean mountain ranges (42º3'N and 0º44'E, 1570 m.a.s.l.). It has been operative from November 2005 and the results obtained provide important information about continental aerosols and long range transport of aerosols at a continental scale. Results obtained during the project have encouraged the *Generalitat de Catalunya* to install a monitoring cabin and to include the site in the Network of Control and Surveillance of Air Quality of the *Direcció General de Qualitat Ambiental* of *the Conselleria de Medi Ambient* of the *Generalitat de Catalunya*.

In this chapter, PM levels and speciation recorded at the MSC continental background site are presented and discussed. PM levels and speciation time series will be evaluated to detect possible daily and seasonal trends. The influence of different meteorological situations and air mass transport episodes at the continental scale on the day to day variability of PM levels and speciation will be also evaluated, with a special focus on African dust outbreaks. Finally, source apportionment techniques will be applied to the speciation dataset to identify the main PM_{10} sources.

4.3.1. Atmospheric dynamics and transport of pollutants to the area

4.3.1.1. Meteorology and atmospheric dynamics in Montsec

The climate at Montsec site is typical of a mountainous area in the Southern Mediterranean. Monthly mean temperatures during the period considered ranged from

0-4ºC in winter (December, January and February) to 13-20ºC in the summer (June, July and August) and annual mean precipitations ranged from 280 mm during 2005 to 1200 mm during 2007, with a much higher precipitation rate than the rest of the years considered (Figure 4.3.1). The months registering the highest precipitations were spring (April, May and June) and autumn (September to November).

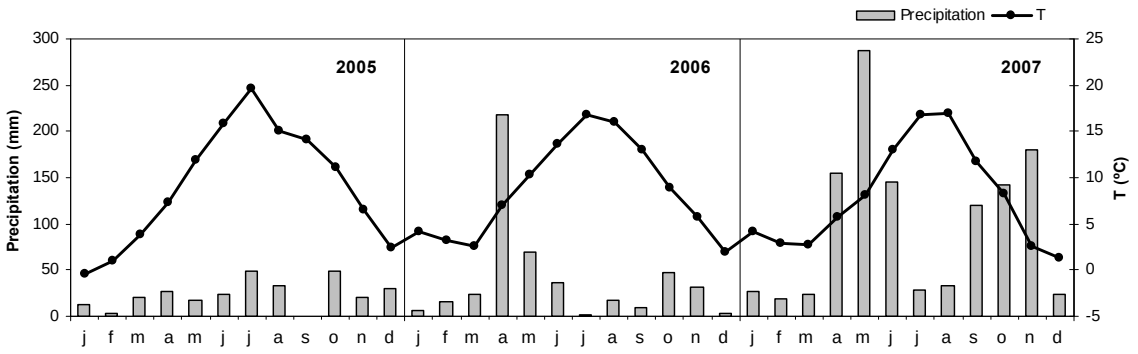

Figure 4.3.1. Mean monthly temperatures (ºC) and total precipitation (mm) registered at Montsec Meteorological station (Servei Meteorologic de Catalunya) from 2005 to 2007.

The MSC station (1570 m.a.s.l.) is located outside of the boundary layer during the colder months of the year (October to March, Figure 4.3.2) and therefore may not be affected by regional pollution events. However, from April to September, the boundary layer increases during the central hours of the day reaching the MSC site height. At these times the MSC site may be affected by regional pollution. Moreover, polluted air masses may be occasionally transported by mountain breezes to the site when the conditions are favourable.

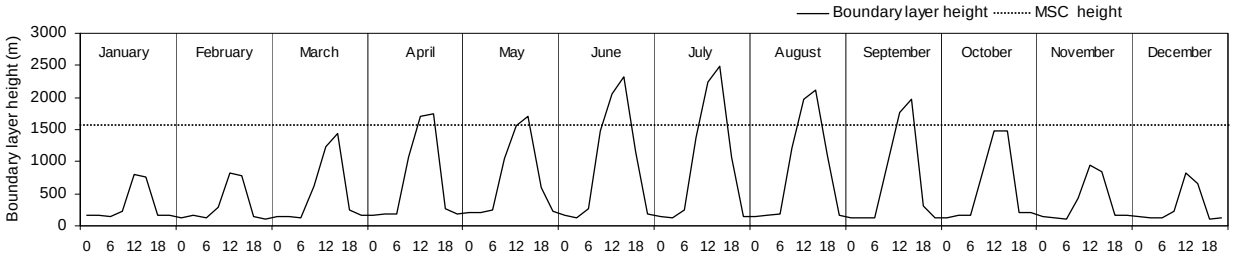

Figure 4.3.2. Modelled boundary layer height at MSC during 2006-2007 (ARL-READY meteorological tools).

The analysis of air mass circulation at a local scale was performed by analyzing wind directions and speed from the Montsec Meteorological station (Servei Meteorologic de Catalunya, Figure 4.3.3 and Figure 4.3.4). Atmospheric dynamics at MSC are typical of a mountain site, conditioned by the orography and mountain breezes. Main wind directions registered were NW-NE (around 40% of the cases) and SW (around 25%). During the winter months (November to March) the main wind component is north and

north-west, corresponding to Atlantic advections, predominant during this period of the year. From April to May and August to October, mountain breezes develop during the day, with a SSW direction and reaching the maximum wind speeds at midday, and a North-Eastern direction during the night with lower wind speeds, corresponding to the drainage flows. During June and July in 2006, the breeze cycle is less marked and during June and July in 2007 constant SSW winds develop, with maximum wind speeds are recorded at midday. This behaviour may be the consequence of the frequency of African dust outbreaks occurring during these months, registering southern winds during the episode, but may also be due to regional circulations induced by the thermal low situated over the Iberian Peninsula during this period of the year, together with the orography (Pyrenees, central depression and Ebro valley). A thermal low is formed over the central depression, that, together with wind canalizations by the orography induce a cyclonic circulation producing regional winds with a southern component (SE-S-SE) that arrive to MSC during the night (Oriol Jorba, personal communication).

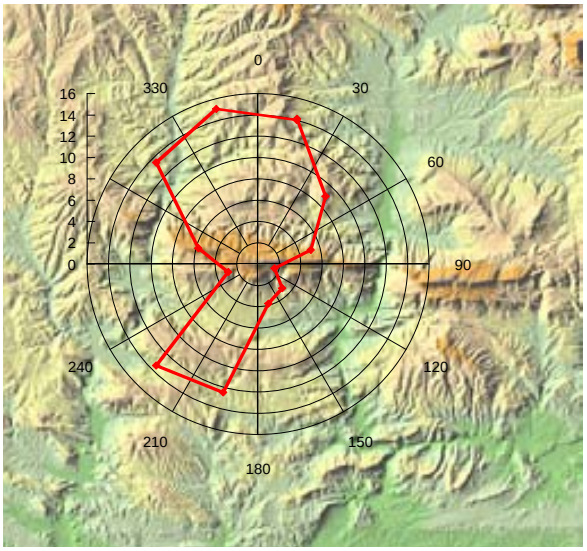

Figure 4.3.3. Relative frequencies of main wind directions at Montsec Meteorological station (Servei Meteorològic de Catalunya) during 2006-2007.

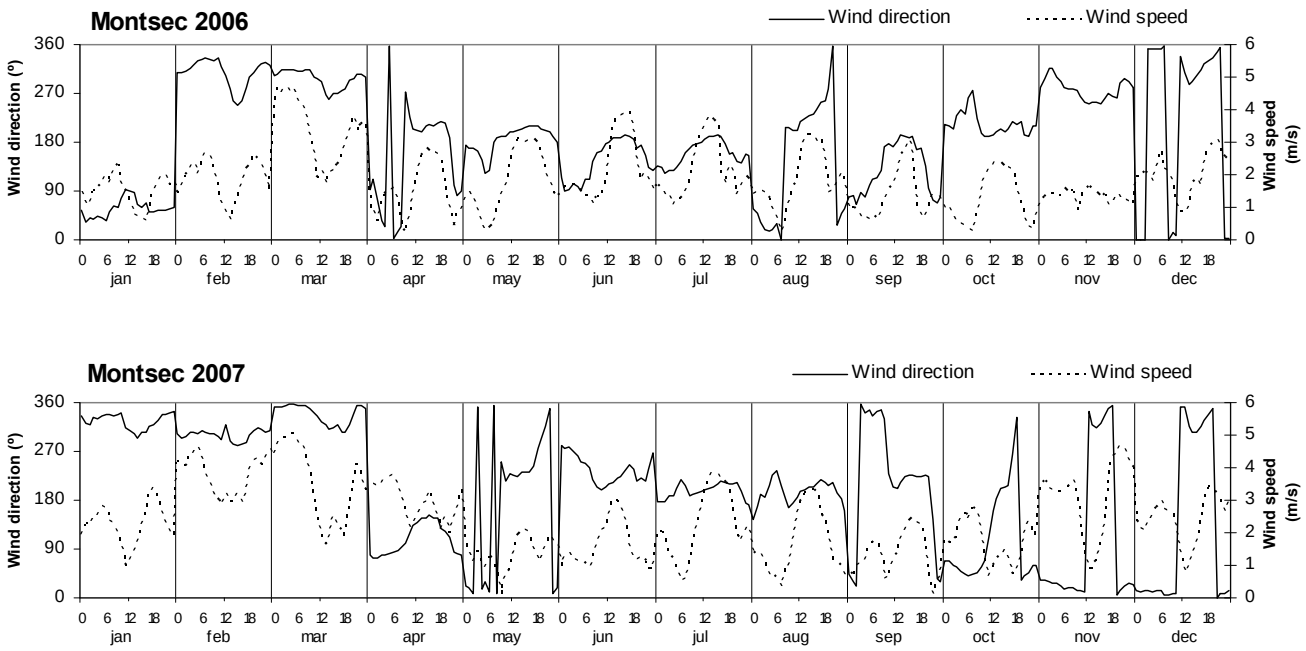

Figure 4.3.4. Annual evolution of the mean daily cycles of wind direction and speed measured at Montsec Meteorological station during 2006 and 2007.

4.3.1.2. Origin of air masses and atmospheric transport scenarios

Day to day variation of PM levels and speciation at MSC is driven by the concatenation of different meteorological scenarios that may increase or reduce the levels and size of atmospheric particulate matter. In line with prior studies these scenarios are as follows: Atlantic advective conditions, African dust episodes, regional recirculation episodes, European and Mediterranean transport episodes, and local pollution episodes (Millán et al., 1997; Rodríguez et al., 2002a and 2003, Escudero et al., 2005 and 2007a). Escudero et al. (2007a) defined the summer anticyclonic episodes, equivalent to the regional recirculation episodes, and the winter anticyclonic episodes, equivalent to the local pollution episodes. The latter have a major influence in urban and industrial areas but also influence remote mountain sites owing to the high stability of these scenarios, giving rise to the frequent formation of near ground inversion layers (Rodríguez et al., 2003, Escudero et al., 2007a). Frequencies of the episodes that affect the study area were calculated for the 2002-2007 period (Figure 4.3.5). Atlantic advection (NWA and WA) is the most frequent situation (39-40%), followed by summer regional recirculation episodes (REG, 15-18%) and African dust outbreaks (NAF, 12-15%). Then, European air mass origins (EU, 9-10%) and winter anticyclonic episodes (WAE, 8-11%) occur with a significant frequency. Finally, the Mediterranean air mass transport (MED, 4%), North-Atlantic (NA, 5-8%) and South-Western Atlantic (SWA, 3%) advection occur with lower frequencies.

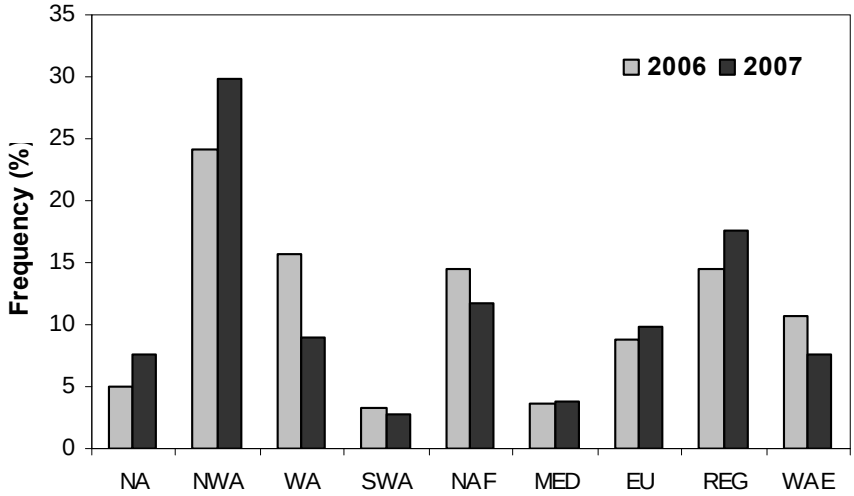

Figure 4.3.5. Annual frequency of the main air mass origins registered at MSC for 2006 and 2007. Atlantic advection (NA, NWA, WA, SWA), African dust episodes (NAF), Mediterranean (MED) and European (EU) air mass transport, summer regional recirculation episodes (REG) and winter anticyclonic episodes (WAE).

4.3.2. PM levels at the continental background

4.3.2.1. Mean PM levels at MSC and other CB sites

PM_{10}, $PM_{2.5}$ and PM_1 levels have been registered at MSC from November 2005 to September 2007 by means of an optical particle counter (GRIMM dust monitor), with levels being corrected with the factors obtained by comparison with the simultaneous gravimetric monitoring using a PM_{10} high volume sampler (MCV and DIGITEL). Daily PM_{10}, $PM_{2.5}$ and PM_1 levels recorded at this site are shown in Figure 4.3.6, where days with African dust influence are marked. The mean real-time and gravimetric annual PM_{10}, $PM_{2.5}$ and PM_1 mean levels registered at MSC are shown in Table 4.3.1.

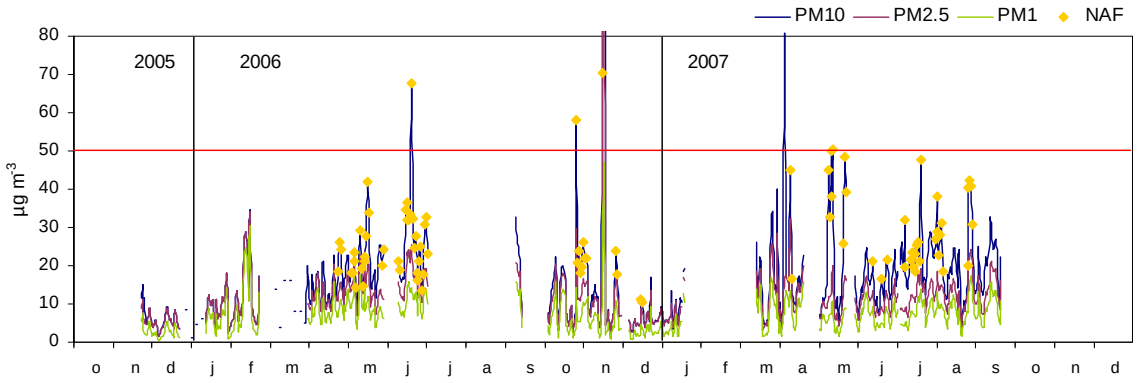

Figure 4.3.6. PM daily levels time series recorded at MSC from November 2005 to September 2007. Days with African dust outbreak influence are marked with yellow diamonds. The 50 µg m^{-3} daily limit is marked with a red line.

The annual variation of PM levels at remote sites typically depends on the meteorology and the frequency of African dust episodes during a year. At MSC, the main differences were observed in the coarsest fraction (PM_{10}), with higher levels recorded in 2007, compared with 2006, while $PM_{2.5}$ and PM_1 did not show a significant variation between 2006 and 2007 (Table 4.3.1). In this case the differences may be also a consequence of the disparity in data availability during different months of the year in 2006 and 2007, as in 2007 most data was registered during the summer months, coinciding with intense African dust outbreaks over the Mediterranean, while in 2006 available data was more spread along the year.

To account for these differences and also the fact that during 2007 sampling frequency was higher than during 2006, an annual mean was calculated using data from 2006 and 2007 to account for the different months of the year at a rate of 1 sample every 4 days. The difference using this calculated mean is only observed in PM_{10} with levels between the obtained for 2006 and 2007. $PM_{2.5}$ and PM_1 do not present significant variations.

When comparing annual means, gravimetric PM_{10} levels are a little higher than automatic levels. This is the consequence of the continuous monitoring of automatic levels compared to the sampling of PM_{10} filters performed every four days.

Table 4.3.1. PM mean annual levels registered at MSC during 2006 and 2007 and total mean levels (November 2005 to September 2007) registered at MSC using optical particle counters and gravimetric methods (November 2005 to November 2007). Calculated annual mean levels with data from 2006 and 2007.

	Optical particle counter				Gravimetry	
µg m^{-3}	PM_{10}	$PM_{2.5}$	PM_1	Data availability (%)	PM_{10}	Number of samples
2006	14.5	11.6	7.5	59	12.1	35
2007	18.4	11.8	7.5	52	20.4	64
Total	15.5	11.3	7.2	65	16.0	110
Annual mean	16.4	11.6	7.2	83	14.1	72

Mean PM levels measured at MSC are similar to the continental background calculated in the previous chapter for the Western Mediterranean Basin, when considering the nocturnal PM levels measured at the regional background site at Montseny (MSY, 13, 10 and 8 µg m^{-3} for PM_{10}, $PM_{2.5}$ and PM_1 respectively). The slightly higher levels measured at MSC in PM_{10} and $PM_{2.5}$ are probably the consequence of the fact that

during the summer, the MSC is located inside the boundary layer during the central hours of the day and may be thus affected by regional pollution, but also to the transport of dust at different heights in the atmosphere. African dust can be transported at different heights in the atmosphere depending on the meteorological scenario producing the African dust outbreak (Escudero et al., 2005). In most of these episodes African dust is preferentially transported over Southern Europe in atmospheric layers from 1000-5000 m.a.s.l. (Escudero et al., 2005), being highest the influence on surface PM levels in monitoring stations located at higher altitudes as MSC (1570 m.a.s.l.) compared with MSY (720 m.a.s.l.).

However, the mean PM levels recorded at MSC during the period 2006-2007 are between the range of mean levels registered at other CB sites in Southern Europe (here considering monitoring sites at heights >1000 m.a.s.l, Figure 4.3.7). PM levels at the CB were markedly higher in Southern Europe, compared to Central and Northern European sites. This difference is the consequence of the proximity to the African continent that makes African dust outbreaks frequent along the year. The difference is observed especially in the coarser fractions, as dust particles are mainly coarse in size. Viznar, in Southern Spain registers the highest TSP levels, compared to other sites in Central Spain (Campisabalos and Risco Llano, EMEP sites). Southern European sites (Izaña in the Canary Islands (Izaña Atmospheric Observatory) Monte Cimone in Italy (Marenco et al., 2006) and Montsec) register higher levels than the central and northern European monitoring sites (EMEP sites). Conversely, the differences in PM_1 are not very significant, as quite similar levels are registered in Southern and Central European sites.

The height of the monitoring site may also influence the PM concentrations observed (Figure 4.3.7). Jungfraujoch in Switzerland (EMEP, 3578 m.a.s.l.) registers the lowest PM levels, being the highest site of the dataset. Conversely, the highest southern European sites (Izaña, 2373, and Monte Cimone, 2165 m.a.s.l) register high PM_{10} and $PM_{2.5}$ levels as a result of the frequent and intense African dust outbreaks registered.

Mean annual $PM_{2.5}/PM_{10}$ and PM_1/PM_{10} ratios recorded at MSC were of 0.7 and 0.4 respectively. When compared with other sites in Europe, these ratios are intermediate. Southern European sites showed lower ratios ($PM_{2.5}/PM_{10}$=0.6 at Izaña and PM_1/PM_{10}=0.4 at Monte Cimone) than central and Northern European sites ($PM_{2.5}/PM_{10}$=0.7-0.8 in Switzerland and Germany and PM_1/PM_{10}=0.6 in Switzerland).

This is also related to the higher impact of North African dust outbreaks in Southern Europe, increasing in a major extent the coarse PM fraction.

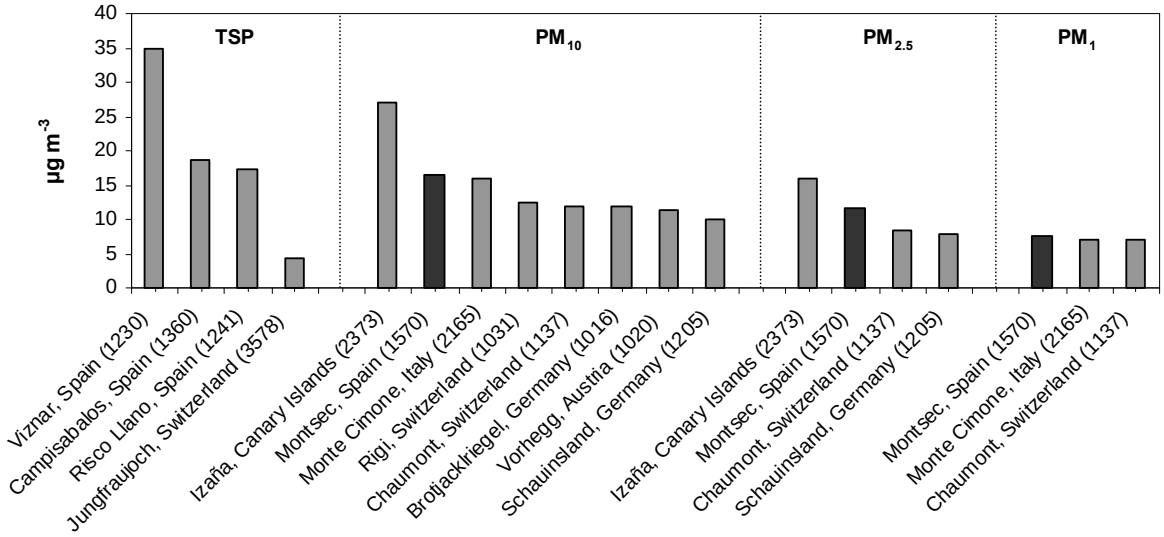

Figure 4.3.7. Mean annual TSP, PM_{10}, $PM_{2.5}$ and PM_1 levels measured at some European CB monitoring sites (height >1000 m.a.s.l. in parentheses) compared with the data from MSC. EMEP (www.emep.int); Marenco et al. (2006); Izaña Atmospheric Observatory and this work.

4.3.2.2. Inter-annual variability

The first thing to consider when studying variability is that sampling at MSC was performed during different periods in the year 2006 and 2007. Figure 4.3.8 shows the mean annual $PM_{2.5-10}$, $PM_{1-2.5}$ and PM_1 levels measured at MSC for 2006 and 2007 for all days (total), days without African dust influence (no NAF) and days with African dust outbreak influence (NAF). The differences between 2006 and 2007 were observed mainly in the coarse fraction ($PM_{2.5-10}$) with higher levels for the total of days, no NAF and NAF days recorded during 2007. These differences are probably due to the different data availability during different seasons in 2006 and 2007, since 2007 available data was mainly recorded from March to September, when coarse PM levels are usually higher, while 2006 available data was more spread along the year, but also to the intense NAF episodes sampled during the summer in 2007.

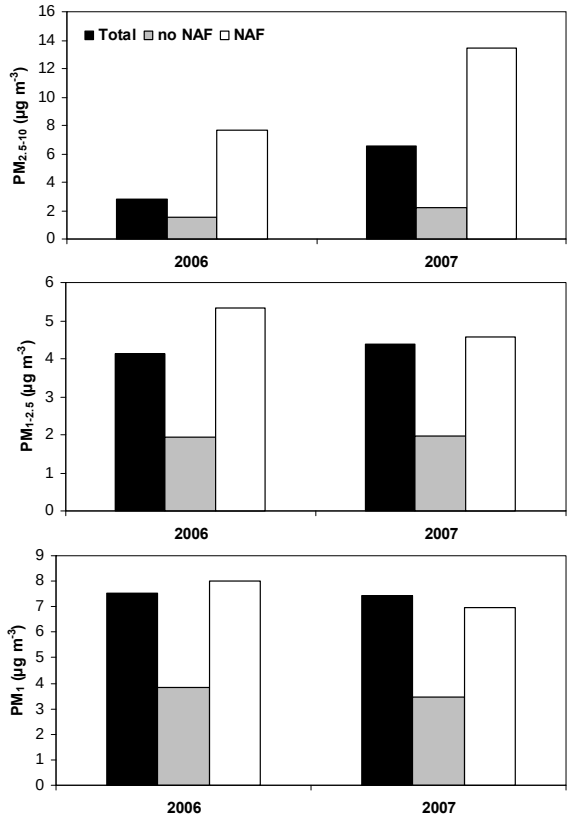

Figure 4.3.8. Mean annual $PM_{2.5-10}$, $PM_{1-2.5}$ and PM_1 levels for all days (total), days without African dust influence (no NAF) and days with African dust influence (NAF) recorded at MSC in 2006 and 2007.

African dust episodes will be described in detail as their impact on levels and composition of aerosols at the CB is very important. Some very intense NAF episodes were detected from the results obtained during the sampling period at MSC. The most significant occurred during July and August in 2007, when mineral dust from Northern Africa was simultaneously transported with the smoke plumes from important forest fires in the Mediterranean (the most important occurred in Greece and Northern Africa). Back-trajectories of the episode registered during 26-29 August 2007 (Figure 4.3.9) show that air masses from Europe crossed the Mediterranean, passing through Greece and then the North of Africa, before reaching the NE Iberian Peninsula. Dust over the Mediterranean and smoke from forest fires over Greece and the North-African coast can even be observed in the Seawifs satellite image (Figure 4.3.9). The influence of this episode is observed all over the rural background sites in the Mediterranean area (Airbase database, http://air-climate.eionet.europa.eu/databases/airbase/), with a specially marked increase in PM_{10} levels for the sites situated at higher altitudes, as Rojen Peak in Bulgary (1750 m.a.sl.) and Chamonix in France (1038 m.a.s.l.).

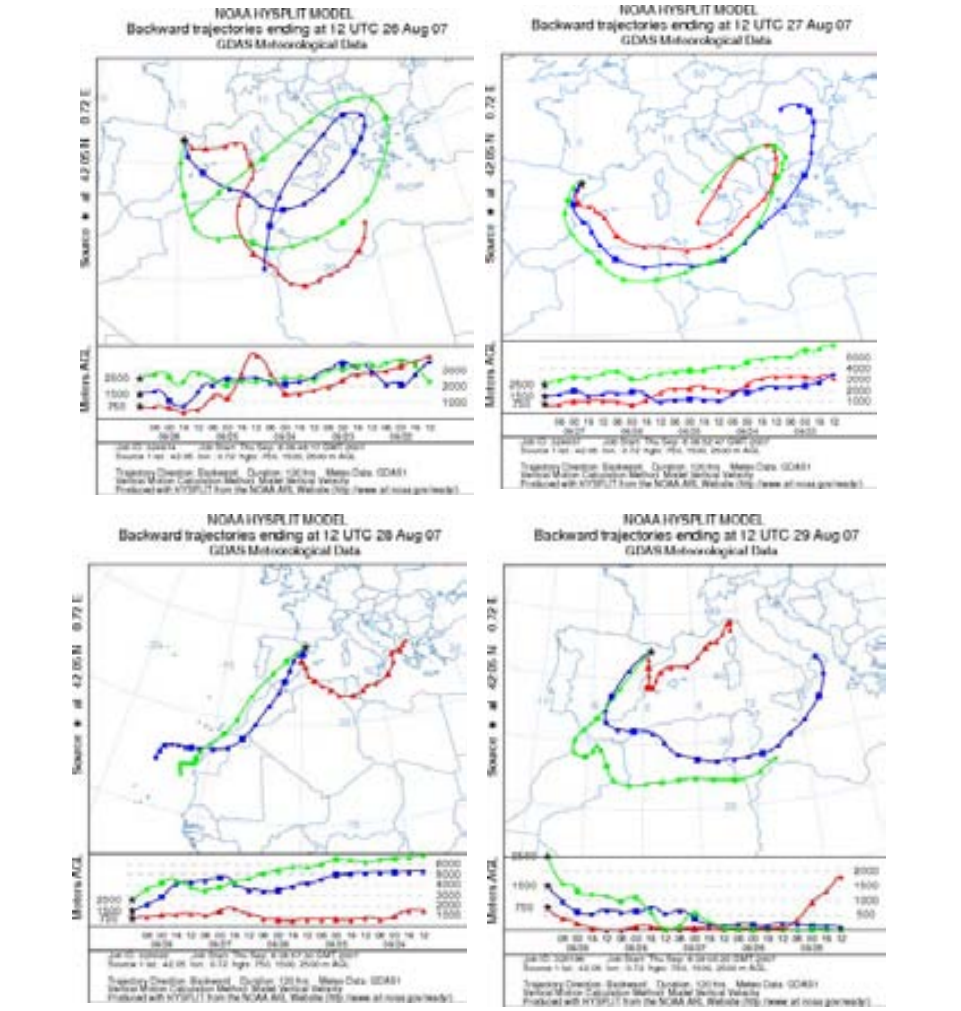

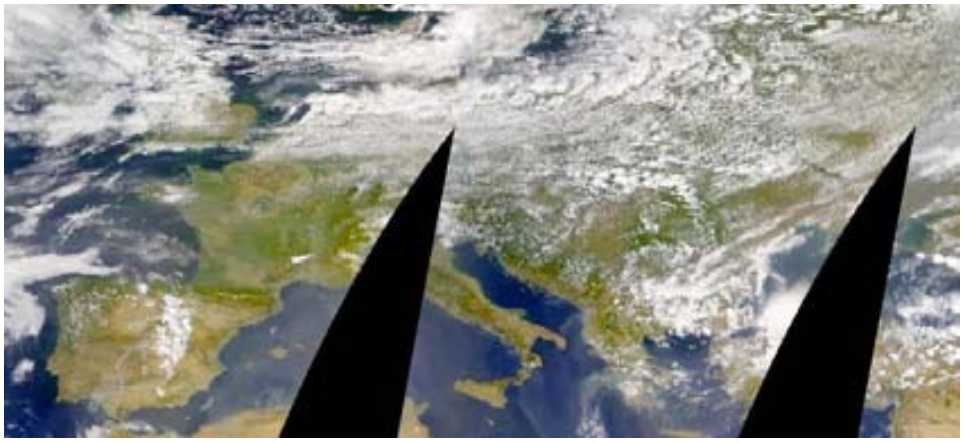

Figure 4.3.9. Back-trajectories of an African dust outbreak episode with simultaneous transport of dust from forest fires in the Mediterranean calculated for MSC from 26 to 29 August 2007 (top). Seawifs satellite image of the same episode for the 27 august 2007 (bottom).

4.3.2.3. Seasonal variability

Monthly mean PM_{10}, $PM_{2.5}$ and PM_1 levels registered at MSC from November 2005 to September 2007 are shown on Table 4.3.2.

Table 4.3.2. Monthly mean PM_{10}, $PM_{2.5}$, PM_1, $PM_{1\text{-}2.5}$ and $PM_{2.5\text{-}10}$ levels registered at MSC from November 2005 to September 2007.

November 05-September 07						
µg m^{-3}	N	PM_{10}	$PM_{2.5}$	PM_1	$PM_{1\text{-}2.5}$	$PM_{2.5\text{-}10}$
January	43	8.1	8.1	4.9	3.2	<0.1
February	22	13.3	13.2	9.7	3.4	0.1
March	17	16.7	13.5	8.5	5.0	3.3
April	50	16.6	12.8	8.5	4.3	3.7
May	52	20.9	12.5	7.9	4.6	8.4
June	51	19.9	13.3	8.5	4.8	6.5
July	30	21.9	11.7	7.3	4.3	10.2
August	31	21.2	13.2	8.4	4.8	8.0
September	20	21.0	13.9	9.3	4.6	7.1
October	28	15.2	11.5	7.2	4.3	3.7
November	39	16.0	12.1	6.2	5.9	3.9
December	53	6.0	5.6	2.8	2.8	0.4

PM levels measured at Montsec showed a significant seasonal evolution (Figure 4.3.10). The highest levels were registered during the warmer months and the lowest during the coldest months of the year. The difference observed between summer and winter was clearly higher for the coarse fraction ($PM_{2.5\text{-}10}$), but was also observed in the finest fraction (PM_1), and was less evident for the $PM_{1\text{-}2.5}$ fraction. The higher PM levels recorded during the summer are related to the higher frequency of African dust outbreaks, the recirculation of air masses, the low precipitations, the higher resuspension and the formation of secondary aerosol occurring in this area during the warmer months of the year (Querol et al., 1998b, 1999 and 2001a; Escudero et al., 2005; Viana et. al., 2005). The summer increase was much more pronounced in the coarse fraction ($PM_{10\text{-}2.5}$) than in the finer fractions ($PM_{1\text{-}2.5}$ and PM_1) because of the coarser size of the mineral dust particles associated to this type of episodes. During December and January the levels registered were much lower and the PM grain size was mainly fine (very low $PM_{2.5\text{-}10}$ levels are observed during winter months). The seasonal variability of PM levels is also affected by the seasonal variation of the boundary layer height. The Montsec site is located outside of the boundary layer during the colder months of the year (October to March) and therefore is less affected by regional pollution episodes. However, from April to September the monitoring site enters the boundary layer during the central hours of the day, coinciding with its maximum development, and making PM levels increase. However, in February and March, the levels of fine aerosols (PM_1) are quite high. This is probably the

consequence of some very intense episodes registered during these months, which increased markedly the levels of PM_1. The most significant episodes were a very intense winter anticyclonic pollution episode that reached the MSC site in February 2006, increasing PM levels noticeably also in BCN and MSY sites, and a very important European episode, that transported pollutants from Europe during March 2007 and reached also MSY and BCN sites.

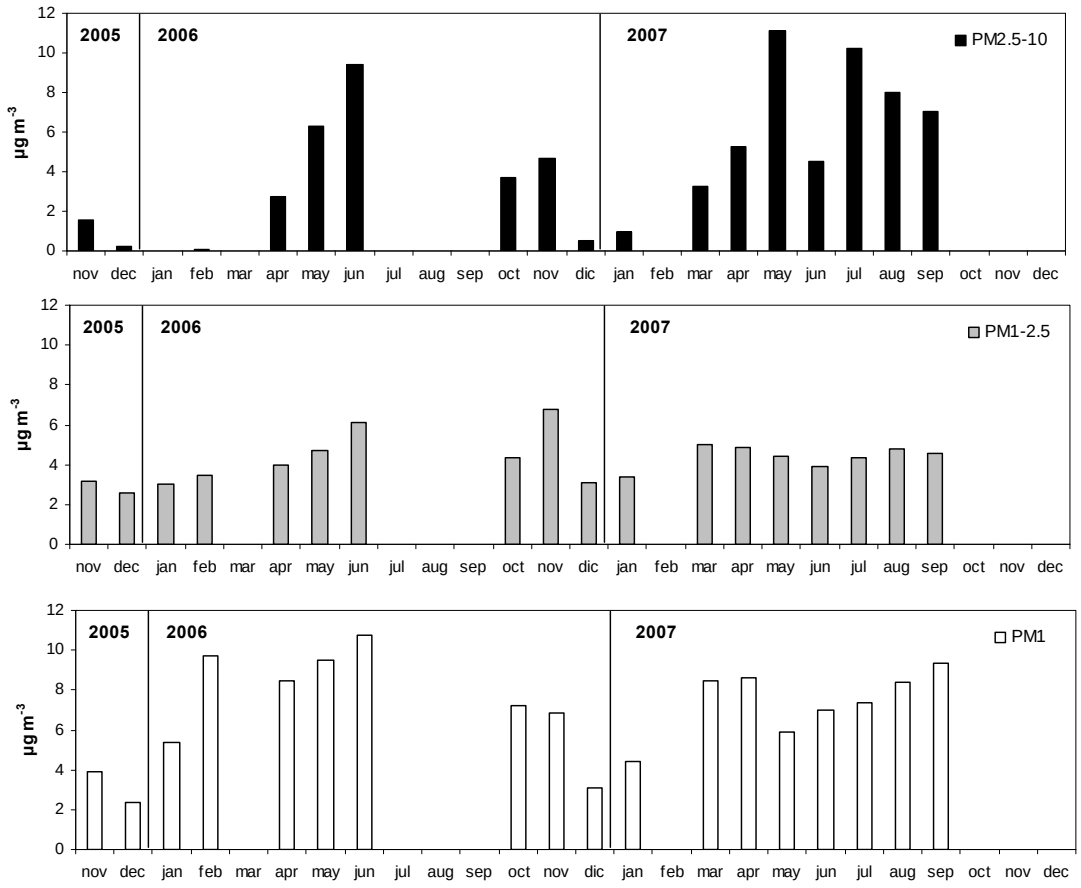

Figure 4.3.10. Monthly $PM_{2.5-10,}$ $PM_{1-2.5}$ and PM_1 means registered at MSC from November 2005 to September 2007.

These important episodes will also be described in detail, as they were detected from the data obtained during these sampling periods at Montsec and had a high impact in the levels and composition of atmospheric aerosols. During the intense anticyclonic pollution episode that occurred during February 2006, air masses with a NW Atlantic origin and passing through the Pyrenees where stagnated when arriving to the region of study by the effect of atmospheric stability (Figure 4.3.11). These polluted air masses reached the MSC site, probably by the effect of mountain breezes, increasing markedly PM levels. During this episode, also registered at MSY and BCN, very high levels of anthropogenic pollutants as sulphate (Figure 4.3.11) and nitrate were

measured at all the sites. The European episode registered in March 2007 also had an important impact at MSC. During this episode polluted air masses were transported from Northern Europe (Poland and Germany) to the site, passing through France and increasing significantly the levels of anthropogenic pollutants (Figure 4.3.12). These episodes were also recorded at some rural background sites in the South of France (Airbase database, http://air-climate.eionet.europa.eu/databases/airbase/), reaching very high PM_{10} peak levels just before the episode was registered at Montsec.

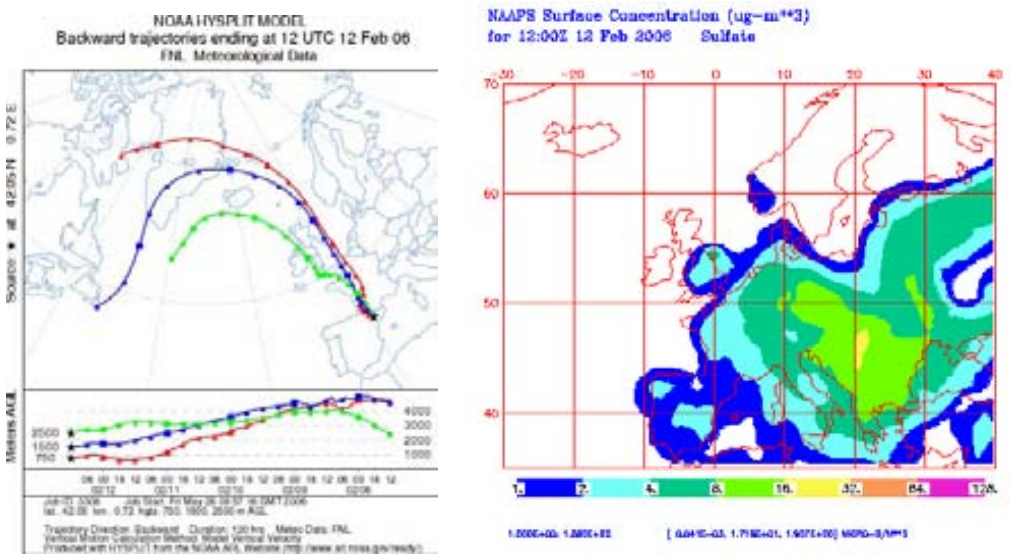

Figure 4.3.11. Back-trajectory of a winter anticyclonic episode calculated for MSC for the 12 February 2006 (left). NAAPS surface concentration map for sulphate for 12 February 2006 (right).

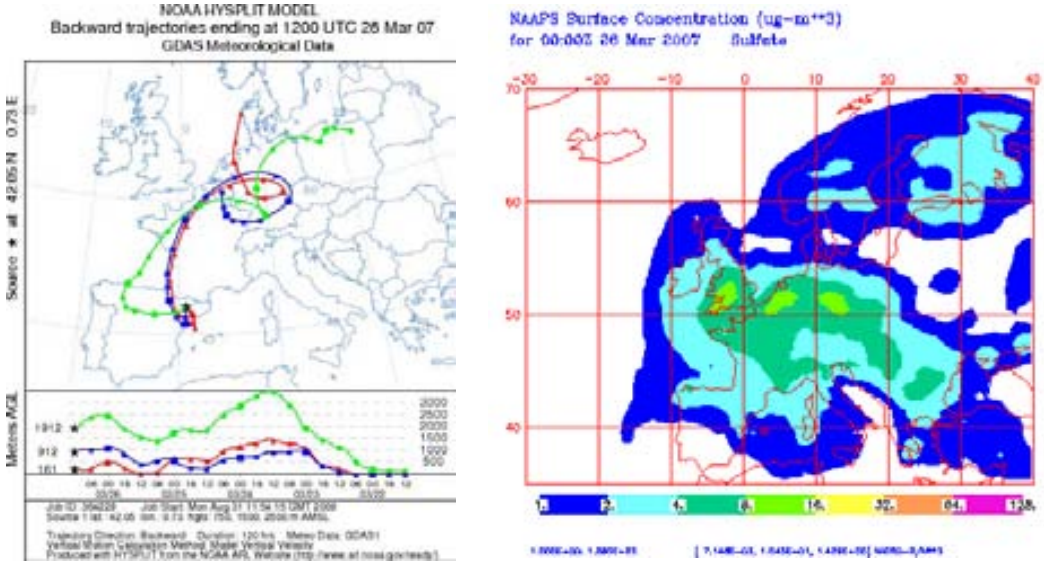

Figure 4.3.12. Back-trajectory of a European episode calculated for MSC for the 26 March 2007 (left). NAAPS surface concentration map for sulphate for 26 March 2006 (right).

The PM_1/PM_{10} and $PM_{2.5}/PM_{10}$ ratios measured at MSC followed also a seasonal trend (Figure 4.3.13). Both ratios were higher during the colder months and decreased during the warmer months, because of the increase in the levels of coarser particles during the summer. At MSC, the ratio PM_1/PM_{10} was markedly lower than the $PM_{2.5}/PM_{10}$ ratio but followed the same trend. The decrease in both PM_1/PM_{10} and $PM_{2.5}/PM_{10}$ ratios when African dust outbreaks occurred was evident as a result of the transport of high concentrations of coarse dust particles to the site.

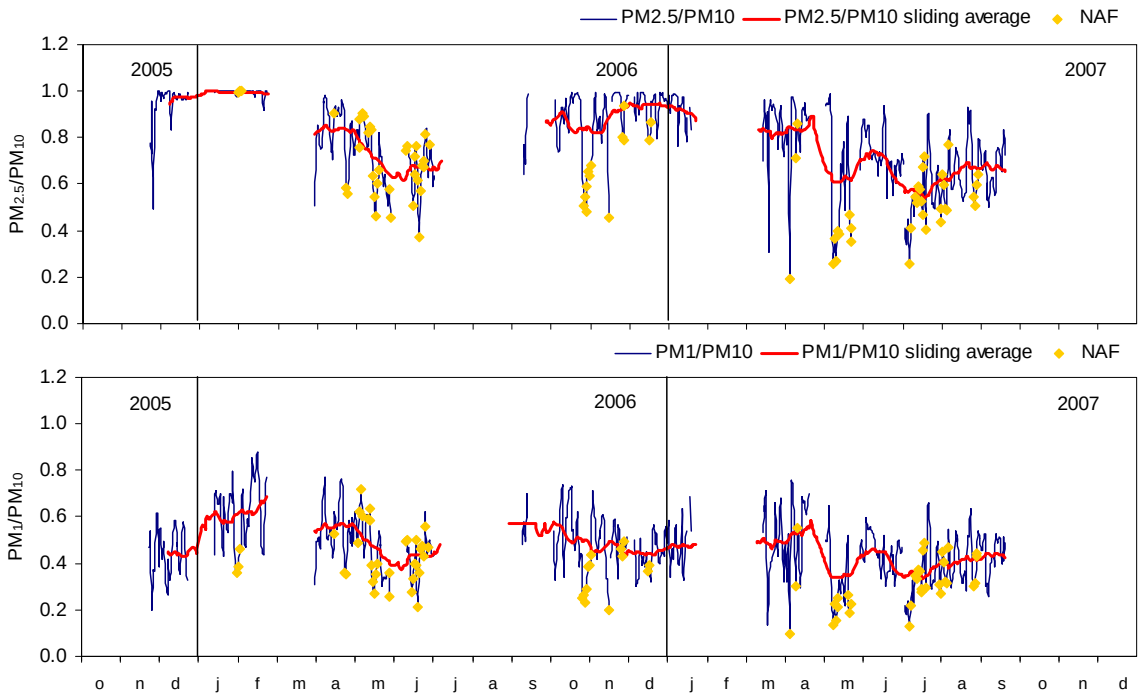

Figure 4.3.13. $PM_{2.5}/PM_{10}$ and PM_1/PM_{10} ratios and 30-day sliding average measured at MSC from November 2005 to September 2007. Days with African dust outbreaks (NAF) are marked.

4.3.2.4. Daily cycles

The daily cycles of PM levels at Montsec followed a very different pattern in summer and winter, especially for the coarse fraction (Figure 4.3.14). The levels of all fractions were markedly lower during the winter months (especially December and January). In winter there was not an important variation of the levels during the day because the site was situated outside the boundary layer and therefore not exposed to regional pollution. However, in February, PM_1 levels showed an increase in the afternoon that may be related to regional pollution transported by mountain breezes as an important anticyclonic pollution episode was registered during February 2006, transporting fine sulphate particles to the site at relatively high atmospheric levels. During the summer,

hourly levels of the finer PM fractions did not present such an important variation during the day. However, a slight increase in PM_1 levels was observed during the central hours of the day, parallel to the coarse fraction.

Coarse PM levels were higher from May to September, presenting a daily cycle with lower levels at night and an increase during the central hours of the day, parallel to the maximum development of the boundary layer and to the highest wind speeds. At this time of the day the site may be located inside the boundary layer and the site may then be affected by regional pollution events and the transport of pollutants and soil resuspension by mountain breezes, increasing coarse PM levels. Moreover, the summer pattern was superposed by high peaks of coarse PM occurring from March to November, related to the occurrence of North-African dust outbreaks, frequent during this period of the year (Escudero et al., 2005).

$PM_{1\text{-}2.5}$ did not show a significant daily cycle during the colder or the warmer months of the year. However during March and November the levels of this fraction varied in accordance with those of $PM_{2.5\text{-}10}$ and PM_1. This is probably the consequence of some European air mass transport episodes occurring during March 2007, increasing the levels of finer sulphate aerosols and also a very intense African dust outbreak occurring in November 2006, increasing PM levels in all size ranges.

The results obtained show that the monitoring of PM_1 and PM_{10} (or PM_1 and $PM_{1\text{-}10}$) may be a better approach for the study of the factors that control air quality. The fraction $PM_{1\text{-}2.5}$ reflects in a lesser way the impact of the factors described above. Moreover, it seems clear that the processes controlling PM_1 are in many occasions different to the processes that control $PM_{1\text{-}10}$ and may thus be important to monitor separately these two PM size fractions.

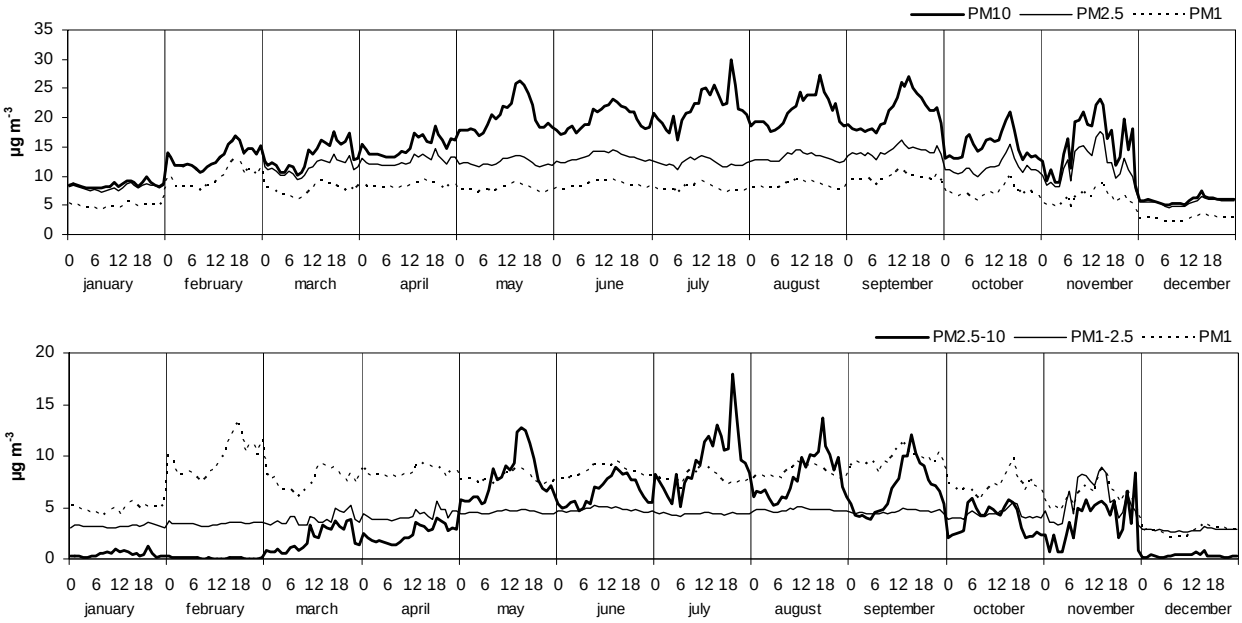

Figure 4.3.14. Annual variability of the mean daily cycles of PM_{10}, $PM_{2.5}$ and PM_1 (top) and $PM_{2.5\text{-}10}$, $PM_{1\text{-}2.5}$ and PM_1 (bottom) recorded at MSC from November 2005 to September 2007.

4.3.2.5. Influence of air mass episodes on PM levels

The different air mass origins and their frequencies arriving to the study region were described above. The mean PM_{10}, $PM_{2.5}$ and PM_1 levels recorded at MSC associated to each of the air mass origin are shown in Table 4.3.3 and Figure 4.3.15.

Table 4.3.3. Mean levels for each air mass origin considered at MSC (November 2005-September 2007).

µg m^{-3}	NA	NWA	WA	SWA	NAF	MED	EU	REG	ANT
PM_{10}	6.1	5.2	5.7	9.0	22.8	7.8	7.2	13.1	6.8
$PM_{2.5}$	4.1	3.7	4.3	6.8	12.5	6.7	6.2	9.3	5.7
PM_1	2.5	2.6	2.6	4.2	7.5	4.4	4.1	6.4	4.2
$PM_{1\text{-}2.5}$	1.6	1.6	1.7	2.5	5.0	2.3	2.1	2.9	1.5
$PM_{2.5\text{-}10}$	2.0	1.4	1.4	2.3	10.3	1.1	1.0	3.7	1.1

At MSC, the highest PM levels in all fractions were associated to African dust outbreaks, but the increase was more important in the $PM_{2.5\text{-}10}$ fraction, owing to the coarse size of mineral dust. At MSC, a CB site with low PM levels in general, these peak PM episodes are clearly evidenced.

The summer regional recirculation episodes (REG) presented also high PM levels that are associated to the accumulation and recirculation of pollutants over the region. The

increase in PM levels at MSC site during these episodes may also be the consequence of the development of the boundary layer during the central hours of the day in the summer months exposing the site to the regional pollution.

The lowest PM levels were observed for Atlantic air mass advections (ATL). Air mass advections renovate the air masses, cleaning the atmosphere from pollutants and generally reducing PM levels. Sometimes Atlantic advections are also associated with precipitations that contribute to wash out the suspended particles and to minimize the dust resuspension.

The European (EU) and Mediterranean (MED) air mass transport episodes are associated to strong winds and precipitations that allow the renovation of air masses, and consequently both types of episode presented low PM levels. However, sometimes the transport of pollutants from Central and Eastern Europe or the Mediterranean coastal urban agglomerations contributes to increment PM levels, especially the finer fractions because the air masses transported are charged with anthropogenic pollutants (mainly ammonium sulphate and nitrate).

Winter anticyclonic episodes (WAE) registered low PM levels in general. During winter months the MSC site is located outside of the boundary layer and the anticyclonic situation favours the stagnation of pollutants in the valley during several days and consequently PM levels remain low. This is one of the most important differences found between the RB and the CB in NE Iberian Peninsula. WAE episodes have a very important incidence in PM levels at the RB (MSY), increasing significantly the levels of fine particles because of the transport of pollution accumulated in the valley by mountain breezes, while at the CB (MSC), PM levels remain very low during these episodes.

In conclusion, the fraction $PM_{2.5-10}$ and PM_1 increased markedly during African dust outbreaks and summer regional recirculation episodes. $PM_{2.5-10}$ levels were higher during Atlantic than during Mediterranean, European or Winter Anticyclonic episodes, probably because of local dust resuspension by wind. Conversely the lowest PM_1 levels were recorded during Atlantic episodes. The variability of the fraction $PM_{1-2.5}$ was less marked.

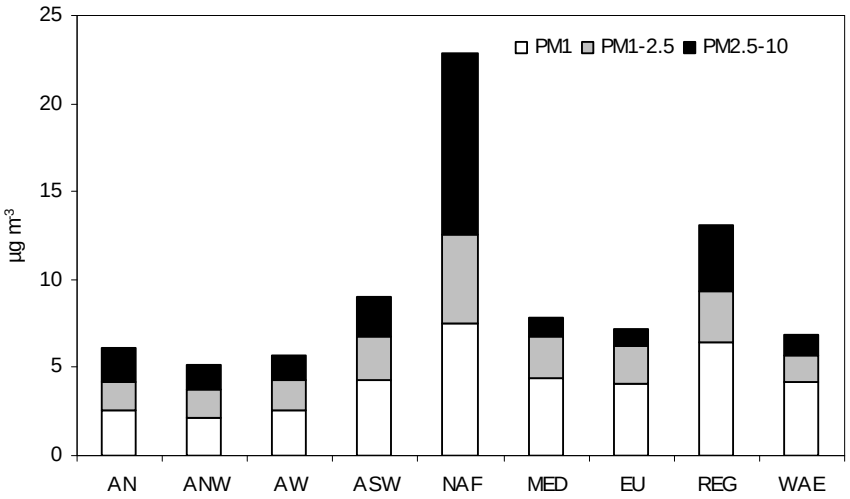

Figure 4.3.15. Mean $PM_{2.5-10,}$ $PM_{1-2.5}$ and PM_1 levels classified by air mass origin registered at MSC from November 2005 to September 2007.

4.3.2.6. Influence of African dust outbreaks on PM levels

The contribution of African mineral dust to the annual PM levels depends on the frequency and intensity of African outbreak episodes (NAF) in a year. In the region considered, the number of days with African dust influence varied from 53 in 2006 to 43 in 2007 (Table 4.3.4).

African dust episodes exert a high influence on PM levels resulting in an important increase on a daily basis, and consequently these may contribute to exceed the PM_{10} daily limit value. At MSC the 50 µgPM_{10} m^{-3} daily limit was exceeded 4 times in 2006 and 3 times in 2007, considering only the available data for each year (59 and 52%, respectively). The exceedances of the PM_{10} daily limit value recorded in 2006 and 2007 at MSC occurred during NAF episodes or during regional recirculation conditions after a dust outbreak had occurred, and may be attributed in all cases to the African dust contribution.

Table 4.3.4. Number of days with African dust influence registered at MSC. Number of exceedances of the 50 µgPM_{10} m^{-3} daily limit value and % of the exceedances recorded during NAF episodes at MSC.

	nº NAF days	Number of days with PM_{10}>50µg m^{-3}/total sampling days	% Exceedances during NAF
2006	53	4/236	100
2007	43	3/191	100
Total (Nov05-Sep07)	96	7/461	100

The difference between the PM mean annual levels and the mean annual levels obtained for days without African dust influence may be considered as the African annual dust contribution to PM levels (Table 4.3.5). In MSC, the mean annual increase of PM levels due to the African dust influence was 3.3, 1.2 and 0.5 μg m^{-3} for PM_{10}, $PM_{2.5}$ and PM_1 respectively, during the period 2006-2007. These contributions are much higher than the mean annual increase of PM levels attributed to African dust outbreaks calculated previously for the MSY regional background site for the years 2006-2007 (0.9, 0.2 and <0.1 μg m^{-3} for PM_{10}, $PM_{2.5}$ and PM_1 respectively). The differences may be attributed to the higher impact of African dust outbreaks at MSC due to the higher altitude (1570 m.a.s.l.) compared with MSY (720 m.a.s.l.). In most of these episodes African dust is preferentially transported over Southern Europe in atmospheric layers from 1000-5000 m.a.s.l. (Escudero et al., 2005), being highest the influence on surface PM levels in monitoring stations located at higher altitudes.

African dust is mainly coarse in size and consequently its contribution to PM levels is much higher for the coarsest fraction (2.1, 0.7 and 0.5 for $PM_{2.5-10}$, $PM_{1-2.5}$ and PM_1 respectively).

Table 4.3.5. Mean annual PM levels calculated at MSC for 2006-2007, mean levels for days without African dust influence (no NAF) and the increase in PM levels attributed to African dust outbreaks.

	PM mean levels (μg m^{-3})	No-NAF PM levels (μg m^{-3})	PM increase related to NAF (μg m^{-3})
PM_{10}	16.4	13.1	3.3
$PM_{2.5}$	11.6	10.3	1.2
PM_1	7.2	6.7	0.5
$PM_{1-2.5}$	4.4	3.7	0.7
$PM_{2.5-10}$	4.8	2.7	2.1

NAF contribution during the year 2006 was slightly higher than the calculated for 2007 (Figure 4.3.16) and the difference was due to the finer fractions, that are higher during the year 2006, conversely to the coarsest fraction that was higher during 2007. These differences are also a consequence of the sampling availability. Mean PM_{10} levels were higher during 2007 than during 2006, due to the sampling performed during the summer months. However, no significant variation was observed for the finer fractions. The sampling availability makes also that no-NAF levels were lower for 2006 in all the fractions. This is the reason for the finer distribution of the NAF contribution calculation during 2006 and the coarser distribution during 2007.

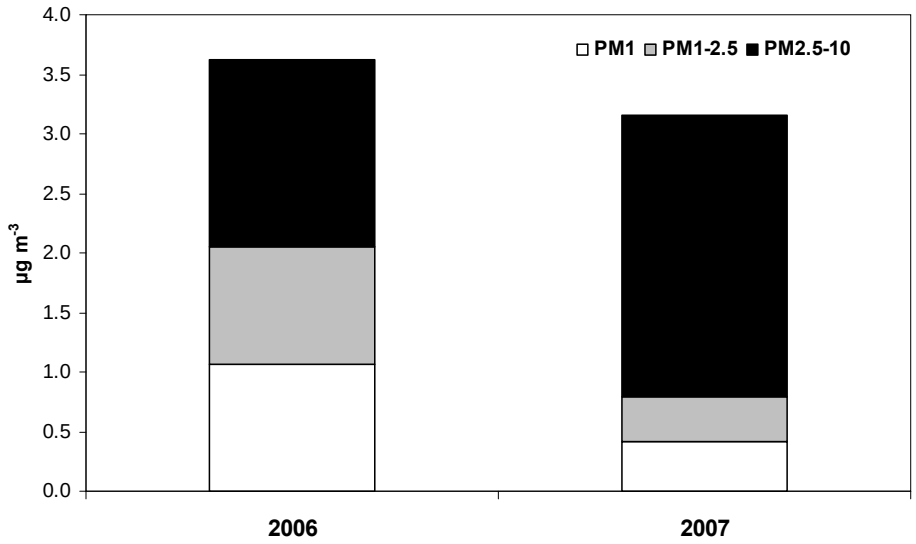

Figure 4.3.16. Annual increment of $PM_{2.5-10}$, $PM_{1-2.5}$ and PM_1 levels attributed to African dust contribution calculated at MSC for 2006 and 2007.

The African dust contribution to annual mean PM levels was also quantified by applying the method proposed by Escudero et al., (2007b). In this method, RB levels are calculated by applying a 30th percentile to the PM mean daily levels measured for the days without African dust transport. Then, the daily African dust load is calculated as the difference between the daily PM levels on days with African dust influence and the calculated RB background. The contributions were very similar to the obtained with the method applied above, 3.2, 1.5 and 0.8 µg m^{-3} for PM_{10}, $PM_{2.5}$ and PM_1, respectively.

4.3.3. PM speciation at the continental background

4.3.3.1. PM_{10} speciation at MSC and other CB sites

The speciation analysis of PM_{10} at Montsec was performed from November 2005 to November 2007. Means for the major components measured during 2006, 2007, and the total sampling period are presented in Table 4.3.6. To account for the differences between 2006 and 2007 sampling frequency and availability, an annual mean was calculated considering data from 2006 and 2007 and accounting the different months of the year at a rate of 1 sample every 4 days. Annual means are presented also in Figure 4.3.17.

Table 4.3.6. Mean levels of PM_{10} and its major components registered at MSC for 2006, 2007, and the total sampling period (November 2005 to November 2007). Annual mean calculated for the period 2006-2007.

	2006	2007	Total (Nov05-Nov07)	Annual mean
N	35	64	110	72
µg m^{-3}	12.1	20.3	16.0	14.1
OC	1.1	3.0	2.2	1.9
EC	0.2	0.4	0.3	0.3
OM+EC	2.6	6.7	4.9	4.3
SO_4^{2-}	1.7	2.8	2.2	1.9
NO_3^-	1.4	1.2	1.2	1.1
NH_4^+	0.4	0.8	0.6	0.5
SIA	3.6	4.8	4.0	3.5
Mineral matter	2.4	5.8	4.2	3.7
Sea spray	0.2	0.4	0.3	0.3
Unaccounted	3.3	2.7	2.7	2.4

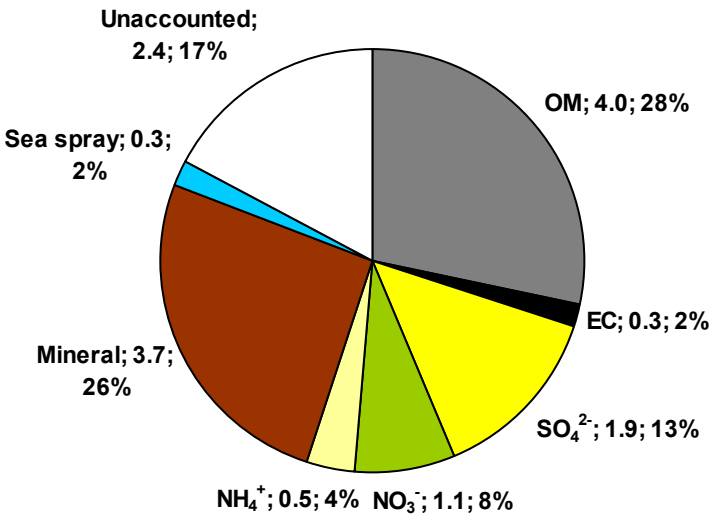

Figure 4.3.17. Mean annual composition of PM_{10} calculated at MSC for 2006 and 2007.

PM_{10} in Montsec was mainly made up of organic matter (OM, 28%), mineral dust (26%), and secondary organic aerosols (SIA, 25%). Sulphate accounted for 13%, Nitrate for 8% and ammonium for 4% of the total mass. Sea spray was found at low levels at this site (2%). Elemental carbon was also found at low levels (2%) due to the lack of a direct influence of combustion emissions. The unaccounted mass is probably due to the occurrence of structural and adsorbed water, and accounted for a 17% of the total mass.

The ion balance between the sum of acid species (nitrate and sulphate) and ammonium, measured in PM_{10} at MSC is shown in Figure 4.3.18 (top). An excess of

acid species indicates that not all nitrate and sulphate are neutralized by ammonium. Around 50% of sulphate and nitrate may then be neutralized by Na (in excess after balance with Cl^-) and Ca, forming coarse nitrate and sulphate (Figure 4.3.18 bottom). After these balances, some of the samples had excess of nitrate and sulphate. These cases may be related to formation of acid species (acid nitrate and sulphates) or the neutralization by Mg or K (not considered in the balance). However, in other cases, an excess of Ca is recorded after this balance, probably related to the local contribution (dust resuspension). The soil of the Montsec d'Ares presents an important proportion of calcite and dolomite, and probably road works and winds contributed to the resuspension of Ca and Mg carbonates.

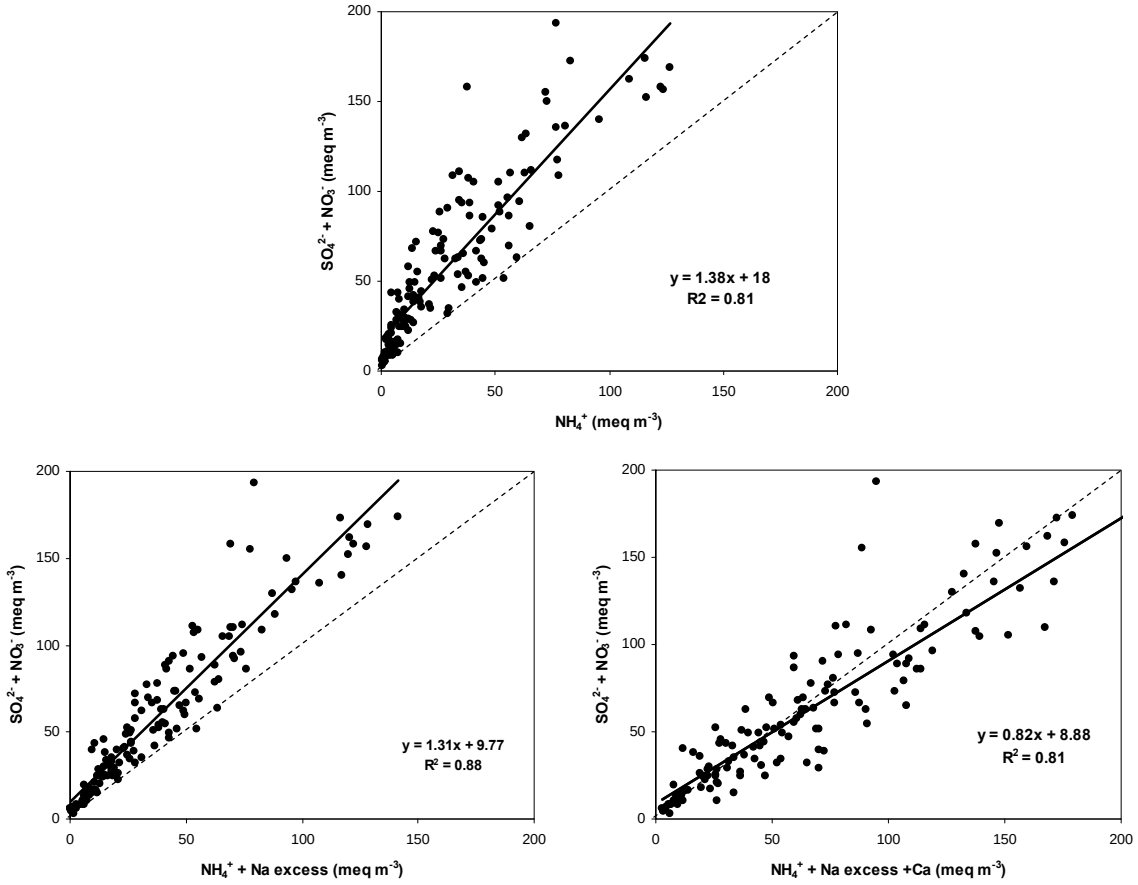

Figure 4.3.18. Ion balance (meq m^{-3}) between acid species (sulphate+nitrate) and ammonium in PM_{10} at Montsec (top), between acid species and the sum of ammonium and excess Na (bottom left) and between acid species and the sum of ammonium, excess Na and Ca (bottom right).

The ratio Al/Ca may then be useful for the detection of African dust outbreaks and to distinguish African from local dust contribution. Figure 4.3.19 shows that the correlation between Al and Ca presents two slopes, a higher slope that may indicate the days with African dust influence, with a higher Al than Ca contribution (Castillo, 2006). The lower

slope represents the days where local contribution was higher, as calcite was the main composition of the Montsec d'Ares soil. This contribution may have been higher because of road works that turned over the land, favouring resuspension.

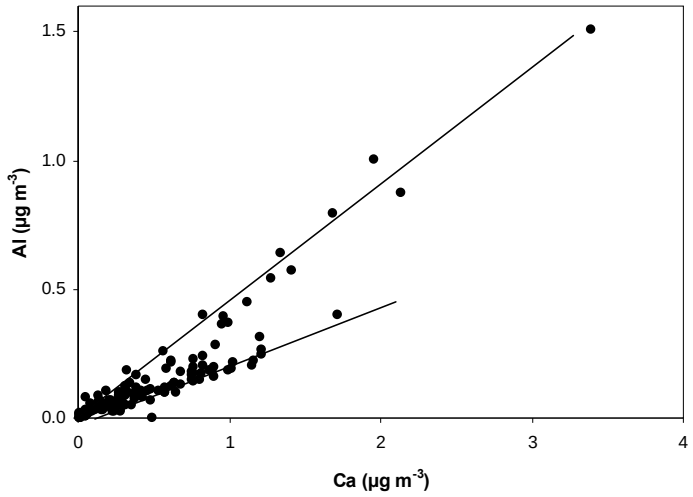

Figure 4.3.19. Correlation between Al and Ca (µg m^{-3}).

Comparing PM_{10} speciation measured at MSC with other continental sites in Europe (considering remote sites at >1000 m.a.s.l, except for Birkenes in Norway at 190 m.a.s.l. (Yttri et al., 2007), Table 4.3.7), the MSC site is comparable to the continental sites in Southern and Central Europe (Monte Cimone in Italy (Marenco et al., 2006) and Chaumont in Switzerland (Hueglin et al., 2005).

Mineral matter levels decreased from south to north, depending on the proximity to the African continent and the frequency of African dust outbreaks occurrence. Izaña, in the Canary Islands (Izaña Atmospheric Observatory) presented the highest levels of mineral matter, given that it is exposed to frequent and intense African dust outbreaks. MSC and Monte Cimone, in Southern Europe, presented intermediate levels, decreasing to the north at Chaumont, in Switzerland to finally, the lowest, at Birkenes in Scandinavia.

The levels of carbonaceous compounds (OM+EC) were higher at MSC than at all the other European sites. This may be the result of the sampling of intense smoke episodes from important forest fires in the Mediterranean during the summer in 2007. However, EC was higher in Switzerland probably because of biomass burning in the area. OC/EC ratios measured at MSC (6.3) were between the ratios measured in

Monte Cimone (7.5) and Birkenes (8.0), and the ratios measured at Izaña (5.5) and Chaumont (2.0).

Sulphate levels were very similar to the levels measured at Chaumont, lower than those measured at Monte Cimone and higher than levels measured at Izaña or Birkenes. The highest nitrate levels were measured at MSC, but were comparable to the levels measured at Monte Cimone and Chaumont. Izaña and Birkenes presented the lowest nitrate levels. Ammonium levels were somewhat higher at Monte Cimone, and ammonium levels at MSC are more comparable to levels measured at Chaumont and Birkenes. Izaña presented much lower ammonium levels. The lowest nitrate/sulphate ratios were measured in Italy (0.2) and ranged from 0.4 in Chaumont and Norway to 0.5 and 0.6 in Izaña and Montsec, respectively.

Sea spray levels were higher at the sites that were situated on the Atlantic coast, as Izaña and Birkenes. The levels at MSC, Monte Cimone and Chaumont were similar.

Table 4.3.7. Mean levels of PM_{10} components measured at MSC and other CB sites in Europe.

	Spain Montsec[1] 1570 m annual 2006-2007	Spain Izaña, Canary Islands[2] 2373 m annual 2005-2007	Italy Monte Cimone[3] 2165 m summer 2004	Switzerland Chaumont[4] 1137 m annual	Norway Birkenes[5] 190 m annual 2004
N	72	141	47	104	
µg m^{-3}	14	28	16	11	5
SO_4^{2-}	1.9	1.0	3.5	2.0	1.1
NO_3^-	1.1	0.5	0.8	0.8	0.4
NH_4^+	0.5	0.1	1.4	0.8	0.8
OC	1.9	1.1	1.5*	1.2	1.6
EC	0.3	0.2	0.2*	0.6	0.2
OC/EC	6.3	5.5	7.5	2.0	8.0
OM[#]+EC	4.3	2.5	3.4	3.2	3.5
Mineral matter	3.7	20.4	3.5	1.6	0.1
Sea spray	0.3	0.6	0.3	0.2	0.8
SIA	3.5	1.7	5.7	3.6	2.2
Unacc.	2.4	3.1	3.1	2.2	-1.2

[1]This work; [2]Izaña Atmospheric Observatory; [3]Marenco et al. (2006); [4]Hueglin et al. (2005); [5]Yttri et al. (2007).
[#]OM=2.1*OC
*OC and EC calculated in PM_1

4.3.3.2. Trace elements

The mean levels of trace elements (including metals) measured at MSC during 2006, 2007 and during the total sampling period (November 2005-November 2007) are shown on Table 4.3.8, together with a calculated annual mean for the years 2006 and 2007, accounting for data availability and sampling frequency. Most of the elements studied presented higher levels during the year 2007 compared with the year 2006,

coincident with the higher levels measured during the year 2007 due to the disparity in data availability during different months of the year in 2006 and 2007. During 2007 the sampling was mostly performed during the summer, when levels of PM_{10} are higher, while in 2006 sampling was performed mostly from January to May, with lower PM_{10} levels. During the summer in 2007 intense African dust outbreaks were sampled. Moreover, during the warmer months of the year the MSC site is situated inside the boundary layer, being exposed to regional pollution and making levels of most trace elements increase.

Table 4.3.8. Mean levels of trace elements registered in PM_{10} at MSC between November 2005 and November 2007.

ng m^{-3}	2006	2007	Total Nov05-Nov07	Annual mean
N	35	64	110	72
P	5.2	15.2	10.5	8.0
Li	0.1	0.3	0.2	0.2
Ti	6.2	22.1	15.1	13.0
V	1.0	2.7	1.9	1.6
Cr	0.3	1.7	1.1	1.0
Mn	3.4	9.4	6.6	5.8
Co	0.1	0.2	0.1	0.1
Ni	0.8	1.2	1.0	1.0
Cu	0.7	3.2	2.2	1.8
Zn	6.1	22.1	15.2	12.2
As	0.1	0.3	0.2	0.2
Se	0.2	0.6	0.2	0.2
Rb	0.2	0.6	0.4	0.4
Sr	0.5	2.8	1.8	1.4
Cd	0.1	0.1	0.1	0.1
Sn	0.2	0.5	0.3	0.3
Sb	0.1	0.2	0.2	0.1
Ba	5.6	11.3	8.6	7.9
La	0.1	0.2	0.2	0.1
Ce	0.2	0.5	0.4	0.3
Tl	0.02	0.03	0.03	0.02
Pb	1.3	2.6	2.0	1.7
Bi	0.02	0.04	0.04	0.03
Th	0.02	0.10	0.06	0.05
U	0.02	0.09	0.06	0.05

Comparing trace elements measured in PM_{10} at MSC with trace elements measured at other sites in Europe (Table 4.3.9), Izaña presented higher levels of elements with a crustal origin (Li, Mn, Sr, Ba, Rb, La and Ce) than the rest of the sites, as this site is more intensely affected by mineral dust outbreaks. MSC, Monte Cimone and Chaumont presented higher levels of some elements with an anthropic origin (Pb, Ni), when compared with Izaña. However, Izaña presented higher V, Cr and Co levels. Cr(III), V(III) and Co(III) can substitute Al(III) in alumino-silicate species, and thus may be related to mineral dust. Chaumont presented lower levels of trace elements in general, except for Cu and Pb levels that were higher.

Table 4.3.9. levels of PM_{10} trace elements measured at MSC and at other European CB sites.

ng m^{-3}	Spain Montsec[1] PM_{10}	Spain Izaña[2] PM_{10}	Italy Mt Cimone[3] PM_{10}	Switzerland Chaumont[4] PM_{10}
N	72	141	47	104
Li	0.2	1.1		
V	2	3	3	1
Cr	1	3		
Mn	6	19	6	2
Co	0.1	0.5		
Ni	1.0	1.1	1.4	1.3
Cu	2		3	7
As	0.2	0.3		0.2
Zn	12	13	10	
Se	0.2	0.1		0.2
Sr	1	8	3	
Ba	8	24		
Pb	2	1	4	5
Rb	0.4	1.9		0.3
Cd	0.1	0.1		0.1
Sb	0.1	0.1		0.2
La	0.1	1.0		0.1
Ce	0.3	2.5		
Tl	0.02	0.02		<0.1
Sn	0.3	0.4		
Th	0.1	0.4		
U	0.1	0.1		

[1]This work; [2]Izaña atmospheric Observatory; [3]Marenco et al. (2006); [4]Hueglin et al. (2005)

4.3.3.3. Seasonal evolution of PM components

PM_{10} components measured at MSC presented a clear seasonal trend. The annual cycles of PM_{10} components measured at MSC from November 2006 to November 2007 in PM_{10} are shown in Figure 4.3.20.

The carbonaceous compounds (OM+EC) presented the maximum levels during the warmer months of the year. These higher concentrations may be related to: 1) the regional background anthropogenic pollution reaching the site during the central hours of the day, as a consequence of the development of the boundary layer; 2) the higher biogenic emissions (Peñuelas et a., 1999) and 3) the lower precipitation rates registered during this period. The transport of smoke from important forest fires occurring during the summer in 2007 in the Mediterranean may also have an important influence in OM+EC levels during the summer. During the winter months OM+EC levels were generally low because of the site being outside of the boundary layer.

The crustal material presented also a seasonal trend related to the seasonality of African dust outbreaks, occurring with a higher frequency during the summer (Escudero et al., 2005), but also to the transport of regional pollution to the site during the warmer months of the year when regional recirculation episodes are important and the site is exposed to the boundary layer pollution (Viana et al., 2005). During the winter months the levels of crustal components were low.

Sea spray presented higher levels also during the summer months. This situation may be related also to regional recirculation episodes carrying sea spray aerosols to the monitoring site (Viana et al., 2005).

Sulphate levels followed the same seasonal pattern than most PM_{10} components, with higher levels recorded during the warmer months. The higher summer sulphate levels are related to the regional pollution arriving to the site but also to the higher oxidation rate of the SO_2 due to the higher photochemical activity (Querol et al., 1998b, 1999 and 2001a).

Conversely, nitrate showed higher levels during February and March. This behaviour is probably due to the thermal instability of particulate ammonium nitrate during the warmer months of the year (Harrison and Pio, 1983; Querol et al., 1998b, 2004a), but probably also to some intense pollution episodes that occurred during these months. During the intense anticyclonic pollution episode that occurred during February 2006, polluted air masses reached MSC, increasing markedly the levels of SIA and carbonaceous compounds, but especially ammonium nitrate. During the episode that occurred during March 2007, polluted air masses transported from Europe increased SIA levels in a high extent.

The seasonal variability of ammonium is related to the cycles of sulphate and nitrate. Ammonium levels increase during February and March due to the formation and stability of particulate ammonium nitrate. Additionally, the formation of ammonium sulphate during the summer accounts for the high ammonium levels observed also during the warmer months.

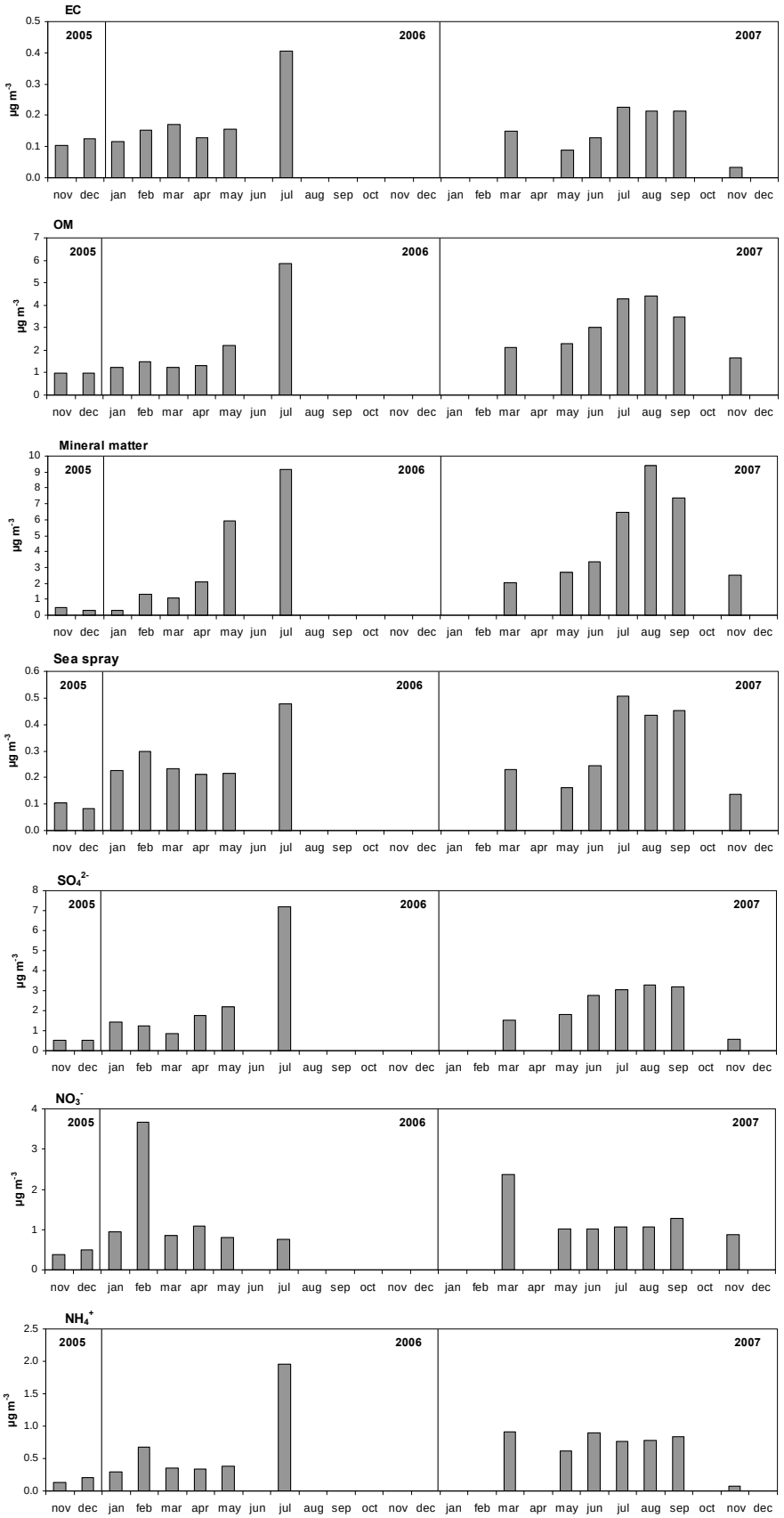

Figure 4.3.20. Mean annual cycle of the main PM_{10} components measured at MSC from November 2006 to November 2007.

4.3.3.4. Day to day variability: PM episodes

The day to day variation of PM levels and speciation at MSC is the consequence of the occurrence of successive air mass transport and meteorological episodes already described for the Western Mediterranean Basin (Rodriguez et al., 2003; Escudero et al. 2007a): Atlantic advection episodes, African dust outbreaks, summer regional recirculations, winter anticyclonic episodes, European and Mediterranean air mass transport events. The mean levels of the main components analyzed in PM_{10} at MSC obtained for each episode considered are shown in Table 4.3.10 and Figure 4.3.21.

Table 4.3.10. Annual frequency, PM_{10} levels and composition (in %) for the main scenarios occurring at MSC during November 2005-November 2007: African dust outbreaks (NAF); winter anticyclonic episodes (WAE); summer regional recirculations (REG), European air mass transport (EU); Mediterranean air mass transport (MED); Atlantic advection episodes (ATL).

	NAF	REG	WAE	MED	EU	ATL
Annual frequency (%days/year)	12-15	15-18	8-11	4	9-10	48-49
N	15	26	10	2	9	46
µg PM_{10} m^{-3}	27	22	14	12	10	10
OM (%)	27	30	19	**37**	29	31
EC (%)	1.7	1.9	1.2	**2.4**	1.9	2.1
SO_4^{2-} (%)	12	**18**	12	10	15	11
NO_3^- (%)	4	6	**19**	10	17	7
NH_4^+ (%)	2	5	5	4	**7**	3
Mineral (%)	**41**	24	9	26	10	20
Sea Spray (%)	1.6	1.8	1.3	1.1	**2.4**	2.0
Unaccounted (%)	9	14	33	8	16	23

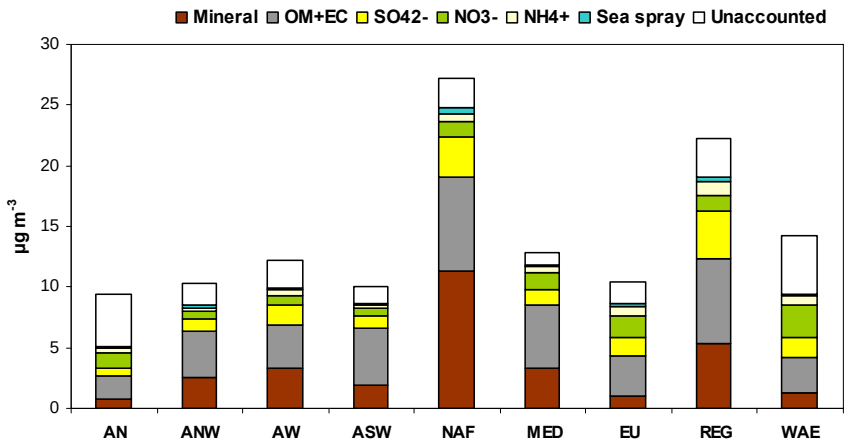

Figure 4.3.21. Mean PM_{10} components measured at MSC during Atlantic advection episodes (AN, ANW, AW, ASW), African dust episodes (NAF), Mediterranean advection (MED), European episodes (EU), summer regional recirculations (REG) and winter anticyclonic episodes (WAE) in the period November 2005-November 2007.

At MSC, African dust outbreaks increased markedly the PM_{10} levels (27 µg m^{-3}). During these episodes the mineral fraction dominated the PM_{10} mass (41%) and OM was also important (27%), probably because of the long-range transport of smoke from important forest fires in the Mediterranean, together with African dust during some intense NAF episodes that occurred in the summer in 2007. SIA accounted for 18% of the PM_{10} mass.

The summer regional recirculations presented also high PM_{10} levels (22 µg m^{-3}). During these episodes PM_{10} was mainly composed of OM (30%), mineral matter (24%) and SIA (29%), registering the highest sulphate proportion of all episodes (18%), because of the higher oxidation rate of the SO_2 due to the higher photochemical activity during the summer months and the low air mass renovation during these episodes (Millán et al, 1997; Querol et al., 1998a and 1999; Rodríguez et al., 2003).

Winter anticyclonic episodes (WAE) registered low PM_{10} levels (14 µg m^{-3}), being mainly composed of OM (19%) and SIA (46%) but registering the highest nitrate levels (19%) of all episodes, because of the thermal stability of particulate ammonium nitrate at lower temperatures (Harrison and Pio, 1983; Querol et al., 1998b, 2004a), but also as a consequence of some intense pollution episodes transporting regional pollution to the site by breezes. Mineral matter presented very low levels during WAE episodes. The general low levels registered for all PM components during these episodes are mainly due to the MSC site being situated outside the boundary layer due to the atmospheric stability. However, in some cases, regional pollution reached the site, increasing markedly the levels of carbonaceous compounds and SIA, especially nitrate.

Mediterranean air mass transport is not very frequent. The samples collected (2) registered low PM_{10} levels (14 µg m^{-3}) and were mainly composed of OM (37%), mineral matter (26%) and SIA (24%). These samples registered the highest OM and EC levels of all episodes (27% and 2.4%, respectively), being probably the consequence of the transport of shipping emissions from the Mediterranean.

European air mass transport also presented low PM_{10} levels (10 µg m^{-3}) and was mainly composed of OM (29%) and SIA (39%). The mineral fraction was low during these episodes (10%) and sea spray registered was higher than in the other episodes described (2.4%). This is probably not due to the transport of sea spray (calculated as the sum of Na + Cl^-) but the consequence of the intense European transport episodes

occurring during March 2007 that increased markedly the levels of secondary pollutants at MSC (with possible formation of ammonium chloride due to the very low temperatures registered).

Atlantic advection episodes presented low PM_{10} levels (10 µg m^{-3}) and was mainly composed of OM (31%), SIA (21%) and mineral dust (20%). Atlantic advections presented also a high proportion of sea spray (2.0%). OM and EC were relatively high (31 and 2.1% respectively) and this may be the consequence of transported shipping emissions or smoke from forest fires.

4.3.4. Source contribution to ambient PM levels

The identification of emission sources influencing ambient PM levels at MSC was carried out by applying two different receptor modelling tools: principal component analysis (PCA) and positive matrix factorization (PMF). PCA results will be briefly discussed and then PMF results will be presented and discussed.

4.3.4.1. PCA

4.3.4.1.1 Components and data for analysis

The components used in the PCA analysis are presented in Table 4.3.11. Some of the components measured were not considered for the analysis because of their low levels measured, frequently under the detection limits or also because the high levels measured in the blank filters. Twenty six PM_{10} components were finally selected for the analysis.

Table 4.3.11. PM_{10} components analyzed and selected for the PCA analysis at MSC. Exclusion causes: very low levels in most cases <DL (●) or very high levels in blanks (○).

Ctotal	**X**	Ni	**X**	Pr	●
Al_2O_3	**X**	Cu	**X**	Nd	●
Ca	**X**	Zn	●	Sm	●
K	**X**	Ga	●	Eu	●
Na	**X**	Ge	●	Gd	●
Mg	**X**	As	**X**	Tb	●
Fe	**X**	Se	○	Dy	●
SO_4^{2-}	**X**	Rb	**X**	Ho	●
NO_3^-	**X**	Sr	**X**	Er	●
Cl^-	**X**	Y	●	Tm	●
NH_4^+	**X**	Zr	○	Yb	●
Li	**X**	Nb	●	Lu	●
Be	●	Mo	○	Hf	●
P	●	Cd	**X**	Ta	●
Sc	●	Sn	**X**	W	●
V	**X**	Sb	**X**	Tl	●
Ti	**X**	Cs	●	Pb	**X**
Cr	○	Ba	○	Bi	●
Mn	**X**	La	**X**	Th	●
Co	●	Ce	**X**	U	●

4.3.4.1.2 Identification of emission sources

The factors identified by the PCA analysis in PM_{10} are shown in Table 4.3.12. Factor loadings associated to each compound are indicated and main tracers are highlighted.

Table 4.3.12. Factors identified by PCA in PM_{10} at MSC, associated factor loadings and % variance of the samples explained by each of the factors obtained at MSC. Main tracers were highlighted in block letters (factor loadings equal or higher than 0.6) and components with factor loadings between 0.4 and 0.6 are written in italics.

Mineral matter		Secondary + anthropogenic		Marine + anthropogenic	
Ti	**1.0**	**NH_4^+**	**0.9**	**Cl^-**	**0.8**
Al	**1.0**	**Sn**	**0.8**	***Na***	**0.7**
Fe	**1.0**	***Sb***	**0.8**	*Cu*	*0.4*
Sr	**0.9**	***Pb***	**0.8**	Sn	0.3
Rb	**0.9**	***SO_4^{2-}***	**0.7**	Ni	0.3
K	**0.9**	**NO_3^-**	**0.6**	Mg	0.3
Ce	**0.9**	***Cd***	**0.6**	V	0.3
Li	**0.9**	**V**	**0.6**	Li	0.2
La	**0.9**	**Ctotal**	**0.6**	As	0.2
Ca	**0.9**	*Cu*	*0.5*	SO_4^{2-}	0.2
As	**0.8**	*Mn*	*0.5*	Sb	0.2
Mg	**0.7**	*As*	*0.4*	Ca	0.2
V	**0.7**	Na	0.3	La	0.2
Ctotal	**0.6**	Li	0.3	Ce	0.2
Mn	**0.6**	Rb	0.3	Sr	0.2
Pb	*0.5*	Mg	0.3	Ctotal	0.2
Cd	*0.5*	Ca	0.3	Rb	0.2
SO_4^{2-}	*0.4*	K	0.3	Ti	0.1
Na	*0.4*	Sr	0.2	Cd	0.1
Sb	*0.4*	Ce	0.2	Pb	0.1
Cu	0.3	Ti	0.2	Al	0.1
Ni	0.2	La	0.2	Fe	0.1
Sn	0.2	Al	0.2	K	0.1
NH_4^+	0.1	Fe	0.2	NH_4^+	0.1
Cl^-	0.0	Ni	0.2	Mn	0.0
NO_3^-	-0.1	Cl^-	0.0	NO_3^-	-0.1
%Var	**63**	**%Var**	**11**	**%Var**	**5**

The main factors identified in PM_{10} at MSC and the characteristic chemical species obtained for each factor (with factor loadings >0.4) are summarized in Table 4.3.13. Three factors were identified, accounting for 78% of the explained variance. Mineral matter explained a 63% of the variance and it was identified by crustal origin elements (Ti, Al, Fe, etc.). The second factor accounted for secondary anthropogenic aerosols (NH_4^+, NO_3^-, SO_4^{2-}) and some anthropogenic trace elements (Sb, Pb, Sn, Cd, etc., Pacyna, 1986) and explained a 11% of the variance. The third factor accounted for elements related to sea spray (Na and Cl^-) and accounted for a 5% of the total variance.

Table 4.3.13. Main factors identified in PM_{10} at MSC. Components with factor loadings higher or equal to 0.6 are highlighted in block letters and components with factor loadings between 0.4 and 0.6 are written in italics.

Mineral matter	**Ti, Al, Fe, Sr, Rb, K, Ce, Li, La, Ca, As, Mg, V, Ctot, Mn,** *Pb, Cd, SO_4^{2-}, Na, Sb*
Secondary/anthropogenic	**NH_4^+, Sn, Sb, Pb, SO_4^{2-}, NO_3^-, Cd, V,** **Ctot**, *Cu, Mn , As*
Marine	**Cl^-, Na,** *Cu*

4.3.4.2. PMF

4.3.4.2.1 Components and data for analysis

Twenty chemical species analyzed in PM_{10} at MSC were selected for the PMF analysis according to their signal to noise ratio (S/N), the % of data over the detection limit (%>DL) and the errors associated to each measurement (explained in the methodology chapter, Table 4.3.14). A total of 110 valid cases were used for the analysis.

Table 4.3.14. Mean concentration for values over the detection limit (Mean>DL), error (%error), signal to noise ratio (S/N) and proportion of values over the detection limit (%>DL) for the main elements used in the PMF analysis measured in PM_{10} at MSC.

	Mean>DL (µg m^{-3})	% error	S/N	%>DL	Selected
Ctot	3.2828	91	2.9	75	X
Al	0.2326	198	4.6	65	X
Ca	0.5950	62	13.0	86	X
K	0.1524	58	6.4	86	X
Na	0.3215	151	3.1	68	X
Mg	0.2078	46	15.5	86	X
Fe	0.1676	23	26.0	100	X
SO_4^{2-}	2.1978	23	94.7	100	X
NO_3^-	1.2121	25	56.9	100	X
Cl^-	0.1265	992	3.4	43	X
NH_4^+	0.6337	29	75.8	99	X
Li	0.0003	1687	5.6	63	X
Ti	0.0160	400	19.5	95	X
V	0.0023	128	6.7	81	X
Cr	0.0019	1475	2.6	51	
Mn	0.0072	156	33.4	93	
Co	0.0002	533	2.0	34	
Ni	0.0018	1439	2.4	49	
Cu	0.0036	2894	2.0	52	
Zn	0.0500	38345	1.1	6	
As	0.0003	214	4.4	67	X
Rb	0.0004	32	14.9	98	X
Sr	0.0028	1804	4.4	62	X
Cd	0.0001	453	1.5	39	
Sn	0.0014	2058	1.4	2	
Sb	0.0007	1573	1.2	3	
La	0.0002	120	3.0	79	X
Ce	0.0005	219	4.4	72	X
Pb	0.0020	32	11.3	99	X

4.3.4.2.2 Identification of emission sources

Source identification and quantification of PM_{10} at MSC was carried out with the PMF model, finding different results than obtained with the PCA.

The most robust solutions were obtained for 3 factors. The main sources identified in PM_{10} were representative of a rural environment without direct anthropogenic emissions: African dust outbreaks, secondary aerosols and a marine and dust resuspension mixed source (sea spray mixed with local crustal elements). The source profiles for the PMF solutions obtained are shown in Figure 4.3.22, together with the explained variances, and a summary of the factors identified is shown in Table 4.3.15.

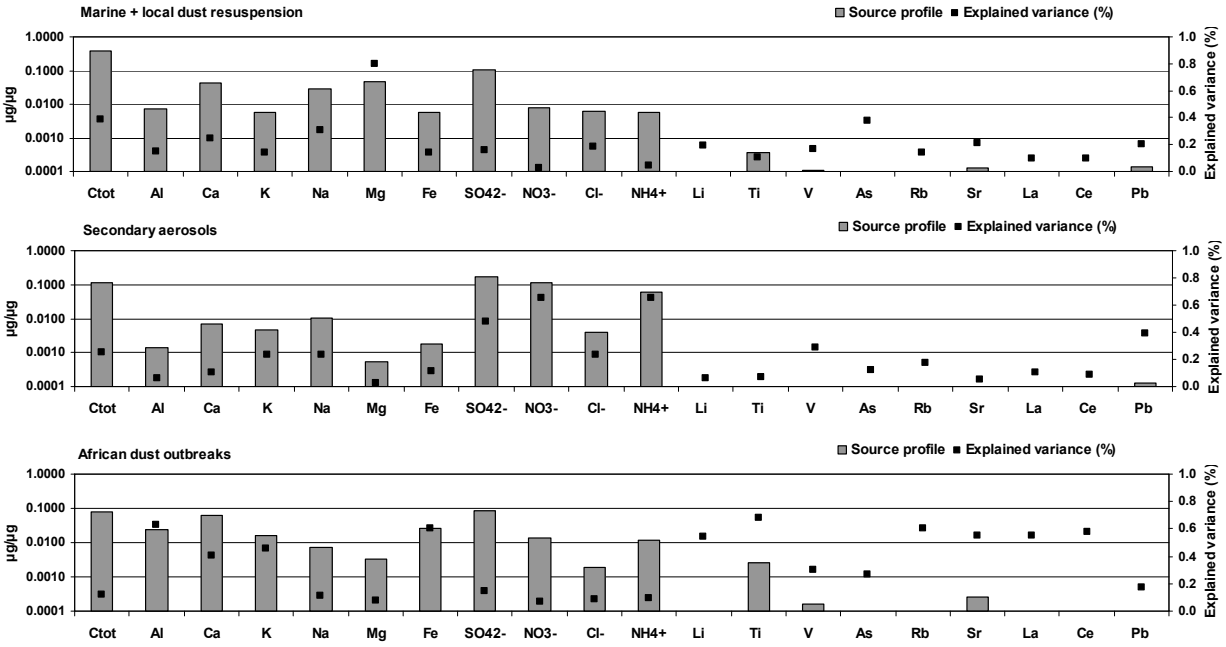

Figure 4.3.22. Source profiles for PMF solutions in PM_{10} for MSC. Explained variance for each element selected.

Table 4.3.15. Factors identified by the PMF model for PM_{10} at MSC. Elements with explained variance >0.5 are in bold letters and elements with variance <0.5 are in italics.

Marine + local dust resuspension	**Mg,** *Ctot, Na, Cl⁻, Ca, SO_4^{2-}, As, Sr, Pb*
Secondary aerosols	**SO_4^{2-}, NO_3^-, NH_4^+,** *Ctot, Cl⁻, V, Pb*
African dust outbreaks	**Al, *K*, Fe, Li, Ti, Rb, Sr, La, Ce,** *Ca, Ctot, V, As*

Marine + local dust resuspension: This factor is a mixed source of marine aerosols with mineral aerosols originated from local dust resuspension processes. The main

tracers of this source were elements from sea spray (Na, Cl^-) and elements with a crustal origin, mainly Mg, Ca, Sr, As and total carbon. These elements are probably associated to local dust resuspension processes because the mineralogical composition of the area of the MSC site is mainly calcite and dolomite (calcium and magnesium carbonates). The local dust resuspension is associated to marine aerosols probably because Atlantic and regional recirculation episodes account for significantly high levels of mineral dust and sea spray. Especially, intense Atlantic episodes transporting air masses charged with sea spray are associated to high wind speeds that probably favour also local resuspension. In addition, regional recirculation episodes reaching the MSC site by the effect of mountain breezes may also contribute to local dust resuspension, and recirculation of air masses around the region may also increase their sea spray content.

Inorganic secondary anthropogenic aerosols: The main tracers of this source were inorganic ions as SO_4^{2-}, NO_3^- and NH_4^+, characteristic of aged air masses. This factor also included total carbon (probably because of the presence of secondary carbonaceous aerosols) and other anthropogenic pollutants as Cl^-, V and Pb.

African dust outbreaks: This factor accounted for mineral matter from long-range transport of mineral dust during African dust outbreaks. The main tracers of this source were elements with a crustal origin as Al, K, Fe, Li, Ti, Rb, Sr, La, Ce and Ca. Total carbon was also associated to this factor, because it includes the mineral carbon from carbonates, but probably also because of some important forest fires that occurred in the Mediterranean simultaneously with African dust outbreaks during the summer in 2007, transporting both mineral dust and smoke to the site. V and As appear also in this factor as they are associated to alumino-silicate species.

4.3.4.2.3 Quantification of source contributions to PM_{10}

The correlation coefficient (r^2) between the measured and PMF-modelled concentrations was 0.87, and a 93% of the PM_{10} mass was simulated in the analysis (Figure 4.3.23).

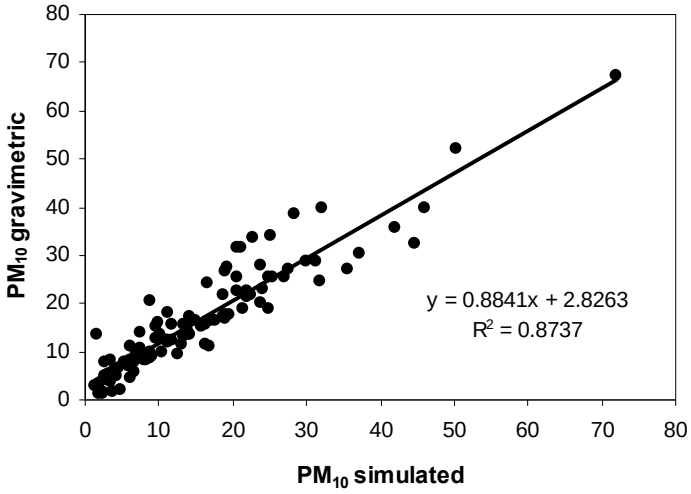

Figure 4.3.23. Correlation between PM_{10} simulated with PMF and gravimetric PM_{10} at MSC.

The main contributions for each factor obtained in the PMF analysis are shown in Figure 4.3.24. Secondary inorganic aerosols were the major contributors to PM_{10} at MSC (42% of the PM_{10} mass). African dust outbreaks were also an important contributing source (30% of the PM_{10} mass). Finally, the marine + dust resuspension aerosols contributed a 21% to the PM_{10} mass. The unaccounted fraction was a 7% of the total PM_{10} mass.

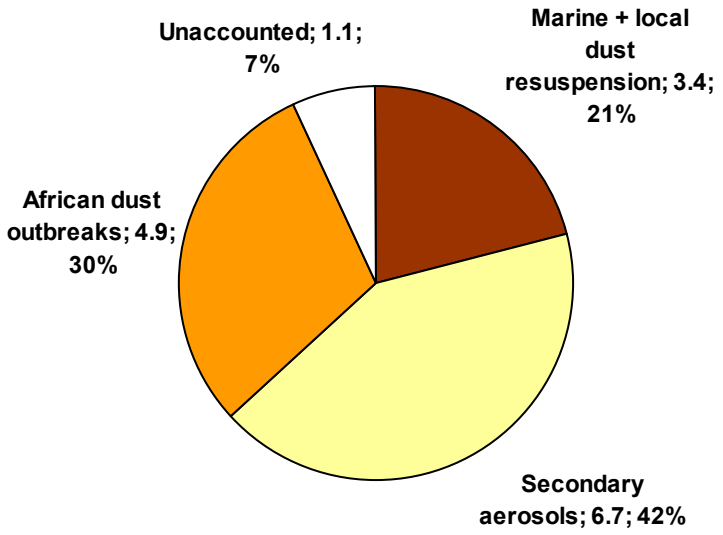

Figure 4.3.24. Average contribution of PM_{10} sources identified by PMF at MSC (µg m^{-3} and %).

The relative contributions of the different species analyzed to each of the factors identified in PM_{10} and $PM_{2.5}$ are shown in Figure 4.3.25, indicating the main sources of each component.

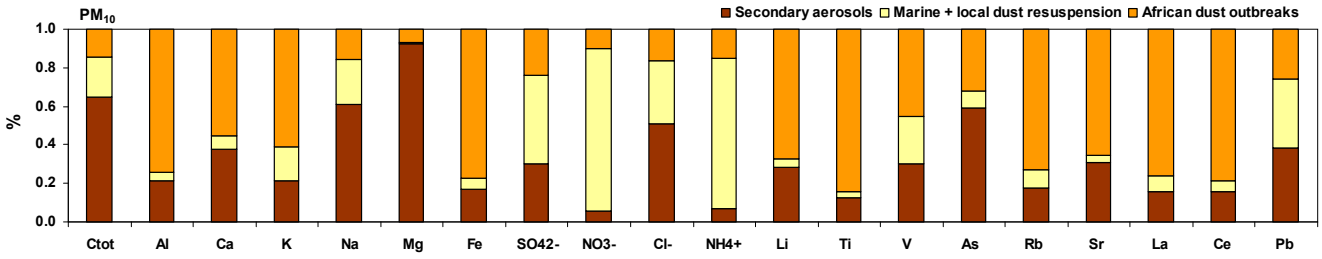

Figure 4.3.25. Relative contribution of each species to the factors identified by PMF in PM_{10} at MSC.

4.3.4.2.4 Seasonal evolution of emission sources

The seasonal evolution of the main daily contributions for each of the factors identified in PM_{10} at MSC is shown in Figure 4.3.26.

The African dust outbreak factor showed a marked seasonal evolution, with the highest contributions from July to September. This is a consequence of the seasonal character of African dust outbreaks (Escudero et al., 2005).

The factor accounting for marine aerosols and local dust resuspension also shows the highest contributions during the warmer months of the year. However, the difference between winter and summer is lower. This is the consequence of the occurrence of summer regional recirculation processes transporting sea spray aerosols to the site by mountain breezes that at the same time favour resuspension processes.

The variability of the secondary aerosol source along the year is less marked, given the different seasonal evolution of SO_4^{2-} and NO_3^-. The contribution of this factor is higher from June to September and much lower during November and December. This is a consequence of the site being exposed to regional pollution during the central hours of the day in the summer or isolated from the boundary layer height in winter. In addition, the formation of sulphate aerosols is favoured during the warmer months of the year as a consequence of an enhanced photochemistry and a low renovation of air masses (Millán et al, 1997; Querol et al., 1998a and 1999; Rodríguez et al., 2003). However, conversely to the other factors, the contribution of secondary aerosols is quite high also during February and March. This may be the consequence of some important pollution episodes occurring during these months, carrying polluted air masses to the site and increasing the levels of secondary aerosols (WAE and European air mass transport),

but also of the thermal stability of ammonium nitrate at lower temperatures (Harrison and Pio, 1983; Querol et al., 1998b, 2004a).

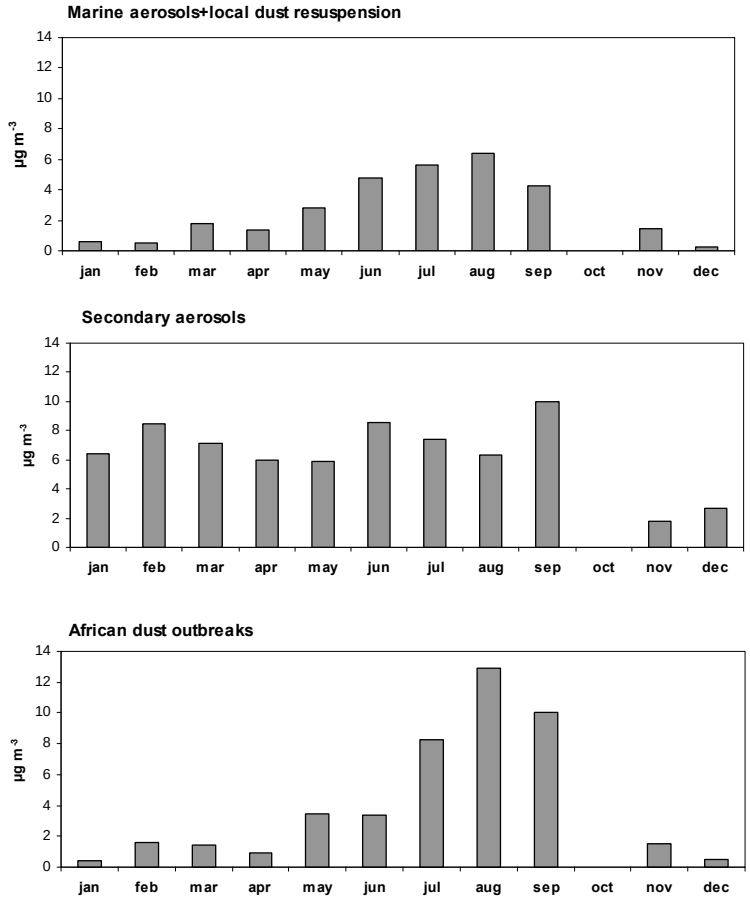

Figure 4.3.26. Seasonal evolution of the main daily contributions for each PM_{10} source identified by PMF at MSC.

4.3.4.3. Differences between PMF and PCA

Source apportionment was carried out for PM_{10} by means of Principal Component analysis (PCA) and Positive Matrix Factorization (PMF) techniques, obtaining different results. In the PCA, three factors explained the sources to PM_{10} at the CB: Mineral matter, a mixed factor with secondary aerosols + anthropogenic contribution and a marine aerosol source. In the PMF analysis also three factors were identified but in this case the mineral matter was separated into two factors: African dust outbreaks, secondary aerosols and a mixed factor accounting for local dust resuspension + marine aerosols.

4.3.5. Summary and conclusions

The Montsec monitoring site (MSC) is a continental background (CB) or remote site for the measurement of atmospheric aerosols. It is located in the Montsec mountain range, which is part of the pre-Pyrenean mountain ranges. The results obtained provide important information about CB aerosols and their long range transport at a continental scale. As a consequence of the results obtained during this work, the site will be integrated in the Network of Control and Surveillance of Air Quality of the *Direcció General de Qualitat Ambiental* of *the Conselleria de Medi Ambient* of the *Generalitat de Catalunya*.

The MSC station (1570 m.a.s.l.) is located outside of the boundary layer during the colder months of the year and therefore may not be affected by regional pollution events. However, from April to September, the boundary layer increases during the central hours of the day reaching the MSC site height. At these times the MSC site may be affected by regional pollution. Moreover, polluted air masses may be occasionally transported by mountain breezes to the site when the conditions are favourable, but this contribution is much lower than the observed at MSY.

Mean annual PM levels at MSC (16, 12 and 7 μg m^{-3} for PM_{10}, $PM_{2.5}$ and PM_1 during 2006-2007) were comparable to the levels calculated for the CB in the NE Iberian Peninsula (nocturnal PM levels at MSY RB site: 13, 10 and 8 μg m^{-3} for PM_{10}, $PM_{2.5}$ and PM_1) when considering the finer fractions. However, PM_{10} at MSC was higher, because of the site being affected by regional pollution during the summer and the higher elevation when compared with MSY, causing a more important impact of African dust episodes, usually transported at high altitudes. PM levels recorded at MSC are between the ranges of mean levels registered at other CB sites in Southern Europe, being markedly higher in Southern Europe, compared to Central and Northern European sites, especially the coarser fractions. This difference is a consequence of the proximity to the African continent that makes dust outbreaks frequent along the year and also a favoured dust resuspension in Southern Europe due to a drier climate. In addition, the variations of the boundary layer height during the warmer months sometimes allow regional pollution to reach the sites. Conversely, the differences in PM_1 are not significant between Southern and Central European CB sites.

Thus, high PM levels were observed for African dust outbreaks, that increased PM levels markedly, even exceeding the 50 μg PM_{10} m^{-3} daily limit, and also during summer regional recirculations. The rest of the episodes presented low levels in

general. The main difference between MSC and MSY sites was observed for the WAE episodes that increased markedly PM levels at MSY because of the transport of regional pollution by mountain breezes, while at MSC the levels remained generally very low because of the stagnation of pollutants at lower altitudes. However, in sporadic episodes, when the pollution episodes were persistent at MSY, regional pollution was also transported to the MSC site.

PM_{10} at MSC was mainly made up of organic matter (OM, 28%), mineral dust (25%), and secondary organic aerosols (SIA, 26%). Sulphate accounted for 14%, Nitrate for 8% and ammonium for 4% of the total mass. Marine aerosol was found at low levels at this site (2%). Elemental carbon was also found at low levels (2%) due to the absence of local combustion emissions. The unaccounted mass, mainly composed of structural and adsorbed water, accounted for a 17% of the total mass. PM_{10} composition at MSC was comparable to other CB sites in Southern and Central Europe, except for mineral and carbonaceous aerosols. Mineral matter levels at the CB in Europe decreased from south to north, depending on the proximity to the African continent and the frequency of African dust outbreaks. High carbonaceous levels were recorded at MSC probably because of the sampling of smoke from large forest fires in the Mediterranean Basin during the summer in 2007.

PM levels and speciation at MSC varied from day to day with the occurrence of successive air mass transport and meteorological episodes, showing a significant seasonal evolution. Most compounds measured in PM_{10} (OM+EC, mineral matter, sulphate, sea spray) registered higher levels during the warmer months, related to the higher frequency of African dust outbreaks, the lower precipitations, the higher soil resuspension processes and the enhanced photochemical formation of secondary aerosols. In addition, regional pollution reaches the site during the central hours of the day, as a consequence of the development of the boundary layer. The summer increase was much more pronounced in the coarse fraction ($PM_{2.5-10}$) than in the finer fractions ($PM_{1-2.5}$ and PM_1) because of the coarse size of mineral dust particles, but probably also because of the interaction of sulphate and nitrate with $CaCO_3$ and NaCl to form coarse sulphate and nitrate. During winter the levels of all PM size fractions and PM_{10} components measured were generally much lower, and the PM grain size was relatively fine.

Some episodes that had a very important incidence in the levels and composition of aerosols at MSC were detected and studied separately. Important African dust

outbreak episodes that transported dust simultaneously with smoke from important forest fires in the Mediterranean basin were recorded during the summer in 2007, strongly increasing PM levels and the levels of crustal elements and carbonaceous compounds markedly. Moreover, an intense winter anticyclonic episode and a European transport episode occurring during February 2006 and March 2007, respectively, transported fine pollutants (ammonium nitrate and sulphate) to the CB site, increasing clearly PM levels.

The results obtained show that the monitoring of the fractions PM_1 and PM_{1-10} may be a better approach for the study of the factors that control air quality than the current approach $PM_{2.5}$ and PM_{10}, as the fraction $PM_{1-2.5}$ reflects in a lesser way the impact of the factors described. Moreover, it seems clear that the processes controlling PM_1 are in many occasions different to the processes that control PM_{1-10} and may thus be important to monitor simultaneously both PM size fractions.

Source apportionment was carried out for PM_{10} by means of Principal Component analysis (PCA) and Positive Matrix Factorization (PMF) techniques, obtaining different results. In the PCA three factors explained the sources to PM_{10} at the CB: Mineral matter, a mixed factor with secondary aerosols + anthropogenic contribution and a marine aerosols source. In the PMF analysis also three factors were identified but in this case the mineral matter was separated into two factors: African dust outbreaks, secondary aerosols and a mixed factor accounting for local dust resuspension + marine aerosols. All sources presented a seasonal trend with higher contributions during the warmer months. However, the secondary aerosol contribution was also high during February and March, as a result of some intense episodes transporting polluted air masses to the MSC (WAE and European episodes).

5. DISCUSSION: URBAN, REGIONAL AND CONTINENTAL BACKGROUNDS

5. DISCUSSION: atmospheric aerosols at urban, regional and continental backgrounds in the Western Mediterranean Basin

The areas surrounding the Western Mediterranean basin (WMB) are characterised by an abrupt topography and complex atmospheric dynamics and meteorological processes that induce the recirculation of air masses and the consequent ageing and accumulation of pollutants at a regional scale (Millán et al.,1997 and 2000; Mantilla et al., 1998; Salvador, 1999; Toll and Baldasano, 2000; Soriano et al., 2001; Gangoiti et al., 2001; Rodríguez et al., 2002a and 2003; Palau, 2003; Jorba et al., 2004; Pérez et al., 2004; Jiménez et al., 2005, 2006 and 2007; Sicard et al., 2006). These recirculations together with a low rainfall, the high solar radiation intensity that favors atmospheric photochemical processes and the increased convective dynamics favoring local soil resuspension, induce a PM seasonal pattern, characterised by a high summer regional background (Bergametti et al., 1989; Querol et al., 1998a and b; Rodríguez et al., 2001 and 2002a; Viana et al., 2005). The high frequency of summer African dust outbreaks (Rodríguez et al., 2001; Viana et al., 2002; Escudero et al., 2005) also contributes to increase summer aerosol levels. These features together with the large atmospheric anthropogenic emissions produced in the Mediterranean coast (mainly arising from densely populated areas, large industrial estates, shipping, agriculture and forest fires, among others) give rise to a scenario with a complex aerosol phenomenology, with large anthropogenic and natural emissions, bulky secondary aerosol formation and transformation and intensive interaction of aerosols and gaseous pollutants.

Therefore, the sources, variability and properties of atmospheric PM urban areas in the WMB may not be fully understood without the characterization of the regional background aerosol. Moreover, information about the continental aerosol background may also be useful to understand the processes taking place at the regional background and to discriminate the possible influence of urban emissions in the regional background. Consequently, a detailed study of PM levels and composition measured simultaneously at urban, regional and continental backgrounds within the same region may be a useful approach to understand the sources, behaviour, transformation and transport patterns of tropospheric aerosols in this area.

Studies using data of simultaneous measurements performed at urban and rural background sites have already been carried out in Europe (Pakkanen et al., 2001;

Röösli et al., 2001; Lenschow et al., 2001; Querol et al., 2004a and b and 2008; Hueglin et al. 2005; Gerasopoulos et al., 2006; Ledoux et al., 2006; Lall et al., 2006; Charron et al., 2007; Yin and Harrison, 2008; Perrino et al., 2008). However, there is a lack of long time PM data from Southern Europe, with differentiated meteorological characteristics including the relevant impact of African dust outbreaks.

Lenschow et al. (2001) estimated the contribution of road traffic and other urban emissions (domestic, residential, industry, etc.), long range transported emissions, natural background or regional emissions by comparing a traffic site, an urban background site and a rural site in the Berlin area. To do this they assumed that the stations selected were considered representative of the type of site (traffic, urban or rural), the differences between the traffic and the urban background site were attributed to traffic emissions and the differences between the urban background and the rural site were attributed to sources emitted in the urban agglomeration. The application of this method to data on PM levels and speciation measured at different types of sites in the WMB may be an interesting approach to understand the main emission sources and processes influencing atmospheric aerosols in such a complex area.

In this direction, the monitoring of PM_{10} levels and chemical characterization was carried out simultaneously at three monitoring stations located in different environments at a regional scale (Figure 5.1): Montsec (MSC, continental background, 1570 m.a.s.l.), Montseny (MSY, regional background, 720 m.a.s.l., EUSAAR site) and Barcelona (BCN-CSIC, urban background, 68 m.a.s.l.). In order to interpret the variability of atmospheric aerosols at these three different scales the main meteorological and atmospheric scenarios affecting the WMB were also characterized, as different episodes may produce the recirculation and mixing of atmospheric pollutants at a regional scale (such as REG), isolate the continental and regional backgrounds (such as WAE), or impact with a different intensity at different heights (such as long range transport: NAF and EU).

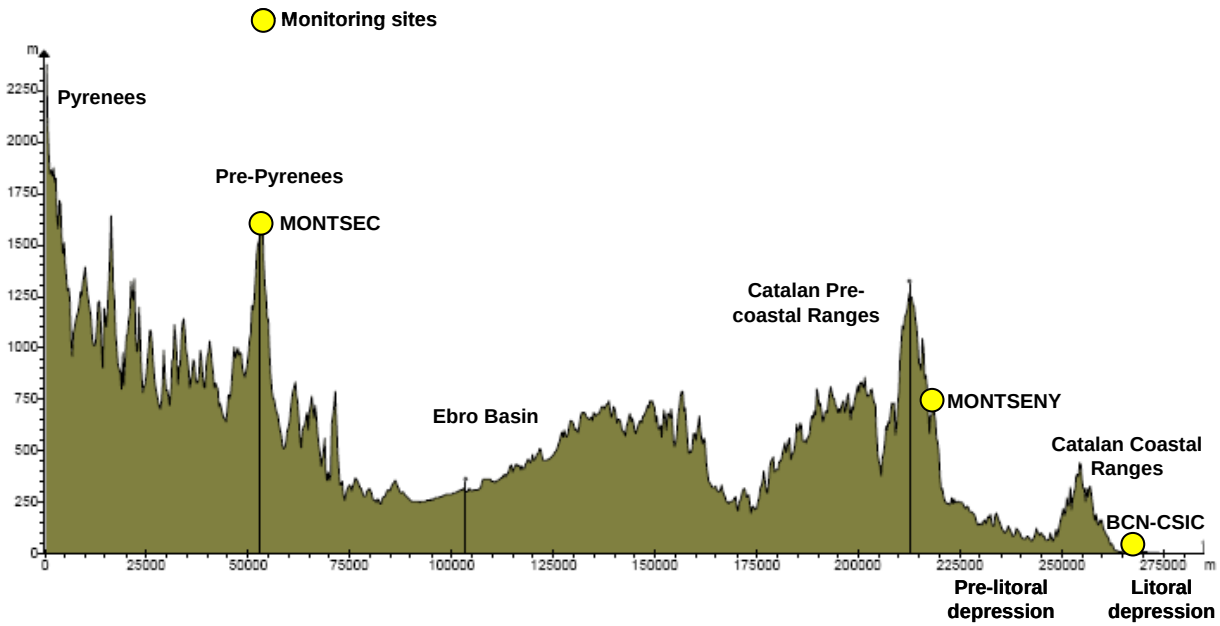

Figure 5.1. Vertical profile of the region of study and location of the three monitoring sites.

5.1. PM levels and speciation at the urban, regional and continental background in the WMB

5.1.1. PM levels

Mean daily PM levels measured at BCN, MSY and MSC during 2006 and 2007, as well as for days with African dust transport, are presented in Figure 5.2. Available simultaneous data were selected for the calculation of the mean daily PM_{10}, $PM_{2.5}$ and PM_1 levels (Table 5.1). Obviously, mean PM levels were much higher at BCN for all fractions, because of the important urban contribution to atmospheric aerosols. Unexpectedly, mean PM_{10} levels were higher at MSC than at MSY. PM_1 levels were higher at MSY, showing the higher influence of anthropogenic pollution on the regional background aerosols measured at this site. Conversely, $PM_{1\text{-}2.5}$ and $PM_{2.5\text{-}10}$ were higher at MSC, reflecting the important impact of African dust and local dust resuspension in the levels of the coarser atmospheric aerosols at this site. No significant differences were observed in the $PM_{2.5}$ fraction.

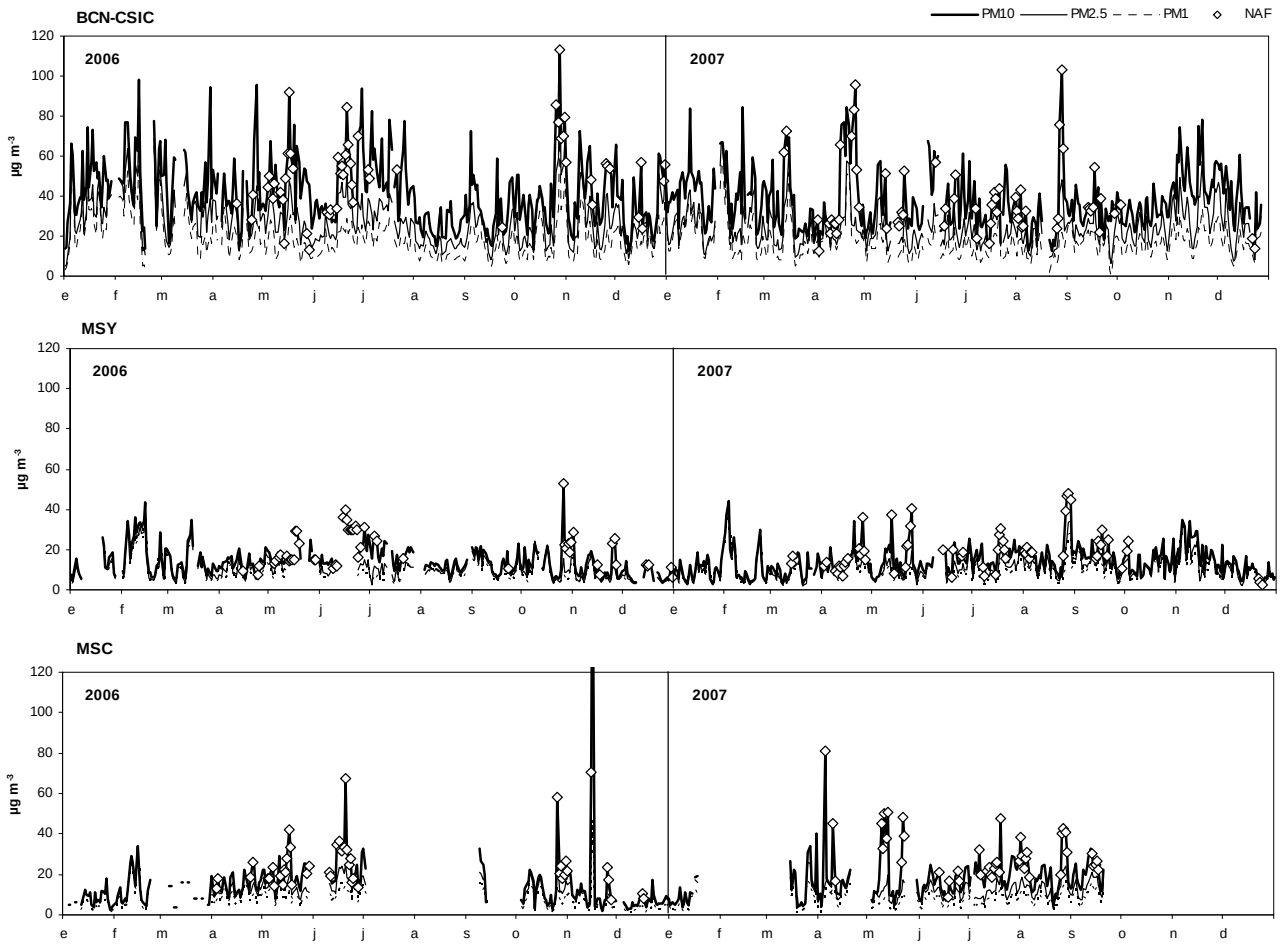

Figure 5.2. Mean daily PM_{10}, $PM_{2.5}$ and PM_1 levels recorded at BCN, MSY and MSC during 2006 and 2007. Days with African dust (NAF) influence are marked with rhombus.

Table 5.1. Mean daily PM_{10}, $PM_{2.5}$ and PM_1 levels and $PM_{1\text{-}2.5}$, $PM_{2.5\text{-}10}$ and $PM_{1\text{-}10}$ fractions recorded simultaneously at BCN, MSY and MSC during 2006 and 2007 during all days (total) and discounting the days with African dust influence (no-NAF). NAF contributions are calculated as the difference between total and no-NAF concentrations.

	Total						**no-NAF**					
	PM_{10}	**$PM_{2.5}$**	**PM_1**	**$PM_{1\text{-}2.5}$**	**$PM_{2.5\text{-}10}$**	**$PM_{1\text{-}10}$**	**PM_{10}**	**$PM_{2.5}$**	**PM_1**	**$PM_{1\text{-}2.5}$**	**$PM_{2.5\text{-}10}$**	**$PM_{1\text{-}10}$**
BCN	40.2	27.1	18.8	8.3	13.1	21.4	38.9	26.1	18.7	7.4	12.8	20.2
MSY	14.9	11.1	9.0	2.1	3.8	5.9	13.5	10.7	9.0	1.7	2.8	4.5
MSC	16.9	11.8	7.4	4.4	5.1	9.5	13.3	10.5	6.8	3.7	2.8	6.5

	NAF contributions					
	PM_{10}	**$PM_{2.5}$**	**PM_1**	**$PM_{1\text{-}2.5}$**	**$PM_{2.5\text{-}10}$**	**$PM_{1\text{-}10}$**
BCN	1.3	1.0	0.1	0.9	0.3	1.2
MSY	1.4	0.4	<0.1	0.4	1.0	1.4
MSC	3.6	1.3	0.6	0.7	2.3	3.0

Mean PM levels recorded at MSC were quite high when considering that this site is situated at 1570 m.a.s.l., isolated from PM sources, and therefore it should not be affected by regional or local pollution. PM_{10} levels measured at MSC are sometimes even higher than PM levels recorded at MSY (situated at 720 m.a.s.l.), especially when considering summer months, being more important the increase observed for the coarser fractions. However, the main sources behind these differences are probably not anthropogenic and may be more related to natural PM contributions as long-range dust transport from Africa, and local or regional dust resuspension, but also to the location of the monitoring sites. The main factors explaining this behaviour will be outlined:

1. The MSC site is more intensely affected by African dust outbreaks than MSY and BCN. African dust outbreaks reach the Iberian Peninsula transporting dust at different heights in the atmosphere depending on the meteorological scenario producing the episode (Escudero et al., 2005). In most of these episodes African dust is preferentially transported over Southern Europe in atmospheric layers from 1000-5000 m.a.s.l., being highest the impact on surface PM levels at monitoring stations located at higher altitudes. The MSC site may then be more intensively affected by African dust outbreaks. This may be at the origin of the higher coarse PM levels measured at MSC. In many of these episodes, when African dust was detected, much higher PM_{10} levels were frequently recorded at MSC than at MSY, and in some occasions even higher than at BCN.
2. The MSC site is situated very often outside of the boundary layer height during the colder months of the year (October to March) and thus it is rarely affected by regional pollution and recirculation processes. However, during the warmer months (April to September), the site enters the boundary layer during the central hours of the day, coinciding with its maximum development, and the highest temperatures and wind speed. This leaves the site exposed to regional pollution and summer recirculation processes at a regional scale, increasing importantly PM levels at the site during the summer, in occasions registering even higher levels than at the MSY site. Also, recirculation processes inject polluted air mass layers at a considerable altitude, reaching the MSC site.
3. The MSC site was affected by road works in the area for some periods during the year 2007, leaving areas with uncovered land which may have favoured local dust resuspension during the warmer months, when the precipitation was lower and the land was drier.

4. The MSY site is situated in an area covered by vegetation, with a lower local resuspension influence than the MSC site, which is situated in a dryer area with poor vegetation coverage. In addition, MSC may be affected by sporadic dust transport at a regional scale from resuspension processes occurring in the Ebro Valley.

After discounting the days with African dust influence to the datasets (Table 5.1), the levels of PM_{10} and $PM_{2.5}$ decreased at MSC, but at MSY the decrease was not very significant. Difference between total concentrations and levels when discounting the NAF episodes enabled us to quantify the NAF contributions (Table 5.1). In MSC, with a low anthropogenic influence, this contribution has been estimated in 3.6, 1.3, and 0.6 for PM_{10}, $PM_{2.5}$ and PM_1, respectively. Therefore, 64% of the NAF contribution is accumulated in $PM_{2.5-10}$, 19% in $PM_{1-2.5}$ and 17% in PM_1. This contribution is clearly lower in MSY and BCN, where the impact in PM_1 is not evident. These results illustrate the important influence that African dust outbreaks have on continental background aerosols in Southern Europe when measured at high altitudes (MSC).

The fact that PM_1 measured at MSY is higher than PM_1 at MSC demonstrates the higher anthropogenic emissions reaching MSY, due to its proximity to urban agglomerations and industrial estates. Transformation of aerosols during transport may also be behind the higher difference in PM_1 between MSY and MSC and the lower differences in $PM_{2.5}$ and PM_{10} (thus $PM_{1-2.5}$ and $PM_{2.5-10}$). PM_1 may grow to coarser fractions during transport because of the interaction between particles and other gaseous pollutants.

The seasonal variability of $PM_{2.5-10}$, $PM_{1-2.5}$ and PM_1 levels measured at BCN, MSY and MSC is shown in Figure 5.3 (mean daily variability for each month) and Figure 5.4 (monthly means after discount of the days with African dust influence). $PM_{2.5-10}$ and PM_1 levels present a marked seasonal trend, while the levels of $PM_{1-2.5}$ are more regular along the year, especially at MSY and MSC. A similar seasonal trend in the levels of all PM fractions considered was observed for MSY and MSC, showing the influence of atmospheric episodes and regional processes on the levels of atmospheric aerosols at both sites, independently of local emissions. However PM_1 daily cycles were more marked at MSY and $PM_{2.5-10}$ cycles at MSC. PM_1 levels were always higher at MSY than at MSC, increasing with mountain breezes carrying pollutants during the day, but $PM_{1-2.5}$ levels were higher at MSC, as it was already observed above. $PM_{2.5-10}$ levels were higher during the warmer months of the year at both sites. $PM_{2.5-10}$ levels

were higher at MSY than at MSC during the winter, but during the warmer months coarse PM levels at MSC increased, even when discounting days with African dust influence, due to the favoured resuspension processes and regional dust transport to the site. $PM_{2.5-10}$ levels were very affected by road dust resuspension by traffic at BCN, increasing markedly during the day. High levels were observed during the summer, decreasing during august and September because of the effect of road traffic reduction by holidays and the frequent precipitations, but also during winter, due to the intense pollution episodes recorded during these months, when anticyclonic episodes and the lack of precipitation favour the accumulation of pollutants in the urban area. The PM_1 fraction presents higher levels during winter at the urban site. In MSY, high PM_1 levels were registered during February and September-October, due to regional pollution accumulated during anticyclonic episodes and reaching the site when breezes developed. However this evolution is less clear at MSC, where the PM_1 daily evolution is less marked.

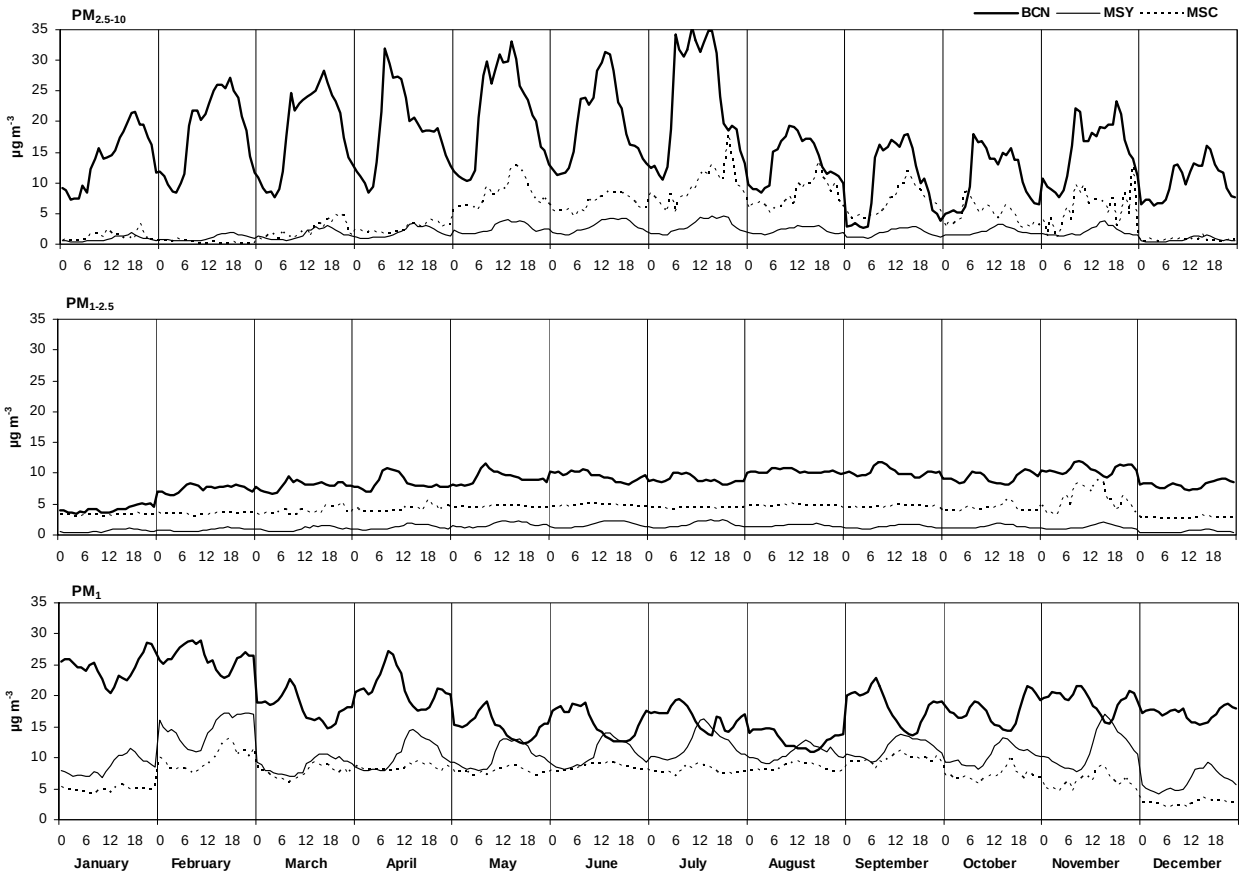

Figure 5.3. Seasonal variability of the mean daily variation of $PM_{2.5-10}$, $PM_{1-2.5}$ and PM_1 levels measured at BCN, MSY and MSC during 2006 and 2007.

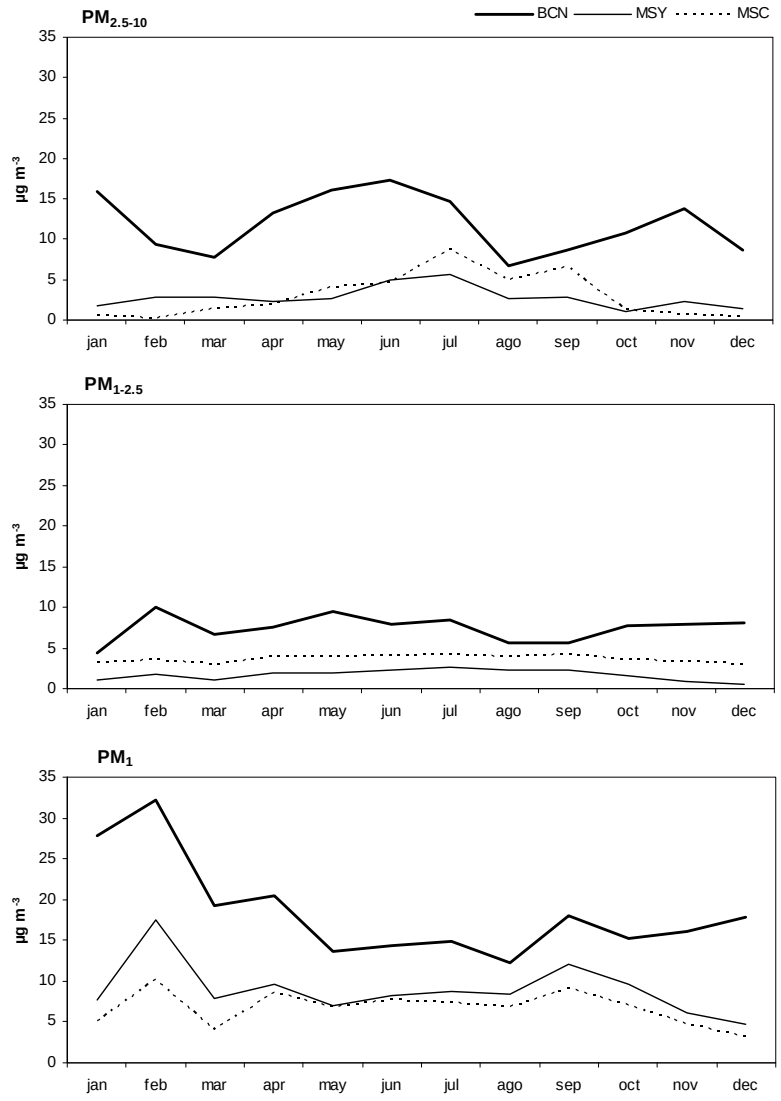

Figure 5.4. Seasonal variability of $PM_{2.5-10,}$ $PM_{1-2.5}$ and PM_1 components measured simultaneously at BCN, MSY and MSC during the period November 2005-November 2007 after discounting African dust episodes.

5.1.2. PM speciation

Mean levels of major components measured in PM_{10} simultaneously at BCN-CSIC, MSY and MSC from November 2005 to November 2007, for all days and excluding days with African dust influence (no-NAF) are presented in Table 5.2. Simultaneous sampling in this case is defined as sampling periods where samples were available at the three sites and were collected at a similar sampling rate. This approach permits to account for a higher number of samples, as sampling days at the three sites were not always coincident.

As expected, the highest levels of all components were observed at Barcelona, because of the important urban anthropogenic emission sources and their contribution to atmospheric aerosols (especially carbonaceous compounds and gaseous precursors). Mineral matter has also a very important contribution due to dust resuspension by road traffic and construction works at the urban site. Moreover, sea spray was also higher at the urban site due to its proximity to the coast. MSY presented higher levels of all components than MSC, except for the mineral matter and EC. However, the difference was not very significant. This is the consequence, as explained above, of some factors that contribute to increase PM levels at MSC: 1) Long range transport episodes (African dust outbreaks and some European episodes transported at high levels in the atmosphere), 2) Boundary layer height variability in the summer, 3) Road works at MSC and 4) Poor vegetation coverage.

When subtracting the days with African dust influence, the levels of mineral matter decreased at all sites, but in a higher proportion at MSC, remaining lower than the levels measured at MSY. The levels of OM+EC at MSC also decreased when discounting African dust outbreaks. The reason for this is the important forest fires that occurred in the Mediterranean area during the summer in 2007, simultaneously with intense African dust outbreaks that transported air masses in higher atmospheric levels. It should be also mentioned the influence of the NAF episodes in the levels of sulphate in Barcelona, and in a lower proportion in MSY and MSC.

Table 5.2. Major components measured in PM_{10} (µg m^{-3}) simultaneously at BCN-CSIC, MSY and MSC from November 2005 to November 2007 for all days and excluding days with African dust influence (no-NAF).

	Mean			**no-NAF**		
	BCN	**MSY**	**MSC**	**BCN**	**MSY**	**MSC**
N	91	99	80	69	82	69
µg m^{-3}	44.8	15.2	13.5	42.7	14.6	12.1
OC	4.3	2.1	1.8	4.8	2.1	1.6
EC	2.1	0.2	0.3	2.7	0.2	0.2
OM+EC	10.2	4.7	4.1	10.4	4.6	3.6
SO_4^{2-}	4.6	2.4	1.8	4.0	2.2	1.7
NO_3^-	5.6	1.7	1.1	5.9	1.9	1.1
NH_4^+	1.3	0.9	0.5	1.3	0.9	0.5
SIA	11.4	5.0	3.3	11.2	5.0	3.3
Mineral matter	14.2	3.2	3.5	12.9	2.8	2.4
Sea spray	2.1	0.5	0.3	2.1	0.5	0.2
Unaccounted	6.4	2.9	2.3	5.6	2.9	2.3

African dust contribution to mineral matter levels may be calculated as the difference between the crustal loads for the total period and for the days without African dust influence. Accordingly, the African dust contribution to mineral matter in PM_{10} was 1.3 µg m^{-3} at BCN, 0.5 µg m^{-3} at MSY and 1.1 µg m^{-3} at MSC. If we apply the same method for PM levels determined by gravimetry (same period as the speciation data), the African contributions are 2.1 µg PM_{10} m^{-3} at BCN, 0.6 at MSY and 1.4 at MSC. The difference observed between the increase in PM_{10} levels and the increase in mineral matter levels attributed to African dust outbreaks may be due to the formation of secondary aerosols favoured by the presence of high concentrations of mineral dust (condensation of precursor gases on dust particle surfaces, Querol et al., 2004a and b; Putaud et al. 2004; Alastuey et al., 2005). This mechanism explains the significant difference determined for BCN (0.8 µg m^{-3}). Al MSY and MSC, this difference is clearly lower (0.2 µg m^{-3} in MSY and 0.3 µg m^{-3} in MSC), and could be related to the long-range or regional transport of polluted air masses together with mineral dust, such as smoke from forest fires or secondary aerosols.

The representation of the chemical composition of PM_{10} in a ternary diagram in ppm (µg/g of PM_{10} sample, Figure 5.5) shows that in the samples of BCN there is a higher proportion of elements derived from traffic emissions (EC) and dust resuspension processes (Fe, Ca). Sea spray (Na and Cl^-) also present a higher proportion in BCN samples because of the proximity to the coast. Secondary aerosols (ammonium sulphate and nitrate) are more equilibrated among the three sites. However, there is a little more nitrate in BCN (derived from traffic emissions) and a little more ammonium and sulphate in MSY (from the regional background). The proportion of OM was a little lower at MSC than at the other sites. Other crustal elements as K and Al_2O_3 were similar at all sites and Mg was a little higher at MSC, probably derived from the mineralogical composition of the area (calcites and dolomites).

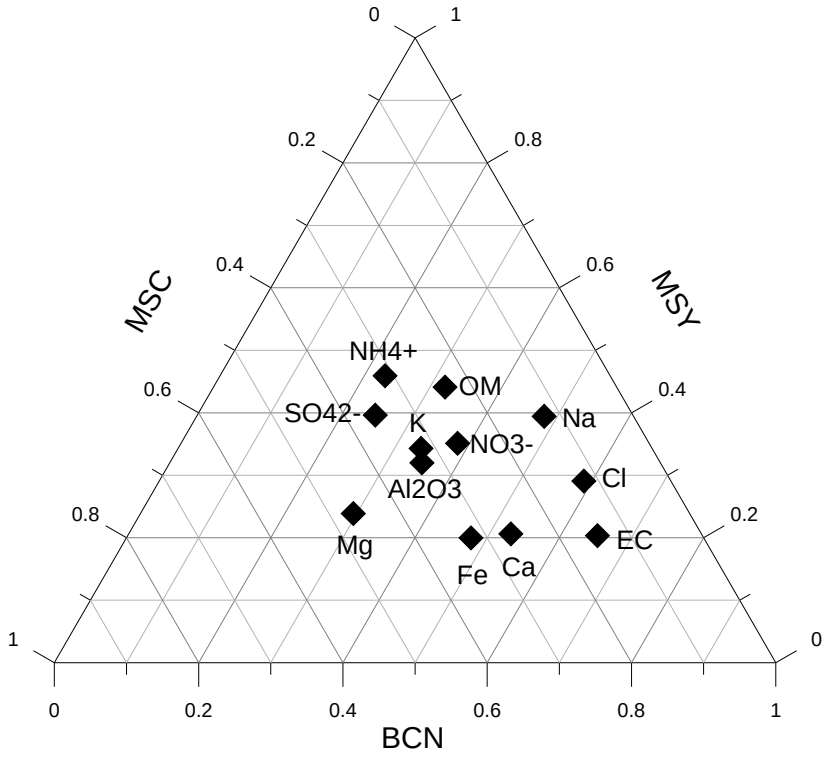

Figure 5.5. Ternary diagram showing major composition in ppm (µg/g) in PM_{10} measured simultaneously in BCN, MSY and MSC during the November 2005-November 2007 period, after excluding days with African dust influence.

Mean levels of trace elements measured simultaneously in BCN, MSY and MSC after excluding days with African dust influence are presented in Table 5.3. As expected, levels of all trace elements were much higher at BCN urban site. For some metals, such as Zn, Cu, Pb, Sb, Sn and Cr, the proportions measured in PM_{10} are much higher at the urban than at the regional site. These elements have an anthropic origin (traffic or industrial emissions). For other elements, such as Ti, P, Sr, Rb, Ce and La, even presenting higher levels in Barcelona, the differences are not so important between BCN and MSY. This fact is attributed to their natural or regional origin (associated with a crustal component). The levels of most elements decreased from MSY to MSC, with the exception of Mn, Zn and U, with presented higher levels at MSC than MSY. However, the differences are not very important for most elements, because of the important influence of the factors described above during the warmer months of the year, when the regional pollution reaches the site and local dust resuspension processes were favoured.

Table 5.3. Mean levels of trace elements in PM_{10} (ng m^{-3} and ppm) measured simultaneously in BCN, MSY and MSC during the November 2005-November 2007 period, after the discount of days with African dust influence.

	ng m^{-3}			ppm (µg/g)		
	BCN	**MSY**	**MSC**	**BCN**	**MSY**	**MSC**
Li	0.5	0.2	0.1	13	12	10
P	24	11	7	565	737	558
Ti	37	11	8	875	745	628
V	10	3	1	239	220	107
Cr	6	1	1	135	72	68
Mn	19	4	5	441	260	408
Co	0.3	0.1	0.1	7	6	6
Ni	4.5	1.4	0.9	107	94	78
Cu	86	3	2	2013	226	128
Zn	101	10	11	2370	712	947
As	0.9	0.3	0.1	20	17	11
Se	0.7	0.2	0.2	16	17	13
Rb	1.1	0.4	0.2	27	24	20
Sr	5.3	1.1	0.9	125	77	77
Cd	0.4	0.1	0.1	8	6	5
Sn	7.2	0.7	0.3	170	50	23
Sb	5.3	0.4	0.1	125	29	10
Ba	31	7	7	717	469	579
La	0.4	0.1	0.1	9	8	8
Ce	0.9	0.3	0.2	20	17	17
Tl	0.21	0.03	0.02	5	2	2
Pb	23.5	3.7	1.5	551	252	127
Bi	0.42	0.06	0.03	10	4	2
Th	0.17	0.05	0.04	4	4	3
U	0.10	0.04	0.05	2	3	4

The representation of trace elements contents in a ternary diagram in ppm (µg/g of PM_{10}, Figure 5.6) shows that the highest proportion of trace elements with an anthropic origin, such as Sb, Sn, Cu, Pb, Bi, Tl, Zn and Cr, tracers of industrial or road traffic emissions, is registered in BCN. Elements with a natural origin, such as crustal elements (Rb, Ti, Ba, Sr, Th, Li, Mn and P) are found at approximately at a similar proportion at all sites. V and Ni, tracers of fuel oil combustion and related to the regional background, are also found in similar proportions at all sites.

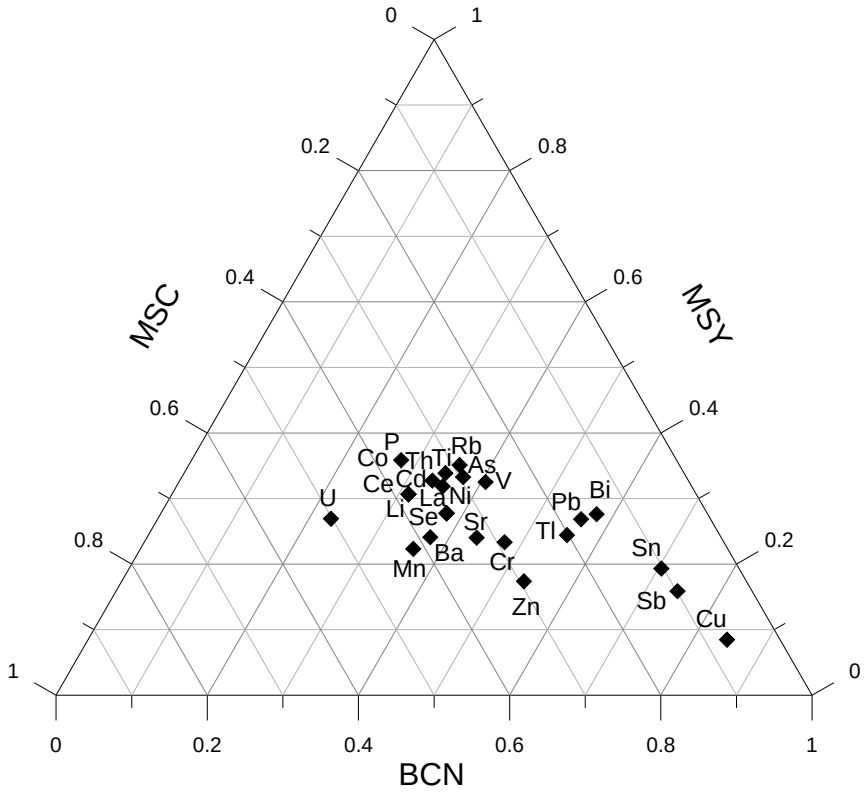

Figure 5.6. Ternary diagrams showing trace elements in ppm (µg/g) in PM_{10} measured simultaneously in BCN, MSY and MSC during the November 2005-November 2007 period, after the discount of days with African dust influence.

Seasonal variability of major components of PM_{10} at BCN, MSY and MSC (Figure 5.7) showed that the higher differences between the levels of most components measured at the urban site and the rural sites were observed during the winter months, when anticyclonic stability favours the accumulation of pollutants at BCN (especially OM+EC, nitrate and ammonium). During summer the differences between the urban and the rural sites were reduced. Summer regional recirculations favour the mixing of pollutants in the region. As a consequence, the levels of OM+EC, nitrate and ammonium are lower at the BCN area. Conversely, OM+EC levels increase at the rural sites, probably because of the regional recirculation of pollutants, occurrence of forest fires during the summer in the Mediterranean area, but also to the enhanced biogenic emissions. With the exception of the month of August at Barcelona (usual holiday month in the region), mineral matter levels increase at all sites, because of the favoured conditions for dust resuspension processes (enhanced breezes and low precipitation rates). Sulphate also increases during the summer at all sites, as it is highly influenced by photochemistry. However, nitrate decreases at all sites during the warmer months, because of the thermal instability of ammonium nitrate. In contrast, ammonium levels decrease during the summer in BCN and MSY, but at MSC the levels increase, due to regional pollution reaching the site. It is important to highlight the high difference between nitrate and

sulphate at the urban site with respect to the regional and continental sites, especially during the colder months. The fact that levels are much higher at BCN may indicate that the formation of SIA occurs mainly in situ from traffic gaseous precursors (ammonia and nitrogen oxides) when atmospheric stability is more important. This is possible considering the high emissions of NH_3 by traffic exhausts and the fact that diesel vehicle emissions result in a high NO_2/NO_x ratio. In the case of sulphate, the enhanced formation of ammonium sulphate at the urban background may be due to the nearby sources of SO_2 from shipping emissions and other disperse urban sources. Finally, sea spray levels are higher during the summer months as a consequence of enhanced sea breezes in the area.

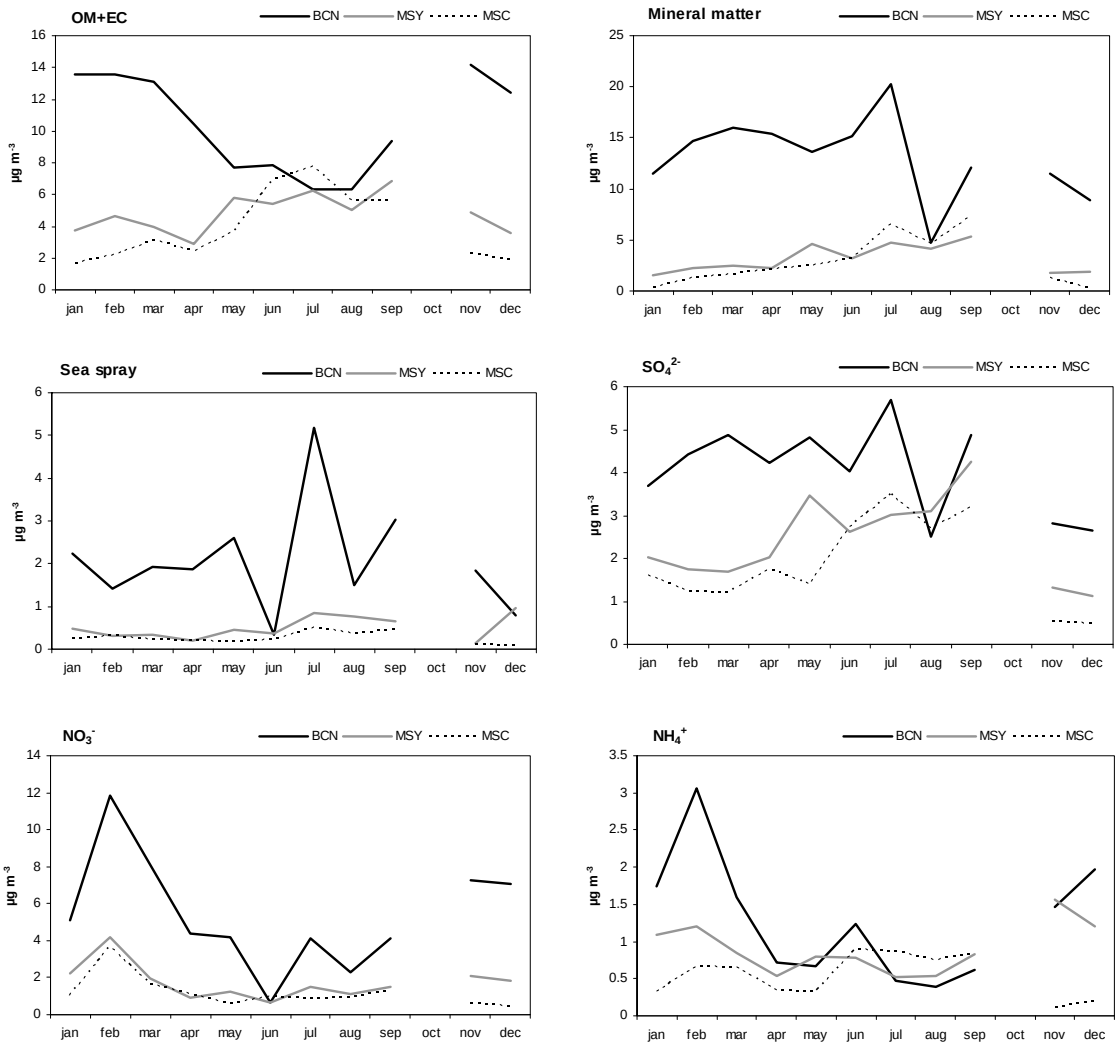

Figure 5.7. Seasonal variability of major PM_{10} components measured simultaneously at BCN, MSY and MSC during the period November 2005-November 2007, after discount of African dust episodes.

5.2. Estimation and quantification of the continental background and the regional and urban contributions to ambient PM in the WMB

The methodology proposed by Lenschow et al. (2001) was applied to the dataset obtained at BCN, MSY and MSC sites, in order to estimate the contribution of the continental background and the regional and urban increments to the aerosol load at the urban site. To do this estimation, the following assumptions were made: a) the sites selected are representative of the type of background (urban, rural and continental); b) the aerosol load at the urban site is a superposition of urban local emissions, regional recirculation of air masses and long-range transport of aerosols; and c) the differences between the urban and the regional background site may be attributed to the influence of urban emissions (emission sources from the urban agglomeration, such as road traffic and other anthropogenic sources), and the differences between the regional and continental background to the regional contribution to the aerosol load.

However, this methodology was initially addressed to quantify road traffic and urban contributions to PM in air quality studies in Northern Europe. The WMB has a complex atmospheric behavior when compared with Northern Europe, with a higher frequency of synoptic winds and rainfall, and the direct application of this methodology to the Mediterranean area might be difficult. Nevertheless, the methodology was applied to the dataset obtained in this study, taking these differences in consideration in the attempt to estimate the continental background and the regional and urban contributions to the bulk aerosols in the region. The application of this method may be helpful to better understand the aerosol phenomenology in the WMB and the differences observed with Northern European studies.

The following points are important and may be taken in account in the discussion in order to investigate how these factors affect the urban, regional and continental backgrounds in the WMB:

a) Air mass transport between the sites: the different backgrounds considered are not closed compartments, as transport of air masses occurs at a regional scale. Accordingly, urban air pollution may influence the regional background due to the proximity and the transport of pollutants at a regional scale. In addition, regional pollution may also reach the continental background.

b) Transformation processes of atmospheric aerosols during transport: aerosols may undergo changes of particle size or chemical composition by condensation, volatilization or agglomeration processes and chemical reactions.
c) Different local sources and atmospheric processes may prevail in different types of backgrounds: Sites situated at higher altitudes may be affected by long-range transport (for example African dust transport) at a different extent than lower altitudes. In addition, local processes, such as dust resuspension or other local emissions may differ from site to site.

5.2.1. PM levels

The urban, regional and continental contributions to PM_{10}, $PM_{2.5}$ and PM_1, and the fractions $PM_{1\text{-}2.5}$, $PM_{2.5\text{-}10}$ and $PM_{1\text{-}10}$ in the region of study were calculated using the simultaneous PM data recorded during the years 2006 and 2007 at BCN, MSY and MSC, after excluding days with African dust influence (Table 5.4). The calculations were made as follows: the urban background contribution was calculated as the difference between the simultaneous data measured at BCN (urban site) and MSY (regional site); the regional background contribution was calculated as the difference between levels measured at MSY and MSC (continental background) and the continental contribution was considered as the levels measured at MSC site.

Table 5.4. Mean levels of PM_{10}, $PM_{2.5}$ and PM_1 and $PM_{1\text{-}2.5}$, $PM_{2.5\text{-}10}$ and $PM_{1\text{-}10}$ fractions recorded simultaneously at BCN, MSY and MSC during the period 2006-2007, after removal of African dust episodes. Calculated urban, regional and continental contributions to mean levels of PM_{10}, $PM_{2.5}$ and PM_1 and $PM_{1\text{-}2.5}$, $PM_{2.5\text{-}10}$ and $PM_{1\text{-}10}$ fractions.

	PM_{10}	**$PM_{2.5}$**	**PM_1**	**$PM_{1\text{-}2.5}$**	**$PM_{2.5\text{-}10}$**	**$PM_{1\text{-}10}$**
BCN	38.9	26.1	18.7	7.4	12.7	20.2
MSY	13.5	10.7	9.0	1.8	2.8	4.5
MSC	13.3	10.5	6.8	3.7	2.8	6.5
Urban	25.3	15.4	9.7	5.7	10.0	15.6
Regional	0.3	0.3	2.2	-1.9	0.0	-1.9
Continental	13.3	10.5	6.8	3.7	2.8	6.5

The quantification of the regional background PM levels presented a few problems, as the mean PM_{10} and $PM_{2.5}$ levels measured at MSC and MSY for the sampling period considered were very similar, even after excluding days with African dust influence. In order to account for the factors rising coarse PM levels at MSC, the contributions of aerosols to the three backgrounds of study considered have been calculated for the

winter and summer months separately. The results of the calculations made with this method are presented in Table 5.5 and Figure 5.8.

Table 5.5. Winter (October to March) and summer (April to September) mean levels of PM_{10}, $PM_{2.5}$ and PM_1 and $PM_{1\text{-}2.5}$, $PM_{2.5\text{-}10}$ and $PM_{1\text{-}10}$ fractions recorded simultaneously at BCN-CSIC, MSY and MSC during the period 2006-2007, after removal of African dust episodes. Urban, regional and continental contributions to mean levels of PM_{10}, $PM_{2.5}$ and PM_1 and the $PM_{1\text{-}2.5}$, $PM_{2.5\text{-}10}$ and $PM_{1\text{-}10}$ fractions during winter and summer.

	Winter						Summer					
	PM_{10}	**$PM_{2.5}$**	**PM_1**	**$PM_{1\text{-}2.5}$**	**$PM_{2.5\text{-}10}$**	**$PM_{1\text{-}10}$**	**PM_{10}**	**$PM_{2.5}$**	**PM_1**	**$PM_{1\text{-}2.5}$**	**$PM_{2.5\text{-}10}$**	**$PM_{1\text{-}10}$**
BCN	40.5	28.8	21.6	7.2	11.7	18.9	37.4	23.8	16.1	7.7	13.7	21.4
MSY	12.2	10.3	8.9	1.3	1.9	3.2	14.7	11.1	9.0	2.1	3.5	5.7
MSC	9.6	8.9	5.6	3.3	0.7	3.9	16.3	11.8	7.8	4.0	4.6	8.6
Urban	28.3	18.6	12.7	5.9	9.8	15.6	22.8	12.6	7.1	5.6	10.1	15.7
Regional	2.6	1.4	3.3	-1.9	1.2	-0.7	-1.7	-0.6	1.2	-1.9	-1.0	-2.9
Continental	9.6	8.9	5.6	3.3	0.7	3.9	16.3	11.8	7.8	4.0	4.6	8.6

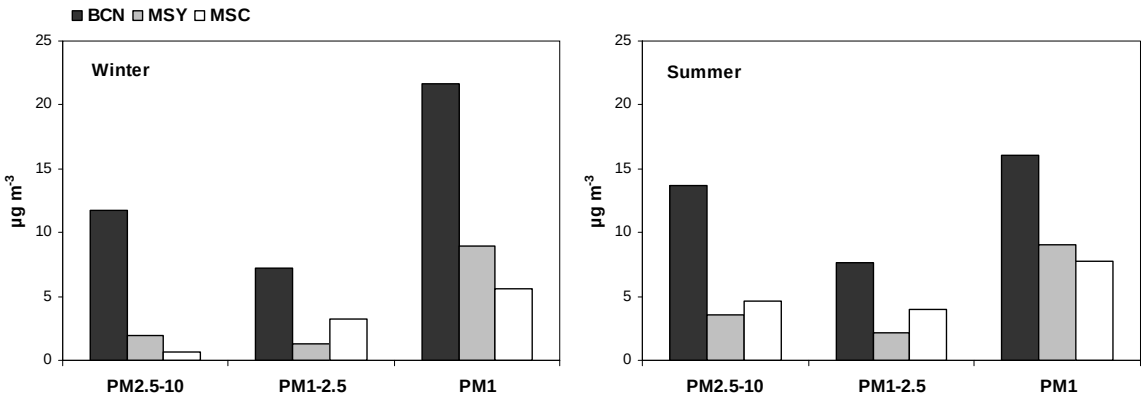

Figure 5.8. Mean $PM_{2.5\text{-}10}$, $PM_{1\text{-}2.5}$ and PM_1 levels recorded at BCN, MSY and MSC during winter and summer, after removal of the days with African dust influence.

The results of these calculations show that, during the summer, the levels of PM_{10} and $PM_{2.5}$ (and also the fractions $PM_{1\text{-}2.5}$, $PM_{2.5\text{-}10}$ and $PM_{1\text{-}10}$) recorded at MSC exceeded the levels recorded at MSY, even after the discount of days with African dust influence. This is probably the consequence, as previously commented, of local resuspension processes, regional pollution reaching the MSC site during the day and the major homogenization of aerosols at a higher scale (regional episodes) during the warmer months of the year. Conversely, during the winter months, the levels of the coarser fractions (PM_{10}, $PM_{2.5}$ and the fraction $PM_{2.5\text{-}10}$) are higher at MSY. This is probably due to the atmospheric decoupling caused by the frequent anticyclonic stability episodes occurring during winter, leaving MSC isolated from regional pollution during longer

periods. However, the levels of the fractions $PM_{1-2.5}$ or PM_{1-10} remain higher at MSC during the winter months.

The levels of PM_1 are higher at MSY during both summer and winter as a consequence of the closer anthropogenic emissions affecting the MSY site, when compared to MSC. The difference was much higher during the winter given that the regional pollution frequently reaches MSC during the warmer months. PM_1 is transformed during transport by reaction, condensation and agglomeration processes, reaching sizes higher than 1 micron. This may be the consequence of the higher levels of the $PM_{1-2.5}$ fraction (and also PM_{1-10}), measured at the MSC site during both winter and summer when comparing with MSY, with closer anthropogenic emissions. Thus, there is no regional increment of $PM_{1-2.5}$ with respect to the MSC, as transport processes (regional and long range) make the levels of the fractions $PM_{1-2.5}$ and PM_{1-10} higher at MSC than MSY, being the calculations of the regional contributions not possible for these size fractions.

These results show that the continental background is affected by regional pollution mainly during the summer, because of the more frequent atmospheric regional recirculations in the WMB. Thus, there is aerosol transport between the regional and continental backgrounds. Therefore, the summer continental PM background levels are partially augmented by the contribution of regional pollution reaching the MSC site, as a result of the higher aerosol mixing between compartments during this period of the year. Thus, the discrimination between the continental background and the regional PM increment may only be possible when considering some periods of the year (mainly winter months), when the MSC site is often situated outside of the boundary layer and therefore it is less affected by regional pollution and local resuspension processes and may then be considered representative of the continental background.

The urban contributions to PM_{10}, $PM_{2.5}$ and PM_1 are higher during winter. This is probably the consequence of atmospheric stability that induces intense pollution episodes during the coldest months. However, during summer, atmospheric mixing and intense breeze circulations produce the dispersion and recirculation of pollutants around the region, increasing PM regional background levels and thus decreasing the relative importance of the urban contribution to ambient PM levels at the urban site. Thus, the regional background is affected by the transport of pollutants from the urban site, especially during the summer months. This may also happen during the winter anticyclonic episodes. Therefore, in these scenarios, the urban contributions calculated

as the difference between BCN and MSY data may be underestimated when urban pollution may affect the regional background. Then, as concluded for the regional contribution, the urban contribution should only be estimated for the winter period.

With this in mind, the mean contributions to PM_1 measured at the urban site during winter are estimated to be 5.6 µg m^{-3} (26%) from the continental background, the regional increment contributing 3.3 µg m^{-3} (15%) and the urban increment 12.7 µg m^{-3} (59%). Regarding $PM_{2.5-10}$ the continental background contributes 0.7 µg m^{-3} (6%), the increment due to regional pollution was 1.2 µg m^{-3} (10%) and the urban increment 9.8 µg m^{-3} (84%). As previously commented, the differentiation of continental and regional contributions is not possible for the $PM_{1-2.5}$ fraction.

In conclusion, the method proposed by Lenschow et al., (2001) is a useful and simple method for estimating the urban and regional contribution, but its direct application in the WMB may be limited given the complex atmospheric processes in this area. Summer regional recirculations around the WMB produce the atmospheric transport, mixing and aging of pollutants at a regional scale. In this scenario, the continental and regional backgrounds are characterised by similar levels of aerosols. In addition, local or regional sources, such as dust resuspension, may influence regional and continental backgrounds to different extents. Furthermore, African dust episodes may impact more intensely at MSC because of its higher altitude.

Besides, given the meteorological characteristics of the WMB, the urban and industrial emissions, concentrated in the coastal areas, may have a considerable impact in PM levels and composition in rural and remote areas located at different altitudes, both in summer, with important atmospheric recirculation and mixing of air masses at a regional scale, and also occasionally during winter, with breeze-activated transport of stagnated urban pollutants.

Nevertheless, the parallel monitoring of PM at an urban, a regional and a continental background site was a useful approach to understand the phenomenology of atmospheric aerosols in the WMB.

5.2.2. Speciation

The urban, regional and continental contributions to PM_{10} components in the study area were calculated using the simultaneous PM_{10} composition data recorded from November 2005 to November 2007 at BCN, MSY and MSC, after subtraction of days with African dust influence (Table 5.6 and Figure 5.9). The calculations were made as above: the urban background contribution was calculated as the difference between the simultaneous data measured at BCN (urban site) and MSY (regional site), the regional background contribution was calculated as the difference between levels measured at MSY and MSC (continental background), and the continental contribution was obtained from the levels measured at the MSC site. As performed for PM levels above, in order to minimize the effects of local dust resuspension and the regional pollution reaching MSC during the warmer months, summer and winter data were separately treated for the calculation of the urban, regional and continental backgrounds.

Table 5.6. Major components (μg m^{-3}) measured in PM_{10} simultaneously at BCN, MSY and MSC during winter and summer months from November 2005 to November 2007 during days without African dust influence (no-NAF). Calculated urban, regional and continental background.

Winter						
	BCN	**MSY**	**MSC**	**Urban**	**Regional**	**Continental**
μg m^{-3}	47.4	14.4	9.5	33.0	4.9	9.5
OC	5.7	1.8	1.1	3.9	0.7	1.1
EC	2.7	0.2	0.2	2.5	0.1	0.2
OM+EC	12.8	4.1	2.5	8.8	1.6	2.5
SO_4^{2-}	4.3	1.8	1.1	2.5	0.7	1.1
NO_3^-	8.7	2.6	1.5	6.1	1.0	1.5
NH_4^+	2.1	1.0	0.5	1.1	0.5	0.5
SIA	15.0	5.3	3.0	9.7	2.3	3.0
Mineral matter	13.7	2.2	1.1	11.5	1.2	1.1
Sea spray	1.9	0.4	0.2	1.5	0.2	0.2
Unaccounted	6.3	3.6	2.2	1.6	<0.1	2.2
Summer						
	BCN	**MSY**	**MSC**	**Urban**	**Regional**	**Continental**
μg m^{-3}	37.2	16.6	15.7	20.6	0.9	15.7
OC	3.4	2.4	2.3	1.0	0.1	2.3
EC	1.8	0.3	0.3	1.5	<0.1	0.3
OM+EC	7.6	5.3	5.1	2.2	0.3	5.1
SO_4^{2-}	4.1	3.0	2.5	1.2	0.5	2.5
NO_3^-	3.4	1.1	1.0	2.3	0.2	1.0
NH_4^+	0.6	0.7	0.6	<0.1	<0.1	0.6
SIA	8.2	4.8	4.1	3.4	0.7	4.1
Mineral matter	13.4	3.7	4.0	9.5	<0.1	4.0
Sea spray	2.6	0.6	0.3	2.1	0.2	0.3
Unaccounted	5.2	3.3	2.1	9.6	<0.1	2.1

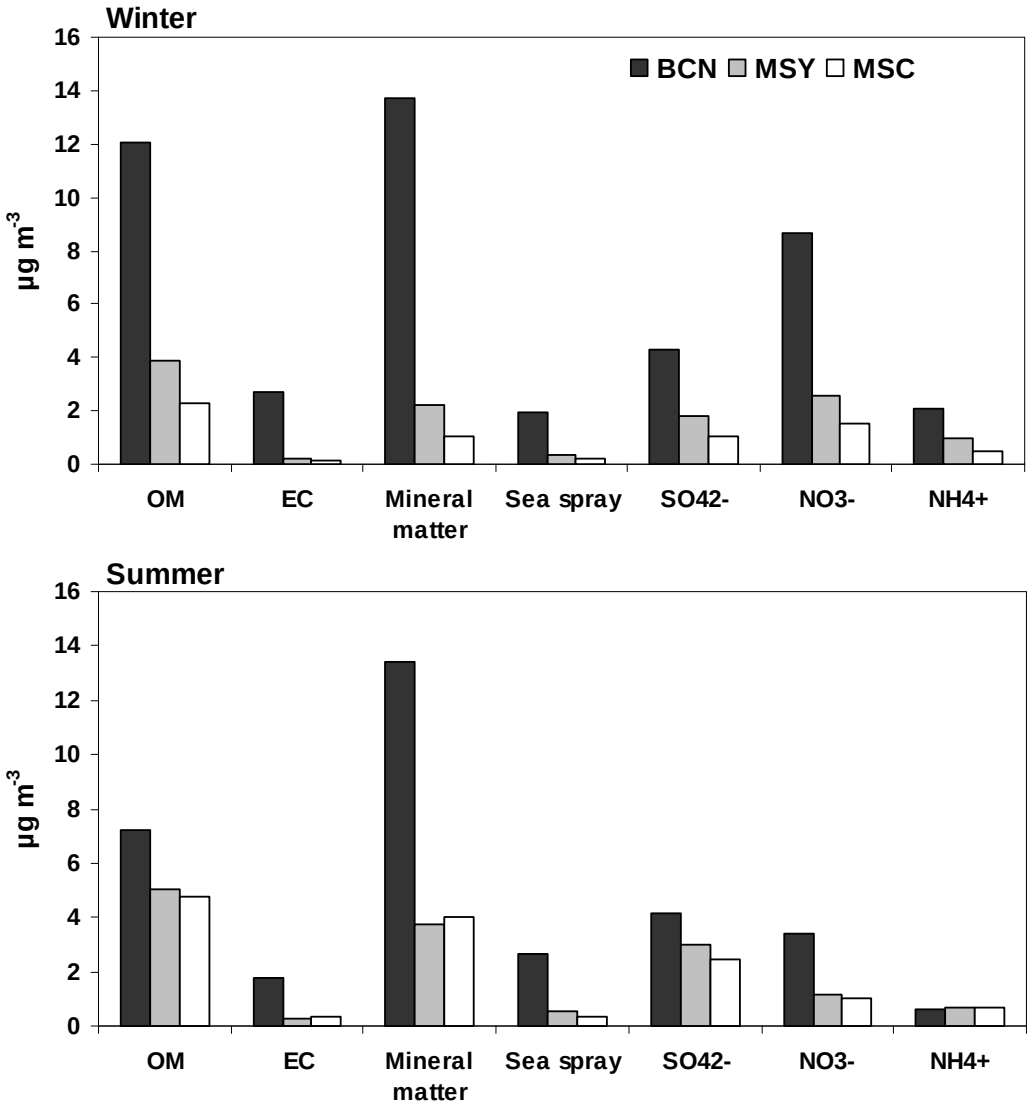

Figure 5.9. PM_{10} major components measured at BCN, MSY and MSC during winter and summer months, discounting the days with African dust influence (November 2005-November 2007).

These results show that during the summer, the important atmospheric mixing and low renovation of air masses at a regional scale induce very similar concentration levels of most of the components measured in PM_{10} at MSC and MSY. Consequently, the regional contribution obtained during the summer months is very low. As observed above for the estimation of the contributions to PM levels, the continental background and regional contributions to the different PM components may be distinguished only during the winter months, when local and regional contributions are less significant at MSC. Thus, during the winter the regional increment of the levels of some of the components measured at MSY with respect to MSC were 40% for OM+EC, 42% for sulphate, 41% for nitrate, 55% for ammonium and 52% for mineral matter (Table 5.6 and Figure 5.9). During winter, the secondary aerosol contribution at the regional

background almost doubled the levels of most compounds at MSC, due to the proximity to urban agglomerations and industrial estates, with higher emissions of aerosols and precursors. Levels of mineral matter also doubled as a result of the transport of regional dust to the site. The increment of sea spray was 45% due to the proximity of MSY to the coast.

At BCN, during the winter months, the urban contribution to all PM_{10} major components was higher of 50% in all cases (Table 5.6 and Figure 5.9). The urban contribution to some of the components, such as EC (93%), mineral dust (85%), OM (73%) and NO_3^- (70%), was very high as a result of road traffic direct and indirect emissions. Mineral matter origin at the urban site was mainly road dust and construction dust. The urban contributions to SO_4^{2-} (59%) and NH_4^+ (51%) were lower than the contributions of other compounds because secondary aerosols are important at the regional background in the WMB. Road traffic, industrial, agricultural, farming and shipping emissions, together with the recirculation of air masses in the region, photochemical oxidation and other processes produce the formation of secondary aerosols and aging of air masses at a regional scale. Moreover, aerosols in the accumulation mode as ammonium sulphate have a long residence time in the atmosphere. However, the urban contributions estimated for the secondary species (59% of sulphate, 70% of nitrate and 51% of ammonia, in winter) may be considered as very high if compared to previous studies that attributed a major regional origin for these compounds (Querol et al., 2004a and b). This is probably the consequence of vehicle exhaust emissions of ammonia at the urban site (Livingston et al., 2009) producing the rapid formation of secondary aerosols (ammonium sulphate and nitrate) in situ. During the summer the levels of most components are reduced at Barcelona (except sea spray) and the urban contributions decrease, due to the more frequent renovation of air masses by atmospheric dispersion processes, and the regional recirculation episodes. However the urban contributions are still important, except for ammonia. Therefore, as commented in the previous chapters, the presence of coarse sulphate and/or nitrate aerosols formed by the reaction with coarse mineral and sea spray particles could be deduced.

Given the aforementioned limitations, the compositions of the continental background and of the regional and urban increments have been estimated for the winter period but not for summer (Figure 5.10).

Therefore, the continental background (Figure 5.10) is mainly composed of OM (24%), NO_3^- (16%), mineral matter (11%), SO_4^{2-} (11%) and NH_4^+ (5%), reflecting a background

composed of natural aerosols (mineral dust and biogenic emissions) together with the long-range transport of aerosols (secondary ammonium nitrate and sulphate and secondary carbonaceous compounds). Both sea spray and EC accounted for 2%. The unaccounted mass was 29% of the total PM_{10} mass, clearly higher than measured at MSY and BCN.

The regional increment (Figure 5.10) is mainly composed of OM (30%), mineral matter (22%) and SIA (nitrate 20%, sulphate 14% and ammonia 10%), reflecting a natural background together with regional pollution (secondary aerosols are in a high proportion). Sea spray (3%) and EC (1%) are in lower proportions as MSY is not by the coast and direct combustion emission sources are low. The unaccounted mass is negligible.

The urban contribution during the winter months (Figure 5.10) is mainly composed of mineral dust (34%), OM (23%) and nitrate (18%), reflecting the important road traffic direct and indirect emissions. Both EC and SO_4^{2-} accounted for 7%. Sea spray accounted for a 4% and ammonia for a 3%. The unaccounted mass was 4% of the total PM_{10} mass.

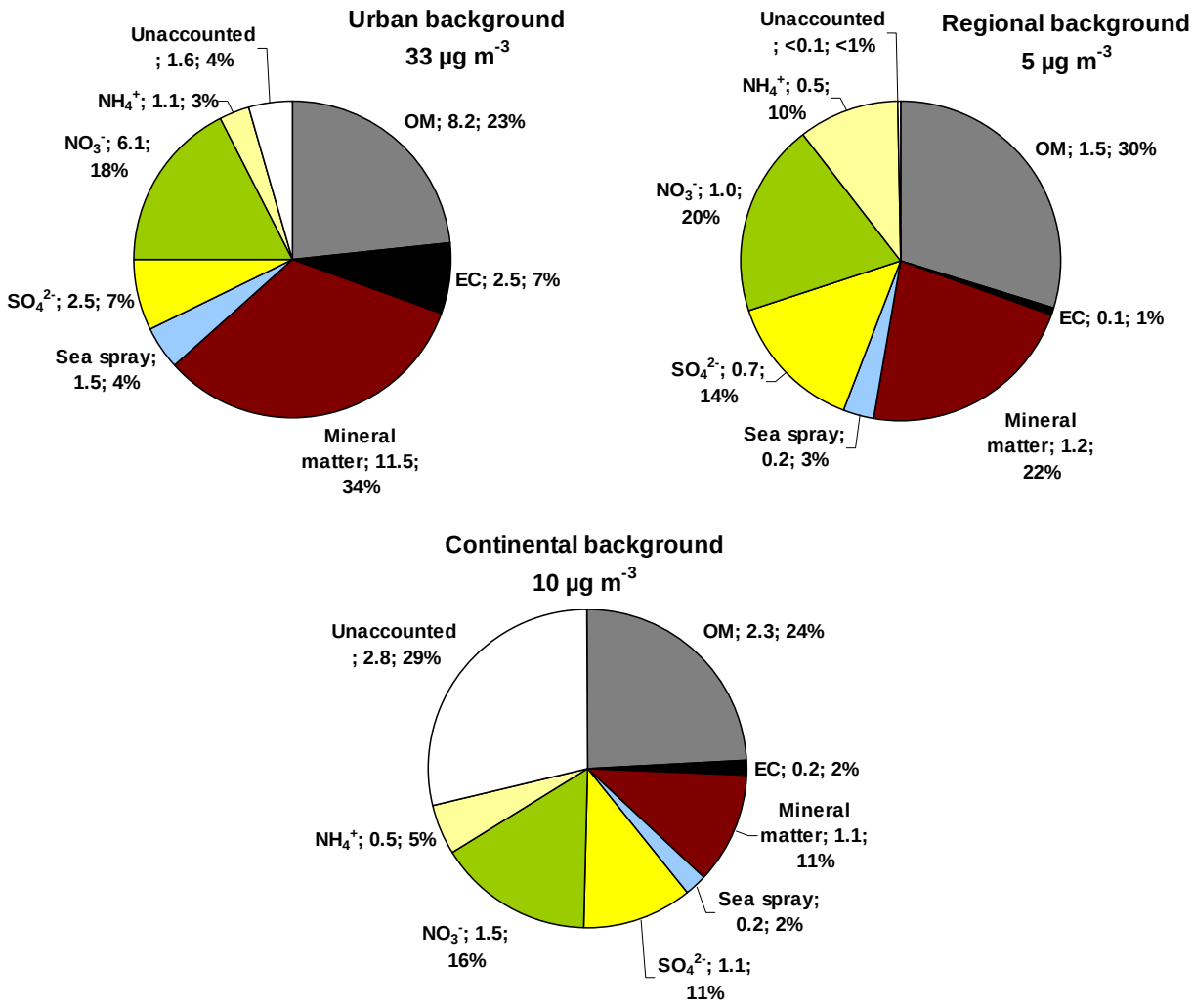

Figure 5.10. Major composition of the urban, regional and continental contributions calculated from BCN, MSY and MSC data during winter from November 2005 to November 2007, excluding days with African dust influence.

Regarding the trace elements, calculations of the continental background and the regional and urban contributions are carried out using winter data, as it was performed with major components (Table 5.7 and Figure 5.11).

Elements typical of urban emissions presented increments higher than a 50% in ppm (µg/g of PM_{10}) at the urban background, with respect to the regional background. These elements were mainly associated to road traffic emissions (Cu, Cr, Zn, Sn and Sb) and other urban emissions, such as industries or road dust resuspension by traffic (Tl, Sr and Bi). Other elements associated to industrial emissions or fuel oil combustion, such as V, Ni, Cd, Mn or Pb, presented important regional and urban increments, as well as significant levels at the continental background, probably due to

the important atmospheric mixing of these pollutants at a regional scale. Some of these elements have anthropic origins and are probably transported to MSC with regional pollution by breezes. However, elements with very high continental background proportions had a crustal origin (Ba, U, Li, La and Ce).

Table 5.7. Mean levels of trace elements in ppm (µg/g of PM_{10}) measured simultaneously in BCN, MSY and MSC during the winter months from November 2005-November 2007, excluding days with African dust influence. Urban, regional and continental contributions calculated from these data.

	ppm (µg/g)			%		
	BCN	**MSY**	**MSC**	**Urban**	**Regional**	**Continental**
Li	8	9	6	0	25	75
P	522	700	394	0	44	56
Ti	770	507	469	34	5	61
V	264	158	85	40	28	32
Cr	152	36	66	56	0	44
Mn	457	226	333	27	0	73
Co	9	5	7	21	0	79
Ni	130	91	90	30	1	69
Cu	2147	185	121	91	3	6
Zn	2001	413	948	53	0	47
As	20	20	8	0	62	38
Se	19	21	16	0	24	76
Rb	25	19	14	23	22	55
Sr	116	56	45	52	9	39
Cd	10	7	6	29	9	61
Sn	175	41	25	77	9	14
Sb	144	28	10	80	13	7
Ba	588	339	639	0	0	100
La	10	7	9	12	0	88
Ce	23	14	18	21	0	79
Tl	6	2	2	64	7	29
Pb	462	250	151	46	21	33
Bi	10	4	3	62	8	29
Th	4	3	2	29	8	63
U	2	2	4	0	0	100

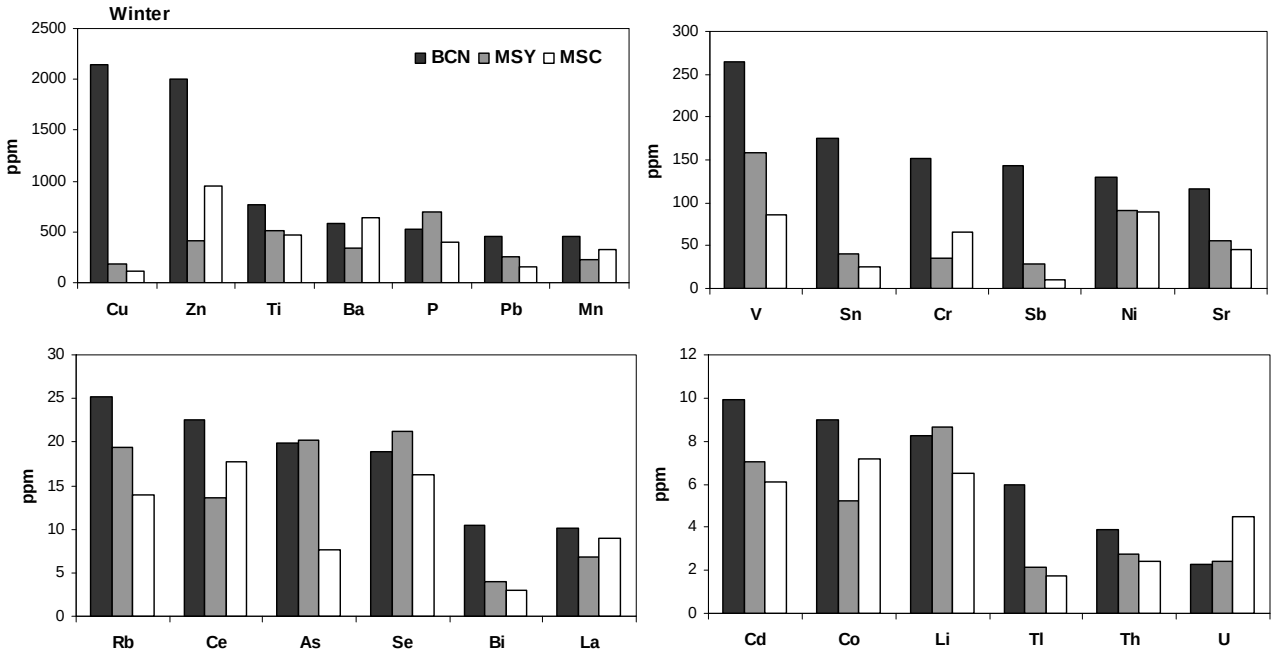

Figure 5.11. Levels of trace elements in ppm (µg/g PM_{10}) at BCN, MSY and MSC calculated from simultaneous PM_{10} samples during winter in the November 2005-November 2007 period, excluding the days with African dust influence.

The high levels of some compounds recorded in PM_{10} at the urban background are attributed to urban local emissions, being traffic the source that has a strongest impact on carbonaceous compounds, nitrate and mineral matter levels. Moreover, other disperse punctual sources in the urban area (small industries, domestic emissions, etc.) result in the increase of sulphate, nitrate and carbonaceous compounds. Fugitive emissions from construction and demolition activities have also a great impact on mineral matter concentrations, mainly in the coarse fraction. Therefore, taking into account the relatively low regional and continental background levels we can conclude that an adequate monitoring and the setting of strategies to control urban emissions could considerably reduce the ambient PM levels registered in Barcelona. The high sulphate, ammonia and nitrate concentrations in the urban background with respect to the regional and continental backgrounds indicates that important precursors are emitted in the urban area, mainly from road traffic (NO_x) but also from many small and disperse sources. NH_3 is also emitted by vehicle exhaust emissions (Livingston et al., 2009) producing the rapid formation of secondary aerosols (ammonium sulphate and nitrate) in situ. However, the continental background and the regional contribution present also important proportions of these compounds, due to transport processes and the formation of secondary compounds in the regional background. The trace elements that are related to traffic emissions presented higher increments at the urban

background, mainly due to the urban contribution. However, tracers related to mineral matter (from African dust outbreaks and resuspension processes) and regional recirculation of pollutants (as V and Ni, tracers from fuel oil combustion) presented important regional increments and also high levels at the continental background.

5.3. Simultaneous PM episodes

The characterization of different meteorological and atmospheric episodes in the WMB and the study of the variability of atmospheric aerosols under these different scenarios have shown their important influence on aerosol levels and speciation. In this direction, a detailed analysis of the variability of PM levels and speciation data registered at BCN, MSY and MSC during characteristic episodes is presented and the most important episodes are described.

5.3.1. PM levels

The analysis of PM levels during the different atmospheric scenarios identified in the region (Figure 5.12) shows that the continental, regional and urban backgrounds are influenced to different extents by the different air mass origin or meteorological conditions registered, but also by local emissions. In general, PM levels at the urban background were more variable than at the regional or continental backgrounds.

The variability of PM_1 as a function of the atmospheric scenario is less significant at the regional and continental backgrounds than at the urban background (Figure 5.12). Levels of PM_1 at the urban background were lower during summer regional recirculation episodes (more effective dispersion of local pollutants) and higher during winter anticyclonic episodes (atmospheric stability associated with intense pollution episodes) and Mediterranean episodes; however the latter are not very significant because of their low frequency. PM_1 levels were frequently higher at MSY than at MSC. However, during the regional episodes, PM_1 levels were similar at both sites given the mixing of air masses at a regional scale. During NAF episodes, the continental PM_1 levels are slightly higher that the regional ones.

The levels of the $PM_{1\text{-}2.5}$ fraction present a low variability at the three sites, increasing during NAF and REG episodes at all sites.

Conversely, the $PM_{2.5\text{-}10}$ fraction presents the most important variability at the three sites, with levels much lower for Mediterranean episodes (frequently associated with

rainfall) and higher during African dust episodes and summer regional recirculations. In BCN, $PM_{2.5-10}$ levels are also high for Atlantic and European episodes, probably due to the favoured dust resuspension by strong winds. $PM_{2.5-10}$ levels were similar at MSY and MSC during most episodes with the exception of NAF, when much higher levels were recorded at MSC, almost reaching levels measured at the urban site. Conversely, during winter anticyclonic episodes, the levels measured at MSC were lower than at MSY, due to atmospheric stability frequently leaving MSC outside of the boundary layer.

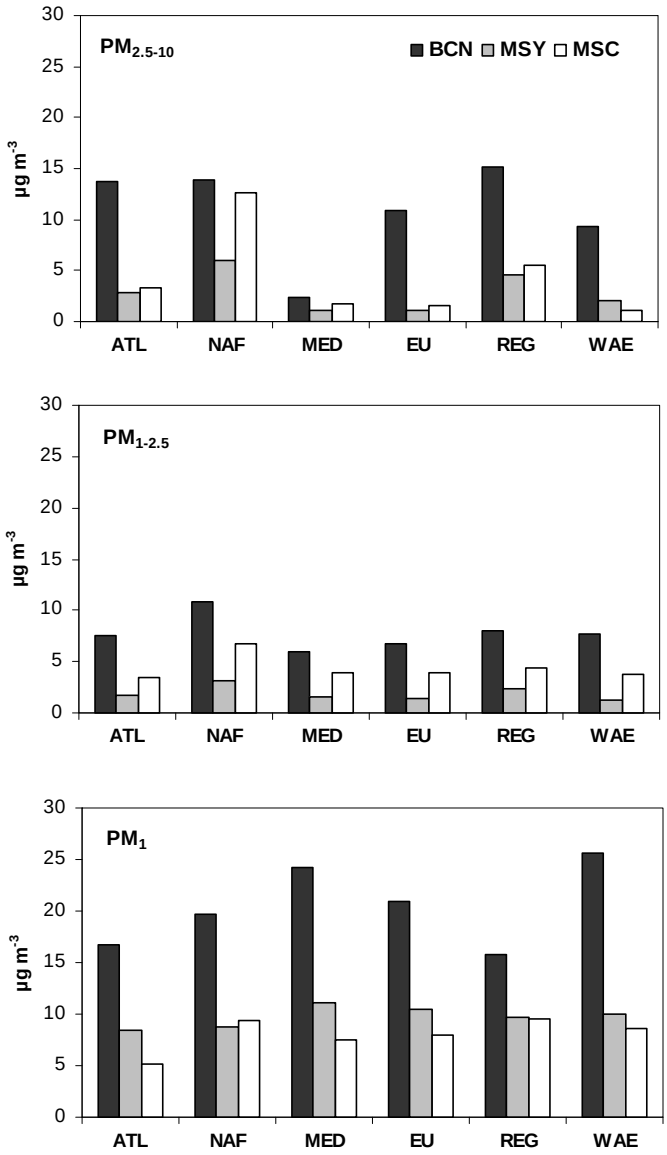

Figure 5.12. $PM_{2.5-10}$, $PM_{1-2.5}$ and PM_1 levels measured at BCN, MSY and MSC during Atlantic advections (ATL), African dust episodes (NAF), Mediterranean (MED) and European (EU) air mass transport, summer regional recirculations (REG) and winter anticyclonic episodes (WAE).

5.3.2. PM_{10} speciation

The different atmospheric-meteorological episodes identified at the region of study also influence the main composition of atmospheric aerosols at the three sites considered. The levels of major PM_{10} components recorded at BCN, MSY and MSC for the different atmospheric scenarios considered are presented in Figure 5.13. In general, the levels of most components present a higher variability at BCN than at MSY and MSC. The number of samples collected during Mediterranean episodes was not significant because of their low frequency and these episodes will not be commented.

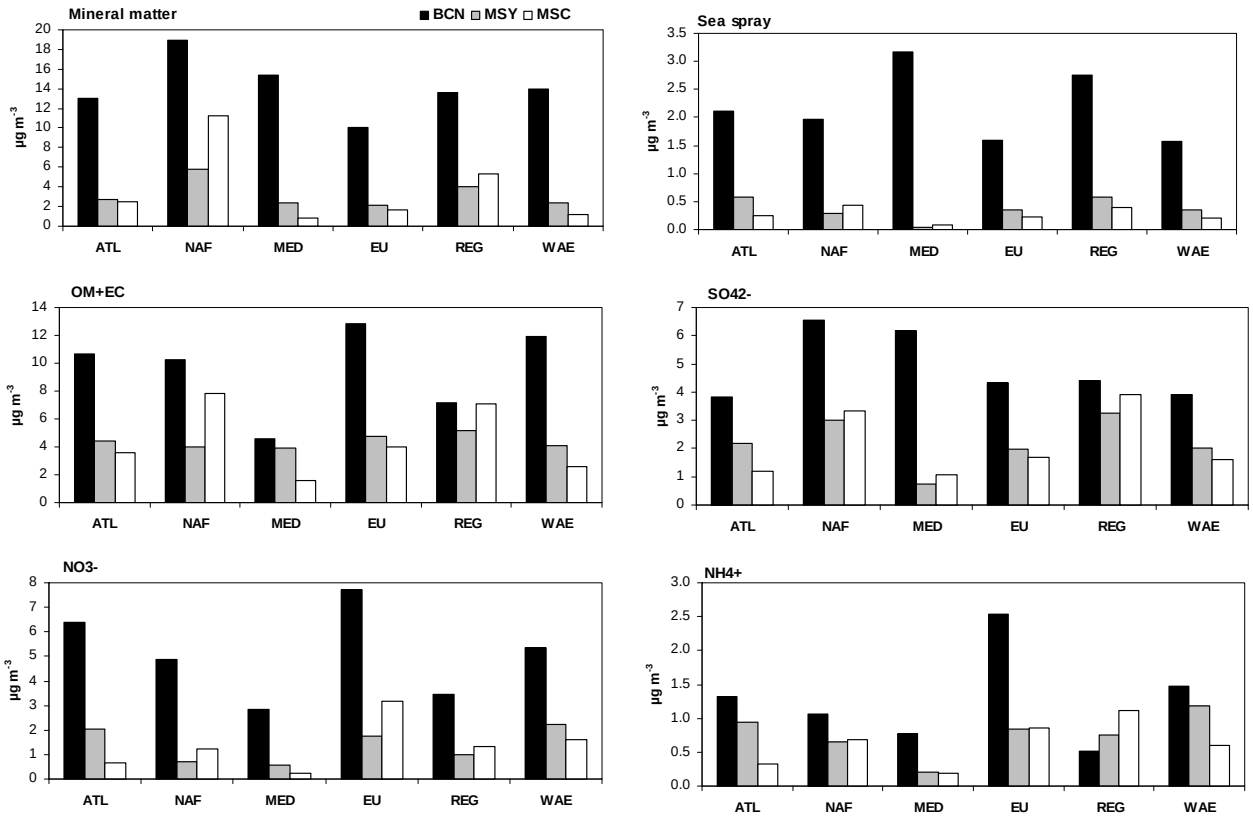

Figure 5.13. Major components measured in PM_{10} in BCN, MSY and MSC during Atlantic advections (ATL), African dust episodes (NAF), Mediterranean (MED) and European (EU) air mass transport, summer regional recirculations (REG) and winter anticyclonic episodes (WAE).

The levels of mineral matter recorded in BCN were higher during African dust episodes due to the long range transport of mineral dust. At the urban site, the levels of mineral matter were always higher than at the continental and regional backgrounds, as a consequence of the important resuspension of road dust by traffic. However, the difference decreased during African dust episodes or regional recirculation episodes, due to the regional and long-range transport of dust to the rural sites. The levels of

mineral matter registered at the continental background were much higher during African dust episodes, due to the transport of dust at high altitudes. In addition, regional dust transport and dust resuspension by wind during the summer episodes increase the levels measured at MSC over the levels recorded at MSY during regional recirculation episodes.

The levels of sea spray at BCN were always much higher than the levels measured at the regional or the continental background for all episodes considered, because of the proximity of BCN to the coast. The levels of sea spray increased for regional recirculation episodes at all sites.

The levels of carbonaceous compounds at the urban site were higher during winter anticyclonic episodes and European air mass transport. During African dust episodes and summer regional recirculations the levels of carbonaceous compounds were higher at the continental than at the regional background, probably due to the regional and long-range transport of smoke from forest fires, frequent during the summer. In addition, the levels of OM+EC registered at MSY for the different episodes present a lower variability. At the urban site, the lowest levels of OM+EC were recorded during regional recirculations and in these cases the urban increment was not very high due to the high atmospheric mixing at a regional scale.

The higher sulphate levels measured at the three sites were recorded during African dust episodes, being clearly higher in BCN. This indicates that during NAF episodes, the formation of secondary sulphate by interaction of mineral particles with gaseous precursors is enhanced. At MSY and MSC, relatively high sulphate levels are recorded also during summer regional recirculations. It should be highlighted that levels of sulphate are very similar between the three sites during regional recirculation episodes, showing a high dispersion and homogenization at a regional scale. During Atlantic, European and winter anticyclonic episodes the levels of sulphate were higher at MSY than MSC, probably due to atmospheric decoupling avoiding regional pollution to reach the MSC site.

Nitrate levels at the urban site were much higher during European episodes, Atlantic advection and winter anticyclonic episodes, probably due to the higher frequency of these episodes during colder months, avoiding the volatilization of particulate ammonium nitrate, but also during African dust outbreaks, probably due to an enhanced formation of coarse nitrate. The levels of nitrate measured at MSY were

higher than at MSC during Atlantic and winter anticyclonic episodes. However they were higher at the continental site during African dust outbreaks, European and regional recirculation episodes, due to the long range and regional transport of secondary pollutants to the MSC site.

Ammonium levels were much higher at Barcelona during European episodes and the urban increment was much higher than during the rest of the scenarios considered. Levels at the regional and continental background were very similar during African and European episodes. The higher regional increment of ammonium levels was found during Atlantic and winter anticyclonic episodes, when atmospheric decoupling leaves MSC isolated from regional pollution. However, the levels measured during summer regional episodes were higher at MSC than at MSY and those higher than at BCN. Given the similar levels of sulphate recorded at the three sites during this scenario and the higher levels of nitrate determined for BCN, this suggests the presence of coarse Na or Ca nitrates and/or sulphates in Barcelona, formed by interaction of gaseous precursors with sea spray and mineral particles. Moreover, the high NH_3 emissions in the area of Lleida, related to farming activities, may account for the higher ammonium and even for the relatively high concentration of nitrate in MSC with respect to MSY.

Given the important influence that certain atmospheric scenarios, such as WAE, REG and NAF, have on aerosol variability in the WMB, some of these characteristic episodes registered simultaneously at BCN, MSY and MSC during the study period will be presented individually. The study of concrete episodes in detail may allow a better interpretation of the aerosol phenomenology in each case and a better understanding of the simultaneous variability of atmospheric aerosols at the three sites.

5.3.3. Winter anticyclonic episodes

Anticyclonic situations are characterized by vertical atmospheric stability that favours the accumulation of pollutants in the boundary layer. These episodes occur mainly during winter and last a few days. Intense pollution episodes are registered at urban sites, where atmospheric pollutants accumulate near emission sources favoured by the poor dispersing conditions. However, at rural sites, the impact of these episodes depends on the altitude of the site and distance from the emissions. Sites located inside the boundary layer may be exposed to winter regional pollution, reaching very high PM levels. However, a site situated outside the boundary layer may be isolated

from regional pollution. Under this scenario, when mountain breezes develop, they may transport upward pollutants that are accumulated at low altitudes during a few days.

An important anticyclonic episode affected simultaneously the continental, regional and urban background sites in the WMB from 1 to 16 February 2006 (Figure 5.14 and Figure 5.15). Air masses with a NW Atlantic origin passing through France and the Pyrenees arrived to the NE Iberian Peninsula, where they stagnated by the effect of atmospheric stability that lasted a few days. This scenario produced an intense pollution episode in BCN, reaching very high levels of PM (up to 110 µg PM_{10} m^{-3}). The stagnation of pollutants at a regional scale produced the accumulation and transformation of aerosols at low altitudes in the regional background. These polluted air masses reached MSY when mountain breezes developed, increasing markedly PM levels, especially the finer fractions. During this period, marked daily cycles were observed at MSY, with very high hourly levels of PM_1 registered in the afternoon (up to 50 µg PM_1 m^{-3}), even higher than at BCN, and low levels during the night. As a result, it may be deduced that during the transport of urban pollutants there is an increase in the concentrations of fine secondary particles, probably by the interaction with other pollutants emitted by industrial or rural activities. However, at the MSC site PM levels remained low, given that this site was isolated from the boundary layer and was not affected by local and regional emissions.

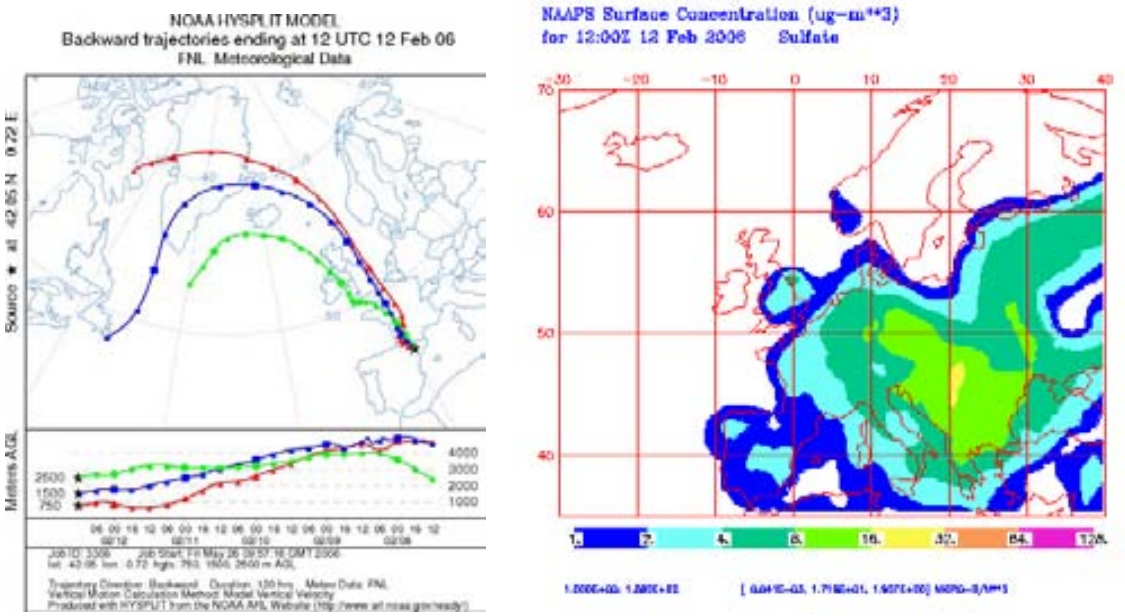

Figure 5.14. Back-trajectory of a winter anticyclonic episode calculated for MSC for the 12 February 2006 (left). NAAPS surface concentration map for sulphate for 12 February 2006 (right).

Since the 9th February this scenario modified slightly. At MSY, the daily cycle was not as marked and PM background levels remained high even during the night. The polluted air masses were stagnated at a certain height, and in this situation the regional pollution reached higher altitudes as MSC, where PM levels increased considerably.

Finally, from the 16th February, atmospheric conditions changed and an Atlantic advection transported clean air masses with high wind speeds producing the dispersion of pollutants in Barcelona and the decrease of PM levels at the three sites.

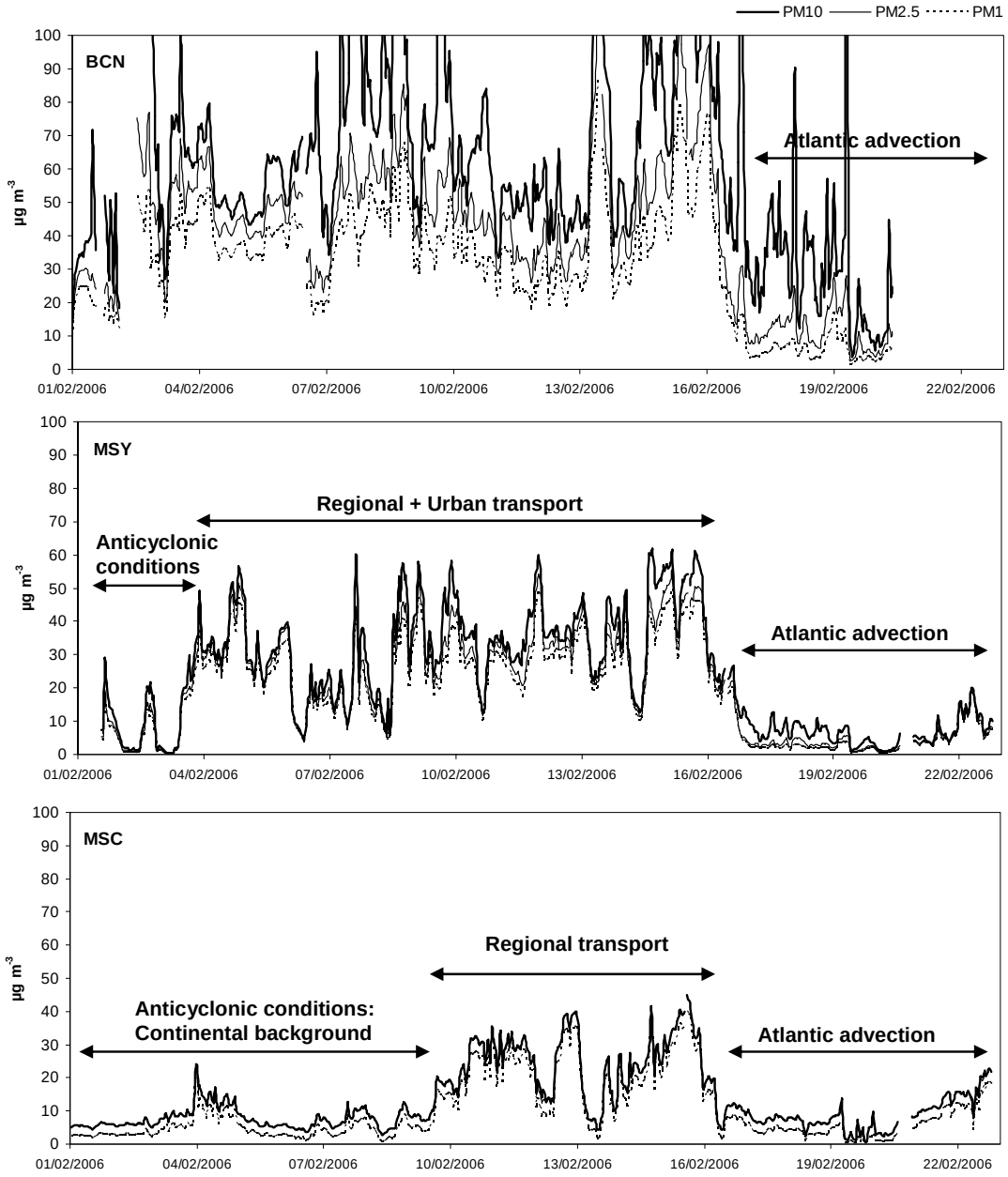

Figure 5.15. Hourly PM_{10}, $PM_{2.5}$ and PM_1 levels registered simultaneously at BCN, MSY and MSC from 1/2/2006 to 22/2/2006.

It is important to draw attention to the very fine main aerosol size that these episodes present, with a PM_1/PM_{10} ratio next to 1 at the regional and continental sites, but also high at the urban site, when compared with other episodes as summer regional recirculations, with a coarser aerosol main size. This is probably due to the enhanced formation of secondary aerosols, mainly in the accumulation mode. During this winter anticyclonic episode a very important increase in the levels of anthropogenic compounds, such as ammonium nitrate and sulphate, and carbonaceous compounds were registered at all sites (Figure 5.16). As observed, daily levels of PM compounds were always higher at Barcelona. However, it is expected that during short periods, mainly in the afternoon, the levels of some compounds such as fine ammonium nitrate could be higher at MSY. To demonstrate this it is necessary to perform hourly-resolved chemical characterization and this was not available during the period of this study.

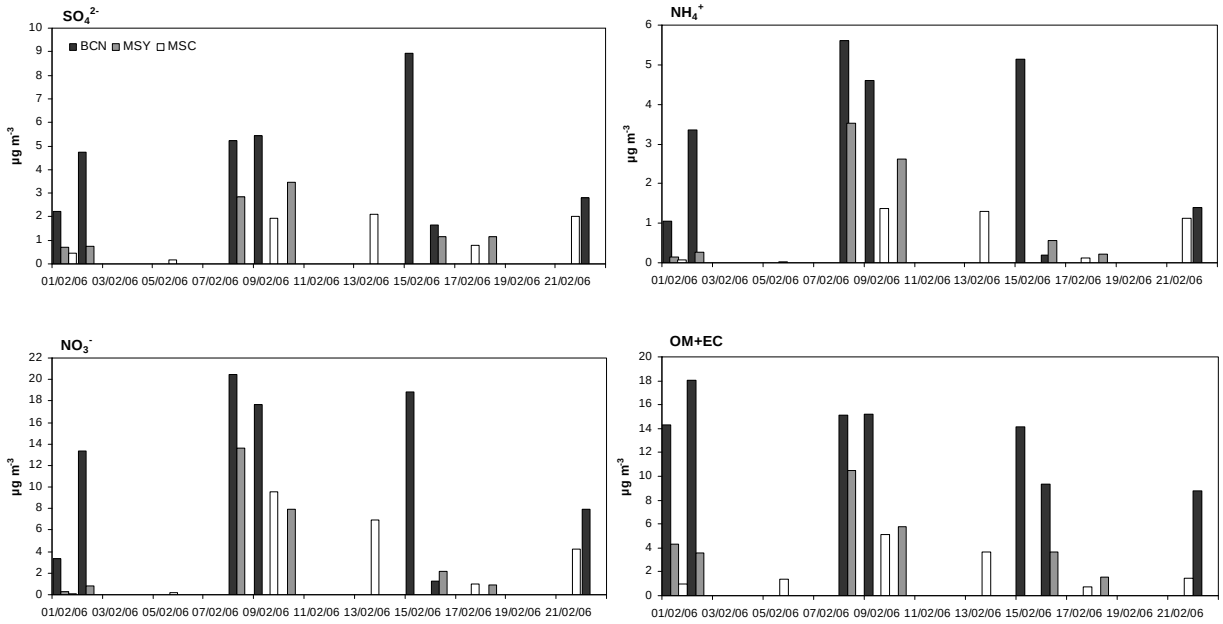

Figure 5.16. Daily sulphate, nitrate, ammonium and OM+EC levels measured simultaneously at BCN, MSY and MSC during 1-22/02/2006.

5.3.4. African dust episodes and summer regional recirculation episodes

African dust outbreaks are frequent in the WMB during the summer months. African dust outbreaks influence decisively the levels of mineral matter registered in the WMB atmosphere, increasing markedly PM levels and sometimes carrying exceedances of the PM_{10} daily limit levels established. African dust may be transported at different heights in the atmosphere depending on the meteorological scenario causing such a transport towards Southern Europe (Escudero et al., 2005). Therefore, as explained before, the three sites may be affected differently by African dust outbreaks and the African dust contributions at BCN, MSY and MSC may be different.

Atmospheric recirculations at a regional scale are also very frequent during summer months in the WMB, producing the accumulation, mixing and aging of air masses, leading to transformation of pollutants by interaction between particles and gases, (condensation, agglomeration, oxidation or photochemical processes). Fine PM levels recorded during these episodes are usually high due to the high production of secondary compounds.

Frequently, in the WMB these scenarios occur simultaneous or consecutively during the summer, giving rise to a complex scenario. This was the case of the summer in 2007. Intensive African dust outbreaks were registered in the region during July and August 2007, when mineral dust from Northern Africa was simultaneously transported with the smoke plumes from important forest fires in the Mediterranean (the most important occurred in Greece and Northern Africa). Back-trajectories of the episode registered during 26-29 August 2007 (Figure 5.17) show that air masses from Europe crossed the Mediterranean, passing through Greece and then the North of Africa, before reaching the NE Iberian Peninsula. Dust over the Mediterranean and smoke from huge forest fires over Greece and the North-African coast can even be observed in the Seawifs satellite image (Figure 5.18). The influence of these episodes on the levels of atmospheric aerosols in the WMB was very important. The simultaneous increase of PM levels registered during this dust outbreak, especially affecting the coarser fractions at the three sites considered in this study, is shown in Figure 5.19. The most intense African dust transport episodes were registered during 7-8 July, 16-21 July, 1-6 August and 26-31 August and affected also other rural and background sites in the Mediterranean area (Figure 5.20, Airbase database, http://air-climate.eionet.europa.eu/databases/airbase/), with a specially marked increase in PM_{10} levels for the sites situated at higher altitudes, as Rojen Peak in Bulgary (1750 m.a.sl.) and Chamonix in France (1038 m.a.s.l.). The episodes during 7-8 July and 1-6 August

impacted mainly at high altitudes as deduced from the high PM levels recorded at MSC (PM_{10} daily means of 27 µg m^{-3} at MSC vs. 16 µg m^{-3} at MSY, Figure 5.19). However, during the 16-21 July and 26-31 August episodes, PM levels were similar at MSY and MSC reflecting the impact of the African dust at all levels (PM_{10} daily means of 31 µg m^{-3} at MSC vs. 32 µg m^{-3} at MSY).

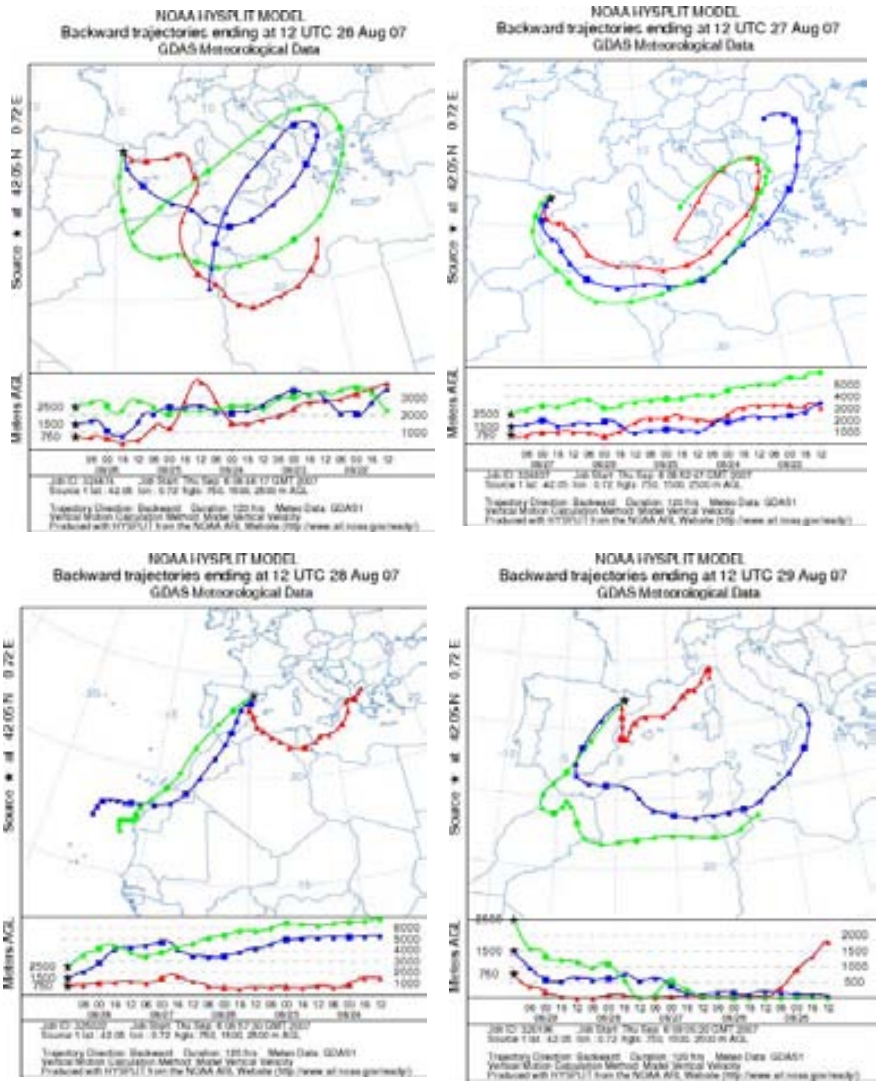

Figure 5.17. Back-trajectories of an African dust outbreak episode with simultaneous transport of dust from forest fires in the Mediterranean calculated for MSC from 26 to 29 August 2007.

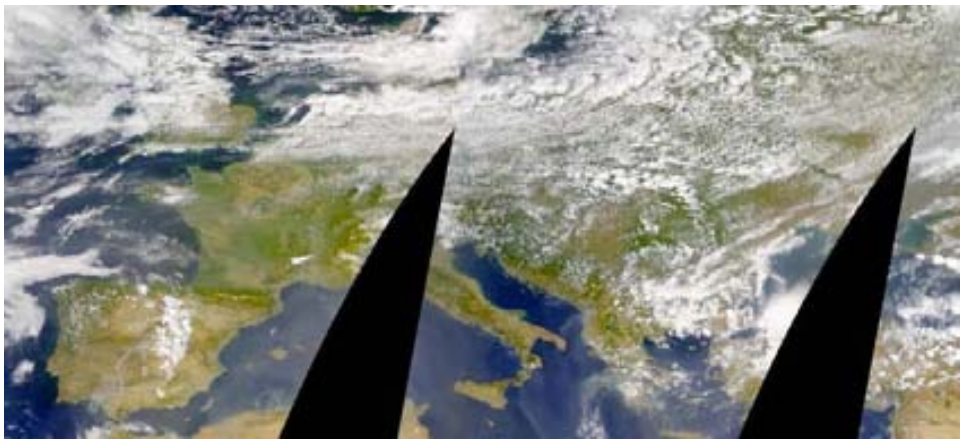

Figure 5.18. Seawifs satellite image of the same episode for the 27 august 2007.

In between the important dust outbreaks, the occurrence of regional recirculation episodes hindered air mass renovation, favouring aging and interaction of aerosols and resulting in high PM levels for relatively long periods. Examples of these episodes are those from 24-30 July and 7-16 August (Figure 5.19). PM levels recorded at MSY and MSC were similar, as the MSC site is situated inside the boundary layer and exposed to regional pollution (PM_{10} daily means of 20 µg m^{-3} at MSC vs. 17 µg m^{-3} at MSY). However the levels measured at MSC presented a coarser grain size than at MSY, closer to anthropogenic emission sources (industry and urban agglomerations). The parallel evolution of PM levels at MSY and MSC, driven by mountain breezes, reflects the mixing of air masses at a regional scale. PM levels at MSY and MSC increased in the afternoon and decreased during the night, being the magnitude of the increase parallel due to regional pollution reaching both sites. At the urban site, the local emissions, mainly road traffic, are superimposed over the regional background giving rise to a different evolution of PM levels.

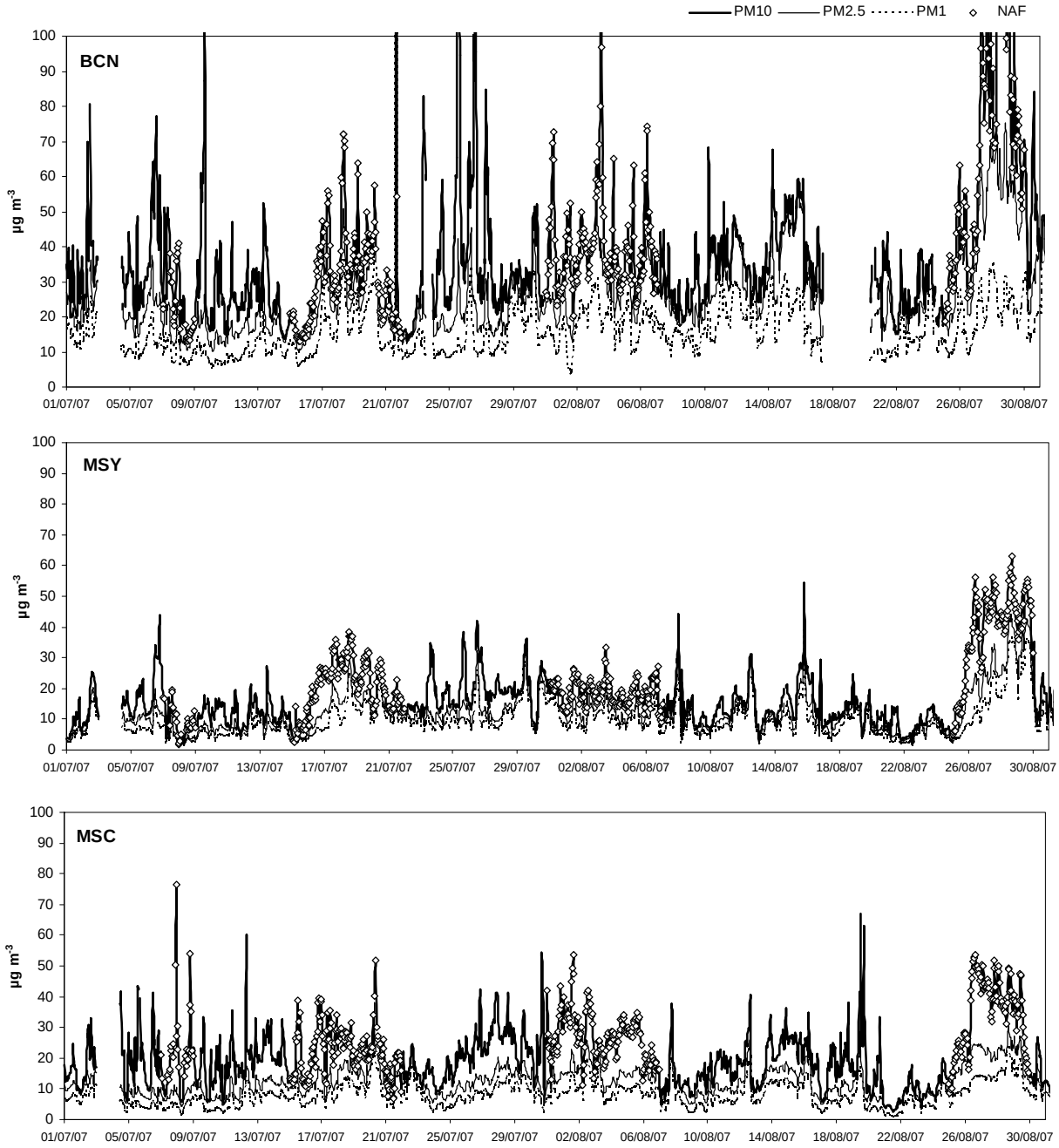

Figure 5.19. Hourly PM_{10}, $PM_{2.5}$ and PM_1 levels registered simultaneously at BCN, MSY and MSC from 1/07/2007 to 31/08/2007.

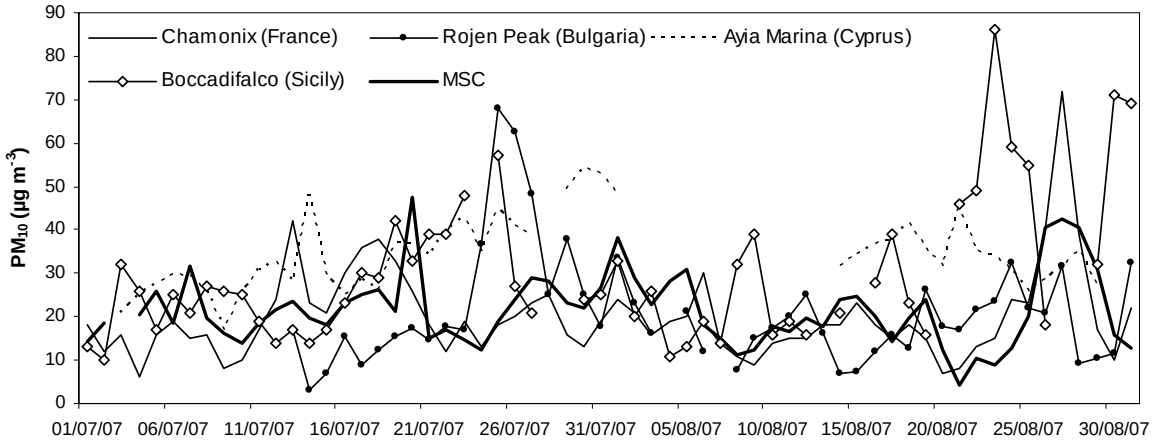

Figure 5.20. Daily PM_{10} levels registered simultaneously at MSC and other rural sites in the WMB from 1/07/2007 to 31/08/2007.

Regarding PM_{10} speciation, the important impact of these African dust episodes was observed on the ambient levels of mineral matter measured at the three sites considered, but especially at MSC, due to its higher altitude (Figure 5.21). The influence of smoke from forest fires was also evident from the finding that levels of OM+EC were also very high at the background sites during these episodes (Figure 5.21). As an example, during the episode registered on the 16-21 August, levels of mineral matter and OM+EC recorded at MSC were 9 and 8 µg m^{-3}, respectively, and those measured at MSY 6 and 6 µg m^{-3}, respectively. This is caused by the concatenation of African dust and regional recirculation episodes in the WMB, resulting in a mixture of pollutants with different origins and a wide spatial distribution. High concentrations of these compounds were recorded during long periods. During the July-August period average concentrations of mineral matter and OM+EC at MSC were 8 and 8 µg m^{-3}, respectively and at MSY 5 and 5 µg m^{-3}, respectively. They are high when compared with annual means (mineral matter and OM+EC levels were 6 and 4 µg m^{-3} at MSC, and 3 and 5 µg m^{-3} at MSY, respectively). It should also be mentioned that during the period July-August 2007, the levels of OM+EC were usually higher at MSC than at MSY and BCN, reflecting the impact at high altitudes of the high number of forest fire episodes occurring in the Mediterranean Basin during the summer 2007.

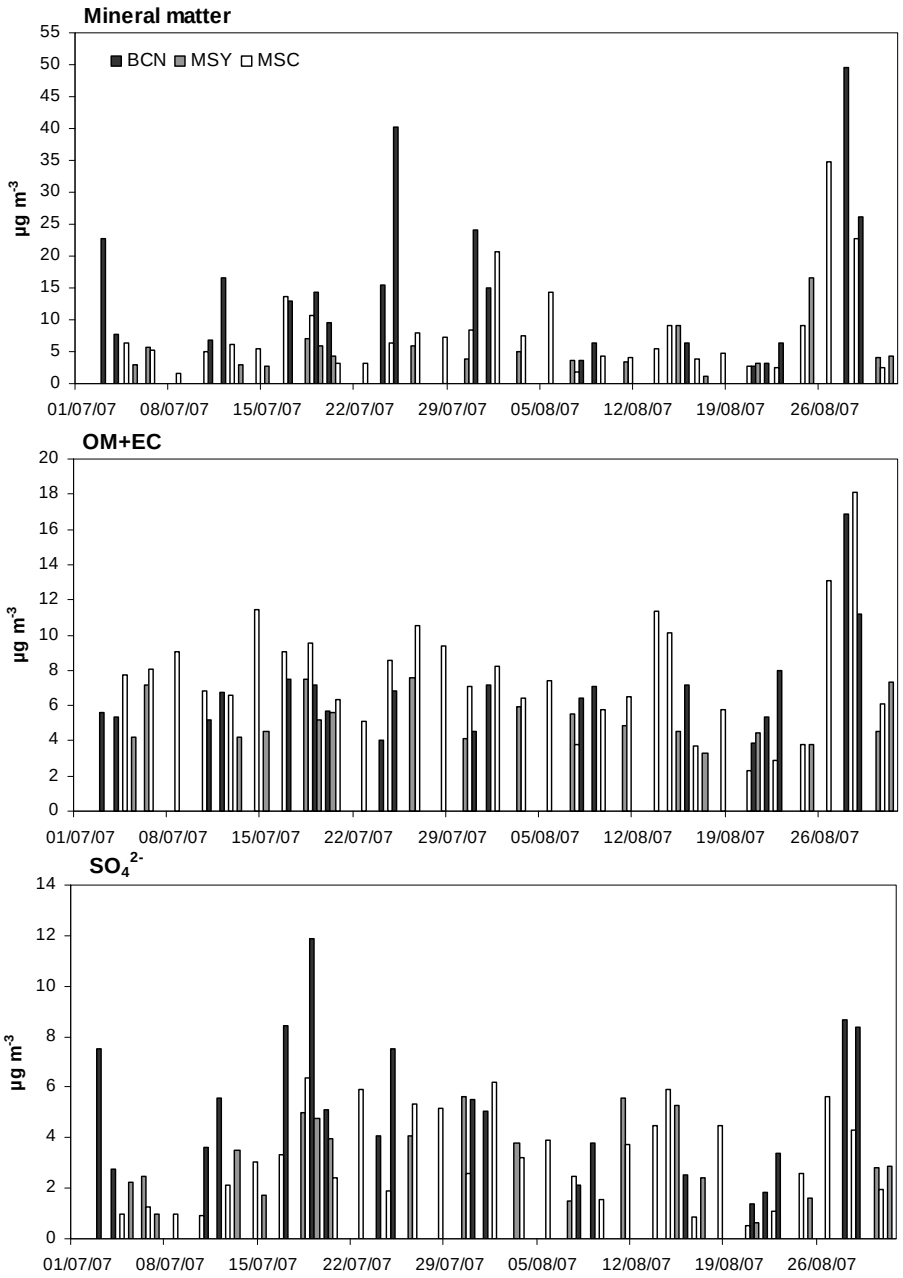

Figure 5.21. Daily mineral matter, OM+EC and sulphate levels measured simultaneously at BCN, MSY and MSC during July-August 2007.

In between the outbreaks (for example during the periods 24-30 July and 7-16 August), high levels of secondary aerosols (mainly ammonium sulphate and carbonaceous compounds) were also recorded at MSY and MSC. Levels of mineral matter measured at MSY and MSC were also high, given that the mineral matter previously transported by the NAF dust outbreaks remains in recirculation around the region (6 and 5 µg m^{-3} at MSC and MSY, respectively).

It should be observed that the levels of sulphate are very similar at the three sites during the regional recirculation episodes considered (4, 4 and 3 μg m^{-3} in PM_{10} at BCN, MSY and MSC, respectively). Conversely, during the NAF episodes considered the levels of sulphate are clearly higher in Barcelona, with concentrations also higher than during the recirculation episodes (8, 3 and 4 μg m^{-3} in PM_{10} at BCN, MSY and MSC, respectively). This illustrates that the input of mineral dust favours the formation of secondary compounds by interaction with precursors.

5.4. Source contribution: PMF at a regional scale

Source identification and quantification of contributions to simultaneous PM_{10} at BCN, MSY and MSC (November 2005-December 2007) was carried out with the PMF model to account for the common aerosol sources at a regional scale. A dataset with simultaneous PM_{10} speciation data from the three sites was considered together in the analysis in an attempt to unify the common sources affecting the WMB.

5.4.1. Components and data for analysis

Twenty-nine chemical species analyzed simultaneously in PM_{10} at BCN, MSY and MSC were selected for the PMF analysis according to their signal to noise ratio (S/N), the % of data over the detection limit (%>DL) and the errors associated to each measurement (explained in the methodology chapter, Table 5.8). A total of 570 valid cases (daily PM_{10} samples) were used for the analysis.

Table 5.8. Mean concentration for values over the detection limit (Mean>DL), error (%error), signal to noise ratio (S/N) and proportion of values over the detection limit (%>DL) for the main elements used in the PMF analysis measured in PM_{10} at BCN, MSY and MSC.

	Mean>DL (µg m^{-3})	% error	S/N	%>DL	Selected
Ctot	5.2070	61	5	92	X
Al	0.4651	83	9	83	X
Ca	1.2948	32	28	96	X
K	0.2460	32	10	97	X
Na	0.6778	74	7	86	X
Mg	0.2033	30	15	96	X
Fe	0.5120	16	80	100	X
SO_4^{2-}	3.1190	19	134	100	X
NO_3^-	2.9632	22	139	99	X
Cl^-	0.4865	593	13	66	X
NH_4^+	0.8490	24	102	100	X
Li	0.0005	365	8	87	X
Ti	0.0281	106	34	98	X
V	0.0066	43	19	96	X
Cr	0.0041	865	5	68	X
Mn	0.0111	42	52	98	X
Co	0.0003	233	3	54	X
Ni	0.0034	497	5	76	X
Cu	0.0340	745	19	78	X
Zn	0.1083	17172	2	29	X
As	0.0005	72	8	92	X
Rb	0.0008	20	28	99	X
Sr	0.0039	427	6	85	X
Cd	0.0003	205	3	63	X
Sn	0.0064	606	6	49	X
Sb	0.0045	430	8	49	X
La	0.0003	65	7	92	X
Ce	0.0007	98	6	88	X
Pb	0.0090	17	50	100	X

5.4.2. Identification of emission sources

The most robust solutions were obtained for 5 factors. The main sources identified in PM_{10} were representative of the region of study: mineral matter, secondary aerosols (ammonium sulphate and nitrate, separately), aged aerosols (composed of sea spray and secondary anthropogenic aerosols) and a primary PM traffic source mainly detected at the urban site. The source profiles for the PMF solutions obtained, together with the explained variances, are shown in Figure 5.22, and a summary of the factors identified is shown in Table 5.9.

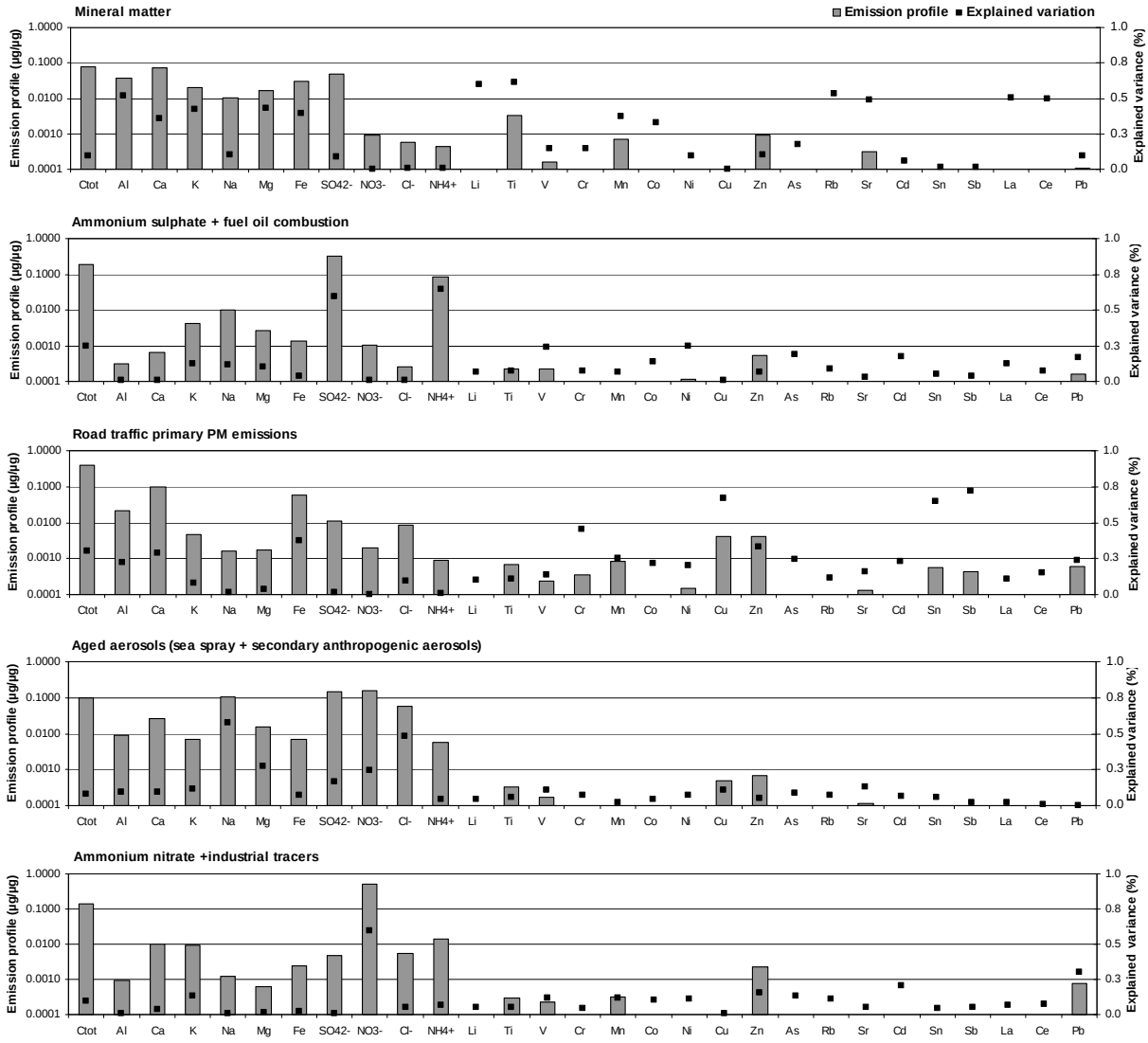

Figure 5.22. Source profiles for PMF solutions in PM_{10} for BCN, MSY and MSC data from November 2005 to December 2007. Explained variance for each element selected.

Table 5.9. Factors identified by the PMF model for PM_{10} at BCN, MSY and MSC. Elements with explained variance >0.4 are in bold letters and elements with variance <0.4 are in italics.

Mineral matter	**Al, Li, Ti, Rb, Sr, La, Ce,** *Ca, K, Mg, Fe, Mn, Co, As*
Ammonium sulphate + fuel oil combustion	**SO_4^{2-}, NH_4^+,** *Ctot, V, Ni, As, Cd, Pb*
Road traffic (primary PM emissions)	**Cu, Sn, Sb, Cr,** *Ctot, Fe, Ca, Al, Mn, Co, Ni, Zn, As, Sr, Cd, Pb*
Aged aerosols (sea spray + secondary anthropogenic)	**Na, Cl^-,** *Mg, NO_3^-, SO_4^{2-}*
Ammonium nitrate + industrial tracers	**NO_3^-,** *Zn, Cd, Pb*

Mineral matter: This factor accounted for mineral matter from long-range transport of dust during African dust outbreaks, natural mineral dust from soil resuspension and anthropogenic mineral dust at the urban area (road dust resuspension by vehicles and resuspension of dust from demolition/construction works by wind). The main tracers of this source were elements with a crustal origin, such as Al, Li, Ti, Rb, Sr, La, Ce, Ca, K, Mg, Fe and Mn. Co and As appear also in this factor as they are sometimes associated to alumino-silicate species.

Ammonium sulphate + fuel oil combustion: The main tracers of this source were inorganic ions, such as SO_4^{2-} and NH_4^+, characteristic of aged air masses. This factor also included total carbon (probably because of the presence of secondary carbonaceous aerosols) and other anthropogenic pollutants, such as V and Ni (tracers of fuel oil combustion, mainly from industry and shipping), and As, Cd and Pb (tracers of industrial emissions).

Primary PM Road traffic: This factor is identified by the presence of total carbon (Ctotal, from primary vehicle exhaust emissions) and trace elements, such as Fe, Cu, Cr, Sn and Sb (from the mechanical abrasion of road pavement and vehicle components). Other tracers appear in this factor, such as Ca, Fe, Al, Mn, Co, As, Sr, associated to mineral matter, because of the resuspension of road dust by vehicles, and Ni, Zn, Cd, Pb associated to road traffic and industrial emissions.

Aged aerosols (sea spray + secondary anthropogenic): This factor is a mixed source of marine aerosols and secondary aerosols originated by interaction of sea spray and gaseous pollutants in the urban atmosphere or during transport and aging of air masses in the region. The main tracers of this source were elements from sea spray (Na, Cl^- and Mg) and secondary compounds (NO_3^- and SO_4^{2-}).

Secondary nitrate + industrial tracers: The main tracer of this source was NO_3^- (mainly from the oxidation of NO_x traffic exhaust emissions), and additionally Zn, Cd and Pb (tracers of industrial emissions). It has to be clarified that the above road traffic source refers to the primary only traffic emissions, whereas most of the secondary PM from traffic are included in this source.

5.4.3. Quantification of source contributions to PM_{10}

The correlation coefficient (r^2) between the measured and PMF-modelled concentrations was 0.93. PM_{10} mass simulated in the analysis was 100%, 95% and 77% at BCN, MSY and MSC, respectively (Figure 5.23).

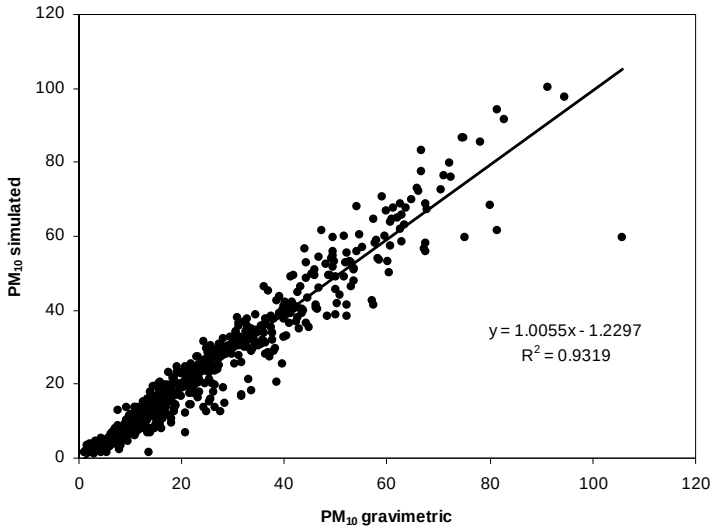

Figure 5.23. Correlation between PM_{10} simulated with PMF and gravimetric PM_{10} at BCN, MSY and MSC.

The main contributions to each factor obtained in the PMF analysis are shown in Table 5.10. In BCN, primary road traffic was the most important factor (27% of the PM_{10} mass); however the rest of factors presented also very high contributions. Mineral matter accounted for 22%, ammonium sulphate for 19%, aged air masses for 18% (this source accounting for a mixture of sea spray and secondary aerosols formed in the urban atmosphere), secondary nitrate for 15% (mostly derived from vehicle exhaust emissions of NO_x) and the unaccounted fraction was not significant (0.2%).

Secondary aerosols were the major contributors to PM_{10} at MSY (38% ammonium sulphate + fuel oil combustion and 16% ammonium nitrate), although an important proportion of the nitrate at the regional background may also be originated from road traffic NO_x emissions (an important proportion from traffic related pollutants transported from BCN, but also from the region). The contribution of mineral matter accounted for 27%, aged marine aerosols for 10% and primary road traffic 4%. The unaccounted fraction was 5% of the total mass.

Secondary inorganic aerosols were also the major contributors to PM_{10} mass at MSC (30% ammonium sulphate + fuel oil combustion and 7% ammonium nitrate). Mineral matter was also a very important contributing source (25% of the PM_{10} mass). The aged marine source contributed 13% to the total mass due to the formation of secondary aerosols during the transport of air masses. Primary road traffic had a very low contribution at MSC (2%) and its detection may also be related to transport of

carbonaceous compounds from important forest fires in the Mediterranean. The unaccounted fraction was 23% of the total PM_{10} mass, much higher than measured at MSY and BCN, probably due to the presence of a high proportion of hydrophilic compounds (Jimenez et al., 2009). The contribution of the secondary nitrate source is much higher at MSY than MSC (16 vs. 7%) and may be the consequence of the lower contribution of road traffic emissions at MSC.

Table 5.10. Average contribution of PM_{10} sources identified by the simultaneous PMF analysis performed at BCN, MSY and MSC (µg m^{-3} and %).

	µg m^{-3}			%		
	BCN	**MSY**	**MSC**	**BCN**	**MSY**	**MSC**
Mineral matter	9.4	4.0	4.0	22	27	25
Ammonium sulphate + fuel oil combustion	8.2	5.5	4.9	19	38	30
Road traffic (primary PM emissions)	11.9	0.6	0.3	27	4	2
Aged aerosols (sea spray + secondary anthropogenic)	7.7	1.5	2.0	18	10	13
Ammonium nitrate + industrial tracers	6.4	2.4	1.1	15	16	7
Unaccounted	<0.1	0.8	3.8	<1	5	23

5.4.4. Seasonal variability

The seasonal evolution of the five factors identified by PMF at the three sites is presented in the next figures. Mineral matter was higher during the warmer months at the three sites due to favoured resuspension processes and the higher frequency of African dust outbreaks (Figure 5.24). However this trend is more marked at MSY and MSC due to the higher local contribution at BCN during all the year.

Ammonium sulphate was higher during the warmer months due to the higher photochemical activity and the higher frequency of regional recirculation episodes producing the aging of air masses (Figure 5.25). The trend was also more marked at MSY and MSC, due to the higher local emissions recorded in BCN. Similar levels are observed in MSY and MSC during the summer, due to the regional pollution reaching MSC, but higher levels are recorded in MSY during the winter.

The contribution of the road traffic factor was much higher at BCN and decreased from MSY to MSC, with extremely low contribution recorded at MSC (Figure 5.26). This factor presents a clear seasonal trend at BCN, increasing during the winter months due

to the intense pollution episodes produced by anticyclonic conditions during the winter. However at MSY and MSC no trend is observed. The higher contributions observed in MSC during the summer 2007 may be due to the detection of carbonaceous compounds due to the transport of smoke from important forest fires in the Mediterranean.

The aged aerosol factor increased during the summer months because of the more intense breezes during this period (Figure 5.27). The levels were much higher in BCN and decreased from MSY to MSC due to the distance to the coast and the high contribution of secondary aerosols due to the interaction of sea spray with gaseous pollutants at the urban site.

The secondary nitrate factor was much higher in Barcelona, due to the higher road traffic emissions and increased during the winter because of the higher frequency of anticyclonic pollution episodes recorded during this period of the year and the thermal instability of ammonium nitrate during the warmer months (Figure 5.28). At MSY, the increase of ammonium nitrate levels during the winter was also related to the transport of pollutants accumulated during winter anticyclonic episodes.

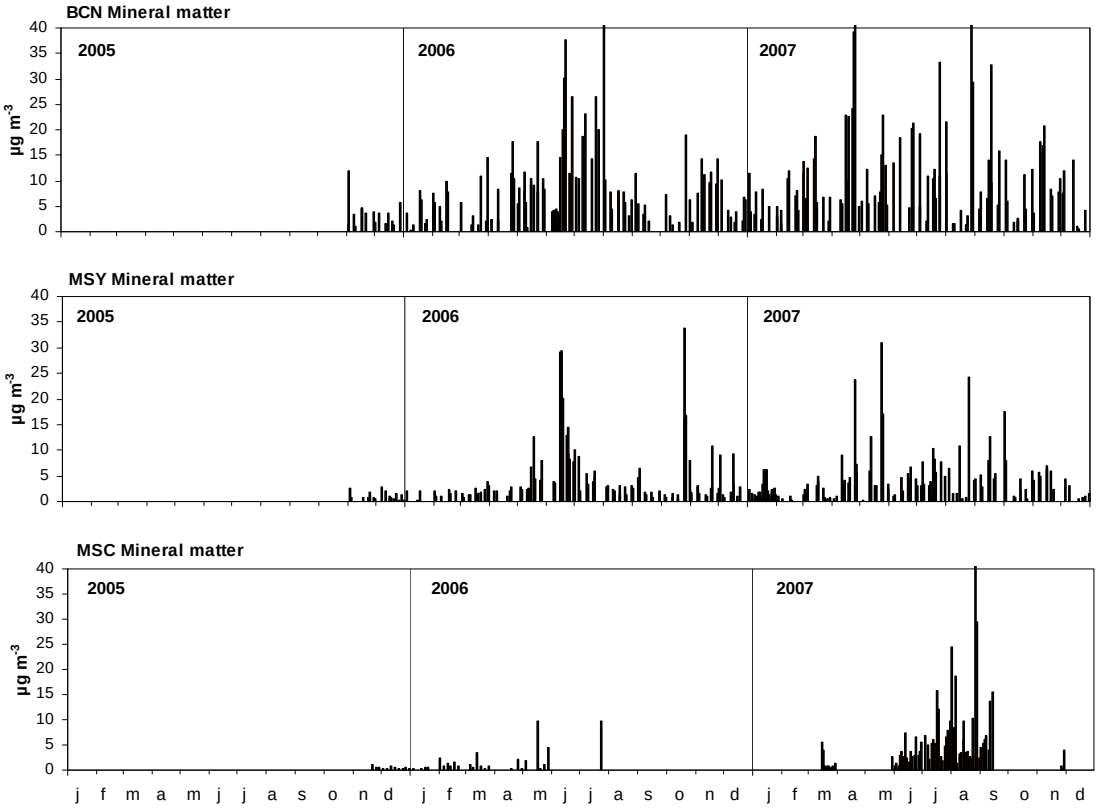

Figure 5.24. Seasonal evolution of the main daily contributions for the mineral matter source identified in PM_{10} by PMF at BCN, MSY and MSC.

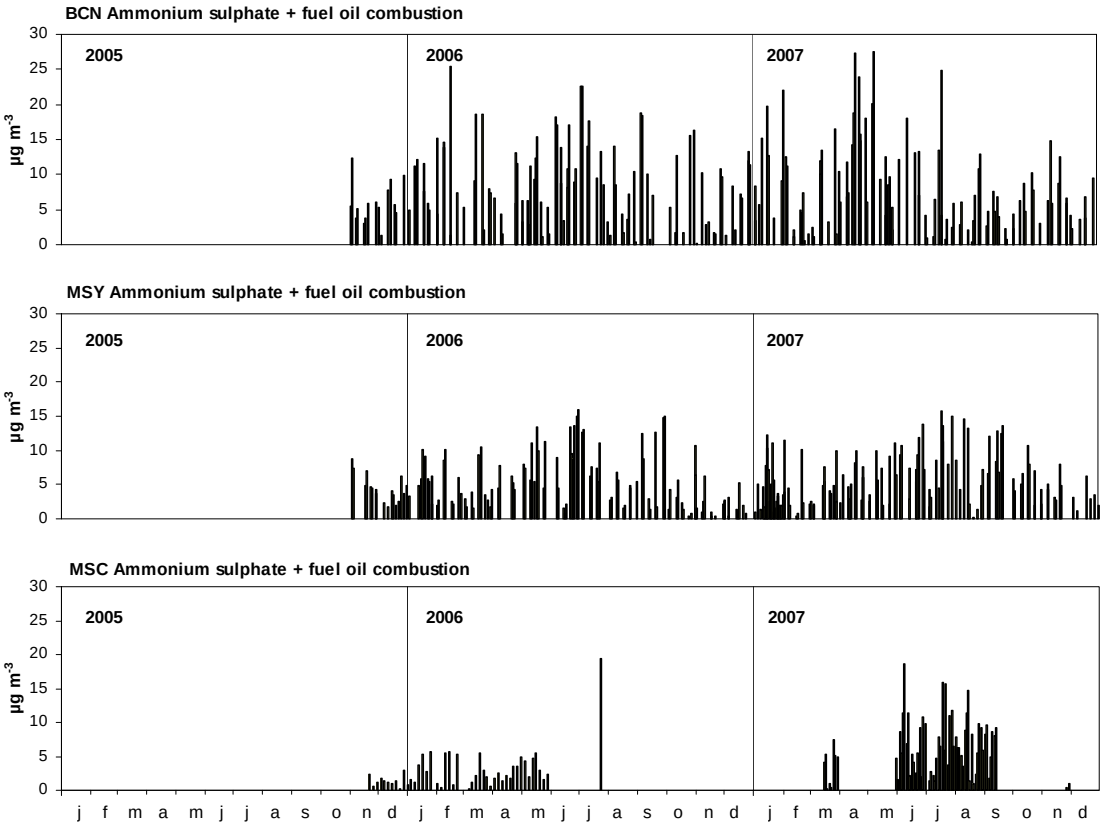

Figure 5.25. Seasonal evolution of the main daily contributions for the ammonium sulphate + fuel oil combustion source identified in PM_{10} by PMF at BCN, MSY and MSC.

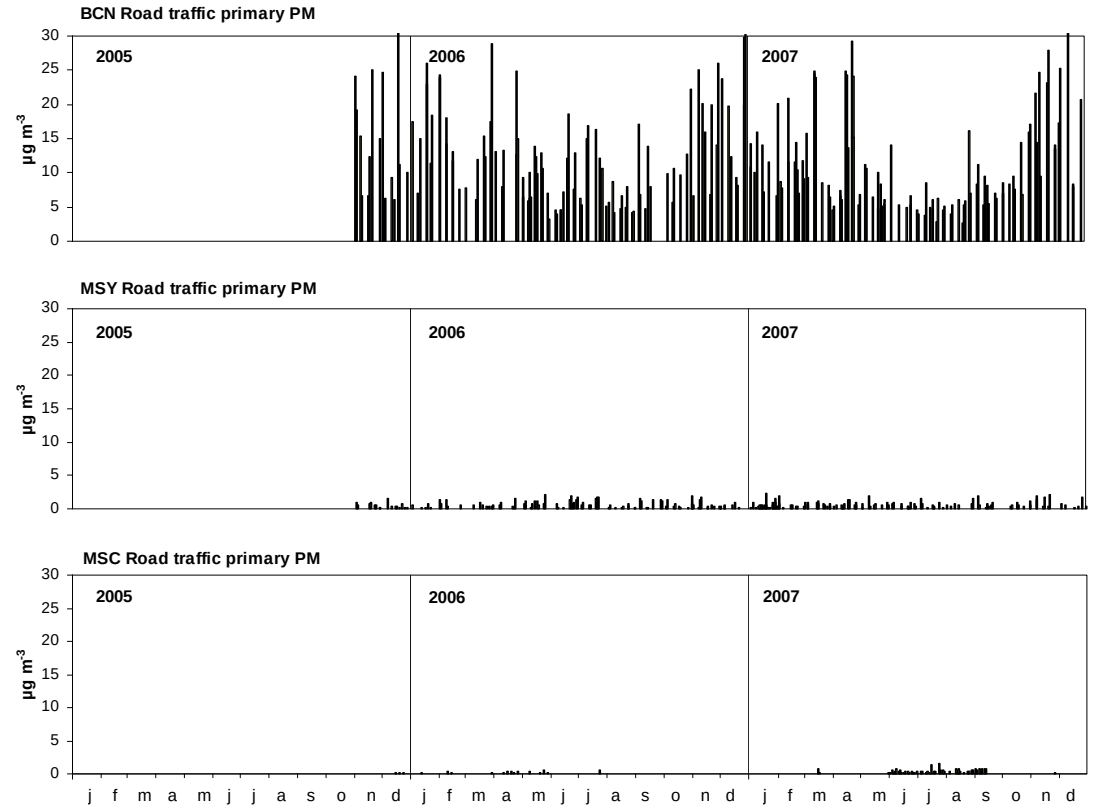

Figure 5.26. Seasonal evolution of the main daily contributions for the primary road traffic source identified in PM_{10} by PMF at BCN, MSY and MSC.

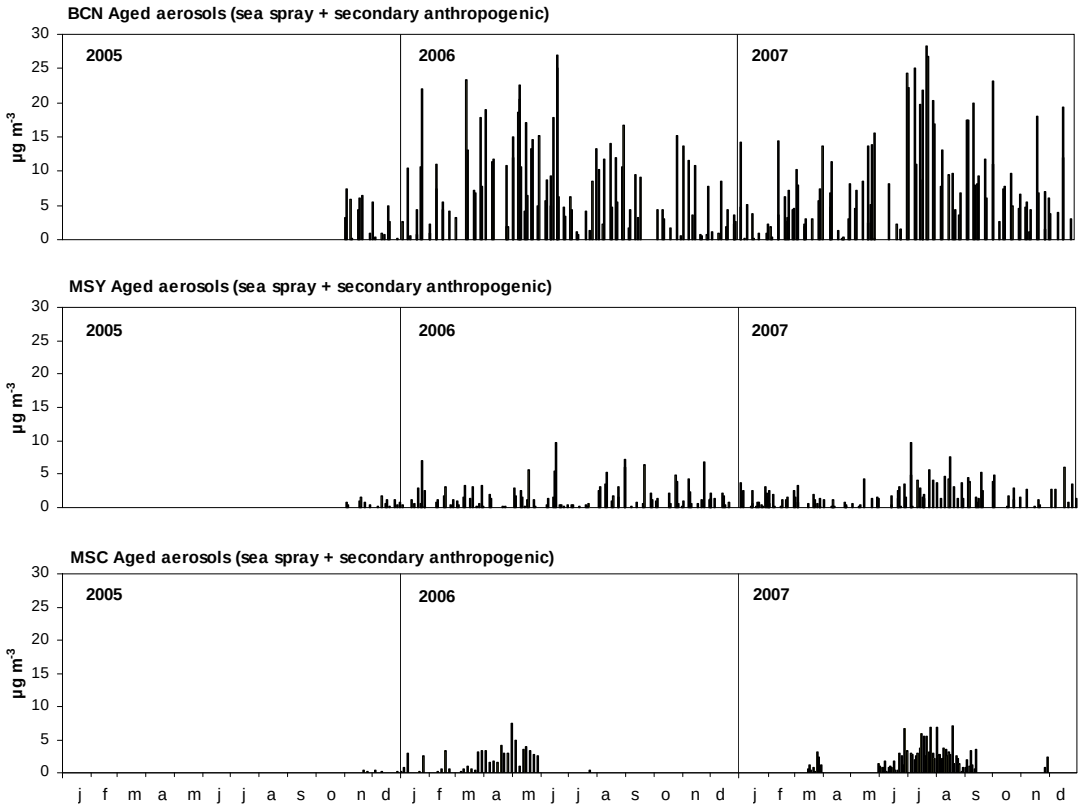

Figure 5.27. Seasonal evolution of the main daily contributions for the aged aerosol source identified in PM_{10} by PMF at BCN, MSY and MSC.

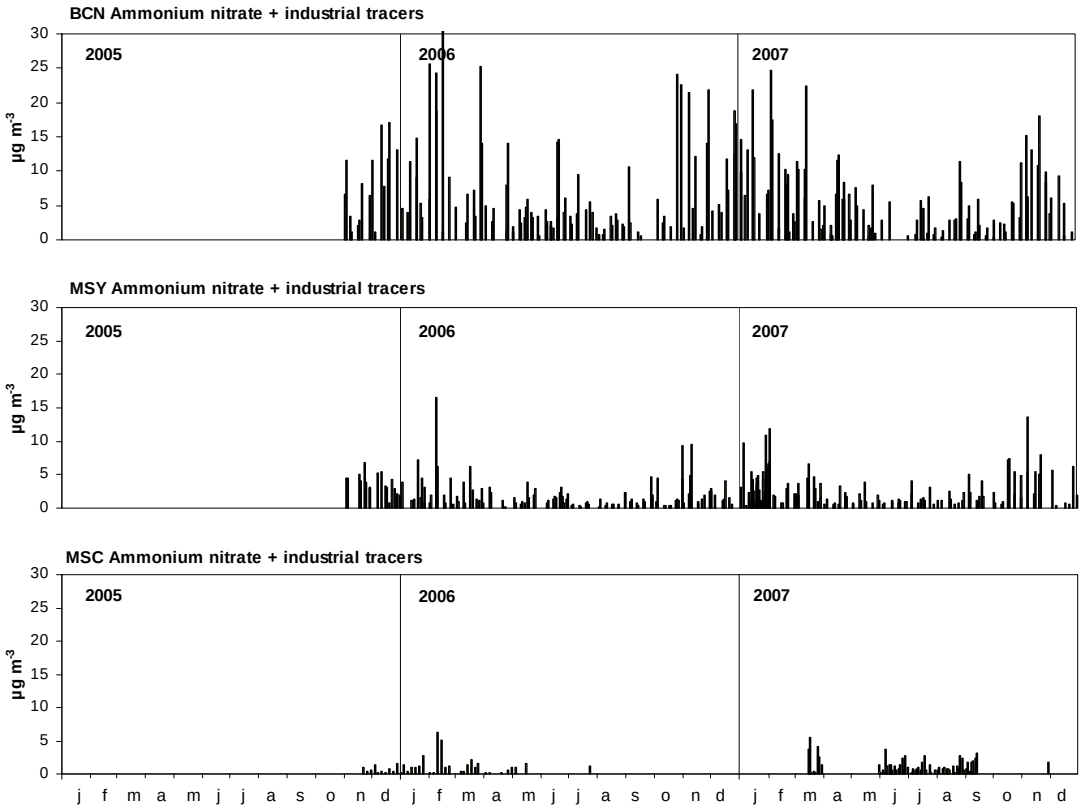

Figure 5.28. Seasonal evolution of the main daily contributions for the ammonium nitrate + industrial tracers source identified in PM_{10} by PMF at BCN, MSY and MSC.

5.4.5. Estimation of urban/local and regional contributions of the PM sources

The contribution of the main PM_{10} sources identified in BCN is the result of the addition of long range/continental, regional and local contributions. In order to quantify these contributions in the following the main sources identified will be divided by subtracting the regional contribution (contribution of each source at MSY) from the urban background. The continental contribution has not been subtracted from the regional background given that we have considered both summer and winter dataset, including the African data, in order to account for a representative number of cases. Nevertheless, the contributions determined for MSC have been taken into account for interpretation.

The African dust contribution to mineral matter was previously calculated as the difference between the crustal load for the total period and for the days without African dust influence (section 5.1.2). This African dust contribution was of 1.3 µg m^{-3} at BCN, 0.5 at MSY and 1.1 µg m^{-3} at MSC. However, in order to simplify the calculations the contribution obtained for MSY will also be used in BCN.

Thus, in MSC, the mineral matter source (4.0 µg m^{-3}, 25% of the total PM_{10} mass) may be divided in the African contribution (7% of PM_{10}) and regional dust transport + local dust resuspension (18%, Table 5.11 and Figure 5.29). In MSY, the contribution of the mineral matter source (4.0 µg m^{-3}, 27% of the total PM_{10} mass) may be divided in the African contribution (3% of PM_{10}) and regional dust transport + local dust resuspension (24%).

The mineral matter source identified for BCN (9.4 µg m^{-3}, 22% of the total PM_{10}) may also be divided in the African dust contribution (1%), the regional dust resuspension (dust source contribution in MSY discounting the African dust increment, 8%) and the anthropogenic dust (road dust resuspension at the urban site by road traffic, wind and construction/demolition works, calculated as the difference between BCN and MSY dust source contributions, 13%, Table 5.11 and Figure 5.29). Thus, part or the mineral matter source at the urban site may also have an important contribution from road traffic indirect emissions. However, the anthropogenic contribution to mineral dust is divided between the primary traffic factor and the mineral matter factor in the analysis and it is difficult to quantify.

The secondary nitrate source was identified at the three sites. The contribution of this source is relatively higher in MSY (2.4 µg m^{-3}) than in MSC (1.1 µg m^{-3}), reflecting a certain impact of urban and industrial emissions in MSY (Table 5.10). Nevertheless, assuming a major regional origin of nitrate in MSY, at least 62% of the secondary nitrate source (9% of the total PM_{10}) estimated in BCN may be originated from local traffic exhaust emissions (difference of this source contribution between BCN and MSY, Table 5.11and Figure 5.29).

At the three sites, the aged aerosol source (Table 5.11 and Figure 5.29) includes sea spray secondary aerosols originated by interaction of sea spray and gaseous pollutants in the urban atmosphere or during transport and aging of air masses in the region. The difference between sea spray levels (calculated as the sum of Na^+ and Cl^-, see Table 5.2) and the contribution of this source is more important in BCN, where the aged aerosol contribution (5.6 µg m^3) is clearly higher than the mean sea spray levels (2.1 µg m^{-3}). Therefore, in BCN, 30% of the aged aerosol source detected may be due only to sea spray, and 70% of this factor may be attributed to secondary aerosol formation, probably from the high emissions of precursors from road and port traffic at the urban site (13% of the total PM_{10} mass).

The road traffic source contribution (mainly related to primary emissions) is very low in MSY and MSC. However, in BCN this source accounts for 11.9 µg m^{-3}, (28% of the total PM_{10} mass, Table 5.11 and Figure 5.29). In addition, as discussed above, a high proportion of the secondary nitrate source and of the aged marine aerosols (accounting for 9% and 13% of PM_{10}, respectively) may be attributed to traffic emissions (including port emissions). Therefore, the road traffic source (including primary and secondary emissions) accounts for 50% of the total PM_{10}. It should be taken into account that a fraction of the secondary aerosols from the nitrate and aged marine source may be also be originated from other emissions other than road and port traffic, such as domestic emissions and small industries. However, these contributions are probably low in BCN.

The contribution of the ammonium sulphate + fuel oil combustion source is very similar at MSY and MSC (5.5 and 4.9 µg m^{-3}, respectively). In BCN, this source accounts for 8.2 µg m^{-3} (Table 5.10). Assuming that the contribution of this source at MSY is the regional contribution in the BCN area, the difference (33%) may be attributed to the urban emissions (industries and port). Consequently, the ammonium sulphate source

at BCN may be divided in the regional contribution (12% of the total PM_{10} mass) and the urban increment (6%, Table 5.11 and Figure 5.29).

Table 5.11. Average contribution of PM_{10} sources identified by the simultaneous PMF analysis performed at BCN, MSY and MSC (µg m^{-3}) divided in the estimated contributions of primary, secondary sources, urban, regional or long-range contributions, as explained in the text above.

		µg m^{-3}			%		
		BCN	MSY	MSC	BCN	MSY	MSC
Road traffic emissions	Primary emissions	11.9	0.6	0.3	28	4	2
	Secondary nitrate from traffic	3.9			9		
	Aged secondary aerosols	5.6			13		
Anthropogenic urban emissions	Anthropogenic dust	5.9			13		
	Secondary ammonium sulphate	2.7			6		
Regional + continental contribution	Transport + resuspension of dust	3.5	3.5	2.9	8	24	18
	Ammonium nitrate	2.4	2.4	1.1	5	16	7
	Ammonium sulphate	5.5	5.5	4.9	12	38	30
Sea spray		2.1	0.5	0.3	5	3	2
Aged secondary aerosols			1.0	1.7		7	11
African dust transport (NAF)		0.5	0.5	1.1	1	3	7
Unaccounted		<0.1	0.8	3.8	<1	5	23

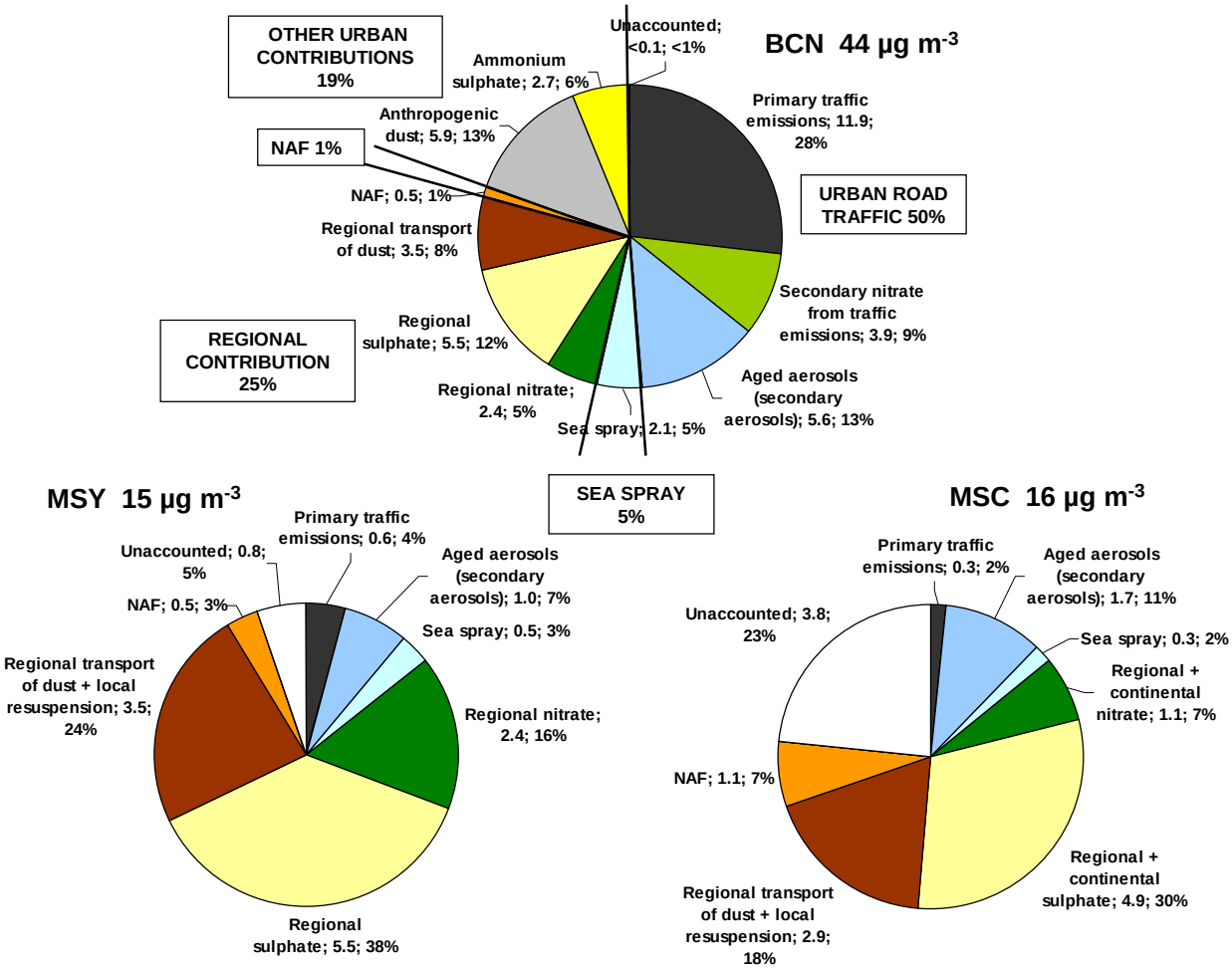

Figure 5.29. Average contribution of PM_{10} sources identified by the simultaneous PMF analysis performed at BCN, MSY and MSC (µg m^{-3} and %) divided in the estimated contributions of primary, secondary sources, urban, regional or long-range, as explained in the text above.

In conclusion, the PMF analysis, applied to the dataset with simultaneous PM data measured at BCN, MSY and MSC, gives information on common sources at the continental, regional and urban backgrounds in the WMB, such as mineral dust from long-range transport during African dust outbreaks, road dust resuspension and regional dust resuspension, secondary aerosols (as ammonium sulphate and nitrate) and aged secondary aerosols due to the recirculation of air masses in the region, together with the presence of sea spray, tracers from fuel oil combustion, industrial processes and primary road traffic.

The results obtained show that the monitoring of atmospheric aerosols at an urban background site is important in order to monitor emissions from the urban agglomeration (road traffic, industrial emissions, fugitive emissions from demolition and construction activities and other domestic emissions). The monitoring of aerosols at the regional background is useful to obtain information on the regional transport and aerosol processes. In addition, the monitoring of the continental background aerosol is also very important in order to monitor the impact of global emissions and long range transport episodes on the levels of ambient aerosols. Finally, the simultaneous aerosol monitoring at urban, regional and continental sites in the same region is very useful for understanding the impact of the different emission sources and processes on the levels of atmospheric aerosols in the area.

6. CONCLUSIONS

6. Conclusions

A detailed study on PM levels and composition in the western Mediterranean basin (WMB) was performed in order to understand the sources, variability of the levels and composition, and transport and transformation patterns of aerosols in the lower troposphere in this area. The WMB presents special and complex characteristics, and a number of studies have been performed in this topic in the last years. However, there is a gap of knowledge on aerosol characterization in this area. In this direction, the monitoring of PM_{10}, $PM_{2.5}$ and PM_1 levels and chemical characterization was carried out at three monitoring stations located in different environments at a regional scale: Montsec (MSC, continental background, 1570 m.a.s.l.), Montseny (MSY, regional background, 720 m.a.s.l.) and Barcelona (BCN, urban background, 68 m.a.s.l.). In addition, levels of particle number concentration (N) and black carbon (BC) were monitored at the BCN site, in order to investigate the major causes of the variability of levels of submicron particles in the urban atmosphere and to interpret atmospheric processes. With respect to previous studies, this is the first time that aerosol characterization has been conducted at a remote site in the WMB simultaneously with other environments. Speciation of PM_1 and continuous and simultaneous monitoring of BC and N are also novel aspects of aerosol research in the WMB.

Sections with a summary of results and conclusions on BCN, MSY and MSC aerosol characterization were previously presented at the end of each chapter. In this section, the most relevant conclusions for each site and on the comparative study of atmospheric aerosols at the urban, regional and continental backgrounds are presented.

The variability of atmospheric aerosols in the WMB is governed by the influence of diverse anthropogenic and natural emissions, and the concatenation of different meteorological scenarios, both of them affecting levels, composition and size distribution of particulate matter. The seasonal distribution of these episodes, together with the characteristic climatic patterns of the WMB, give rise to a marked seasonal pattern for regional background PM levels. In addition, local emissions are superimposed onto this background pattern. In any case, PM levels and composition measured in BCN presented a more important variability than at the regional and continental backgrounds.

Daily atmospheric dynamics at MSY and MSC are highly influenced by the breeze circulation (mountain and sea breezes) which regulates the daily evolution of PM levels. Early in the day atmospheric pollutants accumulate in the pre-coastal (MSY) or Ebro (MSC) depression. Subsequently, the diurnal breeze (activated by insolation) transports aged air masses upwards from the valley, increasing PM levels in elevated RB areas. The impact of this mechanism varies widely along the year with a marked different picture in winter and summer.

During winter, the frequent anticyclonic atmospheric stability induces the stagnation of air masses that, together with road traffic emissions, produce important pollution episodes at BCN. However, atmospheric decoupling leaves MSY and, more frequently MSC, isolated from regional pollution during several days. In specific scenarios, the growth of the boundary layer and development of mountain breezes, activated by solar radiation, result in the transport of highly polluted air masses accumulated in the valley to the rural sites, increasing markedly PM levels (mainly composed of carbonaceous compounds and ammonium nitrate) at a different rate depending on the altitude and distance to the source areas. These scenarios frequently impact MSY increasing PM_1 levels during the afternoon and reaching hourly values up to 50 µg PM_1 m^{-3}, even higher than at BCN. This is due to the formation of secondary aerosols by the interaction between pollutants during transport. After a few days, if the atmospheric conditions persist, PM levels may remain high at MSY for a relatively short period (4-5 days). Given its altitude, MSC is frequently isolated from regional pollution. However, when the high PM_1 episodes are persistent the polluted air masses may also reach distant areas such as MSC.

Due to the predominance of Atlantic advection and local winter stagnation situations, the higher differences between PM levels or most components measured in PM_{10} at the urban and the rural sites were determined for winter. Thus, average levels of PM_{10}, $PM_{2.5}$ and PM_1 (excluding NAF episodes) were 40, 29 and 22 µg m^{-3}, respectively, at BCN, 12, 10 and 9 µg m^{-3} at MSY, and 10, 9 and 6 µg m^{-3} at MSC. Thus, in winter, the urban contribution accounts for more than 70% of the total concentration in BCN for elemental carbon (EC), organic matter (OM), mineral dust and NO_3^- and for more than 50% for SO_4^{2-} and NH_4^+.

It is important to highlight the important differences between the levels of ammonium nitrate and sulphate at the urban site with respect to the regional background, especially during the colder months. The high urban contribution to secondary

inorganic aerosols (SIA) was probably produced by a rapid in-situ formation of secondary aerosols from traffic gaseous precursors (ammonia and nitrogen oxides), sewage fugitive emissions (ammonia) and shipping emissions (SO_2). This is highly relevant, given that many prior studies attributed a major regional origin for these secondary compounds, due to the important agricultural and farming emissions of ammonia.

During summer, intense breeze circulations and atmospheric mixing favour the dispersion, transport, recirculation and ageing of pollutants at a regional scale, reducing the differences in PM levels between the urban and the rural sites. Average levels of PM_{10}, $PM_{2.5}$ and PM_1 (excluding NAF episodes) were 37, 24 and 16 µg m^{-3}, respectively, at BCN and 15-16, 11-12 and 8-9 µg m^{-3} at the rural sites. Similar concentration levels of the main components were measured in PM_{10} at MSY and MSC. During this season, levels of PM and major components are still higher in BCN with respect to the rural sites, but differences are reduced when compared with winter data. Thus, the urban contribution in BCN is reduced with respect to winter, accounting for 30% of the total concentration for carbonaceous compounds (OM+EC), less than 70% for mineral dust and NO_3^- and for less than 30% for SO_4^{2-} and NH_4^+.

The levels of OM+EC were reduced at the BCN area during the warmer months due to the higher dispersion of pollutants, but also probably due to thermal instability of semi-volatile compounds. Conversely, OM+EC levels increase at the rural sites during summer, probably because of the transport and transformation of anthropogenic pollutants around the WMB, enhanced biogenic emissions, and also, the influence of forest fire emissions. Levels of mineral matter increase during the summer at the rural sites, as a consequence of a favoured regional dust resuspension (convective dynamics and scarce precipitations) and a higher frequency of African dust episodes. This increase is more significant at MSC given the higher impact of African dust episodes at higher attitudes, and the favoured local resuspension of dust by wind. Conversely, the summer increase of mineral matter is not as marked in BCN due to the continuous high emissions of local sources, mainly traffic and construction. Regarding SIA, there is a clear decrease on the levels of nitrate at all sites with respect to winter, but this is more marked at BCN. Sulphate levels increase during summer at all sites due to favoured photochemistry, and the differences between the urban and rural sites decrease. It should be noticed that mean levels of sulphate during the regional recirculation episodes are similar at the three sites, proving the regional origin of this compound and the high mixing during these events.

Mean PM_1 levels were higher at MSY than MSC, showing the influence of regional anthropogenic emissions on the regional PM background. However, during the summer, the levels of the coarser fractions ($PM_{2.5-10}$ and $PM_{1-2.5}$) were higher at MSC than at MSY, as a consequence of the higher influence of mineral emissions and sources (African dust and local/regional resuspension).

African dust outbreaks increase markedly the levels of coarse PM in the WMB, leading to exceedances of the PM_{10} daily limit values (50 µg PM_{10} m^{-3}, directive 2008/50/CE). However, at BCN, this increase in coarse PM cannot be exclusively attributed to African dust, due to the important road dust and construction emissions. At the rural sites, almost all the exceedances of the PM_{10} daily limit value recorded were caused by African dust outbreaks, being the impact, as stated above, much higher at MSC. African dust contributions to mean annual PM_{10} levels calculated by gravimetry were 2.1, 0.6 and 1.4 µg m^{-3} at BCN, MSY and MSC, respectively. The increase in mineral matter levels due to NAF was quantified as 1.3, 0.5 and 1.1 µg m^{-3} for BCN, MSY and MSC, respectively. The difference observed between the increase in PM_{10} levels and the increase in mineral matter levels attributed to African dust outbreaks may be due to the formation of secondary aerosols favoured by the presence of high concentrations of mineral dust.

Given the complex scenario of the WMB, the applicability of the Lenshow's (or 'delta') method to this area has some limitations. The discrimination of the continental background contribution to PM levels was possible when considering winter months, when the MSC site is less affected by regional pollution and local resuspension processes. Besides, given that the regional background may be significantly influenced by urban emissions, the urban contribution, estimated by the difference between the urban and regional backgrounds, could be underestimated.

Source apportionment was carried out for simultaneous PM_{10} data measured at BCN, MSY and MSC by Positive Matrix Factorization (PMF). The results obtained showed five common aerosol sources at a regional scale, representative of the region of study: Mineral matter, ammonium sulphate + fuel oil combustion, ammonium nitrate, aged aerosols (sea spray + secondary aerosols) and a primary road traffic + industrial tracers source showing its main contribution at the urban site.

The contribution of the main PM_{10} sources identified in BCN is the result of the addition of long range/continental, regional and local contributions. In order to quantify these contributions the main sources identified were divided by subtracting the regional contribution (contribution of each source at MSY) from the urban background. The contributions determined for MSC were taken into account for interpretation. Results obtained are presented in Figure 6.1.

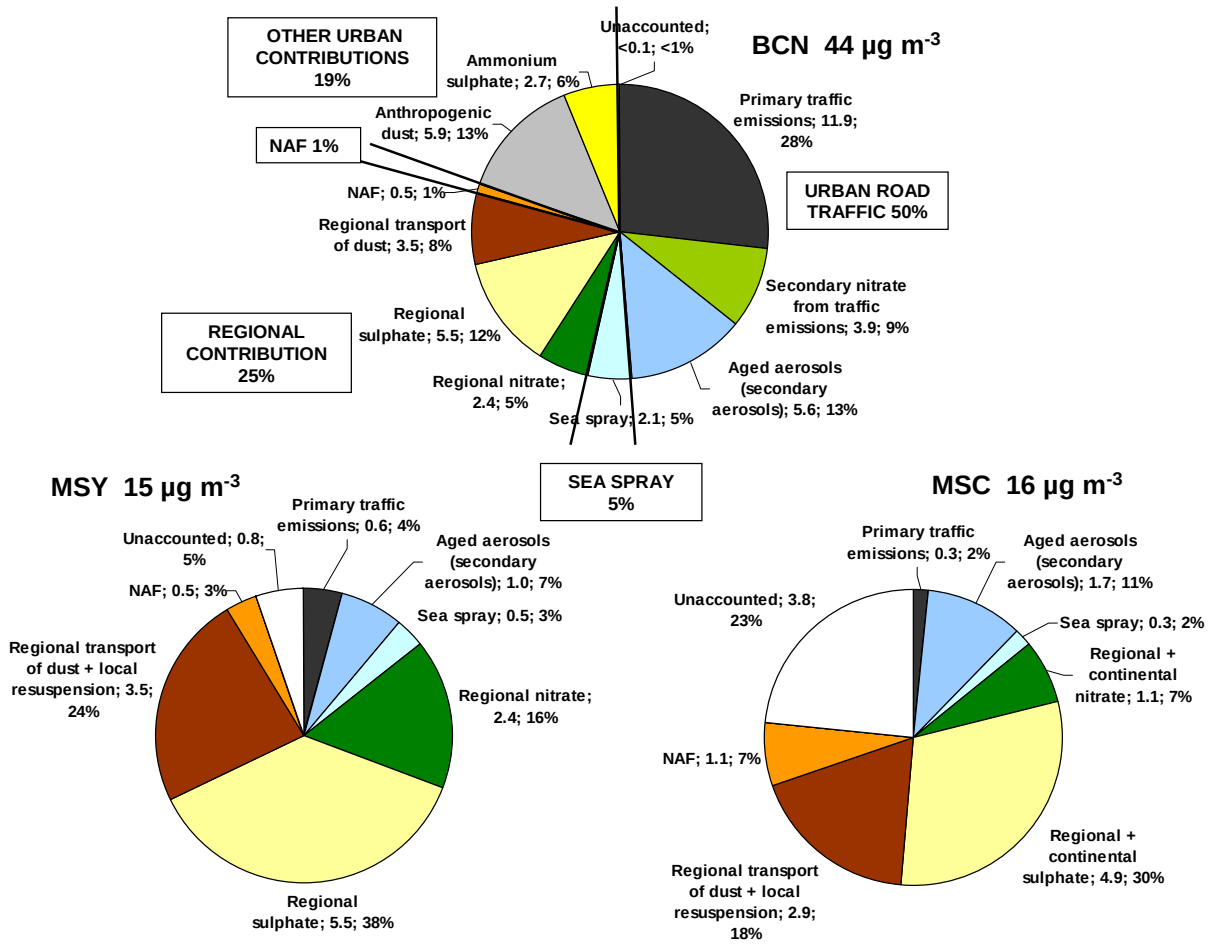

Figure 6.1. Average contribution of PM_{10} sources identified by the simultaneous PMF analysis performed at BCN, MSY and MSC (µg m^{-3} and %) divided in the estimated contributions of primary, secondary sources, urban, regional or long-range contributions.

The urban source is the major contribution to PM_{10} in BCN and is mainly related to particulate and gaseous emissions from road traffic, which accounts for 50% of PM_{10}, resulting from primary traffic emissions (29%), a fraction of the secondary nitrate (9%) and also a fraction of the aged secondary aerosols (13%), although the latter may be partially attributed to other sources. Other urban source identified is the anthropogenic dust (13%) which may be also emitted by traffic in an important extent (road dust resuspension by vehicles) and by wind resuspension and construction/demolition

works. The last urban source identified is urban ammonium sulphate, accounting for 6% of the PM_{10}. The regional contribution to PM_{10} is estimated in 25% of the PM_{10} and it is composed of mineral dust, ammonium sulphate and nitrate species. Finally, the African dust accounts for 1% of the PM_{10}, and the sea spray for 5%.

Major sources at MSY and MSC are mineral and secondary sulphate. Secondary nitrate is an important source in MSY but has a lower relevance in MSC. The African dust source is slightly higher at MSC.

The short time variability of all aerosol metrics (N, BC, PM_x) and gaseous pollutants recorded at BCN urban background is very influenced by road traffic emissions and meteorology (especially the evolution of breezes). PM_x, N, BC, CO and NO_x levels increase markedly during traffic rush hours, reflecting direct exhaust emissions. Then, levels of most parameters decrease at midday due to the reduction of traffic emissions and the changes in wind direction and speed, due to dilution processes. However, the variability of some parameters are not only governed by traffic direct exhaust emissions. Thus, $PM_{2.5-10}$ remains high during all the day due to road dust resuspension processes, but also has contributions from other sources (construction sources and dust resuspension by wind). $PM_{1-2.5}$ and PM_1 levels increase during traffic rush hours but also at night, when the decrease of the boundary layer depth favours condensation and coagulation processes, and consequently N levels decrease and levels of the fine PM fractions increase.

In addition to the traffic peak, N levels show a second but very important peak at noon, reflecting the variation of the solar radiation intensity, which may be attributed to ultrafine particle formation by the photochemical nucleation of precursor urban gaseous pollutants. This peak appears when the levels of BC (primary emissions) are very low. Thus, N is influenced by direct ultrafine particle emissions but also in a very important fraction by the formation of secondary (soluble) particles by photochemical processes. Similar results concerning the formation of secondary particles are expected at MSY and MSC, where these measurements were not available at the time of this study.

The influence of road traffic emissions on the levels of fine particulate matter at the urban background is reflected in PM_1 mean annual levels, which show a statistically significant increasing trend from 2003 to 2007, and a good correlation with the progressive rise in road traffic flow and the growth of the diesel fleet in Barcelona. However the coarse fraction ($PM_{2.5-10}$) showed a decreasing trend. At the regional

background PM_{10} and $PM_{2.5}$ decreasing trends were detected from 2002 to 2007. The decreasing trend observed for the coarser fractions at a regional scale may be attributed to meteorology and the frequency and intensity of African dust outbreaks, but may also be related to temporal changes in anthropogenic emissions, such as road traffic or industrial emissions. A decreasing trend was evidenced in the levels of some industrial and road traffic tracers (Pb, Cd, Zn and Sb in Barcelona from 2002 to 2007 and Sb and As in MSY from 2002 to 2007). In addition, the industrial factor identified in BCN by source apportionment studies also presented a statistically significant decreasing trend form 2003 to 2007. This decreasing trend is probably caused by the influence of the implantation of the IPPC directive 2008/1/EC (integrated pollution prevention and control).

The variety of sources and factors affecting the variability of atmospheric pollutants in the WMB make the simultaneous monitoring of different parameters necessary, in order to better understand emission sources, transformation or transport processes, and to be able to establish effective emission abatement techniques:

• Measurements of ultrafine particle levels (N) allow the monitoring of the variability of primary traffic emissions at BCN, but they are highly influenced by other atmospheric processes such as photochemical nucleation. Therefore, N measurements provide information about the concentration of two major groups of particles with different origins (primary traffic and secondary soluble particles formed by photochemistry nucleation), with different potential health impact. Number concentration depends critically on the size fraction measured which will vary with the instrument size detection limits (usually from 3 to 10 nm). This parameter must be taken in account in the design of measurement standards. Thus, in the study area, an important fraction of the finer particle size ranges detected (<30nm) will mainly consist of soluble particles formed by nucleation processes, whereas the particles in the 30-100nm range are mainly primary insoluble particles from vehicle exhaust emissions.

•The variability of BC levels is highly influenced by vehicle exhaust emissions (soot) and, in a much lower proportion by other combustion processes. Therefore, the measurement of BC permit to better control traffic exhaust emissions, characterised by a high concentration of ultrafine insoluble particles, with a high potential health impact.

•The monitoring of PM levels is necessary to control the influence of the above PM emission sources and other important sources, such as dust resuspension, African dust outbreaks, long range transport of anthropogenic pollutants and other sources of OM and SIA.

•Speciation measurements of fine and coarse PM fractions provide very important information on PM composition and origin, allowing the evaluation and quantification of PM source contributions.

The results also show that the monitoring of PM_1 (or BC) and PM_{10} may be a better strategy for air quality monitoring than the combination of $PM_{2.5}$ and PM_{10} measurements, as air quality standards. PM_1 measurements (nucleation and accumulation modes) and BC provide information about contributions from combustion processes. Simultaneously measured PM_{10} would supply information on the levels of combustion aerosols and also mechanically-generated aerosols, such as mineral dust and sea salt. $PM_{2.5}$ measurements represent an intermediate stage, providing information on particles generated by combustion processes but also with a significant contribution of mechanically generated aerosols. In addition, the fraction $PM_{1\text{-}2.5}$ presents a lower variability and provides less information than the monitoring of PM_1 and $PM_{1\text{-}10}$. Thus, PM_1 may allow monitoring the levels of the same aerosol components (mostly primary and secondary combustion aerosols), whereas the simultaneous monitoring of PM_{10} would allow the monitoring of regional/local aerosol peculiarities, such as high dust or sea spray levels.

In urban areas another optimal combination for PM monitoring in air quality networks may be the measurement of PM_{10} (SIA, OM and EC, crustal) and BC (primary traffic exhaust particles).

The variability of N concentrations is driven by complex processes, not only involving urban emissions, and standardization of N measurements for air quality monitoring at EU levels would be very complex.

Concluding remarks

The parallel monitoring of aerosols at an urban, regional and continental background was a useful strategy in order to understand the phenomenology of aerosols at the WMB. Given the meteorological characteristics of the WMB, the urban and industrial emissions, concentrated in the coastal areas, may have a considerable impact in PM levels and composition in rural and remote areas located at different altitudes, both in summer, with important atmospheric recirculation and mixing of air masses at a regional scale, and during winter, with breeze-activated transport of stagnated urban pollutants.

The application of source apportionment studies simultaneously to the three sites has permitted to demonstrate that urban emissions at BCN account for 70% of PM_{10}, being more than 50% attributed to traffic emissions. The high contribution of urban emissions and the transport of air masses at a regional scale demonstrate the importance of devising and applying emission abatement strategies for urban road traffic, in order to improve efficiently air quality in the study area, not only at a local, but also at a regional scale. To this end, the evaluation of the different aerosol measurement parameters has permitted to conclude that an optimal combination for PM monitoring in an air quality network may be the measurement of PM_{10} (reflecting mineral matter and carbonaceous compounds) and BC (reflecting primary traffic exhaust particles).

7. FUTURE RESEARCH DIRECTIONS

7. Further research directions and open questions

The research carried out in this study leaves many open questions that may lead to additional research directions in the WMB.

- The interest of the results obtained from continuous monitoring of simultaneous aerosol parameters (PM_{10}, $PM_{2.5}$, PM_1 levels and speciation, BC and N levels) and gaseous pollutants in Barcelona has encouraged the continuous monitoring of these parameters in the following years, in order to obtain a larger dataset that would allow the definition and interpretation of temporal trends and to estimate the impact of the reduction emission plans that were established in Barcelona since the year 2008. The results obtained show that PM levels have markedly reduced during 2008 and 2009, and the causes (meteorological, economical crisis, air quality improvement strategies, etc) are being investigated. Moreover, data presented in this study was partially used in an epidemiological study related to traffic and air pollution (Pérez et al., 2009) and has encouraged the continuous collaboration with epidemiology research groups.

- The study of PM_1 speciation and N and BC levels at Barcelona has encouraged the simultaneous monitoring of these parameters at the regional and continental background sites, and it is already being carried out. The results obtained will be useful in order to be able to select the better parameters to use as aerosol standards for air quality measurements.

- The monitoring of ultrafine particle number size distributions at urban, regional and continental background sites would be an additional useful tool to fully understand sources and processes of aerosols at the ultrafine size range. This was carried out in Barcelona during 2003-2004 and is currently being carried out at the MSY site. In addition, the monitoring of BC size distribution would also be interesting. The parallel monitoring of these parameters at the urban and rural sites obtaining longer data series would be very useful to understand aerosol formation and transformation processes.

- Besides, other aerosol measurement parameters could be evaluated, such as particle specific surface. Specific surface measurements are currently being carried out in BCN.

- Day-night or hourly-resolved sampling design for speciation measurements would also be very interesting to understand daily cycles, sources and atmospheric aerosol processes. Sampling campaigns were carried out during winter and summer 2009 at Barcelona and Montseny, in order to address this question. In the future, continuous speciation measurements will be carried out at the MSY site by means of a Aerosol Chemical Speciation Monitor (ACSM).

- The important sampling artefacts that affect the measurement of some of the compounds by high volume filter sampling, mainly due to the thermal stability of some compounds (such as ammonium nitrate or organic carbonaceous compounds) and the retention of VOC as OC by quartz filters, should be addressed, estimated and quantified, in order to characterize accurately atmospheric aerosols.

- The measurements and interpretation of the soluble fraction of major and trace element composition would also be very interesting in order to understand aerosol sources and processes.

- The measurement of EC and OC and the estimation of primary and secondary carbonaceous aerosols (POA and SOA) leave many open questions in the correct measurement of EC and OC, as the differences in the application of the method in different studies are very wide. Therefore, carbonaceous compounds, together with secondary inorganic aerosols, present the major source of uncertainty in models.

- The characterization of the organic carbonaceous fraction (soluble carbon and analysis of important organic compounds, such as sugars, PAHs or n-alkanes) and the isotope analysis of ^{14}C would help to define the origin of organic aerosols and to better estimate the POA and SOA fractions.

- Sampling and analysis of urban road dust is essential to distinguish sources of mineral matter at urban backgrounds. This is already being carried out in our group.

- The investigation of ammonia as a precursor of ammonium sulphate and nitrate is important. Other studies in Europe show that ammonium sulphate and nitrate are usually formed in the atmosphere at a regional scale, mainly from ammonia derived from agricultural and farming emissions. However, this may change at a local scale, as important ammonia emissions at urban areas (from traffic, sewage or dumps) produce the in situ transformation of SO_2 and NO_x precursors in particulate ammonium nitrate and sulphate.

- Results suggested the importance of formation of secondary compounds by interaction with mineral particles. Further research on these processes is needed.

- Background measurements focused on climate, such as aerosol absorption and scattering coefficients, would be very interesting at the regional and continental background sites.

8. DISSEMINATION OF RESULTS

8. DISSEMINATION OF RESULTS

8.1 Publications derived from this study

Pérez N., Pey J., Querol X., Alastuey A., Lopez J.M. and Viana M. (2008). Partitioning of major and trace components in PM_{10}–$PM_{2.5}$–PM_1 at an urban site in Southern Europe. Atmospheric Environment 42, 1677-1691.

Pérez N., Pey J., Castillo S., Viana M., Alastuey A. and Querol X. (2008). Interpretation of the variability of regional background aerosols in the Western Mediterranean. Science of the Total Environment 407, 527- 540.

Pey J., **Pérez N.**, Castillo S., Viana M., Moreno T., Pandolfi M., López-Sebastián J. M., Alastuey A. and Querol X. (2009). Geochemistry of regional background aerosols in the Western Mediterranean. Atmospheric Research 94, 422-435.

Pey J., **Pérez N.**, Querol X., Alastuey A., Cusack M., Reche C. (2010). Intense winter atmospheric pollution episodes affecting the Western Mediterranean. Science of the Total Environment 108, 1951-1959.

Pérez N., Pey J., Cusack M., Reche C., Querol X., Alastuey A. and Viana M.. Variability of particle number, black carbon and PM10, PM2.5 and PM1 levels and speciation: Influence of road traffic emissions on urban air quality. Aerosol Science & Technology. Accepted for publication 2010.

Querol X., Alastuey A., Pey J., Cusack M., **Pérez N.**, Mihalopoulos N., Theodosi C., Gerasopoulos E., Kubilay N. and Kocak M. (2009). Variability in regional background aerosols within the Mediterranean. Atmospheric Chemistry and Physics 9, 4575-4591.

Querol X., Pey J., Pandolfi M., Alastuey A., Cusack M., **Pérez N.**, Moreno T., Viana M., Mihalopoulos N., Kallos G. and Kleanthous S. (2009). African dust contributions to mean ambient PM_{10} levels across the Mediterranean Basin. Atmospheric Environment 43, 4266-4277.

Amato F., Pandolfi M., Escrig A., Querol X., Alastuey A., Pey J., **Pérez N.**, Hopke P. K. (2009). Quantifying road dust resuspension in urban environment by multilinear engine: A comparison with PMF2, Atmospheric Environment 43, 2770-2780.

Pérez L., Medina-Ramón M., Kuenzli N., Alastuey A., Pey J., **Pérez N.**, Tobias A., Querol X. and Sunyer J. (2009). Size fractionate particulate matter, vehicular traffic, and case-specific daily mortality in Barcelona (Spain). Environmental Science & Technology 43, 4707–4714.

8.2 Publications derived from the participation in other studies

Escudero M., Querol X, Pey J, Alastuey A, **Pérez N.**, Ferreira F, Alonso S, Rodriguez S, Cuevas E. (2007). A methodology for the quantification of the net African dust load in air quality monitoring networks. Technical note. Atmospheric Environment 41, 5516-5524.

Querol X., Pey J., Minguillon M. C., **Pérez N.**, Alastuey A., Viana M., Moreno T., Bernabe R. M., Blanco S., Cardenas B., Vega E., Sosa G., Escalona S., Ruiz H., and Artiñano B. (2008). PM speciation and sources in Mexico during the MILAGRO-2006 Campaign. Atmos. Chem. Phys., 8, 111–128.

Moreno T., Querol X., Pey J., Minguillon M. C., **Pérez N.**, Alastuey A., Bernabé R. M., Blanco S., Cardenas B., Eichinger W., Salcido A. and Gibbons W. (2008). Spatial and temporal variations in inhalable CuZnPb aerosols within the Mexico City pollution plume. Journal of Environmental Monitoring 10, 370–378.

Moreno T., Querol X. , Alastuey A. , Pey J. , Minguillón M. C. , **Pérez N.** , Bernabé R. M. , Blanco S., Cárdenas B. and Gibbons W. (2008). Lanthanoid Geochemistry of Urban Atmospheric Particulate Matter. Environ. Sci. Technol. 42, 6502–6507.

Rodríguez, S., Cuevas E., González Y., Ramos R., Romero P. M., **Pérez N.**, Querol X., Alastuey A. (2008). Influence of sea breeze circulation and road traffic emissions on the relationship between particle number, black carbon, PM_1, $PM_{2.5}$ and $PM_{2.5-10}$ concentrations in a coastal city. Atmospheric Environment 42, 6523-6534.

Pérez N., Moreno T., Querol X., Alastuey A., Bhatia R., Spiro B., Hanvey M. (2010). Physicochemical variations in atmospheric aerosols recorded at sea onboard the Atlantic-Mediterranean 2008 Scholar Ship cruise (Part I): particle mass concentrations, size ratios, and main chemical components. Atmospheric Environment. In press. http://dx.doi.org/10.1016/j.atmosenv.2010.04.023

Moreno T., **Pérez N.**, Querol X., Amato F., Alastuey A., Bhatia R., Spiro B., Hanvey M., Gibbons W. (2010). Physicochemical variations in atmospheric aerosols recorded at sea onboard the Atlantic-Mediterranean 2008 Scholar Ship cruise (Part II): natural versus anthropogenic influences revealed by PM_{10} trace element geochemistry. Atmospheric Environment. In press, doi:10.1016/j.atmosenv.2010.04.027

8.3 Contributions to conferences and workshops derived from this study

Pérez N., Pey, J. , Alastuey A., Querol X., Castillo S., Escudero M. Origin of mineral dust in PM levels at an urban and a regional site in North-Eastern Spain. African dust outbreak impact. Primera Reunión Española de Ciencia y Tecnología de Aerosoles, RECTA 2007. Madrid, 5-6 July 2007.

Amato F., Moreno T., Querol X., Alastuey A., **Pérez N**., Pey J. Contribution of local soil dust to the ambient concentrations of trace elements in PM_{10}. Primera Reunión Española de Ciencia y Tecnología de Aerosoles, RECTA 2007. Madrid, 5-6 July 2007.

Querol X., Alastuey A., Moreno T., Viana M., Castillo S., Pey J., **Pérez N.**, Rodríguez S., Artiñano B., Salvador P., Sánchez M., García Dos Santos S., Herce Garraleta M. D., Fernández Patier R., Moreno S., Negral L., Minguillón M. C., Monfort E., Sanz M. J., Palomo-Marin R., Pinilla-Gil E. R., Cuevas E., de la Rosa J., Sánchez de la Campa A. Atmospheric Particulate Matter (PM10 and PM2.5) in Spain (1999-2005): Levels, Composition and Source Origin. RECTA, Primera Reunión Española de Ciencia y Tecnología de Aerosoles 2007, Madrid, Spain, 5-6 July 2007.

Pérez N., Pey, J., Alastuey A., Querol X., Castillo S., Escudero M. Influence of African dust outbreaks on levels and composition of particulate matter in an urban background

in Barcelona, Spain. IAMAS Mineral Dust Aerosol Symposium. IUGG XXIV General Assembly "Earth: our changing planet". Perugia, 9-12 July 2007.

Rodríguez S., Pey J., **Pérez N.**, Querol X., Alastuey A., Van Dingenen R., Putaud J. P. Origin and features of ultrafine particles in Barcelona. UFIPOLNET conference. Dresden, Germany, 23-24 October 2007.

Pérez N., Pey J., Castillo S., Alastuey A., Querol X., Viana M., Moreno T. Variability of atmospheric aerosol levels and composition at a regional background site in NE Iberian Peninsula. EGU 2008. Vienna, Austria, 13-18 April 2008.

Pey J., **Pérez N.**, Alastuey A., Querol X., López J. M., Viana M.. Partitioning of PM10-PM2.5-PM1 at an urban site in the western Mediterranean: trends in PM levels and composition. EGU 2008. Vienna, Austria, 13-18 April 2008.

Pérez N., Pey J., Castillo S., Cusack M., Querol X., Alastuey A., Viana M., López J. M., Moreno T., Pandolfi M. Variabilidad de niveles y composición de aerosoles atmosféricos en el fondo regional del NE de la Península Ibérica. IX Congreso Ingeniería Ambiental, Feria Geo2, Bilbao 4-6 Noviembre 2008. Proceedings no. 444-454.

Querol X., Alastuey A., **Pérez N.**, Pey J., Escudero M., Castillo S., Cristóbal A., Pallarés M., González A., Jiménez S., Alonso N., Alonso S., Cuevas E. Influencia de las intrusiones de masas de aire del Norte de África en los niveles de PM de la Península Ibérica: Un método cuantitativo para la implementación de las directivas de calidad del aire. IX Congreso Ingeniería Ambiental, Feria Geo2, Bilbao 4-6 Noviembre 2008. Proceedings no. 434-443.

Pérez N., J. Pey, Cusack M., Querol X., Alastuey A., Viana M. Variability of particle number, black carbon and PM10, PM2.5 and PM1 levels and speciation: Influence of road traffic emissions on urban air quality. Proceedings nº035. 17th conference Transport and Air pollution (ETTAP 2009). Toulouse, France, 2-4 June 2009.

9. ACKNOWLEDGEMENTS

9. Acknowledgements

This study was supported by the G.D. Environmental Quality and Evaluation from the Spanish Ministry of the Environment, by research projects from the Spanish Ministry of Science and Innovation (INTERREG-CGL2004-05984-C07-02/CLI, DAMOCLES-CGL2005-03428-C04-03/CLI, DAURE-CGL2007-30502-E/CLI, DOASUR-CGL2007-62505/CLI and GRACCIE-CSD2007-00067), the Spanish Ministry of the Environment (CALIOPE, 441/2006/3-12.1), by the European Union (6th framework CIRCE IP, 036961 and EUSAAR RII3-CT-2006-026140) and by the *Departament de Medi Ambient i Habitatge* de Catalunya.

I have been financed by a pre-doctoral fellowship from the *Programa de becas predoctorales para formación de personal investigador* (FPI) of the Spanish Ministry of Science and Innovation associated to the research project INTERREG-CGL2004-05984-C07-02/CLI.

This PhD thesis is presented at the Institut *of Ciencia y tecnologia Ambientals* (ICTA) at the *Universitat Autónoma de Barcelona* (UAB).

First of all, I would like to acknowledge Andrés Alastuey and Xavier Querol for their friendship and support, enthusiastic supervision, useful discussions and general advice during this study.

I would like to express gratitude to the Atmospheric Modelling & Weather Forecasting Group in the University of Athens, the Atmospheric Modelling Laboratory from the Barcelona Supercomputing Centre, the NASA/Goddard Space Flight Center, NOAA Air Resources Laboratory (ARL), the Naval Research Laboratory and the SeaWiFS project (NASA) for the provision of the SKIRON, DREAM, TOMS, NAAPs aerosol maps and the satellite imagery, respectively. The author is also grateful to the Spanish Ministry of the Environment for providing data from EMEP air quality network. Finally, I gratefully acknowledge the NOAA Air Resources Laboratory (ARL) for the provision of HYSPLIT model.

I would like to acknowledge Nuria Cots and the *Departament de Medi Ambient i Habitatge* of the *Generalitat de Catalunya*, for providing data on PM and gaseous pollutants measured at Barcelona, Jeroni Lorente from the *Departament de Física I Química* de la *Universitat de Barcelona* and the *Servei Meteorologic de Catalunya* for

providing data on meteorological variables, the *Council of Barcelona (Serveis de Mobilitat)* and *Dirección General de Tráfico (DGT)* for providing data on road traffic intensity.

I would like to thank Sergio Rodriguez and Mar Viana for providing data on PM levels and speciation measured at Barcelona L'Hospitalet-Gornal during 1999-2000 and at Barcelona La Sagrera during 2001, Jorge Pey for the data on PM levels and speciation and number concentration levels measured at Barcelona-CSIC during 2003-2005, previously to this study. Sonia Castillo and Jorge Pey for the data on PM levels and speciation measured at Montseny previously to this study (2002-2005).

Thanks to Silvia Rico, Patricia Ávila, Sandra Toro, Rebeca Vázquez, Silvia Martínez and Mercé Cabanas for teaching me the laboratory techniques, for their indispensable help in the experimental work of this study, and also for the good moments in the laboratory.

Thanks to Jesús Parga for driving me to Montseny every week, for his company and good conversation and also for his help with sampling and the monitoring equipment.

Thanks to Jorge Pey for his help with sampling, maintenance of equipment and all experimental issues, for the useful discussions and advices, but most of all for all the good times spent together and for being always there when I needed.

Thanks to Sonia Castillo, Marco Pandolfi and Fulvio Amato for their help and patience in teaching me source apportionment methods.

I am grateful to all my colleagues (Xavier, Andrés, Jorge, Mari Cruz, Natalia, Mar, Oriol, Tere, Marco, Fulvio, Alberto, Michael, Cristina, Patricias, Annas, Angeliki, Silvias, Maria, Sonia, Miguel, Merce, Rebeca, Iria, Sandra, Jesús, Oscar, Alex, Flavia, Olga and anyone that I may have forgotten) for their important support and friendship and for the good moments spent together.

I am very thankful to my family because they have always been there, even if they were far away. My parents because they have raised me, supported me, taught me, loved me and given me the opportunity to study. My sisters because they have always been my best friends.

I am very grateful to Amaury Hazan for being always by my side, for encouraging me everyday and for all the adventures we have shared together.

I wish to thank everybody with whom I have shared any experiences in my life. I am tempted to individually thank all of my friends. However, because the list might be too long and by fear of leaving someone out, I will simply say thank you very much to you all.

Finally, I would like to thank all the people that I have met on the way and that have made me and my life better.

10. REFERENCES

10. REFERENCES

Aalto P., Hämeri K., Paatero P., Kulmala M., Bellander T., Berglind N., Bouso L., Castaño-Vinyals G., Cattani G., Cyrys J., Von Klot S., Lanki T., Marconi A., Nyberg F., Pekkanen J., Peters A., Sjövall B., Sunyer J., Zetzsche K. and Forastiere F. (2005). Aerosol particle number concentration measurements in five European cities using TSI-3022 condensation particle counter over a three year period during HEAPSS (Health Effects of Air Pollution on Susceptible Subpopulations). Journal of the Air and Waste Management Association 55, 8, 1064-1076

Ackerman S., Toon O. B., Stevens D. E., Heymsfield A. J., Ramanathan V. and Welton E. J. (2000). Reduction of Tropical Cloudiness by Soot. Science 288, 5468, 1042-1047.

Adams P. J., Seinfeld J. H. and Koch D. M. (1999). Global concentrations of tropospheric sulphate, nitrate, and ammonium aerosol simulated in a general circulation model. Journal of Geophysical Research 104, 13791-13823.

Adams P. J., Seinfeld J. H., Koch D., Mickley L. and Jacob D. (2001). General circulation model assessment of direct radiative forcing by the sulfate-nitrate-ammonium-water inorganic aerosol system. J. Geophys. Res. 106 , D1 ,1097.

Alastuey A. (1994). Caracterización mineralógica y alterológica de morteros de revestimiento en edificios de Barcelona. PhD thesis. Facultat de Geología, Universitat de Barcelona.

Alastuey A., Querol X., Rodríguez S., Plana F., López-Soler A., Ruiz C. and Mantilla E. (2004). Monitoring of atmospheric particulate matter around sources of secondary inorganic aerosol. Atmospheric Environment 38, 4979-4992.

Alastuey A., Querol X., Castillo S., Escudero M., Avila A., Cuevas E., Torres C., Romero P. M., Exposito F., García O., Diaz J. P., Van Dingenen R. and Putaud J. P. (2005). Characterisation of TSP and $PM_{2.5}$ at Izaña and Sta. Cruz de Tenerife (Canary Islands, Spain) during a Saharan Dust Episode (July 2002). Atmospheric Environment 39, 26, 4715-4728.

Allen A. G., Nemitz E., Shi J. P., Harrison R. M. and Greenwood J. C. (2001). Size distribution of trace metals in atmospheric aerosols in the United Kingdom. Atmospheric Environment 35, 4581-4591.

Amato F., Pandolfi M., Viana M., Querol X., Alastuey A. and Moreno T. (2009). Spatial and chemical patterns of PM_{10} in road dust deposited in urban environment. Atmospheric Environment, 43, 9, 1650-1659.

Arimoto R. (2001). Eolian dust and climate: relationships to sources, tropospheric chemistry, transport and deposition. Earth-Science Reviews 54, 29–42.

Ariola V., D'Alessandro A., Lucarelli F., Marcazzan G., Mazzei F., Nava S., Garcia-Orellana I., Prati P., Valli G., Vecchi R. and Zucchiatti A. (2006). Elemental characterization of PM_{10}, $PM_{2.5}$ and PM_1 in the town of Genoa (Italy). Chemosphere 62, 226–232.

Ávila A. (1996). Time trends in the precipitation chemistry at a mountain site in Northeastern Spain for the period 1983–1994. Atmospheric Environment 30, 9, 1363-1373.

Ávila A., Queralt I, and Alarcón M. (1997). Mineralogical composition of African dust delivered by red rains over North-Eastern Spain. Journal of Geophysical Research 102, 21977-21996.

Ávila A., Alarcón M. and Queralt I. (1998). The chemical composition of Dust transported in Red Rains: its contribution to the Biogeochemical Cycle of a holm oak forest in Catalonia (Spain). Atmospheric Environment 32, 179-191.

Bergametti G., Gomes L., Coudé-Gaussen G., Rognon P. and Coustumer M.N.L. (1989). African dust observed over Canary Islands: Source regions identification and transport pattern for some summer situation. Journal of Geophysical Research 94, 14855-14864.

Bi X., Feng Y., Wu J., Wang Y. and Zhu T. (2007). Source apportionment of PM_{10} in six cities of northern China. Atmospheric Environment, 41, 5, 903-912.

Birch M. E. and Cary R. A. (1996). Elemental carbon-based method for monitoring occupational exposures to particulate diesel exhaust. Aerosol Science and Technology 25, 221–241.

Birmili W. and Wiedensohler A. (2000). New particle formation in the continental boundary layer: Meteorological and gas phase parameter influence. Geophysical Research Letters, 27, 20, 3325-3328.

Birmili W., Wiedensohler A., Heitzenber J. and Lehmann K. (2001). Atmospheric particle number size distribution in Central Europe: statistical relationship to air masses and meteorology. Journal of Geophysical Research 106 (D26), 32005–32018.

Bonelli P., Marcazzan G.M.B. and Cereda E. (1996). Elemental composition and air trajectories of African Dust transported in Northern Italy. In The impact of Desert Dust across the Mediterranean, Vol. 11 (ed. S. Guerzoni and R. Chester), pp. 275-283.

Boy M. and Kulmala M. (2002) Nucleation events in the continental boundary layer: influence of physical and meteorological parameters. Atmospheric Chemistry and Physics 2, 1-16.

Brandenbergera S., Mohra M., Grobb K. and Neukomb H. P. (2005) .Contribution of unburned lubricating oil and diesel fuel to particulate emission from passenger cars. Atmospheric Environment, 39, 6985-6994.

Brimblecombe P. (2001). Urban air pollution. In The Urban Atmosphere and Its Effects (Brimblecombe P. and Maynard R., eds.). Vol 1, Air Pollution Reviews. Imperial College Press, London, UK.

Brimblecombe P. and Camuffo D. (2003). Long term damage to the built environment. In: The Effects of Air Pollution on the Built Environment (P Brimblecombe, ed.). Vol 2, Air Pollution Reviews. Imperial College Press, London, UK.

Bruinen de Bruin Y., Koistinen K., Yli-Tuomi T., Kephalopoulos S., and Jantunen M. (2006). A review of source apportionment techniques and marker substances available for identification of personal exposure, indoor and outdoor sources of chemicals (54p.). JRC-European Commission.

Burtscher H. (2005). Physical characterization of particulate emissions from diesel engines: a review. Journal of Aerosol Science, 36, 7, 896-932.

Butler T. J. and Likens G. E. (1991). The impact of changing regional emissions on precipitation chemistry in the Eastern United States, Atmospheric environment, 25(2), 305-315.

Cabada J. C., Rees S., Takahama S., Khlystov S. A., Pandis S. N., Davidson C. I. and Robinson A. L. (2004). Mass size distributions and size resolved chemical composition of fine particulate matter at the Pittsburgh supersite. Atmospheric Environment, 38, 3127-3141.

CAFE (Clean Air for Europe, 2004). Second Position Paper on Particulate Matter. CAFE Working Group on Particulate Matter December 20th, 2004.

Cao J.J., Lee S.C., Ho K.F., Zhang X.Y., Zou S.C., Fung K.K., Chow J.C. and Watson J.G. (2003). Characteristics of carbonaceous aerosol in Pearl River delta region, China during 2001 winter period. Atmospheric Environment 37, 1451–1460.

Cao J.J., Lee S.C., Ho K.F., Zou S.C., Fung K., Li Y., Watson J.G. and Chow J.C. (2004). Spatial and seasonal variations of atmospheric organic carbon and elemental carbon in Pearl River Delta Region, China. Atmospheric Environment 38, 4447–4456.

Casati R., Scheer V., Vogt R. and Benter T. (2007). Measurement of nucleation and soot mode particle emission from a diesel passenger car in real world and laboratory in situ dilution. Atmospheric Environment 41, 2125–2135.

Castillo S. (2006). Impacto de las masas de aire africano sobre los niveles y composición del material particulado atmosférico en Canarias y el NE de la Península Ibérica. PhD Thesis, Universitat Politécnica de Catalunya (UPC).

Charlson R. J., Schwartz S. E., Hales J. M., Cess R. D., Coakley Jr. J. A., Hansen J. E. and Hofmann D. J. (1992). Climate Forcing by Anthropogenic Aerosols. Science 255, 5043, 423–430.

Charron A. and Harrison R.M. (2003). Primary particle formation from vehicle emissions during exhaust dilution in the roadside atmosphere. Atmospheric Environment 37, 4109–4119.

Charron A., Harrison R. M. and Quincey P. (2007). What are the sources and conditions responsible for exceedences of the 24 h PM_{10} limit value (50 mg m^{-3}) at a heavily trafficked London site? Atmospheric Environment 41, 1960–1975.

Chester R., Nimmo M. and Keyse S. (1996). The influence of Saharan and Middle Eastern Desert-Derived dust on the Trace Metal Composition of Mediterranean Aerosols and Rainwaters: an overview. In The impact of Desert Dust across the Mediterranean, Vol. 11 (ed. S. Guerzoni and R. Chester), 253-273.

Chow J.C., Watson J.G., Lowenthal D. H., Chen L.-W. A. and Magliano K.L. (2006). Particulate carbon measurements in California's San Joaquin Valley. Chemosphere 62, 337–348.

Cong Z., Kang S., Liu X. and Wang G. (2007). Elemental composition of aerosol in the Nam Co region, Tibetan Plateau, during summer monsoon season. Atmospheric Environment 41, 1180–1187.

Costa M. and Baldasano J.M. (1996). Development of a source emission model for atmospheric pollutants in the Barcelona area. Atmospheric Environment 30, 2, 309-318.

Cunningham W. C. and Zoller W. H. (1981). The Chemical Composition of Remote Area Aerosols. J. Aerosol Sci. 12, 4, 367-384.

Currie L. A. (1995). Pure & Applied. Chemistry Vol. 67, No. 10,1699-1723.

Cyrys J., Pitz M., Heinrich J., Wichmann H. E. and Peters A. (2008). Spatial and temporal variation of particle number concentration in Augsburg, Germany. Science of The Total Environment 401, 1-3,168-175.

Dayan U., Heffter J., Miller J. and Gutman G. (1991). Dust Intrusion into the Mediterranean Basin. Journal of Applied Meteorology 30, 1185-1199.

Decesari S., Facchini M.C., Matta E., Lettini F., Mircea M., Fuzzi S., Tagliavini E., Putaud J. P. (2001). Chemical features and seasonal variation of fine aerosol water-soluble organic compounds in the Po Valley, Italy. Atmospheric Environment 35, 3691–3699.

de Gouw J. and Jimenez J. L. Organic Aerosols in the Earth's Atmosphere. Environmental Science and Technology, 43, 7614–7618.

de Meij A., Thunis P., Cuvelier C., Vignati E., Dentener F., and Krol M. (2006). The sensitivity of aerosol in Europe to two different emission inventories and temporal distribution of emissions. Atmos. Chem. Phys., 6:4287-4309.

Deng X., Tie X., Wu D., Zhou X., Bi X., Tan H., Li F. and Jiang C. (2008). Long-term trend of visibility and its characterizations in the Pearl River Delta (PRD) region, China. Atmospheric Environment 42, 7, 1424-1435.

Docherty K. S., Stone E. A., Ulbrich I. M., DeCarlo P. F., Snyder D. C.,Schauer J. J., Peltier R., E., Weber R. J., Murphy S. M., Seinfeld J. H., Grover B. D., Eatough D. J. and Jimenez J. L. (2008). Apportionment of primary and secondary aerosols in Southern California during the 2005 Study of Organic Aerosols in Riverside (SOAR-1). Environ. Sci. Technol., 42, 7655-7662.

Dockery D. W. (2001). Epidemiologic evidence of cardiovascular effects of particulate air pollution. Environmental health perspectives 109: 483-486.

Dockery D. W. and Stone P. H. (2007). Cardiovascular risks from fine particulate air pollution. The New England Journal of Medicine 365, 5, 511-513.

Donaldson K., Li X.Y. and MacNee W. (1998). Ultrafine (nanometre) particle mediated lung injury. Journal of Aerosol Science 29, 553-560.

Dongarrà G., Manno E., Varrica D. and Vultaggio M. (2007). Mass levels, crustal component and trace elements in PM_{10} in Palermo, Italy. Atmospheric Environment 41, 7977–7986.

Draxler R. R. and Rolph G. D. (2003). HYSPLIT (HYbrid Single-Particle Lagrangian Integrated Trajectory) Model access via NOAA ARL READY Website (http://www.arl.noaa.gov/ready/hysplit4.html). NOAA Air Resources Laboratory, Silver Spring, MD.

Duan J., Tan T., Cheng D., Bi X., Deng W., Sheng G., Fu J. and Wong M.H. (2007). Sources and characteristics of carbonaceous aerosol in two largest cities in Pearl River delta region, China. Atmospheric Environment 41, 2895–2903.

Duarte R.M.B.O., Mieiro C.L., Penetra A., Pio C.A., Duarte A.C. (2008). Carbonaceous materials in size-segregated atmospheric aerosols from urban and coastal-rural areas at the Western European Coast. Atmospheric Research 90 (2008) 253–263.

Duce R. A. (1995). Sources, distributions and fluxes of mineral aerosols and their relationship to climate. In Aerosol forcing of climate (Charlson R. J. & Heinzenberg J. eds.), pp. 43-72. John Wiley & Sons.

Dulac F., Tanre D., Bergametti G., Buat-Menard P., Desbois M. and Sutton D. (1992) Assessment of the African airborne dust mass over the western Mediterranean Sea using Meteosat data. Journal of Geophysical Research 101 (D14), 19, 515-531.

Eberly S. (2005). EPA-PMF 1.1 User's Guide. U.S. Environmental Protection Agency.

EC (European Comission, 1980). Council Directive 80/779/EEC on air quality limit values and guide values for sulphur dioxide and suspended particulates. Official Journal of the European Communities L 229, 30.8.1980, p. 30.

EC (1996). Council Directive 96/62/EC on ambient air quality assessment and management. Official Journal of the European Communities L 296, 21.11.1996, 55-63.

EC (1999). European Directive 1999/30/EC. Council Directive relating to limit values for sulphur dioxide, nitrogen dioxide and oxide of nitrogen, particulate matter and lead in ambient air. Official Journal of the European Communities L 163, 29.6.1999, 41-60.

EC (2000). European Directive 2000/69/EC. Council Directive relating to limit values for benzene and carbon monoxide in ambient air. Official Journal of the European Communities L 313, 13.12.2000, 12-21.

EC (2004). Directive 2004/107/EC of the European Parliament and of the Council relating to arsenic, cadmium, mercury, nickel and polycyclic aromatic hydrocarbons in ambient air. Official Journal of the European Union L 23, 26.1.2005, 3-16.

EC (2007). Regulation No. 715/2007 of the European Parliament and of the Council of 20 June 2007 on type approval of motor vehicles with respect to emissions from light passenger and commercial vehicles (Euro 5 and Euro 6) and on access to vehicle repair and maintenance information. Official Journal of the European Communities L 171, 29.6.2007.

EC (2008). Council Directive 2008/50/EC of the European Parliament and of the Council of 21 May 2008 on ambient air quality and cleaner air for Europe. Official Journal of the European Union. L152, 11.6.2008, 1-44.

EC (2008). Directive 2008/1/EC of the European Parliament and of the Council of 15 January 2008 concerning integrated pollution prevention and control. Official Journal of the European Union L 24/8, 29.1.2008,

Emberson L., Murray F. and Ashmore M. R. (2003). Air pollution impacts on crops and forests: An introduction. In: Air Pollution Impacts on Crops and Forests A Global Assessment (Emberson L., Ashmore M. and Murray F., eds.). Vol 4, Air Pollution Reviews. Imperial College Press, London, UK.

EMEP (2007). Particulate Matter Assessment Report, Part B, Annex A, NILU, report EMEP/CCC-Report 8/2007, ref. O-7726, August 2007, 370 pp.

EMEP (2008). Technical Report CEIP 1/2008. Inventory review 2008. Emission data reported under the LRTAP convention and NEC directive. Mareckova K., Wankmueller R., Anderl M., Muik B., Poupa S. and Wieser M. Umweltbundesamt GmbH, Vienna.

EN 12341 (1999). European Standard EN 12341, Air Quality—Determination of the PM_{10} Fraction of Suspended Particulate Matter—Reference Method and Field Test Procedure to Demonstrate Reference Equivalence of Measurement Methods, European Committee for Standardization, Brussels.

EN 14907 (2005). European Standard EN 14907, Ambient Air Quality—Standard Gravimetric Measurement Method for the Determination of the $PM_{2.5}$ Mass Fraction of Suspended Particulate Matter, European Committee for Standardization, Brussels.

Escudero, M., Castillo S., Querol X., Avila A., Alarcón M., Viana M., Alastuey A., Cuevas E. and Rodríguez S. (2005). Wet and dry African dust episodes over Eastern Spain, Journal of Geophysical Research, 110 (D18S08), 202-224.

Escudero M., Querol X., Avila A. and Cuevas E. (2007a). Origin of the exceedances of the European daily PM limit value in regional background areas of Spain. Atmospheric Environment, 41, 4, 730-744.

Escudero M., Querol X, Pey J, Alastuey A, Perez N, Ferreira F, Alonso S, Rodriguez S and Cuevas E. (2007b). A methodology for the quantification of the net African dust load in air quality monitoring networks. Technical note. Atmospheric Environment 41, 5516-5524.

Favez O., Cachier H., Sciare J., Alfaro S. C., El-Araby T.M., Harhash M. A. and Abdelwahab M. M. (2008). Seasonality of major aerosol species and their transformations in Cairo megacity. Atmospheric Environment 42, 1503–1516.

Feng J., Chan C.K., Fang M., Hu M., He L. and Tang X. (2006). Characteristics of organic matter in $PM_{2.5}$ in Shanghai. Chemosphere 64, 1393–1400.

Fraser M. P., Buzcu B., Yue Z. W., McGaughey G. R., Desai N. R., Allen D. T., Seila R. L., Lonneman W. A. and Harley R. A. (2003). Separation of fine particulate matter emitted from gasoline and diesel vehicles using chemical mass balancing techniques. Environmental Science & Technology 37, 3904–3909.

Gangoiti G., Millán M., Salvador R. and Mantilla E. (2001). Long range transport and recirculation of pollutants in the Western Mediterranean during the RECAPMA Project. Atmospheric Environment 35, 6267-6276.

Gatari M. J. and Bomana J. (2003). Black carbon and total carbon measurements at urban and rural sites in Kenya, East Africa. Atmospheric Environment 37, 1149-1154.

Gerasopoulos E., Kouvarakis G., Babasakalis P., Vrekoussis M., Putaud J. P. and Mihalopoulos N. (2006). Origin and variability of particulate matter (PM_{10}) mass concentrations over the Eastern Mediterranean. Atmospheric Environment 40 (25), 4679–4690.

Gilbert R. O. (1987). Statistical Methods for Environmental Pollution Monitoring. John Wiley & Sons, Inc. 336pp.

Glaccum R. A. and Prospero J. M. (1980). Saharan aerosols over the tropical North-Atlantic - mineralogy. Mar. Geol. 37, 295-321.

Glavas S. D., Nikolakis P., Ambatzoglou D. and Mihalopoulos N. (2008). Factors affecting the seasonal variation of mass and ionic composition of $PM_{2.5}$ at a central Mediterranean coastal site. Atmospheric Environment 42, 5365– 5373.

Gobbi G. P., Barnaba F. and Ammannato L. (2007). Estimating the impact of Saharan dust on the year 2001 PM_{10} record of Rome, Italy. Atmospheric Environment 41 (2), 261–275.

Götschi T., Hazenkamp-von Arx M. E., Heinrich J., Bono R., Burney P., Forsberg B., Jarvis D., Maldonado J., Norbäck D., Stern W. B., Sunyer J., Torén K., Verlato G., Villani S., Künzli N. (2005). Elemental composition and reflectance of ambient fine particles at 21 European locations. Atmospheric Environment 39, 32, 5947-5958.

Guerzoni S., Molinaroli E. and Chester R. (1997). Saharan dust inputs to the Western Mediterranean Sea: depositional patterns, geochemistry and sedimentological implications. Deep-Sea Research 44, 631-654.

Gustafsson M., Blomqvist G., Gudmundsson A., Dahl A., Swietlicki E., Bohgard M., Lindbom J. and Ljungman A. (2008). Properties and toxicological effects of particles from the interaction between tyres, road pavement and winter traction material. Science of the total environment 393, 226-240.

Hallquist M., Wenger J. C., Baltensperger U., Rudich Y., Simpson D., Claeys M., Dommen J., Donahue N. M., George C., Goldstein A. H., Hamilton J. F., Herrmann H., Hoffmann T., Iinuma Y., Jang M., Jenkin M., Jimenez J. L., Kiendler-Scharr A., Maenhaut W., McFiggans G., Mentel Th. F., Monod A., Prévôt A. S. H., Seinfeld J. H., Surratt J. D., Szmigielski R. and Wildt J. (2009). The formation, properties and impact of secondary organic aerosol: current and emerging issues. Atmos. Chem. Phys. Discuss., 9, 3555–3762.

Hämeri K., Kulmala M., Aalto P., Leszczynski K., Visuri R., Hämekoski K. (1996). The investigations of aerosol particle formation in urban background area of Helsinki. Atmospheric Research 41, 3-4, 281-298.

Han Y.M., Han Z.W., Cao J.J., Chow J.C., Watson J.G., An Z.S., Liu S.X. and Zhang R.J. (2008). Distribution and origin of carbonaceous aerosol over a rural high-mountain lake area, Northern China and its transport significance. Atmospheric Environment 42, 2405–2414.

Harris J. S. and Maricq M. M. (2001). Signature size distributions for diesel and gasoline engine exhaust particulate matter. Journal of Aerosol Science, 32, 749-764.

Harrison R. M. and C. Pio (1983). Size differentiated composition of inorganic aerosol of both marine and continental polluted origin. Atmospheric Environment 17, 1733-1738.

Harrison R. M. and Kito A. M. N. (1990). Field intercomparison of filter pack and denuder sampling methods for reactive gaseous and particulate pollutants. Atmospheric Environment 24: 2633-2640.

Harrison R. M., Smith D. J. T., Pio C. A. and Castro L. M. (1997). Comparative receptor modelling study of airborne particulate pollutants in Birmingham (United Kingdom), Coimbra (Portugal) and Lahore (Pakistan). Atmospheric Environment, 31, 20, 3309-3321.

Harrison R. M., Jones M. and Collins G. C. (1999). Measurements of the physical properties of particles in the urban atmosphere. Atmospheric Environment 33, 309-321.

Harrison R. M., Shi J. P., Xi S., Khan A., Mark D., Kinnersley R. and Yin J. (2000). Measurement of Number, Mass and Size Distribution of Particles in the Atmosphere. Philosophical Transactions: Mathematical, Physical and Engineering Sciences, Vol. 358, No. 1775, Ultrafine Particles in the Atmosphere, pp. 2567-2580.The Royal Society.

Harrison R. M. and Jones A. M. (2005). Multisite study of particle number concentrations in urban air. Environmental Science and Technology, 39, 6063-6070.

Harrison R. M. and Yin J. (2008). Sources and processes affecting carbonaceous aerosol in central England. Atmospheric Environment 42, 1413–1423.

Hauck H., Berner A., Frischer T., Gomiscek B., Kundi M. Neuberger M., Puxbaum H. and Preining O. (2004). AUPHEP-Austrian Project on Health Effects of Particulates: general overview. Atmospheric Environment 38, 3905-0915.

Henry R. C., Lewis C. W., Hopke P. K. and Williamson H. J. (1984). Review of receptor model fundamentals. Atmospheric Environment 18, 8, 1507-1515.

Hidy G. M. (1994). Atmospheric sulfur and nitrogen oxides: Eastern North American source-receptor relationsips. Academic Press, San Diego, 447p.

Highwood E. J. and Kinnersley R. P. (2006). When smoke gets in your eyes: the multiple impact of atmospheric black carbon on climate, air quality and health. Environment International 32, 560-566.

Ho K. F., Lee S. C.,T, Cao J.J., Chow J. C., Watson J. G., Chan C. K. (2006). Seasonal variations and mass closure analysis of particulate matter in Hong Kong. Science of the Total Environment 355, 276– 287.

Hoek G., Brunekreef B., Goldbohm S., Fischer P., van den Brandt P. A. (2002). The association between mortality and indicators of traffic-related air pollution in a Dutch Cohort Study. Lancet 360, 1203–1209.

Hoornaert S., Moreton Godoi R. H. and Van Grieken R. (2004). Elemental and Single Particle Aerosol Characterisation at a Background Station in Kazakhstan. Journal of Atmospheric Chemistry 48, 301–315.

Hoose C., Lohmann U., Erdin R. and Tegen I. (2008). The global influence of dust mineralogical composition on heterogeneous ice nucleation in mixed-phase clouds. Environ. Res. Lett. 3, 025003 (14pp).

Hopke P. K. (2000). A guide to positive matrix factorization, 16pp. <http://www.epa.gov/ttnamti1/files/ambient/pm25/workshop/laymen.pdf>.

Hopke P. K., Ramadan Z., Paatero P., Norris G. A., Landis M. S., Williams R. W., Lewis C. W. (2003). Receptor modelling of ambient and personal exposure samples: 1998 Baltimore particulate mater epidemiology-exposure study. Atmospheric Environment 37 (23), 3289-3302.

Hopke P. K., Ito K., Mar T., Christensen W. F., Eatough D. J., Henry R. C., Kim E., Laden F., Lall R., Larson T. V., Liu H., Neas L., Pinto J., Stölzel M., Suh H., Paatero P. and Thurston G. D. (2006). PM source apportionment and health effects: 1. Intercomparison of source apportionment results. Journal of Exposure Science and Environmental Epidemiology 16, 275–286.

Horvath H. (1992). Effects on visibility, weather and climate. In Atmospheric Acidity. Sources, Consequences and Abatement (ed. M. Radojevic and R.M. Harrison), pp. 435-466. Elsevier Applied Science.

Horvath H. (1998). Influence of atmospheric aerosols upon the global radiation balance. In Atmospheric Particles. Harrison R. M. and Van Grieken R. eds. Wiley.

Hueglin C., Gehrig R., Baltensperger U., Gysel M., Monn C. and Vonmont H. (2005). Chemical characterisation of $PM_{2.5}$, PM_{10} and coarse particles at urban, near-city and rural sites in Switzerland. Atmospheric Environment 39, 637–651.

Husar R. B., Holloway J. M., Patterson D. E., Wilson W. E. (1981). Spatial and temporal pattern of eastern U.S. haziness: A summary. Atmospheric Environment 15, 10-11, 1919-1928.

Hussein T., Puustinen A., Aalto P., Mäkelä J. M., Hämeri K. and Kulmala M. (2004). Urban aerosol number size distributions. Atmos. Chem. Phys. 4, 391-411.

Hussein T., Hämeri K., Aalto P., Paatero P. and Kulmala M. (2005). Modal structure and spatial–temporal variations of urban and suburban aerosols in Helsinki—Finland. Atmospheric Environment 39, 9,1655-1668.

Hussein T., Johansson C., Karlsson H. and Hansson H. C. (2008). Factors affecting non-tailpipe aerosol particle emissions from paved roads: On-road measurements in Stockholm, Sweden. Atmospheric Environment 42, 688–702.

IMPROVE reports, Interagency Monitoring of Protected Visual Environments, http://vista.cira.colostate.edu/improve/).

IPCC, 2001. Climate Change 2001: The Scientific Basis. Contribution of Working Group I to the Third Assessment Report of the Intergovernmental Panel on Climate Change. Houghton J.T., Ding Y., Griggs D.J., Noguer M., van der Linden P.J., Dai X., Maskell K. and Johnson C.A. (eds.). Cambridge University Press.

IPCC, 2007. Climate Change 2007: The Physical Science Basis. Contribution of Working Group I to the Fourth Assessment Report of the Intergovernmental Panel on Climate Change. Solomon S., Qin D., Manning M., Chen Z., Marquis M., Averyt K.B., Tignor M. and Miller H.L. (eds.). Cambridge University Press.

Jacobson M. Z. (2001). Strong radiative heating due to the mixing state of Black Carbon in Atmospheric Aerosols. Nature 409, 672-695.

Jacobson M. Z. Kittelson D. B. and Watts W. F. (2005). Enhanced Coagulation Due to Evaporation and Its Effect on Nanoparticle Evolution. Environ. Sci. Technol., 39, 9486-9492.

Jalava P. I., Salonen R. O., Pennanen A. S., Sillanpää M., Hälinen A. I., Happo M. S., Hillamo R., Brunekreef B., Katsouyanni K., Sunyer J. and Hirvonen M. R. (2007). Heterogeneities in Inflammatory and Cytotoxic Responses of RAW 264.7 Macrophage Cell Line to Urban Air Coarse, Fine, and Ultrafine Particles From Six European Sampling Campaigns', Inhalation Toxicology, 19:3, 213–225.

Jalava P. I., Salonen R. O., Pennanen A. S., Happo M. S., Penttinen P., Hälinen A. I., Sillanpää M., Hillamo R., Hirvonen M. R. (2008). Effects of solubility of urban air fine and coarse particles on cytotoxic and inflammatory responses in RAW 264.7 macrophage cell line. Toxicology and Applied Pharmacology 229,146–160.

Jamriska M., Morawska L. and Mergersen K. (2008). The effect of temperature and humidity on size segregated traffic exhaust particle emissions. Atmospheric Environment 42, 2369–2382.

Jickells T. D., An Z. S., Andersen K. K., Baker A. R., Bergametti G., Brooks N., Cao J. J., Boyd P. W., Duce R. A., Hunter K. A., Kawahata H., Kubilay N., laRoche J., Liss P. S., Mahowald N., Prospero J. M., Ridgwell A. J., Tegen I. and Torres R. (2005). Global Iron Connections between Desert Dust, Ocean Biogeochemistry and Climate. Science 308, 5718, 67–71.

Jimenez J. L., Canagaratna M. R., Donahue N. M., Prevot A. S. H., Zhang Q., Kroll J. H., DeCarlo P. F., Allan J. D., Coe H., Ng N. L., Aiken A. C., Docherty K. S., Ulbrich, I. M., Grieshop A. P., Robinson A. L., Duplissy J., Smith J. D., Wilson K. R., Lanz V. A., Hueglin C., Sun Y. L., Tian J., Laaksonen A., Raatikainen T., Rautiainen J., Vaattovaara P., Ehn M., Kulmala M., Tomlinson J. M., Collins D. R., Cubison M. J., Dunlea E. J., Huffman J. A., Onasch T. B., Alfarra M. R., Williams P. I., Bower K., Kondo Y., Schneider J., Drewnick F., Borrmann S., Weimer S., Demerjian K., Salcedo D., Cottrell L., Griffin R., Takami A., Miyoshi T., Hatakeyama S., Shimono A., Sun J. Y., Zhang Y. M., Dzepina K., Kimmel J. R., Sueper D., Jayne J. T., Herndon S. C., Trimborn A. M., Williams L. R., Wood E. C., Middlebrook A. M., Kolb C. E., Baltensperger U., Worsnop D. R. (2009). Evolution of Organic aerosols in the Atmosphere. Science 326, 1525.

Jiménez P., Jorba O., Parra R., Pérez C., Viana M., Alastuey A., Querol X. and Baldasano J. M. (2005). High-resolution modelling of gaseous photochemical pollution and particulate matter in Barcelona air basin. In: Urban Air Quality 2005. Valencia, Spain, March 28-April 1, 2005.

Jiménez P., Lelieveld J. and Baldasano J. M. (2006). Multiscale modelling of air pollutants dynamics in the North-Western Mediterranean basin during a typical summertime episode. Journal of Geophysical Research 111, D18306.

Jiménez P., Jorba O. and Baldasano J.M. (2007). Modelling the dynamics of air pollutants over the Iberian Peninsula under typical meteorological situations. Developments in Environmental Science, Volume 6. Borrego C. and Renner E. (eds.). Elsevier Ltd.

Johnson R. W. (1981). Daytime visibility and nephelometer measurements related to its determination. Atmospheric Environment 15, 10-11, 1835-1845.

Jorba O., Pérez C., Rocadenbosch F. and Baldasano J. M. (2004). Cluster Analysis of 4-Day Back Trajectories Arriving in the Barcelona Area (Spain) from 1997 to 2002, Journal of Applied Meteorology 43, 6: 887-901.

Kallos G., Kotroni V. and Lagouvardos K. (1997). The Regional Weather Forecasting System SKIRON: an overview. Proceedings of the Symposium on Regional Weather Prediction on Parallel computer Environments. University of Athens, Greece, 109-122.

Kampa M. and Castanas E. (2008). Human health effects of air pollution. Environmental Pollution, 151, 2, 362-367.

Katsouyanni K., Touloumi G., Spix C., Schwartz J., Balducci F., Medina S., Rossi G., Wojtyniak B., Sunyer J., Bacharova L., Schouten J. P., Ponka A. and Anderson H. R. (1997). Short-term effects of ambient sulphur dioxide and particulate matter on mortality in 12 European cities: results from time series data from the APHEA project. Air pollution and health: a European approach. British Medical Journal 314, 1658–1663.

Ketzel M., Wåhlin P., Kristensson A., Swietlicki E., Berkowicz R., Nielsen O. J. and Palmgren F. (2004). Particle size distribution and particle mass measurements at urban, near-city and rural level in the Copenhagen area and Southern Sweden. Atmospheric Chemistry and Physics 4, 281-292.

Ketzel M., Omstedt G., Johansson C., Düring I., Pohjola M., Oettl D., Gidhagen L., Wåhlin P., Lohmeyer A., Haakana M. and Berkowicz R. (2007). Estimation and validation of $PM_{2.5}/PM_{10}$ exhaust and non-exhaust emission factors for practical street pollution modelling. Atmospheric Environment 41, 40, 9370-9385.

Kim E., Hopke P. K., Larson T. V. and Covert D. S. (2004). Analysis of ambient particle size distributions using UNMIX and positive matrix factorization. Environmental Science and Technology 38, 202–209.

Kim E. and Hopke P. K. (2008). Source characterization of ambient fine particles at multiple sites in the Seattle area. Atmospheric Environment 42, 6047– 6056.

Kittelson D. B. (1998). Engines and nanoparticles: a review. Journal of Aerosol Science, 29, 575- 588.

Koçak M., Mihalopoulos N. and Kubilay N. (2007). Chemical composition of the fine and coarse fraction of aerosols in the northeastern Mediterranean. Atmospheric Environment 41, 34, 7351-7368.

Koponen I. K., Asmi A., Keronen P., Puhto K. and Kulmala M. (2001). Indoor air measurement campaign in Helsinki, Finland 1999: The effect of outdoor air pollution on indoor air. Atmospheric Environment 35, 1465-1477.

Krol M., Houweling S., Bregman B., van den Broek M., Segers A., van Velthoven P., Peters W., Dentener F., and Bergamaschi P. (2005). The two-way nested global chemistry-transport zoom model TM5: algorithm and applications. Atmos. Chem. Phys., 5(2):417-432.

Kulmala M., Mäkelä J. M., Koponen I. and Pirjola L. (1998). Formation of cloud condensation nuclei in boreal forest area. Journal of Aerosol Science, 29, 1, S567-S568.

Kulmala M., Vehkamäki H., Petäjä T., Dal Maso M., Lauri A., Kerminen V. M., Birmili W., McMurry P.H. (2004). Formation and growth rates of ultrafine atmospheric particles: a review of observations. Aerosol Science 35,143–176.

Kulmala M. and Kerminen V. M. (2008). On the formation and growth of atmospheric nanoparticles. Atmospheric Research 90, 132–150.

Künzli N., Kaier R., Medina S., Studnicka M., Chanel O., Filliger P., Herry M., Horak Jr. F., Puybonniewx-Texier V., Quénel P., Schneider J., Seethaler R., Vergnaud J. C., and Sommer H. (2000). Public health impact of outdoor and traffic related air pollution: a European assessment. The Lancet, 356:795-801.

Künzli N., Mudway I. S., Götschi T., Shi T., Kelly F. J., Cook S., Burney P., Forsberg B., Gauderman J. W., Hazenkamp M. E., Heinrich J., Jarvis D., Norbäck D., Payo-Losa F., Poli A., Sunyer J. and Borm P. J. A. (2006). Comparison of Oxidative Properties, Light Absorbance, and Total and Elemental Mass Concentration of Ambient $PM_{2.5}$ Collected at 20 European Sites. Environ Health Perspect. 114(5): 684–690.

Kupiainen K. (2007). Road dust from pavement wear and traction sanding. Monographs of the Boreal Environment Research, 26. Finnish Environment Institute, Finland.

Laaksonen A., Hamed A., Joutsensaari J., Hiltunen L., Cavalli F., Junkermann W., Asmi A., Fuzzi S. and Facchini M. C. (2005). Cloud condensation nucleus production from nucleation events at a highly polluted region. Geophysical Research Letters 32, L06812.

Lall R. and Thurston G. D. (2006). Identifying and quantifying transported vs. local sources of New York City $PM_{2.5}$ fine particulate matter air pollution. Atmospheric Environment 40, S333–S346.

Larssen S., Sluyter R. and Helmis C. (1999). Criteria for EUROAIRNET, the EEA air quality monitoring and information network. http://reports.eea.eu.int/TEC12/en.

Ledoux F., Courcot L., Courcot D., Aboukaïs A. and Puskaric E. (2006). A summer and winter apportionment of particulate matter at urban and rural areas in northern France. Atmospheric Research 82, 633–642.

Lee E., Chan C. K. and Paatero P. (1999). Application of positive matrix factorization in source apportionment of particulate pollutants in Hong Kong. Atmospheric Environment 33, 3201-3212.

Lee M. L. T., Whitmore G.A., Laden F., Hart J. E. and Garshick E. (2009). A case–control study relating railroad worker mortality to diesel exhaust exposure using a threshold regression model. Journal of Statistical Planning and Inference 139, 5, 1633-1642.

Lee S., Liu W., Wang Y., Russell A. G. and Edgerton E. S. (2008). Source apportionment of $PM_{2.5}$: Comparing PMF and CMB results for four ambient monitoring sites in the southeastern United States. Atmospheric Environment 42, 18, 4126-4137.

Lenschow P., Abraham H. J., Kutzner K., Lutz M., Preuß J. D., Reichenbächer W. (2001). Some ideas about the sources of PM_{10}. Atmospheric Environment 35, Supplement 1, S23–S33.

Levin Z., Ganor E. and Gladstein V. (1996). The effects of desert particles coated with sulphate on rain formation in the eastern Mediterranean. J. Appl. Meteorol., 35, 1511-1523.

Likens G. E. and Bormann F. H. (1974). Acid rain: a serious regional environmental problem. Science 184:1176-1179.

Lin J. J. and Lee L.-C. (2004). Characterization of the concentration and distribution of urban submicron (PM1) aerosol particles. Atmospheric Environment 38, 3, 469-475.

Livingston C., Rieger P. and Winer A. (2009). Ammonia emissions from a representative in-use fleet of light and medium-duty vehicles in the California South Coast Air Basin. Atmospheric Environment 43, 3326–3333.

Lonati G., Giugliano M., Butelli P., Romele L. and Tardivo R. (2005). Major chemical components of $PM_{2.5}$ in Milan (Italy). Atmospheric Environment 39, 1925-1934.

Lonati G., Ozgen S. and Giugliano M. (2007). Primary and Secondary carbonaceous species in $PM_{2.5}$ samples in Milan (Italy). Atmospheric Environment 41, 4599-4610.

Löye-Pilot M. D., Martin J. M. and Morelli J. (1986). Influence of Saharan Dust on the rain acidity and Atmospheric imput to the Mediterranean. Nature 321, 427-428.

Mäkelä J. M., Koponen I. K., Aalto P. and Kulmala M. (2000). One-year data of submicron size modes of tropospheric background aerosol in Southern Finland. Journal of Aerosol Science 31, 595-611.

Mamane Y. and Mehler M. (1987). On the nature of nitrate particles in a coastal urban area. Atmospheric Environment 21, 9, 1989-1994.

Mantilla E., Millán M., Salvador R., Sanz M. J. and Palau J. L. (1998). Tracking the dynamics of an elevated plume in the Spanish Levantine coast. 10th Joint Conference on the Applications of Air Pollution Meteorology (AMS). Phoenix, Arizona (USA).

Marenco F., Bonasoni P., Calzolari F., Ceriani M., Chiari M., Cristofanelli P., D'Alessandro A., Fermo P., Lucarelli F., Mazzei F., Nava S., Piazzalunga A., Prati P., Valli G. and Vecchi R. (2006). Characterization of atmospheric aerosols at

Monte Cimone, Italy, during summer 2004: Source apportionment and transport mechanisms. Journal Of Geophysical Research 111, D24202.
Maricq M. M. (2007) Chemical characterization of particulate emissions from diesel engines: A review. Aerosol Science 38, 1079–1118.
Mathis U., Mohr M., and Forss A. M. (2005). Comprehensive particle characterization of modern gasoline and diesel passenger cars at low ambient temperatures. Atmospheric Environment 39, 107-117.
McClain C. R., Cleave M. L., Feldman G. C., Gregg W. W., Hooker S. B. and Kuring N. (1998). Science Quality SeaWiFS Data for Global Biosphere Research. Sea Technology 39 (9), 10-15.
Mejía J. F., Wraith D., Mengersen K. and Morawska L. (2007). Trends in size classified particle number concentration in subtropical Brisbane, Australia, based on a 5 year study. Atmospheric Environment 41, 5, 1064-1079.
Mészáros E. and Horváth L. (1984). Concentration and dry deposition of atmospheric sulphur and nitrogen compounds in Hungary. Atmospheric Environment 18, 1725-1730.
Mészáros E. (1999). Fundamentals of Atmospheric Aerosol Chemistry. Akadémiai Kiado.
Middleton N., Yiallouros P., Kleanthous S., Kolokotroni O., Schwartz J., Dockery D. W., Demokritou P. and Koutrakis P. (2008). A 10-year time-series analysis of respiratory and cardiovascular morbidity in Nicosia, Cyprus: the effect of short-term changes in air pollution and dust storms. Environmental Health 7:39.
Mildford J. B. and Davidson C. I. (1987). The sizes of particulate sulphate and nitrate in the Atmosphere: A review. Journal of Air Pollution Control Association 37, 2, 125-134.
Millán M., Salvador R., Mantilla E. and Kallos G. (1997). Photo-oxidant dynamics in the Mediterranean basin in summer: results from European research projects. Journal of Geophysical Research 102, 8811-8823.
Millán M., Mantilla E., Salvador R., Carratalá A., Sanz M. J., Alonso L., Gangoiti G. and Navazo M. (2000). Ozone cycles in the Western Mediterranean Basin: Interpretation of monitoring data in complex coastal terrain. Journal of Applied Meteorology 39, 487-508.
Miller K. A., Siscovick D. S., Sheppard L., Shepherd K., Sullivan J. H., Anderson G. L. and Kaufman J. D. (2007). Long term exposure to air pollution and incidence of cardiovascular events in women. The New England Journal of Medicine 365, 5, 447-457.
Minoura H. and Takekawa H. (2005). Observation of number concentrations of atmospheric aerosols and analysis of nanoparticle behavior at an urban background area in Japan. Atmospheric Environment 39, 5806–5816.
Möhler O., Benz S., Saathoff H., Schnaiter M., Wagner R., Schneider J., Walter S., Ebert V. and Wagner S. (2008). The effect of organic coating on the heterogeneous ice nucleation efficiency of mineral dust aerosols. Environ. Res. Lett. 3, 025007.
Mohr C., Huffman A., Cubison M. J., Aiken A. C., Docherty K. S., Kimmel J. R., Ulbrich I. M., Hannigan M. and Jimenez J. L. (2009). Characterization of Primary Organic Aerosol Emissions from Meat Cooking, Trash Burning, and Motor Vehicles with High-Resolution Aerosol Mass Spectrometry and Comparison with Ambient and Chamber Observations. Environ. Sci. Technol. 43, 2443–2449.
Molinaroli E., Gerzoni S. and Giacarlo R. (1993). Contribution of Saharan Dust to the Central Mediterranean Basin. In Processes Controlling the Composition of the Clastic Sediments, Vol. 284 (Jhonson N. J. and Basu A. eds.), 303-312. Geologica Society of America Special Paper.
Molnár P., Janhäll S. and Hallquist M. (2002) Roadside measurements of fine and ultrafine particles at a major road north of Gothenburg. Atmospheric Environment 36, 4115–4123.

Morawska L., Thomas S., Bofinger N., Wainwright D. and Neale D. (1998). Comprehensive characterization of aerosols in a subtropical urban atmosphere: particle size distribution and correlation with gaseous pollutants. Atmospheric Environment, 32, 2467-2478.

Morawska L., Keogh D. U., Thomas S. B., Mengersen K. (2008a). Modality in ambient particle size distributions and its potential as a basis for developing air quality regulation. Atmospheric Environment, 42, 7, 1617-1628.

Morawska L., Ristovski Z., Jayaratne E. R., Keogh D. U. and Ling X. (2008b). Ambient nano and ultrafine particles from motor vehicle emissions: Characteristics, ambient processing and implications on human exposure. Atmospheric Environment 42, 35, 8113-8138.

Morawska L., Wang H., Ristovski Z., Jayaratne E. R., Johnson G., Cheung H. C. Ling X. and He C. (2009). JEM Spotlight: Environmental monitoring of airborne nanoparticles. Journal of Environmental Monitoring 11, 1758-1773.

Moreno T., Querol X., Alastuey A., Viana M., Salvador P., Sánchez De La Campa A., Artiñano B., De La Rosa J. and Gibbons W. (2006). Variations in atmospheric PM trace metal content in Spanish towns: illustrating the chemical complexity of the inorganic urban aerosol cocktail. Atmospheric Environment 40, 6791-6803.

Nickovic S., Papadopoulos A., Kakaliagou O. and Kallos G. (2001). Model for prediction of desert dust cycle in the atmosphere. Journal of Geophysical Research 106, 18113-18129.

Nriagu J. O. (1989). A global asssessment of natural sources of atmospheric trace metals. Nature 338, 47-49.

Nyanganyura D., Maenhaut W., Mathuthu M., Makarau A. and Meixner F. X. (2007). The chemical composition of tropospheric aerosols and their contributing sources to a continental background site in northern Zimbabwe from 1994 to 2000. Atmospheric Environment 41, 2644–2659.

Olivares G., Johansson C., Ström J. and Hansson H.C. (2007). The role of ambient temperature for particle number concentrations in a street canyon. Atmospheric Environment 41, 2145–2155.

Ostro B., Feng W. Y., Broadwin R., Green S. and Lipsett M. (2007). The effects of components of fine particulate air pollution on mortality in California: results from CALFINE. Environ Health Perspect 14:13–19.

Ovrevik J. and Schwarze P. E. (2006). Chemical composition and not only total surface area is important for the effects of ultrafine particles. Mutation Research 594, 201-202.

Paatero P. and Tapper U. (1993). Analysis of different modes of factor analysis as least squares fit problems. Chemometrics and Intelligent Laboratory Systems 18, 183-194.

Paatero P and Tapper U. (1994). Positive matrix factorization: a non-negative factor model with optimal utilization of error estimates of data values. Environmetrics 5, 111-126.

Paatero P. (1999). The multilinear engine—a table-driven least squares program for solving multilinear problems, including the n-way parallel factor analysis model. Journal of Computational and Graphical Statistics 8 (4), 854–888.

Paatero P., Hopke P. K., Song X. H. and Ramadan Z. (2002). Understanding and controlling rotations in factor analytic models. Chemometrics and Intelligent Laboratory Systems 60, 253-264.

Paatero P. and Hopke P. K. (2003). Discarding or downweighting high-noise variables in factor analytic models. Anal. Chim. Acta 490, 277-289.

Paatero P., Hopke P. K., Hoppenstock J. and Eberly S. I. (2003). Advanced factor analysis of spatial distributions of $PM_{2.5}$ in the Eastern United States. Environmental Science and Technology 37 (11), 2460-2476.

Paatero P., Hopke P. K., Begum B. A. and Biswas S. K. (2005). A graphical diagnostic method for assessing the rotation in factor analysis models of atmospheric pollution. Atmospheric Environment 39, 193–201.

Pacyna J. M. (1986). Toxic metals in the atmosphere. Nriagu J. O. and Davidson C. I. (Eds.). Wiley, New York, 33-52.

Pakkanen T. A., Loukkola K., Korhonen C. H., Aurela M., Mäkelä T., Hillamo R. E., Aarnio P., Koskentalo T., Kousa A. and Maenhaut W. (2001). Sources and chemical composition of atmospheric fine and coarse particles in the Helsinki area. Atmospheric Environment 35, 5381–5391.

Pakkanen T. A., Kerminen V. M. Loukkola K., Hillamo R. E., Aarnio P., Koskentalo T. and Maenhaut W. (2003). Size distributions of mass and chemical components in street-level and rooftop PM_1 particles in Helsinki. Atmospheric Environmment 37, 12, 1673-1690.

Palau J. L. (2003). Dispersión atmosférica de las emisiones de una chimenea alta en terreno complejo. Tesis Doctoral. Universidad de Valencia.

Papadimas C. D., Hatzianastassiou N., Mihalopoulos N., Querol X. and Vardavas I. (2008). Spatial and temporal variability in aerosol properties over the Mediterranean basin based on 6-year (2000-2006) MODIS data. J. Geophys. Res. 113, D11205.

Parra R., Jiménez P. and Baldasano J.M. (2006). Development of the high spatial resolution EMICAT2000 emission model for air pollutants from the north-eastern Iberian Peninsula (Catalonia, Spain). Environmental Pollution 140, 200-219.

Peñuelas J., Llusià J. and Gimeno B.S. (1999). Effects of ozone concentrations on biogenic volatile organic compounds emission in the Mediterranean region. Environmental Pollution 105, 17-23.

Pérez C., Sicard M., Jorba O., Comeron A., Baldasano J.M. (2004). Summertime re-circulations of air pollutants over the north-eastern Iberian coast observed from systematic EARLINET lidar measurements in Barcelona. Atmospheric Environment 38 (24), 3983–4000.

Pérez L., Tobias A., Querol X., Kunzli N., Pey J., Alastuey A., Viana M., Valero N., Gonzalez-Cabre M. and Sunyer J. (2008). Coarse Particles from Saharan Dust and Daily Mortality. Epidemiology, 19(6):800-807.

Pérez L., Medina-Ramón M., Kuenzli N., Alastuey A., Pey J., Pérez N., Tobias A., Querol X. and Sunyer J. (2009). Size fractionate particulate matter, vehicular traffic, and case-specific daily mortality in Barcelona (Spain). Environmental Science & Technology 43, 4707–4714.

Pérez N., Pey J., Querol X., Alastuey A., López J. M. and Viana M. (2008a). Partitioning of major and trace components in PM_{10}–$PM_{2.5}$–PM_1 at an urban site in Southern Europe. Atmospheric Environment 42, 1677–1691.

Pérez N., Castillo S., Pey J., Alastuey A., Viana M. and Querol X. (2008b). Interpretation of the variability of regional background aerosols in the Western Mediterranean. Science of the Total Environment 407, 527- 540.

Perrino C., Catrambone M. and Pietrodangelo A. (2008). Influence of atmospheric stability on the mass concentration and chemical composition of atmospheric particles: A case study in Rome, Italy. Environment International 34, 621–628.

Peters A., von Klot S., Heier M., Trentinaglia I., Hörmann A., Wichmann E., Löwell H. (2004). Exposure to traffic and the onset of myocardial infarction. New Engl. J. Med. 351, 1721-1730.

Pey J. (2007). Caracterización físico-química de los aerosols atmosféricos en el Mediterráneo Occidental. PhD Thesis. Universitat Politècnica de Catalunya.

Pey J., Rodríguez S., Querol X., Alastuey A., Moreno T., Putaud J. P., Van Dingenen R. (2008). Variations of urban aerosols in the western Mediterranean. Atmospheric Environment 42, 9052-9062.

Pio C. A., Nunes T. V., Borrego C. A. and Martins J. (1989). Assessment of air pollution sources in an industrial atmosphere using principal component/multilinear regression analysis. Science of the Total Environment 80, 279–292.

Pio C. A., Legrand M., Oliveira T., Afonso J., Santos C., Caseiro A., Fialho P., Barata F., Puxbaum H., Sanchez-Ochoa A., Kasper-Giebl A., Gelencsér A., Preunkert S., Schock M. (2007). Climatology of aerosol composition (organic versus inorganic) at non-urban areas on a West-East transect across Europe, J. Geophysical Research, 112, D23S02.

Plaza J., Gomez-Moreno F. Z., Nuñez L., Pujadas M., Artiñano B. (2006). Estimation of secondary organic aerosol formation from semicontinuous OC-EC measurements in a Madrid suburban area. Atmospheric Environment 40, 1134-1147.

Polissar A.V., Hopke P.K., Paatero P., Malm W.C. and Sisler J.F. (1998). Atmospheric Aerosol over Alaska 2. Elemental Composition and Sources. Journal of Geophysical Research 103, 19045–19057.

Pope C. A. and Dockery D. W. (1999). Epidemiology of particle effects. In: Air Pollution and Health (Holgate S. T., Samet J. M., Koren H. S., Maynard R. L., eds.). Academic Press, San Diego CA.

Pope C., Burnet R., Thun M. J., Calle E. E., Krewski D., Ito K. and Thurston G. D. (2002). Lung cancer, cardiopulmonary mortality, and long term exposure to fine particulate air pollution. Journal of the American Medical Association 287, 1132-1141.

Pope C., Burnett R., Thurston G., Thun M., Calle E., Krewski D., and Godleski J. (2004). Cardiovascular mortality and long-term exposure to particulate air pollution. Circulation 109: 71-77.

Pope C. and Dockery W. (2006). Health Effects of Fine Particulate Air Pollution: Lines that Connect. Journal of the Air & Waste Management Association, 56, 709-742.

Prospero J. M., Glaccum R. A. and Nees R. T. (1981). Atmospheric transport of soil dust from Africa to South America. Nature 289, 570-572.

Prospero J. M., Schmitt R., Cuevas E., Savoie D. L., Graustein W. C., Turekian K. K., Volz-Thomas A., Diaz A., Oltmans S. J., Levy II H. (1995). Temporal variability of summer-time ozone and aerosols in the free troposphere over the eastern North Atlantic. Geophysical research letters, 22, 2925-2928.

Prospero J. M. (1999) Long range transport of mineral dust in the global atmosphere: impact of African dust on the environment of the south-eastern United States. Proceedings of the National Academy of Science USA 96, 3396-3403.

Prospero J. M., Ginoux P., Torres O. and Nicholson S. (2002). Environmental characterization of global sources of atmospheric soil dust derived from the NIMBUS7 TOMS absorbing aerosol product. Reviews of Geophysics 40 (1), 2-1:2-27.

Prospero J. M. and Lamb P. J. (2003). African Droughts and Dust Transport to the Caribbean: Climate Change Implications. Science 302, 1024-1027.

Putaud J. P., Van Dingenen R., Mangoni M., Virkkula A., Raes F, Maring H., Prospero J.M., Swietlicki E,. Berg O. H., Hillamo R and Makela T. (2000). Chemical mass closure and assessment of the origin of the submicron aerosol in the marine boundary layer and the free troposphere at Tenerife during ACE-2. Tellus 52B, 141–168.

Putaud J. P., Van Dingenen R., Dell'Acqua A., Raes F., Matta E., Decesari S., Facchini M. C. and Fuzzi S. (2003). Size-segregated aerosol mass closure and chemical composition in Monte Cimone (I) during MINATROC. Atmos. Chem. Phys. Discuss. 3, 4097-4127.

Putaud, J. P., Raes, F., van Dingenen, R., Baltensperger, U., Bruggemann, E., Facchini, M.C., Decesari, S., Fuzzi, S., Gehrig, R., Hansson, H.C., Huglin, C., Laj, P., Lorbeer, G., Maenhaut, W., Mihalopoulos, N., Muller, K., Querol, X., Rodriguez, S., Schneider, J., Spindler, G., ten Brink, H., Tørseth, K., Wehner, B. and Wiedensohler, A. (2004). European Aerosol Phenomenology II: Chemical

characteristics of particulate matter at kerbside, urban, rural and background sites in Europe. Atmospheric Environment 38, 2579-2595.

Puustinen A., Hämeri K., Pekkanen J., Kulmala M., de Hartog J., Meliefste K., ten Brink H., Kos G., Katsouyanni K., Karakatsani A., Kotronarou A., Kavouras I., Meddings C., Thomas S., Harrison R., Ayres J. G., van der Zee S. and Hoek G. (2007). Spatial variation of particle number and mass over four European cities. Atmospheric Environment 41, 6622–6636.

Puxbaum H., Gomiscek B., Kalina M., Bauer H., Salam A., Stopper S., Preining O. and Hauck H. (2004). A dual site study of $PM_{2.5}$ and PM_{10} aerosol chemistry in the larger region of Vienna, Austria. Atmospheric Environment 38, 3949–3958.

Querol X., Alastuey A., Lopez-Soler A., Mantilla E. and Plana F. (1996). Mineralogy of atmospheric particulates around a large coal-fired power station. Atmospheric Environment, 30, 21, 3557-3572

Querol X., Alastuey A., Puicercus J.A., Mantilla E., Miró J.V., López-Soler A., Plana F. and Artíñano B. (1998a) Seasonal evolution of atmospheric suspended particles around a coal-fired power station: TSP levels and source origins. Atmospheric Environment, 32, 11, 1963-1978.

Querol X., Alastuey A., Lopez-Soler A., Plana F., Puicercus J.A, Ruiz C.R., Mantilla E. Juan R. (1998b). Seasonal evolution of atmospheric suspended particles around a coal-fired power station: Chemical Characterization. Atmospheric Environment, 32, 4, 719-731.

Querol X., Alastuey A., Lopez-Soler A., Plana F., Puicercus J. A., Mantilla E. and Palau J. L. (1999). Daily evolution of sulphate aerosols in a rural area, northeastern Spain-elucidation of an atmospheric reservoir effect. Environmental Pollution 105, 397-407.

Querol X., Alastuey A., Rodríguez S., Plana F., Mantilla E., Ruiz C.R. (2001a). Monitoring of PM_{10} and $PM_{2.5}$ around primary particulate anthropogenic emission sources. Atmospheric Environment 35, 845-858.

Querol X., Alastuey A., Rodríguez S., Plana F., Ruiz C.R., Cots N., Massagué G., Puig O. (2001b). PM_{10} and $PM_{2.5}$ source apportionment in the Barcelona Metropolitan Area, Catalonia, Spain. Atmospheric Environment 35/36, 6407-6419.

Querol X., Alastuey A., Rodríguez S., Viana M.M., Artíñano B., Salvador P., Mantilla E., Santos S.G.D., Patier R.F., Rosa J.D.L., Campa A.S.D.L. and Menedez M. (2002). Interpretación de series temporales (1996-2000) de niveles de partículas en suspensión en España. Ministerio de Medio Ambiente.

Querol X., Alastuey A., Viana M., Rodriguez S., Artiñano B., Salvador P., Garcia do Santos S., Fernandez Patier R., Ruiz C. R., and de la Rosa J. (2004a). Speciation and origin of PM_{10} and $PM_{2.5}$ in Spain. Journal of Aerosol Science 35, 1151-1172.

Querol, X., Alastuey, A., Ruiz, C. R., Artiñano, B., Hansson, H. C., Harrison, R. M., Buringh, E. ten Brink, H. M., Lutz, M. Bruckmannh, P., Straehl, P., Schneider, J. (2004b). Speciation and origin of PM_{10} and $PM_{2.5}$ in selected European cities Atmospheric Environment 38, 6547-6555.

Querol X., Viana M., Alastuey A., Amato F., Moreno T., Castillo S., Pey J., de la Rosa J., Sánchez de la Campa A., Artiñano B., Salvador P., García dos Santos S., Fernández-Patier R., Moreno-Grau S., Negral L., Minguillón M.C., Monfort E., Gil J. I., Inza A., Ortega L. A., Santamaría J. M. and Zabalza J. (2007). Source origin of trace elements in PM from regional background, urban and industrial sites of Spain. Atmospheric environment 41, 7219-7231.

Querol X., Alastuey A., Moreno T., Viana M., Castillo S., Pey J., Rodriguez S., Artiñano B., Salvador P., Sanchez M., Garcia do Santos S., Herce Garraleta M. D., Fernandez Patier R., Moreno-Grau S., Minguillon M. C., Monfort E., Sanz M.J., Palomo-Marin R., Pinilla-Gil E. and Cuevas E. (2008a). Spatial and temporal variations in airborne particulate matter (PM_{10} and $PM_{2.5}$) across Spain 1999-2005. Atmospheric Environment 42, 3964–3979.

Querol X., Pey J., Minguillon M. C., Perez N., Alastuey A., Viana M., Moreno T., Bernabe R. M., Blanco S., Cardenas B., Vega E., Sosa G., Escalona S., Ruiz H., and Artiñano B. (2008b). PM speciation and sources in Mexico during the MILAGRO-2006 Campaign. Atmos. Chem. Phys., 8, 111–128.

Querol X., Alastuey A., Moreno T. and Viana M. (2008c). New Directions: Legislative considerations for controlling exposure to atmospheric aerosols in rural areas. Atmospheric Environment 42, 8979–8984.

Querol X., Alastuey A., Pey J., Cusack M., Pérez N., Mihalopoulos N., Theodosi C., Gerasopoulos E., Kubilay N. and Kocak M. (2009). Variability in regional background aerosols within the Mediterranean. Atmospheric Chemistry and Physics 9: 4575.

Raes F., Van Dingenen R., Vignati E., Wilson J., Putaud J. P., Seinfeld J. H., Adams P. (2000). Formation and cycling of aerosols in the global troposphere. Atmospheric Environment 34, 4215–4240.

Raman R. S. and Hopke P. K. (2007). Source apportionment of fine particles utilizing partially speciated carbonaceous aerosol data at two rural locations in New York State. Atmospheric Environment 41, 7923–7939.

Raman R. S., Hopke P. K. and Holsen T. M. (2008). Characterization of fine aerosol and its inorganic components at two rural locations in New York State. Environmental Monitoring and Assessment 144, 1-3, 351-366.

Ramanathan V., Crutzen P. J., Kiehl J. T. and Rosenfeld D. (2001). Aerosols, Climate, and the Hydrological Cycle. Science 294, 2119–2124.

Robinson A. L., Donahue N. M., Shrivastava M. K., Weitkamp E. A., Sag, A. M. Grieshop A. P., Lane T. E., Pierce J. R. and Pandis S. N. (2007). Rethinking Organic Aerosols: Semivolatile Emissions and Photochemical Aging. Science 315, no. 5816, 1259–1262.

Rodríguez S., Querol X., Alastuey A., Kallos G. and Kakaliagou O. (2001). Saharan dust contributions to PM_{10} and TSP levels in Southern and Eastern Spain. Atmospheric Environment 35, 2433-2447.

Rodríguez S. (2002). Sources and processes affecting levels and composition of atmospheric particulate matter in the Western Mediterranean. PhD Thesis, Universitat Politècnica de Catalunya, Barcelona.

Rodríguez S., Querol X., Alastuey A. and Plana F. (2002a). Sources and processes affecting levels and composition of atmospheric aerosol in the Western Mediterranean. Journal of Geophysical Research 107, AAC 12-1-12-14.

Rodríguez S., Querol X., Alastuey A. and Mantilla E. (2002b). Origin of high summer PM_{10} and TSP concentrations at rural sites in Eastern Spain. Atmospheric Environment 36(19):3101-3112.

Rodríguez S., Querol X., Alastuey A., Viana M. and Mantilla E. (2003). Events affecting levels and seasonal evolution of airborne particulate matter concentrations in the Western Mediterranean. Environmental Science and Technology 37, 216-222.

Rodríguez S., Querol X., Alastuey A., Viana M., Alarcón M., Mantilla E. and Ruiz C. R. (2004). Comparative PM_{10}–$PM_{2.5}$ source contribution study at rural, urban and industrial sites during PM episodes in Eastern Spain. Science of the Total Environment 328, 95–113.

Rodríguez S, Van Dingenen R, Putaud JP, Martins-Dos Santos S, and Roselli D (2005). Nucleation and growth of new particles in the rural atmosphere of Northern Italy-relationship to air quality monitoring. Atmospheric Environment, 39, 6734-6746.

Rodríguez S. and Cuevas E. (2007). The contributions of 'minimum primary emissions' and 'new particle formation enhancements' to the particle number concentration in urban air. Aerosol Science 38, 12, 1207-1219.

Rodríguez S., Van Dingenen R., Putaud J. P., Dell'Acqua A., Pey J., Querol X., Alastuey A., Chenery S., Kin-Fai H., Harrison R. M., Tardivo R., Scarnato B. and Gianelle V. (2007). A study on the relationship between mass concentrations,

chemistry and number size distribution of urban fine aerosols in Milan, Barcelona & London. Atmospheric Chemistry and Physics Discussions, 7, 605–639.

Rodríguez S., Cuevas E., González Y., Ramos R., Romero P. M., Pérez N., Querol X. and Alastuey A. (2008). Influence of sea breeze circulation and road traffic emissions on the relationship between particle number, black carbon, PM_1, $PM_{2.5}$ and $PM_{2.5-10}$ concentrations in a coastal city. Atmospheric Environment 42, 6523-6534.

Rönkkö T., Virtanen A., Vaaraslahti K., Keskinen J., Pirjola L. and Lappi M. (2006). Effect of dilution conditions and driving parameters on nucleation mode particles in diesel exhaust: Laboratory and on-road study, Atmospheric Environment 40, 2893–2901.

Röösli M., Theis G., Künzli N., Staehelin J., Mathys P., Oglesby L., Camenzind M. and Braun-Fahrländer Ch. (2001). Temporal and spatial variation of the chemical composition of PM_{10} at urban and rural sites in the Basel area, Switzerland. Atmospheric Environment 35, 3701-3713.

Rose D., Wehner B., Ketzel M., Engler C., Voigtländer J., Tuch T. and Wiedensohler A. (2006). Atmospheric number size distributions of soot particles and estimation of emission factors. Atmospheric Chemistry and Physics 6, 1021-1031.

Rosenfeld D., Lohmann U., Raga G. B., O'Dowd C. D., Kulmala M., Fuzzi S., Reissell A. and Andreae M. O. (2008). Flood or Drought: How Do Aerosols Affect Precipitation? Science 321, 1309-1313.

Russell L. M. (2003). Aerosol Organic-Mass-to-Organic-Carbon Ratio Measurements. Environmental Science & Technology 37, 2982-2987.

Ruuskanen J., Tuch T., Ten Brink H., Peters A., Khlystov A., Mirme A., Kos G. P. A., Brunekreef B., Wichmann H. E., Buzorius G., Vallius M., Kreyling W. G. and Pekkanen J. (2001). Concentrations of ultrafine, fine and $PM_{2.5}$ particles in three European cities. Atmospheric Environment, 35, (21), 3729-3738.

Salma I., Chi X. and Maenhaut W. (2004). Elemental and organic carbon in urban canyon and background environments in Budapest, Hungary. Atmospheric Environment, 38, 1, 27-36.

Salma I, Ocskay R., Raes N. and Maenhaut W. (2005). Fine structure of mass size distributions in an urban environment. Atmospheric Environment 39, 5363–5374.

Salmi T., Määttä A., Anttila P., Ruoho-Airola T. and Amnell T. (2002). Detecting trends of annual values of atmospheric pollutants by the Mann-Kendall test and Sen's slope estimates-the Excel template application MAKESENS. In Publications on Air Quality No. 31 (ed. Finnish Meteorological Institute), pp. 35. Finnish Meteorological Institute.

Salvador P., Artíñano B., Querol X., Alastuey A. and Costoya M. (2007). Characterisation of local and external contributions of atmospheric particulate matter at a background coastal site. Atmospheric Environment 41, 1–17.

Salvador R. (1999). Análisis y modelización de los procesos atmosféricos durante condiciones de brisa en la costa mediterránea occidental: zona de Castellón. Tesis Doctoral. Universidad Politécnica de Catalunya.

Sánchez de la Campa A., de la Rosa J., Querol X., Alastuey A. and Mantilla E. (2007). Geochemistry and origin of PM_{10} at a rural background site in South-Western Spain. Environmental Research 103, 305-316.

Satheesh S. K. and Moorthy K. K. (2005). Radiative effects of natural aerosols: A review. Atmospheric Environment 39, 2089–2110.

Schauer J. J., Lough G. C., Shafer M. M., Christensen W. F., Arndt M. F., DeMinter J. T. and Park J. S. (2006). Characterization of metals emitted from motor vehicles. Health Effects Institute. Research report No. 133.

Schins R. P. F., Lightbody J. H., Borm P. J. A., Shi T. Donaldson K. and Stone V. (2004). Inflammatory effects of coarse and fine particulate matter in relation to chemical and biological constituents. Toxicology and Applied Pharmacology 195, 1–11.

Schwartz J. (1996). Air pollution and hospital admissions for respiratory disease. Epidemiology 7, 20–28

Schwartz J. and Neas L. M. (2000). Fine particles are more strongly associated than coarse particles with acute respiratory health effects in schoolchildren. Epidemiology 11, 6–10.

Schwarze P. E., Øvrevik J., Hetland R. B., Becher R., Cassee F. R., Lăg M., Løvik M., Dybing E. and Refsnes M. (2007). Importance of Size and Composition of Particles for Effects on Cells in Vitro. Inhalation Toxicology 19, S1, 17–22.

Seaton A., MacNee W., Donaldson K. and Godden D. (1995). Particulate air pollution and acute health effects. Lancet, 345, 176-178.

Seguel R., Morales R. G. E. and Leiva M. A. (2009). Estimations of primary and secondary organic carbon formation in $PM_{2.5}$ aerosols of Santiago City, Chile. Atmospheric Environment 43, 2125-2131.

Seidl W., Brunnemann G., Kins E., Kölher E., Reusswig K., Ruoss K., Seiler T. and Dlugi R. (1996). Nitrate in the accumulation mode; data from measurement campaigns in eastern Germany. En Nucleation and Atmospheric Aerosols (ed. M Kulmala and P E Wagner), pp. 431-434. Pergamon Press.

Seinfeld J. H. and Pandis S. N. (1998). Atmospheric Chemistry and Physics: From air pollution to climate change. John Wiley and Sons, Inc.

Sekiguchi M., Nakajima T., Suzuki K., Kawamoto K., Higurashi A., Rosenfeld D., Sano I. and Mukai S. (2003). A study of the direct and indirect effects of aerosols using global satellite data sets of aerosol and cloud parameters. Journal of Geophysical Research 108, D22, 4699.

Sicard M., Perez C., Rocadenbosch F., Baldasano J. M. and Garcia-Vizcaino D. (2006). Mixed-layer depth determination in the Barcelona coastal area from regular lidar measurements: methods, results and limitations. Boundary-Layer Meteorology 119, 135-157.

Sillanpää M., Hillamo R., Saarikoski S., Frey A., Pennanen A., Makkonen U., Spolnik Z., Van Grieken R., Braniš M., Brunekreef B., Chalbot M. C., Kuhlbusch T., Sunyer J., Kerminen V. M., Kulmala M. and Salonen R. O. (2006). Chemical composition and mass closure of particulate matter at six urban sites in Europe. Atmospheric Environment 40, S212–S223.

Spindler G., Müller K., Brüggemann E., Gnauk T. and Herrmann H. (2004). Long-term size-segregated characterization of PM_{10}, $PM_{2.5}$, and PM_1 at the IfT research station Melpitz downwind of Leipzig (Germany) using high and low-volume filter samplers. Atmospheric Environment 38, 5333–5347.

Spindler G., Brüggemann E., Gnauk T., Grüner A., Müller K., Tuch Th.M., Wallasch M.B., Wehner A., Herrmann H. (2007). Size-segregated physical and chemical long-time characterization of particles depending from air mass origin at German lowlands (Saxony, Melpitz site). EMEP Particulate Matter Assessment Report, Part B, Annex A, NILU, report EMEP/CCC-Report 8/2007, ref. O-7726, August 2007, 178-221.

Sunyer J., Kerminen V. M., Kulmala M., Salonen R. O. (2006). Chemical composition and mass closure of particulate matter at six urban sites in Europe. Atmospheric Environment 40, S212–S223.

Song X. H., Polissar A. V. and Hopke P. K. (2001). Sources of fine particle composition in the northeastern US. Atmospheric Environment 35, 5277–5286.

Soriano C., Baldasano J. M., Buttler W. T. and Moore K. (2001). Circulatory patterns of air pollutants within the Barcelona air basin in a summertime situation. Proceedings 2nd Urban Environment Symposium, American Meteorological Society.

Srivastava A. and Jain V. K. (2007). Seasonal trends in coarse and fine particle sources in Delhi by the chemical mass balance receptor model. Journal of Hazardous Materials 144, 283–291.

Stanier C. O., Khlystov A. Y. and Pandys S. N. (2004). Ambient aerosol size distribution and number concentrations measured during the Pittsburg air quality study (PAQS). Atmospheric Environment 38, 3275-3284.

Stelson A. W., Friedlender S. K. and Seinfeld J. H. (1979). A note on the equilibrium relationship between ammonia and nitric acid and particulate ammonium nitrate. Atmospheric Environment 13, 369-371.

Sternbeck J., Sjödin A. and Andréasson K. (2002). Metal emissions from road traffic and the influence of resuspension - results from two tunnel studies. Atmospheric Environment 36, 4735-4744.

Szidat S., Jenk T. M., Gäggeler H. W., Synal H. H., Fisseha R., Baltensperger U., Kalberer M., Samburova V., Reimann S., Kasper-Giebl A. and Hajdas I. (2004). Radiocarbon (14C)-deduced biogenic and anthropogenic contributions to organic carbon (OC) of urban aerosols from Zürich, Switzerland. Atmospheric Environment 38, 4035-4044.

Teller A. and Levin Z. (2005). The effects of aerosols on precipitation and dimensions of subtropical clouds; a sensitivity study using a numerical cloud model. Atmos. Chem. Phys. Discuss., 5, 7211-7245.

Thorpe A. and Harrison R. M. (2008). Sources and properties of non-exhaust particulate matter from road traffic: A review. Science of the total environment 400, 270-282.

Thurston G. D. and Spengler J. D. (1985). A quantitative assessment of source contributions to inhalable particulate matter pollution in metropolitan Boston. Atmospheric Environment 19, 1, 9-25.

Toll I. and Baldasano J. M. (2000). Modelling of photochemical air pollution in the Barcelona area with highly disaggregated anthropogenic and biogenic emissions. Atmospheric Environment 34, 3069-3084.

Tuch T. M., Wehner B., Pitz M., Cyrys J., Heinrich J., Kreyling W. G., Wichmann H. E. and Wiedensohler A. (2003). Long-term measurements of size-segregated ambient aerosol in two German cities located 100 km apart. Atmospheric Environment 37, 4687-4700.

Tunved P., Hansson H. C., Kerminen V. M., Ström J., Dal Maso M., Lihavainen H., Viisanen Y., Aalto P., Komppula M. and Kulmala M. (2006). High Natural Aerosol Loading over Boreal Forests. Science 312, 5771, 261-263.

Türküm A., Pekey B., Pekey H. and Tuncel G. (2008). Comparison of sources affecting chemical compositions of aerosol and rainwater at different locations in Turkey. Atmospheric Research 89, 4, 306-314.

Turpin B. J. and Lim H. J. (2001). Species Contributions to $PM_{2.5}$ Mass Concentrations: Revisiting Common Assumptions for Estimating Organic Mass. Aerosol Science and Technology 35, 602-610.

US-EPA (1987). Protocol for applying and validating the CMB model (ed. Office for Air Quality Planning and Standards).

US-EPA (2004). Air Quality Criteria for Particulate Matter. EPA 600/P-99/002aF-bF U.S. Environmental Protection Agency, Washington, DC. October 2004.

US-NIOSH -National Institute for Occupational Safety and Health, Centres for Disease Control and Prevention-guidelines.

Van Dingenen R., Raes F., Putaud J-P., Baltensperger U., Charron A., Facchini M-C., Decesari S., Fuzzi S., Gehrig R., Hansson H-C., Harrison R. M., Hüglin C., Jones A.M., Laj P., Lorbeer G., Maenhaut W., Palmgren F., Querol X., Rodriguez S., Schneider J., ten Brink H., Tunved P., Tørseth K., Wehner B., Weingartner E., Wiedensohler A., Wåhlin P. (2004). A European aerosol phenomenology—1: physical characteristics of particulate matter at kerbside, urban, rural and background sites in Europe. Atmospheric Environment 38, 2561-2577.

Vardoulakis S. and Kassomenos P. (2008). Sources and factors affecting PM_{10} levels in two European cities: Implications for local air quality management. Atmospheric Environment 42, 3949–3963.

Vecchi R., Marcazzan G., Valli G., Ceriani M. and Antoniazzi C. (2004). The role of atmospheric dispersion in the seasonal variation of PM_1 and $PM_{2.5}$ concentration and composition in the urban area of Milan (Italy). Atmospheric Environment 38, 4437–4446.

Vecchi R., Chiari M., D'Alessandro A., Fermo P., Lucarelli F., Mazzei F., Nava S., Piazzalunga A., Prati P., Silvani F. and Valli G. (2008). A mass closure and PMF source apportionment study on the sub-micron sized aerosol fraction at urban sites in Italy. Atmospheric Environment 42, 9, 2240-2253.

Viana M., Querol X., Alastuey A., Cuevas E. and Rodríguez S. (2002). Influence of African dust on the levels of atmospheric particulates in the Canary Islands air quality network. Atmospheric Environment 36, 5861-5875.

Viana M. (2003). Niveles, composición y origen del material particulado atmosférico en los sectores norte y este de la Península Ibérica y Canarias. PhD Thesis. Universitat de Barcelona, Barcelona.

Viana M., Pérez C., Querol X., Alastuey A. and Baldasano J. M. (2005) .Monitoring of PM levels in a complex summer atmospheric scenario in Barcelona (NE Spain), Atmospheric Environment 39, 5343-5361.

Viana M., Chi X., Maenhaut W., Querol X., Alastuey A., Mikuška P. and Vecera Z. (2006a). Organic and elemental carbon concentrations during summer and winter sampling campaigns in Barcelona, Spain. Atmospheric Environment 40, 2180-2193.

Viana M., Querol X., Götschi T., Alastuey A., Sunyer J., Forsberg B., Heinrich J., Norbäck D., Payo F., Maldonado J.A. and Künzli N. (2007). Source apportionment of ambient $PM_{2.5}$ at five Spanish centres of the European community respiratory health survey (ECRHS II). Atmospheric Environment 41, 1395–1406.

Viana M., Kuhlbusch T. A. J., Querol X., Alastuey A., Harrison R. M., Hopke P. K., Winiwarter W., Vallius M., Szidat S., Prévôt A. S. H., Hueglin C., Bloemenk H., Wåhlin P., Vecchi R., Miranda A. I., Kasper-Giebl A., Maenhaut W., Hitzenbergerq R. (2008a). Source apportionment of particulate matter in Europe: A review of methods and results. Aerosol Science 39, 827–849.

Viana M., Querol X., Ballester F., Llop S., Esplugues A., Fernández Patier R., García Dos Santos S. and Herce M.D. (2008b). Characterising exposure to PM aerosols for an epidemiological study. Atmospheric Environment 42, 1552–1568.

Visser H., Buringh E. and van Breugel P.B. (2001). Composition and origin of airborne particulate matter in the Netherlands. National Institute for Public Helath and the Environment, RIVM. The Netherlands. Report 650010029. 104 p.

Von Klot S, Peters A, Aalto P, Bellander T, Berglind N, D'Ippoliti D, Elosua R, Hörmann A, Kulmala M, Lanki T, Löwel H, Pekkanen J, Picciotto S, Sunyer J, Forastiere F; Health Effects of Particles on Susceptible Subpopulations (HEAPSS) Study Group (2005). Ambient air pollution is associated with increased risk of hospital cardiac readmissions of myocardial infarction survivors in five European cities. Circulation 112 (20):3073-9. Erratum in: Circulation. 2006 113(5):e71.

Wåhlin P. (2003). COPREM—a multivariate receptor model with a physical approach. Atmospheric Environment 37, 4861–4867.

Wåhlin P., Berkowicz R. and Palmgren F. (2006). Characterisation of traffic-generated particulate matter in Copenhagen. Atmospheric Environment 40, 2151–2159.

Wakamatsu S., Utsunomiya A., Suk Han J., Mori A., Uno I., Uehara K. (1996). Seasonal variation in atmospheric aerosol concentration covering Northern Kyushu, Japan and Seoul, Korea. Atmospheric Environment 30, 13, 2343-2354.

Wall S. M., John W. and Ondo J. L. (1988). Measurement of aerosol size distribution for nitrate and major ionic species. Atmospheric Environment 22, 8, 1649-1656.

Warneck P. (1988). Chemistry of the natural atmosphere. International Geophysics Series. Wiley & Sons. Vol. 41. Academy Press, pp. 757.

Wehner B. and Wiedensohler A. (2003). Long term measurements of submicrometer urban aerosols: statistical analysis for correlations with meteorological conditions and trace gases. Atmospheric Chemistry and Physics 3, 867–879.

Wehner B., Uhrner U., von Löwis S., Zallinger M. and Wiedensohler A. (2009). Aerosol number size distributions within the exhaust plume of a diesel and a gasoline passenger car under on-road conditions and determination of emission factors. Atmospheric Environment 43, 6, 1235-1245.

Whitby K. T. (1978). The physical characteristics of sulphur aerosols. Atmospheric Environment 12, 135-159.

WHO (2002). Guidelines for concentration and exposure-response measurement of fine and ultra fine particulate matter for use in epidemiological studies. WHO Dietrich Schwela, Lidia Morawska, QUT, Dimitrios Kotzias, EC JRC. Published on behalf of the European Commission.

WHO (2003). Health aspects of air pollution with particulate matter, ozone and nitrogen dioxide. World Health Organization.

WHO (2006). Health risks of particulate matter from long-range transboundary air pollution. Regional Office for Europe. World Health Organization.

Wichmann H. E., Spix C., Tuch T., Wölke G., Peters A., Heinrich J., Kreyling W. G. and Heyder J. (2000). Daily Mortality and Fine and Ultrafine Particles in Erfurt, Germany. Part I: Role of Particle Number and Particle Mass. Health Effects Institute, 98.

Willison M. J., Clarke A. G. and Zeki E. M. (1985). Seasonal variations in atmospheric aerosol concentration and composition at urban and rural sites in northern England. Atmospheric Environment 19, 1081-1089.

Wilson W. E. and Suh H. H. (1997). Fine particles and coarse particles: concentration relationships relevant to epidemiologic studies. J. Air Waste Manage. Assoc. 47: 1238-1249.

Wittig A. E., Takahama S., Khlystov A. Y., Pandis S. N., Hering S., Kirby B. and Davidson C. (2004). Semi-continuous $PM_{2.5}$ inorganic composition measurements during the Pittsburg air quality study. Atmospheric Environment 38, 3201–3213.

Woo K. S., Chen D. R., Pui D. Y. H. and McMurry P. H. (2001). Measurement of Atlanta aerosol size distributions: observations of ultrafine particle events. Aeros. Sci. Technol. 34, 75-87.

Wright R. F. and Schindler D. W. (1995). Interaction of acid rain and global changes: Effects on terrestrial and aquatic ecosystems. Water, Air & Soil Pollution 85, 1, 89-99.

Wu D., Tieb X., Li C., Ying Z., Kai-Hon Lau A., Huang J., Deng X. and Bi X. (2005). An extremely low visibility event over the Guangzhou region: A case study. Atmospheric Environment 39, 6568–6577.

Wu Z., Hu M., Lin P., Liu S., Wehner B. and Wiedensohler A. (2008). Particle number size distribution in the urban atmosphere of Beijing, China. Atmospheric Environment 42, 7967–7980.

Xie Y. L., Hopke P. K., Paatero P., Barrie L. A. and Li S. M. (1999). Identification of source nature and seasonal variations of Arctic aerosol by positive matrix factorization. Journal of Atmospheric Science, 56, 249-260.

Yatkin S. and Bayram A. (2008). Source apportionment of PM_{10} and $PM_{2.5}$ using positive matrix factorization and chemical mass balance in Izmir, Turkey. Science of The Total Environment 390, 1, 109-123.

Yin J. and Harrison R. M. (2008). Pragmatic mass closure study for $PM_{1.0}$, $PM_{2.5}$ and PM_{10} at roadside, urban background and rural sites. Atmospheric Environment 42, 980–988.

Yttri K.E. (2007).Concentrations of particulate matter (PM_{10}, $PM_{2.5}$) in Norway. Annual and seasonal trends and spatial variability. EMEP Particulate Matter Assessment Report, Part B, Annex A, NILU, report EMEP/CCC-Report 8/2007, ref. O-7726, August 2007, 292-307.

Yttri K. E., Aas W., Bjerke A., Ceburnis D., Dye C., Emblico L., Facchini M. C., Forster C., Hanssen J. E., Hansson H. C., Jennings S. G., Maenhaut W., Putaud J. P. and Tørseth K. (2007). Elemental and organic carbon in PM10: a one year measurement campaign within the European Monitoring and Evaluation Programme EMEP. Atmos. Chem. Phys. Discuss. 7, 3859–3899.

Zhang K. M. and Wexler A. S. (2004). Evolution of particle number distribution near roadways. Part I: analysis of aerosol dynamics and its implications for engine emission measurement. Atmospheric Environment 38, 6643–6653

Zhang K. M., Wexler A. S., Zhu Y.F., Hinds W. C. and Sioutas C. (2004). Evolution of particle number distribution near roadways. Part II: the 'Road-to-Ambient' process. Atmospheric Environment 38, 6655–6665.

Zhao W. and Hopke P. K. (2004). Source apportionment for ambient particles in the San Gorgonio wilderness. Atmospheric Environment 38, 5901-5910.

Zhou L., Kim E., Hopke P. K., Stanier C. O. and Pandis S. (2004). Advanced factor analysis on Pittsburg particle size-distribution data. Aerosol Science and Technology 38, 118-132.

Zhu Y., Hinds W.C., Kim S., Shen S. and Sioutas C. (2002). Study of ultrafine particles near a major highway with heavy-duty diesel traffic. Atmospheric Environment 36, 4323-4335.

Zhuang H., Chan C. K., Fang M., Wexler A. S. (1999). Formation of nitrate and non-sea-salt sulfate on coarse particles. Atmospheric Environment 33, 4223-4233.